

Application of an Oxygen Stitching Strategy in the Syntheses of Complex
Terpenoids

By

Xirui Hu

A dissertation submitted in partial satisfaction of the

requirements for the degree of

Doctor of Philosophy

in

Chemistry

in the

Graduate Division

of the

University of California, Berkeley

Committee in Charge:

Professor Thomas Maimone, Chair

Professor Richmond Sarpong

Professor John Hartwig

Professor Daniel Nomura

Spring 2018

Abstract

Application of an Oxygen Stitching Strategy for the Syntheses of Complex Terpenoids

by

Xirui Hu

Doctor of Philosophy in Chemistry

University of California, Berkeley

Professor Thomas J. Maimone, Chair

In the first chapter of this dissertation, a three-step total synthesis of the antimalarial (+)-cardamom peroxide, an endoperoxide-containing monoterpene dimer, is reported. This concise synthesis utilized (–)-myrtenal as an inexpensive terpene building block, and applied a novel oxygen stitching strategy to install all the oxygen atoms in the natural product from molecular oxygen. This strategy has enabled the preparation of large quantities of (+)-cardamom peroxide, and subsequent studies have determined its absolute configuration, and this molecule's reactivity in iron(II)-induced reductive cleavage. Additionally, the antimalarial activities of cardamom peroxide against the clinical isolates of *Plasmodium falciparum* from several Cambodia provinces have been evaluated.

In the second chapter, a double allylation strategy for the construction of the [5,7,5]-fused carbocyclic system found in guaianolide sesquiterpenoids is disclosed. This strategy features a robust intramolecular allylation mediated by tin(II) chloride to assemble the seven-membered core. An efficient and scalable total synthesis of the *trans*-fused 8,12-guaianolide (+)-mikanokryptin via this strategy is reported in nine to ten steps from the abundant monoterpene (+)-carvone, which constitutes the first example of gram-scale total synthesis of any guaianolide natural product.

Subsequently, the oxygen stitching strategy has been expanded from the synthesis of endoperoxides to the strategic installation of multiple oxygen atoms on complex guaianolides in a stereocontrolled manner. A concise total synthesis of (–)-nortrilobolide and a formal synthesis of the anticancer agent (–)-thapsigargin are achieved by merging the oxygen stitching strategy and double allylation strategy.

Preliminary studies on a modular synthesis of guaianolides from the Apiaceae family of plants are also disclosed via an intramolecular allylation strategy. These studies include concise total syntheses of (–)-sinodielide A and (–)-grilactone from chiral-pool building block linalool, and studies towards the total syntheses of prutenin, ammolactone A, and montanolide. Notably, this strategy has the potential to access the Apiaceae guaianolides encompassing all the oxidation levels in this family.

TABLE OF CONTENTS

Acknowledgements	ii
List of Abbreviations	v
Chapter 1. Total Synthesis of (+)-Cardamom Peroxide via an Oxygen Stitching Strategy	1
1.1. Background and Introduction	2
1.2. Initial Forays into the Synthesis of (+)-Cardamom Peroxide	3
1.3. Total Synthesis of (+)-Cardamom Peroxide	6
1.4. Mechanistic Studies of the Polyoxygenation Cascade	9
1.5. Reductive Activation of (+)-Cardamom Peroxide	10
1.6. Antimalarial Evaluation of (+)-Cardamom Peroxide	11
1.7. Conclusions	13
1.8. References	14
1.9. Experimental Procedures and Characterization Data	18
Appendix 1. NMR Spectra and X-ray Crystallography Data for Compounds Discussed in Chapter 1	27
Chapter 2. Expansion of the Oxygen Stitching Strategy: Total Syntheses of Complex Guaianolides	93
2.1. Background and Introduction	94
2.2. Previous Synthetic Studies of Guaianolides	99
2.3. A Model Study for the Polyoxygenation Cascade	123
2.4. Initial Forays into the Construction of the [5,7,5]-fused Ring System	125
2.5. Revision of the Synthetic Plan: A Double Allylation Strategy for Efficient and Scalable Guaianolide Production	131
2.6. Total Synthesis of (-)-Nortrilobolide and a Formal Synthesis of (-)-Thapsigargin via an Oxygen Stitching Strategy	136
2.7. Synthetic Studies on Guaianolides from the Apiaceae Family	145
2.8. Conclusions	155
2.9. References	156
2.10. Experimental Procedures and Characterization Data	163
Appendix 2. NMR Spectra and X-ray Crystallography Data for Compounds Discussed in Chapter 2	207

ACKNOWLEDGEMENTS

To Tom: Thank you for letting me join your lab and your help throughout my graduate study. I learned a lot from you in chemistry, presentation, and many things. Without your help in my GRS and job talk, I would not be able to handle them well. I still remember the first time we practiced my GRS talk, and how broken it was. Thanks for being supportive. I also remember the first reaction you helped me to set up in grad school, the pinene–singlet oxygen reaction, and the prep TLCs we did together for the fragmentation of cardamom peroxide. You spent a lot of efforts in training us and we really appreciated it. Best wishes to the Maimone lab.

To Danny and Kenn: Thank you for editing the first draft of my thesis, Danny. I had a great time since I moved to 909. People say when you are happy time goes fast, and it truly applies to my time in this room. I enjoyed how we make fun of each other in lab, and the time we hang out outside of Latimer. Kenn, “don’t tell people”, you’ve been a great friend to share thoughts and frustrations. You are always positive, supportive, and willing to listen. I wish you guys the best of luck in finishing the ophiobolin project, and hammering new targets in the near future. “Despite what you did” and “hv”, still “Chinese like” you.

To Rachel: When I said 909, I meant 909 plus Rachel. I still remember the first time you drove us to Safeway to buy ice cream, but can’t remember how many times I got drunk with you guys since that. We’ll definitely do hot pot again in Boston, and probably I will tell you what Zach told me when I visited him☺. Btw thank you, Danny, and Fernando for tolerating my poor cello practicing.

To Drew: It is great to have you joined the Guaianolide team. From our collaboration in the past semester I can tell you are a great team player. I enjoyed our daily discussions about chemistry. Hope we can finish this project soon, and see you in Boston (I hope at BMS).

To Silong: You are the man who can give me 10 grams of material whenever I ask you. I could not imagine without your support how much longer it would take to get the project to work. Thank you for the great food, and the help to assemble my furniture. Best wishes to you, your family, and your new baby!

To Zach: Thank you for all the advice through these years, and being a nice friend outside of lab. Having hot pot and beer with you guys were one of the most fun moments in graduate school. Best of luck at Merck and I am sure you will do the greatest. See you in Boston soon.

To Matt Kolaczowski: Thank you for being a nice friend throughout these years. I enjoyed the Hanukkah dinner and the Matzah ball soup very much. Best wishes to you and Lauren. Good luck in finishing up at LBNL and hope you find your dream job near home.

To Huck and Michael: Thank you for listening to my questions all the time, and for the beers. I hope I can meet you guys later this year. Let me know if you need more hot pot sauce☺. Best wishes to you and your family.

To Chi: Hope you are having a great time at UIUC, and I am sure the projects all become easy in your hands. Thank you for the guidance in the early days.

To Kevin and Matt: I can tell you two are a good match for chemistry, and video games. Wish you guys keep producing nice work in industry.

To Karl: You've been my longest bench-mate in grad school. I enjoyed our time in 907 and our conversations about life and chemistry. "I just need attention.☺" Good luck with your project, I have confidence you will conquer it.

To Bingqi and Nick: Thank you guys for the advice about chemistry and music. Both of you are well knowledgeable and have great personalities. Good luck with your projects and life in general.

To Linus: You are a great guy but keep saying "but" to me. "But" let me know if you need my help in the future. Hope you have a successful career and enjoy your time at Berkeley.

To Claire, Vasil, and Fernando: It is nice to know you guys at the end of my graduate study. I hope you had a great time, and best wishes to your career and life in general.

To Yuming and Gong: You are one of the most efficient chemists I know. Thank you for the guidance in chemistry, and good luck with your research as professors.

To Yujia: Good luck to your graduate study in the Reisman lab. I know that is your dream place from the very beginning. Remember our last conversation, always ask yourself "why" when a reaction is not working.

To Daniel, Hywel, Malte, and Angus: During the semester you worked with me, I hope you had a good time and learned what you needed. Hywel and Malte, and Angus if you go to UK for your PhD, I will see you guys in Europe at some point.

To Guangxin: Thank you for introducing me to chemistry. I enjoyed my time as an undergraduate student in your lab, although at that time I did not understand organic chemistry much. It was a great experience to learn chemistry from you, and my mentors Tong and Xiao. I especially appreciate the time you spend in discussing ideas of total synthesis with me after I started at BU.

To Heng and Bin: It is my fortune to know you at BU and have you as friends over the past years. There are so many funny stories I can remember, but I hope we will have even more after I move to Boston. Thank you for the phone calls throughout these years. Boss Cai, you better finish your PhD and postdoc soon, and come back to Boston.

To Wen and Feng: I wish we will end up working at the same place again. Otherwise I will visit you two and Huluwa every year if possible. Good luck to your project, I have faith in you.

To Jing and Ping: Thank you for taking me out on weekends during the two years, and for hosting me last summer. Thank you for your tremendous help last year. Let me know if you need a new lawn cutter☺.

To Tian, Yingxue, Mingyou, Lihong, Yuzhu, Li-ke, Xiaoli, Chen, Miao, Chang, Lingling: I really appreciate your support in the past years and in my life. Thank you for being there for me.

To Mom and Dad: Thank you for your support though these years. I would say this degree is not only for myself, but also for both of you.

To Grandmother and Grandfather: Thank you for raising me up till my second grade and teaching me the values of being a good person. I really wish I spent more time with you.

List of Abbreviations

Ac	acetate
acac	acetylacetonate
AD	asymmetric dihydroxylation
AIBN	azobisisobutyronitrile
AZADO	2-azaadamantane- <i>N</i> -oxyl
BINAP	2,2'-bis(diphenylphosphino)-1,1'-binaphthyl
brsm	based on recovered starting material
Bz	benzoyl
cap	caprolactamate
cod	1,5-cyclooctadiene
Cp	cyclopentadienyl
Δ	heat
DABCO	1,4-diazabicyclo[2.2.2]octane
dba	dibenzylideneacetone
DBPO	di- <i>tert</i> -butyl peroxyoxalate
DBU	1,8-diazabicyclo[5.4.0]undec-7-ene
DCE	1,2-dichloroethane
DCM	dichloromethane
DDQ	2,3-dichloro-5,6-dicyano-1,4-benzoquinone
DEAD	diethyl azodicarboxylate
DHP	3,4-dihydropyran
DIAD	diisopropyl azodicarboxylate
DIBAL-H	diisobutylaluminum hydride
DIPA	diisopropylamine
DIPEA	<i>N,N</i> -diisopropylethylamine
DMAP	4-dimethylaminopyridine
DMDO	dimethyldioxirane
DME	dimethoxyethane
DMF	dimethylformamide
DMP	Dess–Martin periodinane
3,5-DMP	3,5-dimethylpyrazole
DMS	dimethyl sulfide
DMSO	dimethyl sulfoxide
dpdb	dicyclo-hexylphosphano-2',6'-dimethoxybiphenyl
dpm	dipivaloylmethanato
dppb	1,4-bis(diphenylphosphino)butane
dppBz	1,2-bis(diphenylphosphino)benzene

dppf	1,1'-ferrocenediyl-bis(diphenylphosphine)
dppp	1,3-bis(diphenylphosphino)propane
EDC	<i>N</i> -(3-dimethylaminopropyl)- <i>N'</i> -ethylcarbodiimide
EDTA	ethylenediaminetetraacetic acid
Fe(PDP)	(2 <i>S</i> ,2' <i>S</i> -(−)-[<i>N,N'</i> -bis(2-pyridylmethyl)]-2,2'-bipyrrrolidinebis(acetonitrile)iron(II) hexafluoroantimonate
G-II <i>or</i> Grubbs II	Grubbs catalyst™ second generation
[H]	reduction
HMDS	bis(trimethylsilyl)amide
HMPA	hexamethylphosphoramide
hν	light
HRMS	high-resolution mass spectrometry
IBX	2-iodoxybenzoic acid
imid.	imidazole
IPNBSH	<i>N</i> -isopropylidene- <i>N'</i> -2-nitrobenzenesulfonyl hydrazine
IR	infrared spectroscopy
LDA	lithium diisopropylamide
<i>m</i> -CPBA	<i>meta</i> -chloroperoxybenzoic acid
MEM	2-methoxyethoxymethyl
MMPP	magnesium monoperoxyphthalate
modp	4,4-dimethyl-1-(morpholinocarbonyl)pentane-1,3-dionato
MOM	methoxymethyl
MS	molecular sieve
NBS	<i>N</i> -bromosuccinimide
NMF	<i>N</i> -methylformamide
NMM	<i>N</i> -methylmorpholine
NMO	<i>N</i> -Methylmorpholine <i>N</i> -oxide
NMR	nuclear magnetic resonance
[O]	oxidation
ox	oxalate
Pc	phthalocyanine
PCC	pyridinium chlorochromate
PDB code	protein data bank code
PDC	pyridinium dichromate
Ph	phenyl
PIDA	(diacetoxyiodo)benzene
pin	pinacol
PPTS	pyridinium <i>para</i> -toluenesulfonate
PSMA	prostate-specific membrane antigen
PTSA	<i>para</i> -toluenesulfonic acid

py	pyridine
RCM	ring-closing metathesis
rsm	recovered starting material
rt	room temperature
SEM	[2-(trimethylsilyl)ethoxy]methyl
SERCA	sarco/endoplasmic reticulum Ca ²⁺ ATPase
2,4,6-TCBC	2,4,6-trichlorobenzoyl chloride
TBAF	tetrabutylammonium fluoride
TBDPS	<i>tert</i> -butyldiphenylsilyl
TBHP	<i>tert</i> -butyl hydroperoxide
TBS	<i>tert</i> -butyldimethylsilyl
TCCA	trichloroisocyanuric acid
TEMPO	(2,2,6,6-tetramethylpiperidin-1-yl)oxyl
TES	triethylsilyl
Tf	triflate <i>or</i> trifluoromethanesulfonate
TFA	trifluoroacetic acid
TFE	trifluoroethanol
THF	tetrahydrofuran
TIPS	triisopropylsilyl
TLC	thin layer chromatography
TMEDA	tetramethylethylenediamine
TMS	trimethylsilyl
TPAP	tetrapropylammonium perruthenate
TPP	tetraphenylporphyrin
X-ray	X-radiation <i>or</i> Röntgen radiation

Chapter 1

Total Synthesis of the Antimalarial (+)-Cardamom Peroxide via an Oxygen Stitching Strategy

1.1 Background and Introduction

Cardamom peroxide (**1**) was isolated in 1995 by Clardy and coworkers from the *Amomum krevanh* fruit (Siam cardamom) (Figure 1.1).¹ Initial *in vitro* assays indicated that this terpene endoperoxide exhibited strong antimalarial activities against *Plasmodium falciparum* (EC₅₀ = 170 nM), approximately at the same level of potency as the synthetic antimalarial arteflene. Despite several synthetic studies that have been reported,² no chemical synthesis of **1** was available prior to our work. We viewed **1** as an intriguing synthetic target for the development of a novel synthetic strategy, which could potentially elucidate its biosynthetic origin, as well as for further investigation of its activities against malaria.

Malaria is an infectious parasitic disease transmitted by the *Anopheles* mosquito. Based on studies from the World Health Organization (WHO), more than 3 billion people over 99 countries are at risk of acquiring this disease, and an estimated 445,000 deaths occurred as a result of malaria in 2016, mostly due to the infection from *P. falciparum*.³ Humanity's fight against malaria dates back to the 1600s, when Peruvian Indians were observed chewing on Cinchona bark to stop shivering.⁴ The Cinchona bark, from which the first antimalarial drug quinine was isolated, was introduced into Europe as a treatment for malaria in the early 17th century.⁵ Since then, many quinine-type antimalarial drugs have been applied to infected patients, but resistance to these drugs rapidly developed in malaria parasites.⁶ The isolation of the terpene peroxide artemisinin (**2**) in the 1970s represented a landmark breakthrough in the development of antimalarials.⁷ For decades, artemisinin-based combination therapies (ACTs) have served as the front-line treatment for uncomplicated and severe *P. falciparum* infections. In the past decade, however, continually growing reports of artemisinin resistance have surfaced, an observation which severely threatens the global malaria control.⁸

Continuous efforts in this field have sought new antimalarials, and numerous endoperoxide-containing natural products have been discovered in the past decades (Figure 1.1A).⁹ Some fully synthetic antimalarials such as the ozonide arterolane and the yingzhaosu-type endoperoxide arteflene were also investigated.¹⁰ Although the potency of these peroxide-containing antimalarials remain inferior to that of **2** and its congeners, these ongoing efforts have led to many innovative chemical syntheses as well as the development of peroxidation methodology.¹¹

Structurally, cardamom peroxide (**1**) contains a rare seven-membered endoperoxide motif (1,2-dioxepane) that is distinct from many of the aforementioned antimalarials. Given that the endoperoxide moiety found in artemisinin (**2**) was proposed to be assembled in nature via a non-enzymatic process,¹² we speculated whether **1** could be constructed likewise in a biomimetic setting. We envisioned that **1** might arise from chemoselective reduction of diperoxide **3** (Figure 1.1B), which may in turn derive from a peroxide or peroxy radical precursor (*i.e.* **4** or **5**), via a 7-*endo-trig* cyclization followed by oxygenation of the resulting enolate or α -keto radical respectively. The peroxy intermediate (**4** or **5**) could then come from an air oxidation process of diketone **6**, which resembles a pinene-type monoterpene dimer. It is worth noting that various pinene-derived monoterpenes were also isolated alongside **1** from the *A. krevanh* fruit.¹

We suspected that from diketone **6**, the α -oxygenation event and the subsequent polyoxygenation cascade would occur diastereoselectively as controlled by the neighboring pinane ring system, and such control would not require a chiral enzymatic environment. Nevertheless, literature precedent suggested that the 7-*endo* cyclization would be challenging, and we were

aware that Mayrargue and coworkers could not forge the 1,2-dioxepane unit (see **8**, $n = 3$) from the corresponding pinene-derived model peroxide **7**.^{2c} In contrast, this model radical cyclization was competent in forging the 1,2-dioxolane and 1,2-dioxane structures (Figure 1.1C).

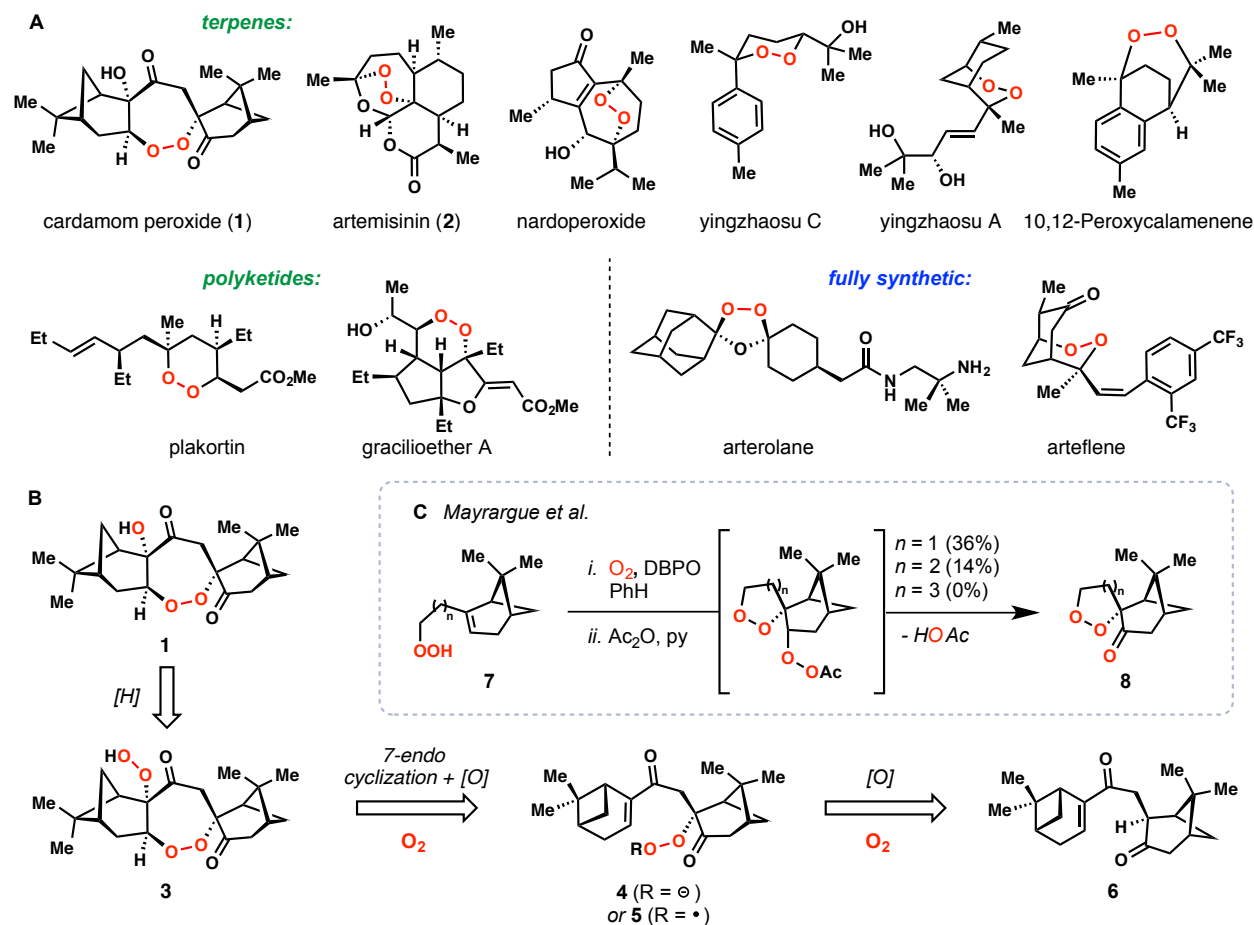
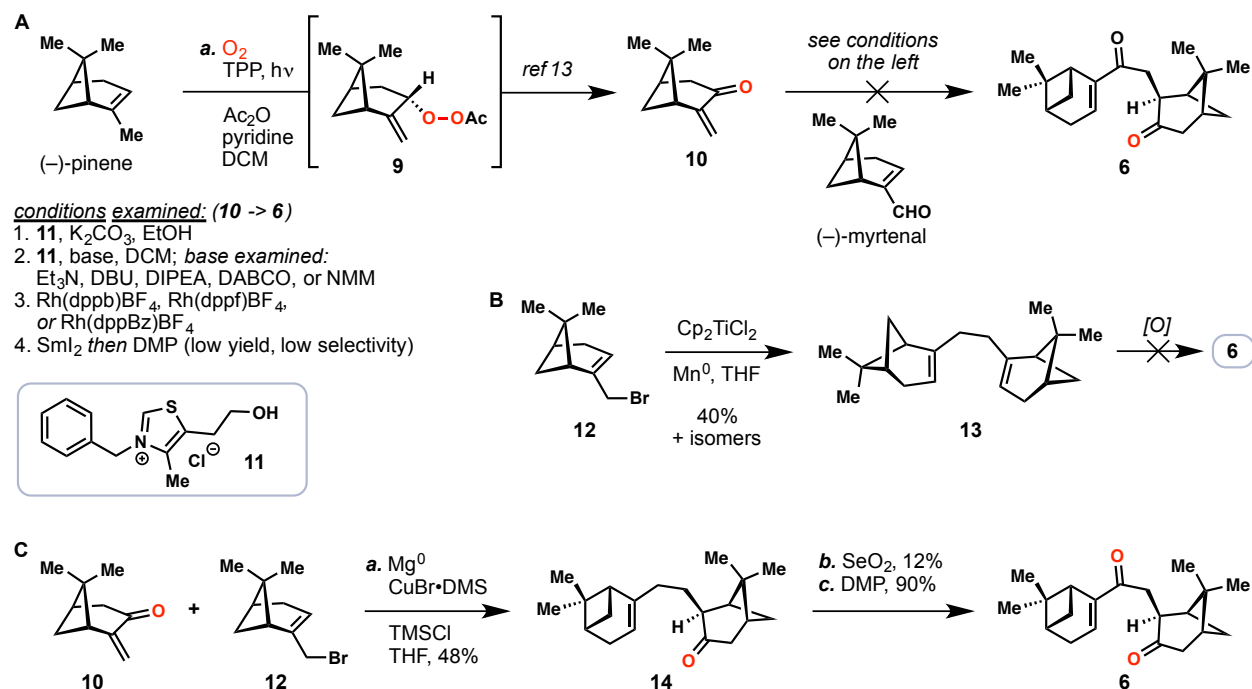


Figure 1.1. **A**) Antimalarials containing an oxygen-oxygen bond: endoperoxide-containing natural products and fully synthetic molecules inspired by natural products. **B**) Our initial retrosynthesis. **C**) Studies by Mayrargue and coworkers demonstrates the challenge in forming the 1,2-dioxepane unit found in **1**.

1.2 Initial Forays into the Synthesis of (+)-Cardamom Peroxide

Our initial forays into the construction of cardamom peroxide (**1**) began with the assembly of the dimeric carbon skeleton found in diketone **6** (Scheme 1.1). To this end, enone **10** was prepared in one step from pinene via peroxide intermediate **9**.¹³ A Stetter-type coupling of enone **10** and (–)-myrtenal under the conditions mediated by thiazolium salt **11** and base was examined, but failed to provide the desired coupled product (Scheme 1.1A). Subsequent attempts using Rh-catalyzed hydroacylation or SmI_2 -mediated reductive coupling to react (–)-myrtenal with enone **10** were also found to be unfeasible.¹⁴ In an alternative approach, bromopinene **12** was dimerized under titanocene-mediated reductive conditions to give diene **13**,¹⁵ which we envisioned as a plausible biogenetic precursor to **1**, but achieving the desired oxidation patterns found in **6** proved problematic (Scheme 1.1B). Nevertheless, by using a copper-mediated conjugate addition to

connect the two fragments **10** and **12**, we gained our initial success in forging **6** (Scheme 1.1C). The cuprate derived from bromopinene **12** was prepared under the conditions developed by Lipshutz and coworkers (Mg^0 , *cat.* dibromoethane; $\text{CuBr}\cdot\text{Me}_2\text{S}$, TMSCl),¹⁶ which was then treated with enone **10** *in situ*, affording the 1,4-addition product **14** in 48% yield as a single diastereomer after acidic work-up. Subsequent SeO_2 -mediated allylic oxidation followed by Dess–Martin oxidation successfully provided the proposed peroxidation precursor **6**. However, the low yield encountered in the SeO_2 oxidation (12%, unoptimized) was a bottleneck for material throughput to examine the following peroxidation cascade.

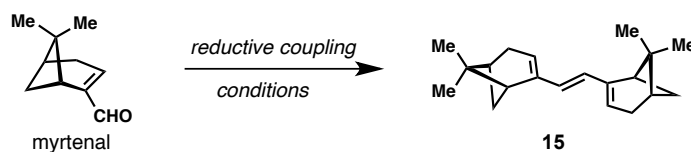


Scheme 1.1. Synthetic studies towards diketone **6**.

In order to prepare diketone **6** in larger quantities, I developed an alternative sequence to **6** based on the chemistry shown in Scheme 1.2. In this route, (–)-myrtenal was dimerized under reductive coupling conditions, which produced triene **15** bearing the desired functionality for further redox manipulations. A number of established protocols inducing McMurry-type carbonyl coupling were examined (Table 1.1). While the reductive coupling conditions based on aluminum¹⁷ and chromium¹⁸ failed to produce triene **15** (entries 1 and 2), several titanium-based systems were found to be applicable to this transformation. In our initial attempts, a small amount of **15** (<10% yield) was obtained under the conditions employing excess amounts of titanium powder (entry 3).¹⁹ The use of stoichiometric quantities of titanocene dichloride with reducing agents (Mn^0 or Zn^0) produced **15** in low yield (~20%) (entries 4 and 5), whereas the catalytic version of this system failed to produce any desired product (entry 6).²⁰ Under the conditions wherein Cp_2TiCl_2 was replaced by freshly distilled TiCl_4 , triene **15** was obtained in a more synthetically useful yield (35%, entry 7).²¹ This enhancement of reaction yield led us to consider the classic McMurry coupling condition [TiCl_3 , Zn–Cu alloy] (entry 8),²² which provided an improved yield of **15** (51%), and also featured a relatively straightforward workup protocol compared to the aforementioned conditions. However, due to the high cost of titanium(III) trichloride, this protocol was not directly applied in our synthesis, but slightly modified by using less expensive titanium

(IV) tetrachloride and higher equivalents of the metal reductant (entry 9). The modified procedure offered 62% yield of **15** on small scales, and could be reproducibly performed on 3-gram scales in 53% yield. It is worth noting that triene **15** was found to be unstable, and decomposed to complex mixtures upon standing in air, or in solution of mildly acidic CDCl₃.

Table 1.1. Investigation of the reductive coupling of myrtenal.



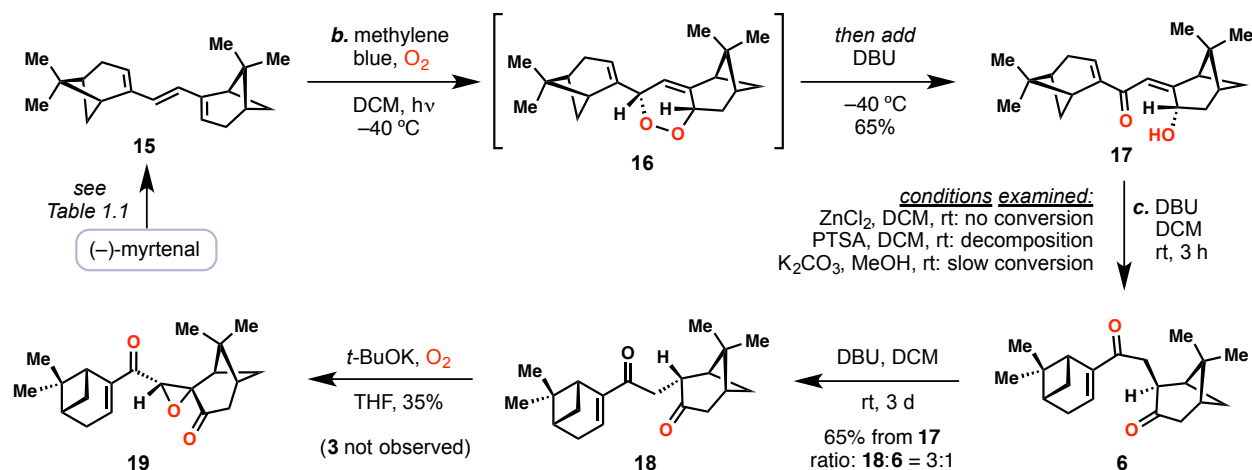
Entries	Conditions ^[a]	Yield [%]
1	AlCl ₃ (2 equiv), Zn ⁰ (2 equiv), MeCN (0.1 M)	0
2	CrCl ₂ (4 equiv), HSiCl ₃ (5 equiv), THF (0.07 M)	0
3	Ti ⁰ (30 equiv), TMSCl (30 equiv), DME (0.07 M)	<10 ^[b]
4	Cp ₂ TiCl ₂ (1.2 equiv), Mn ⁰ (2.4 equiv), THF (0.1 M)	17 ^[b]
5	Cp ₂ TiCl ₂ (1.2 equiv), Zn ⁰ (2.4 equiv), THF (0.1 M)	18 ^[b]
6	Cp ₂ TiCl ₂ (0.3 equiv), TMSCl (4 equiv), Mn ⁰ (8 equiv), THF (0.1 M)	0
7	TiCl ₄ (1.2 equiv), Zn ⁰ (2.4 equiv), THF (0.1 M)	35 ^[b]
8	TiCl ₃ (11 equiv), Zn–Cu (30 equiv), DME (0.01 M)	51 ^[c,d]
9	TiCl₄ (10 equiv), Zn–Cu (40 equiv), DME (0.01 M)	62^[c,d,e]

[a] Reaction performed on a 100-mg scale, conditions detailed in references unless otherwise stated. [b] NMR yield, with dibromomethane as internal standard. [c] Isolated yield. [d] Myrtenal was added in two portions over 24 h. [e] Reaction afforded 53 % of **15** on a 3-gram scale.

From triene **15**, a [4+2] cycloaddition with singlet oxygen smoothly desymmetrized this C₂-symmetric dimer, and delivered endoperoxide **16** (Scheme 1.2). This sensitive intermediate was then subjected to Kornblum–DeLaMare fragmentation (DBU, –40 °C),²³ furnishing dienone alcohol **17** in 65% yield. Subsequently, a redox-neutral isomerization was envisioned to forge diketone **6** via a sequence of γ -deprotonation of **17** and protonation of the resulting bis-enol intermediate.²⁴ A brief screening of conditions revealed that under basic conditions (K₂CO₃, MeOH), a small amount of diketone **6** was formed under extended reaction time. Ensuing efforts in optimization of this transformation led to the discovery of an improved procedure, in which excess amounts of DBU in DCM were used, and partially conversion of **17** to **6** was observed within hours at room temperature. After stirring at room temperature for 3 days, a mixture of **6** and its diastereomer **18** could be obtained in 65% yield (1:3 *dr*).

With sufficient amounts of **6** and **18** in hand, I subsequently investigated the proposed polyoxygenation cascade. Both isomers were reacted under conditions known to elicit ketone α -peroxidation (*t*-BuOK, O₂).²⁵ Unfortunately, formation of the desired diperoxide **3** was not observed under these conditions; the major product isolated was determined to be epoxide **19**. These findings led us to speculate that anion **4** did not undergo the 7-*endo* cyclization at a rate comparable to the formation of epoxide.²⁶ This hypothesis was also corroborated by our later findings, wherein we suspect that protonated **4** favors the formation of a peroxy hemiacetal intermediate (*i.e.* **26**, see Figure 1.2) instead of undergoing the intramolecular conjugate addition

to the enone moiety. While unsuccessful in forging dperoxide **3**, this work led us to consider alternative ways of generating **3** via radical **5** instead of anion **4** (see Figure 1.1); such efforts ultimately enabled a rapid synthesis of **1**.



Scheme 1.2. Improved synthesis of diketone **6** and failed conversion to dperoxide **3**.

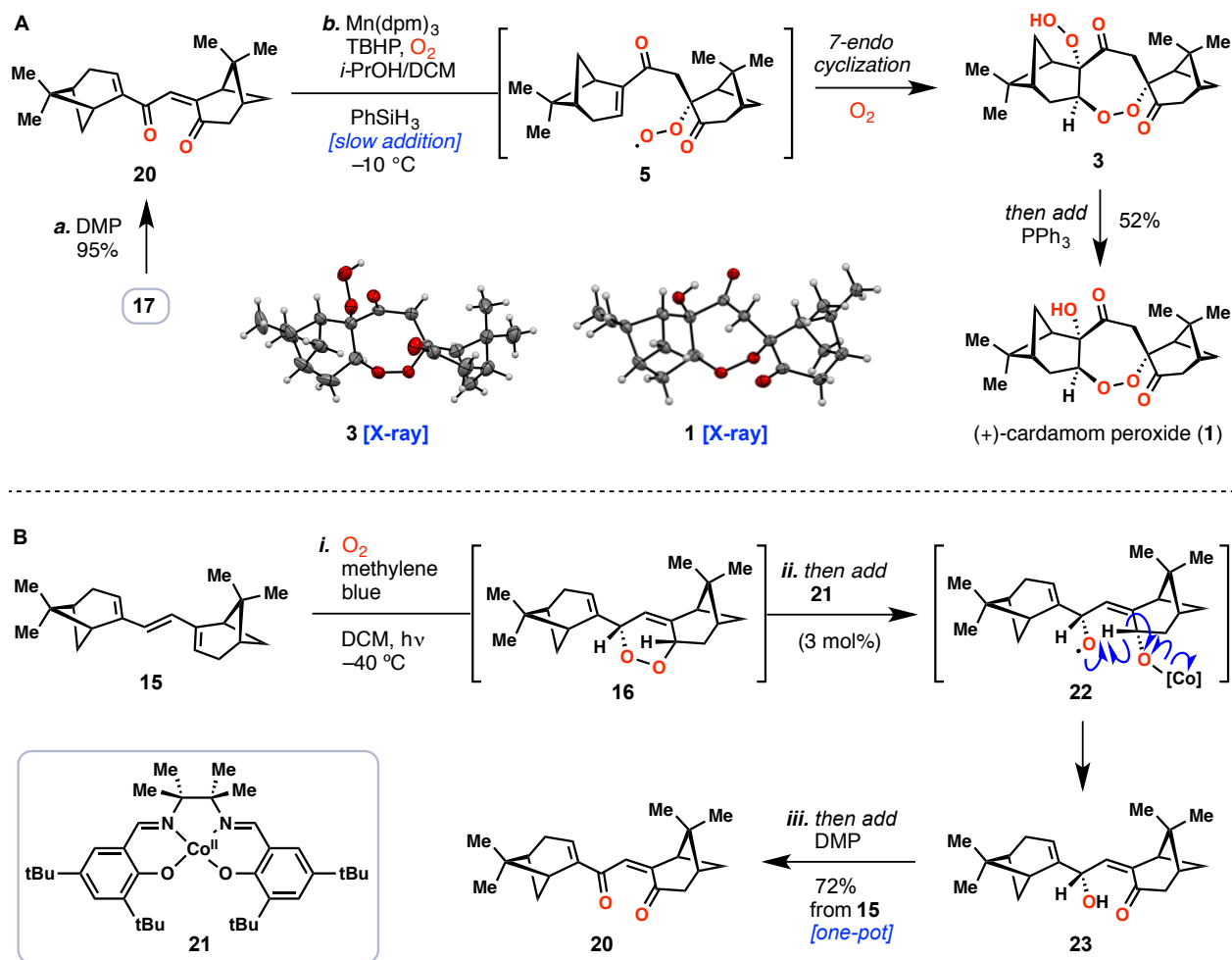
1.3 Total Synthesis of (+)-Cardamom Peroxide

Our successful route to dperoxide **3** (and ultimately **1**) commenced with a Dess–Martin oxidation to generate bisenone **20** from the previously prepared dienone alcohol **17** (Scheme 1.3A). Alternatively, we also developed a one-pot procedure to prepare **20** directly from triene **15** (Scheme 1.3B). In this protocol, the initial [4+2]-adduct between triene **15** and single oxygen (*i.e.* **16**) was subjected to the Taylor’s conditions utilizing catalytic amounts of Co(II)-salen complex **21**.²⁷ The Co(II)-catalyst induced a single-electron fragmentation of endoperoxide **16**, presumably arriving at radical **22**, which then underwent a 1,5-hydrogen atom abstraction to produce enone **23** and regenerate the Co(II)-complex. Enone **23** could ultimately be oxidized *in situ* upon the addition of Dess–Martin periodinane, affording bisenone **20** in 72% overall yield.

With a sufficient amount of **20** in hand, we turned towards the examination of a tandem hydroperoxidation reaction to generate dperoxide **3** or cardamom peroxide (**1**). We envisioned that if the initial metal-catalyzed hydroperoxidation of bisenone **20** occurred in a regio- and stereoselective manner, the proposed radical **5** could be produced via a subsequent homolytic cleavage of the transient peroxymetallo species. The regioselectivity of this process (**20** → **5**) may be achieved by tuning the metal-hydride generating conditions favoring the formal addition of metal hydride at the more electron-deficient alkene,²⁸ while the stereoselectivity of the peroxidation would be controlled by the steric constraints caused by the surrounding pinane unit. From radical **5**, if our previously discussed hypothesis is correct, dperoxide **3** could then be forged after the tandem cyclization–oxygenation process.

Our initial screening of metal precatalysts for this tandem process began with several reported conditions for the Mukaiyama-type hydration or hydroperoxidation.²⁹ As shown in Table 2, the iron-based system developed by Boger and coworkers,³⁰ which employed excess amounts of iron(III) oxalate in combination with NaBH₄, remained unreactive to the conjugated bisenone system found in **20** (entry 1). In contrast, bisenone **20** was particularly reactive under the conditions

utilizing $\text{Fe}^{\text{II}}(\text{PC})$ and NaBH_4 (entry 2).³¹ Under these conditions, complete consumption of **20** was observed after 15 minutes, affording a complex mixture of products, and the major product was identified as nopinone (39%, GC yield). The use of $\text{Fe}(\text{acac})_3$ and $\text{Co}(\text{acac})_2$ as the precatalysts resulted in low conversion of bisenone **20** at 0 °C (entries 3 and 4), and therefore the reaction mixtures were warmed to room temperature.^{29,32} Complete conversion of the starting material was achieved after stirring at room temperature for 16 hours and 36 hours, respectively. Nopinone was again predominately formed under these conditions.



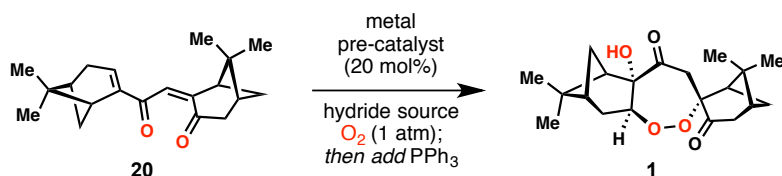
Scheme 1.3. A) Total synthesis of (+)-cardamom peroxide. B) One-pot synthesis of **20** from **15**.

To our delight, cardamom peroxide (**1**) was isolated in the cobalt- and manganese-catalyzed reactions after reductive workup in 6% and 34% yield, respectively (entries 4 and 5, Table 1.2). My efforts to optimize this transformation (*i.e.* **20** → **1**) then focused on variation of other reaction parameters in the manganese-based system.^{29e,33-35} The product composition of this tandem process was found to be highly dependent on the concentration of reductant and oxygen. Decreasing the ratio of reductant and oxygen by slow addition of PhSiH_3 as a solution in dichloromethane over 12 hours improved the yield to 41% with fewer side products formed (entry 6). Incorporation of *tert*-butyl hydroperoxide (TBHP) further increased the yield to 52% (entry 7), presumably due to faster oxidation of the $\text{Mn}(\text{II})(\text{dpm})_2$ intermediate to the functional $\text{Mn}(\text{III})$

complex, a process that would otherwise consume molecular oxygen in the solution. Under this optimized condition, nopinone, hydration product **24**, and diol **25** were obtained in 9% (GC yield), 11%, and 13% yields respectively (entries 7).

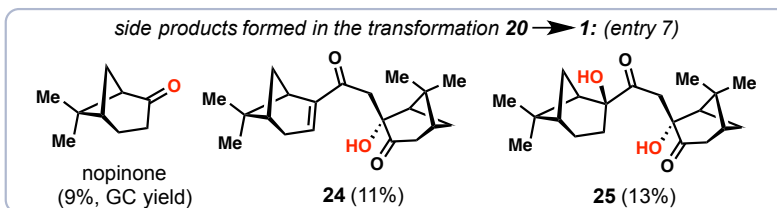
Synthetic cardamom peroxide (**1**) prepared from (-)-myrtenal displayed an optical rotation of +123.2° (*c* = 0.005 g/mL, hexanes), which is in agreement with the reported value of $[\alpha]_D = +111.35^\circ$ (concentration not reported). The absolute configuration of synthetic **1** was unambiguously determined by X-ray analysis, and is opposite to that previously suggested by Clardy and coworkers.¹ Taking the one-pot transformation of triene **15** to bisenone **20** into account, our synthesis of **1** only requires three steps. This concise synthesis provided large quantities of **1** (>500 mg prepared), which enabled the subsequent studies that will be discussed in sections 1.5 and 1.6.

Table 1.2. Optimization of the tandem peroxidation reaction.



Entries	Conditions ^[a]	Yield [%] ^[b]
1	Fe ₂ (ox) ₃ •6H ₂ O (5.0 equiv), NaBH ₄ (6.4 equiv), EtOH/H ₂ O, 0 °C	0
2	Fe ^{II} (Pc), NaBH ₄ (3.0 equiv), EtOH, 0 °C	0
3	Fe(acac) ₃ , PhSiH ₃ (2.5 equiv), EtOH, 0 °C to rt	0
4	Co(acac) ₂ , PhSiH ₃ (2.5 equiv), DCM/ <i>i</i> -PrOH, -10 °C to rt	6
5	Mn(dpm) ₃ , PhSiH ₃ (2.5 equiv), DCM/ <i>i</i> -PrOH, -10 °C	34
6	Mn(dpm) ₃ , PhSiH ₃ (2.5 equiv), DCM/ <i>i</i> -PrOH, -10 °C	41 ^[b]
7	Mn(dpm)₃, PhSiH₃ (2.5 equiv), <i>t</i>-BuOOH (1.5 equiv), DCM/<i>i</i>-PrOH, -10 °C	52^[b]

[a] Reaction performed on a 0.1 mmol scale using 20 mol% of metal catalyst unless otherwise stated. [b] PhSiH₃ added slowly over 12 h as a solution in DCM. Pc = phthalocyanine, ox = oxalate, acac = acetylacetonate, dpm = dipivaloylmethanato.



1.4 Mechanistic Studies of the Polyoxygenation Cascade

Intrigued by the formation of nopinone and other side products observed in the tandem peroxidation reaction, we sought to better understand the mechanisms by which these compounds may be formed (Figures 1.2 and 1.3). In a key experiment, I treated bisenone **20** with stoichiometric amounts of $\text{Mn}(\text{dpm})_3$, and added PhSiH_3 in a single portion (Figure 1.2). With an increased ratio of reductant and oxygen compared to the aforementioned condition (Table 1.2, entry 7), a rapid consumption of enone **20** was observed within 10 minutes and only a small amount of diperoxide **3** was detected based on TLC analysis. Before the reductive work-up, the major component of the reaction mixture was a mystery intermediate existing as two unstable and interconvertible isomers, which we tentatively assigned as peroxy hemiacetal **26** based on ^1H NMR analysis. Upon addition of PPh_3 to the mixture, both **3** and **26** were consumed, and cardamom peroxide (**1**) and the mono-hydration product **24** were obtained in 9% and 40% yields, respectively.

In subsequent studies, the sensitive intermediate **26** was isolated after a rapid column chromatography (as a mixture of two isomers), and was immediately subjected to the conditions employing catalytic amounts of $\text{Mn}(\text{dpm})_3$. Nopinone and diol **25** were isolated under these conditions, along with a complex mixture of decomposition products. In contrast, when the mono-hydration product **24** was resubjected to the manganese-catalyzed condition, a clean conversion to diol **25** was obtained, while the formation of nopinone was not observed.

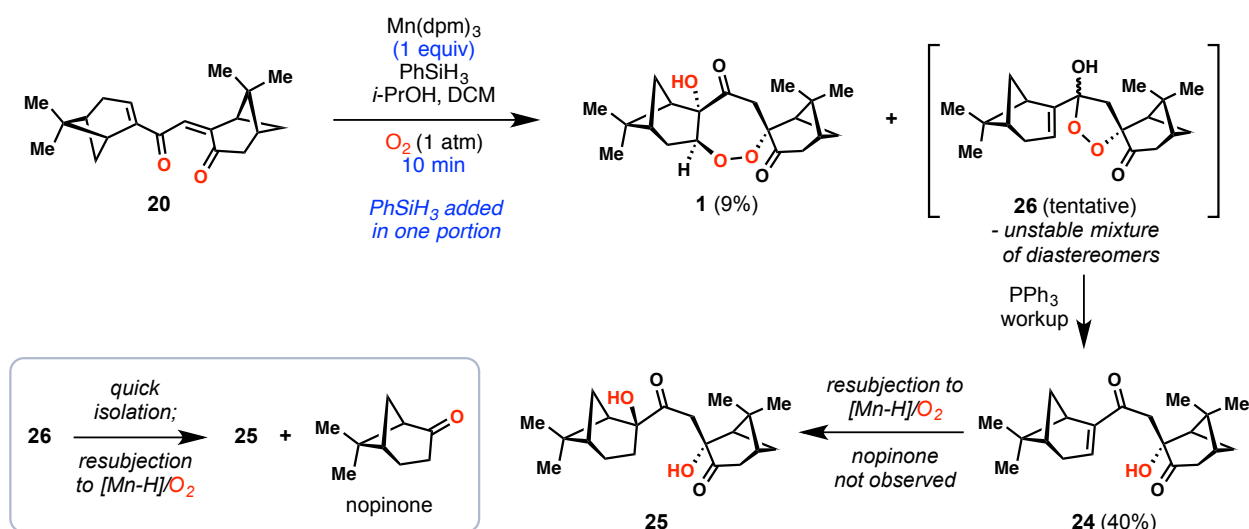


Figure 1.2. Investigation into the formation of side products during the polyoxygenation cascade.

Based on these mechanistic studies, we hypothesize that the radical intermediate **5** upon generation from bisenone **20**, encounters two competing pathways under the manganese-catalyzed system (Figure 1.3). With sufficient amounts of molecular oxygen in the solution, the α -keto radical form of **5** (*i.e.* **27**) can be oxygenated to an α -peroxy radical intermediate, and subsequently reduced to diperoxide **3**. With lower amounts of molecular oxygen or increased amounts of reductant, however, peroxy hemiacetal **26** is predominantly formed, which triggers the downstream processes to deliver mono-hydration product **24** after reduction, or intermediate **28** after an additional hydroperoxidation. The ensuing hydroperoxidation of **24** then delivers diol **25** as its downstream product via a peroxide intermediate **29**; while the fragmentation of β -hydroxy

hydroperoxide **28** results in the formation of nopinone,³⁶ as well as other decomposition products presumably via peroxy ester **30**.

It should be noted that we have not isolated peroxy ester **30** to date from the reactions utilizing the combination of $\text{Mn}(\text{dpm})_3$ and PhSiH_3 . However, under the cobalt-catalyzed conditions $[\text{Co}(\text{acac})_2, \text{PhSiH}_3]$ (Table 1.2, entry 4), we have isolated small amounts (~5%) of dione **31** alongside nopinone.³⁷ We wondered whether **31** is a downstream product from the decomposition of peroxy ester **30**. To gain more mechanistic insight, dione **31** was subjected to the manganese-catalyzed conditions $[\text{Mn}(\text{dpm})_3, \text{PhSiH}_3]$. However, extensive decomposition was observed, affording a complex mixture of unidentifiable products. Presumably, the enol form of **31** (*i.e.* **32**) underwent hydroperoxidation under these conditions, which was followed by fragmentation of the resulting peroxide. This result suggested that **31** would not be isolable under the manganese-based conditions if it was produced, thus evading initial detection.

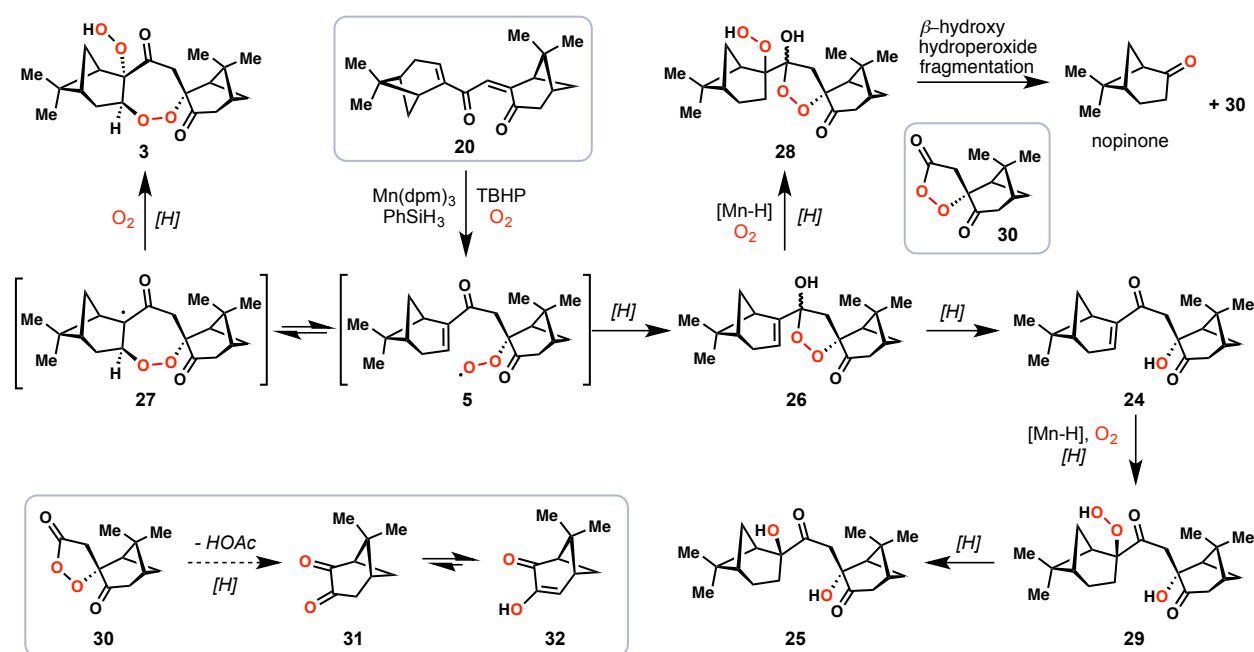


Figure 1.3. Potential mechanism of the polyoxygenation cascade.

1.5 Reductive Activation of (+)-Cardamom Peroxide

Despite the longstanding and ongoing debate over the mechanism of action of artemisinin (**2**) and other peroxide-containing antimalarials,³⁸ a pathway involving single-electron peroxide O–O bond cleavage has been documented as the origin of their oxidative damages to the malaria parasites. Many studies have suggested that upon activation by a single-electron reductant, such as intracellular iron(II)-species, organic peroxides undergo fragmentations to generate oxygen-centered radicals, which then lead to various downstream processes, including radical β -scission.³⁹ The active carbon-centered radicals derived from radical β -scission ultimately triggers oxidative damages through various pathways such as heme alkylation, protein alkylation, or inducing apoptotic cell death (Figure 1.4).⁴⁰ As disclosed by previous studies, artemisinin (**2**) produces a primary radical intermediate upon reductive activation, whereas synthetic antimalarials arteflene and arterolane generate secondary radical intermediates.⁴¹

In order to examine the reductive activation mode of cardamom peroxide (**1**), we treated **1** with iron(II) chloride in a solvent mixture of water and acetonitrile under deoxygenated conditions (Figure 1.5A). Upon addition of the iron(II) salt, a rapid solution color change of yellow/green to red was observed. After **1** was consumed as judged by TLC, three major products, vinyllogous acid **36**, pyranone **37**, and furanone **38**, were isolated in yields of 20%, 5–10%, and 42% respectively. Presumably, iron(II) chloride approaches the endoperoxide from the less-hindered side, and generates oxygen-centered radical **33** that selectively cleaves the neighboring carbon-carbonyl bond. Oxidation of the resulting acyl radical **34** by the iron(III) center then leads to acylium ion **35**, followed by addition of H₂O, arriving at carboxylic acid **36**, and the further cyclized products **37** and **38**. Notably, the structures of pyranone **37** and furanone **38** were unambiguously confirmed by X-ray crystallographic analysis.

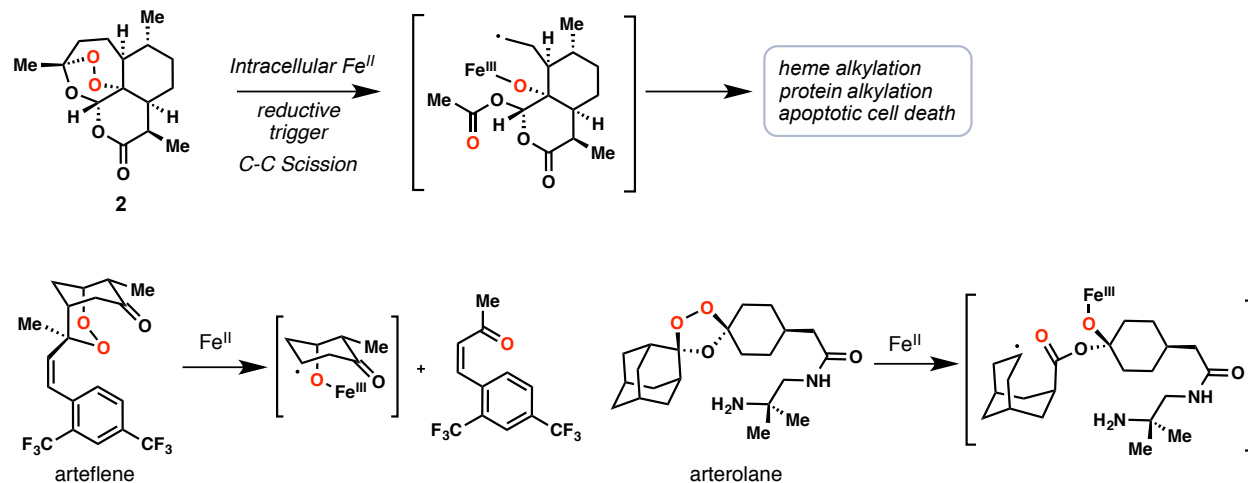


Figure 1.4. Known Fe(II)-induced activation of O–O bond-containing antimalarials.

According to the heme alkylation model for artemisinin's mechanism of action, the primary radical derived from **2** forms a covalent C–C bond with the iron-porphyrin complexes thus inhibiting hemozoin formation.^{40a} We therefore conducted a biologically relevant reaction by treating cardamom peroxide (**1**) with hemin dimethyl ester and an abundant intracellular reductant glutathione (Figure 1.5B).^{41d} From this reaction, pyranone **38** was isolated as the major product, along with three presumed hemin-containing adducts as judged by TLC analysis and high-resolution mass spectrometry (see **39**, $m/z = 974.3963$, C₅₆H₆₂FeN₄O₈). Unfortunately to date, attempts to demetallate these complexes for NMR characterization have led only to decomposition, and we have not been able to grow single crystals of **39** for X-ray diffraction studies.

1.6 Antimalarial Evaluation of (+)-Cardamom Peroxide

Recent reports of artemisinin resistance in *P. falciparum* have surfaced in western Cambodia,⁸ historically an epicenter for antimalarial drug resistance. The resistance to endoperoxides found in this region was proposed as a result of mutations which increase the ability of the parasite to manage oxidative damage.⁴²

Evaluation of cardamom peroxide (**1**) against clinical isolates from three provinces in the Cambodia region were performed in collaboration with Dr. Pharath Lim and Dr. Rick Fairhurst

from the National Institutes of Health (NIH). The mean IC_{50} s were measured as 613.3, 502.7, and 339.0 nM for Pursat (western region), Preah Vihear (central), and Ratanakiri (eastern), respectively. While **1** has not been used clinically, it shows western Cambodian field isolates being the least sensitive to its effects. Similar trends were also observed in the survey of several other commonly used or historically used antimalarials.⁴³

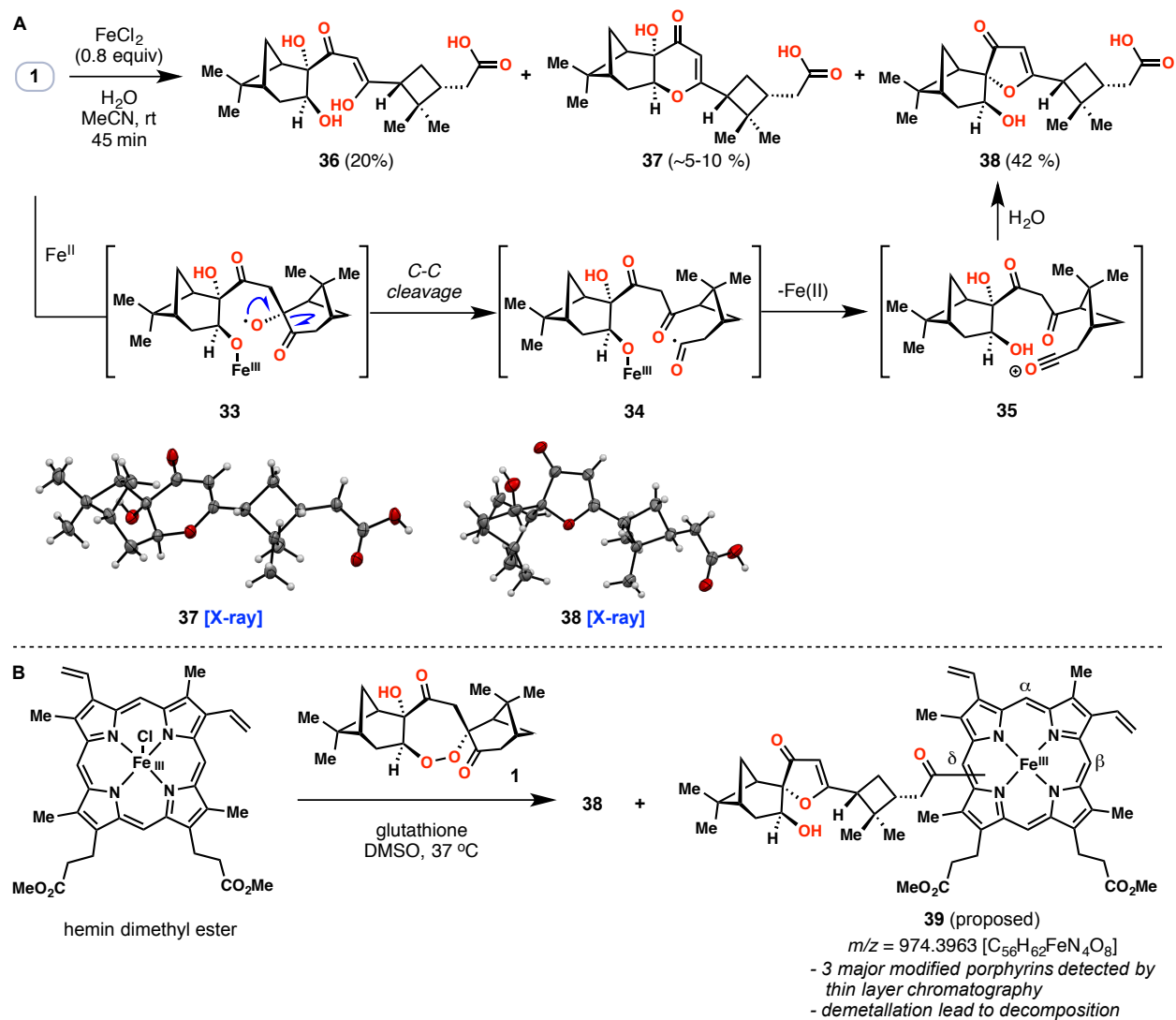


Figure 1.6. Activation modes of **1** in the presence of various Fe^{II} sources.

1.7 Conclusion and Acknowledgements

In conclusion, we have developed a practical 3-step synthesis of (+)-cardamom peroxide (**1**) from (-)-myrtenal. Although the antimalarial activity of **1** proved insufficient for further clinical consideration, a variety of interesting chemical discoveries were unearthed during our synthetic studies. These findings include the investigation of the tandem peroxidation reaction, determination of the reductive activation mode of **1** in comparison to those of the previously reported endoperoxides, and determination of the absolute configuration of **1**. This work also inspired us to envision a novel stereocontrolled trihydroxylation transformation that will be discussed in the next chapter.

The synthesis was designed by Professor Thomas Maimone and myself, and executed by me under the guidance of Thomas Maimone. Bioassay of **1** on clinical isolates of *P. falciparum* from Cambodia was performed by Dr. Pharath Lim and Dr. Rick Fairhurst. All X-ray crystal structures were obtained by Dr. Antonio DiPasquale, and the suitable crystalline samples were prepared and submitted by Thomas Maimone and myself.

The content of this chapter was published as a communication in 2014,⁴⁴ and as a full research account recently.⁴⁵

1.8 References

1. Kamchonwongpaisan, S.; Nilanonta, C.; Tarnchompoo, B.; Thebtaranonth, C.; Thebtaranonth, Y.; Yuthavong, Y.; Kongsaree, P.; Clardy, J., *Tetrahedron Lett.* **1995**, *36*, 1821.
2. (a) Berrien, J. F.; Provot, O.; Mayrargue, J.; Coquillay, M.; Ciceron, L.; Gay, F.; Danis, M.; Robert, A.; Meunier, B., *Org. Biomol. Chem.* **2003**, *1*, 2859; (b) Cointeaux, L.; Berrien, J. F.; Mahuteau, J.; Huu-Dau, M. E.; Ciceron, L.; Danis, M.; Mayrargue, J., *Bioorg. Med. Chem.* **2003**, *11*, 3791; (c) Cointeaux, L.; Berrien, J. F.; Mayrargue, J., *Tetrahedron Lett.* **2002**, *43*, 6275.
3. World Health Organization, *World Malaria Report*. World Health Organization: Geneva, Switzerland, 2017.
4. Rosenthal, P. J., *Antimalarial Chemotherapy: Mechanisms of Action, Resistance, and New Directions in Drug Discovery*. Humana Press: Totowa, NJ, 2011.
5. Poser, C. M.; Bruyn, G. W., *An Illustrated History of Malaria*. the Parthenon Publishing Group: Carnforth, UK, 1999.
6. (a) Wellems, T. E.; Plowe, C. V., *J. Infect. Dis.* **2001**, *184*, 770. (b) Hastings, I. M., *Trends Parasitol* **2004**, *20*, 512. (c) Ginsburg, H., *Acta Tropica* **2005**, *96*, 16.
7. (a) Liu, J.-M.; Ni, M.-Y.; Fen, J.-F.; Tu, Y.-Y.; Wu, Z.-H.; Wu, Y.-L.; Zhou, W.-S., *Huaxue Xuebao* **1979**, *37*, 129. (b) Tu, Y.-Y., *Angew. Chem. Int. Ed.* **2016**, *55*, 10210.
8. (a) Dondorp, A. M. *et al.*, *Engl. J. Med.* **2009**, *361*, 455. (b) Ashley, E. A. *et. al.*, *New Engl. J. Med.* **2014**, *371*, 411. (c) Imwong, M. *et al.*, *Lancet Infect Dis* **2017**, *17*, 491. (d) Imwong, M.; Hien, T. T.; Thuy-Nhien, N. T.; Dondorp, A. M.; White, N. J., *Lancet Infect Dis* **2017**, *17*, 1022. (e) Rossi, G.; De Smet, M.; Khim, N.; Kindermans, J. M.; Menard, D., *Lancet Infect Dis* **2017**, *17*, 1233. (f) Lu, F. *et al.*, *N. Engl. J. Med.* **2017**, *376*, 991.
9. (a) Spittler, G., *Free Radic. Biol. Med.* **2006**, *41*, 362. (b) Dembitsky, V. M.; Glorizova, T. A.; Poroikov, V. V., *Mini Rev. Med. Chem.* **2007**, *7*, 571. (c) Chaturvedi, D.; Goswami, A.; Saikia, P. P.; Barua, N. C.; Rao, P. G., *Chem. Soc. Rev.* **2010**, *39*, 435. (d) Schwikkard, S.; van Heerden, F. R., *Nat. Prod. Rep.* **2002**, *19*, 675. (e) Kaur, M.; Jain, M.; Kaur, T.; Jain, R., *Bioorg. Med. Chem. Lett.* **2009**, *17*, 3229. (f) Dembitsky, V. M., *J. Mol. Genet. Med.* **2015**, *9*, 163.
10. (a) Slack, R. D.; Jacobine, A. M.; Posner, G. H., *Med. Chem. Commun.* **2012**, *3*, 281. (b) Schlitzer, M., *ChemMedChem* **2007**, *2*, 944. (c) Hofheinz, W.; Burgin, H.; Gocke, E.; Jaquet, C.; Masciadri, R.; Schmid, G.; Stohler, H.; Urwyler, H., *Trop. Med. Parasitol.* **1994**, *45*, 261. (d) Vennerstrom, J. L. *et. al.*, *Nature*, **2004**, *430*, 900. For recent examples of non-peroxidic antimalarials, see: (e) Flannery, E. L.; Chatterjee, A. K.; Winzeler, E. A., *Nat. Rev. Microbiol.* **2013**, *11*, 849. (f) Baragana, B. *et al.*, *Nature*, **2015**, *522*, 315. (g) Kato, N. *et al.*, *Nature* **2016**, *538*, 344. (h) Cowell, A. N. *et al.*, *Science*, **2018**, *359*, 191.
11. For total syntheses of the structures shown in Figure 1.1, see: (a) Schmid, G.; Hofheinz, W., *J. Am. Chem. Soc.* **1983**, *105*, 624. (b) Xu, X. X.; Zhu, J.; Huang, D. Z.; Zhou, W. S., *Tetrahedron* **1986**, *42*, 819. (c) Avery, M. A.; Chong, W. K. M.; White, C. J., *J. Am. Chem. Soc.* **1992**, *114*, 974. (d) Avery, M. A.; White, C. J.; Chong, W. K. M., *Tetrahedron Lett.* **1987**, *28*, 4629. (e) Liu, H. J.; Yeh, W. L.; Chew, S. Y., *Tetrahedron Lett.* **1993**, *34*, 4435. (f) Constantino, M. G.; Beltrame, M., Jr.; da Silva, G. V. J., *Synth. Commun.* **1996**, *26*, 321. (g) Yadav, J. S.; Babu, R. S.; Sabitha, G., *Tetrahedron Lett.* **2003**, *44*, 387. (h) Yadav, J. S.; Thirupathiah, B.; Srihari, P., *Tetrahedron* **2010**, *66*, 2005. (i) Zhou, W.-S.; Xu, X.-X., *Acc. Chem. Res.* **1994**, *27*, 211. (j) Zhu, C.; Cook, S. P., *J. Am. Chem. Soc.* **2014**, *134*, 13577. (k)

- Hilf, J. A.; Witthoft, L. W.; Woerpel, K. A., *J. Org. Chem.* **2015**, *80*, 8262. (l) Xu, X.-X.; Dong, H.-Q., *Tetrahedron Lett.* **1994**, *35*, 9429. (m) Szpilman, A. M.; Korshin, E. E.; Rozenberg, H.; Bachi, M. D., *J. Org. Chem.* **2005**, *70*, 3618. (n) Xu, X.-X.; Zhu, J.; Huang, D.-Z.; Zhou, W.-S., *Tetrahedron Lett.* **1991**, *32*, 5785. (o) Li, Q.; Zhao, K.; Peuronen, A.; Rissanen, K.; Enders, D.; Tang, Y., *J. Am. Chem. Soc.* **2018**, *140*, 1937. For reviews on the synthesis of endoperoxides, see: (p) Korshin, E. E.; Bachi, M. D. in *Synthesis of Cyclic Peroxides*, *Patai's Chemistry of Functional Groups, Online*, Wiley, **2009**, 1-117. (q) Dussault, P., *Synlett* **1995**, 997.
12. Czechowski, T.; Larson, T. R.; Catania, T. M.; Harvey, D.; Brown, G. D.; Graham, I. A., *Proc. Natl. Acad. Sci.* **2016**, *113*, 15150.
 13. Mazzega, M.; Fabris, F.; Cossu, S.; De Lucchi, O.; Lucchini, V.; Valle, G., *Tetrahedron* **1999**, *55*, 4427.
 14. (a) Willis, M. C., *Chem. Rev.* **2010**, *110*, 725. (b) Nicolaou, K. C.; Ellery, S. P.; Chen, J. S., *Angew. Chem. Int. Ed.* **2009**, *48*, 7140.
 15. Barrero, A. F.; Herrador, M. M.; del Moral, J. F.; Arteaga, P.; Arteaga, J. F.; Dieguez, H. R.; Sanchez, E. M., *J. Org. Chem.* **2007**, *72*, 2988.
 16. Lipshutz, B. H.; Hackmann, C., *J. Org. Chem.* **1994**, *59*, 7437.
 17. Dutta, D. K.; Konwar, D., *Tetrahedron Lett.* **2000**, *41*, 6227.
 18. Baati, R.; Mioskowski, C.; Barma, D.; Kache, R.; Falck, J. R., *Org. Lett.* **2006**, *8*, 2949.
 19. Furstner, A.; Hupperts, A., *J. Am. Chem. Soc.* **1995**, *117*, 4468.
 20. Dieguez, H. R.; Lopez, A.; Domingo, V.; Arteaga, J. F.; Dobado, J. A.; Herrador, M. M.; Quilez del Moral, J. F.; Barrero, A. F., *J. Am. Chem. Soc.* **2010**, *132*, 254.
 21. Mukaiyama, T.; Sato, T.; Hanna, J., *Chem. Lett.* **1973**, 1041.
 22. (a) McMurry, J. E.; Fleming, M. P.; Kees, K. L.; Krepski, L. R., *J. Org. Chem.* **1978**, *43*, 3255. (b) McMurry, J. E., *Chem. Rev.* **1989**, *89*, 1513.
 23. (a) Kornblum, N.; Delamare, H. E., *J. Am. Chem. Soc.* **1951**, *73*, 880. (b) Nicolaou, K. C.; Totokotsopoulos, S.; Giguere, D.; Sun, Y.; Sarlah, D., *J. Am. Chem. Soc.* **2011**, *133*, 8150. (c) Yaremenko, Y. A.; Vil, V. A.; Demchuk, D. V.; Terent'ev, A. O., *Beilstein J. Org. Chem.* **2016**, *12*, 1647.
 24. (a) Nokami, J.; Nishimura, A.; Sunami, M.; Wakabayashi, S., *Tetrahedron Lett.* **1987**, *28*, 649. (b) Atasoy, B.; Balci, M., *Tetrahedron* **1986**, *42*, 1461.
 25. (a) Gersmann, H. R.; Bickel, A. F.; Nieuwenhuis, H. J. W., *Proc. Chem. Soc.* **1962**, 279. (b) Novkovic, L.; Trmcic, M.; Rodic, M.; Bihelovic, F.; Zlatar, M.; Matovic, R.; Saicic, R. N., *Rsc Advances* **2015**, *5*, 99577. For elegant syntheses that employed this transformation, see: (c) Chumoyer, M. Y.; Danishefsky, S. J., *J. Am. Chem. Soc.* **1992**, *114*, 8333. (d) Magnus, P.; Booth, J.; Magnus, N.; Tarrant, J.; Thom, S.; Ujjainwalla, F., *Tetrahedron Lett.* **1995**, *36*, 5331. (e) Nickel, A.; Maruyama, T.; Tang, H.; Murphy, P. D.; Greene, B.; Yusuff, N.; Wood, J. L., *J. Am. Chem. Soc.* **2004**, *126*, 16300. (f) Schottner, E.; Wiechoczek, M.; Jones, P. G.; Lindel, T., *Org. Lett.* **2010**, *12*, 784. (g) Gampe, C. M.; Carreira, E. M., *Angew. Chem. Int. Ed.* **2011**, *50*, 2962.
 26. House, H. O.; Ro, R. S., *J. Am. Chem. Soc.* **1958**, *80*, 2428.
 27. Greatrex, B. W.; Jenkins, N. F.; Taylor, D. K.; Tiekink, E. R., *J. Org. Chem.* **2003**, *68*, 5205.
 28. Crossley, S. W. M.; Obradors, C.; Martinez, R. M.; Shenvi, R. A., *Chem. Rev.* **2016**, *116*, 8912.
 29. (a) Mukaiyama, T.; Isayama, S.; Inoki, S.; Kato, K.; Yamada, T.; Takai, T., *Chem. Lett.* **1989**, 449. (b) Inoki, S.; Kato, K.; Takai, T.; Isayama, S.; Yamada, T.; Mukaiyama, T., *Chem. Lett.*

- 1989, 515. (c) Isayama, S.; Mukaiyama, T., *Chem. Lett.* **1989**, 1071. (d) Isayama, S., *Bull. Chem. Soc. Jpn.* **1990**, *63*, 1305. (e) Inoki, S.; Kato, K.; Isayama, S.; Mukaiyama, T., *Chem. Lett.* **1990**, 1869.
30. (a) Leggans, E. K.; Barker, T. J.; Duncan, K. K.; Boger, D. L., *Org. Lett.* **2012**, *14*, 1428. (b) Sears, J. E.; Boger, D. L., *Acc. Chem. Res.* **2015**, *48*, 653.
31. Sugimori, T.; Horike, S.; Tsumura, S.; Handa, M.; Kasuga, K., *Inorg. Chim. Acta* **1998**, 283, 275.
32. (a) Lo, J. C.; Yabe, Y.; Baran, P. S., *J. Am. Chem. Soc.* **2014**, *136*, 1304. (b) Lo, J. C.; Gui, J.; Yabe, Y.; Pan, C. M.; Baran, P. S., *Nature* **2014**, *516*, 343. (c) Gui, J.; Pan, C. M.; Jin, Y.; Qin, T.; Lo, J. C.; Lee, B. J.; Spergel, S. H.; Mertzman, M. E.; Pitts, W. J.; La Cruz, T. E.; Schmidt, M. A.; Darvatkar, N.; Natarajan, S. R.; Baran, P. S., *Science* **2015**, *348*, 886. (d) Dao, H. T.; Li, C.; Michaudel, Q.; Maxwell, B. D.; Baran, P. S., *J. Am. Chem. Soc.* **2015**, *137*, 8046.
33. (a) Magnus, P.; Payne, A. H.; Waring, M. J.; Scott, D. A.; Lynch, V., *Tetrahedron Lett.* **2000**, *41*, 9725. (b) Magnus, P.; Scott, D. A.; Fielding, M. R., *Tetrahedron Lett.* **2001**, *42*, 4127. (c) Magnus, P.; Waring, M. J.; Scott, D. A., *Tetrahedron Lett.* **2000**, *41*, 9731. (d) Magnus, P.; Fielding, M. R., *Tetrahedron Lett.* **2001**, *42*, 6633.
34. For mechanistically related hydrofunctionalization methodology, see: (a) Waser, J.; Carreira, E. M. *J. Am. Chem. Soc.* **2004**, *126*, 5676. (b) Waser, J.; Carreira, E. M. *Angew. Chem. Int. Ed.* **2004**, *43*, 4099. (c) Waser, J.; Nambu, H.; Carreira, E. M. *J. Am. Chem. Soc.* **2005**, *127*, 8294. (d) Waser, J.; Gaspar, B.; Nambu, H.; Carreira, E. M. *J. Am. Chem. Soc.* **2006**, *128*, 11693. (e) Gaspar, B.; Carreira, E. M. *Angew. Chem. Int. Ed.* **2007**, *46*, 4519. (f) Gaspar, B.; Carreira, E. M. *Angew. Chem. Int. Ed.* **2008**, *120*, 5842. (g) Gaspar, B.; Carreira, E. M. *J. Am. Chem. Soc.* **2009**, *131*, 13214. (h) Barker, T. J.; Boger, D. L. *J. Am. Chem. Soc.* **2012**, *134*, 13588. (i) Tokuyasu, T.; Kunikawa, S.; Masuyama, A.; Nojima, M. *Org. Lett.* **2002**, *4*, 3595. (j) Shigehisa, H.; Aoki, T.; Yamaguchi, S.; Shimizu, N.; Hiroya, K. *J. Am. Chem. Soc.* **2013**, *135*, 10306. (k) Hashimoto, T.; Hirose, D.; Taniguchi, T. *Angew. Chem. Int. Ed.* **2014**, *53*, 2730. (l) Ma, X.; Herzon, S. B. *J. Org. Chem.* **2016**, *81*, 8673. (m) Ma, X.; Herzon, S. B. *J. Am. Chem. Soc.* **2016**, *138*, 8718. (n) Ma, X.; Dang, H.; Rose, J. A.; Rablen, P.; Herzon, S. B. *J. Am. Chem. Soc.* **2017**, *139*, 5998.
35. For reduction of unactivated alkenes, see: (a) Iwasaki, K.; Wan, K. K.; Oppedisano, A.; Crossley, S. W.; Shenvi, R. A., *J. Am. Chem. Soc.* **2014**, *136*, 1300-1303. (b) C. Obradors, R. M. Martinez, R. A. Shenvi, *J. Am. Chem. Soc.*, **2016**, *138*, 4962-4971. (c) King, S. M.; Ma, X.; Herzon, S. B. *J. Am. Chem. Soc.* **2014**, *136*, 6884. (d) Ma, X.; Herzon, S. B. *Chem. Sci.* **2015**, *6*, 6250.
36. (a) Gu, X.; Zhang, W.; Salomon, R. G., *J. Org. Chem.* **2012**, *77*, 1554-1559. (b) A direct Hock-Criegee-type fragmentation of **26** could also ultimately lead to nopinone and dione **31**, see ref 23c.
37. For chemical synthesis of **31**, see: Michon, C.; Djukic, J. P.; Ratkovic, Z.; Pfeffer, M., *Tetrahedron Lett.* **2002**, *43*, 5241.
38. (a) Golenser, J.; Waknine, J. H.; Krugliak, M.; Hunt, N. H.; Grau, G. E. *Int. J. Parasitol.* **2006**, *36*, 1427. (b) O'Neill, P. M.; Barton, V. E.; Ward, S. A. *Molecules* **2010**, *15*, 1705. (c) Posner, G. H.; O'Neill, P. M. *Acc. Chem. Res.* **2004**, *37*, 397.
39. For selected examples, see: (a) Posner, G. H.; O'Neill, P. M., *Acc. Chem. Res.* **2004**, *37*, 397. (b) Wu, W.-M.; Wu, Y.; Wu, Y.-L.; Yao, Z.-J.; Zhou, C.-M.; Li, Y.; Shan, F., *J. Am. Chem. Soc.* **1998**, *120*, 3316. (c) O'Neill, P. M.; Stocks, P. A.; Pugh, M. D.; Araujo, N. C.; Korshin,

- E. E.; Bickley, J. F.; Ward, S. A.; Bray, P. G.; Pasini, E.; Davies, J.; Verissimo, E.; Bachi, M. D., *Angew. Chem., Int. Ed.* **2004**, *43*, 4193. (d) Tang, Y.; Dong, Y.; Wang, X.; Sriraghavan, K.; Wood, J. K.; Vennerstrom, J. L., *J. Org. Chem.* **2005**, *70*, 5103.
40. (a) Weissbuch, I.; Leiserowitz, L., *Chem. Rev.* **2008**, *108*, 4899. (b) Percário, S.; Moreira, D. R.; Gomes, B.; Ferreira, M.; Gonçalves, A.; Laurindo, P.; Vilhena, T.; Dolabela, T.; Green, M. D., *Int. J. Mol. Sci.* **2012**, *13*, 16346.
41. (b) Posner, G. H.; Cumming, J. N.; Ploypradith, P.; Chang, H. O., *J. Am. Chem. Soc.* **1995**, *117*, 5885-5886. (b) Wu, W.-M.; Wu, Y.; Wu, Y.-L.; Yao, Z.-J.; Zhou, C.-M.; Li, Y.; Shan, F., *J. Am. Chem. Soc.* **1998**, *120*, 3316-3325. (c) Robert, A.; Cazelles, J.; Meunier, B., *Angew. Chem. Int. Ed.* **2001**, *40*, 1954. (d) Robert, A.; Coppel, Y.; Meunier, B., *Chem. Commun.* **2002**, 414.
42. (a) Straimer, J. *et al. Science*, **2015**, *347*, 428. (b) Ariey, F. *et al. Nature*, **2014**, *505*, 50. (c) Mbengue, A. *et al. Nature*, **2015**, *520*, 683.
43. (a) Lim, P. *et al. Antimicrob. Agents Chemother.* **2013**, *57*, 5277. (b) Paloque, L.; Ramadani, A. P.; Mercereau-Puijalon, O.; Augereau, J.-M.; Benoit-Vical, F. *Malaria J.* **2016**, *15*, 149.
44. Hu, X.; Maimone, T. J., *J. Am. Chem. Soc.* **2014**, *136*, 5287.
45. Hu, X.; Lim, P.; Fairhurst, R. M.; Maimone, T. J. *Tetrahedron*, **2018**, *in press*.

Supplementary Information

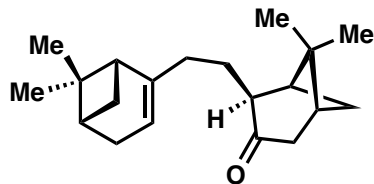
For

Chapter 1

Total Synthesis of the Antimalarial (+)-Cardamom Peroxide
via an Oxygen Stitching Strategy

General Procedures

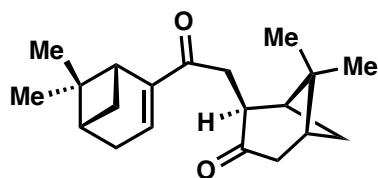
Unless otherwise stated, all reactions were performed in oven-dried or flame-dried glassware under an atmosphere of dry nitrogen or argon. Dry tetrahydrofuran (THF), dichloromethane (DCM), toluene, hexane, acetonitrile, and diethyl ether were obtained by passing these previously degassed solvents through activated alumina columns. Amines and alcohols were distilled from calcium hydride prior to use. 1,2-Dimethoxyethane (DME) was distilled from sodium and benzophenone. TiCl_4 was distilled prior to use. (-)-Pinene, (-)-myrtenol, and (-)-myrtenal was purchased from Sigma Aldrich and used directly without further purification. Reactions were monitored by thin layer chromatography (TLC) on Silicycle Siliaplate™ G TLC plates (250 μm thickness, 60 Å porosity, F-254 indicator) and visualized by UV irradiation and staining with *p*-anisaldehyde or potassium permanganate developing agents. Volatile solvents were removed under reduced pressure using a rotary evaporator. Flash column chromatography was performed using Silicycle F60 silica gel (60Å, 230-400 mesh, 40-63 μm). Proton nuclear magnetic resonance (^1H NMR) and carbon nuclear magnetic resonance (^{13}C NMR) spectra were recorded on Bruker AV-300, AVB-400, AV-500, or AV-600 spectrometers operating respectively at 300, 400, 500, and 600 MHz for ^1H , and 75, 100, 125, and 150 MHz for ^{13}C . Chemical shifts are reported in parts per million (ppm) with respect to the residual solvent signal CDCl_3 (^1H NMR: $\delta = 7.26$; ^{13}C NMR: $\delta = 77.16$), and CD_2Cl_2 (^1H NMR: $\delta = 5.32$; ^{13}C NMR: $\delta = 53.84$). Peak multiplicities are reported as follows: *s* = singlet, *brs* = broad singlet, *d* = doublet, *t* = triplet, *dd* = doublet of doublets, *ddd* = doublet of doublet of doublets, *dddd* = doublet of doublet of doublet of doublets, *m* = multiplet, *app* = apparent. Melting points were determined using MEI-TEMP™ apparatus and are uncorrected. IR spectra were recorded on a Nicolet 380 FT-IR spectrometer. High-resolution mass spectra (HRMS) were obtained by the qb3 mass spectrometry facility at the University of California, Berkeley (a VG Prospec Micromass spectrometer for EI). Optical rotations were measured on a Perkin-Elmer 241 polarimeter. X-ray crystallographic analyses were performed at the UC-Berkeley College of Chemistry X-ray crystallography facility (MicroSTAR-H APEX II, ChexSTAR: RUA # 1091).



Ketone 14: This procedure was adapted from previous conditions reported by Lipshutz and coworkers (*J. Org. Chem.* **1994**, *59*, 7437.) A 50 mL round-bottom flask was charged with Mg⁰ turnings (1.25 g) and THF (5 mL). A drop of 1,2-dibromoethane was added to the reaction flask at 0 °C, and the resulting mixture was stirred for 10 minutes. A solution of bromide **12** (0.50 g, 2.5

mmol) in THF (5 mL) was then added dropwise over 2 hours at –10 °C. After the addition was complete, the reaction mixture was warmed to room temperature, and was stirred for an additional 30 minutes. The resulting grey solution was then transferred to a 20 mL syringe.

A separate 50 mL round-bottom flask was charged with CuI (0.524 g, 2.75 mmol), Me₂S (0.5 mL, 13.75 mmol), dry LiCl (117 mg, 2.75 mmol), and THF (5 mL). The resulting mixture was vigorously stirred at –78 °C over an acetone–dry ice bath, and the aforementioned grey solution was added dropwise. The resulting mixture was stirred at –78 °C for 10 minutes, followed by the addition of freshly distilled TMSCl (0.35 mL, 2.75 mmol) and a solution of enone **10** (0.30 g, 2 mmol) in THF (1 mL). After the consumption of enone **10** was complete as judged by TLC (DCM:hexane 1:2), the reaction was quenched by addition of *sat.* NH₄Cl (15 mL). The mixture was extracted with EtOAc (20 mL × 2), and the combined organic phase was washed with brine (30 mL), dried over Na₂SO₄, and concentrated *in vacuo*. The crude mixture was purified by flash column chromatography (EtOAc/hexanes, 1:20), affording ketone **14** (0.27 g, 48% yield) as a colorless oil: ¹H NMR (300 MHz, CDCl₃) δ 5.18 (ddd, J = 3.0, 3.0, 1.5 Hz, 1H), 2.69 – 2.56 (m, 2H), 2.50 (dd, J = 19.3, 2.4 Hz, 1H), 2.34 (ddd, J = 8.5, 5.6, 5.6 Hz, 1H), 2.29 – 1.90 (m, 11H), 1.31 (s, 3H), 1.26 (s, 3H), 1.12 (m, 2H), 0.85 (s, 3H), 0.80 (s, 3H); ¹³C NMR (75 MHz, CDCl₃) δ 214.8, 147.9, 116.5, 56.5, 45.8, 44.9, 41.9, 41.0, 39.3, 38.8, 38.1, 35.4, 34.1, 31.8, 31.4, 28.7, 27.2, 26.5, 22.2, 21.3.

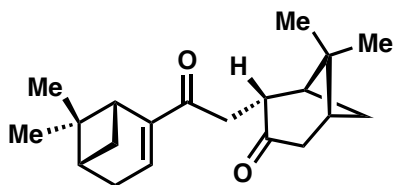


Keto-enone 6 (and 18): [Procedure A] A 25 mL round-bottom flask was charged with ketone **14** (270 mg, 0.95 mmol), 2-hydroxybenzoic acid (14.0 mg, 0.1 mmol), and DCM (5 mL). SeO₂ (11.0 mg, 0.1 mmol) and TBHP (0.57 mL, 3.4 mmol, 6 M in decane) were then added sequentially to the reaction flask. The resulting mixture was stirred at room temperature for 3 days, and

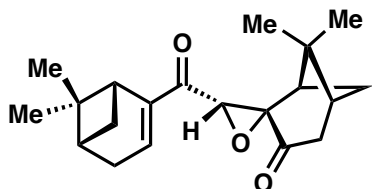
the reaction was then quenched by addition of *sat.* Na₂S₂O₃ (2 mL). The mixture was extracted with DCM (5 mL × 2), and the combined organic phase was washed with brine (10 mL), dried over Na₂SO₄, and concentrated *in vacuo*. The crude mixture was purified by flash column chromatography, affording the corresponding allylic alcohol (33.0 mg, 0.11 mmol) as a colorless oil. The alcohol was then dissolved in DCM (1.1 mL) in a 10 mL round-bottom flask, followed by the addition of solid NaHCO₃ (10 mg, 0.11 mmol) and DMP (56 mg, 0.132 mmol). After the consumption of the alcohol intermediate was complete as judged by TLC (DCM:hexane 1:2), the reaction was quenched by addition of brine (5 mL). The mixture was extracted with EtOAc (5 mL × 2), and the combined organic phase was washed with brine (10 mL), dried over Na₂SO₄, and concentrated *in vacuo*. The crude mixture was purified by flash column chromatography (EtOAc/hexanes, 1:20), affording enone **5** (30.0 mg, 11% yield from **14**) as a colorless oil: ¹H NMR (500 MHz, CDCl₃) δ 6.76 (dddd, J = 3.2, 3.2, 1.5, 1.5 Hz, 1H), 3.47 (dd, J = 16.9, 3.4 Hz, 1H), 3.12 – 3.08 (m, 1H), 2.93 (ddd, J = 5.6, 5.6, 1.6 Hz, 1H), 2.70 – 2.61 (m, 2H), 2.60 – 2.54 (m, 1H), 2.54 (dd, J = 16.9, 9.1 Hz, 1H), 2.50 (ddd, J = 19.9, 3.2, 3.2 Hz, 1H), 2.47 – 2.41 (m, 2H), 2.15 – 2.11 (m, 2H), 2.09 (ddd, J = 6.2, 6.2, 2.0 Hz, 1H), 1.32 (s, 3H), 1.30 (d, J = 10.6 Hz,

1H), 1.29 (s, 3H), 1.03 (d, J = 9.1 Hz, 1H), 0.88 (s, 3H), 0.74 (s, 3H); ¹³C NMR (125 MHz, CDCl₃) δ 214.0, 197.2, 149.1, 137.0, 52.3, 44.9, 43.3, 40.4, 39.8, 39.8, 39.1, 38.9, 37.6, 34.5, 32.7, 31.3, 26.9, 26.0, 22.2, 21.0. IR (thin film, cm⁻¹) 2922, 1714, 1666, 1615, 1468, 1410, 1369; HRMS (EI) *calcd.* for [C₂₀H₂₈O₂]: *m/z* 300.2089, found 300.2089.

[Procedure B] A 25 mL round-bottom flask was charged with DBU (0.6 ml, 3.67 mmol) and DCM (7.2 ml). The resulting solution was degassed by bubbling of argon for 20 min, and was then added via cannula to a separate 25 mL round-bottom flask pre-charged with a stir bar and dienone **17** (110 mg, 0.367 mmol) under an argon atmosphere. The reaction mixture was stirred at room temperature for 3 days, and the reaction was then quenched by addition of *aq.* HCl (20 mL, 1 N). The aqueous phase was extracted with DCM (20 mL × 3), and the combined organic phase was washed with *sat.* NaHCO₃ (40 mL × 2) and brine (40 mL), dried over Na₂SO₄, and concentrated *in vacuo*. The crude mixture was purified by flash column chromatography (EtOAc/hexanes, 1:20), affording recovered dienone **17** (27 mg, 25%), and a mixture of **6** and **18** (60 mg, 55% yield, 1:3 *dr*) as a colorless oil. The diastereomeric ratio (*dr*) was determined by ¹H NMR analysis.



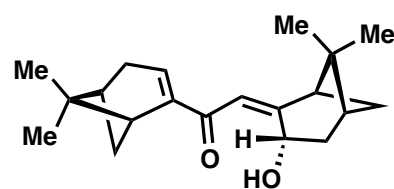
Keto-enone 18: ¹H NMR (600 MHz, CDCl₃) δ 6.75 (dddd, J = 3.2, 3.2, 1.5, 1.5 Hz, 1H), 3.20 – 3.17 (m, 1H), 3.15 (dd, J = 16.3, 3.2 Hz, 1H), 2.92 (ddd, J = 5.7, 5.7, 1.6 Hz, 1H), 2.71 – 2.63 (m, 2H), 2.50 (ddd, J = 19.9, 3.2, 3.2 Hz, 1H), 2.48 – 2.40 (m, 4H), 2.15 – 2.10 (m, 2H), 1.96 (ddd, J = 6.2, 6.2, 2.1 Hz, 1H), 1.31 (s, 3H), 1.31 (s, 3H), 1.11 (d, J = 10.9 Hz, 1H), 1.03 (d, J = 9.2 Hz, 1H), 0.95 (s, 3H), 0.72 (s, 3H); ¹³C NMR (100 MHz, CDCl₃) δ 214.3, 197.3, 149.3, 137.0, 48.7, 44.6, 42.3, 40.4, 39.9, 39.5, 38.3, 37.4, 36.9, 32.7, 31.2, 29.4, 26.4, 26.0, 21.0, 20.0.



Epoxide 19: A 25 mL round-bottom flask was charged with a stir bar, **6** and **18** (30 mg, 0.1 mmol, as a mixture of two diastereomers), and a solvent mixture of THF (4 mL) and *t*-BuOH (1 mL). The resulting solution was cooled to –40 °C, and bubbled with a stream of oxygen for 10 minutes. The mixture was then vigorously stirred at –40 °C under an oxygen atmosphere (balloon), and potassium *tert*-butoxide (45 mg, 0.4 mmol) was added as solid in one portion. The reaction mixture was further stirred for 30 minutes, and the reaction was then quenched by addition of *aq.* HCl (10 mL, 1 N). The mixture was extracted with DCM (10 mL × 3), and the combined organic phase was washed with brine (20 mL × 2), dried over Na₂SO₄, and concentrated *in vacuo*. The crude mixture was purified by flash column chromatography (EtOAc/hexanes, 1:15 to 1:10), affording a small amount of recovered starting material, and **19** (11 mg, 35% yield) as a colorless oil: [α]_D²⁰ = +170.6° (c 0.005 g/ml, CHCl₃); ¹H NMR (500 MHz, CDCl₃) δ 6.93 (dddd, J = 3.1, 3.1, 1.4, 1.4 Hz, 1H), 2.95 (ddd, J = 5.7, 5.7, 1.6 Hz, 1H), 2.78 – 2.62 (m, 3H), 2.52 – 2.50 (m, 2H), 2.47 (ddd, J = 9.2, 5.7, 5.7 Hz, 1H), 2.25 (dddd, J = 6.1, 6.1, 2.9, 2.9 Hz, 1H), 2.16 (dddd, J = 5.7, 5.7, 2.8, 2.8 Hz, 1H), 2.01 (dd, J = 6.0, 6.0 Hz, 1H), 1.58 (d, J = 11.1 Hz, 1H), 1.33 (s, 3H), 1.28 (s, 3H), 0.97 (d, J = 9.2 Hz, 1H), 0.85 (s, 3H), 0.77 (s, 3H); ¹³C NMR (100 MHz, CDCl₃) δ 206.5, 189.8, 149.1, 140.8, 67.5, 61.5, 42.8, 40.5, 40.5, 40.4, 39.6, 38.2, 37.5, 33.1, 31.3, 29.9, 26.2, 25.9, 21.6, 21.1; IR (thin film, cm⁻¹) 2935,

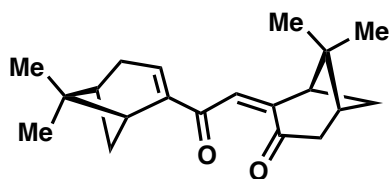
1730, 1671, 1611, 1467, 1419, 1370, 1274; HRMS (EI) *calcd.* for [C₂₀H₂₆O₃]: *m/z* 314.1882, found 314.1885.

Triene 15: This procedure was adapted from previous conditions reported by McMurry and co-workers (*J. Org. Chem.* **1978**, *43*, 3255.) A flame-dried 1 L three-necked round-bottom flask equipped with a reflux condenser was charged with a large stir bar and freshly prepared Zn–Cu couple (44 g, 0.67 mol, 40 equiv). The system was evacuated and backfilled with argon three times. Freshly distilled DME (600 mL) was then added via cannula, followed by the dropwise addition of freshly distilled TiCl₄ (24 mL, 200 mmol, 10 equiv) to the rapidly stirring slurry. The mixture was sonicated at room temperature for 1 hour, and was vigorously stirred at reflux temperature for 5 hours. The mixture was then cooled to room temperature, and a solution of (–)-myrtenal (3.0 g, 20 mmol, 1 equiv) in degassed DME (50 mL) was added slowly over 12 hours via syringe pump. After the addition of myrtenal was complete, the reaction mixture was sonicated at room temperature for 1 hour, and was then vigorously stirred at reflux temperature for 48 hours. The resulting mixture was cooled to room temperature, and filtered through a pad of Florisil® eluting with diethyl ether. The filtration was repeated to give a clear solution, which was then concentrated *in vacuo*, and purified by flash column chromatography (hexanes:Et₃N, 200:1), affording triene **15** (1.41 g, 53% yield) as a colorless oil: $[\alpha]_D^{20} = +31.70^\circ$ (c 0.010 g/mL, CHCl₃); ¹H NMR (500 MHz, CDCl₃) δ 6.14 (s, 2H), 5.53 (m, 2H), 2.62 (ddd, J = 5.7, 5.7, 1.6 Hz, 2H), 2.42 (ddd, J = 8.8, 5.7, 5.7 Hz, 2H), 2.39 (ddd, J = 19.2, 3.0, 3.0 Hz, 2H), 2.32 (ddd, J = 19.2, 2.7, 2.7 Hz, 2H), 2.12 (m, 2H), 1.33 (s, 6H), 1.13 (d, J = 8.8 Hz, 2H), 0.81 (s, 6H); ¹³C NMR (150 MHz, CDCl₃) δ 146.9, 126.4, 123.7, 41.3, 41.2, 37.9, 32.2, 31.6, 26.6, 21.0; IR (thin film, cm⁻¹) 2931, 2360, 1705, 1650, 1628, 1369, 1331; HRMS (EI) *calcd.* for [C₂₀H₂₈]: *m/z* 268.2191, found 268.2191.



Dienone alcohol 17: A 500 mL round-bottom flask was charged with triene **15** (1.3 g, 4.84 mmol, 1 equiv) and DCM (145 mL). The solution was cooled to –40 °C and methylene blue (15 mg, 0.05 mmol, 0.01 equiv) in DCM (1 mL) was added in one portion. The reaction mixture was irradiated with a 500 W halogen lamp, while vigorously bubbled with a stream of oxygen. After 1 hour of irradiation and bubbling of oxygen at –40 °C, a second portion of methylene blue (15 mg) in DCM (1 mL) was added, and the irradiation was continued until TLC indicated complete consumption of the starting material (~2 hours). The solution was then bubbled with a stream of nitrogen for 30 minutes. At this point, DBU (3.7 mL, 24 mmol, 5 equiv) was added dropwise at –40 °C. The resulting mixture was allowed to gradually warm to –20 °C and stirred for an additional 4 hours at this temperature. After the consumption of the endoperoxide intermediate was complete as judged by TLC, the reaction was quenched by addition of *aq.* HCl (100 mL, 1 N). The mixture was extracted with DCM (100 mL × 2), and the combined organic phase was washed with *sat.* NaHCO₃ (200 mL), H₂O (200 mL), and brine (200 mL), dried over MgSO₄, and concentrated *in vacuo*. The crude mixture was purified by column chromatography (hexanes/EtOAc, 20:1 to 10:1), affording dienone **17** (816 mg, 56% yield) as white solid: mp 118.4 – 119.6 °C; $[\alpha]_D^{20} = +246.02^\circ$ (c 0.005 g/mL, CHCl₃); ¹H NMR (500 MHz, CDCl₃) δ 6.76 (dddd, J = 3.3, 3.3, 1.5, 1.5 Hz, 1H), 6.40 (d, J = 0.8 Hz, 1H), 5.11 (d,

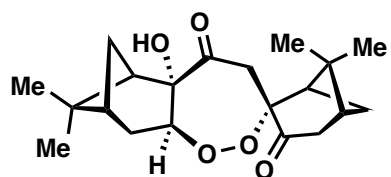
$J = 3.0$ Hz, 1H, D₂O exchangeable), 4.66 – 4.62 (m, 1H), 2.94 (ddd, $J = 5.7, 5.7, 1.5$ Hz, 1H), 2.56 – 2.50 (m, 2H), 2.49 – 2.40 (m, 3H), 2.38 – 2.31 (m, 1H), 2.16 – 2.11 (m, 1H), 2.07 (dddd, $J = 6.0, 6.0, 6.0, 2.2$ Hz, 1H), 1.95 (dd, $J = 14.6, 3.6$ Hz, 1H), 1.72 (d, $J = 10.0$ Hz, 1H), 1.34 (s, 3H), 1.31 (s, 3H), 1.07 (d, $J = 9.2$ Hz, 1H), 0.75 (s, 3H), 0.69 (s, 3H); ¹³C NMR (125 MHz, CDCl₃) δ 191.2, 168.3, 150.6, 137.3, 120.4, 62.9, 53.5, 40.8, 40.3, 40.2, 40.0, 37.5, 33.8, 32.7, 31.2, 27.4, 26.0, 25.9, 22.7, 21.0; IR (thin film, cm⁻¹) 3421, 2916, 1636, 1591, 1393, 1366; HRMS (EI) *calcd.* for [C₂₀H₂₈O₂]: m/z 300.2089, found 300.2094.



Bisenone 20: Dienone alcohol **17** (816 mg, 2.72 mmol, 1.0 equiv) was dissolved in DCM (27 mL) in a 50 mL round-bottom flask, and solid NaHCO₃ (228 mg, 2.72 mmol, 1.0 equiv) and Dess–Martin periodinane (1.5 g, 3.54 mmol, 1.3 equiv) were added sequentially. The resulting mixture was stirred at room

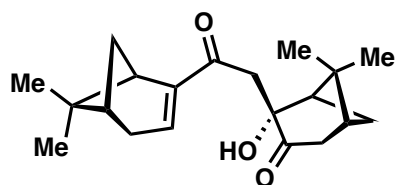
temperature for 1 hour (monitored by TLC for complete consumption of **17**). The reaction was then quenched by addition of *aq.* NaOH (30 mL, 1 N), and the mixture was extracted with DCM (30 mL \times 2). The combined organic phase was washed with H₂O (30 mL \times 2) and brine (30 mL), dried over MgSO₄, and purified by flash column chromatography (hexanes/EtOAc, 20:1 to 10:1), affording **20** (770 mg, 95% yield) as white solid: mp 137.1 – 138.4 °C; $[\alpha]_D^{20} = +27.20^\circ$ (c 0.005 g/mL, CHCl₃); ¹H NMR (500 MHz, CDCl₃) δ 6.55 (ddd, $J = 3.4, 1.8, 1.8$ Hz, 1H), 6.00 (s, 1H), 3.05 (dd, $J = 5.5, 5.5$ Hz, 1H), 2.77 – 2.68 (m, 2H), 2.64 (ddd, $J = 19.2, 2.4, 2.4$ Hz, 1H), 2.54 – 2.41 (m, 3H), 2.39 (ddd, $J = 19.9, 2.9, 2.9$ Hz, 1H), 2.21 (dddd, $J = 6.1, 6.1, 2.8, 2.8$ Hz, 1H), 2.15 – 2.10 (m, 1H), 1.42 (dd, $J = 2.9, 2.9$ Hz, 1H), 1.40 (s, 3H), 1.35 (s, 3H), 1.08 (d, $J = 9.1$ Hz, 1H), 0.91 (s, 3H), 0.81 (s, 3H); ¹³C NMR (125 MHz, CDCl₃) δ 198.4, 195.0, 149.7, 145.0, 138.3, 132.8, 48.9, 42.6, 41.3, 40.8, 39.3, 38.4, 37.9, 32.7, 32.3, 31.2, 26.0, 26.0, 22.0, 21.0; IR (thin film, cm⁻¹) 2931, 1705, 1651, 1628, 1465, 1421, 1368; HRMS (EI) *calcd.* for [C₂₀H₂₆O₂]: m/z 298.1933, found 298.1937.

Cardamom peroxide (1), hydration product 24, and diol 25: A flame-dried round-bottom flask was charged with bisenone **20** (30 mg, 0.1 mmol, 1.0 equiv), Mn(dpm)₃ (12 mg, 0.02 mmol, 20 mol %), DCM (1.6 mL), and *i*-PrOH (0.4 mL). The solution was vigorously bubbled with oxygen for 5 minutes, followed by the addition of TBHP (5M in decane, 30 μ L, 1.5 equiv) in one portion. The mixture was cooled to –10 °C under an atmosphere of oxygen (balloon), and a solution of PhSiH₃ (30 μ L, 0.24 mmol, 2.4 equiv) in DCM (1 mL) was added dropwise over 12 hours via syringe pump. After the addition was complete, a solution of PPh₃ (56 mg, 0.21 mmol) in DCM was added dropwise at –10 °C. The reaction mixture was diluted with H₂O (5 mL), and extracted with DCM (3 \times 10 mL). The combined organic phase was washed with brine (30 mL), dried over Na₂SO₄, and concentrated *in vacuo*. The crude mixture was purified by flash column chromatography (pure DCM) to afford **1** (18.2 mg, 52% yield) as a white solid, along with mono-hydration product **24** (3.5 mg, 11% yield), diol **25** (4.4 mg, 13% yield), and nopinone (9% GC yield using an internal standard of dodecane). [Note: the reaction afforded 48% of **1** on a 150 mg scale].

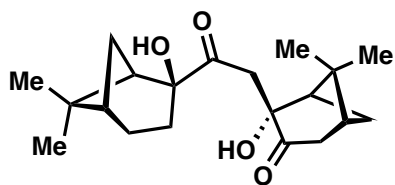


(+)-Cardamom peroxide (1): white solid: mp 154.9 – 156.2 °C; $[\alpha]_D^{20} = +123.20^\circ$ (c 0.005 g/mL, hexanes); ¹H NMR (500 MHz, CDCl₃) δ 4.28 (s, 1H), 4.22 (d, $J = 11.3$ Hz, 1H), 4.18 (d, $J = 8.7$ Hz, 1H), 2.78 (dd, $J = 18.9, 2.4$ Hz, 1H), 2.69 (ddd, $J = 18.9, 3.0,$

3.0 Hz, 1H), 2.58 (dd, $J = 15.4, 8.9$ Hz, 1H), 2.46 (dddd, $J = 11.0, 5.8, 2.9, 2.9$ Hz, 2H), 2.40 (d, $J = 11.2$ Hz, 1H), 2.41 – 2.35 (m, 1H), 2.30 (dd, $J = 6.1, 6.1$ Hz, 1H), 2.15 – 2.05 (m, 2H), 1.97 – 1.92 (m, 1H), 1.84 – 1.74 (m, 2H), 1.69 (d, $J = 11.2$ Hz, 1H), 1.38 (s, 3H), 1.27 (s, 3H), 1.06 (s, 3H), 0.86 (s, 3H); ^{13}C NMR (100 MHz, CDCl_3) δ 208.8, 204.5, 84.3, 84.2, 83.3, 49.6, 43.9, 43.3, 42.9, 41.0, 40.7, 39.0, 38.3, 30.7, 27.9, 27.5, 26.9, 26.6, 24.1, 22.5; IR (thin film, cm^{-1}) 3447, 3021, 2909, 1722, 1692, 1441, 1406, 1371; HRMS (ESI) calcd. for $[\text{C}_{20}\text{H}_{28}\text{O}_5\text{Na}]^+$ ($\text{M}+\text{Na}$) $^+$: m/z 371.1829, found 371.1837. Vapor diffusion of an ether solution of **1** with pentane afforded X-ray quality crystals.

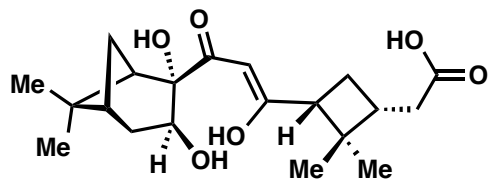


Hydration product **24**: colorless oil; $[\alpha]_{\text{D}}^{20} = -56.7^\circ$ (c 0.006 g/ml, CHCl_3); ^1H NMR (500 MHz, CDCl_3) δ 6.70 (ddd, $J = 3.4, 1.8, 1.8$ Hz, 1H), 3.38 (d, $J = 15.7$ Hz, 1H), 2.99 (ddd, $J = 5.7, 5.7, 1.6$ Hz, 1H), 2.68 (dd, $J = 19.0, 2.4$ Hz, 1H), 2.59 (ddd, $J = 19.0, 3.2, 3.2$ Hz, 1H), 2.53 (dt, $J = 20.2, 3.2, 3.2$ Hz, 1H), 2.50 – 2.41 (m, 3H), 2.39 (d, $J = 15.8$ Hz, 1H), 2.22 (dd, $J = 6.2, 6.2$ Hz, 1H), 2.15 (dddd, $J = 5.9, 3.0, 3.0, 1.2$ Hz, 1H), 2.11 (dddd, $J = 6.1, 6.1, 3.0, 3.0$ Hz, 1H), 1.92 (d, $J = 11.0$ Hz, 1H), 1.36 (s, 3H), 1.35 (s, 3H), 1.02 (d, $J = 9.1$ Hz, 1H), 0.95 (s, 3H), 0.82 (s, 3H); ^{13}C NMR (100 MHz, CDCl_3) δ 210.6, 200.6, 150.4, 138.8, 79.8, 50.0, 43.3, 40.4, 40.3, 39.6, 39.3, 38.6, 37.6, 32.9, 31.2, 27.9, 27.4, 26.0, 22.9, 21.0; IR (thin film, cm^{-1}) 3359, 2924, 1721, 1640, 1613, 1421, 1370; HRMS (EI) calcd. for $[\text{C}_{20}\text{H}_{28}\text{O}_3]$: m/z 316.2038, found 316.2040.

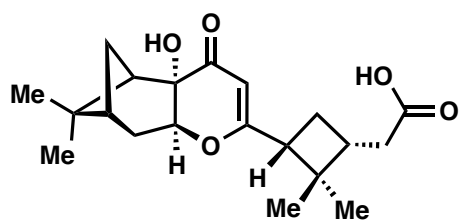


Diol **25**: white solid (acid sensitive): mp 132.9 – 134.1 $^\circ\text{C}$; $[\alpha]_{\text{D}}^{20} = -33.2^\circ$ (c 0.010 g/ml, CD_2Cl_2); ^1H NMR (600 MHz, CD_2Cl_2) δ 5.49 (s, 1H), 3.37 (d, $J = 15.3$ Hz, 1H), 2.78 (ddd, $J = 15.8, 10.5, 3.5$ Hz, 1H), 2.69 – 2.62 (m, 2H), 2.57 (ddd, $J = 19.1, 3.2, 3.2$ Hz, 1H), 2.41 (dddd, $J = 11.0, 6.2, 6.2, 3.1$ Hz, 1H), 2.26 (dddd, $J = 10.1, 6.0, 6.0, 1.8$ Hz, 1H), 2.21 (dd, $J = 6.1, 4.8$ Hz, 1H), 2.18 – 2.14 (m, 2H), 2.08 (dddd, $J = 6.1, 6.1, 2.9, 2.9$ Hz, 1H), 1.99 – 1.90 (m, 2H), 1.85 (d, $J = 10.9$ Hz, 1H), 1.87 – 1.81 (m, 1H), 1.61 (ddd, $J = 16.0, 11.0, 5.2$ Hz, 1H), 1.58 (d, $J = 10.1$ Hz, 1H), 1.35 (s, 3H), 1.22 (s, 3H), 0.90 (s, 3H), 0.72 (s, 3H); ^{13}C NMR (150 MHz, CD_2Cl_2) δ 213.2, 213.1, 82.5, 80.4, 50.7, 49.0, 43.6, 41.7, 41.1, 39.7, 39.0, 38.3, 28.0, 27.5, 27.3, 26.2, 24.6, 24.3, 22.8, 22.0; IR (thin film, cm^{-1}) 3410, 3005, 2925, 2360, 2341, 1823, 1708, 1463, 1408, 1326; HRMS (ESI) calcd. for $[\text{C}_{20}\text{H}_{30}\text{O}_4\text{Na}]^+$ ($\text{M}+\text{Na}$) $^+$: m/z 357.2036, found 357.2035.

Acid 36, pyranone 37, and furanone 38: In a nitrogen-filled glovebox, **1** (12 mg, 0.03 mmol, 1.0 equiv) was dissolved in thoroughly degassed acetonitrile (750 μL) and H_2O (7 μL , 0.4 mmol, 13.0 equiv) in a 10 mL round-bottom flask. Solid FeCl_2 (3.5 mg, 0.028 mmol, 0.8 equiv) was added to the resulting solution in one portion, and the reaction mixture was stirred at room temperature for 45 minutes. The resulting red colored solution was then removed from the glovebox, opened to air, and diluted with DCM (15 mL). The mixture was washed with brine (2 \times 25 mL), and the organic phase was concentrated *in vacuo*. The crude mixture was purified by preparative TLC (DCM/MeOH, 100:12), affording acids **36** (2.5 mg, 20% yield), **38** (5 mg, 42% yield), and a small amount of **37** (ca. 0.5–1.0 mg, 5–10% yield).

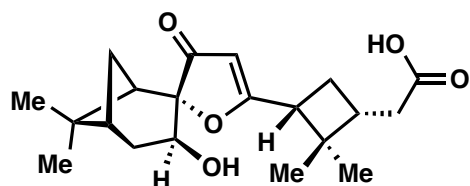


Acid **36**: white foam (unstable over extended periods in CDCl_3 , converts to **37** and **38**); $[\alpha]_{\text{D}}^{20} = +48.0^\circ$ (c 0.001 g/ml, CH_2Cl_2); $^1\text{H NMR}$ (600 MHz, CD_2Cl_2) δ 5.25 (d, $J = 0.8$ Hz, 1H), 4.48 – 4.40 (m, 1H), 2.98 (ddd, $J = 10.4, 7.6, 0.8$ Hz, 1H), 2.91 (d, $J = 11.0$ Hz, 1H), 2.83 (dd, $J = 18.1, 6.7$ Hz, 1H), 2.73 (dd, $J = 18.1, 7.9$ Hz, 1H), 2.73 – 2.68 (m, 1H), 2.50 – 2.43 (m, 1H), 2.26 (ddd, $J = 11.1, 7.9, 7.9$ Hz, 1H), 2.26 – 2.21 (m, 1H), 2.10 (d, $J = 11.2$ Hz, 1H), 2.02 – 1.96 (m, 2H), 1.80 – 1.69 (m, 2H), 1.26 (s, 3H), 1.24 (s, 3H), 1.02 (s, 3H), 0.89 (s, 3H); $^{13}\text{C NMR}$ (125 MHz, CD_2Cl_2) δ 206.0, 199.0, 192.8, 102.9, 96.7, 68.2, 50.3, 44.7, 43.9, 40.3, 40.0, 39.0, 38.0, 37.4, 30.6, 26.9, 25.8, 24.7, 23.7, 18.0; IR (thin film, cm^{-1}) 3061, 2926, 2349, 1724, 1598, 1548, 1484, 1379; HRMS (ESI) *calcd.* for $[\text{C}_{20}\text{H}_{27}\text{O}_5]^-$ (M-H) $^-$: m/z 347.1864, found 347.1863.



Pyranone **37**: white solid: mp 154.3 – 156.0 $^\circ\text{C}$; $^1\text{H NMR}$ (600 MHz, CD_2Cl_2) δ 5.27 (s, 1H), 4.98 (dd, $J = 9.1, 3.9$ Hz, 1H), 2.77 – 2.71 (m, 1H), 2.71 (dd, $J = 10.8, 7.6$ Hz, 1H), 2.43 – 2.35 (m, 2H), 2.34 – 2.25 (m, 2H), 2.22 (dd, $J = 5.8, 5.8$ Hz, 1H), 2.14 (ddd, $J = 11.0, 7.5, 7.5$ Hz, 1H), 1.99 (dddd, $J = 5.7, 5.7, 3.3, 3.3$ Hz, 1H), 1.90 (ddd, $J = 14.6, 3.8, 3.8$ Hz, 1H), 1.79 (dd, $J = 10.6, 10.6$ Hz, 1H), 1.27 (s, 3H), 1.22 (s, 3H), 1.10 (ddd, $J = 6.1, 3.8, 3.8$ Hz, 1H), 1.05 (s, 3H), 0.95 (s, 3H); IR (thin film, cm^{-1}) 3457, 2997, 2923, 2667, 2365, 1677, 1591, 1367; HRMS (ESI) *calcd.* for $[\text{C}_{20}\text{H}_{27}\text{O}_5]^-$ (M-H) $^-$: m/z 347.1864, found 347.1863.

Vapor diffusion of an ether solution of **37** with pentane afforded X-ray quality crystals.

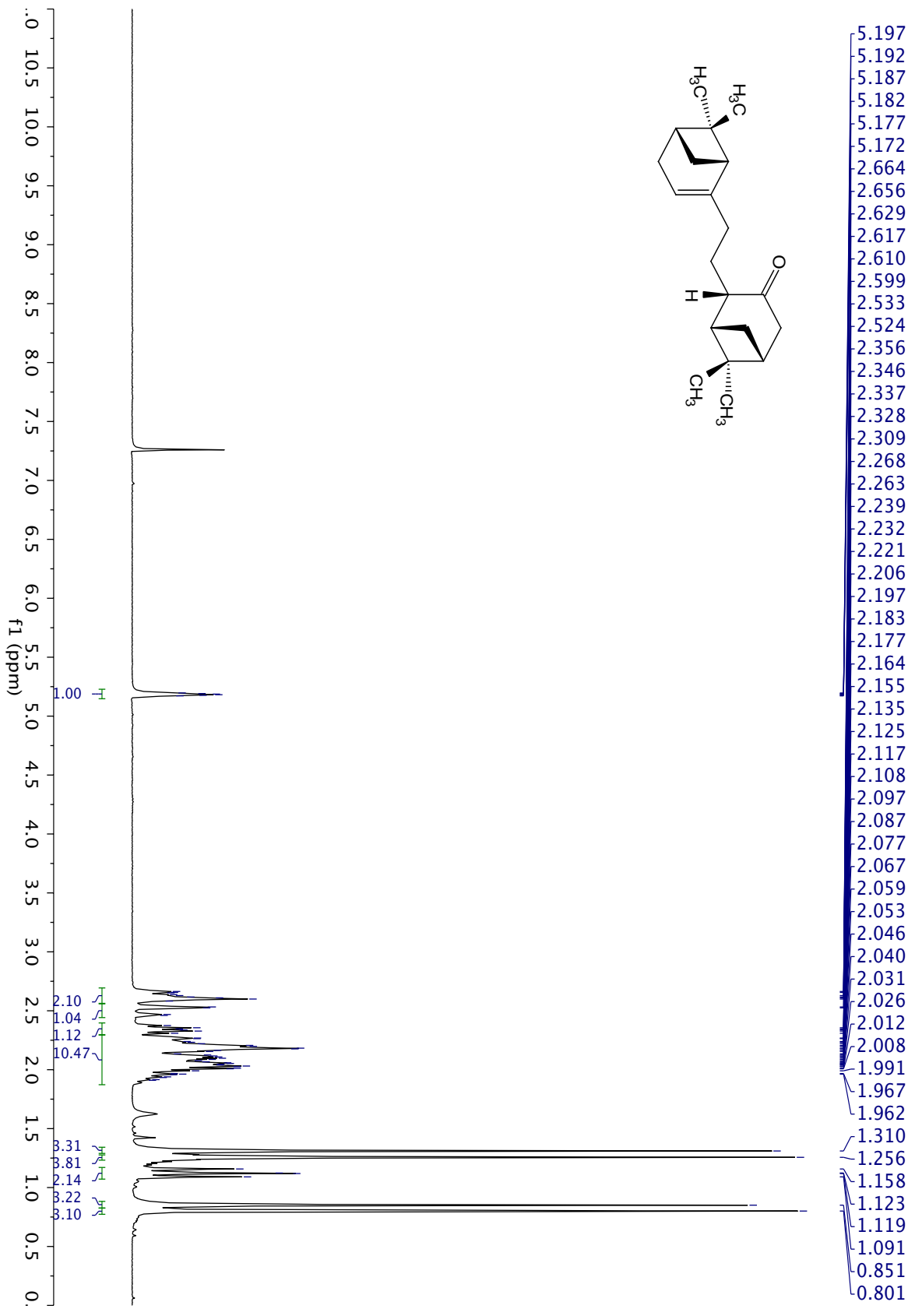


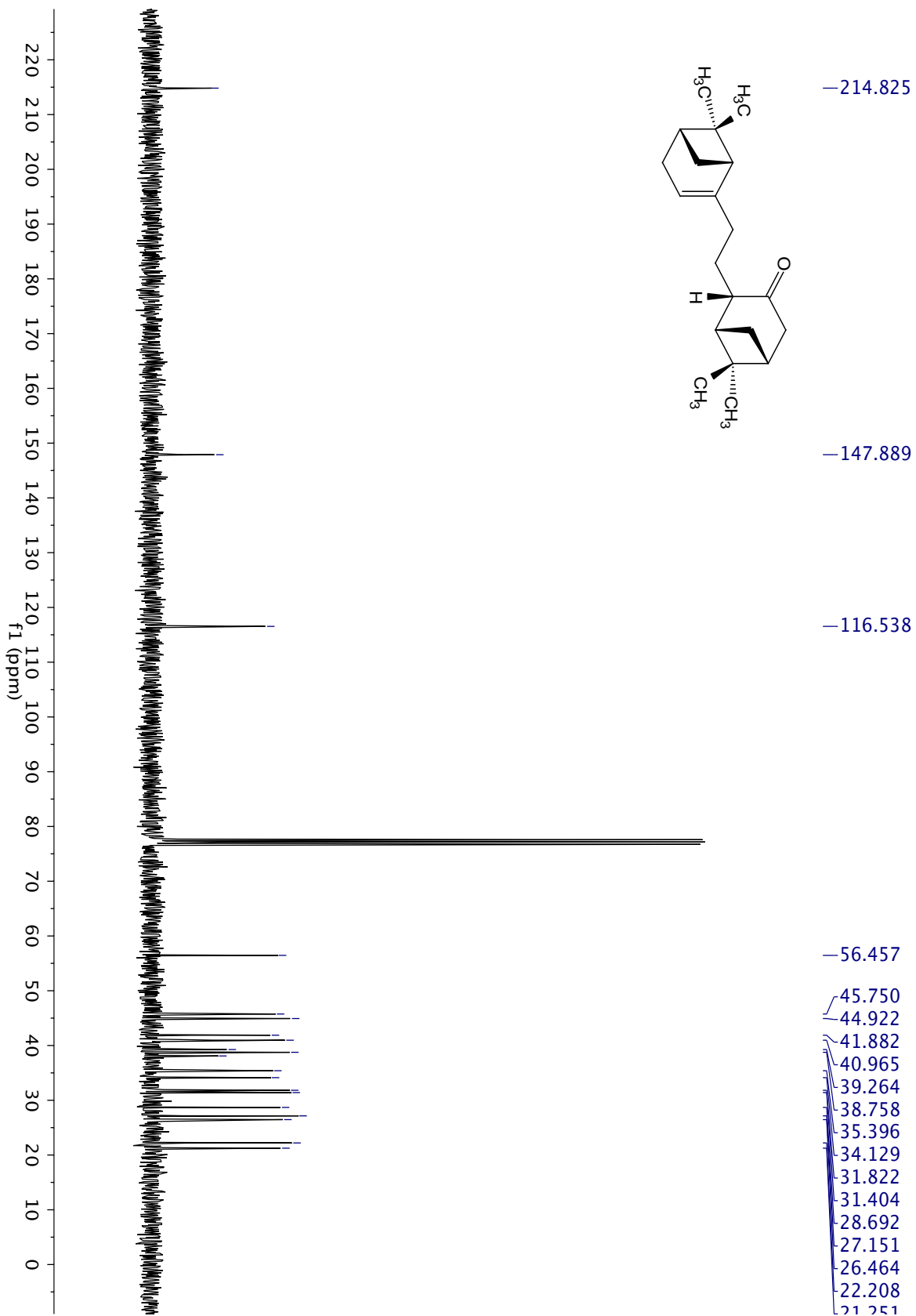
Furanone **38**: white solid: mp 147.5 – 149.8 $^\circ\text{C}$; $[\alpha]_{\text{D}}^{20} = +77.50^\circ$ (c 0.002 g/ml, CD_2Cl_2); $^1\text{H NMR}$ (600 MHz, CDCl_3) δ 5.30 (s, 1H), 4.50 (dd, $J = 9.7, 4.3$ Hz, 1H), 2.95 (dd, $J = 10.6, 7.7$ Hz, 1H), 2.73 (dddd, $J = 14.8, 9.8, 2.8, 2.8$ Hz, 1H), 2.49 (dddd, $J = 10.3, 7.8, 7.8, 7.7$ Hz, 1H), 2.43 (dd, $J = 15.8, 7.2$ Hz, 1H), 2.34 (dd, $J = 15.8, 8.0$ Hz, 1H), 2.30 (ddd, $J = 11.3, 7.8, 7.8$ Hz, 1H), 2.26 (dddd, $J = 11.9, 6.2, 3.0, 3.0, 2.3$ Hz, 1H), 2.15 (d, $J = 11.3$ Hz, 1H), 2.03 – 1.97 (m, 2H), 1.83 – 1.74 (m, 2H), 1.27 (s, 3H), 1.25 (s, 3H), 1.03 (s, 3H), 0.93 (s, 3H); $^{13}\text{C NMR}$ (125 MHz, CDCl_3) δ 206.0, 192.5, 176.9, 102.8, 96.5, 67.9, 50.0, 44.3, 43.4, 39.9, 39.5, 38.7, 38.6, 34.8, 30.4, 26.8, 25.5, 24.4, 23.6, 17.5; IR (thin film, cm^{-1}) 3849, 3105, 2997, 2924, 2361, 1682, 1587, 1484, 1368; HRMS (ESI) *calcd.* for $[\text{C}_{20}\text{H}_{27}\text{O}_5]^-$ (M-H) $^-$: m/z 347.1864, found 347.1861.

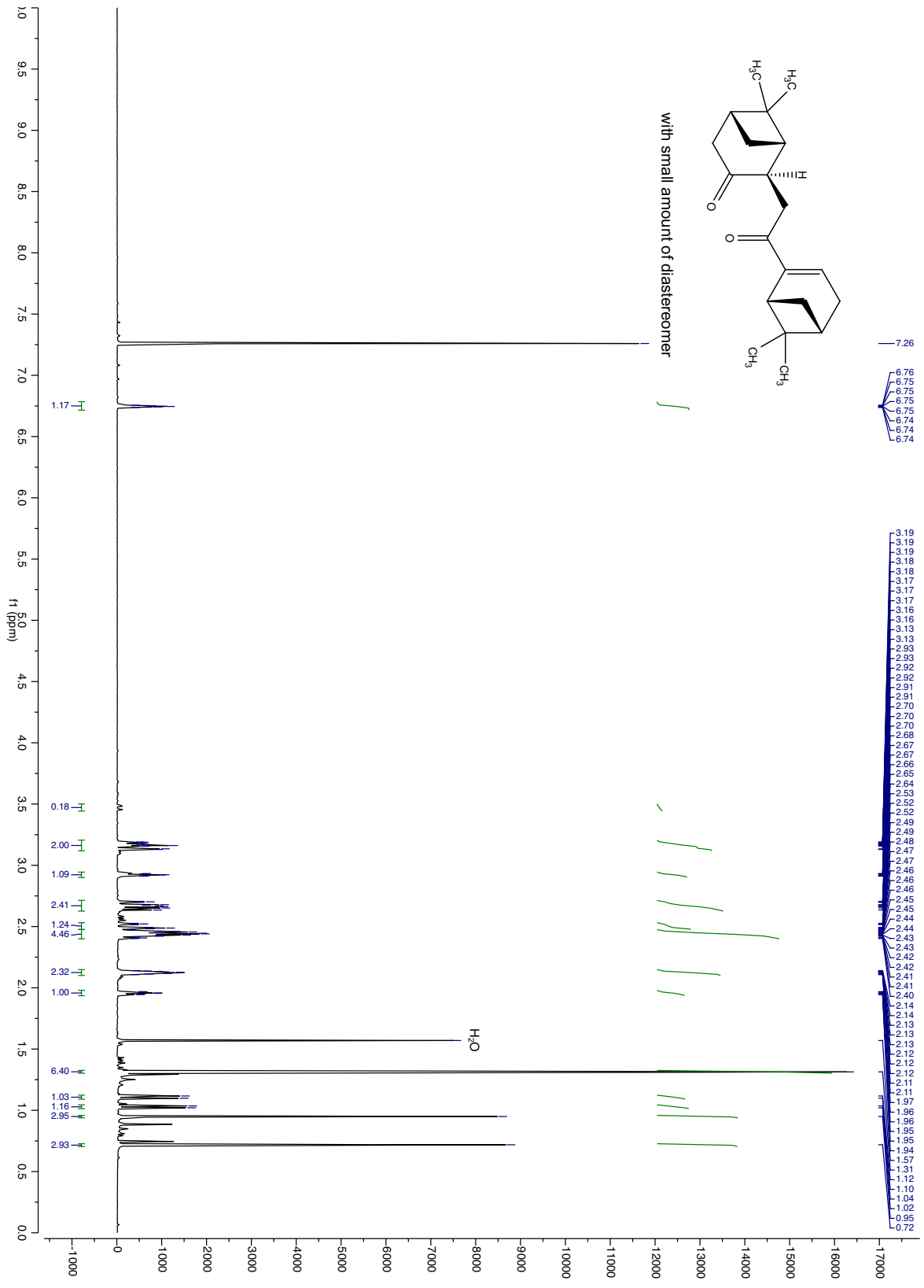
Vapor diffusion of an ether solution of **38** with pentane afforded X-ray quality crystals.

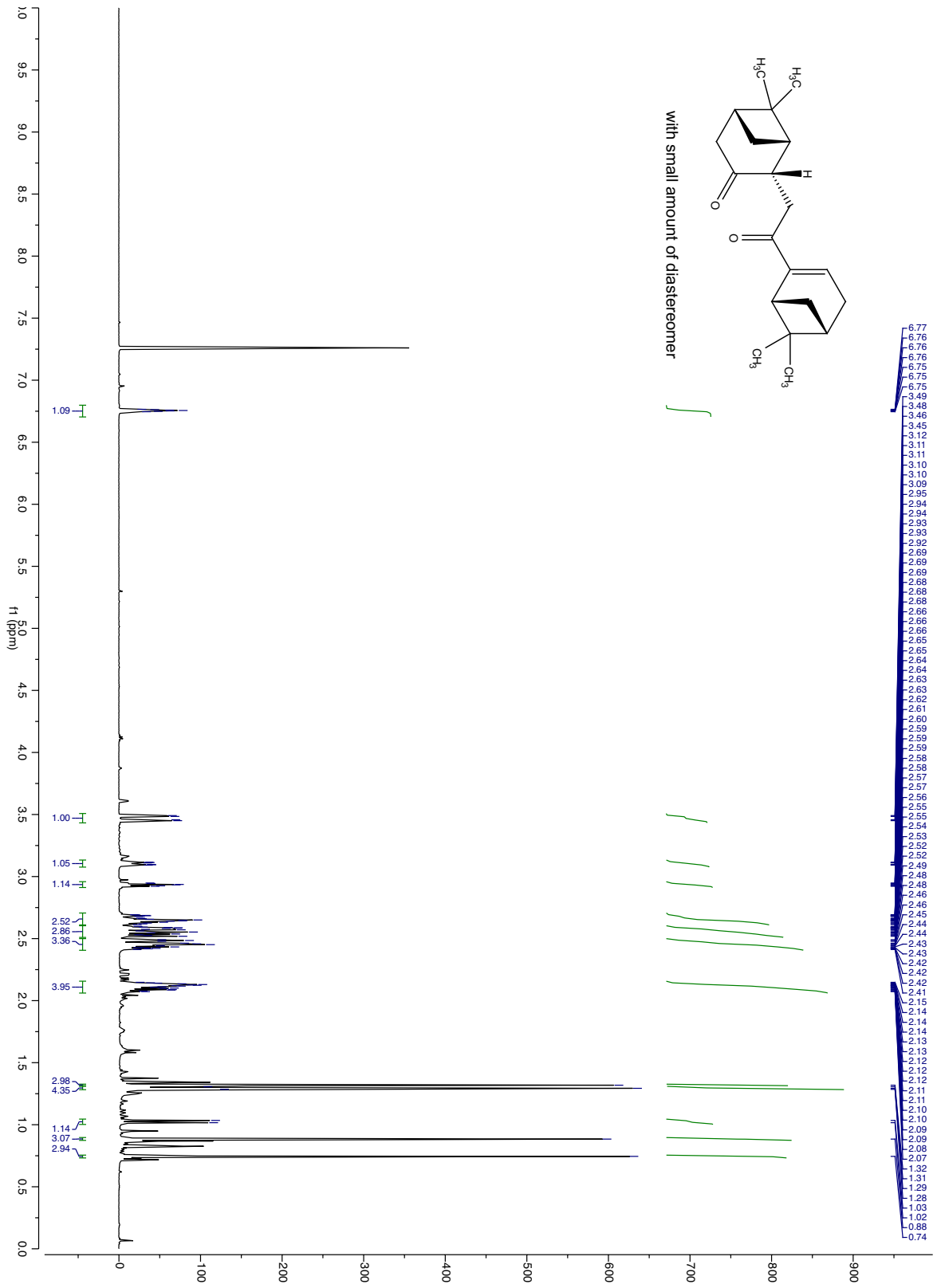
Reaction of 1 with hemin dimethyl ester: In a nitrogen-filled glove box, a 20 mL reaction vial was charged with hemin dimethyl ester (68 mg, 0.1 mmol), **1** (42 mg, 0.12 mmol), and glutathione (307 mg, 1 mmol). Degassed DMSO (3 mL) was added to the reaction vial at room temperature. The vial was then removed from glovebox, and was stirred at 37 $^\circ\text{C}$ for 8 hours. The reaction was monitored by TLC analysis (MeOH/ CHCl_3 1:15 and acetone/hexane 1:5, for the consumption of hemin dimethyl ester and **1**, respectively). After the reaction was complete as judged by TLC, the mixture was mixed with H_2O (10 mL), and extracted with DCM (10 mL \times 2)

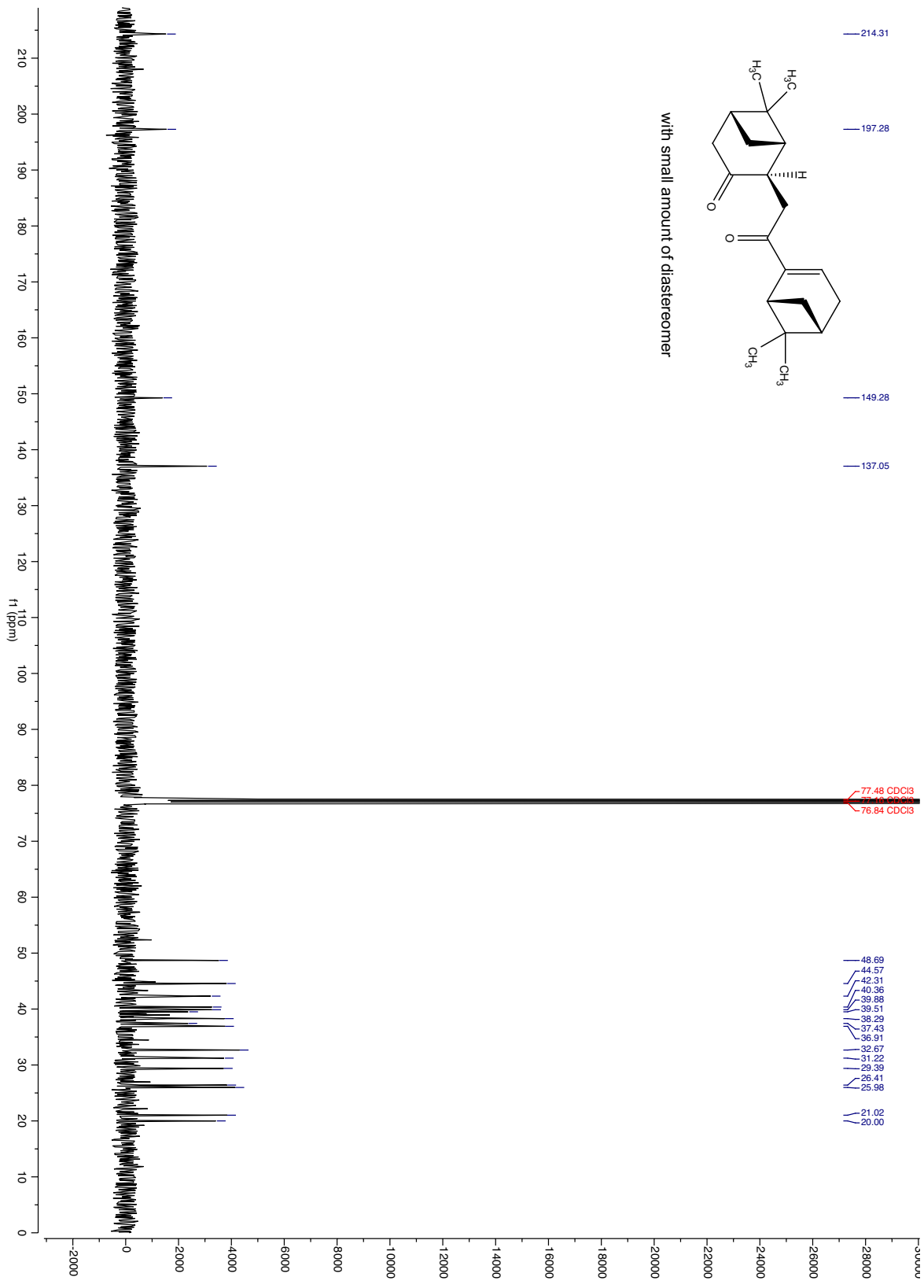
and EtOAc (10 mL × 2). The combined organic phase was washed with brine (20 mL × 2), dried over Na₂SO₄, and concentrated *in vacuo*. The crude mixture was purified by column chromatography, affording furanone **38** as the major product, along with a mixture of three paramagnetic, colored, hemein-containing products, potentially as the regioisomers of Fe(III)-PPIX adduct **39**: HRMS (ESI) *calcd.* for [C₅₆H₆₂FeN₄O₈]⁺ (M-Cl)⁺ : *m/z* 974.3918, found 974.3963.

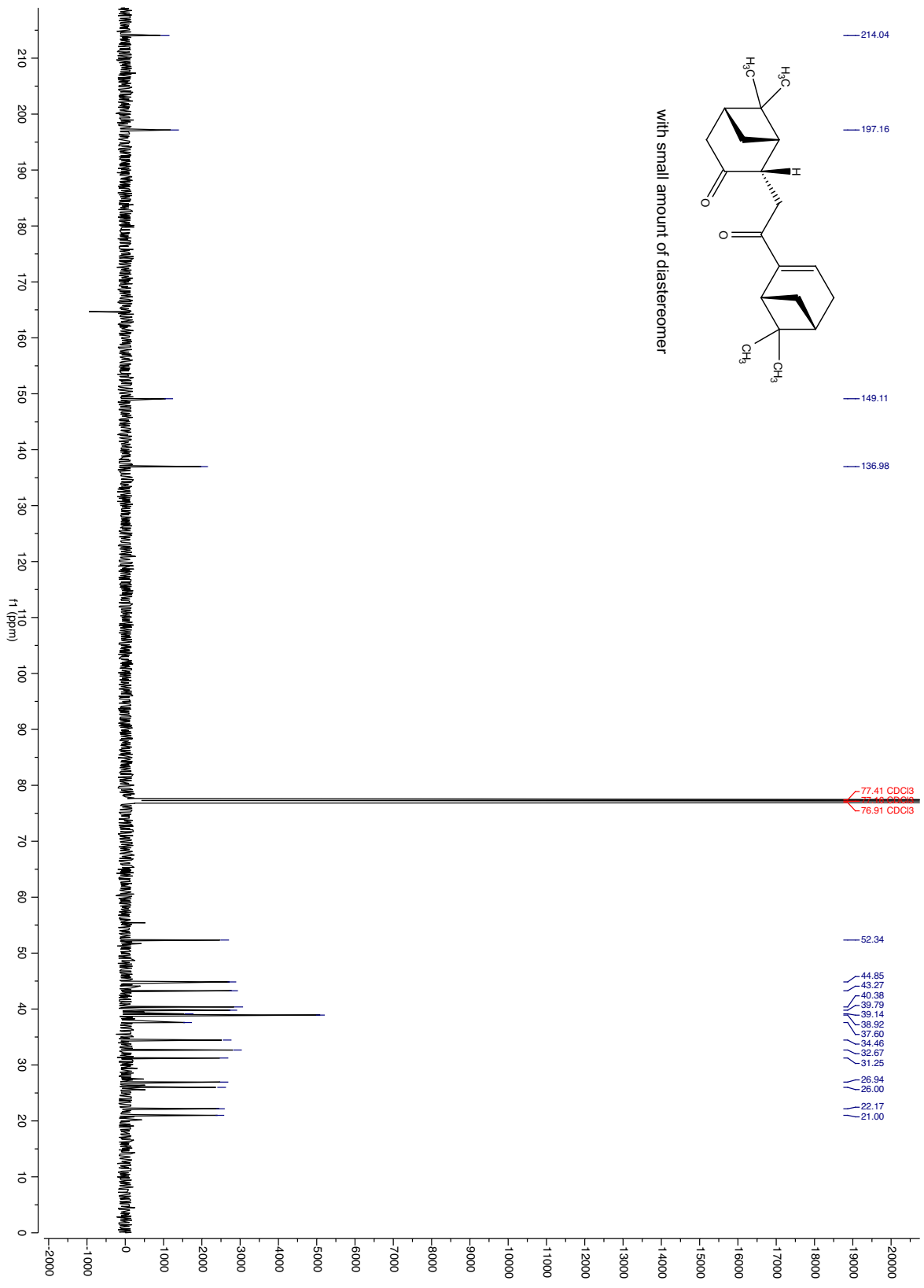


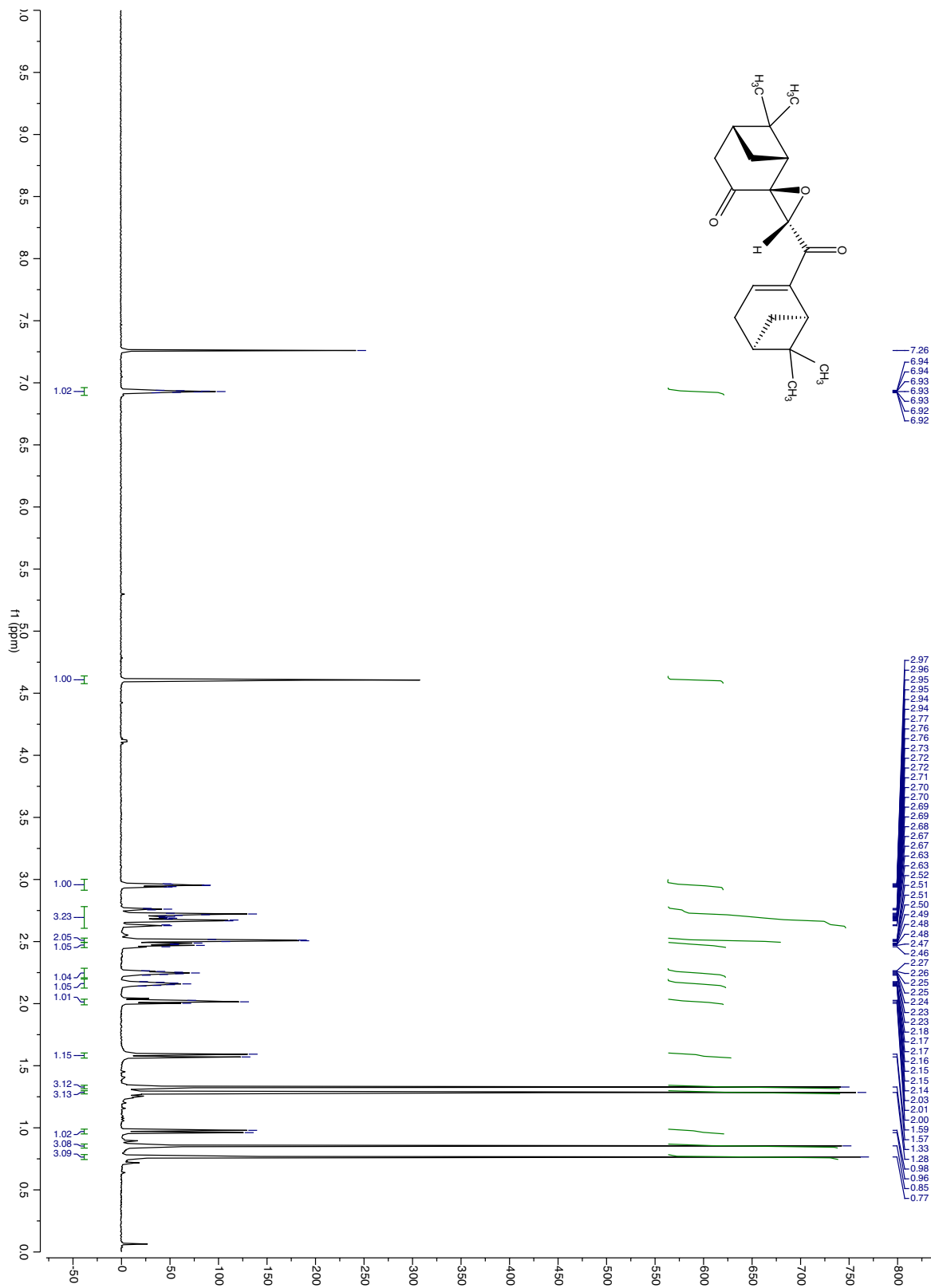


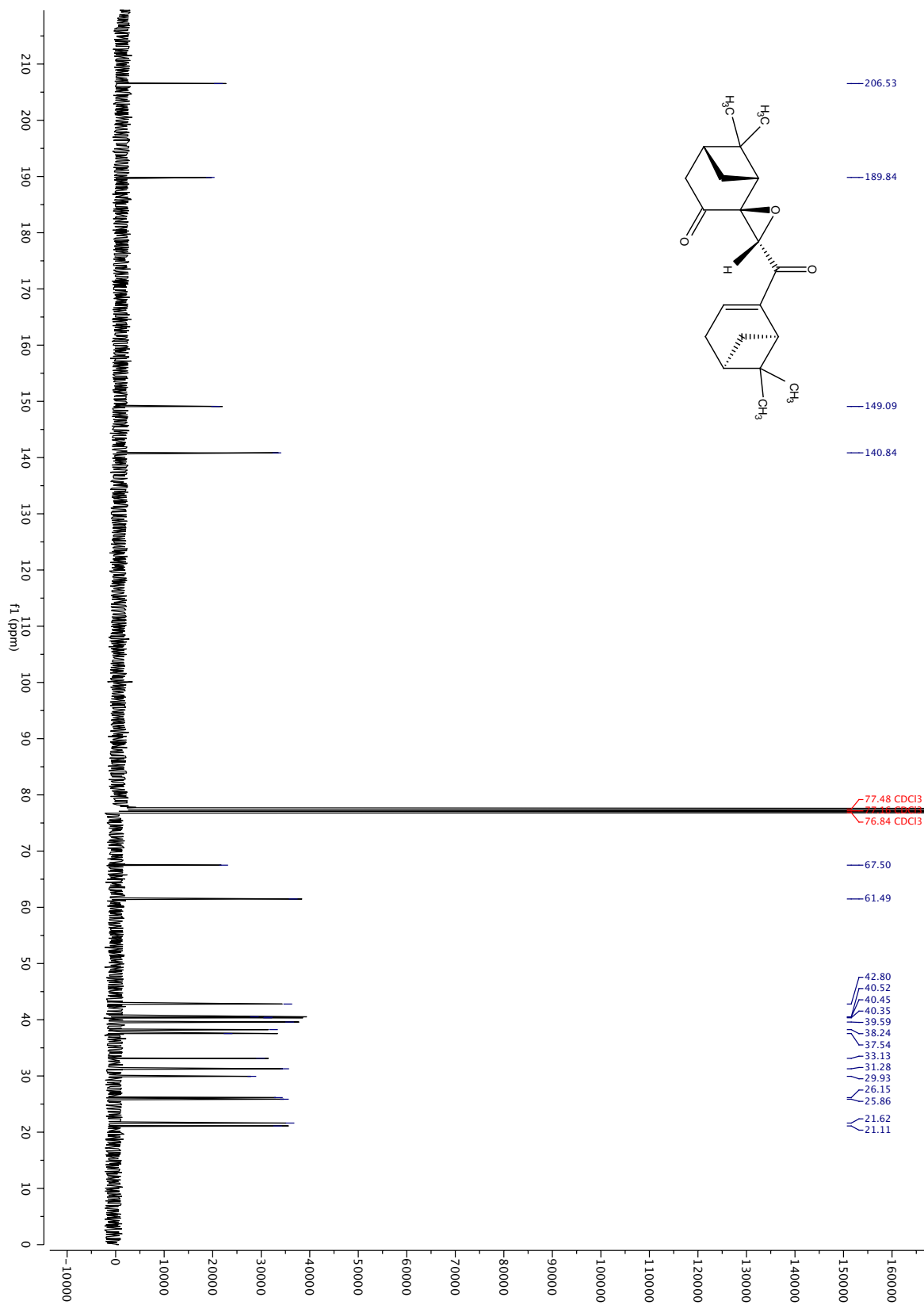


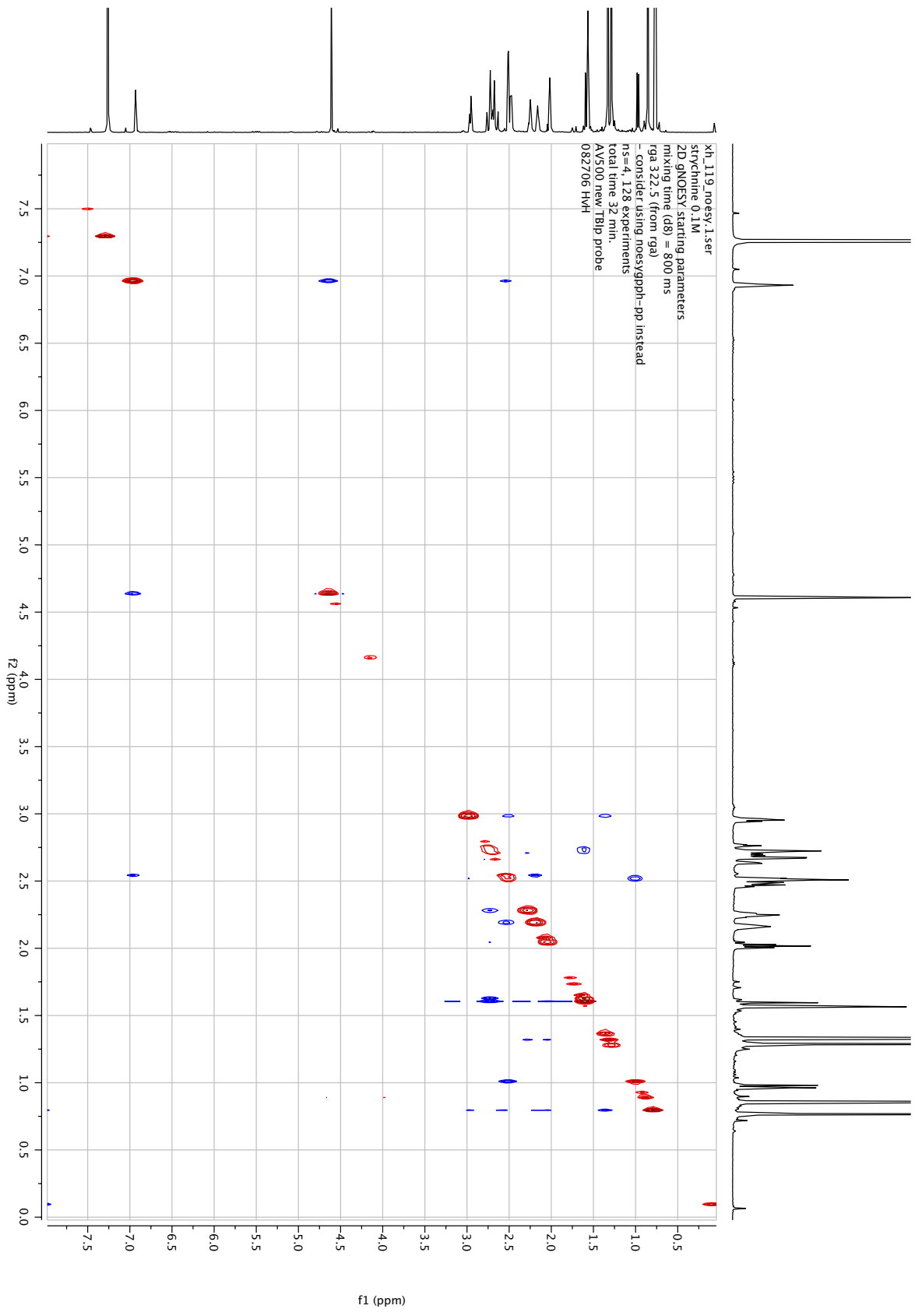


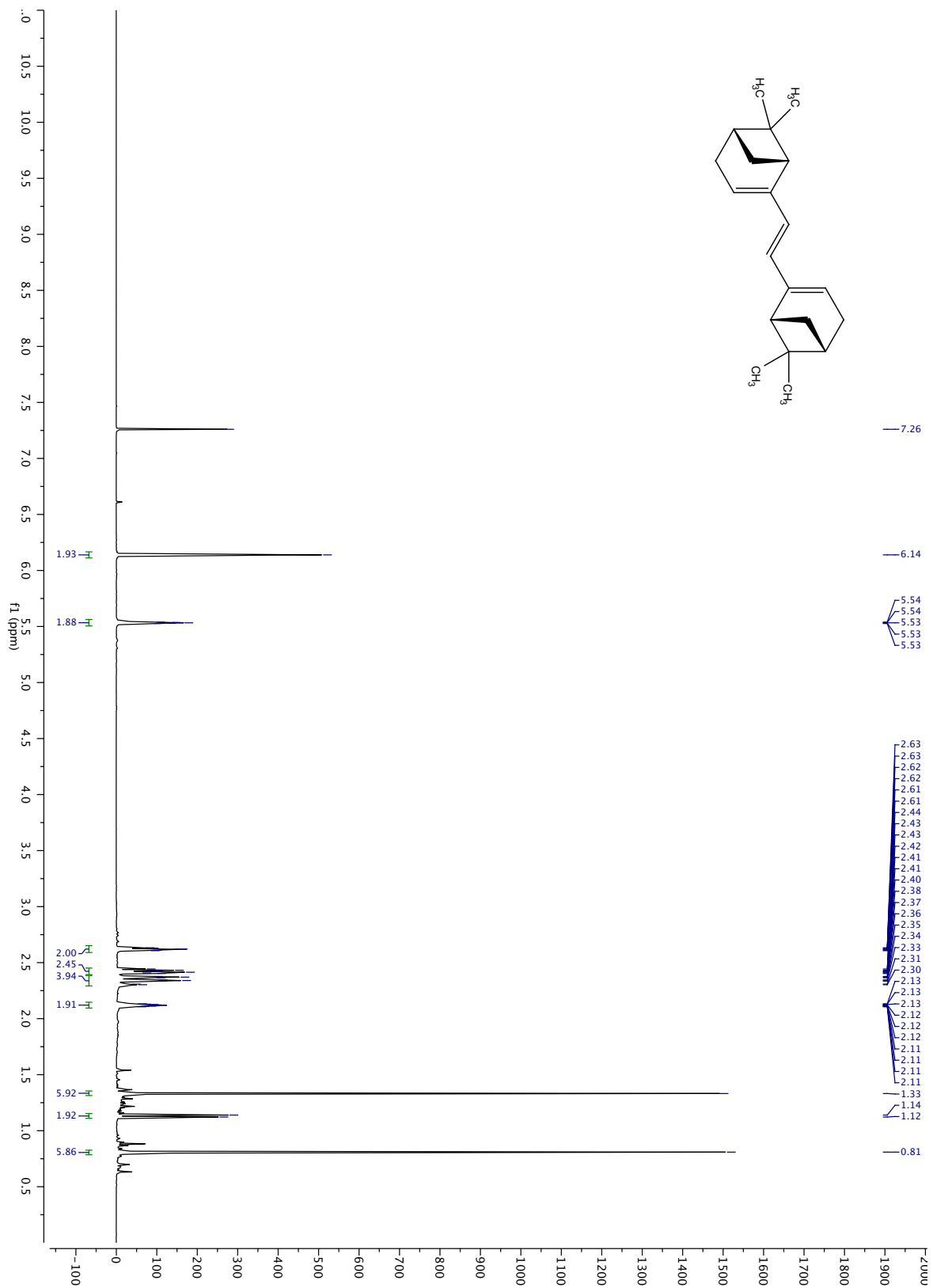


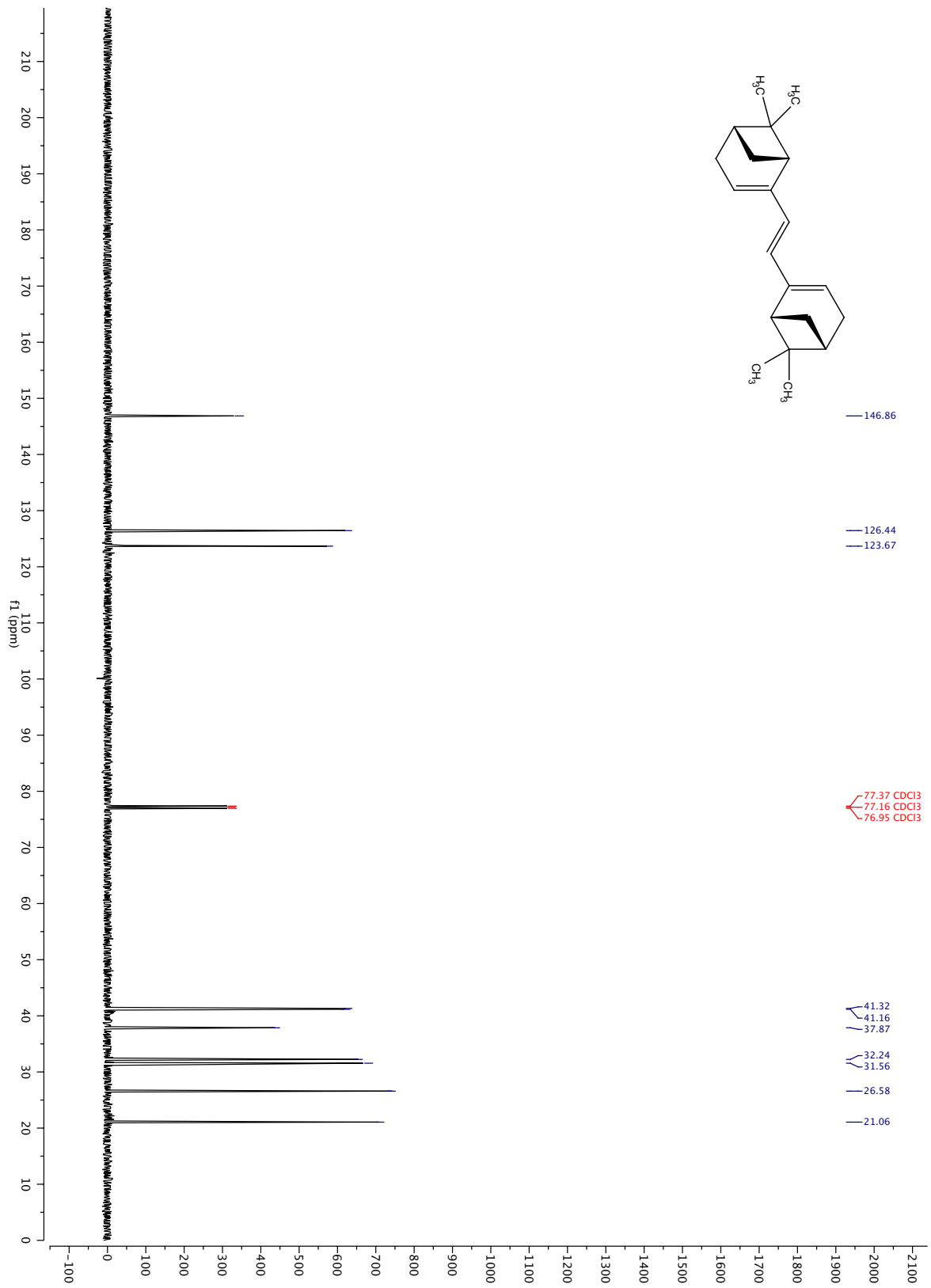


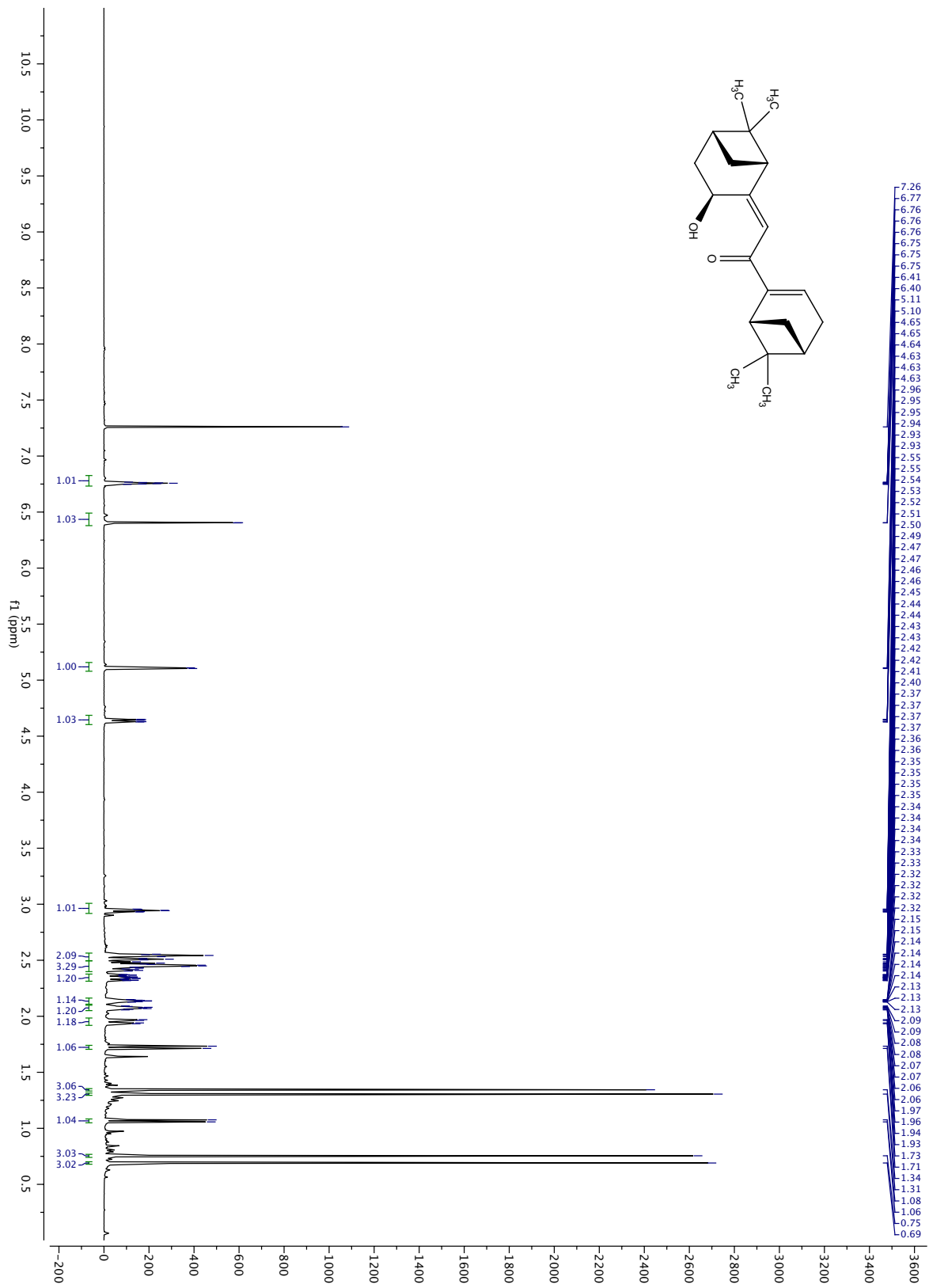


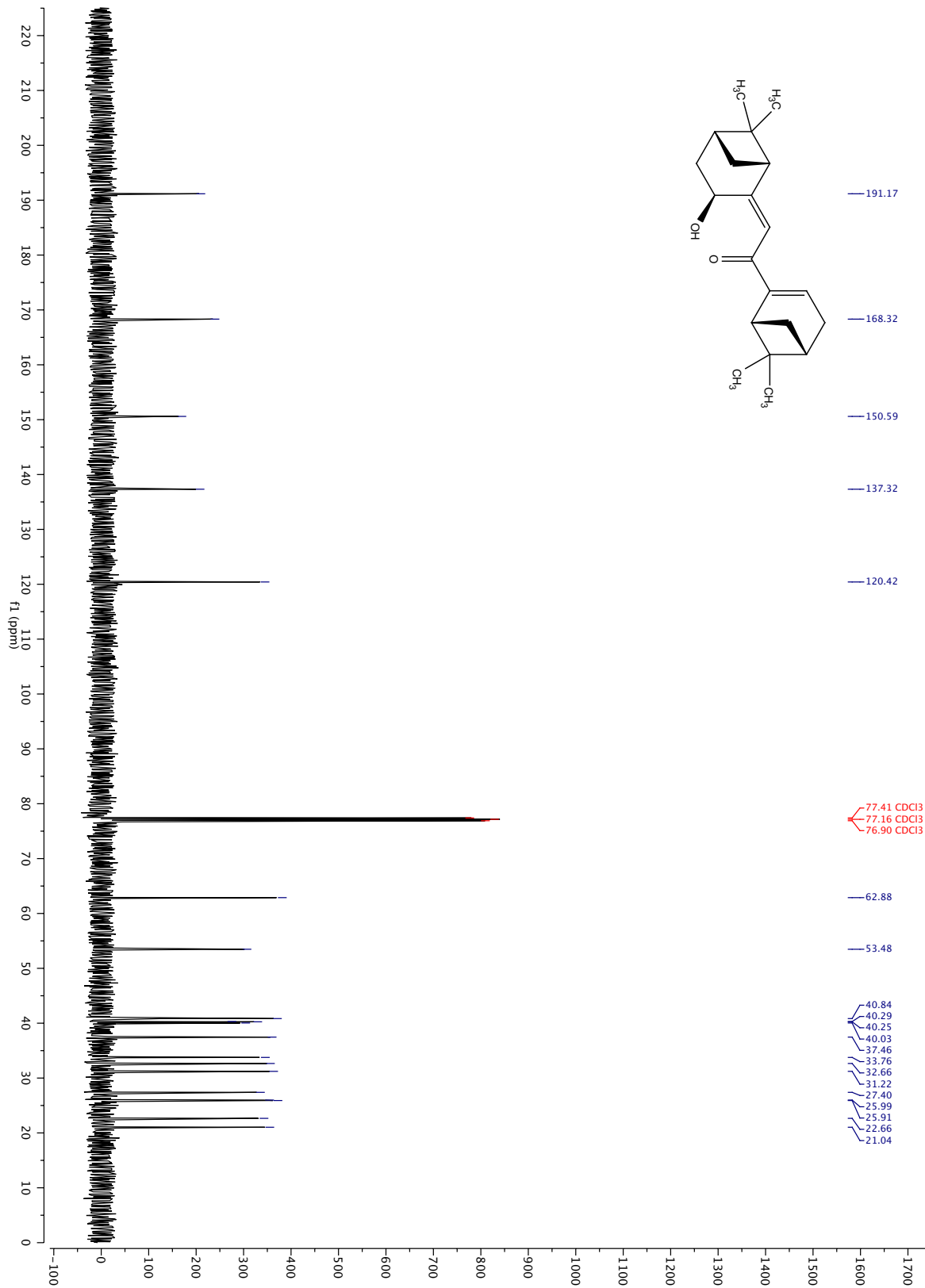


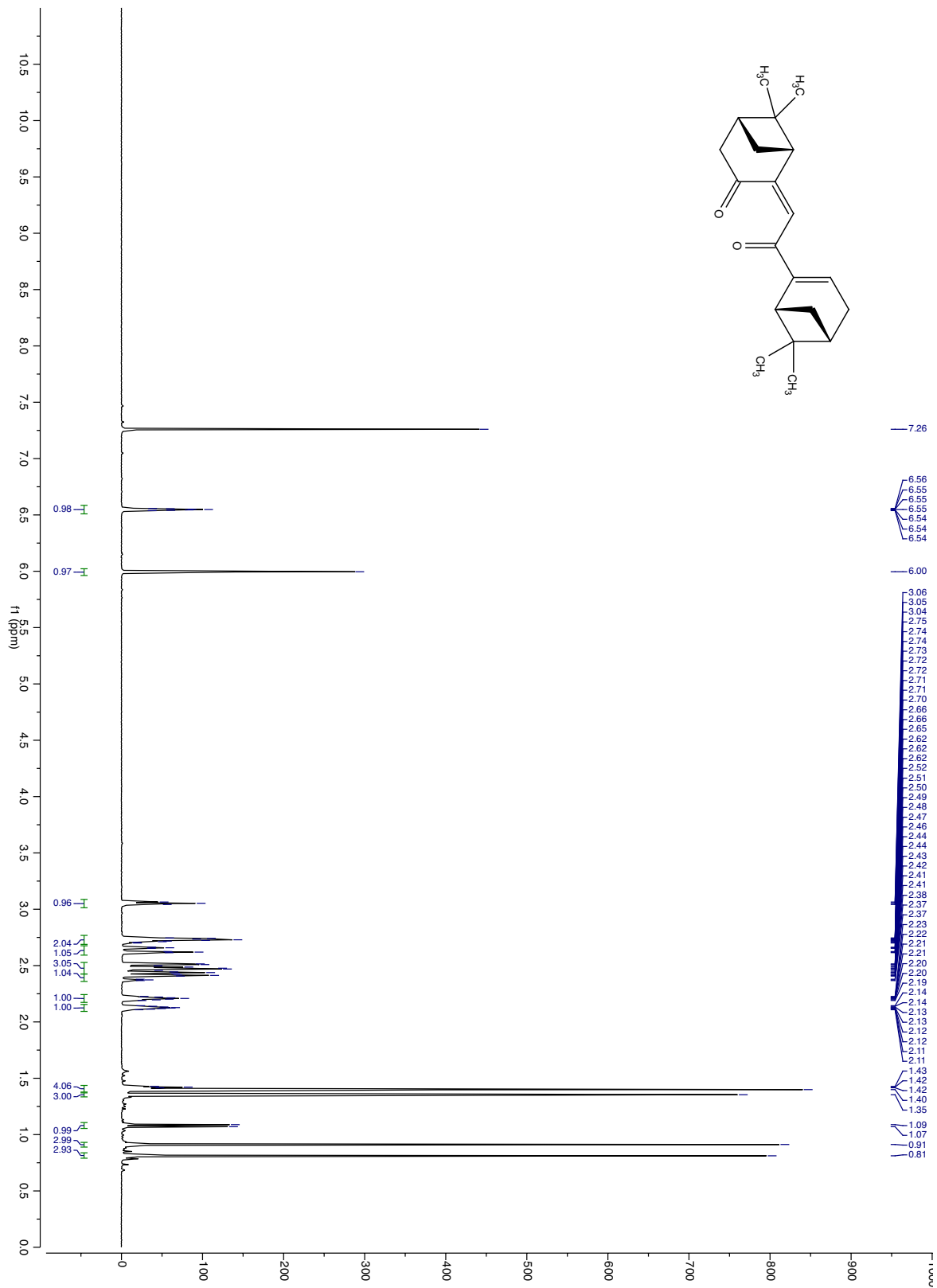


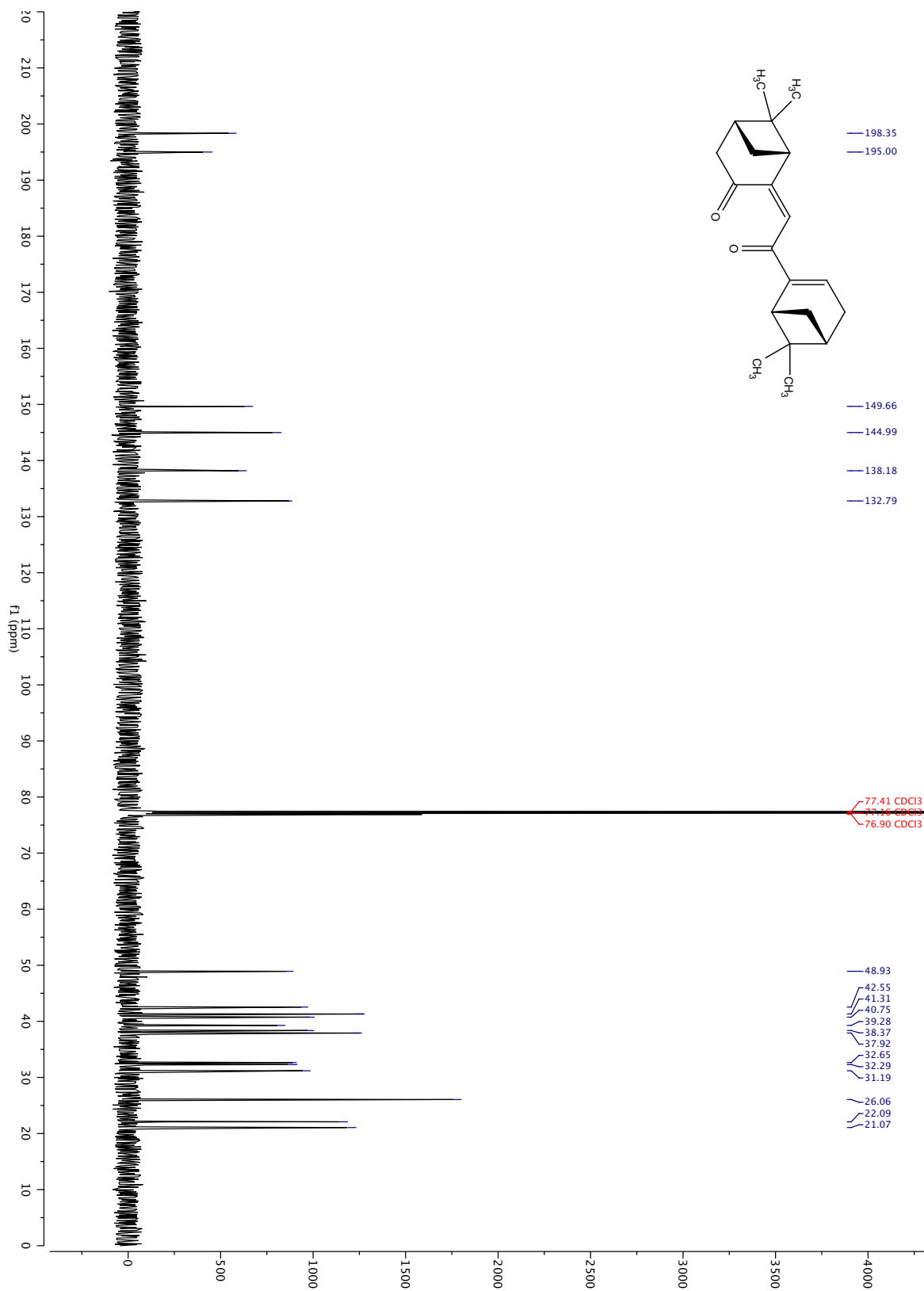


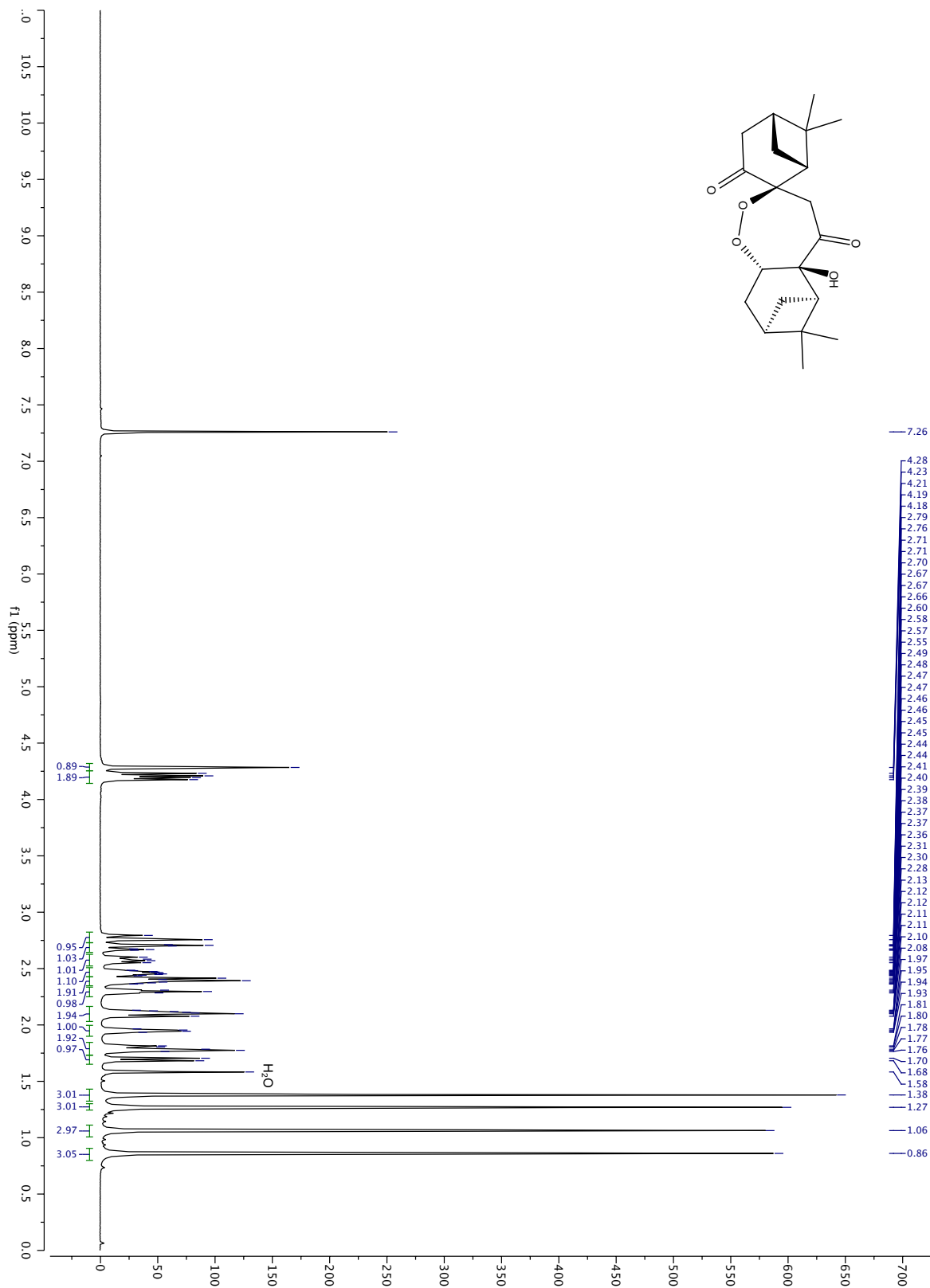


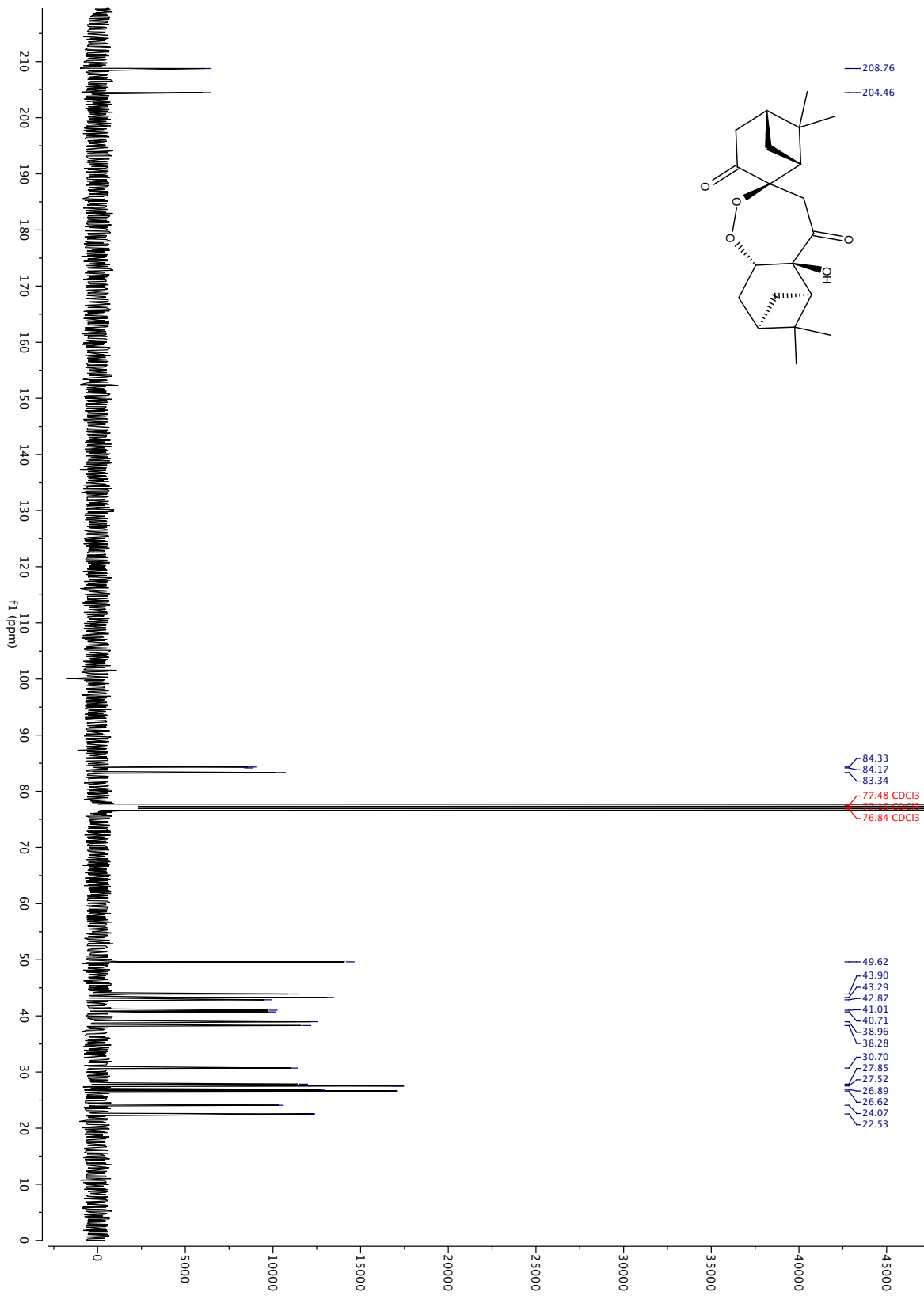


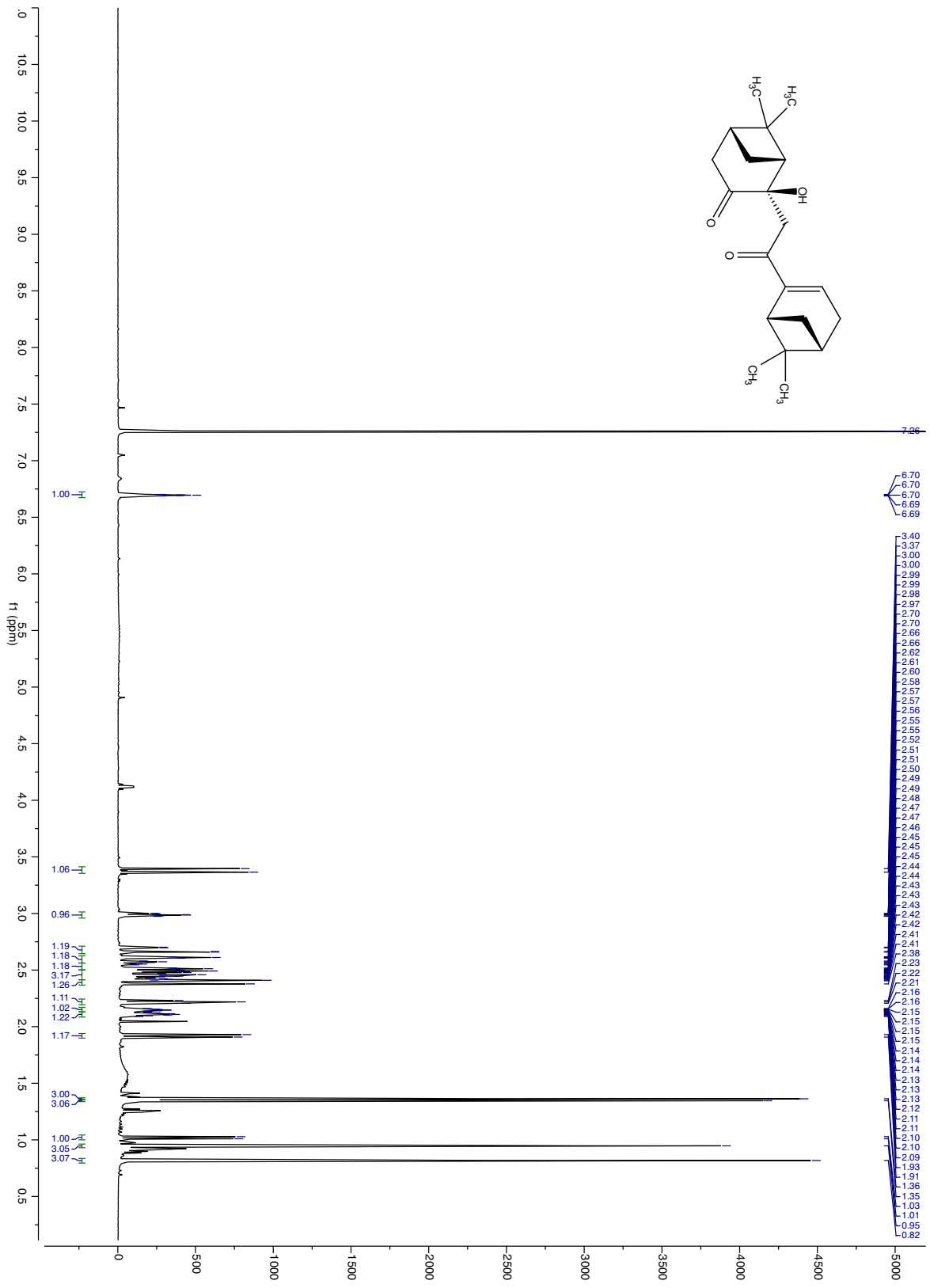


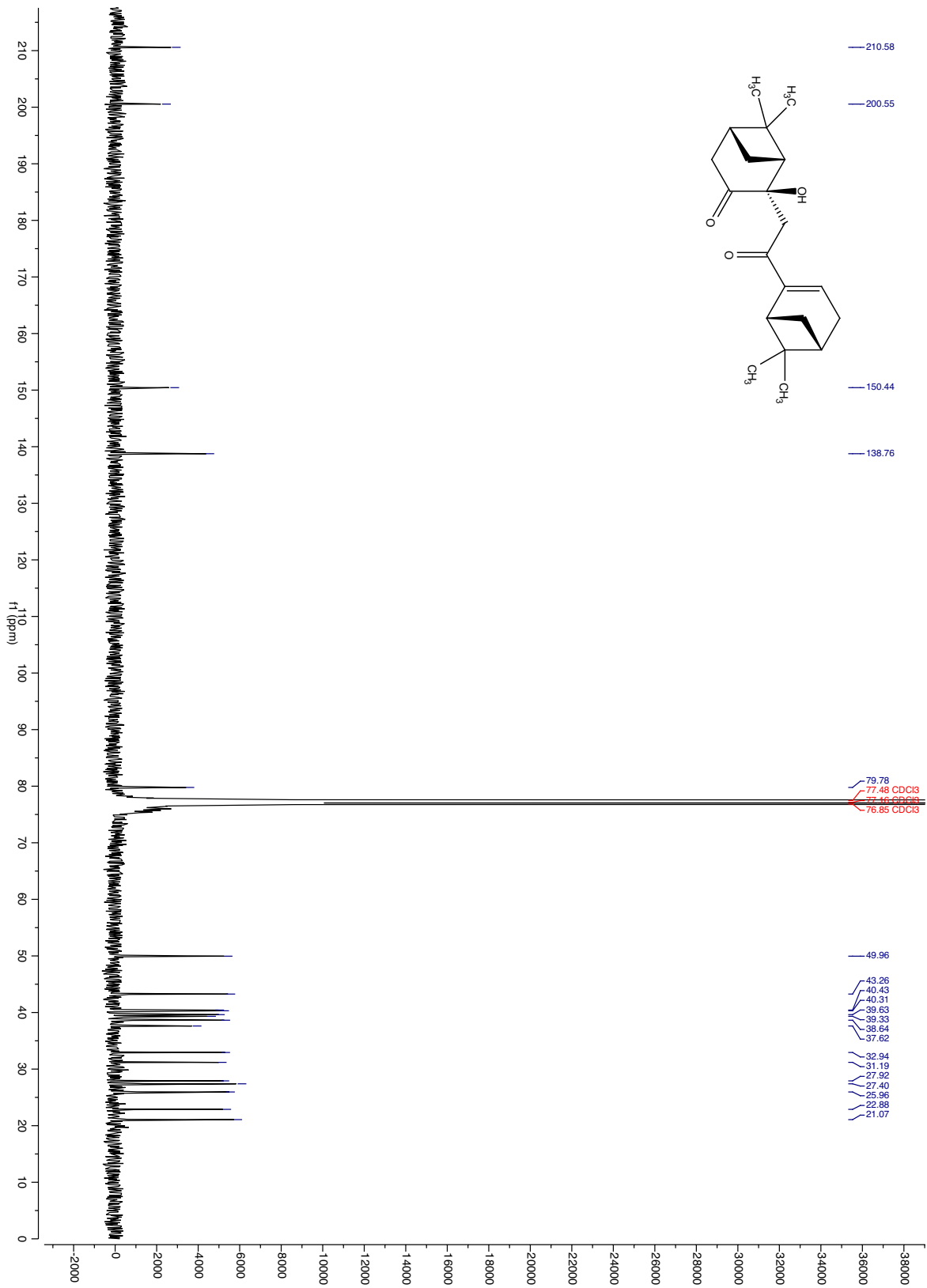


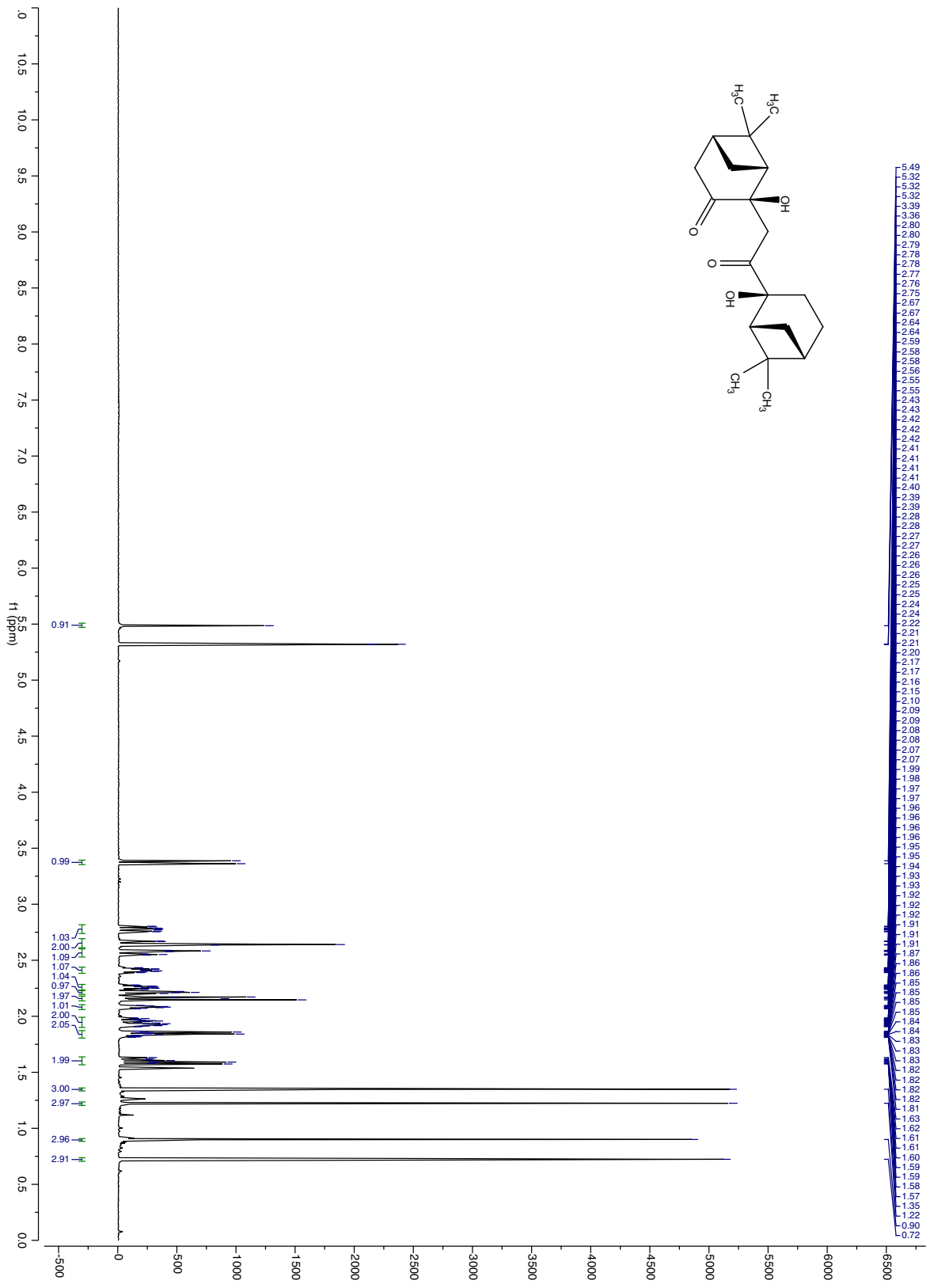


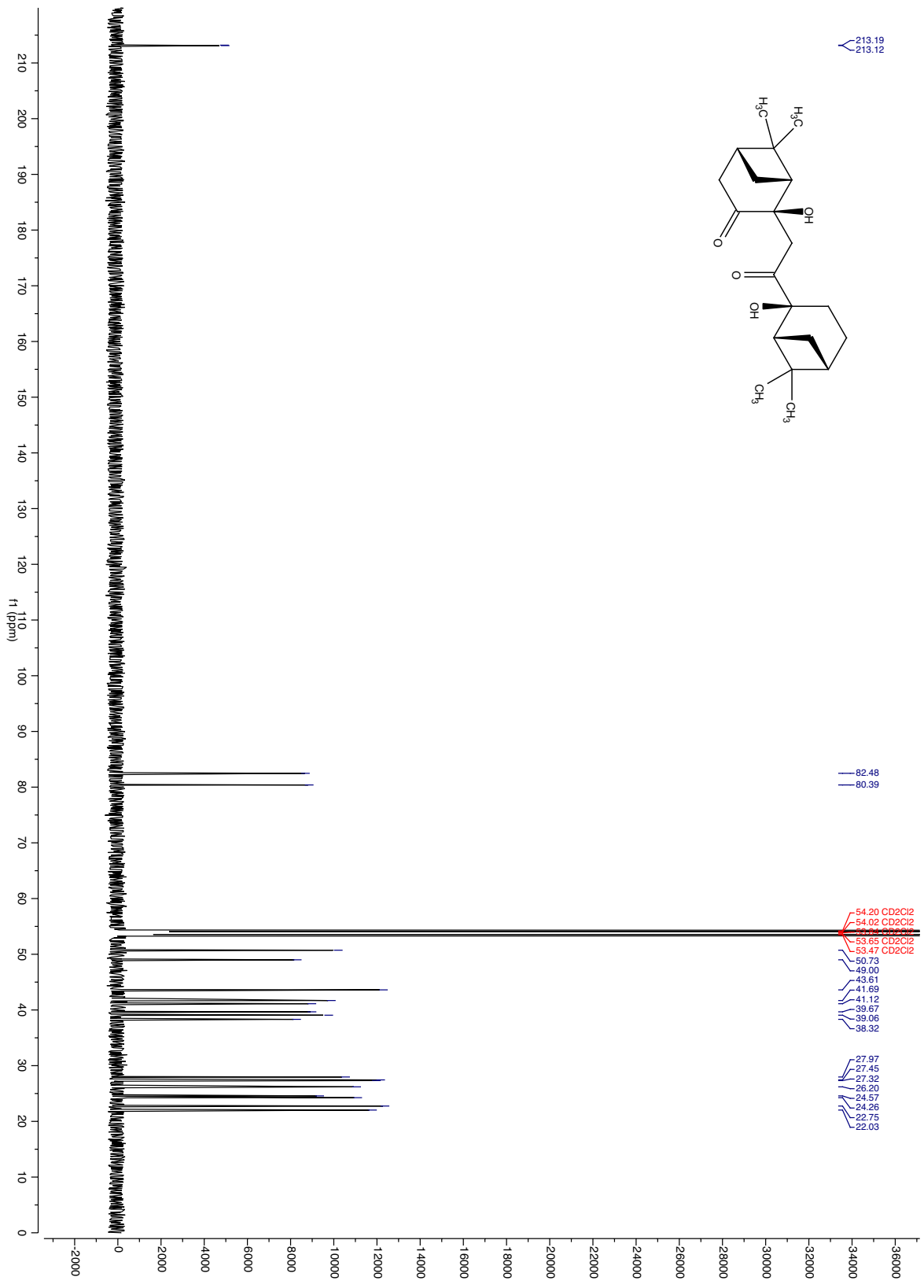


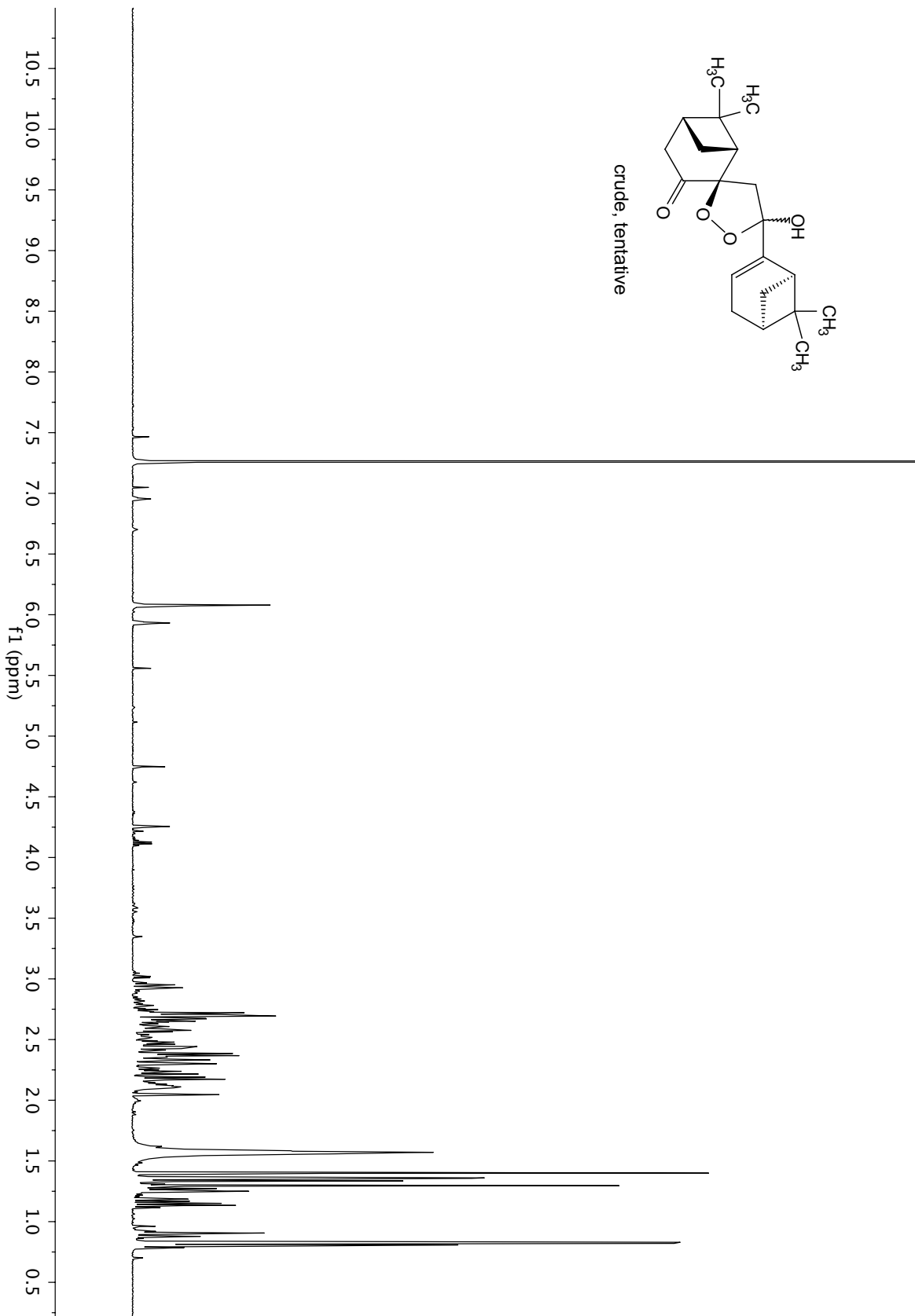
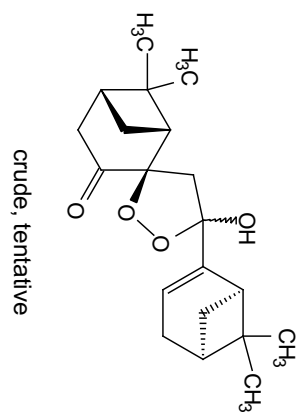


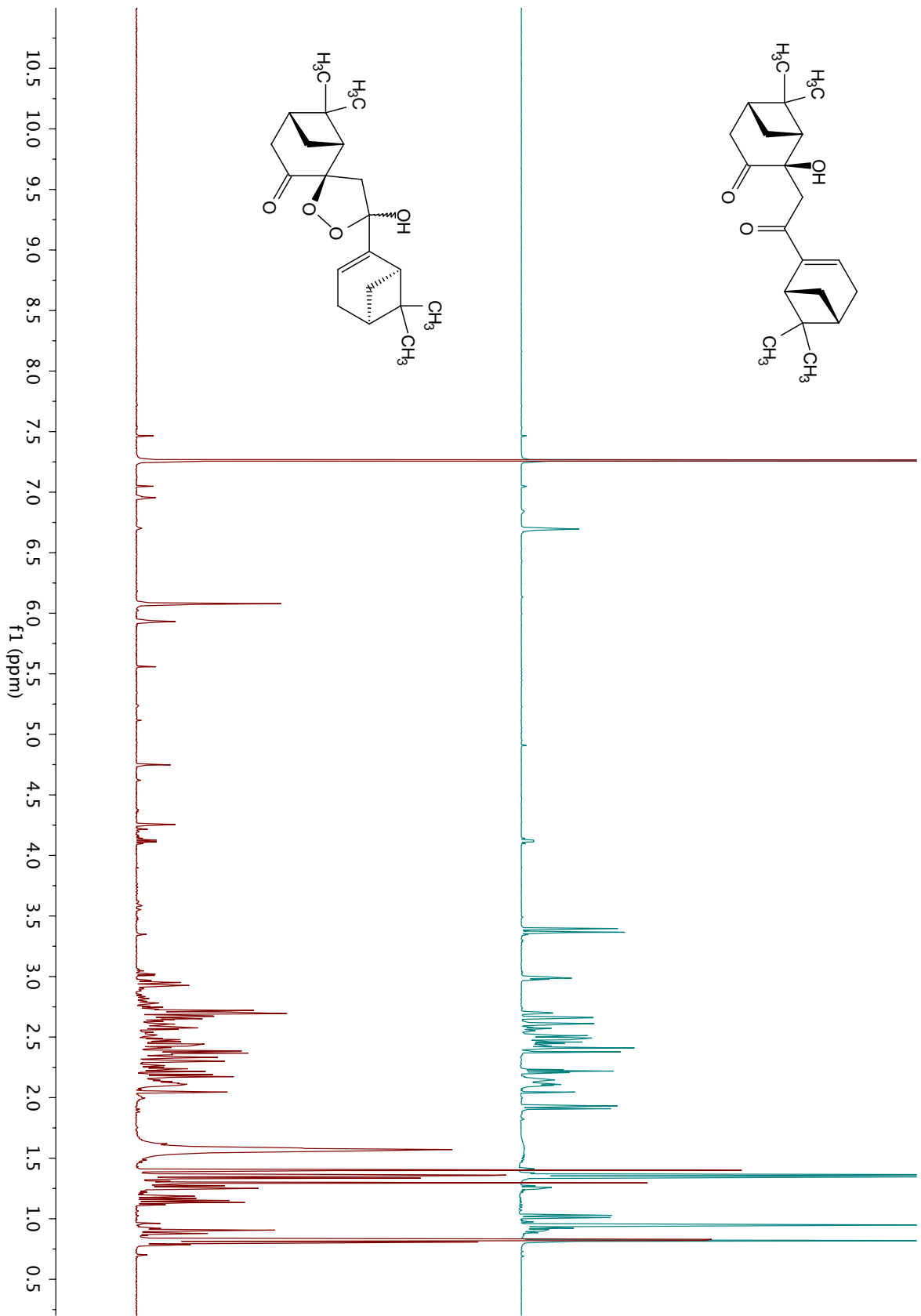


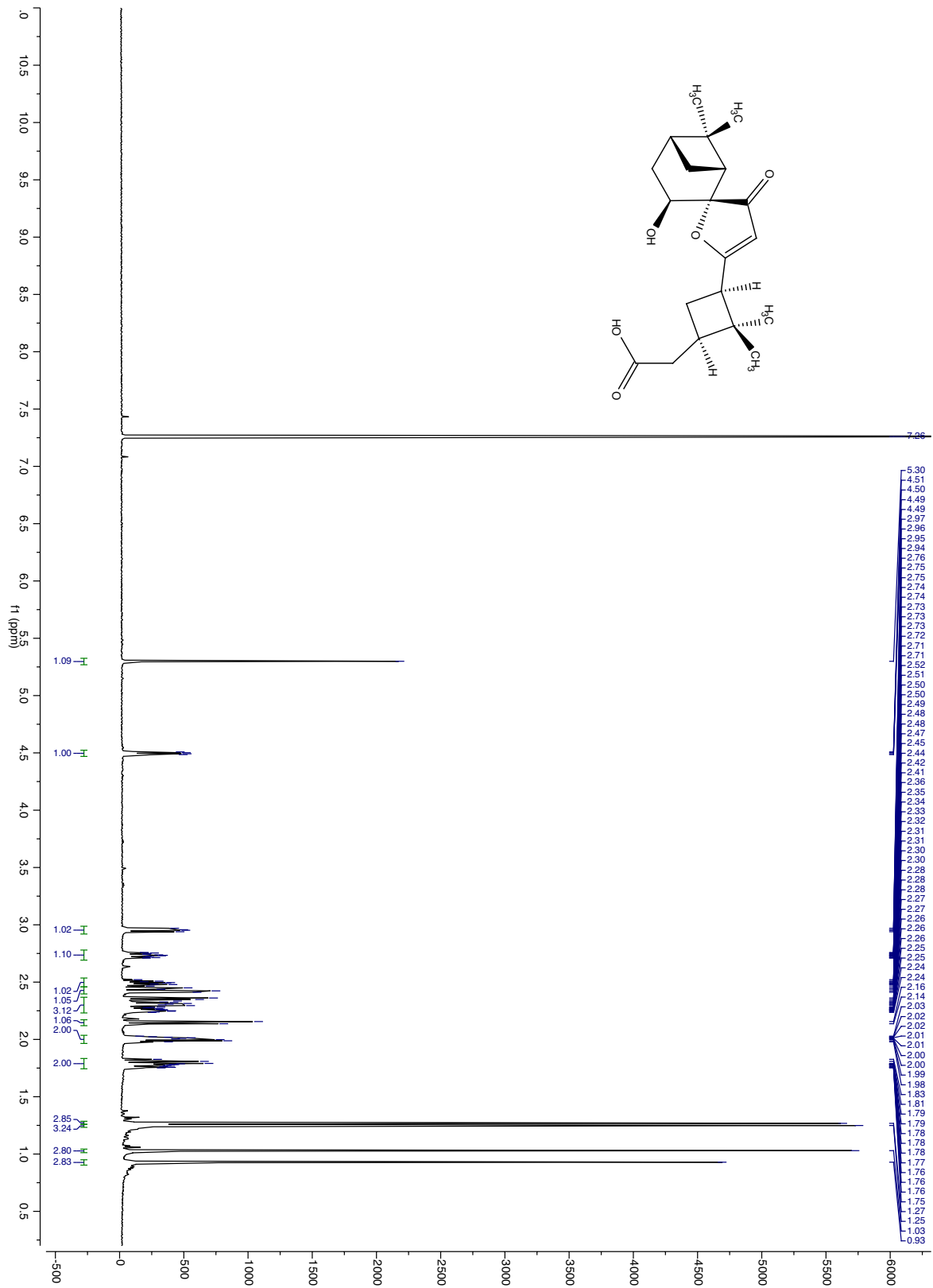


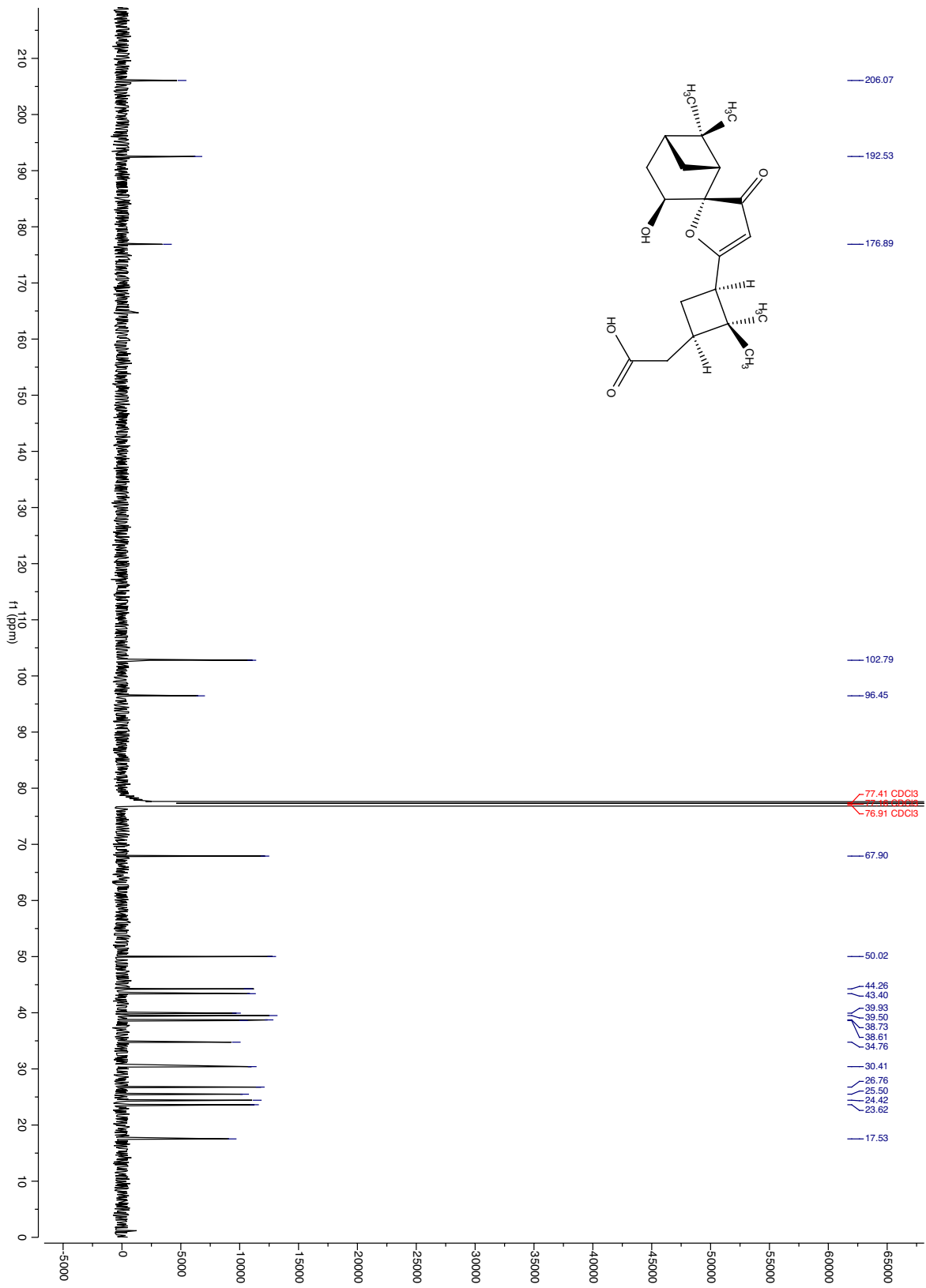


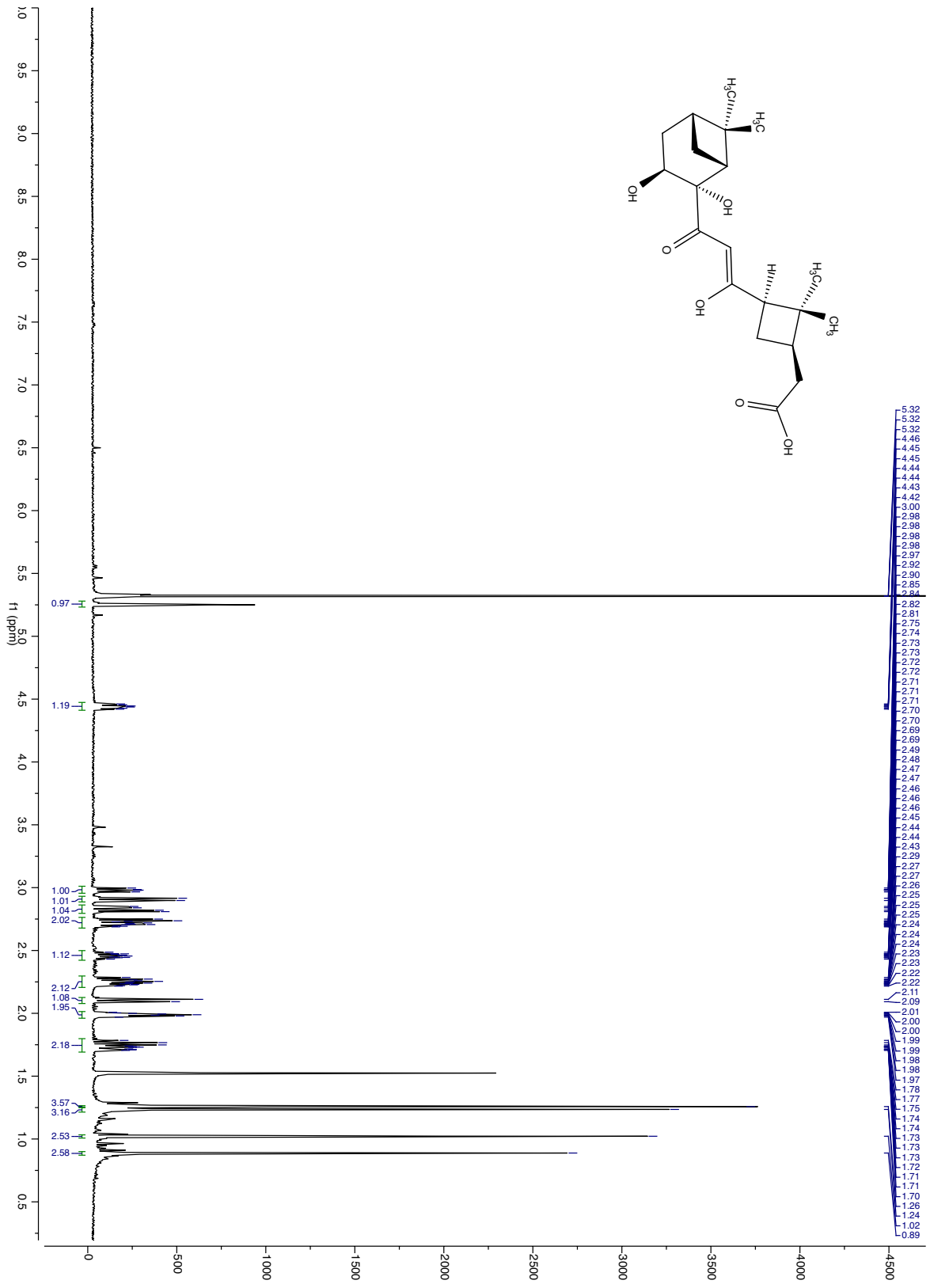


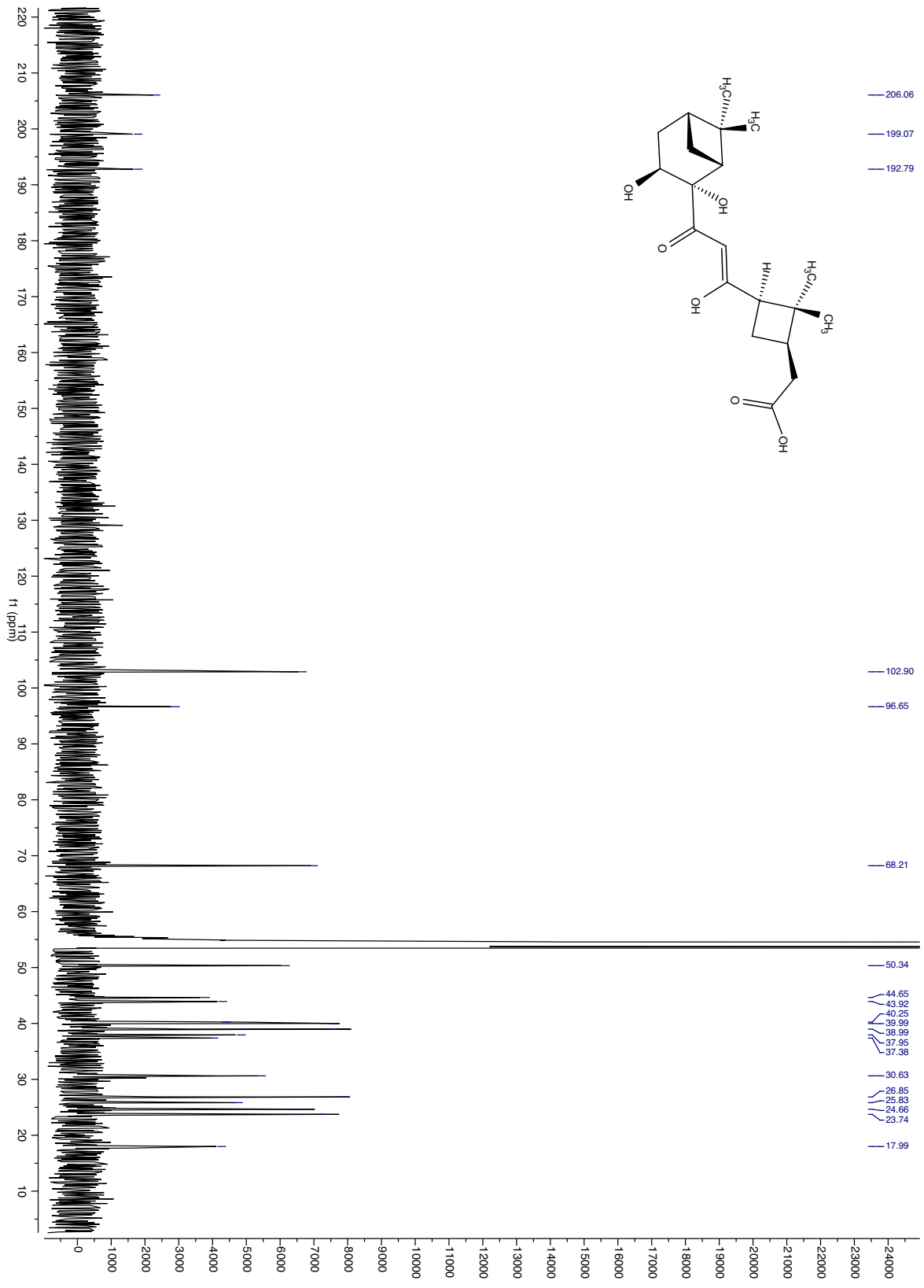


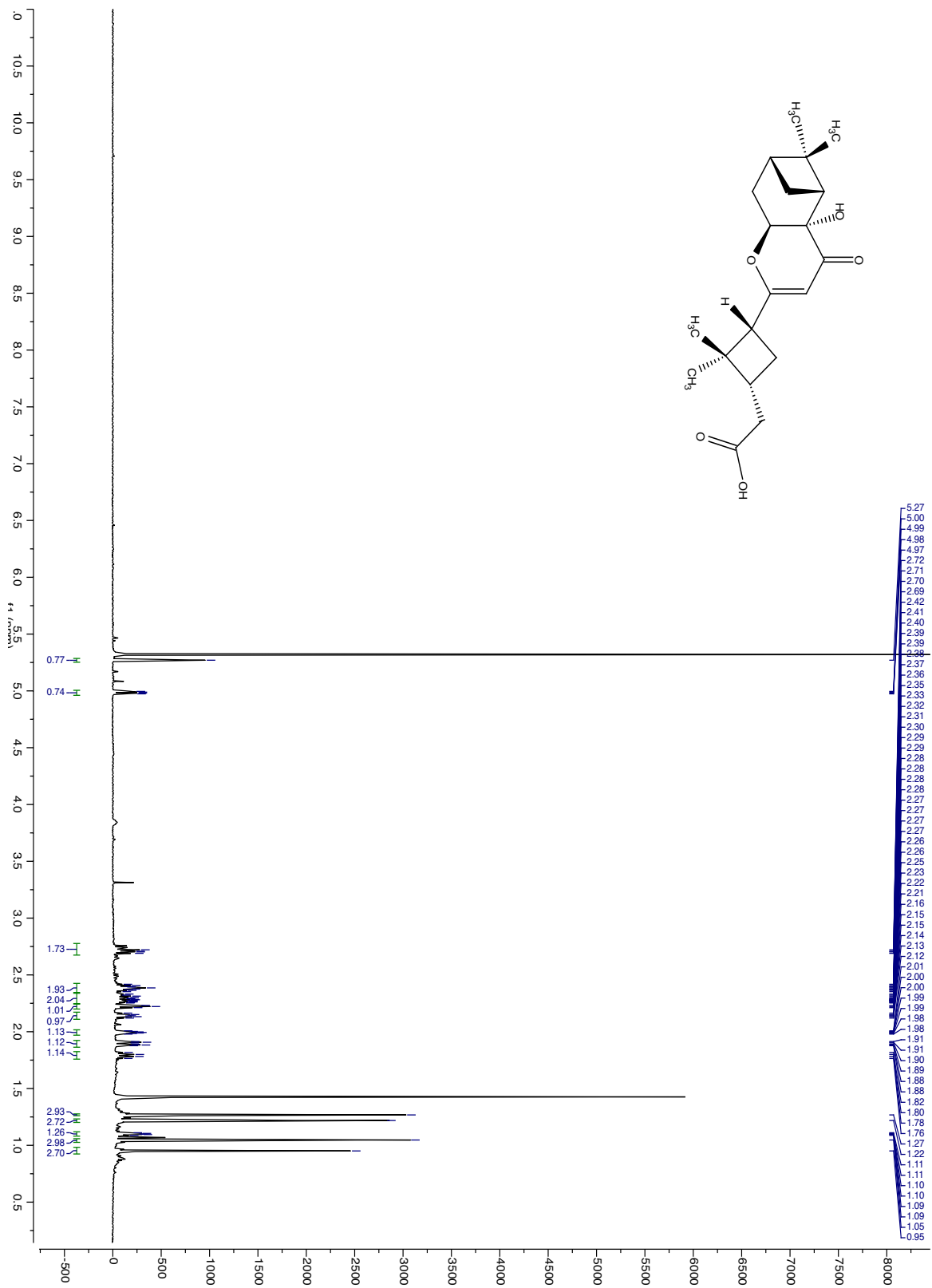




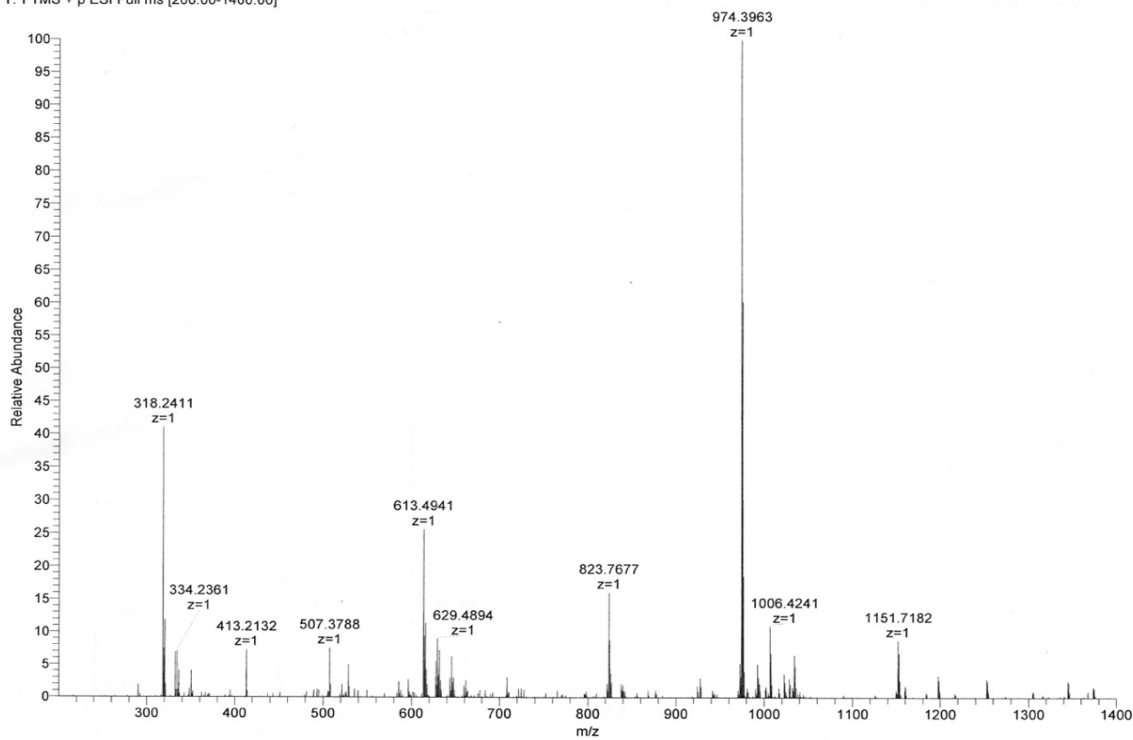




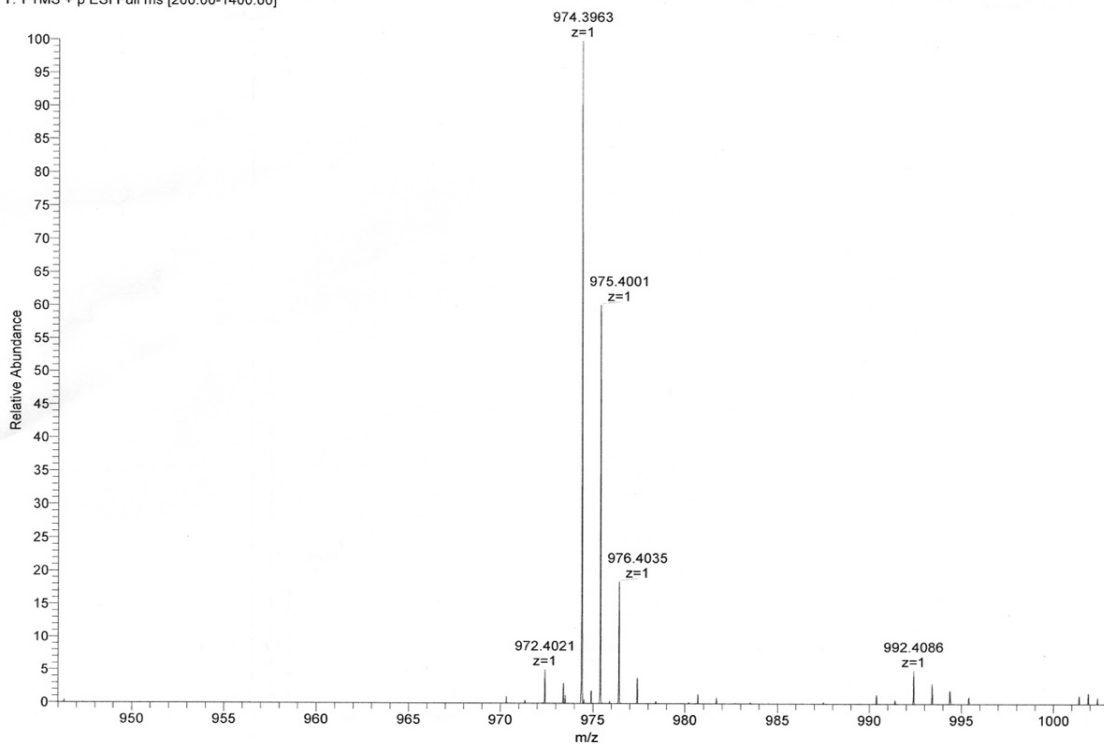




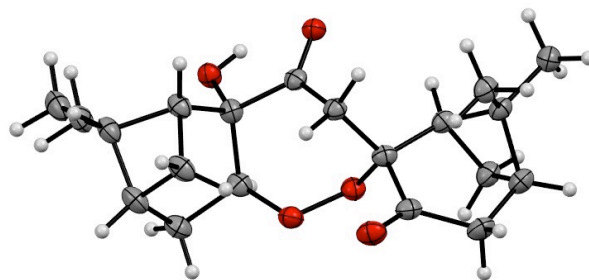
LFT2512 #1-67 RT: 0.01-0.99 AV: 67 NL: 2.50E6
T: FTMS + p ESI Full ms [200.00-1400.00]



LFT2512 #1-67 RT: 0.01-0.99 AV: 67 NL: 2.50E6
T: FTMS + p ESI Full ms [200.00-1400.00]



X-Ray crystallographic Analysis of Cardamom Peroxide (1)



A colorless needle 0.060 x 0.030 x 0.020 mm in size was mounted on a Cryoloop with Paratone oil. Data were collected in a nitrogen gas stream at 100(2) K using phi and omega scans. Crystal-to-detector distance was 60 mm and exposure time was 10 seconds per frame using a scan width of 1.0°. Data collection was 100.0% complete to 67.000° in θ . A total of 25275 reflections were collected covering the indices, $-7 \leq h \leq 7$, $-15 \leq k \leq 14$, $-25 \leq l \leq 26$. 3253 reflections were found to be symmetry independent, with an R_{int} of 0.0218. Indexing and unit cell refinement indicated a primitive, orthorhombic lattice. The space group was found to be P 21 21 21 (No. 19). The data were integrated using the Bruker SAINT software program and scaled using the SADABS software program. Solution by iterative methods (SHELXT) produced a complete heavy-atom phasing model consistent with the proposed structure. All non-hydrogen atoms were refined anisotropically by full-matrix least-squares (SHELXL-2013). All hydrogen atoms were placed using a riding model. Their positions were constrained relative to their parent atom using the appropriate HFIX command in SHELXL-2013. Absolute stereochemistry was unambiguously determined to be *R* at C3, C5, C9, C12 and C14, and *S* at C1 and C6, respectively.

Table 1. Crystal data and structure refinement for compound **1**.

X-ray ID	maimone18	
Sample/notebook ID	XH_NP_1	
Empirical formula	C20 H28 O5	
Formula weight	348.42	
Temperature	100(2) K	
Wavelength	1.54178 Å	
Crystal system	Orthorhombic	
Space group	P 21 21 21	
Unit cell dimensions	a = 6.4066(3) Å	$\alpha = 90^\circ$.
	b = 12.6083(6) Å	$\beta = 90^\circ$.
	c = 22.0227(11) Å	$\gamma = 90^\circ$.
Volume	1778.91(15) Å ³	
Z	4	
Density (calculated)	1.301 Mg/m ³	
Absorption coefficient	0.750 mm ⁻¹	
F(000)	752	
Crystal size	0.060 x 0.030 x 0.020 mm ³	
Crystal color/habit	colorless needle	
Theta range for data collection	4.014 to 68.277°.	
Index ranges	-7 ≤ h ≤ 7, -15 ≤ k ≤ 14, -25 ≤ l ≤ 26	
Reflections collected	25275	
Independent reflections	3253 [R(int) = 0.0218]	
Completeness to theta = 67.000°	100.0 %	
Absorption correction	Semi-empirical from equivalents	
Max. and min. transmission	0.929 and 0.863	
Refinement method	Full-matrix least-squares on F ²	
Data / restraints / parameters	3253 / 0 / 231	
Goodness-of-fit on F ²	1.045	
Final R indices [I > 2σ(I)]	R1 = 0.0388, wR2 = 0.1028	
R indices (all data)	R1 = 0.0392, wR2 = 0.1032	
Absolute structure parameter	0.04(4)	
Extinction coefficient	n/a	
Largest diff. peak and hole	0.339 and -0.166 e.Å ⁻³	

Table 2. Atomic coordinates ($\times 10^4$) and equivalent isotropic displacement parameters ($\text{\AA}^2 \times 10^3$) for maimone18. $U(\text{eq})$ is defined as one third of the trace of the orthogonalized U^{ij} tensor.

	x	y	z	$U(\text{eq})$
C(1)	2027(4)	4887(2)	8864(1)	26(1)
C(2)	1676(4)	5217(2)	8196(1)	30(1)
C(3)	3043(4)	4591(2)	7749(1)	30(1)
C(4)	2565(4)	3383(2)	7776(1)	29(1)
C(5)	4012(4)	3387(2)	8359(1)	25(1)
C(6)	2827(4)	3725(2)	8940(1)	23(1)
C(7)	4297(4)	3577(2)	9489(1)	22(1)
C(8)	6225(4)	4249(2)	9568(1)	23(1)
C(9)	5575(4)	5219(2)	9943(1)	24(1)
C(10)	7098(4)	6169(2)	9846(1)	26(1)
C(11)	7592(4)	6845(2)	10402(1)	31(1)
C(12)	6925(4)	6320(2)	10993(1)	28(1)
C(13)	7424(4)	5106(2)	10979(1)	24(1)
C(14)	5303(4)	4997(2)	10620(1)	23(1)
C(15)	5149(4)	4359(2)	8069(1)	29(1)
C(16)	4584(4)	6030(2)	10942(1)	27(1)
C(17)	3653(5)	2749(2)	7271(1)	37(1)
C(18)	273(4)	3052(2)	7781(1)	32(1)
C(19)	9487(4)	4749(2)	10701(1)	28(1)
C(20)	7215(4)	4590(2)	11606(1)	29(1)
O(1)	3504(3)	5550(1)	9755(1)	26(1)
O(2)	3488(3)	5666(1)	9090(1)	27(1)
O(3)	1088(3)	3054(1)	9027(1)	26(1)
O(4)	3864(3)	2904(1)	9862(1)	26(1)
O(5)	7832(3)	6350(1)	9352(1)	32(1)

Table 3. Bond lengths [Å] and angles [°] for maimone18.

C(1)-O(2)	1.445(3)	C(11)-H(11A)	0.9900
C(1)-C(2)	1.546(3)	C(11)-H(11B)	0.9900
C(1)-C(6)	1.561(3)	C(12)-C(16)	1.548(4)
C(1)-H(1)	1.0000	C(12)-C(13)	1.563(3)
C(2)-C(3)	1.536(4)	C(12)-H(12)	1.0000
C(2)-H(2A)	0.9900	C(13)-C(19)	1.524(3)
C(2)-H(2B)	0.9900	C(13)-C(20)	1.532(4)
C(3)-C(15)	1.550(3)	C(13)-C(14)	1.578(3)
C(3)-C(4)	1.556(4)	C(14)-C(16)	1.553(3)
C(3)-H(3)	1.0000	C(14)-H(14)	1.0000
C(4)-C(18)	1.526(4)	C(15)-H(15A)	0.9900
C(4)-C(17)	1.537(4)	C(15)-H(15B)	0.9900
C(4)-C(5)	1.584(3)	C(16)-H(16A)	0.9900
C(5)-C(6)	1.547(3)	C(16)-H(16B)	0.9900
C(5)-C(15)	1.563(4)	C(17)-H(17A)	0.9800
C(5)-H(5)	1.0000	C(17)-H(17B)	0.9800
C(6)-O(3)	1.411(3)	C(17)-H(17C)	0.9800
C(6)-C(7)	1.544(3)	C(18)-H(18A)	0.9800
C(7)-O(4)	1.213(3)	C(18)-H(18B)	0.9800
C(7)-C(8)	1.508(3)	C(18)-H(18C)	0.9800
C(8)-C(9)	1.533(3)	C(19)-H(19A)	0.9800
C(8)-H(8A)	0.9900	C(19)-H(19B)	0.9800
C(8)-H(8B)	0.9900	C(19)-H(19C)	0.9800
C(9)-O(1)	1.451(3)	C(20)-H(20A)	0.9800
C(9)-C(14)	1.528(3)	C(20)-H(20B)	0.9800
C(9)-C(10)	1.560(3)	C(20)-H(20C)	0.9800
C(10)-O(5)	1.207(3)	O(1)-O(2)	1.472(2)
C(10)-C(11)	1.526(3)	O(3)-H(3A)	0.8400
C(11)-C(12)	1.520(4)		
O(2)-C(1)-C(2)	103.82(19)	C(2)-C(1)-H(1)	108.7
O(2)-C(1)-C(6)	112.87(19)	C(6)-C(1)-H(1)	108.7
C(2)-C(1)-C(6)	113.7(2)	C(3)-C(2)-C(1)	112.9(2)
O(2)-C(1)-H(1)	108.7	C(3)-C(2)-H(2A)	109.0

C(1)-C(2)-H(2A)	109.0	H(8A)-C(8)-H(8B)	108.6
C(3)-C(2)-H(2B)	109.0	O(1)-C(9)-C(14)	103.08(18)
C(1)-C(2)-H(2B)	109.0	O(1)-C(9)-C(8)	109.0(2)
H(2A)-C(2)-H(2B)	107.8	C(14)-C(9)-C(8)	114.3(2)
C(2)-C(3)-C(15)	107.6(2)	O(1)-C(9)-C(10)	108.17(18)
C(2)-C(3)-C(4)	111.5(2)	C(14)-C(9)-C(10)	110.18(19)
C(15)-C(3)-C(4)	88.2(2)	C(8)-C(9)-C(10)	111.7(2)
C(2)-C(3)-H(3)	115.5	O(5)-C(10)-C(11)	122.5(2)
C(15)-C(3)-H(3)	115.5	O(5)-C(10)-C(9)	120.8(2)
C(4)-C(3)-H(3)	115.5	C(11)-C(10)-C(9)	116.7(2)
C(18)-C(4)-C(17)	107.5(2)	C(12)-C(11)-C(10)	112.7(2)
C(18)-C(4)-C(3)	117.2(2)	C(12)-C(11)-H(11A)	109.1
C(17)-C(4)-C(3)	113.1(2)	C(10)-C(11)-H(11A)	109.1
C(18)-C(4)-C(5)	123.9(2)	C(12)-C(11)-H(11B)	109.1
C(17)-C(4)-C(5)	108.8(2)	C(10)-C(11)-H(11B)	109.1
C(3)-C(4)-C(5)	85.02(19)	H(11A)-C(11)-H(11B)	107.8
C(6)-C(5)-C(15)	110.5(2)	C(11)-C(12)-C(16)	108.3(2)
C(6)-C(5)-C(4)	112.56(19)	C(11)-C(12)-C(13)	110.6(2)
C(15)-C(5)-C(4)	86.76(18)	C(16)-C(12)-C(13)	88.05(18)
C(6)-C(5)-H(5)	114.6	C(11)-C(12)-H(12)	115.5
C(15)-C(5)-H(5)	114.6	C(16)-C(12)-H(12)	115.5
C(4)-C(5)-H(5)	114.6	C(13)-C(12)-H(12)	115.5
O(3)-C(6)-C(7)	107.65(18)	C(19)-C(13)-C(20)	108.1(2)
O(3)-C(6)-C(5)	109.53(19)	C(19)-C(13)-C(12)	118.3(2)
C(7)-C(6)-C(5)	108.33(18)	C(20)-C(13)-C(12)	112.4(2)
O(3)-C(6)-C(1)	108.53(19)	C(19)-C(13)-C(14)	121.3(2)
C(7)-C(6)-C(1)	113.40(19)	C(20)-C(13)-C(14)	109.8(2)
C(5)-C(6)-C(1)	109.34(19)	C(12)-C(13)-C(14)	85.36(18)
O(4)-C(7)-C(8)	120.2(2)	C(9)-C(14)-C(16)	109.1(2)
O(4)-C(7)-C(6)	118.3(2)	C(9)-C(14)-C(13)	112.02(19)
C(8)-C(7)-C(6)	121.5(2)	C(16)-C(14)-C(13)	87.34(18)
C(7)-C(8)-C(9)	106.71(19)	C(9)-C(14)-H(14)	115.1
C(7)-C(8)-H(8A)	110.4	C(16)-C(14)-H(14)	115.1
C(9)-C(8)-H(8A)	110.4	C(13)-C(14)-H(14)	115.1
C(7)-C(8)-H(8B)	110.4	C(3)-C(15)-C(5)	85.91(19)
C(9)-C(8)-H(8B)	110.4	C(3)-C(15)-H(15A)	114.3

C(5)-C(15)-H(15A)	114.3	C(4)-C(18)-H(18C)	109.5
C(3)-C(15)-H(15B)	114.3	H(18A)-C(18)-H(18C)	109.5
C(5)-C(15)-H(15B)	114.3	H(18B)-C(18)-H(18C)	109.5
H(15A)-C(15)-H(15B)	111.5	C(13)-C(19)-H(19A)	109.5
C(12)-C(16)-C(14)	86.74(18)	C(13)-C(19)-H(19B)	109.5
C(12)-C(16)-H(16A)	114.2	H(19A)-C(19)-H(19B)	109.5
C(14)-C(16)-H(16A)	114.2	C(13)-C(19)-H(19C)	109.5
C(12)-C(16)-H(16B)	114.2	H(19A)-C(19)-H(19C)	109.5
C(14)-C(16)-H(16B)	114.2	H(19B)-C(19)-H(19C)	109.5
H(16A)-C(16)-H(16B)	111.4	C(13)-C(20)-H(20A)	109.5
C(4)-C(17)-H(17A)	109.5	C(13)-C(20)-H(20B)	109.5
C(4)-C(17)-H(17B)	109.5	H(20A)-C(20)-H(20B)	109.5
H(17A)-C(17)-H(17B)	109.5	C(13)-C(20)-H(20C)	109.5
C(4)-C(17)-H(17C)	109.5	H(20A)-C(20)-H(20C)	109.5
H(17A)-C(17)-H(17C)	109.5	H(20B)-C(20)-H(20C)	109.5
H(17B)-C(17)-H(17C)	109.5	C(9)-O(1)-O(2)	108.54(16)
C(4)-C(18)-H(18A)	109.5	C(1)-O(2)-O(1)	106.23(16)
C(4)-C(18)-H(18B)	109.5	C(6)-O(3)-H(3A)	109.5
H(18A)-C(18)-H(18B)	109.5		

Symmetry transformations used to generate equivalent atoms:

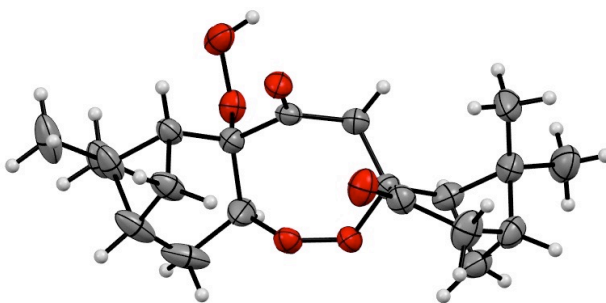
Table 4. Anisotropic displacement parameters ($\text{\AA}^2 \times 10^3$) for maimone18. The anisotropic displacement factor exponent takes the form: $-2\pi^2 [h^2 a^{*2} U^{11} + \dots + 2 h k a^* b^* U^{12}]$

	U ¹¹	U ²²	U ³³	U ²³	U ¹³	U ¹²
C(1)	21(1)	29(1)	28(1)	1(1)	0(1)	3(1)
C(2)	28(1)	30(1)	31(1)	6(1)	-3(1)	4(1)
C(3)	27(1)	38(1)	23(1)	9(1)	0(1)	3(1)
C(4)	28(1)	35(1)	23(1)	4(1)	-2(1)	7(1)
C(5)	22(1)	29(1)	24(1)	3(1)	-1(1)	5(1)
C(6)	21(1)	26(1)	23(1)	0(1)	1(1)	0(1)
C(7)	23(1)	21(1)	22(1)	-2(1)	3(1)	4(1)
C(8)	23(1)	22(1)	25(1)	0(1)	0(1)	1(1)
C(9)	22(1)	21(1)	28(1)	1(1)	1(1)	-1(1)
C(10)	25(1)	20(1)	32(1)	2(1)	-1(1)	1(1)
C(11)	34(1)	20(1)	38(1)	-2(1)	0(1)	-5(1)
C(12)	30(1)	22(1)	31(1)	-5(1)	0(1)	-2(1)
C(13)	23(1)	22(1)	27(1)	-4(1)	-1(1)	-2(1)
C(14)	20(1)	21(1)	26(1)	-2(1)	1(1)	-1(1)
C(15)	24(1)	38(1)	26(1)	8(1)	3(1)	3(1)
C(16)	26(1)	25(1)	30(1)	-5(1)	0(1)	1(1)
C(17)	41(2)	47(2)	23(1)	0(1)	-2(1)	13(1)
C(18)	32(1)	37(1)	26(1)	2(1)	-8(1)	3(1)
C(19)	22(1)	29(1)	33(1)	-2(1)	-2(1)	-2(1)
C(20)	32(1)	28(1)	27(1)	-2(1)	-3(1)	0(1)
O(1)	26(1)	25(1)	26(1)	0(1)	-1(1)	3(1)
O(2)	30(1)	23(1)	28(1)	4(1)	-1(1)	1(1)
O(3)	25(1)	29(1)	23(1)	2(1)	0(1)	-4(1)
O(4)	30(1)	22(1)	25(1)	2(1)	-3(1)	-2(1)
O(5)	32(1)	27(1)	36(1)	4(1)	7(1)	-3(1)

Table 5. Hydrogen coordinates ($\times 10^4$) and isotropic displacement parameters ($\text{\AA}^2 \times 10^{-3}$) for maimone18.

	x	y	z	U(eq)
H(1)	681	4964	9090	31
H(2A)	190	5107	8090	36
H(2B)	1984	5983	8152	36
H(3)	3153	4899	7331	35
H(5)	4902	2740	8407	30
H(8A)	6773	4473	9167	28
H(8B)	7326	3844	9782	28
H(11A)	9112	6983	10416	37
H(11B)	6872	7537	10364	37
H(12)	7340	6700	11372	33
H(14)	4465	4351	10719	27
H(15A)	5585	4909	8364	35
H(15B)	6301	4170	7789	35
H(16A)	3764	6515	10681	33
H(16B)	3886	5912	11337	33
H(17A)	3557	1989	7362	55
H(17B)	5125	2958	7249	55
H(17C)	2973	2895	6882	55
H(18A)	-373	3242	7393	48
H(18B)	-453	3419	8112	48
H(18C)	173	2284	7843	48
H(19A)	10641	4970	10964	42
H(19B)	9653	5072	10299	42
H(19C)	9492	3975	10662	42
H(20A)	7168	3817	11560	43
H(20B)	5927	4836	11800	43
H(20C)	8416	4787	11857	43
H(3A)	1066	2841	9388	39

X-Ray crystallographic Analysis of Compound 3



A colorless plate 0.060 x 0.040 x 0.030 mm in size was mounted on a Cryoloop with Paratone oil. Data were collected in a nitrogen gas stream at 100(2) K using phi and omega scans. Crystal-to-detector distance was 60 mm and exposure time was 10 seconds per frame using a scan width of 1.0°. Data collection was 100.0% complete to 67.000° in θ . A total of 27487 reflections were collected covering the indices, $-7 \leq h \leq 7$, $-16 \leq k \leq 16$, $-24 \leq l \leq 24$. 3318 reflections were found to be symmetry independent, with an R_{int} of 0.0290. Indexing and unit cell refinement indicated a primitive, orthorhombic lattice. The space group was found to be P 21 21 21 (No. 19). The data were integrated using the Bruker SAINT software program and scaled using the SADABS software program. Solution by iterative methods (SHELXT) produced a complete heavy-atom phasing model consistent with the proposed structure. All non-hydrogen atoms were refined anisotropically by full-matrix least-squares (SHELXL-2013). All hydrogen atoms were placed using a riding model. Their positions were constrained relative to their parent atom using the appropriate HFIX command in SHELXL-2013. Absolute stereochemistry was unambiguously determined to be *R* at C3, C5, C6, C12, and C14, respectively.

Table 1. Crystal data and structure refinement for compound **3**.

X-ray ID	maimone15	
Sample/notebook ID	XH_54_SPS	
Empirical formula	C20 H28 O6	
Formula weight	364.42	
Temperature	100(2) K	
Wavelength	1.54178 Å	
Crystal system	Orthorhombic	
Space group	P 21 21 21	
Unit cell dimensions	a = 6.4231(5) Å	$\alpha = 90^\circ$.
	b = 13.8311(9) Å	$\beta = 90^\circ$.
	c = 20.3077(14) Å	$\gamma = 90^\circ$.
Volume	1804.1(2) Å ³	
Z	4	
Density (calculated)	1.342 Mg/m ³	
Absorption coefficient	0.807 mm ⁻¹	
F(000)	784	
Crystal size	0.060 x 0.040 x 0.030 mm ³	
Crystal color/habit	colorless plate	
Theta range for data collection	3.867 to 68.463°.	
Index ranges	-7<=h<=7, -16<=k<=16, -24<=l<=24	
Reflections collected	27487	
Independent reflections	3318 [R(int) = 0.0290]	
Completeness to theta = 67.000°	100.0 %	
Absorption correction	Semi-empirical from equivalents	
Max. and min. transmission	0.929 and 0.846	
Refinement method	Full-matrix least-squares on F ²	
Data / restraints / parameters	3318 / 0 / 259	
Goodness-of-fit on F ²	1.104	
Final R indices [I>2sigma(I)]	R1 = 0.0714, wR2 = 0.1882	
R indices (all data)	R1 = 0.0725, wR2 = 0.1901	
Absolute structure parameter	0.02(6)	
Extinction coefficient	n/a	
Largest diff. peak and hole	0.518 and -0.243 e.Å ⁻³	

Table 2. Atomic coordinates ($\times 10^4$) and equivalent isotropic displacement parameters ($\text{\AA}^2 \times 10^3$) for maimone15. $U(\text{eq})$ is defined as one third of the trace of the orthogonalized U^{ij} tensor.

	x	y	z	$U(\text{eq})$
C(1)	-2499(9)	4845(3)	5749(2)	57(1)
C(2)	-2206(8)	5938(4)	5761(3)	62(2)
C(3)	-406(8)	6277(3)	5369(3)	56(1)
C(4)	-519(8)	5921(3)	4647(2)	46(1)
C(5)	469(6)	4970(3)	4916(2)	35(1)
C(6)	-1109(6)	4295(3)	5241(2)	34(1)
C(7)	60(6)	3430(3)	5561(2)	31(1)
C(8)	-1241(7)	2695(3)	5937(2)	37(1)
C(9)	-1707(7)	2966(3)	6657(2)	34(1)
C(10)	276(7)	3022(3)	7096(2)	40(1)
C(11)	75(8)	2582(4)	7791(2)	54(1)
C(12)	-1894(7)	2019(3)	7890(2)	44(1)
C(13)	-2384(7)	1372(3)	7277(2)	43(1)
C(14)	-3320(6)	2321(3)	6972(2)	39(1)
C(15)	1445(8)	5580(3)	5481(2)	46(1)
C(16)	-3733(7)	2666(4)	7685(2)	47(1)
C(17)	1038(10)	6436(4)	4195(3)	67(2)
C(18)	-2628(8)	5900(3)	4297(2)	50(1)
C(19)	-595(10)	840(4)	6950(3)	62(1)
C(20)	-4119(10)	642(4)	7423(3)	61(1)
O(1)	-2850(10)	3884(5)	6697(3)	38(2)
O(2)	-1556(7)	4647(3)	6426(2)	35(1)
O(1A)	-1930(30)	4011(12)	6621(8)	47(4)
O(2A)	-3725(13)	4104(6)	6188(4)	39(3)
O(3)	-2569(4)	3890(2)	4787(1)	40(1)
O(4)	-1372(5)	3407(2)	4270(2)	49(1)
O(5)	1882(4)	3328(2)	5460(1)	39(1)
O(6)	1836(5)	3400(3)	6910(2)	51(1)

Table 3. Bond lengths [Å] and angles [°] for maimone15.

C(1)-C(2)	1.524(7)	C(11)-H(11A)	0.9900
C(1)-O(2)	1.526(6)	C(11)-H(11B)	0.9900
C(1)-C(6)	1.562(5)	C(12)-C(16)	1.539(6)
C(1)-O(2A)	1.570(10)	C(12)-C(13)	1.565(6)
C(1)-H(1)	1.0000	C(12)-H(12)	1.0000
C(2)-C(3)	1.480(8)	C(13)-C(19)	1.518(7)
C(2)-H(2A)	0.9900	C(13)-C(20)	1.533(6)
C(2)-H(2B)	0.9900	C(13)-C(14)	1.571(6)
C(3)-C(15)	1.547(6)	C(14)-C(16)	1.549(6)
C(3)-C(4)	1.548(6)	C(14)-H(14)	1.0000
C(3)-H(3)	1.0000	C(15)-H(15A)	0.9900
C(4)-C(18)	1.531(6)	C(15)-H(15B)	0.9900
C(4)-C(17)	1.532(8)	C(16)-H(16A)	0.9900
C(4)-C(5)	1.558(5)	C(16)-H(16B)	0.9900
C(5)-C(6)	1.528(6)	C(17)-H(17A)	0.9800
C(5)-C(15)	1.556(5)	C(17)-H(17B)	0.9800
C(5)-H(5)	1.0000	C(17)-H(17C)	0.9800
C(6)-O(3)	1.429(5)	C(18)-H(18A)	0.9800
C(6)-C(7)	1.556(5)	C(18)-H(18B)	0.9800
C(7)-O(5)	1.196(5)	C(18)-H(18C)	0.9800
C(7)-C(8)	1.521(5)	C(19)-H(19A)	0.9800
C(8)-C(9)	1.539(5)	C(19)-H(19B)	0.9800
C(8)-H(8A)	0.9900	C(19)-H(19C)	0.9800
C(8)-H(8B)	0.9900	C(20)-H(20A)	0.9800
C(9)-O(1A)	1.455(17)	C(20)-H(20B)	0.9800
C(9)-O(1)	1.469(8)	C(20)-H(20C)	0.9800
C(9)-C(14)	1.510(6)	O(1)-O(2)	1.452(7)
C(9)-C(10)	1.557(6)	O(1A)-O(2A)	1.454(18)
C(10)-O(6)	1.192(5)	O(3)-O(4)	1.463(4)
C(10)-C(11)	1.542(6)	O(4)-H(4)	0.8400
C(11)-C(12)	1.499(7)		
C(2)-C(1)-O(2)	96.6(4)	O(2)-C(1)-C(6)	106.3(4)
C(2)-C(1)-C(6)	115.0(4)	C(2)-C(1)-O(2A)	134.5(5)

C(6)-C(1)-O(2A)	110.1(4)	C(8)-C(7)-C(6)	117.3(3)
C(2)-C(1)-H(1)	112.6	C(7)-C(8)-C(9)	114.9(3)
O(2)-C(1)-H(1)	112.6	C(7)-C(8)-H(8A)	108.5
C(6)-C(1)-H(1)	112.6	C(9)-C(8)-H(8A)	108.5
C(3)-C(2)-C(1)	113.7(4)	C(7)-C(8)-H(8B)	108.5
C(3)-C(2)-H(2A)	108.8	C(9)-C(8)-H(8B)	108.5
C(1)-C(2)-H(2A)	108.8	H(8A)-C(8)-H(8B)	107.5
C(3)-C(2)-H(2B)	108.8	O(1A)-C(9)-C(14)	122.6(7)
C(1)-C(2)-H(2B)	108.8	O(1)-C(9)-C(14)	98.3(4)
H(2A)-C(2)-H(2B)	107.7	O(1A)-C(9)-C(8)	102.4(7)
C(2)-C(3)-C(15)	108.9(4)	O(1)-C(9)-C(8)	111.1(4)
C(2)-C(3)-C(4)	111.8(4)	C(14)-C(9)-C(8)	113.1(3)
C(15)-C(3)-C(4)	88.7(3)	O(1A)-C(9)-C(10)	93.5(7)
C(2)-C(3)-H(3)	114.9	O(1)-C(9)-C(10)	109.5(4)
C(15)-C(3)-H(3)	114.9	C(14)-C(9)-C(10)	110.4(3)
C(4)-C(3)-H(3)	114.9	C(8)-C(9)-C(10)	113.4(3)
C(18)-C(4)-C(17)	107.9(4)	O(6)-C(10)-C(11)	122.2(4)
C(18)-C(4)-C(3)	119.2(4)	O(6)-C(10)-C(9)	121.9(4)
C(17)-C(4)-C(3)	112.8(4)	C(11)-C(10)-C(9)	115.9(4)
C(18)-C(4)-C(5)	120.4(3)	C(12)-C(11)-C(10)	113.5(4)
C(17)-C(4)-C(5)	109.6(4)	C(12)-C(11)-H(11A)	108.9
C(3)-C(4)-C(5)	85.3(3)	C(10)-C(11)-H(11A)	108.9
C(6)-C(5)-C(15)	106.3(3)	C(12)-C(11)-H(11B)	108.9
C(6)-C(5)-C(4)	113.4(3)	C(10)-C(11)-H(11B)	108.9
C(15)-C(5)-C(4)	88.0(3)	H(11A)-C(11)-H(11B)	107.7
C(6)-C(5)-H(5)	115.3	C(11)-C(12)-C(16)	108.0(4)
C(15)-C(5)-H(5)	115.3	C(11)-C(12)-C(13)	111.1(4)
C(4)-C(5)-H(5)	115.3	C(16)-C(12)-C(13)	87.9(3)
O(3)-C(6)-C(5)	113.3(3)	C(11)-C(12)-H(12)	115.5
O(3)-C(6)-C(7)	106.6(3)	C(16)-C(12)-H(12)	115.5
C(5)-C(6)-C(7)	109.3(3)	C(13)-C(12)-H(12)	115.5
O(3)-C(6)-C(1)	104.0(4)	C(19)-C(13)-C(20)	108.4(4)
C(5)-C(6)-C(1)	111.5(3)	C(19)-C(13)-C(12)	118.3(4)
C(7)-C(6)-C(1)	111.9(3)	C(20)-C(13)-C(12)	111.7(4)
O(5)-C(7)-C(8)	123.0(3)	C(19)-C(13)-C(14)	121.4(3)
O(5)-C(7)-C(6)	119.5(3)	C(20)-C(13)-C(14)	110.4(4)

C(12)-C(13)-C(14)	85.0(3)	C(4)-C(18)-H(18A)	109.5
C(9)-C(14)-C(16)	109.4(4)	C(4)-C(18)-H(18B)	109.5
C(9)-C(14)-C(13)	113.5(3)	H(18A)-C(18)-H(18B)	109.5
C(16)-C(14)-C(13)	87.3(3)	C(4)-C(18)-H(18C)	109.5
C(9)-C(14)-H(14)	114.6	H(18A)-C(18)-H(18C)	109.5
C(16)-C(14)-H(14)	114.6	H(18B)-C(18)-H(18C)	109.5
C(13)-C(14)-H(14)	114.6	C(13)-C(19)-H(19A)	109.5
C(3)-C(15)-C(5)	85.4(3)	C(13)-C(19)-H(19B)	109.5
C(3)-C(15)-H(15A)	114.4	H(19A)-C(19)-H(19B)	109.5
C(5)-C(15)-H(15A)	114.4	C(13)-C(19)-H(19C)	109.5
C(3)-C(15)-H(15B)	114.4	H(19A)-C(19)-H(19C)	109.5
C(5)-C(15)-H(15B)	114.4	H(19B)-C(19)-H(19C)	109.5
H(15A)-C(15)-H(15B)	111.5	C(13)-C(20)-H(20A)	109.5
C(12)-C(16)-C(14)	86.7(3)	C(13)-C(20)-H(20B)	109.5
C(12)-C(16)-H(16A)	114.2	H(20A)-C(20)-H(20B)	109.5
C(14)-C(16)-H(16A)	114.2	C(13)-C(20)-H(20C)	109.5
C(12)-C(16)-H(16B)	114.2	H(20A)-C(20)-H(20C)	109.5
C(14)-C(16)-H(16B)	114.2	H(20B)-C(20)-H(20C)	109.5
H(16A)-C(16)-H(16B)	111.4	O(2)-O(1)-C(9)	108.8(5)
C(4)-C(17)-H(17A)	109.5	O(1)-O(2)-C(1)	104.1(4)
C(4)-C(17)-H(17B)	109.5	C(9)-O(1A)-O(2A)	101.3(10)
H(17A)-C(17)-H(17B)	109.5	O(1A)-O(2A)-C(1)	90.3(8)
C(4)-C(17)-H(17C)	109.5	C(6)-O(3)-O(4)	107.3(3)
H(17A)-C(17)-H(17C)	109.5	O(3)-O(4)-H(4)	109.5
H(17B)-C(17)-H(17C)	109.5		

Symmetry transformations used to generate equivalent atoms:

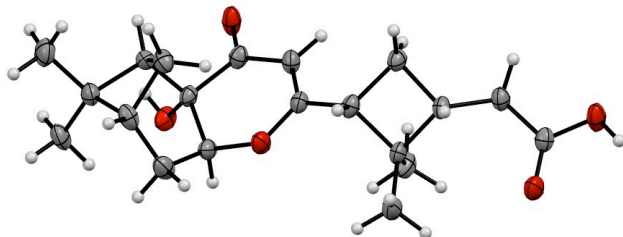
Table 4. Anisotropic displacement parameters ($\text{\AA}^2 \times 10^3$) for maimone15. The anisotropic displacement factor exponent takes the form: $-2\pi^2 [h^2 a^{*2} U^{11} + \dots + 2 h k a^* b^* U^{12}]$

	U ¹¹	U ²²	U ³³	U ²³	U ¹³	U ¹²
C(1)	77(3)	45(2)	49(2)	12(2)	21(2)	32(2)
C(2)	61(3)	59(3)	66(3)	-37(2)	-27(2)	30(2)
C(3)	64(3)	32(2)	72(3)	-19(2)	-33(3)	13(2)
C(4)	59(3)	25(2)	54(2)	2(2)	-22(2)	-4(2)
C(5)	44(2)	26(2)	35(2)	-2(1)	-6(2)	0(2)
C(6)	41(2)	30(2)	32(2)	0(1)	2(2)	4(2)
C(7)	36(2)	28(2)	30(2)	-5(1)	1(1)	5(1)
C(8)	45(2)	32(2)	33(2)	-2(1)	2(2)	0(2)
C(9)	42(2)	29(2)	31(2)	-1(1)	-2(2)	6(2)
C(10)	44(2)	38(2)	39(2)	0(2)	-4(2)	-1(2)
C(11)	51(3)	73(3)	40(2)	11(2)	-12(2)	-8(2)
C(12)	47(2)	54(2)	32(2)	10(2)	1(2)	6(2)
C(13)	49(2)	41(2)	40(2)	5(2)	7(2)	-1(2)
C(14)	35(2)	50(2)	33(2)	-3(2)	0(2)	5(2)
C(15)	56(3)	35(2)	47(2)	-10(2)	-21(2)	8(2)
C(16)	50(2)	56(2)	34(2)	-2(2)	4(2)	8(2)
C(17)	77(4)	40(2)	84(4)	26(2)	-32(3)	-21(2)
C(18)	60(3)	38(2)	53(2)	6(2)	-25(2)	-1(2)
C(19)	83(4)	40(2)	63(3)	16(2)	24(3)	20(2)
C(20)	74(3)	59(3)	51(3)	3(2)	10(2)	-22(3)
O(1)	51(4)	30(3)	33(2)	3(2)	3(3)	11(3)
O(2)	41(2)	31(3)	33(2)	-4(2)	-6(2)	-1(2)
O(1A)	65(10)	37(7)	38(6)	-5(5)	-8(7)	1(8)
O(2A)	35(5)	39(5)	42(5)	-6(4)	0(4)	2(3)
O(3)	37(1)	42(1)	41(1)	7(1)	-1(1)	-4(1)
O(4)	58(2)	50(2)	38(1)	-6(1)	8(1)	-22(1)
O(5)	40(2)	36(1)	41(1)	3(1)	7(1)	9(1)
O(6)	45(2)	59(2)	48(2)	10(1)	-3(1)	-9(2)

Table 5. Hydrogen coordinates ($\times 10^4$) and isotropic displacement parameters ($\text{\AA}^2 \times 10^{-3}$) for maimone15.

	x	y	z	U(eq)
H(1)	-3997	4652	5722	69
H(2A)	-3486	6248	5590	74
H(2B)	-2022	6149	6223	74
H(3)	-65	6978	5422	67
H(5)	1489	4649	4615	42
H(8A)	-503	2067	5931	44
H(8B)	-2579	2607	5702	44
H(11A)	1279	2151	7871	65
H(11B)	133	3110	8120	65
H(12)	-2037	1694	8328	53
H(14)	-4604	2220	6702	47
H(15A)	1447	5257	5916	55
H(15B)	2825	5860	5376	55
H(16A)	-3494	3366	7756	56
H(16B)	-5093	2460	7867	56
H(17A)	1154	6082	3779	100
H(17B)	2403	6461	4410	100
H(17C)	552	7095	4108	100
H(18A)	-3057	6561	4190	76
H(18B)	-3669	5602	4585	76
H(18C)	-2510	5522	3890	76
H(19A)	-128	311	7235	93
H(19B)	561	1290	6875	93
H(19C)	-1061	576	6527	93
H(20A)	-4630	367	7009	92
H(20B)	-5265	968	7651	92
H(20C)	-3572	123	7703	92
H(4)	-1538	2806	4299	73

X-Ray crystallographic Analysis of Compound 37



A colorless plate 0.050 x 0.040 x 0.020 mm in size was mounted on a Cryoloop with Paratone oil. Data were collected in a nitrogen gas stream at 100(2) K using phi and omega scans. Crystal-to-detector distance was 60 mm and exposure time was 10 seconds per frame using a scan width of 1.0°. Data collection was 100.0% complete to 67.000° in θ . A total of 28889 reflections were collected covering the indices, $-8 \leq h \leq 8$, $-10 \leq k \leq 11$, $-33 \leq l \leq 33$. 3424 reflections were found to be symmetry independent, with an R_{int} of 0.0362. Indexing and unit cell refinement indicated a primitive, orthorhombic lattice. The space group was found to be P 21 21 21 (No. 19). The data were integrated using the Bruker SAINT software program and scaled using the SADABS software program. Solution by iterative methods (SHELXT) produced a complete heavy-atom phasing model consistent with the proposed structure. All non-hydrogen atoms were refined anisotropically by full-matrix least-squares (SHELXL-2014). All hydrogen atoms were placed using a riding model. Their positions were constrained relative to their parent atom using the appropriate HFIX command in SHELXL-2014. Absolute stereochemistry was unambiguously determined to be *R* at C3, C5, C13, and C15, and *S* at C1 and C6, respectively.

Table 1. Crystal data and structure refinement for compound **37**.

X-ray ID	maimone24	
Sample/notebook ID	XH-211-3	
Empirical formula	C ₂₀ H ₂₈ O ₅	
Formula weight	348.42	
Temperature	100(2) K	
Wavelength	1.54178 Å	
Crystal system	Orthorhombic	
Space group	P 21 21 21	
Unit cell dimensions	a = 6.8100(3) Å	α = 90°.
	b = 9.9666(4) Å	β = 90°.
	c = 27.5837(12) Å	γ = 90°.
Volume	1872.18(14) Å ³	
Z	4	
Density (calculated)	1.236 Mg/m ³	
Absorption coefficient	0.713 mm ⁻¹	
F(000)	752	
Crystal size	0.050 x 0.040 x 0.020 mm ³	
Crystal color/habit	colorless plate	
Theta range for data collection	3.204 to 68.390°.	
Index ranges	-8 ≤ h ≤ 8, -10 ≤ k ≤ 11, -33 ≤ l ≤ 33	
Reflections collected	28889	
Independent reflections	3424 [R(int) = 0.0362]	
Completeness to theta = 67.000°	100.0 %	
Absorption correction	Semi-empirical from equivalents	
Max. and min. transmission	0.929 and 0.896	
Refinement method	Full-matrix least-squares on F ²	
Data / restraints / parameters	3424 / 0 / 232	
Goodness-of-fit on F ²	1.037	
Final R indices [I > 2σ(I)]	R1 = 0.0364, wR2 = 0.0951	
R indices (all data)	R1 = 0.0377, wR2 = 0.0963	
Absolute structure parameter	0.01(5)	
Extinction coefficient	n/a	
Largest diff. peak and hole	0.260 and -0.139 e.Å ⁻³	

Table 2. Atomic coordinates ($\times 10^4$) and equivalent isotropic displacement parameters ($\text{\AA}^2 \times 10^3$) for maimone24. $U(\text{eq})$ is defined as one third of the trace of the orthogonalized U^{ij} tensor.

	x	y	z	$U(\text{eq})$
C(1)	4048(3)	3660(2)	978(1)	26(1)
C(2)	3849(4)	3972(3)	435(1)	33(1)
C(3)	1713(4)	4016(2)	272(1)	30(1)
C(4)	668(4)	5235(2)	520(1)	27(1)
C(5)	417(3)	4259(2)	964(1)	23(1)
C(6)	2259(3)	4144(2)	1285(1)	23(1)
C(7)	1787(3)	3201(2)	1706(1)	25(1)
C(8)	2528(3)	1868(2)	1701(1)	26(1)
C(9)	3746(3)	1433(2)	1348(1)	24(1)
C(10)	453(4)	3079(2)	594(1)	28(1)
C(11)	-1337(4)	5516(3)	290(1)	39(1)
C(12)	1750(4)	6559(2)	555(1)	34(1)
C(13)	4417(3)	20(2)	1289(1)	25(1)
C(14)	3615(3)	-1093(2)	1618(1)	27(1)
C(15)	5643(3)	-1785(2)	1582(1)	23(1)
C(16)	6563(3)	-401(2)	1446(1)	25(1)
C(17)	7293(4)	382(3)	1885(1)	34(1)
C(18)	8084(4)	-389(3)	1044(1)	36(1)
C(19)	6275(4)	-2602(2)	2019(1)	27(1)
C(20)	8049(4)	-3452(2)	1933(1)	26(1)
O(1)	4437(2)	2210(2)	992(1)	29(1)
O(2)	2852(2)	5388(2)	1486(1)	29(1)
O(3)	706(3)	3606(2)	2036(1)	35(1)
O(4)	9351(3)	-3181(2)	1648(1)	35(1)
O(5)	8050(3)	-4559(2)	2198(1)	36(1)

Table 3. Bond lengths [Å] and angles [°] for maimone24.

C(1)-O(1)	1.470(3)	C(11)-H(11C)	0.9800
C(1)-C(2)	1.536(3)	C(12)-H(12A)	0.9800
C(1)-C(6)	1.559(3)	C(12)-H(12B)	0.9800
C(1)-H(1)	1.0000	C(12)-H(12C)	0.9800
C(2)-C(3)	1.523(4)	C(13)-C(14)	1.533(3)
C(2)-H(2A)	0.9900	C(13)-C(16)	1.581(3)
C(2)-H(2B)	0.9900	C(13)-H(13)	1.0000
C(3)-C(10)	1.548(3)	C(14)-C(15)	1.547(3)
C(3)-C(4)	1.564(3)	C(14)-H(14A)	0.9900
C(3)-H(3)	1.0000	C(14)-H(14B)	0.9900
C(4)-C(12)	1.514(3)	C(15)-C(19)	1.518(3)
C(4)-C(11)	1.531(4)	C(15)-C(16)	1.560(3)
C(4)-C(5)	1.574(3)	C(15)-H(15)	1.0000
C(5)-C(6)	1.539(3)	C(16)-C(18)	1.518(3)
C(5)-C(10)	1.558(3)	C(16)-C(17)	1.525(3)
C(5)-H(5)	1.0000	C(17)-H(17A)	0.9800
C(6)-O(2)	1.417(3)	C(17)-H(17B)	0.9800
C(6)-C(7)	1.528(3)	C(17)-H(17C)	0.9800
C(7)-O(3)	1.239(3)	C(18)-H(18A)	0.9800
C(7)-C(8)	1.421(3)	C(18)-H(18B)	0.9800
C(8)-C(9)	1.351(3)	C(18)-H(18C)	0.9800
C(8)-H(8)	0.9500	C(19)-C(20)	1.495(3)
C(9)-O(1)	1.337(3)	C(19)-H(19A)	0.9900
C(9)-C(13)	1.489(3)	C(19)-H(19B)	0.9900
C(10)-H(10A)	0.9900	C(20)-O(4)	1.215(3)
C(10)-H(10B)	0.9900	C(20)-O(5)	1.323(3)
C(11)-H(11A)	0.9800	O(2)-H(2)	0.8400
C(11)-H(11B)	0.9800	O(5)-H(5A)	0.8400
O(1)-C(1)-C(2)	103.80(19)	C(6)-C(1)-H(1)	107.9
O(1)-C(1)-C(6)	115.56(18)	C(3)-C(2)-C(1)	112.18(19)
C(2)-C(1)-C(6)	113.44(19)	C(3)-C(2)-H(2A)	109.2
O(1)-C(1)-H(1)	107.9	C(1)-C(2)-H(2A)	109.2
C(2)-C(1)-H(1)	107.9	C(3)-C(2)-H(2B)	109.2

C(1)-C(2)-H(2B)	109.2	C(3)-C(10)-H(10A)	114.3
H(2A)-C(2)-H(2B)	107.9	C(5)-C(10)-H(10A)	114.3
C(2)-C(3)-C(10)	110.03(19)	C(3)-C(10)-H(10B)	114.3
C(2)-C(3)-C(4)	109.18(19)	C(5)-C(10)-H(10B)	114.3
C(10)-C(3)-C(4)	88.07(18)	H(10A)-C(10)-H(10B)	111.5
C(2)-C(3)-H(3)	115.5	C(4)-C(11)-H(11A)	109.5
C(10)-C(3)-H(3)	115.5	C(4)-C(11)-H(11B)	109.5
C(4)-C(3)-H(3)	115.5	H(11A)-C(11)-H(11B)	109.5
C(12)-C(4)-C(11)	107.5(2)	C(4)-C(11)-H(11C)	109.5
C(12)-C(4)-C(3)	118.9(2)	H(11A)-C(11)-H(11C)	109.5
C(11)-C(4)-C(3)	111.6(2)	H(11B)-C(11)-H(11C)	109.5
C(12)-C(4)-C(5)	122.8(2)	C(4)-C(12)-H(12A)	109.5
C(11)-C(4)-C(5)	109.8(2)	C(4)-C(12)-H(12B)	109.5
C(3)-C(4)-C(5)	84.82(17)	H(12A)-C(12)-H(12B)	109.5
C(6)-C(5)-C(10)	107.90(18)	C(4)-C(12)-H(12C)	109.5
C(6)-C(5)-C(4)	113.91(18)	H(12A)-C(12)-H(12C)	109.5
C(10)-C(5)-C(4)	87.36(16)	H(12B)-C(12)-H(12C)	109.5
C(6)-C(5)-H(5)	114.8	C(9)-C(13)-C(14)	120.74(19)
C(10)-C(5)-H(5)	114.8	C(9)-C(13)-C(16)	120.30(19)
C(4)-C(5)-H(5)	114.8	C(14)-C(13)-C(16)	88.60(16)
O(2)-C(6)-C(7)	107.54(18)	C(9)-C(13)-H(13)	108.5
O(2)-C(6)-C(5)	113.05(17)	C(14)-C(13)-H(13)	108.5
C(7)-C(6)-C(5)	108.13(18)	C(16)-C(13)-H(13)	108.5
O(2)-C(6)-C(1)	105.07(18)	C(13)-C(14)-C(15)	88.07(17)
C(7)-C(6)-C(1)	112.72(18)	C(13)-C(14)-H(14A)	114.0
C(5)-C(6)-C(1)	110.37(17)	C(15)-C(14)-H(14A)	114.0
O(3)-C(7)-C(8)	121.5(2)	C(13)-C(14)-H(14B)	114.0
O(3)-C(7)-C(6)	118.9(2)	C(15)-C(14)-H(14B)	114.0
C(8)-C(7)-C(6)	119.53(19)	H(14A)-C(14)-H(14B)	111.2
C(9)-C(8)-C(7)	121.7(2)	C(19)-C(15)-C(14)	116.15(19)
C(9)-C(8)-H(8)	119.1	C(19)-C(15)-C(16)	123.41(19)
C(7)-C(8)-H(8)	119.1	C(14)-C(15)-C(16)	88.87(16)
O(1)-C(9)-C(8)	124.0(2)	C(19)-C(15)-H(15)	108.9
O(1)-C(9)-C(13)	111.12(19)	C(14)-C(15)-H(15)	108.9
C(8)-C(9)-C(13)	124.8(2)	C(16)-C(15)-H(15)	108.9
C(3)-C(10)-C(5)	85.93(17)	C(18)-C(16)-C(17)	110.8(2)

C(18)-C(16)-C(15)	117.11(19)	H(18A)-C(18)-H(18C)	109.5
C(17)-C(16)-C(15)	113.15(19)	H(18B)-C(18)-H(18C)	109.5
C(18)-C(16)-C(13)	115.4(2)	C(20)-C(19)-C(15)	113.99(19)
C(17)-C(16)-C(13)	112.51(19)	C(20)-C(19)-H(19A)	108.8
C(15)-C(16)-C(13)	85.91(16)	C(15)-C(19)-H(19A)	108.8
C(16)-C(17)-H(17A)	109.5	C(20)-C(19)-H(19B)	108.8
C(16)-C(17)-H(17B)	109.5	C(15)-C(19)-H(19B)	108.8
H(17A)-C(17)-H(17B)	109.5	H(19A)-C(19)-H(19B)	107.6
C(16)-C(17)-H(17C)	109.5	O(4)-C(20)-O(5)	122.8(2)
H(17A)-C(17)-H(17C)	109.5	O(4)-C(20)-C(19)	124.5(2)
H(17B)-C(17)-H(17C)	109.5	O(5)-C(20)-C(19)	112.7(2)
C(16)-C(18)-H(18A)	109.5	C(9)-O(1)-C(1)	121.64(18)
C(16)-C(18)-H(18B)	109.5	C(6)-O(2)-H(2)	109.5
H(18A)-C(18)-H(18B)	109.5	C(20)-O(5)-H(5A)	109.5
C(16)-C(18)-H(18C)	109.5		

Symmetry transformations used to generate equivalent atoms:

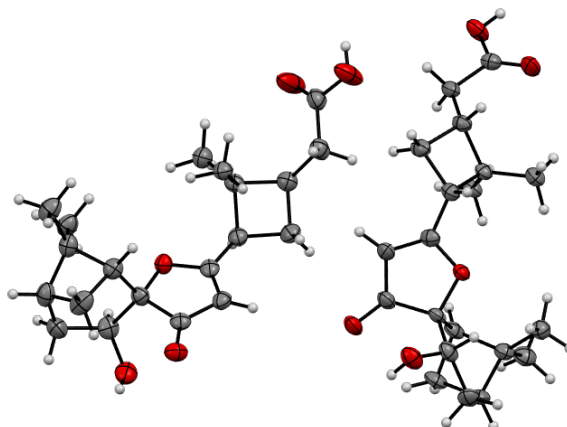
Table 4. Anisotropic displacement parameters ($\text{\AA}^2 \times 10^3$) for maimone24. The anisotropic displacement factor exponent takes the form: $-2\pi^2 [h^2 a^{*2} U^{11} + \dots + 2 h k a^* b^* U^{12}]$

	U ¹¹	U ²²	U ³³	U ²³	U ¹³	U ¹²
C(1)	24(1)	18(1)	36(1)	1(1)	3(1)	2(1)
C(2)	39(1)	24(1)	35(1)	2(1)	14(1)	5(1)
C(3)	44(1)	23(1)	22(1)	1(1)	2(1)	-1(1)
C(4)	32(1)	24(1)	25(1)	5(1)	0(1)	3(1)
C(5)	22(1)	21(1)	25(1)	3(1)	2(1)	0(1)
C(6)	23(1)	17(1)	29(1)	-1(1)	-1(1)	3(1)
C(7)	28(1)	26(1)	22(1)	-1(1)	-1(1)	6(1)
C(8)	31(1)	22(1)	25(1)	3(1)	-2(1)	6(1)
C(9)	24(1)	21(1)	27(1)	2(1)	-3(1)	4(1)
C(10)	34(1)	24(1)	27(1)	2(1)	-4(1)	-4(1)
C(11)	41(1)	42(2)	34(1)	10(1)	-7(1)	9(1)
C(12)	47(2)	21(1)	34(1)	6(1)	7(1)	3(1)
C(13)	27(1)	22(1)	26(1)	-3(1)	-2(1)	6(1)
C(14)	26(1)	20(1)	36(1)	0(1)	-2(1)	3(1)
C(15)	27(1)	19(1)	25(1)	-1(1)	-3(1)	4(1)
C(16)	24(1)	21(1)	29(1)	2(1)	-1(1)	6(1)
C(17)	32(1)	24(1)	45(1)	-3(1)	-9(1)	1(1)
C(18)	33(1)	31(1)	44(1)	11(1)	9(1)	10(1)
C(19)	32(1)	22(1)	26(1)	2(1)	1(1)	5(1)
C(20)	31(1)	24(1)	23(1)	-1(1)	-3(1)	5(1)
O(1)	32(1)	21(1)	35(1)	1(1)	8(1)	8(1)
O(2)	30(1)	21(1)	38(1)	-7(1)	-2(1)	3(1)
O(3)	49(1)	30(1)	26(1)	4(1)	7(1)	17(1)
O(4)	34(1)	27(1)	43(1)	6(1)	7(1)	10(1)
O(5)	48(1)	29(1)	31(1)	6(1)	9(1)	17(1)

Table 5. Hydrogen coordinates ($\times 10^4$) and isotropic displacement parameters ($\text{\AA}^2 \times 10^{-3}$) for maimone24.

	x	y	z	U(eq)
H(1)	5244	4132	1101	31
H(2A)	4474	4848	366	39
H(2B)	4553	3277	247	39
H(3)	1494	3929	-85	35
H(5)	-845	4363	1146	27
H(8)	2157	1268	1952	31
H(10A)	1150	2268	710	34
H(10B)	-846	2851	456	34
H(11A)	-2121	6072	510	59
H(11B)	-2020	4666	231	59
H(11C)	-1154	5990	-18	59
H(12A)	995	7181	757	51
H(12B)	1910	6940	230	51
H(12C)	3045	6411	701	51
H(13)	4212	-252	944	30
H(14A)	2529	-1616	1472	33
H(14B)	3273	-788	1949	33
H(15)	5657	-2376	1289	28
H(17A)	7606	1304	1788	51
H(17B)	8473	-50	2016	51
H(17C)	6268	397	2135	51
H(18A)	8288	534	932	54
H(18B)	7619	-941	773	54
H(18C)	9325	-754	1166	54
H(19A)	6551	-1982	2291	32
H(19B)	5173	-3188	2118	32
H(2)	1857	5817	1578	44
H(5A)	9021	-5034	2122	54

X-Ray crystallographic Analysis of 38



A colorless block 0.040 x 0.030 x 0.030 mm in size was mounted on a Cryoloop with Paratone oil. Data were collected in a nitrogen gas stream at 100(2) K using phi and omega scans. Crystal-to-detector distance was 60 mm and exposure time was 10 seconds per frame using a scan width of 1.0°. Data collection was 98.4% complete to 67.000° in θ . A total of 47377 reflections were collected covering the indices, $-8 \leq h \leq 7$, $-11 \leq k \leq 11$, $-64 \leq l \leq 65$. 6367 reflections were found to be symmetry independent, with an R_{int} of 0.0490. Indexing and unit cell refinement indicated a primitive, orthorhombic lattice. The space group was found to be P 21 21 21 (No. 19). The data were integrated using the Bruker SAINT software program and scaled using the SADABS software program. Solution by iterative methods (SHELXT) produced a complete heavy-atom phasing model consistent with the proposed structure. All non-hydrogen atoms were refined anisotropically by full-matrix least-squares (SHELXL-2013). All hydrogen atoms were placed using a riding model. Their positions were constrained relative to their parent atom using the appropriate HFIX command in SHELXL-2013. Absolute stereochemistry was unambiguously determined to be *R* at C2, C4, C13, C15, C22, C24, C33, and C35, and *S* at C1, C6, C21, and C26, respectively.

Table 1. Crystal data and structure refinement for compound **38**.

X-ray ID	maimone23	
Sample/notebook ID	XH-194-2	
Empirical formula	C ₂₀ H ₂₈ O ₅	
Formula weight	348.42	
Temperature	100(2) K	
Wavelength	1.54178 Å	
Crystal system	Orthorhombic	
Space group	P 21 21 21	
Unit cell dimensions	a = 6.7606(4) Å	α = 90°.
	b = 10.0156(5) Å	β = 90°.
	c = 54.297(3) Å	γ = 90°.
Volume	3676.5(3) Å ³	
Z	8	
Density (calculated)	1.259 Mg/m ³	
Absorption coefficient	0.726 mm ⁻¹	
F(000)	1504	
Crystal size	0.040 x 0.030 x 0.030 mm ³	
Crystal color/habit	colorless block	
Theta range for data collection	3.256 to 68.283°.	
Index ranges	-8 ≤ h ≤ 7, -11 ≤ k ≤ 11, -64 ≤ l ≤ 65	
Reflections collected	47377	
Independent reflections	6367 [R(int) = 0.0490]	
Completeness to theta = 67.000°	98.4 %	
Absorption correction	Semi-empirical from equivalents	
Max. and min. transmission	0.929 and 0.774	
Refinement method	Full-matrix least-squares on F ²	
Data / restraints / parameters	6367 / 0 / 463	
Goodness-of-fit on F ²	1.179	
Final R indices [I > 2σ(I)]	R1 = 0.0571, wR2 = 0.1278	
R indices (all data)	R1 = 0.0576, wR2 = 0.1281	
Absolute structure parameter	0.05(7)	
Extinction coefficient	n/a	
Largest diff. peak and hole	0.336 and -0.186 e.Å ⁻³	

Table 2. Atomic coordinates ($\times 10^4$) and equivalent isotropic displacement parameters ($\text{\AA}^2 \times 10^3$) for maimone23. $U(\text{eq})$ is defined as one third of the trace of the orthogonalized U^{ij} tensor.

	x	y	z	$U(\text{eq})$
C(1)	-2499(7)	14339(4)	3104(1)	31(1)
C(2)	-1623(6)	13796(5)	2866(1)	33(1)
C(3)	-2844(7)	14162(5)	2632(1)	35(1)
C(4)	-1721(7)	15527(5)	2646(1)	40(1)
C(5)	-2622(8)	16477(5)	2831(1)	44(1)
C(6)	-3159(7)	15834(4)	3080(1)	37(1)
C(7)	-8(7)	14780(5)	2777(1)	44(1)
C(8)	-2197(8)	13311(5)	2414(1)	46(1)
C(9)	-5072(7)	14182(5)	2639(1)	42(1)
C(10)	-1076(7)	14051(4)	3318(1)	31(1)
C(11)	-2065(7)	13108(4)	3473(1)	34(1)
C(12)	-3866(7)	12886(4)	3376(1)	31(1)
C(13)	-5513(7)	12024(4)	3461(1)	33(1)
C(14)	-5177(8)	11053(4)	3676(1)	39(1)
C(15)	-6559(7)	10058(4)	3545(1)	34(1)
C(16)	-6163(7)	10799(4)	3298(1)	32(1)
C(17)	-4450(7)	10218(4)	3151(1)	35(1)
C(18)	-7946(7)	11050(5)	3133(1)	39(1)
C(19)	-6089(7)	8587(4)	3577(1)	39(1)
C(20)	-7514(8)	7655(4)	3454(1)	40(1)
C(21)	355(6)	9649(4)	4413(1)	27(1)
C(22)	-1212(7)	10176(4)	4589(1)	32(1)
C(23)	-713(7)	9868(4)	4865(1)	31(1)
C(24)	658(8)	11111(4)	4850(1)	39(1)
C(25)	2634(7)	10796(5)	4737(1)	39(1)
C(26)	2523(7)	9903(4)	4506(1)	35(1)
C(27)	-695(7)	11655(4)	4644(1)	36(1)
C(28)	-2483(8)	10115(4)	5032(1)	41(1)
C(29)	144(7)	8511(4)	4935(1)	34(1)
C(30)	-50(7)	10109(4)	4149(1)	32(1)
C(31)	-592(7)	8945(4)	4013(1)	33(1)

C(32)	-473(6)	7888(4)	4167(1)	29(1)
C(33)	-922(7)	6460(4)	4130(1)	29(1)
C(34)	-1877(7)	5978(4)	3889(1)	37(1)
C(35)	-3147(7)	5009(4)	4041(1)	31(1)
C(36)	-2733(6)	5861(4)	4276(1)	27(1)
C(37)	-2159(7)	5090(4)	4507(1)	36(1)
C(38)	-4311(6)	6885(4)	4331(1)	28(1)
C(39)	-5238(7)	4790(4)	3954(1)	35(1)
C(40)	-6387(7)	3726(4)	4088(1)	33(1)
O(1)	-2556(6)	16622(3)	3282(1)	46(1)
O(2)	-4233(4)	13555(3)	3167(1)	32(1)
O(3)	594(5)	14519(3)	3338(1)	38(1)
O(4)	-8881(7)	7954(4)	3332(1)	82(2)
O(5)	-7096(6)	6400(3)	3505(1)	61(1)
O(6)	3798(5)	10311(3)	4317(1)	41(1)
O(7)	89(4)	8195(2)	4397(1)	28(1)
O(8)	0(5)	11274(3)	4076(1)	40(1)
O(9)	-5782(5)	3105(3)	4261(1)	48(1)
O(10)	-8156(5)	3535(3)	3987(1)	44(1)

Table 3. Bond lengths [Å] and angles [°] for maimone23.

C(1)-O(2)	1.451(5)	C(13)-H(13)	1.0000
C(1)-C(2)	1.523(6)	C(14)-C(15)	1.541(6)
C(1)-C(10)	1.533(6)	C(14)-H(14A)	0.9900
C(1)-C(6)	1.568(6)	C(14)-H(14B)	0.9900
C(2)-C(7)	1.550(7)	C(15)-C(19)	1.517(6)
C(2)-C(3)	1.559(6)	C(15)-C(16)	1.556(6)
C(2)-H(2)	1.0000	C(15)-H(15)	1.0000
C(3)-C(9)	1.507(7)	C(16)-C(18)	1.522(6)
C(3)-C(8)	1.523(6)	C(16)-C(17)	1.522(6)
C(3)-C(4)	1.565(7)	C(17)-H(17A)	0.9800
C(4)-C(5)	1.515(7)	C(17)-H(17B)	0.9800
C(4)-C(7)	1.551(7)	C(17)-H(17C)	0.9800
C(4)-H(4)	1.0000	C(18)-H(18A)	0.9800
C(5)-C(6)	1.541(6)	C(18)-H(18B)	0.9800
C(5)-H(5A)	0.9900	C(18)-H(18C)	0.9800
C(5)-H(5B)	0.9900	C(19)-C(20)	1.498(7)
C(6)-O(1)	1.411(5)	C(19)-H(19A)	0.9900
C(6)-H(6)	1.0000	C(19)-H(19B)	0.9900
C(7)-H(7A)	0.9900	C(20)-O(4)	1.177(6)
C(7)-H(7B)	0.9900	C(20)-O(5)	1.318(5)
C(8)-H(8A)	0.9800	C(21)-O(7)	1.469(4)
C(8)-H(8B)	0.9800	C(21)-C(22)	1.522(6)
C(8)-H(8C)	0.9800	C(21)-C(30)	1.530(5)
C(9)-H(9A)	0.9800	C(21)-C(26)	1.571(6)
C(9)-H(9B)	0.9800	C(22)-C(27)	1.552(5)
C(9)-H(9C)	0.9800	C(22)-C(23)	1.567(6)
C(10)-O(3)	1.228(5)	C(22)-H(22)	1.0000
C(10)-C(11)	1.430(6)	C(23)-C(28)	1.522(6)
C(11)-C(12)	1.343(6)	C(23)-C(29)	1.526(6)
C(11)-H(11)	0.9500	C(23)-C(24)	1.555(6)
C(12)-O(2)	1.344(5)	C(24)-C(25)	1.503(7)
C(12)-C(13)	1.482(6)	C(24)-C(27)	1.542(6)
C(13)-C(14)	1.538(6)	C(24)-H(24)	1.0000
C(13)-C(16)	1.575(6)	C(25)-C(26)	1.544(6)

C(25)-H(25A)	0.9900	C(34)-H(34A)	0.9900
C(25)-H(25B)	0.9900	C(34)-H(34B)	0.9900
C(26)-O(6)	1.401(5)	C(35)-C(39)	1.508(6)
C(26)-H(26)	1.0000	C(35)-C(36)	1.560(5)
C(27)-H(27A)	0.9900	C(35)-H(35)	1.0000
C(27)-H(27B)	0.9900	C(36)-C(38)	1.509(6)
C(28)-H(28A)	0.9800	C(36)-C(37)	1.522(5)
C(28)-H(28B)	0.9800	C(37)-H(37A)	0.9800
C(28)-H(28C)	0.9800	C(37)-H(37B)	0.9800
C(29)-H(29A)	0.9800	C(37)-H(37C)	0.9800
C(29)-H(29B)	0.9800	C(38)-H(38A)	0.9800
C(29)-H(29C)	0.9800	C(38)-H(38B)	0.9800
C(30)-O(8)	1.232(5)	C(38)-H(38C)	0.9800
C(30)-C(31)	1.428(6)	C(39)-C(40)	1.505(6)
C(31)-C(32)	1.351(6)	C(39)-H(39A)	0.9900
C(31)-H(31)	0.9500	C(39)-H(39B)	0.9900
C(32)-O(7)	1.341(5)	C(40)-O(9)	1.199(5)
C(32)-C(33)	1.476(5)	C(40)-O(10)	1.328(5)
C(33)-C(34)	1.536(6)	O(1)-H(1)	0.8400
C(33)-C(36)	1.578(6)	O(5)-H(5)	0.8400
C(33)-H(33)	1.0000	O(6)-H(6A)	0.8400
C(34)-C(35)	1.536(6)	O(10)-H(10)	0.8400
O(2)-C(1)-C(2)	108.6(3)	C(9)-C(3)-C(2)	120.9(4)
O(2)-C(1)-C(10)	103.2(3)	C(8)-C(3)-C(2)	110.5(4)
C(2)-C(1)-C(10)	109.3(3)	C(9)-C(3)-C(4)	118.2(4)
O(2)-C(1)-C(6)	107.9(3)	C(8)-C(3)-C(4)	112.6(4)
C(2)-C(1)-C(6)	112.4(4)	C(2)-C(3)-C(4)	84.9(3)
C(10)-C(1)-C(6)	114.9(4)	C(5)-C(4)-C(7)	107.3(4)
C(1)-C(2)-C(7)	108.3(4)	C(5)-C(4)-C(3)	112.6(4)
C(1)-C(2)-C(3)	113.7(4)	C(7)-C(4)-C(3)	87.8(4)
C(7)-C(2)-C(3)	88.1(3)	C(5)-C(4)-H(4)	115.3
C(1)-C(2)-H(2)	114.6	C(7)-C(4)-H(4)	115.3
C(7)-C(2)-H(2)	114.6	C(3)-C(4)-H(4)	115.3
C(3)-C(2)-H(2)	114.6	C(4)-C(5)-C(6)	114.6(4)
C(9)-C(3)-C(8)	108.3(4)	C(4)-C(5)-H(5A)	108.6

C(6)-C(5)-H(5A)	108.6	O(2)-C(12)-C(13)	114.5(4)
C(4)-C(5)-H(5B)	108.6	C(12)-C(13)-C(14)	119.5(4)
C(6)-C(5)-H(5B)	108.6	C(12)-C(13)-C(16)	119.4(3)
H(5A)-C(5)-H(5B)	107.6	C(14)-C(13)-C(16)	88.6(3)
O(1)-C(6)-C(5)	112.3(4)	C(12)-C(13)-H(13)	109.2
O(1)-C(6)-C(1)	112.8(4)	C(14)-C(13)-H(13)	109.2
C(5)-C(6)-C(1)	113.9(4)	C(16)-C(13)-H(13)	109.2
O(1)-C(6)-H(6)	105.6	C(13)-C(14)-C(15)	88.1(3)
C(5)-C(6)-H(6)	105.6	C(13)-C(14)-H(14A)	114.0
C(1)-C(6)-H(6)	105.6	C(15)-C(14)-H(14A)	114.0
C(2)-C(7)-C(4)	85.7(3)	C(13)-C(14)-H(14B)	114.0
C(2)-C(7)-H(7A)	114.4	C(15)-C(14)-H(14B)	114.0
C(4)-C(7)-H(7A)	114.4	H(14A)-C(14)-H(14B)	111.2
C(2)-C(7)-H(7B)	114.4	C(19)-C(15)-C(14)	116.7(4)
C(4)-C(7)-H(7B)	114.4	C(19)-C(15)-C(16)	121.6(4)
H(7A)-C(7)-H(7B)	111.5	C(14)-C(15)-C(16)	89.2(3)
C(3)-C(8)-H(8A)	109.5	C(19)-C(15)-H(15)	109.2
C(3)-C(8)-H(8B)	109.5	C(14)-C(15)-H(15)	109.2
H(8A)-C(8)-H(8B)	109.5	C(16)-C(15)-H(15)	109.2
C(3)-C(8)-H(8C)	109.5	C(18)-C(16)-C(17)	111.0(3)
H(8A)-C(8)-H(8C)	109.5	C(18)-C(16)-C(15)	116.7(4)
H(8B)-C(8)-H(8C)	109.5	C(17)-C(16)-C(15)	113.6(4)
C(3)-C(9)-H(9A)	109.5	C(18)-C(16)-C(13)	115.0(4)
C(3)-C(9)-H(9B)	109.5	C(17)-C(16)-C(13)	112.3(4)
H(9A)-C(9)-H(9B)	109.5	C(15)-C(16)-C(13)	86.3(3)
C(3)-C(9)-H(9C)	109.5	C(16)-C(17)-H(17A)	109.5
H(9A)-C(9)-H(9C)	109.5	C(16)-C(17)-H(17B)	109.5
H(9B)-C(9)-H(9C)	109.5	H(17A)-C(17)-H(17B)	109.5
O(3)-C(10)-C(11)	129.1(4)	C(16)-C(17)-H(17C)	109.5
O(3)-C(10)-C(1)	124.8(4)	H(17A)-C(17)-H(17C)	109.5
C(11)-C(10)-C(1)	106.0(4)	H(17B)-C(17)-H(17C)	109.5
C(12)-C(11)-C(10)	107.7(4)	C(16)-C(18)-H(18A)	109.5
C(12)-C(11)-H(11)	126.1	C(16)-C(18)-H(18B)	109.5
C(10)-C(11)-H(11)	126.1	H(18A)-C(18)-H(18B)	109.5
C(11)-C(12)-O(2)	114.5(4)	C(16)-C(18)-H(18C)	109.5
C(11)-C(12)-C(13)	131.1(4)	H(18A)-C(18)-H(18C)	109.5

H(18B)-C(18)-H(18C)	109.5	C(26)-C(25)-H(25A)	108.7
C(20)-C(19)-C(15)	114.9(4)	C(24)-C(25)-H(25B)	108.7
C(20)-C(19)-H(19A)	108.6	C(26)-C(25)-H(25B)	108.7
C(15)-C(19)-H(19A)	108.6	H(25A)-C(25)-H(25B)	107.6
C(20)-C(19)-H(19B)	108.6	O(6)-C(26)-C(25)	113.4(4)
C(15)-C(19)-H(19B)	108.6	O(6)-C(26)-C(21)	112.8(3)
H(19A)-C(19)-H(19B)	107.5	C(25)-C(26)-C(21)	113.6(4)
O(4)-C(20)-O(5)	122.0(5)	O(6)-C(26)-H(26)	105.4
O(4)-C(20)-C(19)	126.7(4)	C(25)-C(26)-H(26)	105.4
O(5)-C(20)-C(19)	111.3(4)	C(21)-C(26)-H(26)	105.4
O(7)-C(21)-C(22)	107.2(3)	C(24)-C(27)-C(22)	86.4(3)
O(7)-C(21)-C(30)	102.7(3)	C(24)-C(27)-H(27A)	114.3
C(22)-C(21)-C(30)	111.1(3)	C(22)-C(27)-H(27A)	114.3
O(7)-C(21)-C(26)	107.1(3)	C(24)-C(27)-H(27B)	114.3
C(22)-C(21)-C(26)	113.1(3)	C(22)-C(27)-H(27B)	114.3
C(30)-C(21)-C(26)	114.7(3)	H(27A)-C(27)-H(27B)	111.4
C(21)-C(22)-C(27)	107.2(4)	C(23)-C(28)-H(28A)	109.5
C(21)-C(22)-C(23)	112.5(3)	C(23)-C(28)-H(28B)	109.5
C(27)-C(22)-C(23)	87.4(3)	H(28A)-C(28)-H(28B)	109.5
C(21)-C(22)-H(22)	115.4	C(23)-C(28)-H(28C)	109.5
C(27)-C(22)-H(22)	115.4	H(28A)-C(28)-H(28C)	109.5
C(23)-C(22)-H(22)	115.4	H(28B)-C(28)-H(28C)	109.5
C(28)-C(23)-C(29)	107.1(3)	C(23)-C(29)-H(29A)	109.5
C(28)-C(23)-C(24)	111.7(3)	C(23)-C(29)-H(29B)	109.5
C(29)-C(23)-C(24)	120.0(4)	H(29A)-C(29)-H(29B)	109.5
C(28)-C(23)-C(22)	111.7(4)	C(23)-C(29)-H(29C)	109.5
C(29)-C(23)-C(22)	119.7(3)	H(29A)-C(29)-H(29C)	109.5
C(24)-C(23)-C(22)	85.4(3)	H(29B)-C(29)-H(29C)	109.5
C(25)-C(24)-C(27)	107.9(4)	O(8)-C(30)-C(31)	128.0(4)
C(25)-C(24)-C(23)	112.6(4)	O(8)-C(30)-C(21)	125.4(4)
C(27)-C(24)-C(23)	88.1(3)	C(31)-C(30)-C(21)	106.6(3)
C(25)-C(24)-H(24)	115.1	C(32)-C(31)-C(30)	107.7(4)
C(27)-C(24)-H(24)	115.1	C(32)-C(31)-H(31)	126.2
C(23)-C(24)-H(24)	115.1	C(30)-C(31)-H(31)	126.2
C(24)-C(25)-C(26)	114.2(4)	O(7)-C(32)-C(31)	114.4(4)
C(24)-C(25)-H(25A)	108.7	O(7)-C(32)-C(33)	113.9(3)

C(31)-C(32)-C(33)	131.6(4)	C(36)-C(37)-H(37B)	109.5
C(32)-C(33)-C(34)	120.4(4)	H(37A)-C(37)-H(37B)	109.5
C(32)-C(33)-C(36)	117.4(3)	C(36)-C(37)-H(37C)	109.5
C(34)-C(33)-C(36)	89.0(3)	H(37A)-C(37)-H(37C)	109.5
C(32)-C(33)-H(33)	109.5	H(37B)-C(37)-H(37C)	109.5
C(34)-C(33)-H(33)	109.5	C(36)-C(38)-H(38A)	109.5
C(36)-C(33)-H(33)	109.5	C(36)-C(38)-H(38B)	109.5
C(33)-C(34)-C(35)	88.6(3)	H(38A)-C(38)-H(38B)	109.5
C(33)-C(34)-H(34A)	113.9	C(36)-C(38)-H(38C)	109.5
C(35)-C(34)-H(34A)	113.9	H(38A)-C(38)-H(38C)	109.5
C(33)-C(34)-H(34B)	113.9	H(38B)-C(38)-H(38C)	109.5
C(35)-C(34)-H(34B)	113.9	C(40)-C(39)-C(35)	115.8(4)
H(34A)-C(34)-H(34B)	111.1	C(40)-C(39)-H(39A)	108.3
C(39)-C(35)-C(34)	116.6(4)	C(35)-C(39)-H(39A)	108.3
C(39)-C(35)-C(36)	120.3(3)	C(40)-C(39)-H(39B)	108.3
C(34)-C(35)-C(36)	89.6(3)	C(35)-C(39)-H(39B)	108.3
C(39)-C(35)-H(35)	109.6	H(39A)-C(39)-H(39B)	107.4
C(34)-C(35)-H(35)	109.6	O(9)-C(40)-O(10)	123.6(4)
C(36)-C(35)-H(35)	109.6	O(9)-C(40)-C(39)	124.7(4)
C(38)-C(36)-C(37)	111.2(3)	O(10)-C(40)-C(39)	111.7(4)
C(38)-C(36)-C(35)	114.0(3)	C(6)-O(1)-H(1)	109.5
C(37)-C(36)-C(35)	116.2(3)	C(12)-O(2)-C(1)	108.5(3)
C(38)-C(36)-C(33)	112.9(3)	C(20)-O(5)-H(5)	109.5
C(37)-C(36)-C(33)	114.1(4)	C(26)-O(6)-H(6A)	109.5
C(35)-C(36)-C(33)	86.3(3)	C(32)-O(7)-C(21)	108.5(3)
C(36)-C(37)-H(37A)	109.5	C(40)-O(10)-H(10)	109.5

Symmetry transformations used to generate equivalent atoms:

Table 4. Anisotropic displacement parameters ($\text{\AA}^2 \times 10^3$) for maimone23. The anisotropic displacement factor exponent takes the form: $-2\pi^2 [h^2 a^{*2} U^{11} + \dots + 2 h k a^* b^* U^{12}]$

	U ¹¹	U ²²	U ³³	U ²³	U ¹³	U ¹²
C(1)	28(2)	31(2)	34(2)	2(2)	2(2)	-3(2)
C(2)	29(2)	37(2)	34(2)	0(2)	0(2)	5(2)
C(3)	29(2)	43(2)	32(2)	4(2)	2(2)	4(2)
C(4)	35(3)	52(3)	34(2)	10(2)	2(2)	-2(2)
C(5)	50(3)	37(2)	45(2)	6(2)	-2(2)	-8(2)
C(6)	30(3)	38(2)	43(2)	1(2)	1(2)	8(2)
C(7)	26(2)	71(3)	36(2)	-5(2)	7(2)	-5(2)
C(8)	42(3)	61(3)	36(2)	-3(2)	1(2)	2(3)
C(9)	37(3)	50(3)	38(2)	0(2)	-7(2)	0(2)
C(10)	31(2)	27(2)	33(2)	-7(2)	3(2)	4(2)
C(11)	42(3)	31(2)	28(2)	-4(2)	-2(2)	4(2)
C(12)	39(3)	25(2)	28(2)	-6(2)	5(2)	7(2)
C(13)	38(3)	31(2)	31(2)	-3(2)	2(2)	2(2)
C(14)	49(3)	39(2)	30(2)	-5(2)	2(2)	-1(2)
C(15)	32(3)	33(2)	37(2)	-1(2)	1(2)	1(2)
C(16)	32(2)	30(2)	33(2)	-2(2)	1(2)	1(2)
C(17)	37(3)	33(2)	34(2)	-3(2)	-2(2)	-1(2)
C(18)	41(3)	39(2)	38(2)	2(2)	-3(2)	0(2)
C(19)	39(3)	33(2)	45(2)	7(2)	-4(2)	2(2)
C(20)	47(3)	32(2)	40(2)	5(2)	0(2)	3(2)
C(21)	27(2)	17(2)	37(2)	3(2)	-4(2)	-5(2)
C(22)	29(2)	18(2)	48(2)	4(2)	-7(2)	1(2)
C(23)	32(2)	24(2)	36(2)	-1(2)	-1(2)	-1(2)
C(24)	55(3)	25(2)	38(2)	-5(2)	-8(2)	-11(2)
C(25)	31(3)	39(2)	47(3)	1(2)	-12(2)	-11(2)
C(26)	32(3)	26(2)	46(2)	10(2)	-4(2)	2(2)
C(27)	37(3)	18(2)	55(3)	-1(2)	1(2)	-1(2)
C(28)	44(3)	29(2)	50(3)	-2(2)	-1(2)	3(2)
C(29)	39(3)	31(2)	32(2)	1(2)	-2(2)	2(2)
C(30)	31(2)	26(2)	40(2)	6(2)	-3(2)	-7(2)
C(31)	35(3)	34(2)	31(2)	5(2)	-2(2)	-13(2)

C(32)	26(2)	31(2)	32(2)	-3(2)	5(2)	-4(2)
C(33)	31(2)	24(2)	32(2)	-2(2)	6(2)	-1(2)
C(34)	45(3)	35(2)	30(2)	-6(2)	9(2)	-11(2)
C(35)	32(2)	28(2)	32(2)	-4(2)	8(2)	-8(2)
C(36)	31(2)	18(2)	31(2)	-1(2)	1(2)	1(2)
C(37)	43(3)	26(2)	39(2)	3(2)	0(2)	-2(2)
C(38)	26(2)	21(2)	36(2)	0(2)	5(2)	-2(2)
C(39)	47(3)	25(2)	32(2)	-2(2)	1(2)	-9(2)
C(40)	33(3)	27(2)	37(2)	-5(2)	1(2)	-4(2)
O(1)	60(2)	35(2)	43(2)	-5(1)	2(2)	12(2)
O(2)	30(2)	34(2)	31(1)	2(1)	0(1)	1(1)
O(3)	34(2)	34(2)	48(2)	-7(1)	-6(1)	2(2)
O(4)	94(3)	36(2)	116(3)	15(2)	-68(3)	-13(2)
O(5)	46(2)	32(2)	105(3)	8(2)	-24(2)	-8(2)
O(6)	31(2)	38(2)	56(2)	8(2)	1(2)	-3(2)
O(7)	32(2)	18(1)	32(1)	1(1)	-2(1)	-1(1)
O(8)	43(2)	29(2)	49(2)	12(1)	-10(2)	-10(2)
O(9)	53(2)	44(2)	46(2)	13(2)	-8(2)	-23(2)
O(10)	34(2)	30(2)	66(2)	11(2)	-1(2)	-7(2)

Table 5. Hydrogen coordinates ($\times 10^4$) and isotropic displacement parameters ($\text{\AA}^2 \times 10^{-3}$) for maimone23.

	x	y	z	U(eq)
H(2)	-1191	12842	2875	40
H(4)	-1376	15931	2483	48
H(5A)	-3833	16871	2759	53
H(5B)	-1677	17215	2861	53
H(6)	-4637	15822	3086	44
H(7A)	978	14381	2664	53
H(7B)	637	15296	2910	53
H(8A)	-2630	12387	2440	70
H(8B)	-752	13336	2400	70
H(8C)	-2791	13662	2263	70
H(9A)	-5580	14506	2481	63
H(9B)	-5519	14776	2771	63
H(9C)	-5568	13277	2669	63
H(11)	-1542	12710	3618	41
H(13)	-6695	12592	3497	40
H(14A)	-5690	11379	3836	47
H(14B)	-3794	10738	3692	47
H(15)	-7954	10227	3598	41
H(17A)	-4829	9343	3086	52
H(17B)	-3294	10118	3258	52
H(17C)	-4124	10819	3015	52
H(18A)	-7602	11712	3008	59
H(18B)	-9047	11385	3233	59
H(18C)	-8337	10213	3053	59
H(19A)	-4750	8417	3510	47
H(19B)	-6057	8381	3755	47
H(22)	-2613	10005	4539	38
H(24)	711	11667	5002	47
H(25A)	3465	10344	4862	47
H(25B)	3296	11644	4692	47

H(26)	3025	9009	4559	42
H(27A)	16	12115	4510	44
H(27B)	-1824	12193	4705	44
H(28A)	-3386	9351	5023	62
H(28B)	-3176	10924	4979	62
H(28C)	-2027	10228	5202	62
H(29A)	437	8497	5112	51
H(29B)	1365	8354	4842	51
H(29C)	-817	7809	4896	51
H(31)	-968	8918	3844	40
H(33)	288	5918	4165	35
H(34A)	-943	5531	3776	44
H(34B)	-2650	6674	3803	44
H(35)	-2454	4130	4055	37
H(37A)	-1696	5715	4633	54
H(37B)	-1099	4458	4467	54
H(37C)	-3311	4601	4569	54
H(38A)	-5518	6431	4386	42
H(38B)	-4592	7403	4182	42
H(38C)	-3847	7485	4462	42
H(39A)	-5967	5644	3969	42
H(39B)	-5198	4557	3777	42
H(1)	-1369	16850	3264	69
H(5)	-7893	5897	3431	91
H(6A)	3591	11118	4284	62
H(10)	-8714	2885	4056	65

Chapter 2

Expansion of the Oxygen Stitching Strategy: Total Syntheses of Complex Guaianolides

2.1 Introduction and Background

2.1.1 Expansion of the Oxygen Stitching Strategy to the Synthesis of Complex Guaianolides

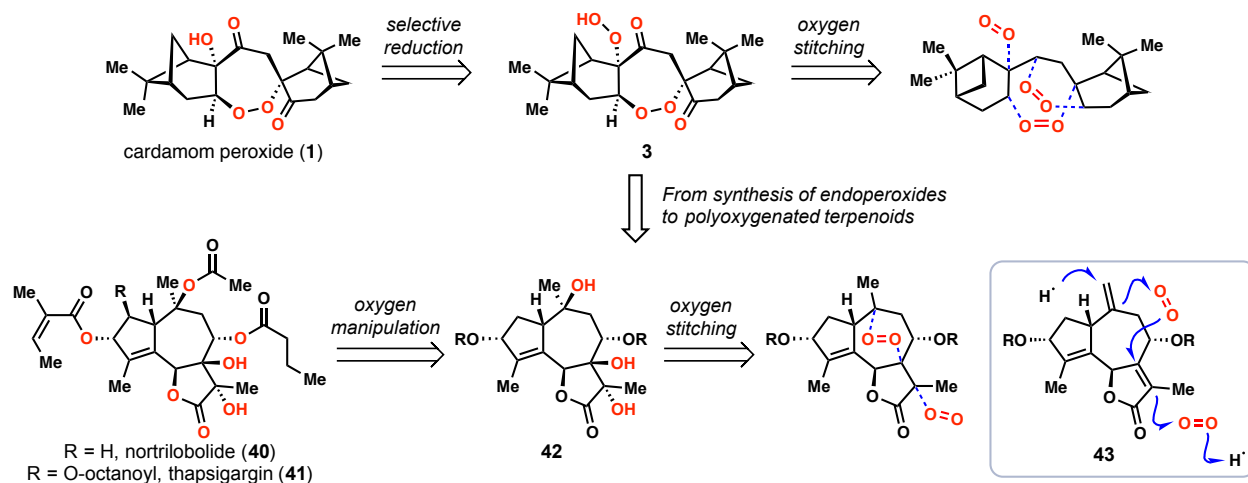


Figure 2.1. Expansion of the oxygen stitching strategy: polyoxygenation in a remotely stereo-controlled manner.

The oxygen stitching strategy is a novel concept developed from my first research project, the total synthesis of antimalarial cardamom peroxide (**1**). Herein, this strategy is applied to the total synthesis of the highly oxygenated terpenoids nortrilobolide (**40**) and thapsigargin (**41**), derivatives of which are entering clinical trials for the treatment of various cancers.¹ In this oxygen stitching strategy, the oxygen atoms in complex terpenoids are assembled from simple molecular oxygen via peroxide-containing intermediates. Subsequent functionalization of the peroxide unit ranges from reduction to an alcohol, to fragmentation of its adjacent carbon-carbon bond. This strategy has the potential to construct a wide array of medicinally relevant terpenes, particularly for the treatment of cancer and malaria, with high efficiency.

In a conventional retrosynthetic analysis of a terpenoid, carbon-carbon bonds or carbon-oxygen bonds are disconnected sequentially until the complex molecule is deduced to simple and commercially available starting materials. In our analyses utilizing the oxygen stitching strategy, the oxygen atoms are carefully selected, and then combined to endoperoxides or extended to hydroperoxides (see **3** and **42**, Figure 2.1). The peroxides ultimately are derived from molecular oxygen by “oxygen stitching” of olefins. The alkene starting materials (e.g. **43**) typically possess much less complexity than the target natural products, and are often easy to synthesize. In conventional synthesis, it is common that multiple steps are conducted to construct each oxygen-attached stereogenic center. The technique to install multiple oxygen-attached stereocenters in one step therefore provides a powerful synthetic tool for the synthesis of densely oxygenated molecules. The power of this strategy is underscored by the ability of the peroxide linkage to enforce the stereochemical information across the molecule. This technique also produces little chemical waste and requires minimal protecting-group manipulations.

2.1.2 Guaianolides of Interest and Their Biological Activities

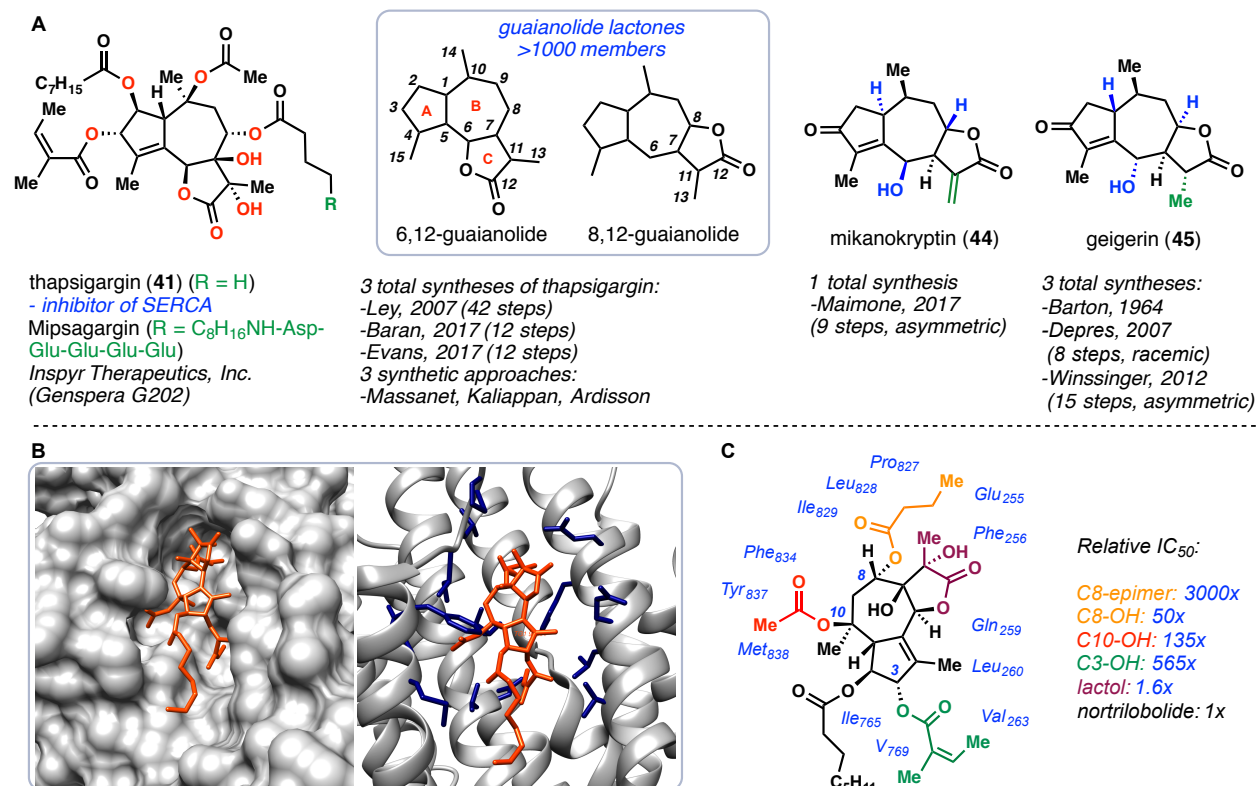


Figure 2.2. A) Numbering system of 6,12-guaianolides and 8,12-guaianolides, and examples of targets of interest. B) Crystal structure of SERCA with **41** bound (PDB code 1XP5, generated by Chimera®). C) Schematic presentation of the interaction between **41** and the amino acid residues of SERCA, and the relative IC₅₀ of thapsigargin analogs versus thapsigargin itself.

The sesquiterpene lactone thapsigargin (**41**) was isolated in 1978 by Christensen and coworkers from the root of *Thapsia garganica* (Apiaceae).² This highly oxygenated terpenoid, as well as the other 16 members in this group that includes **40**, strongly inhibit the sarco/endoplasmic reticulum Ca²⁺ ATPase (SERCA) at low nM levels.³ Thapsigargin (**41**) represents one of the few examples in which only hydrophobic interactions account for the binding affinity between the small molecule and its target protein. The hydrophobic ester side chains of **41**, particularly those at C-3, C-8, and C-10 positions, interact with the amino acid residues of SERCA that are highlighted in blue in Figure 2.2B and also listed in detail in Figure 2.2C.⁴ Saponification or epimerization at the three positions typically results in significant loss of the inhibitory activities of the corresponding analogs. In contrast, nortrilobolide (**40**) bearing one less oxygenation at C-2,⁵ and the lactol derivative of **41**,^{4b} retain similar levels of potency.

Mipsagargin (or G202) is a C-8 derivative prodrug linking **41** with a small peptide chain that can be specifically recognized by prostate-specific membrane antigen (PSMA) and selectively cleaved *in vivo* to release the active drug. The active form then irreversibly inhibits SERCA of the target cancer cells and induces apoptotic cell death. Mipsagargin is now under Phase II clinical trials against prostate, brain, and liver cancers.¹

Structurally, **41** belongs to the *guaianolide* family, a major subset of sesquiterpene lactones. Guaianolides have been intensely investigated from both medicinal and chemical synthesis perspectives for decades.⁶ Members in this family share a [5,7,5]-fused tricyclic ring system with variations at the lactone position, giving rise to 6,12-guaianolides, such as **40** and **41**, and 8,12-guaianolides, such as mikanokryptin (**44**) and geigerin (**45**) (Figure 2.2A). The majority of guaianolides have been isolated from the Asteraceae family of plants, while Apiaceae represents the second largest source.⁷

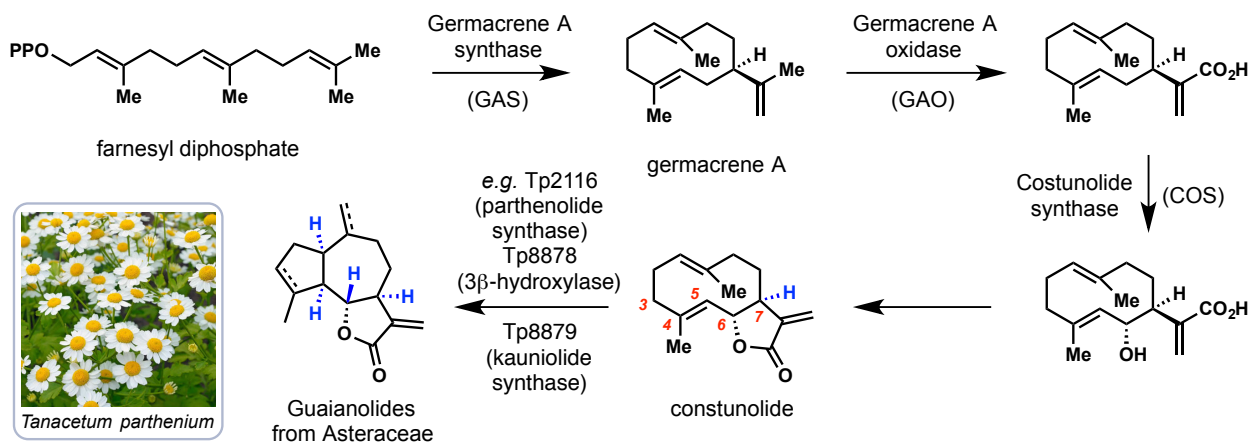
Distinct from the hydrophobic binding mechanism of the polyoxygenated guaianolides **40** and **41** from the Apiaceae family, a characteristic α -methylene- γ -lactone motif has been located in most guaianolides in the Asteraceae family (*e.g.* **44**) due to its formation at the early stage of biosynthesis,⁸ and proven essential for their anticancer, anti-inflammatory, anthelmintic, and anti-migraine activities.⁹ Recently, α -methylene-containing sesquiterpene lactones have been shown to potently inhibit aspects of both the signaling NF- κ B pathway,^{9e, 10} and the pathway of mitogen-activated protein kinases (MAPKs).¹¹ Transcriptional factor NF- κ B is a central mediator of the human immune response, and its deregulation is noted in the development of inflammation and cancer.¹² Current molecular models include: (i) covalent binding of α -methylene lactones to cysteine residues C38 and C120 in the p65 subunit of active NF- κ B,¹³ (ii) stabilization of its inhibitor I κ B in response to inductive stimuli,¹⁴ and (iii) covalent binding to cysteine residue C179 in the catalytic subunit IKK β of I κ B kinase, which therefore deactivates I κ B and up-regulates NF- κ B.¹⁵ Sesquiterpene lactones with more than one alkylating functional group are proposed to crosslink cysteine residues in close vicinity, achieving enhanced inhibitory activities.^{13b, 16}

Overall, the densely oxygenated guaianolides from Apiaceae plants with potent activities against SERCA, and guaianolides from Asteraceae plants containing the α -methylene- γ -lactone moiety with potential for cysteine ligation, both attracted us to develop chemical synthesis pathways.

2.1.3 Biosynthesis

Guaianolides from Asteraceae

also referred to as *Compositae*, commonly known as the aster, daisy, composite, or sunflower family



Guaianolides from Apiaceae

also referred to as *Umbelliferae*, commonly known as the celery, carrot, or parsley family

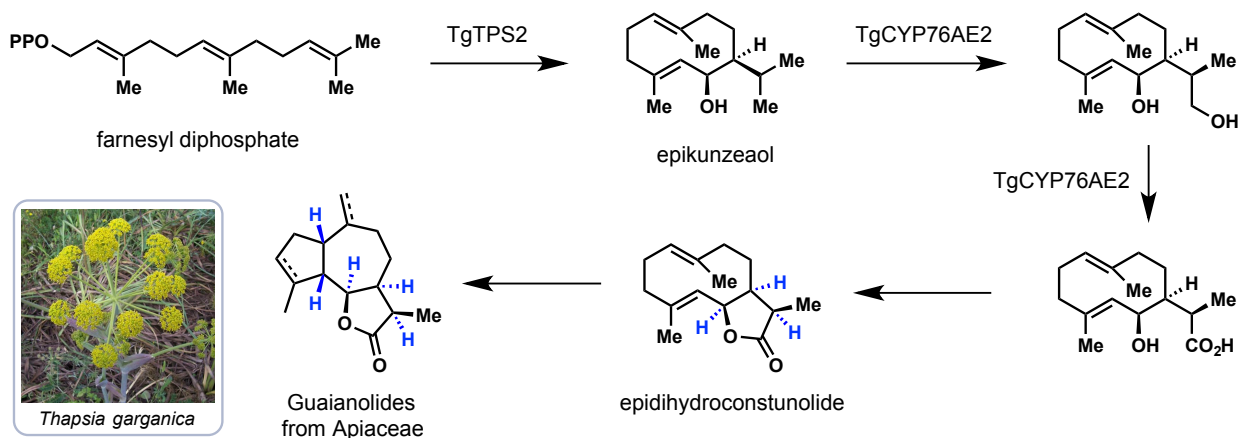


Figure 2.3. Distinct biosynthetic pathways of guaianolides in the Asteraceae and Apiaceae family.

As mentioned above, guaianolides have been predominantly isolated from two families of plants, the *Asteraceae* and the *Apiaceae*, which are historically referred to as *Compositae* and *Umbelliferae*, respectively. Common examples of these families are listed in Figure 2.3, including aster, daisy, composite, and sunflower for the *Asteraceae* family; and celery, carrot, and parsley for the *Apiaceae* family. These two families were found to possess distinct biosynthetic pathways to assemble the [5,7,5]-fused carbon network of guaianolides, both from the same building block farnesyl diphosphate.

The *Asteraceae* plants, such as *Tanacetum parthenium*,¹⁷ utilize germacrene A synthase (GAS), germacrene A oxidase (GAO), and constunolide synthase (COS) to synthesize a key intermediate, constunolide, which contains a characteristic α -methylene- γ -lactone with *trans* configuration at the C6–C7 junction. From this intermediate, $\Delta_{4,5}$ -epoxidation or allylic

hydroxylation at the C-3 position, followed by carbocation generating conditions, leads to formation of the [5,7]-fused carbocyclic system, arriving at a wide variety of guaianolides bearing stereochemical patterns shown in Figure 2.3A. Further oxidations of the cyclized products can then deliver over 1000 distinct guaianolides.^{6a}

The Apiaceae plants utilize a different series of enzymes to construct the lactone moiety and the carbocyclic system of guaianolides (Figure 2.3B). In *Thapsia garganica*,¹⁸ for example, TgTPS2 cyclizes farnesyl diphosphate to epikunzeaol, then TgCYP76AE2 renders site-selective C–H oxidation of the isopropyl moiety to afford a carboxylic acid product. Likely, a spontaneous lactonization occurs in a non-enzymatic manner, providing the key intermediate epidihydroconstunolide. This intermediate differs from constunolide in its *cis* configuration at the lactone junction, and the α -methyl group that comes from epikunzeaol. Cyclization of epidihydroconstunolide potentially leads to a group of ~100 guaianolides isolated to date from the Apiaceae family, including nortrilobolide (**40**) and thapsigargin (**41**).^{7a} Notably, guaianolides from the Apiaceae family bear opposite stereochemistry at the C-1, C-5 and C-6 positions compared to those from the Asteraceae family (if no oxidation occurs at these positions), and are also referred to as *slovanolides* in prior literature.¹⁹ They will be further discussed in detail in Chapter 2.7 and a comprehensive list of slovanolides from the Apiaceae family will be presented.

2.2 Previous Synthetic Studies of Guaianolides

In a literature survey of all published total syntheses and semi-syntheses of guaianolides, chiral-pool building blocks²⁰ were found to be the predominate source of the carbocyclic system. Examples in this section are therefore sorted by the ways of mapping these chiral-pool building blocks onto the [5,7,5]-fused tricyclic system, which include (i) Favorskii rearrangement of carvone derivatives, (ii) photo-induced rearrangement of a dienone, (iii) ozonolysis of carvone derivatives, and (iv) methods using other chiral-pool or achiral building blocks.

2.2.1 Studies Based on the Favorskii Rearrangement of Carvone Derivatives

2.2.1.1 Lee's syntheses of (–)-estafiatin and (+)-cladantholide (1997)

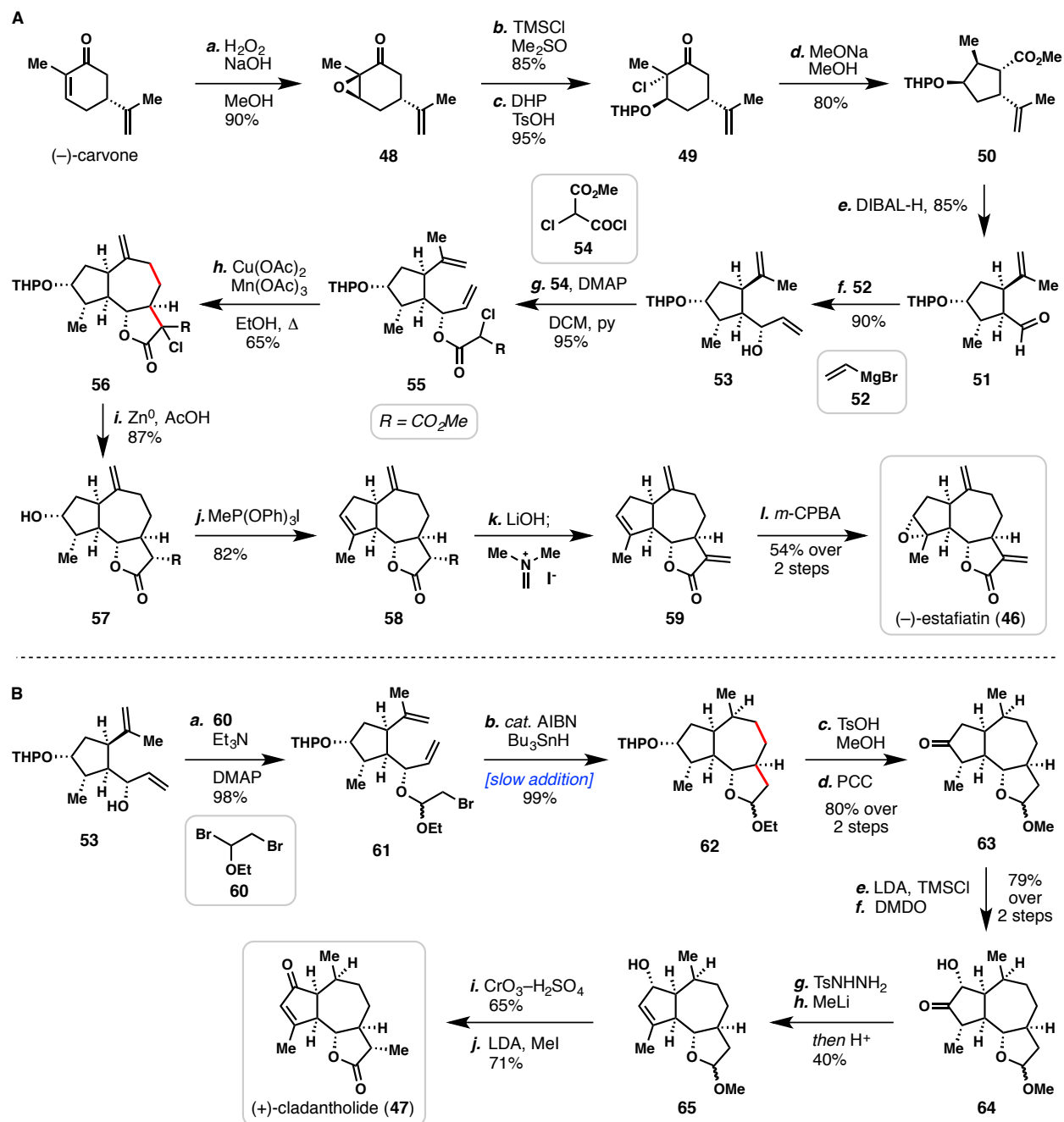
Lee's seminal work on (–)-estafiatin (**46**) and (+)-cladantholide (**47**) in 1997 represents one of the first examples of utilizing a Favorskii rearrangement to assemble the A ring of guaianolide natural products.²¹ This strategy was recapitulated by many researchers in a number of elegant guaianolide syntheses, some of which will be discussed later in this section. (–)-Estafiatin (**46**) was first isolated by Sanchez-Viesca and Romo from *Artemisia mexicana* (Asteraceae) in 1963,²² and (+)-cladantholide (**47**) was isolated later in 1993 by Wichlacz and coworkers from *Cladanthus arabicus* (Asteraceae).²³ While both maintain the stereochemistry derived from the Asteraceae biosynthesis, they differ in oxidation states across the entire carbon network. Lee and coworkers thus strategically utilized two types of radical cascades to access the desired oxidation levels in the natural products (Scheme 2.1).

Lee's synthesis commenced with a three-step procedure to prepare the chlorohydrin derivative **49** from (–)-carvone via nucleophilic epoxidation, chlorohydrin formation, and protection of the resulting alcohol (Scheme 2.1A). Under basic conditions (NaOMe, MeOH), **49** underwent a Favorskii rearrangement, affording highly functionalized cyclopentane **50** in high yield. Reduction of the methyl ester to an aldehyde by DIBAL-H, followed by addition of vinyl Grignard reagent **52**, afforded allylic alcohol **53**, and at this point, the two syntheses diverged.

The synthesis of **46** utilized oxidative radical generating conditions with chloromalonate **55** as the cyclization substrate. Mn(III) acetate oxidized the malonate moiety and the resulting α -keto radical underwent a 5-*exo-trig*/7-*endo-trig* cyclization with the cascade terminated by Cu(II)-mediated oxidation. Subsequent β -deprotonation of the tertiary carbocation afforded exocyclic alkene **56** in overall 65% yield. The remaining redox manipulation and installation of the α -methylene moiety provided (–)-estafiatin (**46**) in four steps.

In the synthesis of (+)-cladantholide (**47**) (Scheme 2.1B), common intermediate **53** was converted to primary bromide **61**. This intermediate was then reacted under the standard reductive radical generating condition (AIBN, *n*-Bu₃SnH) to afford cyclized product **62** in near quantitative yield. With tricycle **62** in hand, an 8-step sequence including functional group manipulations was conducted to arrive at (+)-cladantholide (**47**).

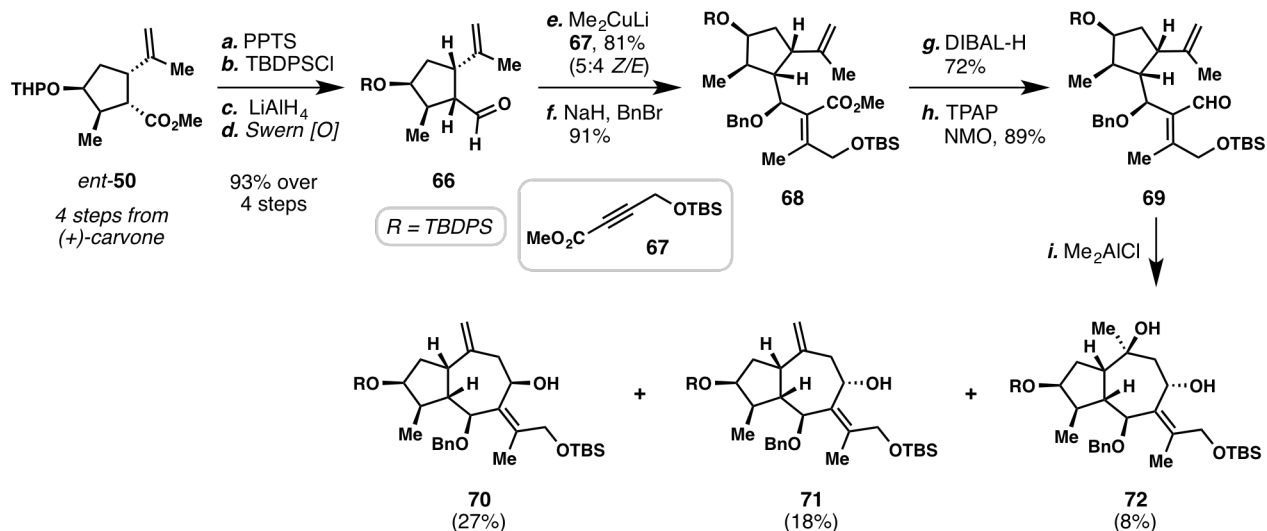
Overall, Lee and coworkers' work demonstrated the power of programmed radical cascades in total synthesis of complex terpenoids,²⁴ and most importantly introduced building blocks **50** and **51** to the field of guaianolide synthesis, as well as to the syntheses of other natural products.²⁵



Scheme 2.1. Lee's seminal syntheses of (-)-estafiatiin (**46**) and (+)-cladantholide (**47**) (1997).

2.2.1.2 Ley's synthesis of (-)-thapsigargin (2007)

In 2004, Ley and coworkers accomplished the first total synthesis of nortrilobolide (**40**).²⁶ In their seminal work, an initial study employing a Prins-type cyclization was investigated prior to their synthesis of **40** (Scheme 2.2).^{26b} Lee's intermediate **50** was utilized as the A ring precursor in its enantiomeric series, and slightly modified in four steps to afford aldehyde **66**. The authors then coupled the ten-carbon fragment **66** and a five-carbon fragment derived from **67** via a cuprate addition. After protection of the resulting alcohol, ester **68** was converted into



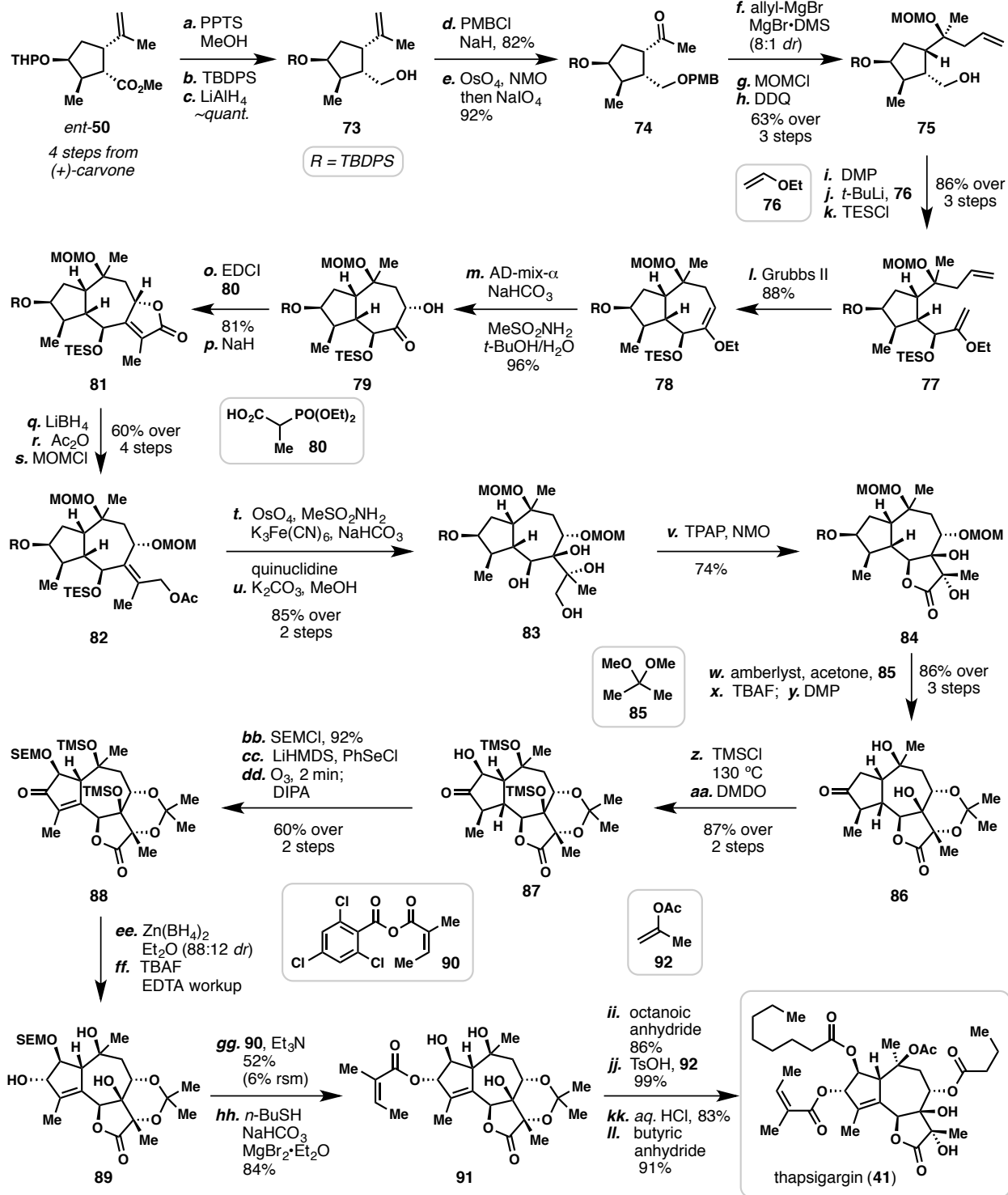
Scheme 2.2. Ley's initial study on thapsigargin (**41**) from (–)-**50** via a Prins cyclization (2004).

aldehyde **69** in a two-step procedure, which was then treated with Lewis acid (Me_2AlCl), affording Prins-type cyclized products **70–72**. Despite the low selectivity of this ring forming event, this strategy discloses an alternative bond disconnection of the seven-membered B ring to the synthetic field.

In 2007, Ley and coworkers reported the synthesis of thapsigargin (**41**) in 42 steps from carvone by modifying the end game of their 2004 work on nortrilobolide (**40**) (Scheme 2.3).²⁷ The total synthesis began with Lee's intermediate **50** and a five-step sequence of redox manipulations offered ketone **74**. In this work, the order and positions of C–C bond formation in assembly of the B ring altered from Ley's initial study. A Grignard addition of the allyl species to ketone **74** followed by protecting group manipulations provided alcohol **75**, which was then oxidized. Subsequent addition of a vinyl lithiate derived from **76** and protection of the alcohol moiety resulted in diene **77**. This intermediate was then subjected to Grubbs ring-closing metathesis (RCM) to construct the B-ring. Asymmetric hydroxylation of the cyclized product provided ketone **79** in good yields. An intramolecular Horner–Wadsworth–Emmons (HWE) reaction was utilized in the formation of last C–C bond, and after a five-step sequence of redox manipulations on the HWE product **81**, tetraol **83** was obtained in good yields. Direct subsection of **83** to oxidation conditions (TPAP, NMO) provided lactone **84** in 74% yield. This efficient strategy of C-ring construction was also adapted by Massanet and Baran's work, which will be discussed in section 2.2.2.

From lactone **84**, a five-step sequence was developed to arrive at the oxidized product **87**. SEM protection of alcohol **87** proved to be essential for the regioselectivity in subsequent enone formation. With enone **88** in hand, stereoselective reduction by zinc borohydride, followed by protecting group manipulations and installation of the angelic moiety with anhydride **90**, afforded **91**. The remainder of the ester groups were installed sequentially, arriving at thapsigargin (**41**) in four steps with excellent yields.

Ley's 2007 synthesis serves as foundation for several later improved syntheses.

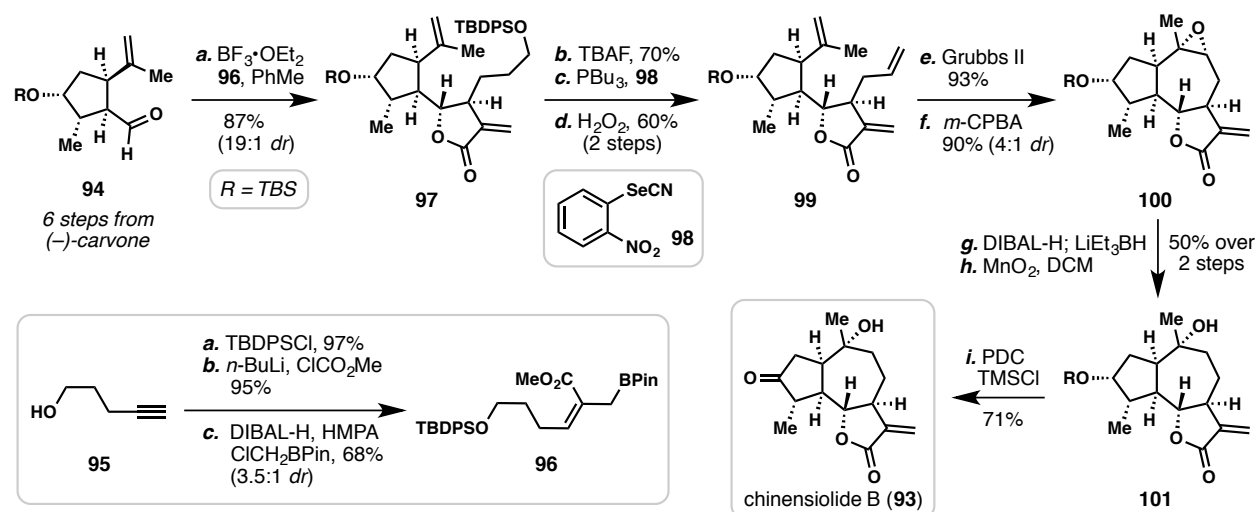


Scheme 2.3. Ley's inaugural total synthesis of thapsigargin (**41**) from intermediate **50** (2007).

2.2.1.3 Hall's synthesis of chinensiolide B (2010)

Chinensiolide B (**93**) was isolated in 2002 by Ando and coworkers from *Ixeris chinensis* (Asteraceae), a perennial plant used in Chinese folk medicine (Siyekucui).²⁸ In 2010, Hall and coworkers presented an elegant synthesis of this Asteraceae guaianolide from building block **94**,²⁹ a compound modified from Lee's intermediate **51** (Scheme 2.4).

Highly functionalized allylic borane **96** was synthesized in 3 steps from commercially available alkyne **95**. Utilizing catalytic amounts of Lewis acid ($\text{BF}_3 \cdot \text{OEt}_2$), the coupling of aldehyde **94** and allylic borane **96** directly afforded *trans*-lactone **97** in one step in 87% yield. From this point, a three-step sequence was developed to generate the terminal alkene moiety in **99**, which was subjected to Grubbs RCM conditions. With the completion of the carbon skeleton, a three-step sequence was utilized to convert the *tri*-substituted alkene into a tertiary alcohol **101**, which consisted of epoxidation (see **100**), global reduction (DIBAL-H; LiEt_3BH) and regeneration of the lactone (MnO_2). Subsequently, oxidation of the TBS-protected alcohol **101** (PDC, TMSCl) directly afforded **93** in 15 steps overall with a 6.7% yield.



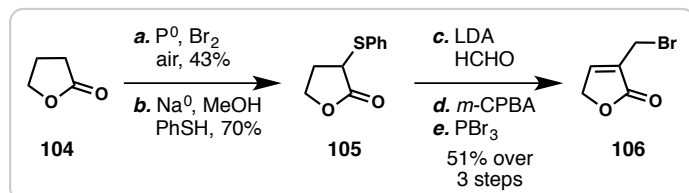
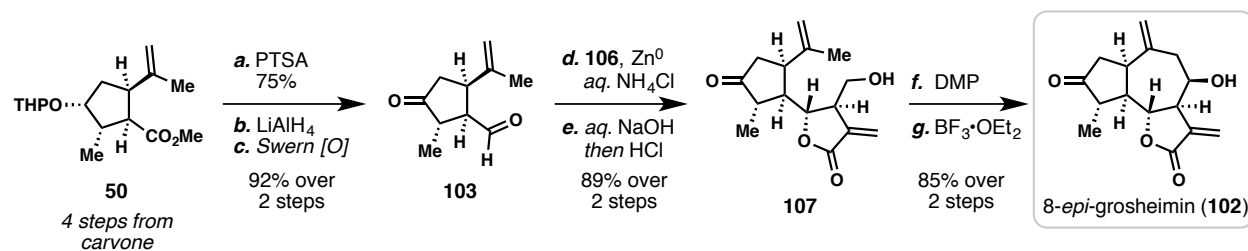
Scheme 2.4. Hall's synthesis of chinensiolide B (**93**) from intermediate **94** (2010).

2.2.1.4. Xu's synthesis of 8-*epi*-grosheimin (2011)

In 2001, Xu and coworkers reported their second generation synthesis of 8-*epi*-grosheimin (**102**) (Scheme 2.5),³⁰ a guaianolide isolated in 1979 by Barbetti and coworkers from *Crepis virens* (Asteraceae).³¹ In this work, the authors started with Lee's intermediate **50**, from which aldehyde **103** was synthesized in three steps via redox manipulations. Aldehyde **103** was then coupled with allylic bromide **106**, which was synthesized in five steps from commercially available lactone **104**. The resulting alcohol then underwent a *trans*-lactonization (*aq.* NaOH ; then *aq.* HCl), affording *trans*-fused 6,12-lactone **107** in 89% yield over 2 steps. It is worth noting that the same process to convert 8,12-lactones to 6,12-lactones might find difficulties when applied to the Apiaceae guaianolides; their properties will be discussed in chapter 2.7.

From **107**, Dess–Martin oxidation smoothly oxidized the alcohol into an aldehyde which was then subjected to Prins-type cyclization conditions ($\text{BF}_3 \cdot \text{OEt}_2$), affording 8-*epi*-grosheimin

(**102**) in 85% yield over 2 steps. This highly concise synthesis of 8-*epi*-grosheimin was achieved in 11 steps from carvone with a remarkable overall 45% yield.³²



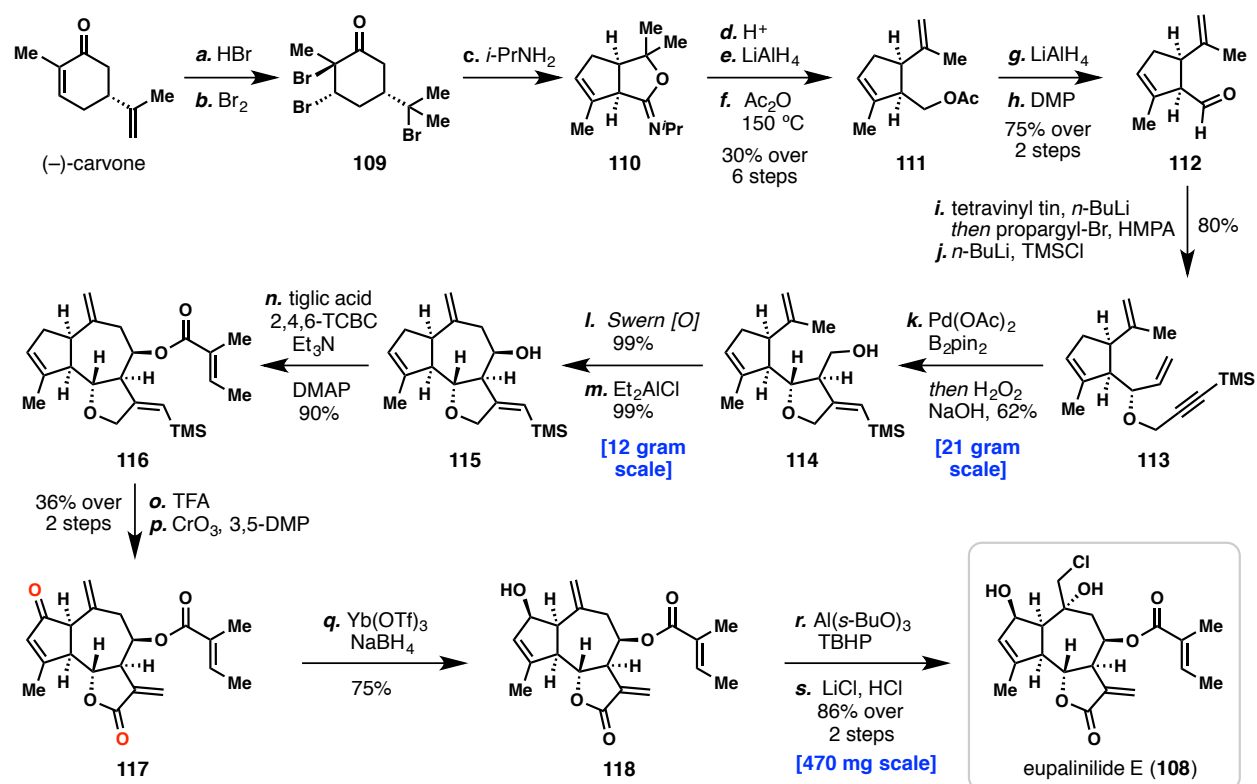
Scheme 2.5. Xu's synthesis of 8-*epi*-grosheimin (**102**) from intermediate **50** (2011).

2.2.1.5. Siegel's synthesis of eupalinilide E (2016)

Eupalinilide E (**108**) was isolated in 2004 by Yue and coworkers from *Eupatorium lindleyanum* DC. (Asteraceae), and exhibits cytotoxicity against P-388 and A-549 tumor cell lines.³³ In a search of natural products to control the differentiation of hematopoietic stem cells (HSPCs), Schultz and coworkers identified **108** out of ~700 natural terpenoids. Eupalinilide E (**108**) possesses inhibitory activities on the differentiation of HSPCs and promotes its expansion.³⁴ In 2016, Siegel and coworkers reported an efficient synthesis of this complex guaianolide (Scheme 2.6).³⁵

Wolinsky's intermediate **110** was identified as a key building block *en route* to **108** and was prepared in four steps from carvone.³⁶ Hydrobromination of the electron-rich alkene (HBr) followed by dibromination of the enone (Br₂) afforded tribromide **109** on large scales. The Favorskii rearrangement of **109** was facilitated by isopropyl amine in a tandem process to arrive at the bicyclic product **110**, which was subsequently hydrolyzed (AcOH, H₂O) to afford the corresponding lactone (not shown) in 50% yield over 4 steps. At this juncture, an additional 4 steps of redox manipulations were conducted to prepare aldehyde **112** bearing the desired Δ_{3,4}-unsaturation. From aldehyde **112**, which possesses a similar level of complexity as **51**, a three-step process was used to install the requisite C ring, which includes a palladium-catalyzed tandem hydroboration/cyclization of enyne **113**. An ensuing oxidation provided alcohol **114**. Swern oxidation smoothly oxidized **114** to the aldehyde which was then subjected to Prins-type cyclization conditions (EtAlCl₂), affording tricycle **115** in near quantitative yields on decagram scales. From this point, a 3-step sequence of esterification, desilylation, and allylic oxidations (CrO₃, 3,5-dimethylpyrazole) unveiled lactone **117**. Finally, a 3-step protocol was applied to install the chlorohydrin moiety in Eupalinilide E (**108**).

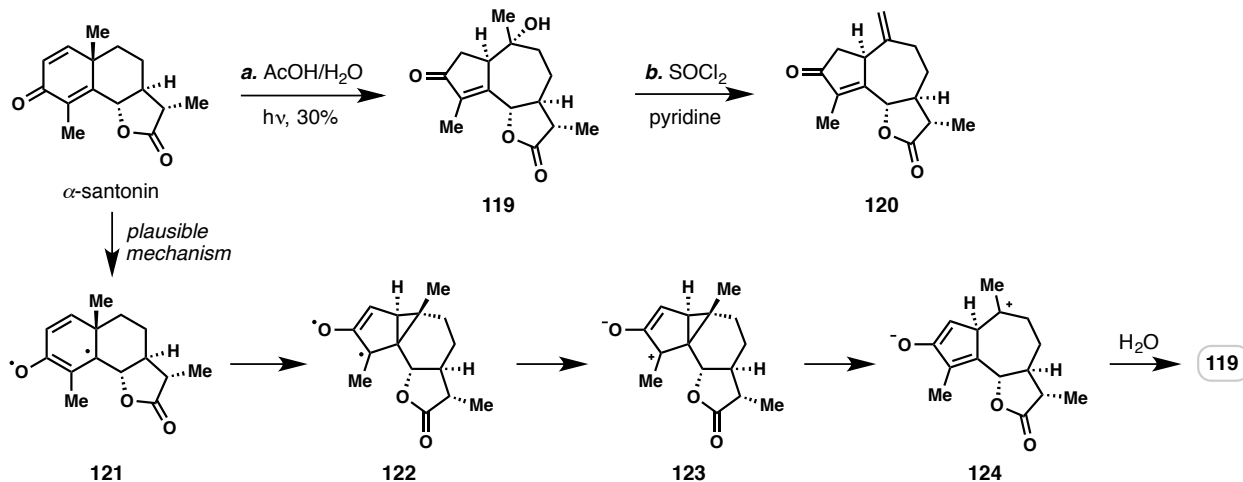
Siegel's efficient 19-step synthesis of **108** allowed a 470-mg scale synthesis of this natural product in a single batch, which secured ample material for further biological studies with HSPCs.



Scheme 2.6. Siegel's synthesis of eupalinilide E (**108**) from Wolinsky's intermediate **110** (2016).

2.2.2 Studies Based on Dienone Rearrangements

Barton's early studies in the 1950s on the photo-induced rearrangement of α -santonin and artemisin popularized this powerful transformation in guaianolide syntheses (Scheme 2.7).³⁷ The solid-state photochemical transformation of this natural terpene that provides different products (not shown) could be dated back to as early as 1834.³⁸ Upon irradiation of ultraviolet light, the dienone moiety in this eudesmane sesquiterpene can be excited, and undergo a series of transformations to provide guaianolide **119** in 30% yield. A plausible mechanism is provided in Scheme 2.7. From **119**, Barton and coworkers examined various derivatizations, including elimination of the tertiary alcohol by thionyl chloride to cleanly afford alkene **120**.

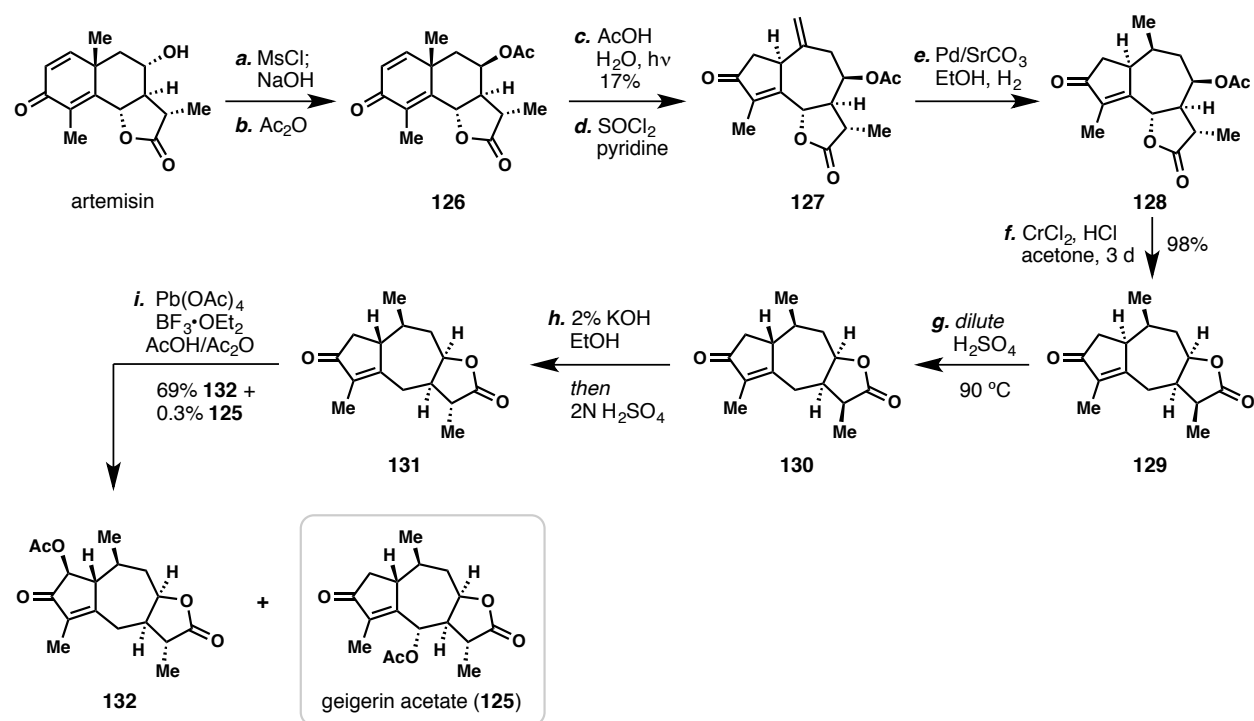


Scheme 2.7. Barton's study on the photo-induced rearrangement of α -santonin (1957).

2.2.2.1. Barton's synthetic study on geigerin (1964)

Geigerin (**45**) was isolated in 1936 by Rimington and coworkers from *Geigeria aspera* (Asteraceae).³⁹ In 1960s, Barton and coworkers reported a series of synthetic studies towards the structural determination of 8,12-guaianolides geigerin (**45**) and geigerin acetate (**125**), which also represents a concise synthesis of **125** from artemisin (Scheme 2.8).⁴⁰ Barton's synthesis commenced with epimerization of artemisin at C-8, followed by acetylation with acetic anhydride. Dienone **126** was then irradiated in the presence of aqueous acetic acid, affording the corresponding guaianolide in 17% yield. It is worth noting that artemisin acetate (*8-epi-126*) only yielded 5% of desired product when treated with the same condition.

After three redox-manipulation steps and two steps to effect epimerization, enone **131** was obtained in excellent yields. Enone **131** can be obtained by treatment of natural **45** or **125** with the reductive conditions utilizing CrCl_2 and acid as well, thus merging the studies of structural determination and semi-synthesis. In the last step of this synthetic study, **131** was subjected to oxidative conditions [$\text{Pb}(\text{OAc})_4$, $\text{BF}_3 \cdot \text{OEt}_2$, AcOH , Ac_2O], affording α - and γ -oxidation products in 69% and 0.3% yield, respectively, completing the synthesis of **125** in 9 steps from artemisin. Despite the low yield of the final step, this landmark 1964 synthesis represents an excellent example of applying synthetic chemistry in structural elucidation of complex natural products.⁴¹



Scheme 2.8. Barton's synthesis of geigerin acetate (**125**) from artemisin (1964).

2.2.2.2. White's synthesis of leukodin (1967)

Leukodin (**133**) was isolated in 1962 by Holub and coworkers from *Artemisia leukodes* (Asteraceae).⁴² In 1967, White and coworkers reported an elegant synthesis of leukodin (**133**) from α -santonin in only 5 steps (Scheme 2.9).⁴³

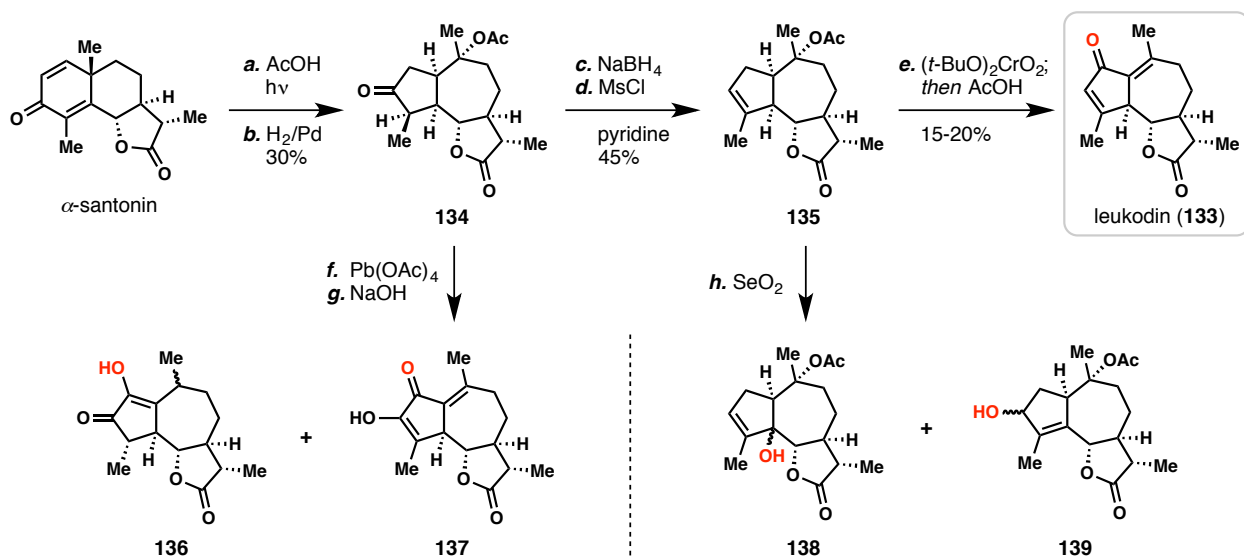
The photo-induced rearrangement, when conducted in glacial acetic acid instead of aqueous solutions, afforded the corresponding acetate of **119** in similar yields (~30%). Hydrogenation of the enone intermediate was then achieved in high yield with palladium on carbon and H₂. From the resulting ketone **134**, $\Delta_{3,4}$ -alkene **135** was prepared in moderate yield (45%) via reduction and elimination. This 3-step process served as foundation for a number of synthetic studies starting from α -santonin. Allylic oxidization of **135** by a chromium(VI) oxidant, follow by concomitant elimination of the acetate moiety, afforded leukodin (**133**) in 15-20% yield from **135**. Other attempts in oxidation of intermediates **134** and **135** rendered several interesting albeit undesired oxidation products **136–139**.

2.2.2.3. Greene's synthesis of oxoisodehydroleucodin (1988)

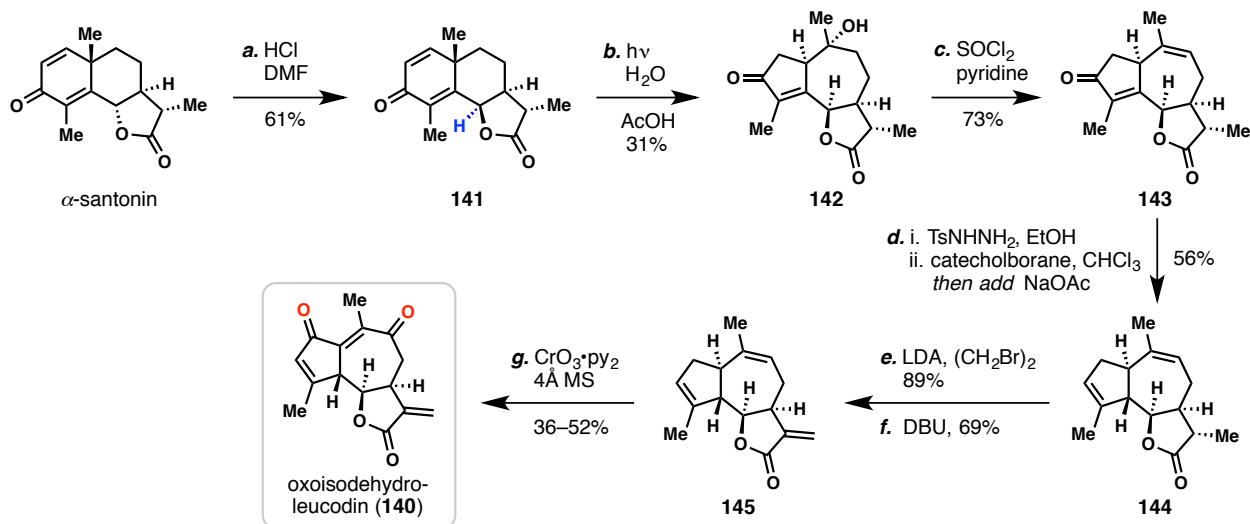
Oxoisodehydroleucodin (**140**) was isolated by Fisher and coworkers in 1986 from *Montanoa imbricata* (Asteraceae).⁴⁴ Two years later, Greene and coworkers reported a rapid synthesis of this highly unsaturated guaianolide (Scheme 2.10),⁴⁵ which was complementary to White's work in guiding the stereocontrolled syntheses employing santonin as a building block.

Greene's synthesis began with epimerization of α -santonin to 6-*epi*-santonin (**141**).⁴⁶ Photo-induced rearrangement of **141** afforded guaianolide **142** in 31% yield, similar to that of the

rearrangement of α -santonin itself. Treatment of **142** with the standard elimination condition (SOCl_2 , base), however, afforded exclusively the endocyclic alkene **143** (*cf.* **119** \rightarrow **120**). To address this peculiarity, the authors proposed that the geometry of the *cis*-fused lactone dictated the stereochemical outcome of this transformation. From **143**, a one-pot procedure was employed with TsNHNH_2 and a reductant to install the requisite α -H at C-5 in diene **144**. Followed by introduction of the unsaturation on the C-ring lactone and an efficient dual oxidation, oxoisodehydroleucodin (**140**) was prepared in 3 steps from **144** with a moderate overall yield.



Scheme 2.9. White's synthesis of leukodin (**133**) from α -santonin (1967).

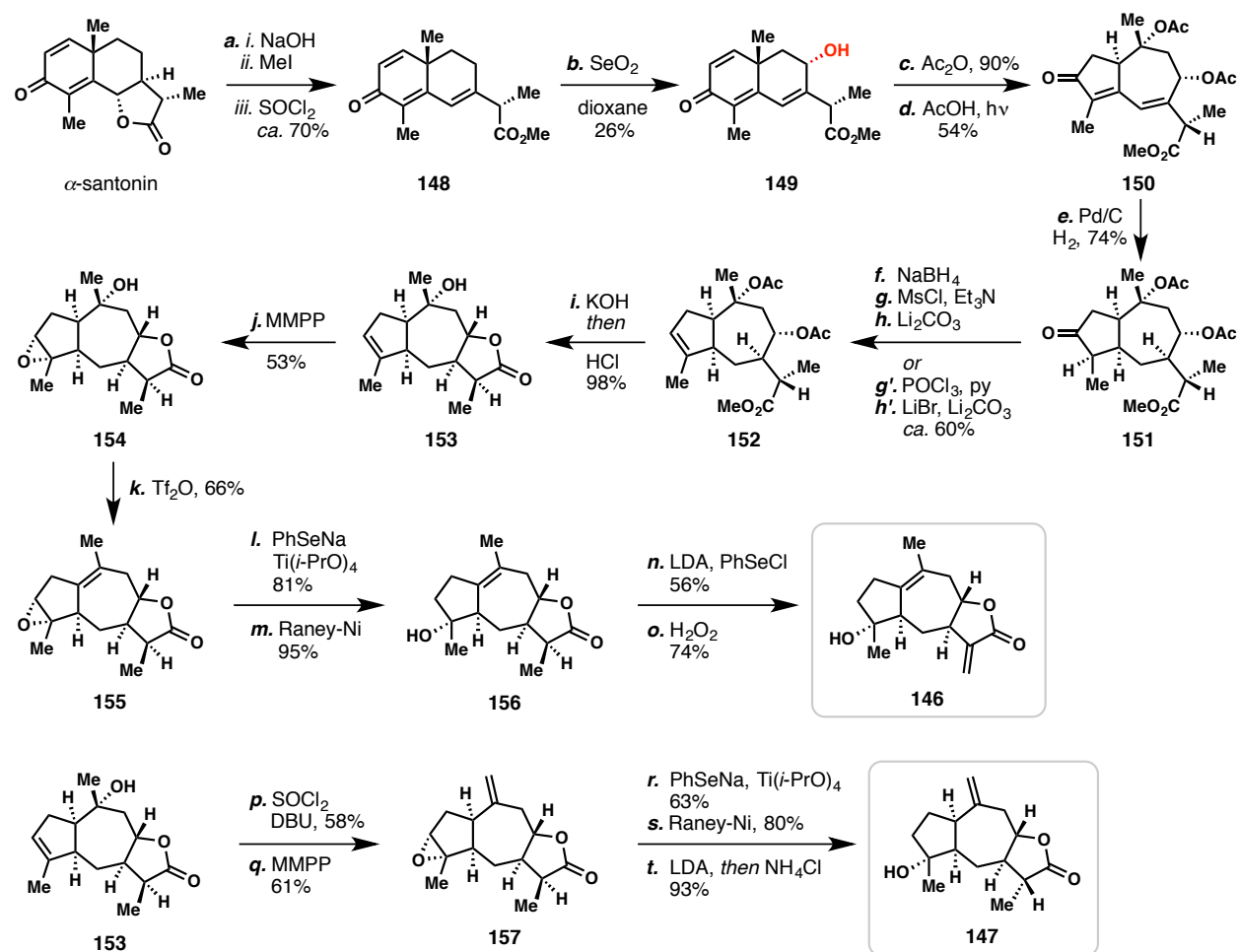


Scheme 2.10. Greene's synthesis of oxoisodehydroleucodin (**140**) from α -santonin (1988).

2.2.2.4. Pedro's synthesis of 8,12-guaianolides (2000)

One could argue that the main drawback of applying the rearrangement of α -santonin in guaianolide syntheses is the lack of C-8 oxygenation present in santonin, and the commercial supply of artemisinin that contains the valuable C-8 oxygen has unfortunately been inconsistent. In contrast, this oxidation pattern can be found in majority of the complex guaianolides isolated to date. In 2000, Pedro and coworkers strategically installed the C-8 oxygen in santonin derivatives, and completed the synthesis of two 8,12-guaianolides **146** and **147** (Scheme 2.11).⁴⁷

To begin their studies, Pedro and coworkers developed a one-pot procedure to convert α -santonin to alkene **148** in ~70% yield. Subsequent SeO₂-mediated allylic oxidation rendered allylic alcohol **149** in 26% yield, as well as other regioisomers. Treatment of acetylated **149** with photo-irradiation offered a cleaner rearrangement (54%) compared to that of the santonin-type substrates, and this enhancement was also observed by Massanet and Baran (see Scheme 2.12 and 2.13). After a series of functional group manipulations (5 steps), $\Delta_{3,4}$ -alkene **153** was prepared, and from this intermediate the authors achieved regioselective eliminations of the tertiary alcohol at C-10. By using Tf₂O after epoxidation of the $\Delta_{3,4}$ -double bond (MMPP), endocyclic alkene **155** was obtained in moderate yields, whereas the condition utilizing SOCl₂ and base, followed by epoxidation, cleanly afforded exocyclic alkene **157**. From **155** and **157**, 8,12-guaianolides **146** and **147** were prepared in 4 steps and 3 steps, respectively.



Scheme 2.11. Pedro's synthesis of 8,12-*trans*-guaianolides **146** and **147** from α -santonin (2000).

2.2.2.5. Syntheses of guaianolides from α -santonin

Additional examples of guaianolide syntheses from α -santonin are listed in Figure 2.4, and those of guaianolide dimers can be found in Figure 2.5. The work from Ando and coworkers does not involve the aforementioned photo-induced rearrangement, instead, Ando and coworkers developed a 12-step process to achieve the [5,7,5]-fused tricyclic system from α -santonin.

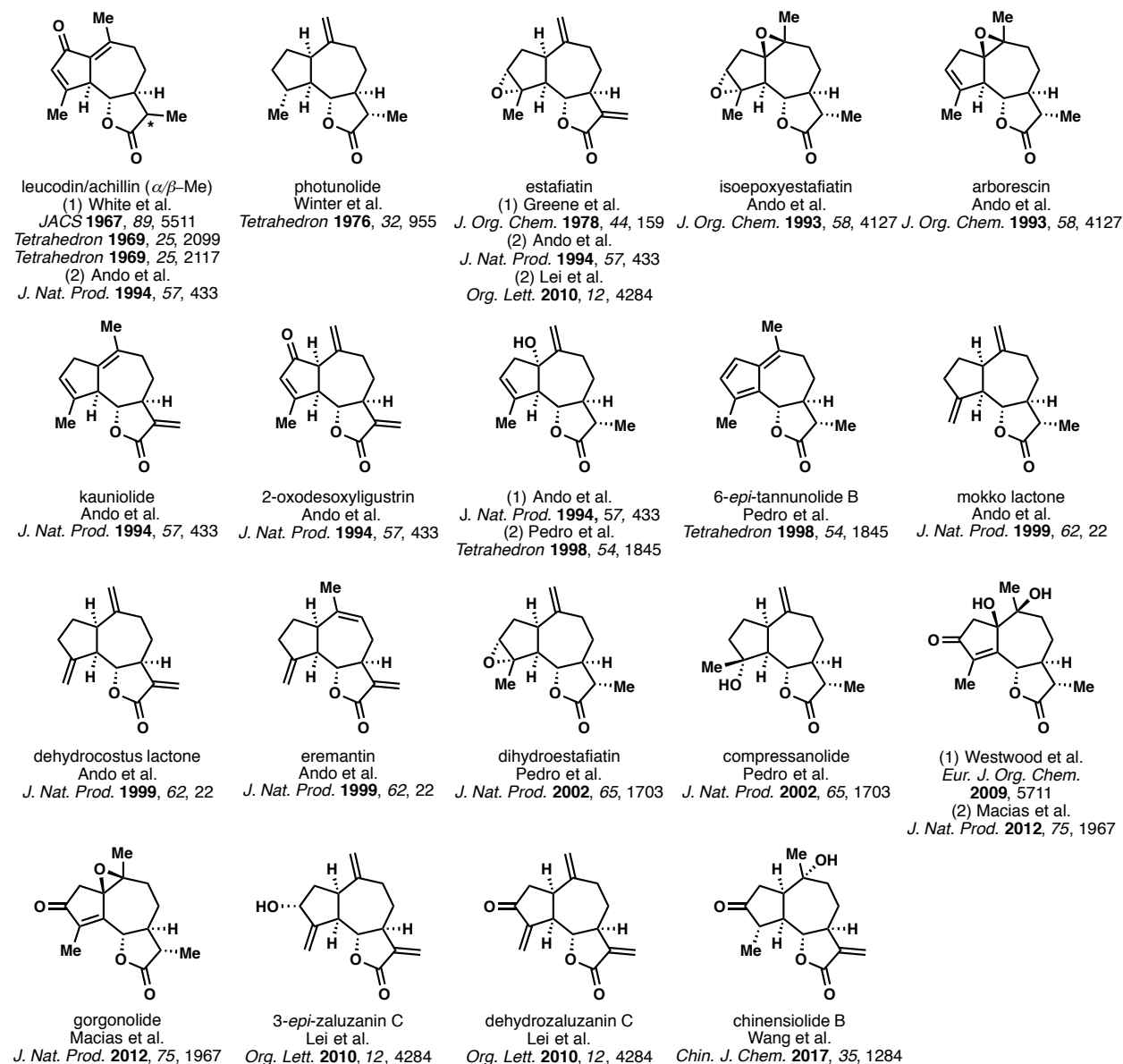
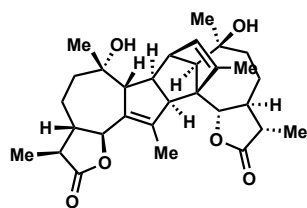
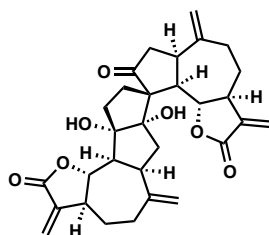


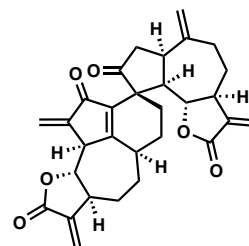
Figure 2.4. Additional examples of guaianolides synthesized from α -santonin.



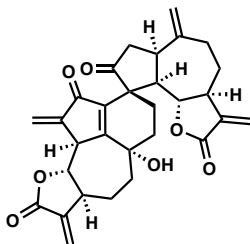
absinthin
Zhai et al.
J. Am. Chem. Soc. **2005**, *127*, 18



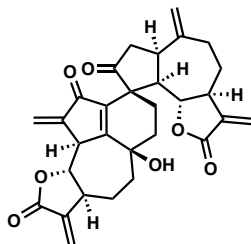
ainsliadimer A
Lei et al.
Org. Lett. **2010**, *12*, 4284



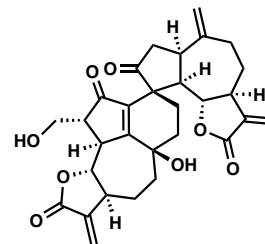
gochnatiolide C
Lei et al.
J. Am. Chem. Soc. **2012**, *134*, 12414



gochnatiolide A
Lei et al.
J. Am. Chem. Soc. **2012**, *134*, 12414



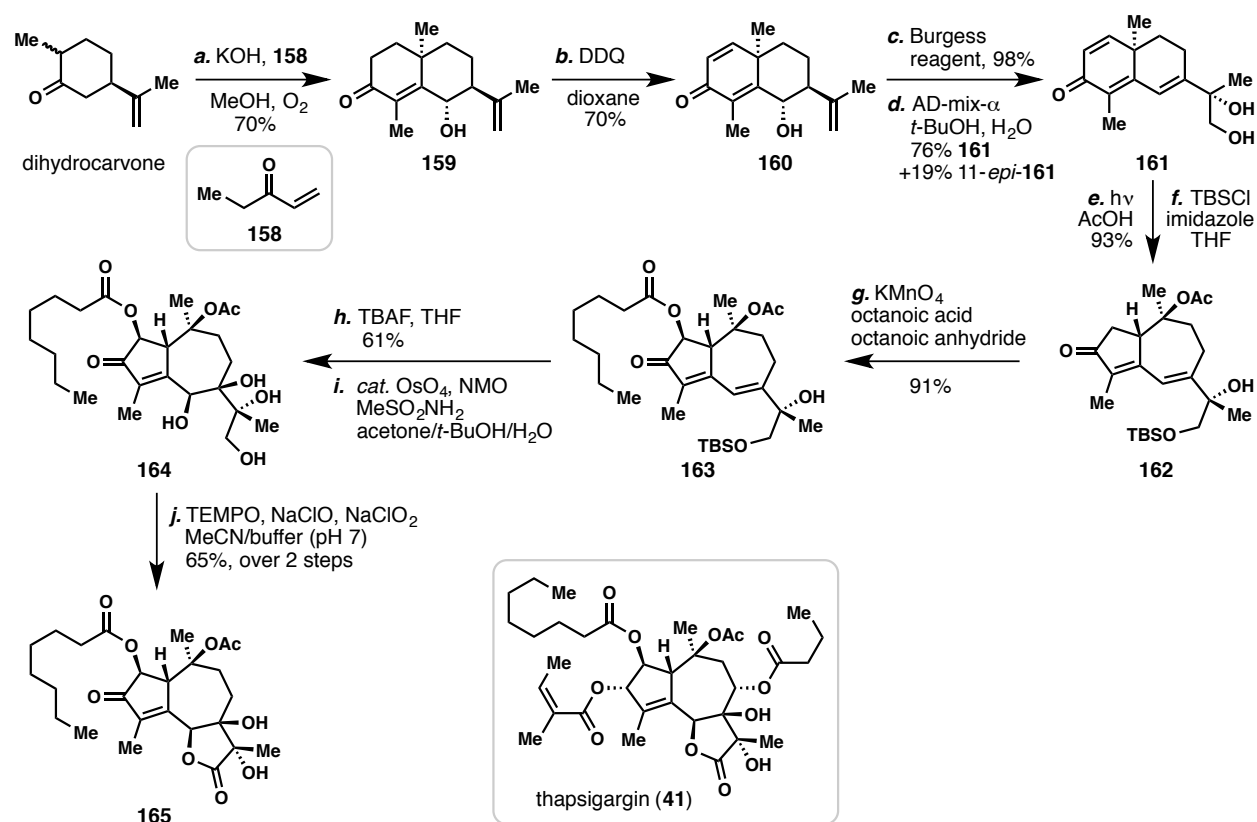
gochnatiolide B
Lei et al.
J. Am. Chem. Soc. **2012**, *134*, 12414



ainsliadimer B
Lei et al.
J. Am. Chem. Soc. **2012**, *134*, 12414

Figure 2.5. Examples of guaianolide dimers synthesized from α -santonin.

2.2.2.6. Massanet's synthetic study towards thapsigargin (2006, 2014)



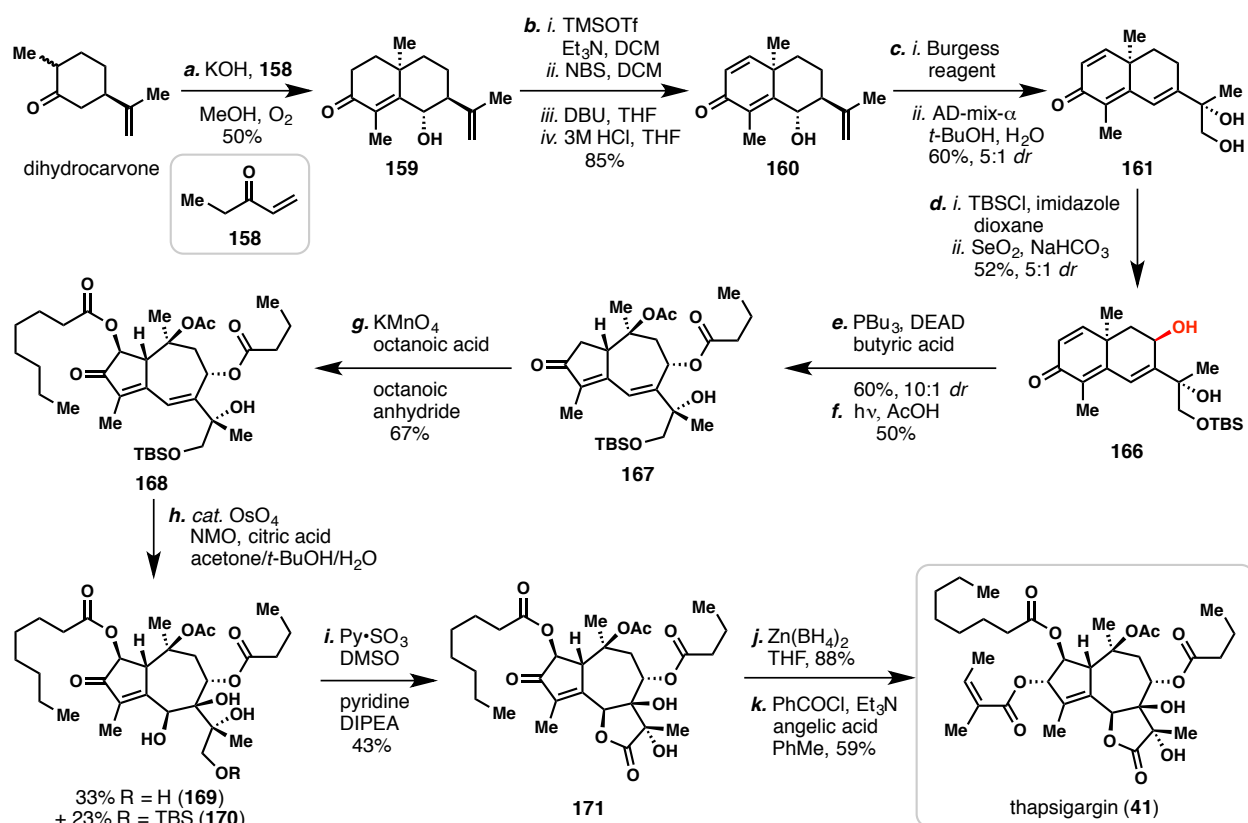
Scheme 2.12. Massanet's synthetic studies towards (–)-thapsigargin (**41**) from dihydrocarvone (2006, 2014).

Massanet and coworkers developed a highly efficient synthetic route towards thapsigargin (**41**) (Scheme 2.12).⁴⁸ The synthesis commenced with a modified Robinson annulation, joining dihydrocarvone with ethyl vinyl ketone (**158**). In the presence of O₂, the annulation condition (KOH, MeOH) also offered γ -oxygenation of the cyclized intermediate, affording **159** in synthetically useful yields. Dienone **160** was generated by DDQ oxidation, followed by two steps of redox manipulation, arriving at diol **161**. Photo-irradiation of this intermediate afforded a remarkable 93% yield of the desired [5,7]-fused bicycle, and after silylation, provided silyl ether **162**. In 2014, the authors updated the synthesis with the C-2 oxidation of **162** and various analogs. This condition efficiently provided octanoate **163** in 91% yield. Subsequent desilylation and Os-catalyzed dihydroxylation arrived at tetraol **164**, which could be directly oxidized in one step to lactone **165** (see also **83** \rightarrow **84**). Given that functionalization of the A ring from enone to allylic angelate is well known, this work only lacks one oxidation at C-8 to complete the total synthesis of **41**.

2.2.2.7. Baran's synthesis of thapsigargin (2016)

In 2016, Baran and coworkers completed the total synthesis of **41** in 12 steps based on precedent efforts in this field (Scheme 2.13).⁴⁹ It is worth noting that the authors expanded the definition of *step count* to tolerate rotary evaporation between conventional steps, for which

there is still ongoing debate in the synthetic community. After conversion of dihydrocarvone to dienone **161** similar to the previously discussed work of Massanet, Baran and coworkers applied a one-pot silylation and SeO₂-mediated allylic oxidation to install the prerequisite C-8 oxygen. The butyrate moiety was then assembled by a Mitsunobu reaction. Subsequent photo-induced rearrangement afforded **167** in moderate yields. Transformation of **167** to **171** was then achieved in three steps (see also **162** → **165**), followed by functionalization of the A ring, efficiently yielding thapsigargin (**41**) in overall 12 steps using the authors' definition of step count.



Scheme 2.13. Baran's total synthesis of (–)-thapsigargin (**41**) from dihydrocarvone (2016).

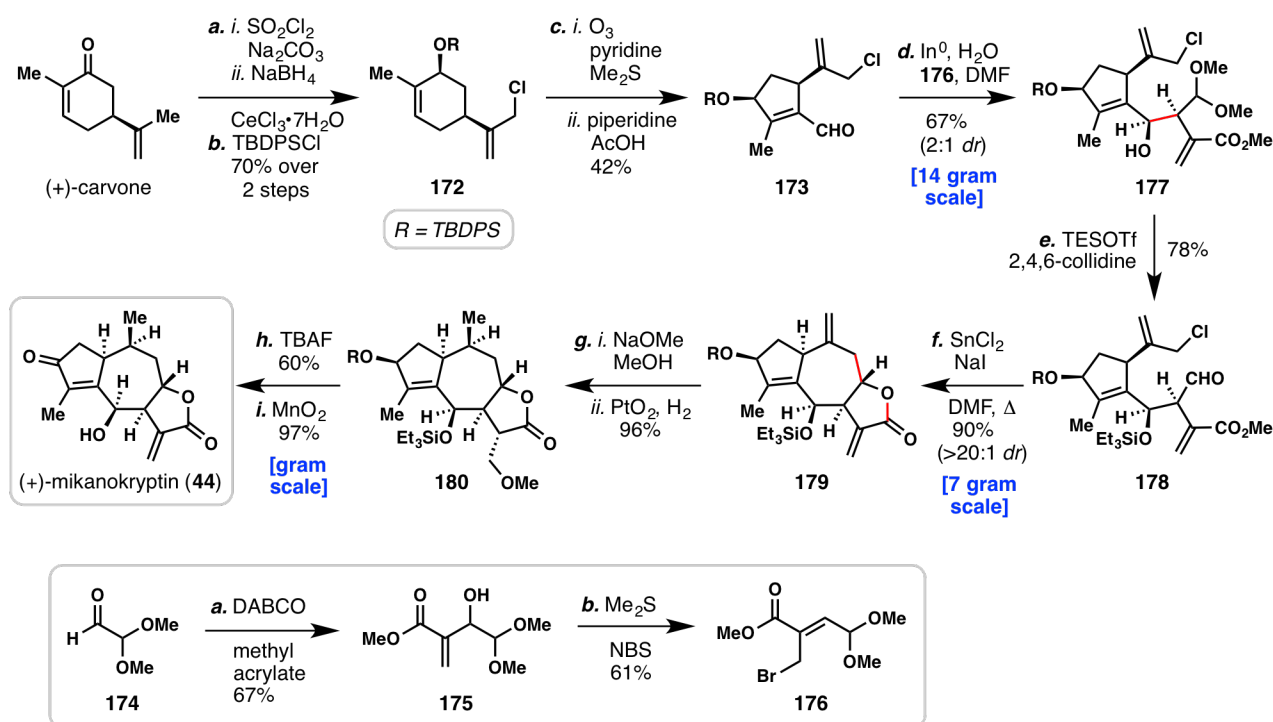
2.2.3 Studies Based on Ozonolysis of Carvone Derivatives

At the beginning of 2017, our research group (submitted Nov. 15, 2016) and Evans' group (submitted Feb. 18, 2017) published back-to-back work employing carvone-ozonolysis products of as the A-ring precursors to guaianolides.⁵⁰ The two syntheses utilized similar logic of bond disconnection, and are therefore both reviewed in this section. More details of my work on mikanokryptin (**44**) and thapsigargin (**41**) will be discussed in chapter 2.5 and 2.6.

2.2.3.1. Maimone's synthesis of mikanokryptin (2017)

Mikanokryptin (**44**) was isolated by Herz and coworkers in 1975 from *Mikania micrantha* (Asteraceae).⁵¹ Despite extensive spectroscopic and crystallographic studies of this complex 8,12-guaianolide,⁵² no chemical synthesis was available for ~40 years prior to our work, nor was the biological activity reported. Our synthesis commenced with a strategic activation of the preexisting isopropenyl moiety in carvone (Scheme 2.14). Similarly, activation of the prenyl moiety in terpene building blocks can be found in other work from our laboratory.⁵³ After a one-pot chlorination and Luche reduction, followed by silylation, silylated chlorocarveol **172** was ozonolyzed (O₃, pyridine; DMS) and subjected to *in situ* condensation (piperidine, AcOH), affording aldehyde **173** in 3 steps. Notably, **173** possesses the desired $\Delta_{4,5}$ -unsaturation, which could serve as complementary to Lee's intermediate **51** and Siegel's intermediate **112** in guaianolide syntheses.

Concurrently, we prepared allylic bromide **176** in 2 steps from commercially available aldehyde **174**.⁵⁴ The ten- and five-carbon fragments were then coupled by sequential allylations, assembling the tricyclic **179** in 3 steps from the two fragments. This work featured a tin(II)-mediated allylation that efficiently forged the cycloheptane B ring and lactone C ring in excellent

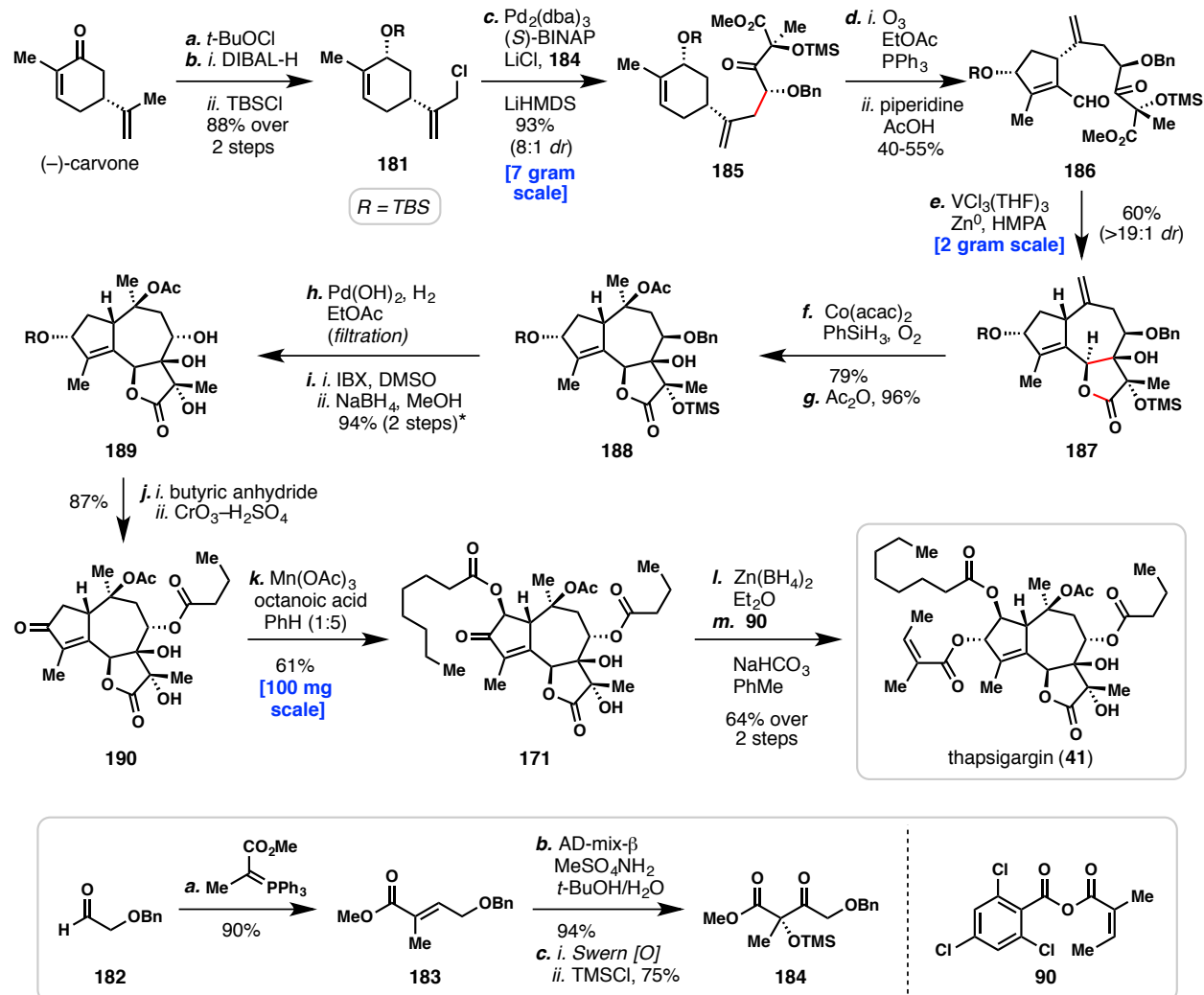


Scheme 2.14. Maimone's synthesis of (+)-mikanokryptin (**44**) from (+)-carvone (2017).

yield and with excellent diastereoselectivity. The remaining 3 steps of redox manipulations afforded mikanokryptin (**44**) in moderate to high yields. One gram of this complex guaianolide was prepared in our laboratory in one single batch. To this end, the synthesis of mikanokryptin (**44**) has enabled subsequent biological studies, which identified a protein target of this natural product.⁵⁵

2.2.3.1. Evans' synthesis of thapsigargin (2017)

Evans and coworkers also developed a two-pot procedure to prepare silylated chlorocarveol **181**, in which the sequence and protecting group were slightly altered (Scheme 2.15). Concurrently, the authors prepared β -keto ester **184** in 3 steps from commercially available aldehyde **182**. Although the authors claimed that the longest linear sequence begins at intermediate **183**, no information was provided indicating from which commercial source they acquired this material. To the best of my knowledge, one can only find **183** from exotic CRO companies in costly estimated prices.

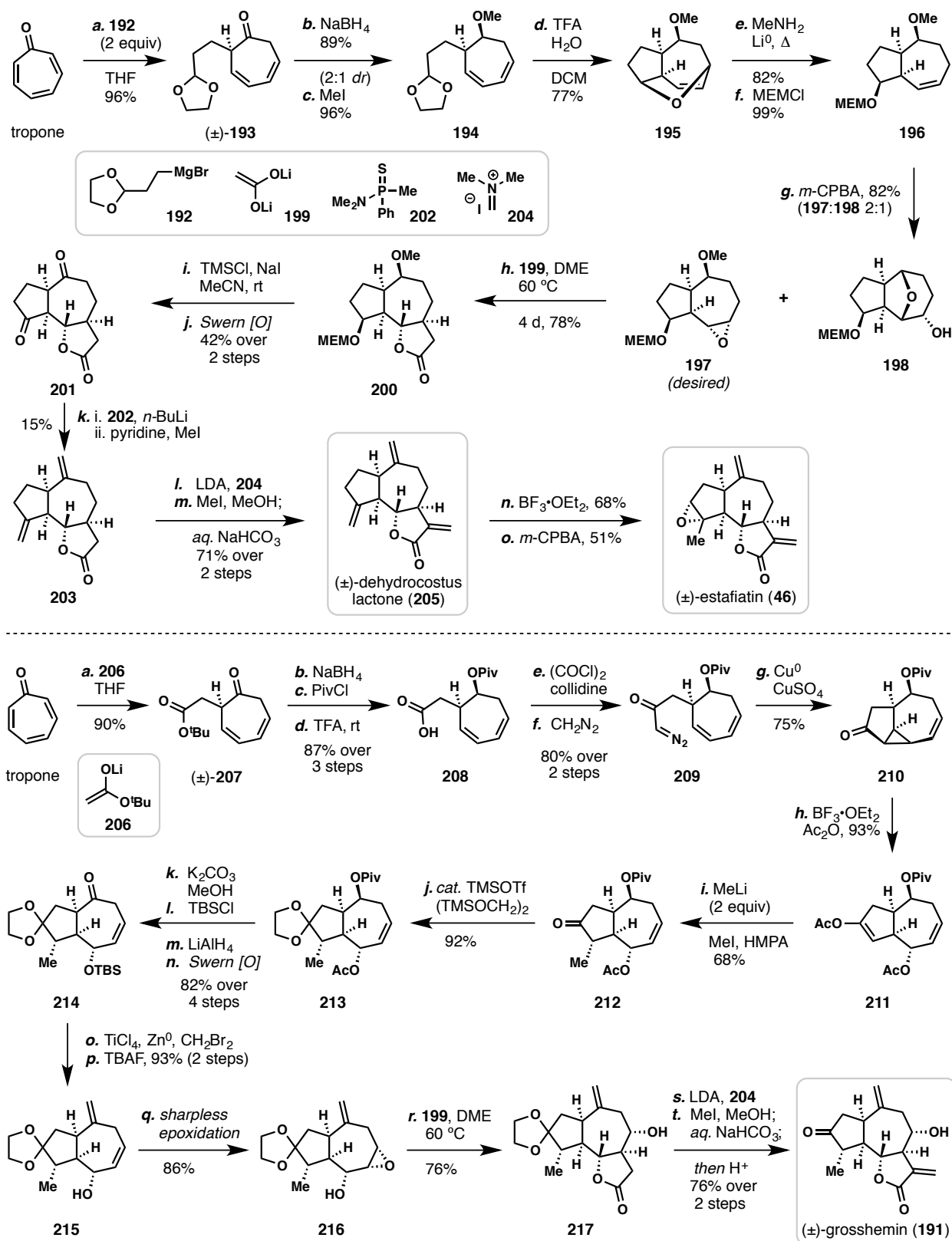


Scheme 2.15. Evan's synthesis of (-)-thapsigargin (**41**) from (-)-carvone (2017) (*steps *h* and *i* counted as one step by the authors).

The two fragments were subsequently coupled by a palladium-catalyzed enolate allylation in excellent yields. The resulting intermediate **185** was ozonolyzed (O_3 ; PPh_3) and condensed *in situ* (piperidinium acetate), affording aldehyde **186** in 2 steps. From this highly functionalized intermediate, vanadium(II)-mediated pinacol coupling conditions efficiently forged the cycloheptane B ring and lactone C ring, arriving at tricycle **187** in synthetically useful yields with excellent diastereoselectivity. Subsequent functional group manipulations provided acetate **188** in two steps. From this point, the authors developed a *one-step* process to generate the C-8 epimerized product **189**, which consisted of hydrogenative cleavage of the benzyl ether (Pd/C , H_2 , $EtOAc$), filtration to remove palladium on carbon, solvent evaporation, oxidation of the resulting alcohol (IBX , $DMSO$), and an *in situ* reduction ($NaBH_4$, $MeOH$). It is worth noting that here the authors further expanded Baran's definition of *step count* to tolerate both rotary evaporation and filtration.

From **189**, A one-pot esterification and oxidation delivered enone **190** in 87% yield. By modification of Christensen's C-2 oxidation conditions,⁵⁶ the requisite C-2 octanoate was successfully installed in 61% yield on a 100-mg scale, arriving at Baran's intermediate **171**. Subsequent 2 steps of A-ring functionalization offered thapsigargin (**41**). Overall, the Evans synthesis of **41** is highly efficient and scalable, and requires only 12 steps using the authors' definition of step count.

2.2.4 Studies Based on Other Building Blocks



Scheme 2.16. Rigby's total syntheses of guaianolides from tropone (1984, 1987).

2.2.4.1. Rigby's synthesis of estafiatin and grosshemin (1984, 1987)

In 1984 and 1987, Rigby and coworkers reported elegant total syntheses of (±)-estafiatin (**46**) and (±)-grosshemin (**191**) from the simple building block tropone (Scheme 2.16).⁵⁷ To date, estafiatin (**46**) has been synthesized by Vandewalle,⁵⁸ Rigby,^{57a} Greene,⁵⁹ Ando,⁶⁰ Lee,^{21b} and Lei;⁶¹ whereas the synthesis of grosshemin (**191**) has only been achieved by Rigby and coworkers.^{57b}

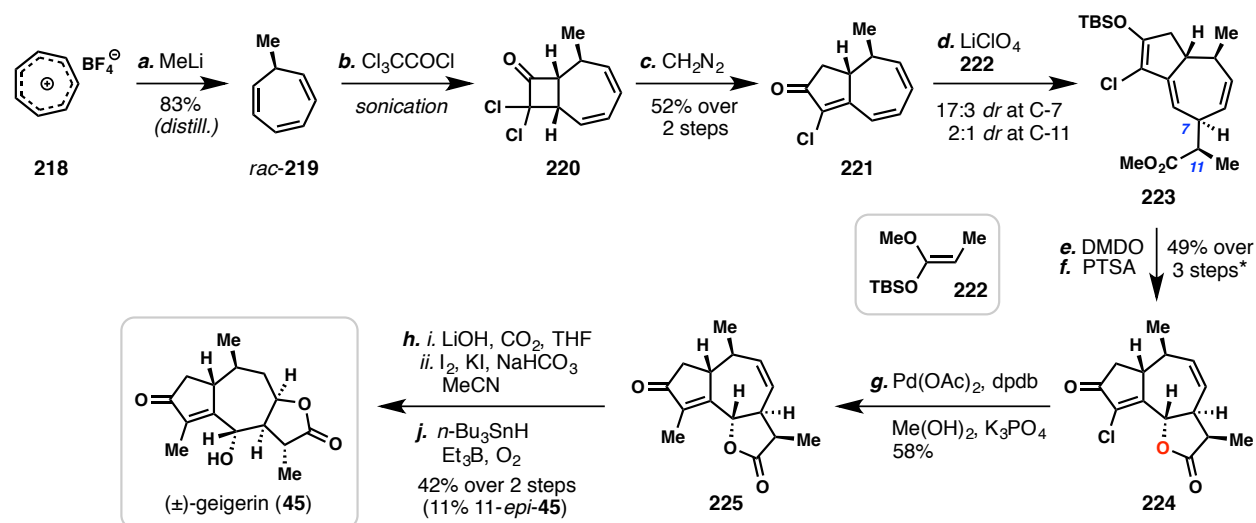
The synthesis of **46** began with a Grignard addition of **192** to tropone, and following reduction and methylation, racemic diene **194** was obtained in high yield. A highly efficient acid-mediated deacetalization with a simultaneous formal [4+2] cyclization of the aldehyde and diene rendered tricyclic ether **195** in 77% yield. A three-step sequence subsequently opened the bridged ether as well as generated the desired epoxide functionality, arriving at the [5,7]-fused bicycle **197**. From this intermediate, the *trans*-fused lactone moiety was assembled in one step by using a large excess of dilithioacetate (**199**), affording lactone **200** in 78% yield. Diene **203** was then synthesized in 3 steps from **200** via dual functionalization of the protected alcohols. From **203**, the requisite α -methylene moiety was generated via alkylation of the lactone with Eschenmoser's salt **204**,⁶² followed by treatment with the standard elimination conditions (MeI; then base). (±)-Dehydrocostus lactone (**205**) was thus prepared in 71% yield. Lewis acid-mediated olefin isomerization, followed by epoxidation with *m*-CPBA, converted **205** to **46** in a regioselective fashion.

Grosshemin (**191**) was isolated in 1964 by Rybalko and coworkers from *Grossheimia Macrocephala* (Asteraceae).⁶³ Rigby's synthesis of **191** commenced with the addition of nucleophile **206** to tropone, followed by functional group manipulations (3 steps), arriving at acid **206**; the diene moiety in this case remained unreactive under TFA-mediated conditions. The A ring was then strategically assembled by cyclopropanation via diazonium intermediate **209**, arriving at tricycle **210**. Treating this cyclopropane with BF₃•OEt₂ and acetic anhydride selectively incorporated the C-6 oxygen. In the presence of the C-6 acetate, activation of the vinyl acetate moiety (MeLi, MeI) highly efficiently afforded methylated product **212** in a remarkable 63% yield over 2 steps. After careful manipulation of functional groups, *trans*-fused lactone **217** was prepared in 10 steps from **212**. Eschenmoser methylenation and hydrolysis of the ketal protecting group subsequently delivered **191** in 76% yield from lactone **217**, thus completing an efficient total synthesis.

2.2.4.2. Deprés' synthesis of geigerin (2007)

In 2007, Deprés and coworkers reported a concise synthesis of (±)-geigerin (**45**) from tropylium cation **218** (Scheme 2.17).⁶⁴ A 3-step sequence consisting of methyl lithium addition, [2+2]-cycloaddition, and ring expansion provided the highly unsaturated [5,7]-fused bicycle **221**. A regio- and stereo-selective 1,6-addition of **221** was then achieved by using silyl enol ether **222** with weakly acidic LiClO₄, affording **223**, which could be selectively oxidized *in situ* with DMDO in a one-pot manner. Formation of the *trans*-fused 6,12-lactone (PTSA) proved essential for the following Suzuki coupling to install the requisite C-15 methyl group. When the oxygenated product (DMDO) or the corresponding acetate was treated with the Suzuki coupling conditions, extensive elimination at C-6 was observed. Finally, conversion of the Suzuki coupling product **225** to **45** was achieved in 2 steps via saponification, *in situ* iodo-lactonization,

and a radical-based reduction of the iodide intermediate (*n*-Bu₃SnH, BEt₃, O₂). Overall, **45** was synthesized in only 8 steps when one-pot procedures are considered.



Scheme 2.17. Deprés' synthesis of (\pm)-geigerin (**45**) from tropylium cation **218** (2007) (*step *d* and *e* can be conducted in one pot, 44% yield).

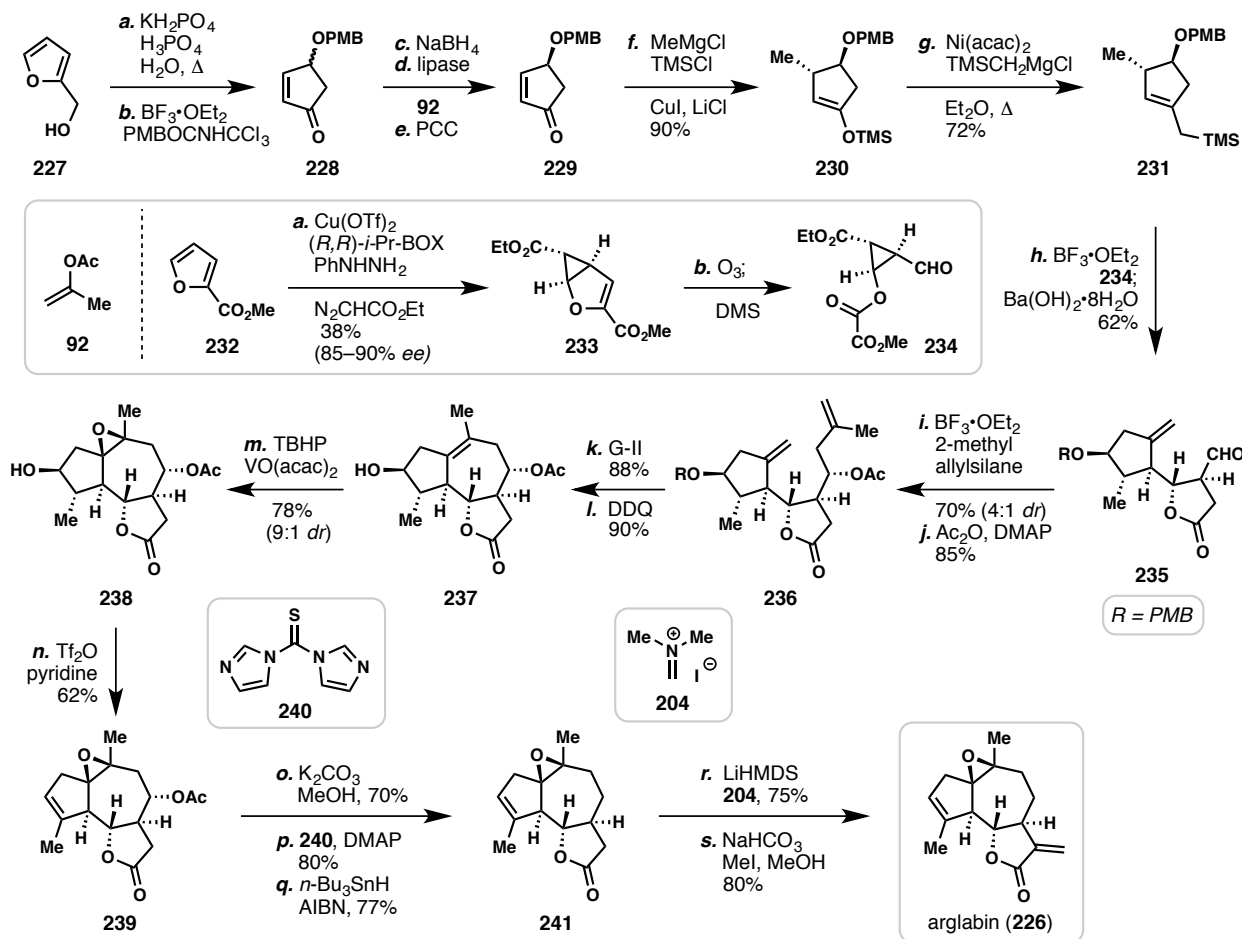
2.2.4.3. Reiser's synthesis of arglabin (2007)

Arglabin (**226**), a potent farnesyl transferase inhibitor,⁶⁵ was isolated in 1982 by Adekenov and coworkers from *Artemisia glabella* (Asteraceae).⁶⁶ In 2007, Reiser and coworkers reported an enantioselective total synthesis of **226** from furan-derived building blocks (Scheme 2.18).⁶⁷ From furan **227**, enantiopure enone **229** can be prepared in 5 steps via a kinetic resolution employing lipase and **92**.⁶⁸ Enone **229** was then converted into allylic silane **231** by a two-step sequence of cuprate addition and nickel-catalyzed cross coupling. Concurrently, copper-catalyzed cyclopropanation of furan **232** afforded **233** in high enantioselectivity, which enabled efficient preparation of enantiopure aldehyde **234** after ozonolysis. A highly stereoselective Hosomi–Sakurai reaction then coupled the two fragments **231** and **234**, and the resulting alcohol intermediate was treated with Ba(OH)₂·8H₂O *in situ*. The basic condition cleaved the oxalate and the newly generated cyclopropanol underwent spontaneous ring opening and formation of the 6,12-lactone, arriving at **235** in an efficient 62% yield. The cycloheptane B ring was then assembled via installation of the second alkene fragment, alcohol protection, and Grubbs ring-closure metathesis (RCM). Removal of PMB protecting group (DDQ) exposed alcohol **237** to the following vanadium-catalyzed directed epoxidation and elimination, affording epoxide **239** in moderate yields. A 5-step sequence of C-8 deoxygenation and the Eschenmoser methylenation ultimately produced **226** in overall 19 steps.

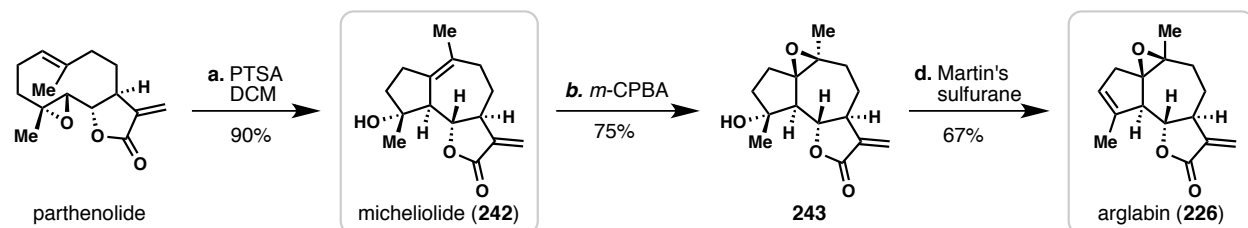
2.2.4.4. Zhang's semi-synthesis of arglabin (2012)

In 2012, the groups of Zhang and Chen reported a biomimetic synthesis of guaianolides micheliolide (**242**) and arglabin (**226**) from parthenolide (Scheme 2.19).⁶⁹ After screening various acidic conditions, the authors identified PTSA as the optimal catalyst to convert parthenolide to **242** in excellent yields. Epoxidation of **242** (*m*-CPBA) effortlessly afforded the

desired epoxide diastereomer, and treatment of **243** with Martin's sulfurane offered **226** in superior yields compared to other dehydrating conditions. It is worth noting that switching the sequence of epoxidation and dehydration led to severely diminished yield and diastereoselectivity in the epoxidation, which may give a hint towards the identification of its biosynthetic pathway. Exceptionally, the dimethylamine adduct of **242** developed by Chen and coworkers has entered clinical trials for selective inhibition of acute myelogenous leukemia stem and progenitor cells.^{9g}

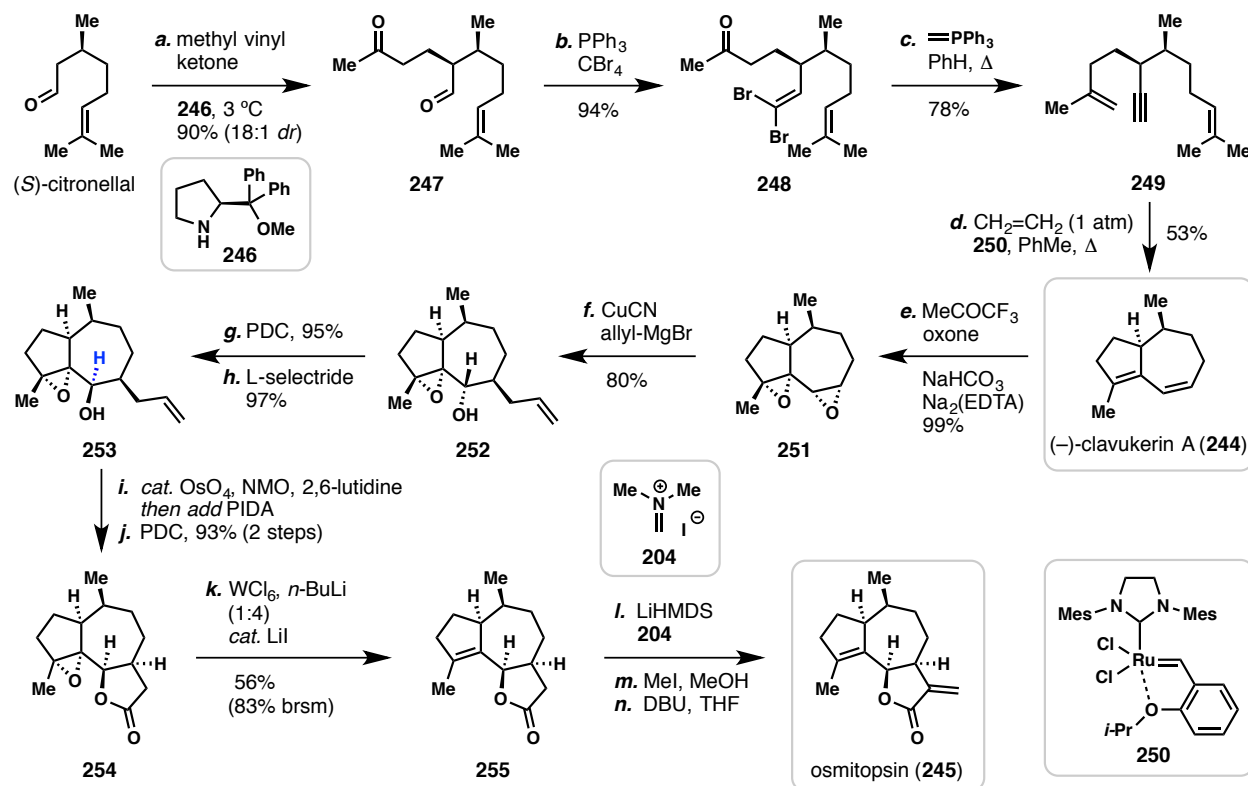


Scheme 2.18. Reiser's synthesis of arglabin (**226**) from furan-derived building blocks (2007).



Scheme 2.19. Zhang's semi-synthesis of arglabin (**226**) from parthenolide (2012).

2.2.4.5. Metz's synthesis of osmitopsin (2016)



Scheme 2.20. Metz's synthesis of (-)-clavukerin A (**244**) (2010) and osmitopsin (**245**) (2016) from (S)-citronellal.

Osmitopsin (**245**) and 4,5-epoxyosmitopsin were isolated in 1985 by Bohlmann and coworkers from *Osmitopsis asteriscoides* (Asteraceae).⁷⁰ In 2016, Metz and coworkers reported a total synthesis of **245** based on their previous work on (-)-clavukerin A (**244**),⁷¹ featuring a key enyne metathesis cascade in construction of the [5,7]-fused bicyclic natural product (Scheme 2.20). (S)-citronellal was employed in this synthesis to introduce the stereochemistry at C-10 and consequently at C-1. The authors also attempted to synthesize 4,5-epoxyosmitopsin, however the diastereomers prepared did not match the isolated guaianolide, a case similar to the report from Posner and coworkers.⁷²

From **244**, the authors developed an efficient diepoxidation, affording **251** in near quantitative yields. However, assembly of the *cis*-fused 6,12-lactone from the epoxide proved less straightforward in this case compared to the one-step transformation in Rigby's synthesis to construct the *trans*-fused lactone (see **197** → **200**). Here, a four-step sequence was utilized to synthesize *cis*-fused lactone **254** via epimerization of **252** to **253**. The Δ_{4,5}-unsaturation was then regenerated by Sharpless' condition involving lower-valent tungsten halides,⁷³ arriving at lactone **255**. The end game of this synthesis employed the venerable Eschenmoser methylation as well, yielding osmitopsin (**245**) in overall 14 steps.

2.2.5. Conclusion

A comprehensive review of the total syntheses and semi-syntheses of complex guaianolides published before the end of 2017 was provided. Two additional unique syntheses of Asteraceae guaianolides that we have not discussed are briefly presented below with highlights of the key steps (Figure 2.6).⁷⁴ Evidently, the synthetic field has primarily focused on the Asteraceae guaianolides, while the thapsigargin group represents the only members of the Apiaceae guaianolides that have been synthetically studied.

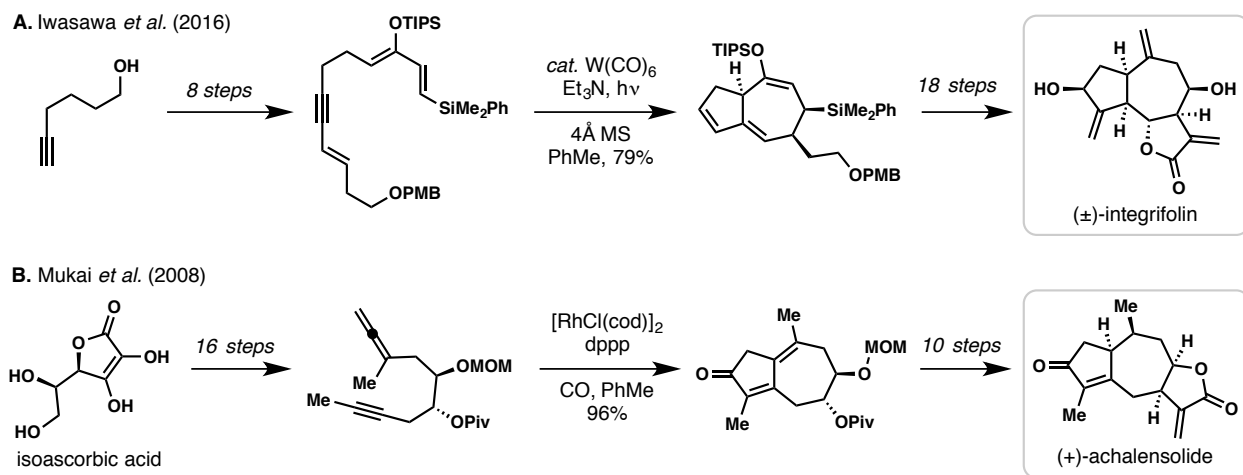


Figure 2.6. Iwasawa's synthesis of (±)-integrifolin (2016) and Mukai's synthesis of (+)-achalensolide (2008).

2.3 A Model Study for the Proposed Polyoxygenation Cascade

At the beginning of this research project, I conducted a model study to test the feasibility of the proposed polyoxygenation cascade on a santonin-derived intermediate **257** (Figure 2.7). The aim of this study was to evaluate: (i) the reactivity of the triene system under the metal-catalyzed hydroperoxidation conditions, specifically with regard to the chemoselectivity between the exocyclic C–C double bond and the electron-deficient butenolide moiety; (ii) whether the desired regioselectivity could be obtained in the addition of the peroxy radical, or the peroxy metallo species, to the remaining two C–C double bonds; and (iii) whether the final hydroxy group could be installed diastereoselectively in *trans*-configuration to the endoperoxide moiety.

The investigation commenced with the preparation of the model substrate **257** based on the modification of established protocols.^{37,61,75} The photochemical transformation of α -santonin to **119** was optimized on a 5-gram scale by using a 1:2:4 solvent mixture of TFA/H₂O/DME (0.15 M) (49% yield). After a SOCl₂-mediated elimination and Luche reduction, the resulting alcohol was silylated (TBSCl) and reacted under Greene's condition to provide butenolide **257**.⁷⁵

With butenolide **257** in hand, I initially screened three metal-catalyzed hydroperoxidation conditions employing Mn(dpm)₃, Co(acac)₂, and Fe(acac)₃ as catalysts. The cobalt-catalyzed conditions [Co(acac)₂, PhSiH₃, O₂] offered the desired endoperoxide **258** in ~10% isolated yield, along with a mixture of decomposition products. The condition employing Mn(dpm)₃ and PhSiH₃ under an oxygen atmosphere afforded mono-hydration product **259** (see Figure 2.8, 34% yield) and the undesired A-ring-cyclized endoperoxide (8% yield). The iron-based system [Fe(acac)₃, PhSiH₃, O₂] only resulted in extensive decomposition; the formation of **258**, **259**, or the undesired isomeric endoperoxide was not observed. To our delight, the stereoselectivity of the cobalt-catalyzed tandem peroxidation was suitable for the target synthesis, which was unambiguously determined by the X-ray diffraction of peroxide **258**.

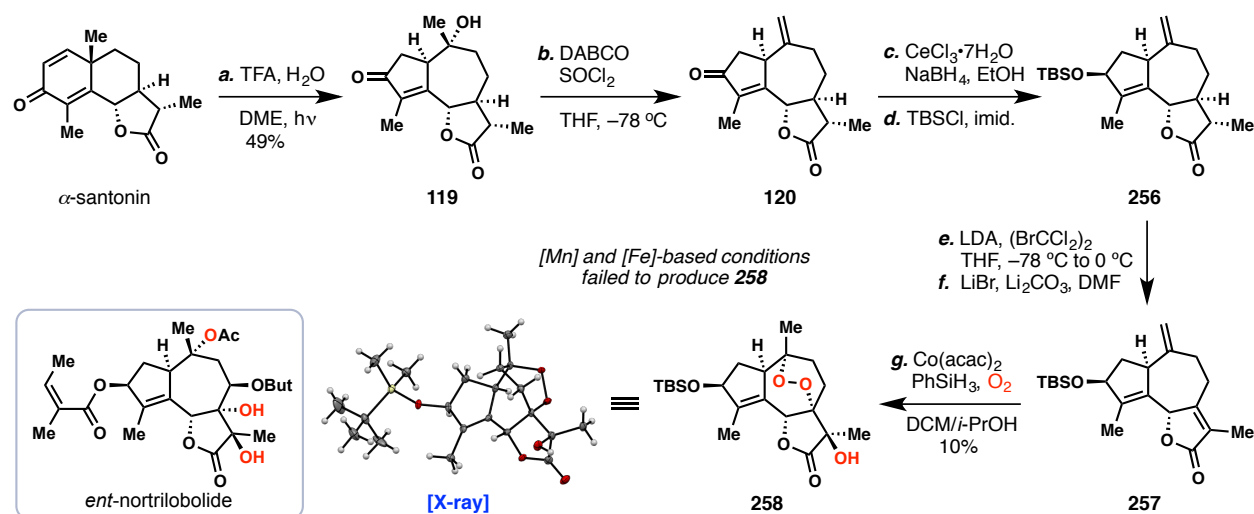


Figure 2.7. A model study of the proposed polyoxygenation cascade.

Although the initial result was promising, this model system lacks the C-8 oxygenation for the synthesis of nortrilobolide (**40**) and thapsigargin (**41**). To understand whether the presence of the C-8 oxygen affects the regio- and stereo-selectivity of this tandem peroxidation, I

then tried to install the requisite C-8 oxygen on butenolide **257** or **259**. Unfortunately, experimentation with these two intermediates failed to provide access to any C-8 oxidized products (Figure 2.8). With triene **257**, allylic oxidation, halogenation, and oxidative generation of the conjugated alkene were attempted,⁷⁶ however, the desired product was not observed in each case. When diene **259** was subjected to the oxidative conditions employing NBS/(BzO)₂ or PIDA/TBHP, the C-3 oxidized product (*i.e.* the corresponding enone) was isolated instead. Therefore, incorporation of amine-borane adducts as polarity reversal catalysts to the hydrogen abstraction conditions were examined in order to adjust the chemoselectivity.⁷⁷ Unfortunately, these conditions did not afford any desired oxidized or halogenated product.

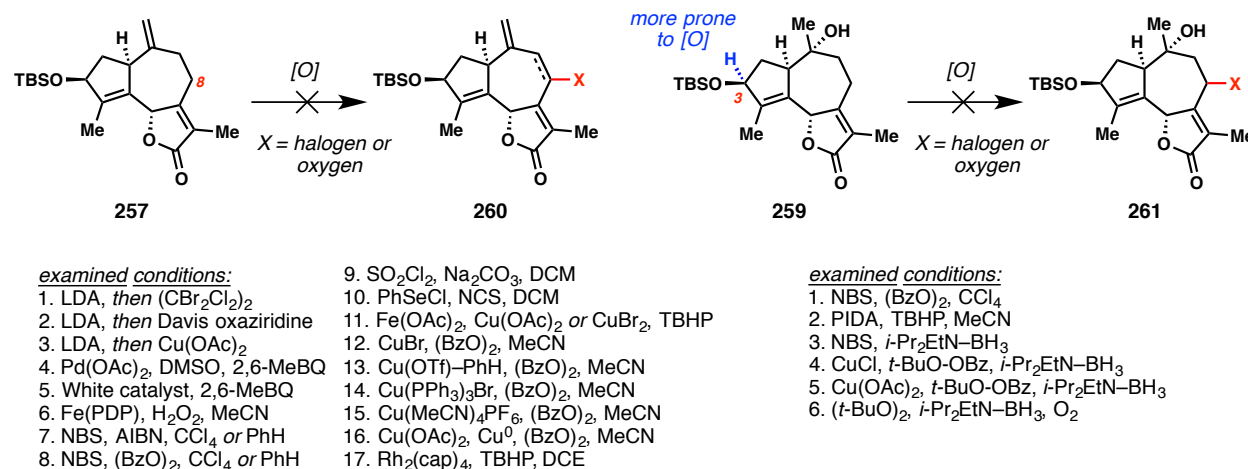


Figure 2.8. Failed attempts to install the C-8 oxygenation on model substrates **257** and **259**.

At this point, we decided to begin the studies towards the total synthesis of **40** and **41** from chiral-pool building blocks. I explored the possibilities of mapping carvone and linalool into the [5,7,5]-fused tricyclic system. The work starting from (+)- and (-)-carvone will be discussed in chapter 2.4-2.6, and the work based on (-)-linalool will be disclosed in chapter 2.7.

2.4 Initial Forays into the Construction of the [5,7,5]-fused Ring System

2.4.1 Synthetic Studies on 6,12-guaianolides

Our initial forays into the synthesis of nortrilobolide (**40**) and thapsigargin (**41**) using carveone as the building block began with the construction of precursor **263** with the preinstalled A-ring functionality. Considering the desire for $\Delta_{4,5}$ -unsaturation, a robust 3-step protocol was developed from (–)-carvone, inspired by precedent work with limonene (Figure 2.9).⁷⁸ It should be noted that at this point, **263** does not contain chlorination on the isopropenyl unit, a motif ultimately required for the synthesis.

Silyl ether **262** was prepared in 2 steps according to known procedures.⁷⁹ This intermediate was then ozonolyzed in the presence of catalytic quantities of pyridine (0.3 equiv),⁸⁰ resulting in chemoselective cleavage of the tri-substituted alkene under carefully monitored cryogenic conditions (8–10 minutes, $-78\text{ }^{\circ}\text{C}$). Extensive undesired oxidation of the isopropenyl moiety was observed under prolonged reaction times or in the absence of pyridine. Nevertheless, the sensitive dicarbonyl intermediate formed after the reductive quench (dimethyl sulfide) underwent intramolecular aldol condensation in the presence of piperidine and acetic acid, affording $\Delta_{4,5}$ -unsaturated aldehyde **263**.

From this key intermediate, I examined various sp^2 -centered nucleophiles for the assembly of the C-ring butenolide. Vinyl triflate **265**, for example, was prepared in two steps from commercially available ester **264**. Claisen condensation of **264** with methyl propionate under basic conditions offered the corresponding β -ketoester on large scales,⁸¹ which was then deprotonated (NaH) and treated with triflic anhydride, affording triflate **265** as a 5:2 mixture of Z/E isomers. Other triflating conditions employing lithium diisopropylamide (LDA) or 2,6-di-*t*-butylpyridine as base, or PhNTf_2 as the triflate source, failed to provide the desired product. Subsequently, the Nozaki–Hiyama–Kishi coupling⁸² successfully connected the two fragments **263** and **265** into butenolide **266** in one step with suitable stereoselectivity and in synthetically useful yields.

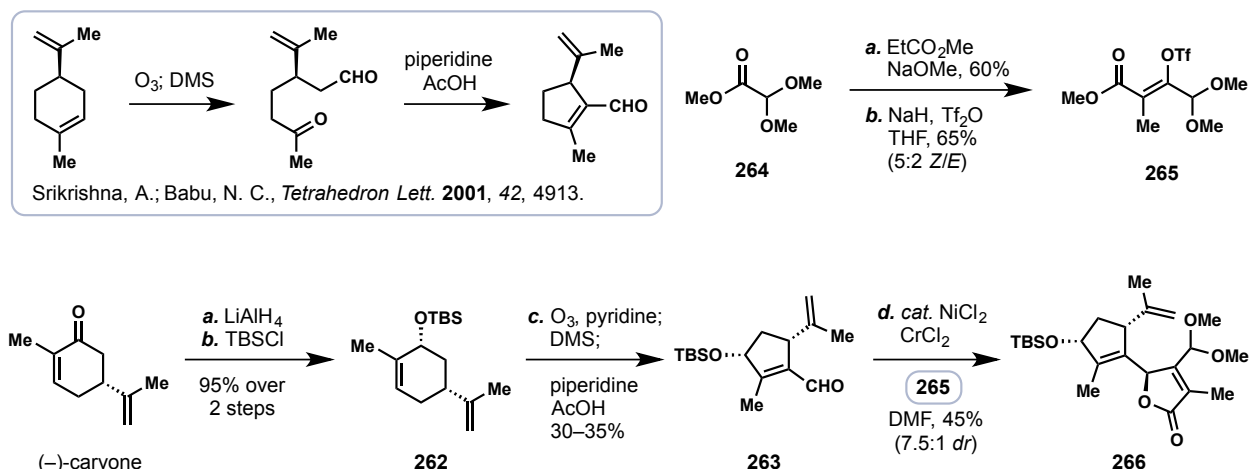


Figure 2.9. Assembly of the A and C rings from carveone and vinyl triflate **265**.

With butenolide **266** in hand, our initial attempts focused on removal of the acetal moiety to unveil aldehyde **267** for a subsequent Prins-type cyclization⁸³ (Figure 2.10). Unfortunately,

this deacetalization was not straightforward. Under mildly acidic conditions employing amberlyst resin or *p*-toluenesulfonic acid (PTSA), **266** underwent desilylation while the acetal moiety remained unreacted. Other conditions resulted in either no conversion of the starting material (entries 3-5) or extensive decomposition to a complex mixture of undesired products (entries 6-11).⁸⁴ Efforts to utilize nickel-catalyzed functionalization of the acetal also proved unsuccessful (entry 12).⁸⁵ Presumably, the electron-deficient butenolide moiety inhibits the formation of an oxonium ion at the C-8 position, which is crucial to initiate the deacetalization process (entries 1-11). It is worth noting that the identity of the major product from the TFA/H₂O system (entry 7), which has a bright yellow color, remained mysterious for a period of time; it was later determined to be **271** with more knowledge gained from the subsequent studies.

The focus of my research then turned towards converting the butenolide moiety into an electron-rich siloxy furan system in order to facilitate the deacetalization. In a key experiment, the butenolide **266** was first treated with TIPSOTf in the presence of triethylamine (in excess) to generate a triisopropylsiloxy furan intermediate. Subsequent addition of more equivalents of TESOTf then triggered the deacetalization,⁸⁶ affording furanyl aldehyde **269** in 50% yield. In contrast, when **266** was treated with TIPSOTf or TBSOTf in the absence of TESOTf, the corresponding silyloxy furan was obtained in high yields while the acetal was not removed. Treating **266** with TESOTf as the silylating agent only led to extensive decomposition, presumably due to the instability of the triethylsiloxy furan intermediate. Subsequently, aldehyde **269** was subjected to Lewis acid [TiCl₂(*i*-PrO)₂] to examine the formation of the last C–C bond. The Prins-type cyclization occurred under this condition, which was, however, followed by a concomitant elimination at the C-3 position and alkene isomerization, affording the highly conjugated tetraene **271** along with minor alkene isomers.

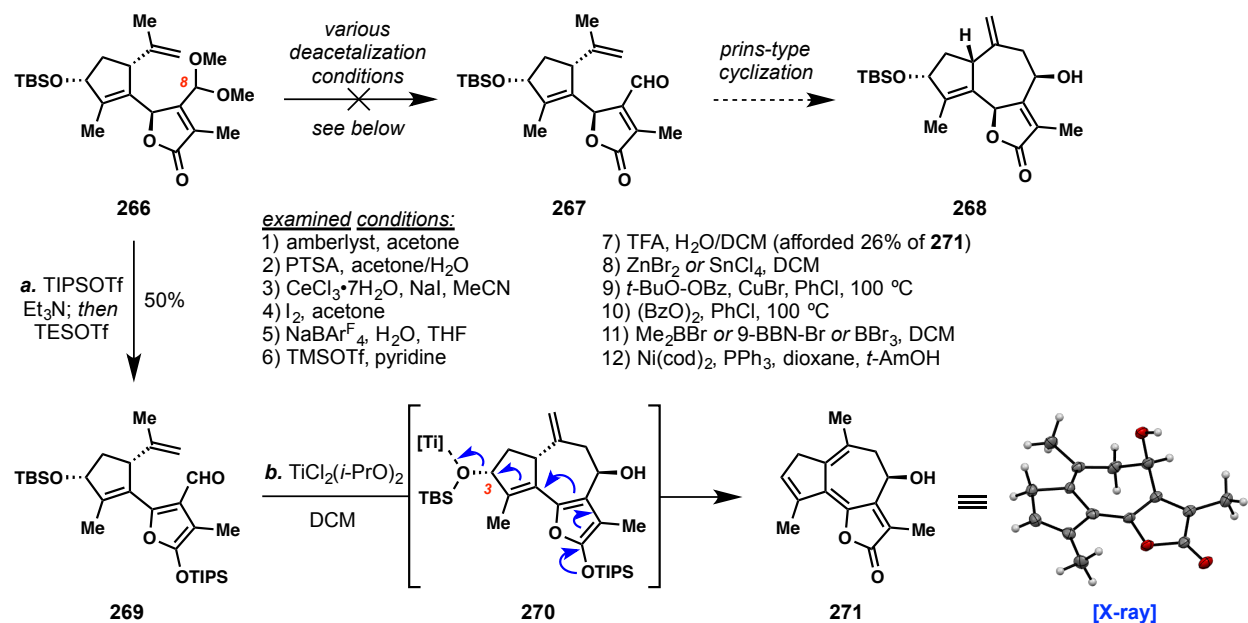


Figure 2.10. A Prins-type cyclization led to simultaneous elimination and isomerization.

This result suggested to us that the the hypothetical intermediate **270** might be labile to acid, therefore an alternative Barbier allylation strategy was pursued (Figure 2.11).⁸⁷ Allylic chlorination of aldehyde **269** (SO₂Cl₂, Na₂CO₃, 23 °C) resulted in extensive decomposition,

whereas the same condition applied to butenolide **266** provided the chlorinated product **272** as an inseparable mixture of regioisomers (2.5:1) in 40% yield. Variation of base (Et₃N, DIPEA, pyridine, and 2,4,6-collidine) or reaction temperature (−78 °C, −20 °C, 0 °C) from the aforementioned condition (SO₂Cl₂, Na₂CO₃, 23 °C) did not improve the yield or regioselectivity. Nevertheless, mild chlorinating condition employing trichloroisocyanuric acid (TCCA)⁸⁸ enhanced the selectivity (6.5:1) of this transformation with an improved 68% yield. Allylic chloride **272** was then treated with the same one-pot process of silylation/deacetalization (TIPSOTf, Et₃N; then TESOTf), affording aldehyde **273** in 65% yield. At this stage, the two alkene isomers could be separated. Subsequently, I examined the Nozaki–Hiyama–Kishi condition on this sensitive intermediate **273**, and obtained small amounts of the cyclized product **270** as a single diastereomer (7%, unoptimized). The unstable tricycle **270** was then subjected to the desilylating condition (TBAF) in order to regenerate the butenolide moiety. Unfortunately, this condition afforded a complex mixture, in which the major product was recognized as **271**. The anionic intermediate **274** appeared to favor the elimination at C-3 as well, instead of the protonation at C-6, and the ensuing alkene isomerization then led to various decomposition products. Nevertheless, the small amount of **271** prepared from **270** was subjected to X-ray analysis, and the stereochemistry at C-8 was unambiguously determined as shown. Notably, this intermediate also has the potential to be used in the preparation of highly unsaturated guaianolide malaphyllidin (**275**).⁸⁹

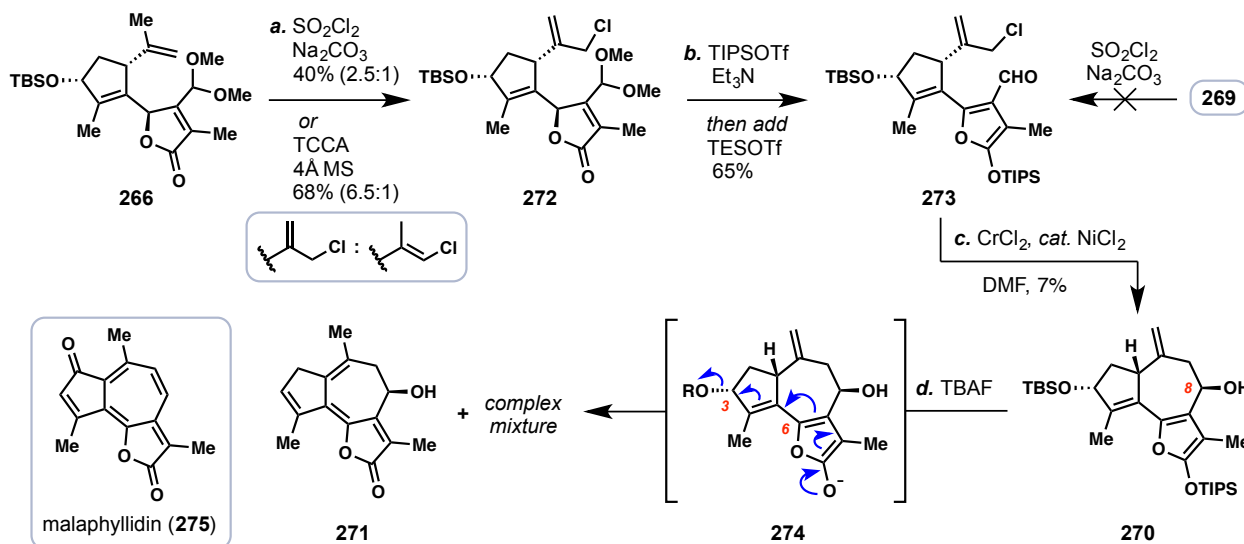


Figure 2.11. A Barbier-type cyclization with an undesired elimination.

Given the general instability of the 2-silyoxy furan intermediates, the conversion of butenolide **266** to relatively stable furanyl aldehyde **276** was also investigated (Figure 2.12). This transformation was achieved by reduction of **266** to the corresponding lactol intermediates, followed by treatment with mildly acidic amberlyst resin. A brief screening of conditions to promote the subsequent Prins-type cyclization did not provide isolable amounts of tricycle **277**. The alternative strategy featuring an intramolecular Barbier allylation led to success in forging the cycloheptane ring found in **277**. However, tricycle **277** again was found to be highly unstable, and decomposed to artemazulene (**279**) in slightly acidic CDCl₃ or neat over extended time. Artemazulene (**279**) is a minor component (~1%) of the *Artemia* essential oil with a blue color,

and served as the characteristic downstream product in detection or identification of guaianolide natural products after a deliberate dehydrogenation (Pd/C, heat).⁹⁰

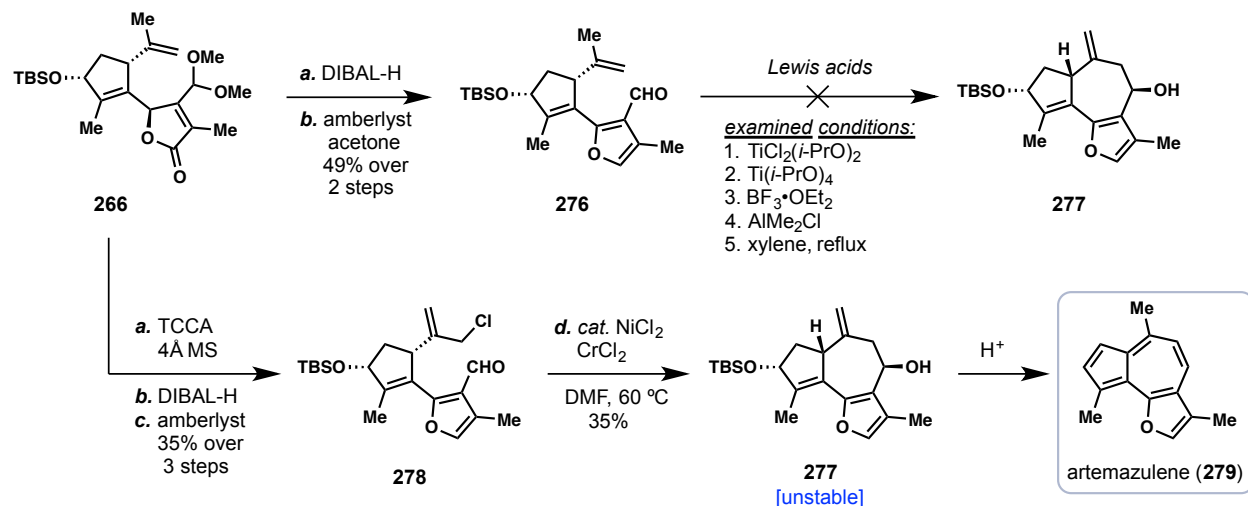


Figure 2.12. Reduction of the butenolide moiety led to furan formation.

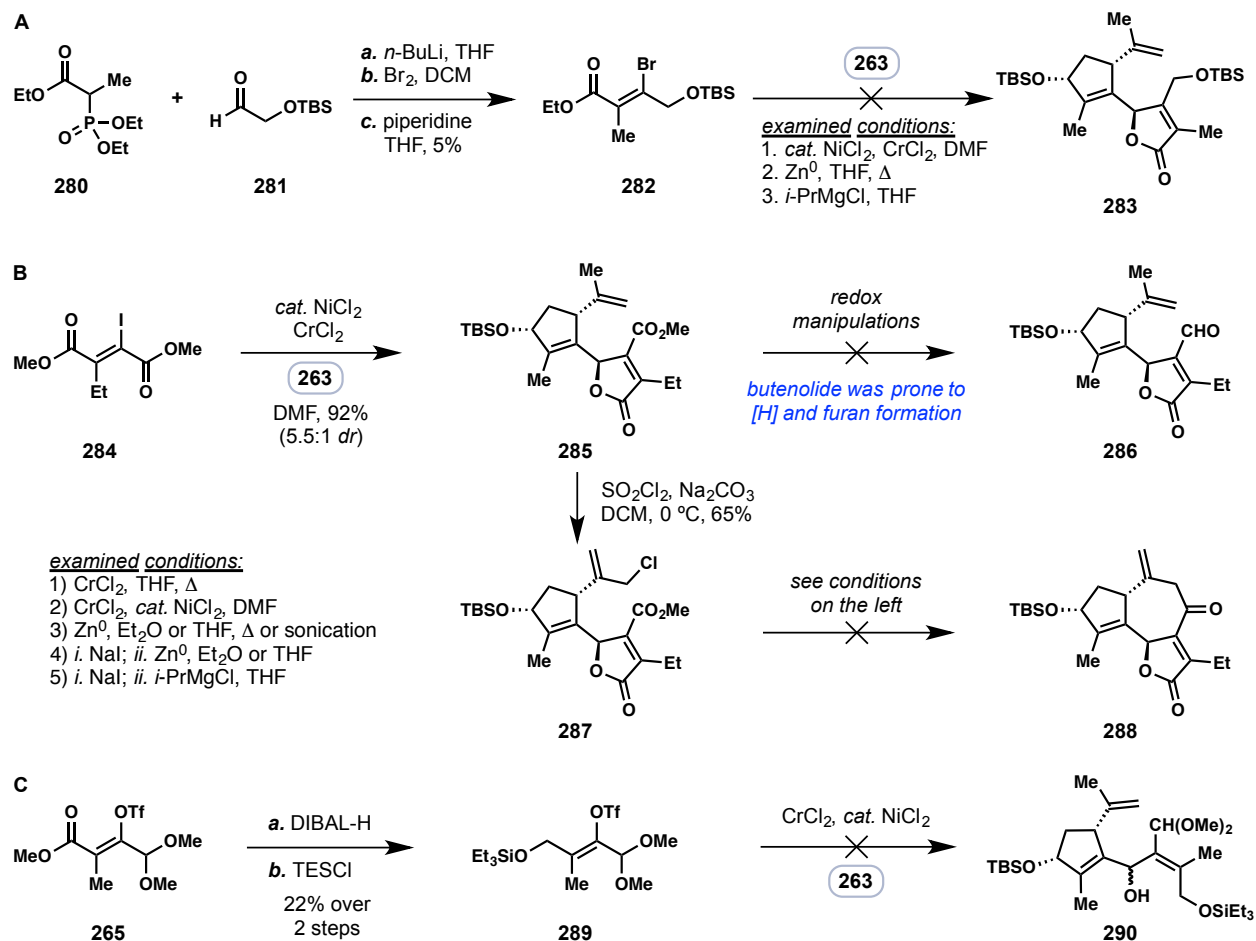


Figure 2.13. Failed strategies with various five-carbon coupling partners.

Last but not least, the coupling of aldehyde **263** with other nucleophiles was also examined, which were generated *in situ* from vinyl bromide **282**,⁹¹ vinyl iodide **284**,⁹² and vinyl triflate **289**, respectively; each of these fragments possesses altered oxidation state and distinct reactivity (Figure 2.13). Experimentation with these fragments failed either in the coupling of two building blocks (Figures 2.13A and 2.13C), or in forging the seven-membered B ring (Figure 2.13B).

2.4.2 Synthetic Studies on 8,12-guaianolides

Besides our initial foray into 6,12-guaianolides, I also investigated several initial strategies towards the synthesis of 8,12-guaianolides (Figure 2.14). Common building block **263** was examined with dihydrofuran (**291**) for a tandem addition/cyclization process (Figure 2.14A). No coupled product was observed however in the presence of various Lewis acids. A similar strategy of adding dioxene-derived lithiate **294** to aldehyde **263**, followed by acid-induced elimination and Prins-type cyclization, failed in forging the desired tricycle **297** as well. Alcohol intermediate **295** underwent dehydration and *in situ* hydrolysis under conditions employing strong Lewis acids [Et_2AlCl , AlMe_3 , $\text{BF}_3\cdot\text{OEt}_2$, or $\text{TiCl}_2(i\text{-PrO})_2$], thus affording aldehyde **298**, as well as its alkene isomer **299**.

At this stage of our research, the chlorinated ten-carbon fragment **173** had emerged as a desirable building block alternative to aldehyde **263** in response to the studies employing the intramolecular Barbier allylation. In preliminary studies using aldehyde **173**, bromofuran **300** was employed as the five-carbon fragment, which could be prepared by silylation of the corresponding bromobutenolide (TIPSOTf, Et_3N).⁹³ A lithium-halogen exchange of **300** followed by the addition to aldehyde **173** cleanly provided the coupled product **301** as a mixture of diastereomers (70% yield, 10:3 *dr*). However, attempts to perform the Finkelstein reaction on **301** resulted in undesired desilylation, and subsequent treatment with base (DBU) failed to regenerate the C-nucleophile on the butenolide unit. Instead, an intramolecular O-allylation was observed.

In an alternative strategy for assembling the seven-membered ring, aldehyde **173** was first protected by TMSCN under solvent-free conditions,⁹⁴ followed by the addition of NaI and acetone. The crude mixture was then immediately treated with silver(I) trifluoroacetate and bromofuran **300**,⁹⁵ affording **305** as a mixture of diastereomers (32% over 2 steps, 1:1 *dr*). Both isomers were subjected to the Nozaki–Hiyama–Kishi condition, but only trace amounts of the desired product **303** could be obtained. The majority of the bromide was reduced under these conditions, presumably due to the presence of the acidic proton on the butenolide moiety, which quenched the active chromium species.

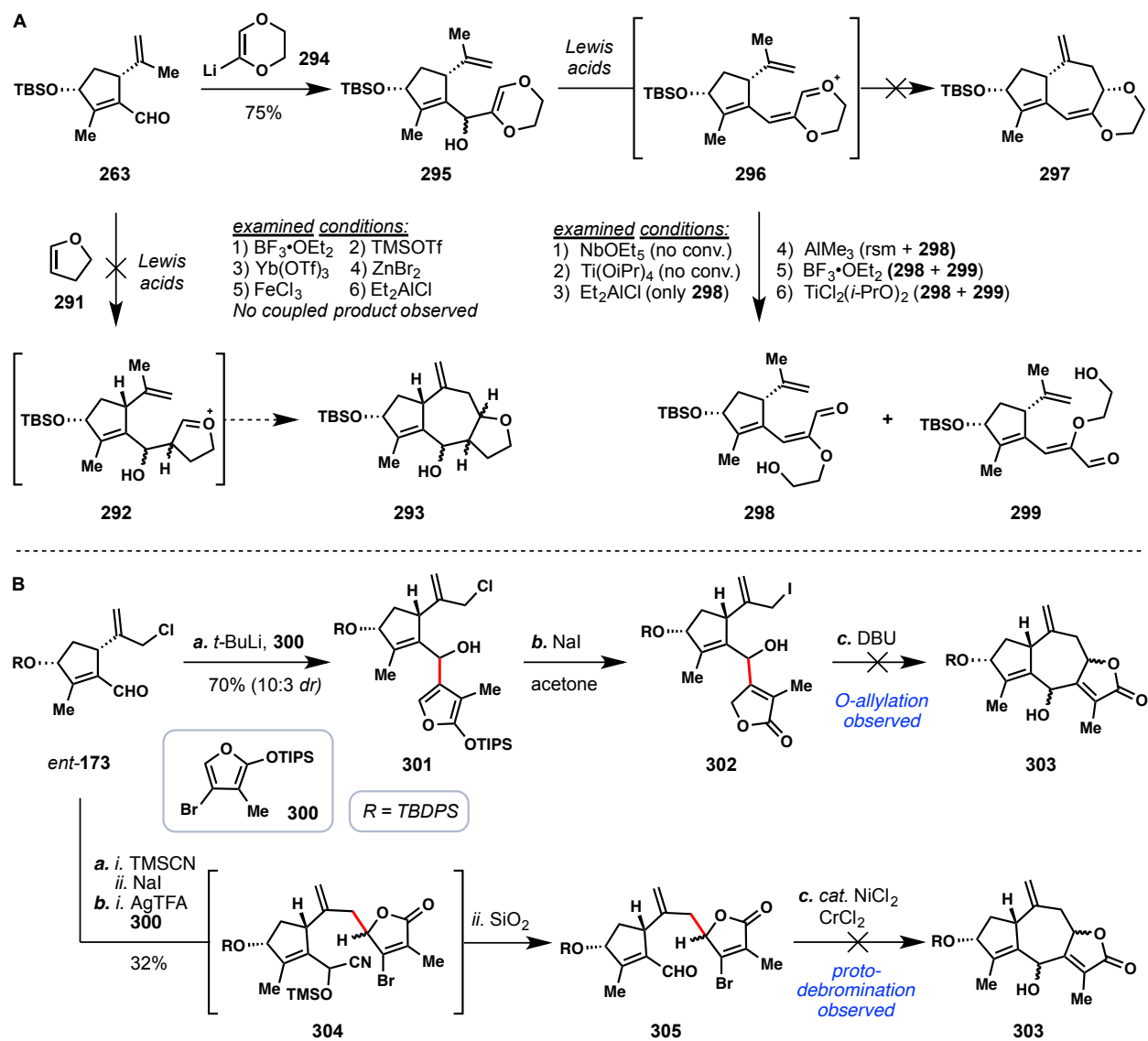


Figure 2.14. Failed attempts in forging the [5,7,5]-fused tricyclic system of 8,12-guaianolides.

2.5 Revision of the Synthetic Plan: A Double Allylation Strategy for Efficient and Scalable Guaianolide Production

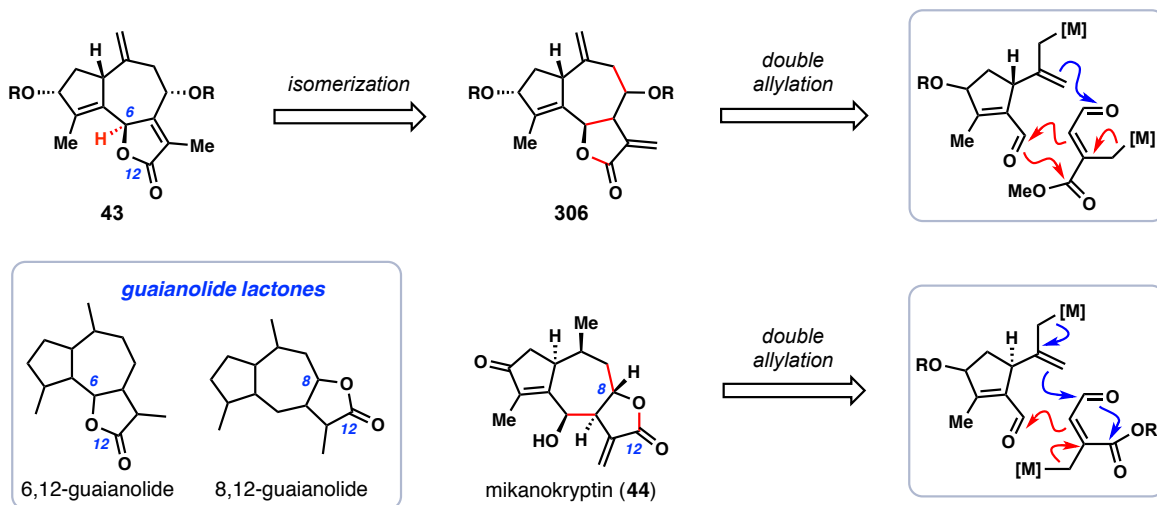


Figure 2.14. A double allylation strategy for the syntheses of 6,12- and 8,12-guaianolides.

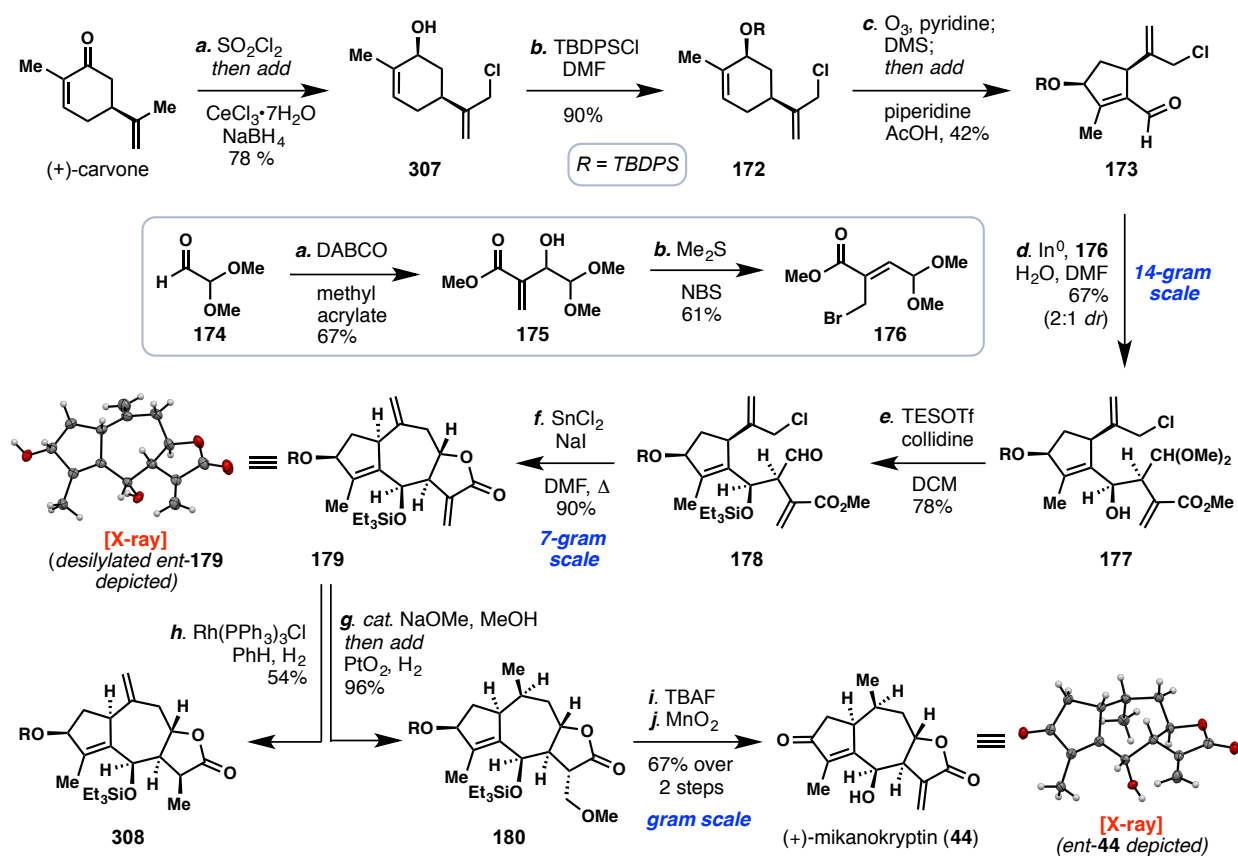
The initial studies discussed in section 2.4.1 have clearly demonstrated the acid- and base-sensitivity of the carbocyclic system related to the hypothetical substrate **43**, particularly at the doubly allylic C-6 position. Therefore, we revised our synthetic plan from assembly of the butenolide moiety at an early stage, to a late-stage isomerization of alkene isomer **306**. In this case the lactone intermediates would potentially be more stable and easily handled.

With this modified blueprint, we envisioned a double allylation strategy for the construction of guaianolides. For 6,12-guaianolides, the first allylation of an aldehyde precursor could ideally assemble the C-ring lactone in one step,⁹⁶ and we have demonstrated the feasibility of the second allylation in the previously discussed work featuring the intramolecular Barbier reaction in the B-ring construction. By tuning the position of lactone formation, 8,12-guaianolides may also be assembled accordingly. Ultimately, this strategy has enabled the total synthesis of mikanokryptin (**44**), nortrilobolide (**40**), and a formal synthesis of thapsigargin (**41**). In this section, I will focus on the synthesis of the 8,12-guaianolide mikanokryptin (**44**).

In our synthesis of **44** (Scheme 2.21), (+)-carvone was initially chlorinated at the isopropenyl moiety (SO_2Cl_2 , Na_2CO_3), and then subjected to Luche reduction conditions *in situ* ($\text{CeCl}_3 \cdot 7\text{H}_2\text{O}$, NaBH_4). This one-pot procedure afforded chlorinated *cis*-carveol **307** reliably on 30-gram scales in ~80% yields. Alcohol protection of **307** with *tert*-butyldiphenylsilyl chloride cleanly afforded silyl ether **172** in excellent yields (90~99%). Ozonolysis of **172** in the presence of catalytic quantities of pyridine (30 mol%), followed by reductive quenching with dimethyl sulfide, and intramolecular aldol condensation in the presence of catalytic amounts of piperidine and acetic acid, afforded enal **173** in a one-pot procedure. Large quantities of **173** (~200 g) have been synthesized in our laboratory through this three-step procedure.

Allylic bromide **176** was subsequently chosen as the allylation precursor, in analogy to vinyl triflate **265**. By adapting Hoffman's protocol,⁵⁴ **176** could be readily prepared in two steps on 30-gram scales from commercially available materials. For mikanokryptin (**44**) and related guaianolides, a *cis* arrangement at the junction of C-6 and C-7 between the hydroxy group and the neighboring acrylate group is required for the construction of the seven-membered B ring.

Previous work relied heavily on the inversion or epimerization of *trans*-configured precursors, as was reviewed in chapter 2.2. Nevertheless, allylic bromide **176** functioned well in setting the desired *cis* configuration. Under indium-mediated Barbier conditions,⁹⁷ **176** could be chemoselectively activated in the presence of allylic chloride **173**, and the proposed allylic indium species could then add to the aldehyde moiety to give **177** (2:1 *dr*) in 67% yield on a decagram scale. Inspection of the other reductive conditions based on Cr, Zn, Pd, Cd, Sn, Pb, and Bi failed to improve the yield or diastereoselectivity.^{96c, 98} It is worth noting that visiting scholar Dr. Silong Xu discovered the importance of adding one equivalent of H₂O during his optimization of this transformation on large scales. The presence of H₂O prevented the rapid formation of the undesired 6,12-lactone framework, whereas excess amounts of H₂O resulted in extensive decomposition of bromide **176**. The sensitive homoallylic alcohol **177** and its minor isomer were then treated with the mild silylation/deacetalization conditions (TESOTf, 2,4,6-collidine),⁸⁶ affording aldehyde **178** in good yield. At this point, the minor isomer could be separated.



Scheme 2.21. Gram-scale total synthesis of (+)-mikanokryptin from (+)-carvone via a double allylation strategy. (All X-ray crystal structures shown were obtained during preliminary studies conducted with (–)-carvone.)

With the densely functionalized intermediate **178** in hand, I then screened various Barbier conditions for the designed second allylation (Table 2.1), commencing with the Nozaki–Hiyama–Kishi conditions that were investigated in our initial studies. The CrCl₂-mediated condition afforded the desired product **179** in this case, albeit in low yield (10%) and with moderate diastereoselectivity (2:1 *dr*) (entry 1). The major product formed under this condition

was identified as cyclooctane **309** as a mixture of two diastereomers (3.3:1 *dr*). Similarly, when a 2-step sequence of the Finkelstein reaction and the SmI₂-mediated cyclization was applied (entry 3),⁹⁹ both cycloheptane **179** (27%, 2:1 *dr*) and cyclooctane **309** (17%, 9:1 *dr*) were isolated. The indium-mediated condition afforded the desired cycloheptane **179** as a single diastereomer (13% yield, entry 2), and the zinc-mediated condition cleanly afforded cyclooctane **309** (51%, 2.5:1 *dr*) and recovered **178** (34%) (entry 4). The magnesium-based conditions proved ineffective for this transformation (entries 5, 6). Nevertheless, the SnCl₂-mediated condition offered **179** in synthetically useful yield (53%) as a single diastereomer from the Finkelstein product (entry 7).¹⁰⁰ A small amount of cycloheptanol **310** (20%) and recovered **178** (9%) were isolated under this condition as well. Finally, the combination of NaI, SnCl₂, and **178** resulted in a clean transformation at 60 °C, affording **179** in 90% yield as a single diastereomer. It is worth noting that in the literature a radical-based mechanism has been proposed for many Barbier transformations, which may contribute to the formation of cyclooctane **309** through an 8-*endo* radical cyclization process.^{82, 99a, 101}

Table 2.1. Investigation of metal-mediated allylation conditions for the synthesis of the 5,7,5-fused guaianolide lactone system.

Entries	Conditions ^[a]	Isolated Yield (%)			
		179	309	310	rsm ^[b]
1	CrCl ₂ , <i>cat.</i> NiCl ₂ , DMF, 60 °C	10 (2:1 <i>dr</i>)	17 (3:3 <i>dr</i>)	–	–
2	In ⁰ , NaI, DMF, 60 °C	13 ^[c]	–	–	–
3 ^[d]	NaI; SmI ₂ , HMPA-THF, –78 °C	27 (2:1 <i>dr</i>)	17 (9:1 <i>dr</i>)	–	–
4 ^[d]	NaI; Zn ⁰ , <i>aq.</i> NH ₄ Cl, THF, rt	0	51 (2.5:1 <i>dr</i>)	–	34
5 ^[d]	NaI; Mg ⁰ , <i>cat.</i> (CH ₂ Br) ₂ , THF, rt	0	–	–	–
6 ^[d]	NaI; <i>i</i> -PrMgCl, THF, 0 °C	0	–	–	–
7 ^[d]	NaI; SnCl ₂ , DMF, rt	53 ^[c]	–	20 ^[c]	9
8^[e]	SnCl₂, NaI, DMF, 60 °C	90^[c]	–	–	–

[a] Reaction performed on a 30-mg scale unless otherwise stated; [b] Recovered starting material [c] Single diastereomer was obtained. [d] The starting material was reacted with NaI in acetone for 8 h, followed by a filtrative workup. [e] The reaction was performed on a 7-gram scale.

The optimized ring-forming condition secured our access to tricyclic intermediate **179** on large scales. For mikanokryptin (**44**), the remaining chemoselective reduction on the seven-membered B ring proved challenging. The conditions employing Adams' catalyst (PtO₂, H₂) provided nonselective hydrogenation of both exocyclic C–C double bonds, whereas under Wilkinson's hydrogenation conditions [RhCl(PPh₃)₃, H₂], only the more reactive α -methylene lactone was reduced (see **308**). Therefore, we treated **179** with basic methanol (10 mol% NaOMe, MeOH) to induce a conjugate addition, and then added the hydrogenating reagents (PtO₂, H₂) to the same flask, affording the mono-reduced product **180** in near quantitative yield. When **180**

was subjected to the subsequent global desilylation (TBAF), a concomitant retro-conjugate addition of methanol was also observed, affording diol **311** and **312** in a 5:2 ratio (Figure 2.15). The elimination of methanol could be driven to completion when additional amounts of base were added, either in a one-pot manner (*t*-BuOK) or a stepwise manner (DBU, toluene), thus simplifying the purification process.

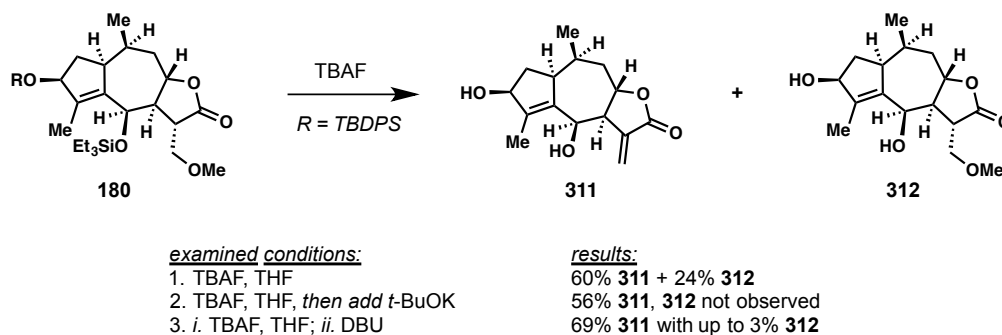


Figure 2.15. Desilylation and the retro-conjugate addition of methanol.

Finally, regioselective allylic oxidation of diol **311** was achieved using excess amounts of MnO_2 , thus affording mikanokryptin (**44**) in near quantitative yield. Therefore, we have completed the total synthesis of (+)-**44** from (+)-carvone in 9 steps on small scales, or in 10 steps on a gram scale by utilizing the stepwise procedure of desilylation and retro-conjugate addition (TBAF; DBU). To the best of our knowledge, this work constitutes the first example of gram-scale production of any guaianolide natural product.

We also envisioned that tricycle **179** may serve as a common intermediate for the syntheses of other 8,12-guaianolides and pseudoguaianolides. Structurally, pseudoguaianolides vary from guaianolides in the position of the C-15 methyl group; a quaternary center is found at the C-5 position in pseudoguaianolides. In a preliminary study towards the synthesis of the pseudoguaianolide isotenulin (**313**) (Figure 2.16),¹⁰² **179** was epoxidized and desilylated, affording **314** in 37% yield over 2 steps. From this intermediate, a 1,2-methyl shift via epoxide opening was envisioned to achieve the carbon network found in the proposed intermediate **315**,¹⁰³ *en route* to the synthesis of isotenulin (**313**).

The Crabtree directed hydrogenation of **314** cleanly afforded the *trans*-configured doubly hydrogenated product.¹⁰⁴ The same condition [H_2 , $\text{Ir}(\text{cod})(\text{PCy}_3)(\text{py})\text{PF}_6$] was also examined on desilylated **179** or acetylated **314**, but both failed to provide the desired product. The hydrogenated product of **314** was then treated with acetic anhydride *in situ*, given that the acetyl moiety exists in isotenulin (**313**) and could also serve as a protecting group in the subsequent transformation. However, treatment of the acetylated product **316** with various Lewis acids resulted in a clean acetate-assisted epoxide opening, arriving at diol **318** in near quantitative yields. This result suggested that a non-participating R' group in **315** is necessary for the examination of the proposed 1,2-methyl shift. Nevertheless, the structure of **318** was unambiguously confirmed by X-ray analysis, which also confirmed the stereoselectivity in the Crabtree hydrogenation. Future work towards the synthesis of **313** or related targets (see Figure 2.17) could start from the hydrogenated product of **314**, and investigate the varied R' group towards the synthesis of intermediate **315**.

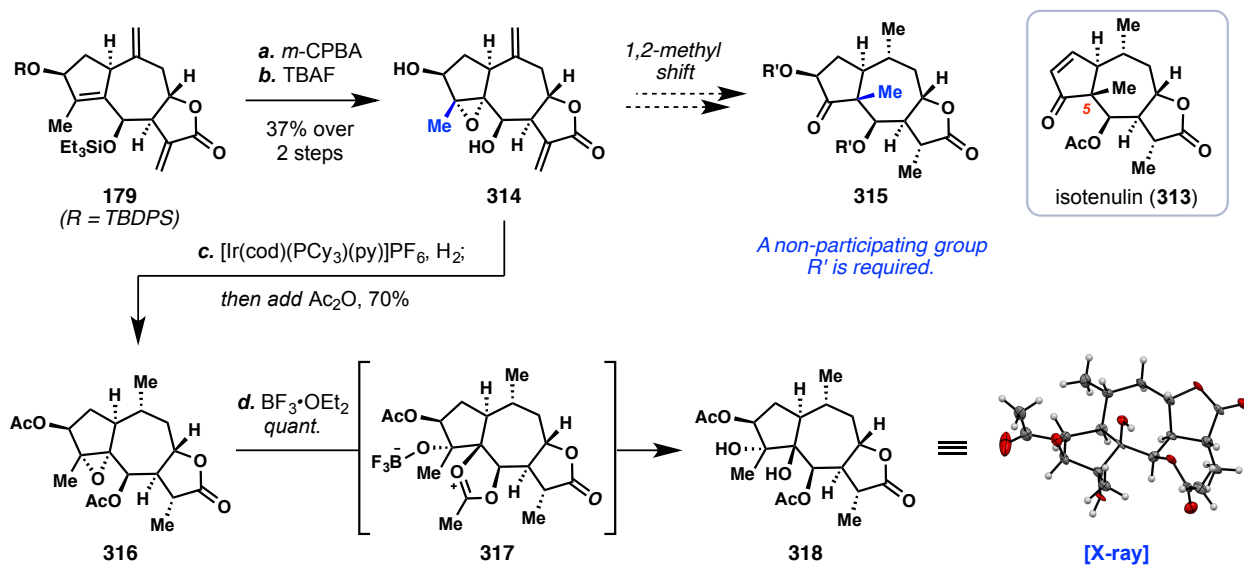


Figure 2.16. Preliminary studies towards the synthesis of the pseudoguaianolide isotenulin (313).

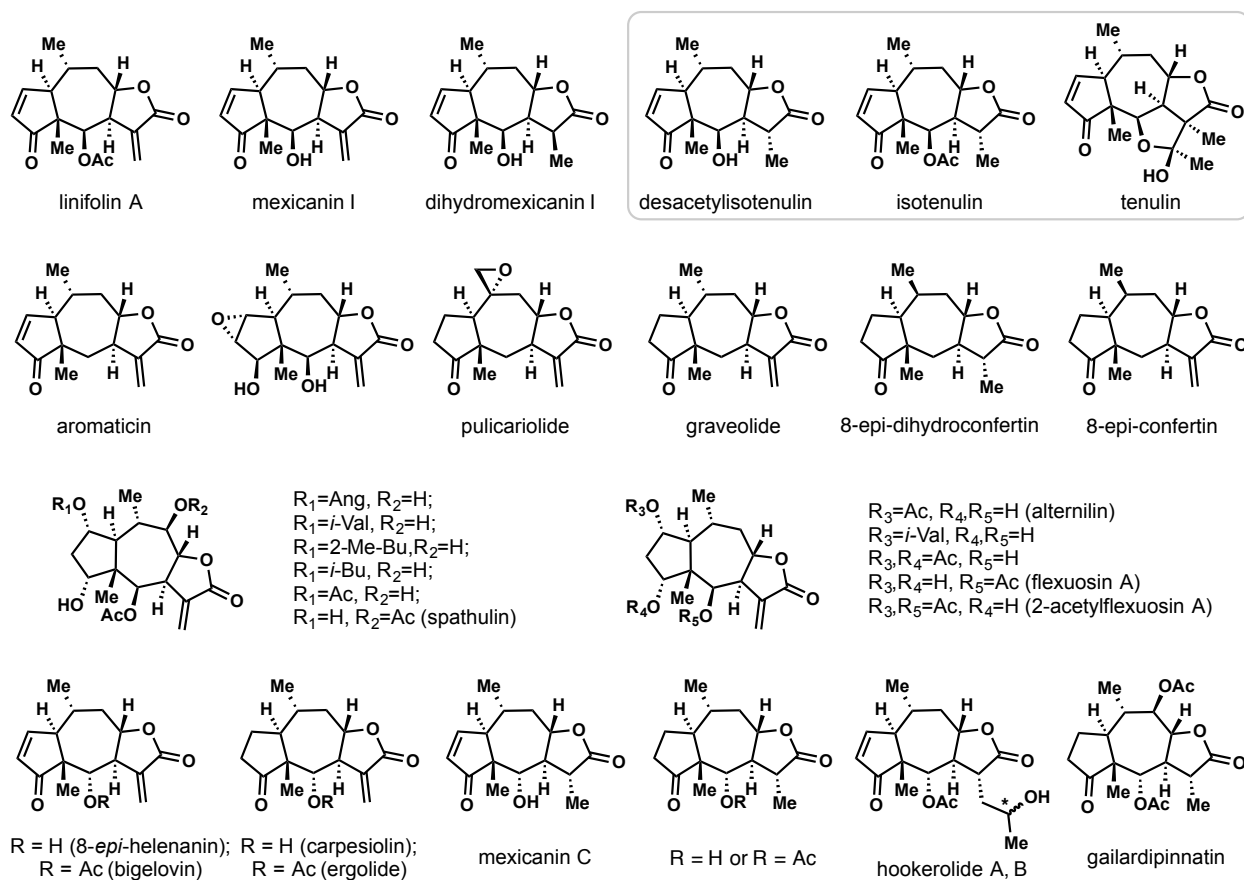
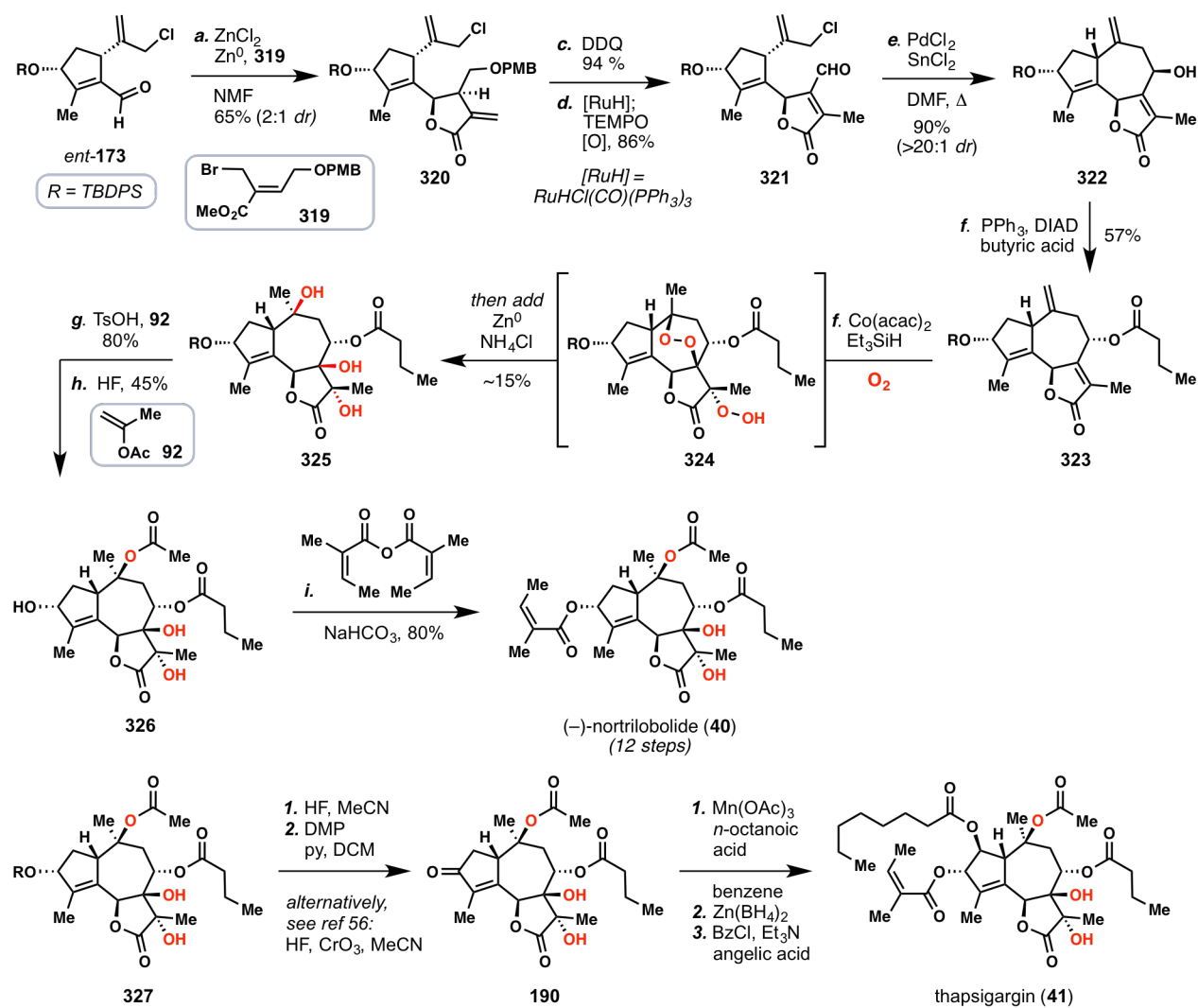


Figure 2.17. Selected *trans*-lactone-containing pseudoguaianolides.

2.6 Total Synthesis of (–)-Nortrilobolide and a Formal Synthesis of (–)-Thapsigargin via an Oxygen Stitching Strategy

By merging the double allylation strategy and oxygen stitching strategy, I have completed the total synthesis of nortrilobolide (**40**) and the formal synthesis of thapsigargin (**41**) as shown in Scheme 2.22. This synthesis utilized common building block **173**, which was synthesized from (–)-carvone, as well as allylic bromide **319**, prepared similarly to **176**. A one-step process of allylation and lactonization afforded α -methylene lactone **320** in synthetically useful yields on decagram scales. Subsequent cleavage of the PMB ether (DDQ) cleanly afforded the corresponding primary alcohol in near quantitative yield. Oxidation of this alcohol, however, proved challenging (see Figure 2.18). After extensive experimentation, a one-pot procedure of alkene isomerization and alcohol oxidation was developed to afford enal **321** in 86% yield. The SnCl₂-mediated intramolecular Barbier allylation continued to be a robust and powerful method to forge the seven-membered B ring, arriving at **322** with excellent yield and stereoselectivity.



Scheme 2.22. Total synthesis of (–)-nortrilobolide (**40**) and a formal synthesis of (–)-thapsigargin (**41**) via an oxygen stitching strategy.

The butyrate ester moiety on the cycloheptane ring was then introduced by a Mitsunobu reaction, providing the key intermediate **323** for the subsequent polyoxygenation. The cobalt-catalyzed tandem peroxidation, followed by reductive cleavage of the endoperoxide, efficiently installed three hydroxy groups with the desired stereochemical pattern in triol **325**. The yield of this transformation (~15%) is currently under optimization in our laboratory. The subsequent acetylation was achieved with careful reaction monitoring under the conditions reported by Ley and coworkers [isopropenyl acetate (**92**), TsOH].^{27b} Notably, in this case the hydroxy groups on the lactone C ring were not protected; over acetylation was observed under extended reaction times. The resulting acetate was then subjected to desilylating conditions to unveil alcohol **326**. The basic TBAF-mediated conditions failed for this purpose, resulting in cleavage of the labile butyrate ester. Fortunately, switching to acidic HF-mediated condition afforded the desired alcohol **326** in 45% yield, along with a minor C-3 epimerized alcohol. This epimerization at C-3 was also observed by Christensen and coworkers in their semi-synthetic studies.⁵⁶ Alcohol **326** represents the known intermediate to complete the syntheses of **40** and **41**. The acylating protocol reported by Baran and coworkers proved reproducible,⁴⁹ and cleanly afforded nortrilobolide (**40**) in *ca.* 80% yield; the remaining steps to convert intermediates **326** and 3-*epi*-**326** to thapsigargin (**41**) were reported by Christensen and coworkers.^{56b}

2.6.1. Optimizations before the Polyoxygenation Step

The optimization of the first transformation in this synthesis (Table 2.2) began with the indium-mediated allylation, which was previously applied to our synthesis of mikanokryptin (**44**). Prior conditions afforded a mixture of two isomeric alcohols and their corresponding lactones in differing ratios (entries 1-3). The crude reaction mixture was therefore treated with catalytic amounts of base in a second step to achieve the complete lactonization, and the diastereoselectivity of the allylation could then be clearly determined by ¹H NMR analysis. Employing conditions conducted under anhydrous *N,N*-dimethylformamide (DMF) as solvent favored the undesired stereoisomer **330**, which represents the mikanokryptin-type stereochemical pattern (entry 1). In contrast, the use of dimethylacetamide (DMA) as solvent improved the stereoselectivity in favoring of **320** (3:2 *dr*), and provided an 82% combined yield over 2 steps (entry 3). Subsequently, anhydrous *N*-methylformamide (NMF) was found to promote a clean allylation with the desired *in situ* lactonization (entry 4),¹⁰⁵ directly affording lactones **320** and **330** as a 1:1 mixture. After screening of several conditions, the combination of zinc powder, ZnCl₂ (10 mol%), and anhydrous NMF appeared to be optimal (entry 8), affording **320** and **330** in one step with a 2:1 diastereomeric ratio in 76% yield on small scale, and in 65% yield on an 8-gram scale.

The next bottle neck I encountered in this synthesis was the oxidation of the primary alcohol group in **331** after DDQ-mediated cleavage of the PMB ether. The conditions I have examined for the oxidation of **331** are listed in an approximately chronological order in Figure 2.18. Under these conditions, a complex mixture of products was typically obtained with the desired product **321** or **332** isolated in low yields, or not observed at all. Presumably, a facile deprotonation of the newly generated aldehyde **332** occurred, which was followed by over oxidation of the sensitive extended enol **333**, leading to extensive decomposition. It is worth noting that a serendipitous use of aged aqueous bleach (entry 12) provided the highest yield in these experiments, which enabled the material throughput to examine the second SnCl₂-mediated allylation for a period of time. However, after the aged bottle of bleach was consumed, we were

Table 2.2. Investigation of the Barbier allylation/lactonization

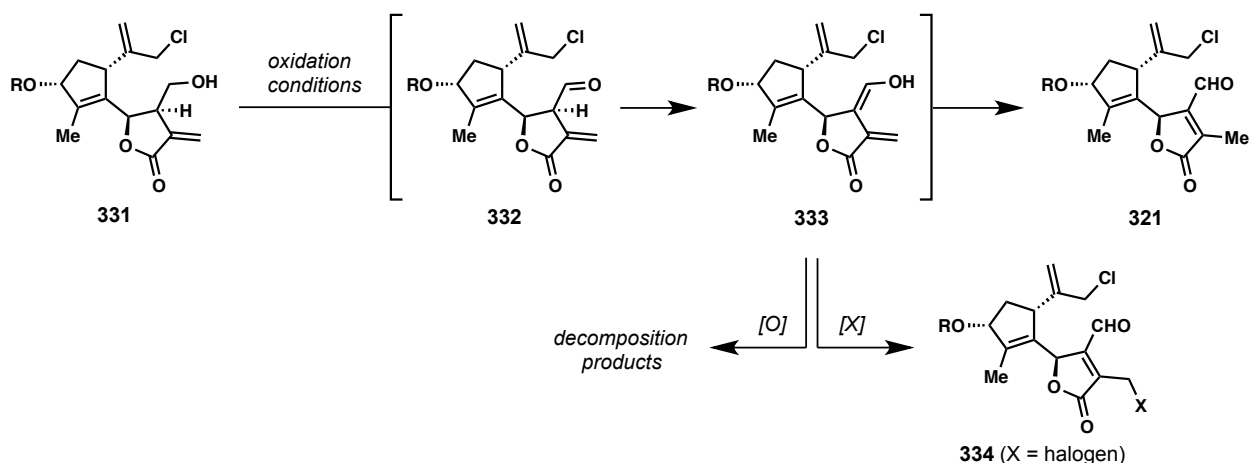
Entries	Conditions ^[a]	Diastereomeric ratio (320:330)	Combined Yield [%] ^[b]
1 ^[c]	In ⁰ , DMF; KHMDS (5 mol%), THF	2:3	ND
2 ^[c]	In ⁰ , DMSO; KHMDS (5 mol%), THF	1:1	ND
3 ^[c]	In ⁰ , DMA; KHMDS (5 mol%), THF	3:2	82
4	In ⁰ , NMF	1:1	90
5	In ⁰ , NMP (no conversion)	–	–
6 ^[c]	Zn ⁰ , <i>aq.</i> NH ₄ Cl/THF; KHMDS (5 mol%), THF	1:1	72
7	Zn ⁰ , NMF	3:2	78
8	Zn⁰, ZnCl₂ (10 mol%), NMF	2:1	76^[d]

[a] Reaction performed on a 100-mg scale unless otherwise stated; [b] Yield of the isolated product; [c] The mixture of resulting alcohols and lactones were treated with 5 mol% KHMDS in an additional step to achieve complete lactonization. [d] This condition afforded 65% of lactones **320** and **330** (2:1 *dr*) on an 8-gram scale.

not able to reproduce this transformation. Additional attempts mostly resulted in halogenation of the presumed intermediate **333**, providing halogen-substituted butenolide **334** in moderate yields. Such efforts include dilution of commercial bleach from various vendors, slow addition of bleach over 12 hours, variation of the catalyst or solvent, and experimentation using electrochemical conditions.¹⁰⁶

Furthermore, I also examined an alternative route towards enal **321** via a chemoselective Mukaiyama hydration of α -methylene lactone **320** to generate **335**.¹⁰⁷ A concomitant trans-lactonization was observed in the subsequent PMB-ether cleavage (DDQ), arriving at similar amounts of the primary alcohol and the corresponding 8,12-lactone (~40% yield). Although the following oxidation cleanly provided enal **321** in 85% yield, the overall yield and reproducibility of this sequence was not satisfactory. Nevertheless, from this study we could gain a glimpse at the importance of avoiding the sensitive intermediate **333** in these oxidative transformations.

Finally, a sequence of isomerization and oxidation solved this problem (Figure 2.19). In our initial studies, a clean isomerization of **331** to butenolide **336** was achieved with stoichiometric amounts of RhH(CO)(PPh₃)₃, but low conversion was observed when catalytic amounts of the rhodium hydride was applied.¹⁰⁸ After a brief screening of the metal catalysts known to promote olefin isomerization, a ruthenium-based system was found to be effective. With catalytic amounts of RuHCl(CO)(PPh₃)₃,¹⁰⁹ primary alcohol **331** was cleanly isomerized to butenolide **336**, which could be oxidized in one pot upon addition of the oxidizing agents, affording enal **321** in 86% yield.



examined conditions:

- 1 DMP, DCM
- 2 DMP, NaHCO₃, DCM
- 3 DMSO, (COCl)₂, Et₃N, DCM
- 4 CrO₃·2py, DCM
- 5 SO₃·py, DMSO, DCM, base (py, collidine, di-^tBu-py, or DIPEA)
- 6 TPAP, NMO, DCM
- 7 IBX, DMSO
- 8 RuCl₂(PPh₃)₃, toluene, Δ
- 9 Ir(dF(CF₃)ppy)₂(dtbbpy)PF₆, visible light
- 10 TEMPO, PIDA, DCM
- 11 AZADO, PIDA, DCM
- 12 TEMPO, KBr, aged aq. NaClO, DCM/aq. NaHCO₃
- 13 TEMPO, KBr, aq. NaClO, DCM/aq. NaHCO₃
- 14 AZADO, KBr, aq. NaClO, DCM/aq. NaHCO₃
- 15 TEMPO, KBr, aq. NaClO, DCM/aq. NaHCO₃
(diluted 10x, 20x, 30x, 50x, or 100x)
- 16 TEMPO, KBr, aq. NaClO, acetone or MeCN
- 17 TEMPO, aq. LiClO₄ (0.2 M), collidine, CH₂Br₂, Ag/AgNO₃, 0.4 V
- 18 TEMPO, Cu(bpy)OTf, NMI, O₂, MeCN
- 19 AZADO, Cu(bpy)OTf, NMI, O₂, MeCN
- 20 TEMPO, PhIO, Yb(OTf)₃, DCM
- 21 TEMPO, Fe(NO₃)₃·9H₂O, NaCl, O₂, DCM
- 22 TEMPO, NCS, *n*-Bu₄NCl, KBr, DCM/aq. NaHCO₃
- 23 TEMPO, *n*-Bu₄NBr, oxone, DCM
- 24 AZADO, H₃O₅, *n*-Bu₄NBr, wet Al₂O₃, DCM
- 25 AZADO, NaClO·5H₂O, *n*-Bu₄NHSO₄, DCM
- 26 Pd(OAc)₂, pyridine, O₂, toluene, 3Å MS
- 27 Pd(OAc)₂, K₂CO₃, O₂, toluene
- 28 Jones reagent, acetone
- 29 PDC, DCM
- 30 PCC, DCM
- 31 PCC over silica gel, DCM
- 32 PCC over Al₂O₃, DCM
- 33 PCC (polymer-based), DCM
- 34 PCC, 3Å MS, DCM
- 35 PCC, 3Å MS, AcOH, DCM

results:

- <10% of **321**
- <10% of **321**
- <10% of **332**
- rsm + trace **321**
- decomp.
- rsm + decomp.
- decomp.
- decomp.
- rsm + decomp.
- rsm + decomp.
- rsm + decomp.
- 35% of **321** (46% brsm)
- no **321**, major **334** (X = Cl)
- no **321**, major **334** (X = Cl)
- trace **321**, major **334** (X = Cl)
- no conv.
- major **334** (X = Br, tentative)
- no conv.
- no conv.
- rsm + decomp.
- decomp.
- decomp.
- decomp.
- rsm + decomp.
- rsm + decomp.
- rsm + decomp.
- decomp.
- decomp.
- rsm + trace **321**
- 10% of **321**
- decomp.
- decomp.
- rsm
- 15-20% of **321**
- decomp.

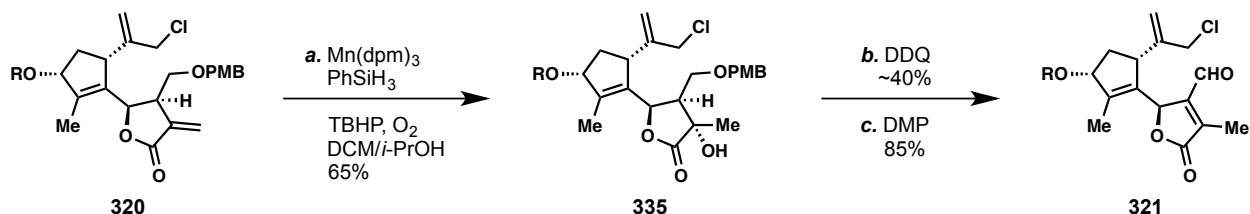
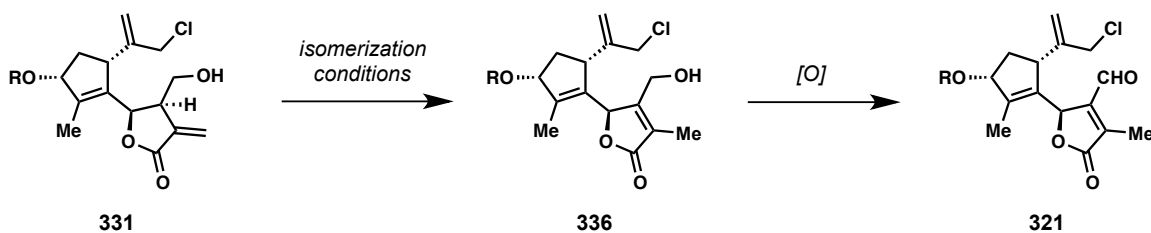


Figure 2.18. Attempted oxidation conditions to access enal **321**.



conditions examined: (331 -> 336)

1. RhH(PPh ₃) ₄ , toluene, Δ	no conv.
2. RhH(CO)(PPh ₃) ₃ (1.2 equiv), toluene, Δ	90%
3. RhH(CO)(PPh ₃) ₃ (0.2 equiv), toluene, Δ (or DMF, DCE, THF, dioxane)	low conv.
4. RuHCl(CO)(PPh ₃) ₃ (0.1 equiv), toluene, Δ	88%
5. RuH ₂ (CO)(PPh ₃) ₃ (0.1 equiv), toluene, Δ	53%

one-pot isomerization/oxidation: (331 -> 321)

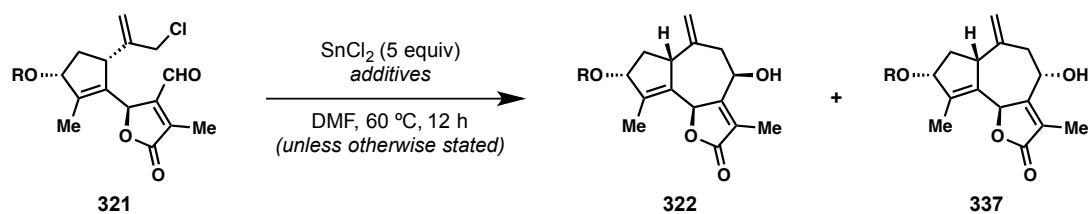
1. RuHCl(CO)(PPh ₃) ₃ (0.1 equiv), DCE, Δ	86%
then add TEMPO, KBr, aq. NaOCl, aq. NaHCO ₃	
2. RuHCl(CO)(PPh ₃) ₃ (0.1 equiv), DCE, Δ	23%
then add KBr, aq. NaOCl, aq. NaHCO ₃	

Figure 2.19. A sequence of isomerization and oxidation afforded enal **321** in high yield.

In retrospect, the preliminary studies on the following ring-forming event to forge tricycle **322** began once we obtained **321** on 100-mg scales from the condition utilizing the aged bleach, which was approximately at the same time when we examined the B-ring formation in the synthesis of mikanokryptin (**44**) (see Table 2.1, **178** → **179**). The Barbier conditions shown in Table 2.1 were also examined on enal **321**, but none of these conditions except the SnCl₂-mediated condition afforded isolable amounts of tricycle **322** or its diastereomer **337**. Under these robust conditions employing combined NaI and SnCl₂ at 60 °C, **322** and **337** could be isolated in near quantitative yield as a 1:1 mixture. The studies were then discontinued due to the availability of enal **321**, and were resumed after the development of the isomerization/oxidation process.

Replacement of NaI from the aforementioned conditions with additives was also examined (Table 2.3). Activation of the allylic chloride was deemed necessary; with no additive, the SnCl₂-mediated condition did not provide noticeable conversion of the starting material (entry 2). Decreasing reaction temperature resulted in incomplete conversion of **321**, and a slight variation of the product ratio in favor of **337** (entry 3). Addition of other Finkelstein-type additives resulted in altered diastereoselectivities as well (entries 4-12).¹¹⁰ Additionally, the combination of SnCl₂ with transition-metal catalysts has been well documented in the literature, including systems based on Cu, Pd, Ti, Co, Cr, and Rh.¹¹¹ To this end, a PdCl₂-based system¹¹² (entry 14) provided excellent diastereoselectivity while preserving the reaction yield on small scales (95%, >20:1 *dr*) or gram scales (90%, >20:1 *dr*).

Table 2.3. Investigation of the Barbier allylation in the synthesis of the cycloheptane B ring.



Entries	Additives ^[a]	Diastereomeric ratio (322:337)	Combined Yield [%] ^[b]
1	NaI (5 equiv)	1:1	97
2	no additive (no conversion)	–	–
3	NaI (5 equiv), 23 °C, 4 d (partial conversion)	1:1.5	60
4	LiI (5 equiv)	1:1	95
5	KI (5 equiv)	1:1.2	90
6	<i>n</i> -Bu ₄ NI (5 equiv) (low conversion)	1:1.4	ND
9	CsI (5 equiv)	1:1.1	90
7	NI ₂ (5 equiv)	1:1	86
10	CuI (5 equiv)	1:1.5	<30
11	ZnI ₂ (5 equiv)	1:1.5	40
12	InI (5 equiv)	–	0
13	CoBr ₂ (5 equiv)	1.1:1	<30
14	PdCl₂(PhCN)₂ (0.15 equiv)	>20:1	95^[c]
15	Pd(OAc) ₂ (0.15 equiv)	>20:1	88
16	TiCl ₃ (0.1 equiv) (low conversion)	ND	ND
17	Rh ₂ (OAc) ₄ (2 equiv)	1:1.6	66
18	Rh ₂ (TFA) ₄ (2 equiv)	>20:1	48
19	Co(acac) ₂ or Cr(acac) ₃ or Cp ₂ TiCl ₂	–	0

[a] Reaction performed on a 10-mg scale unless otherwise stated; [b] Yield of the isolated product; [c] This condition afforded 90% of **322** on a gram scale.

2.6.2. Optimization of the Polyoxygenation Step

With the synthesis completed, the optimization of the key polyoxygenation step remains the last challenge. My efforts to optimize this transformation have primarily focused on the initial tandem peroxidation, in which intermediates **338**, **339**, **340**, and/or **341** were isolated and evaluated (Table 2.4). It should be noted that the *in situ* cleavage of the endoperoxide intermediates (Zn^0 , NH_4Cl) was not performed at this optimization stage, given that this procedure may introduce additional variables. To this end, a one-pot yield of the polyoxygenation (10~15%) will be updated upon arriving at suitable conditions for the initial peroxidation process. It is worth noting that endoperoxides **338** and **339** were found to be unstable on silica gel, and it was necessary to act quickly during the purification.

Throughout the course of my optimization, the highest isolated yield of **338** thus far was obtained under a $\text{Co}(\text{acac})_2$ -based condition (entry 1), in which triethylsilane (5 equiv) was slowly added over 24 hours as a solution in ethanol, while the reaction mixture was vigorously stirred under an oxygen atmosphere. Endoperoxides **338** (16% yield), **339** (10% yield), as well as mono-hydration product **341** (19% yield) were isolated as the main products. Hydroperoxide **340** was also observed during monitoring of the reaction, which could be characteristically converted to **341** on the TLC plate by co-spotting with PPh_3 in dichloromethane.

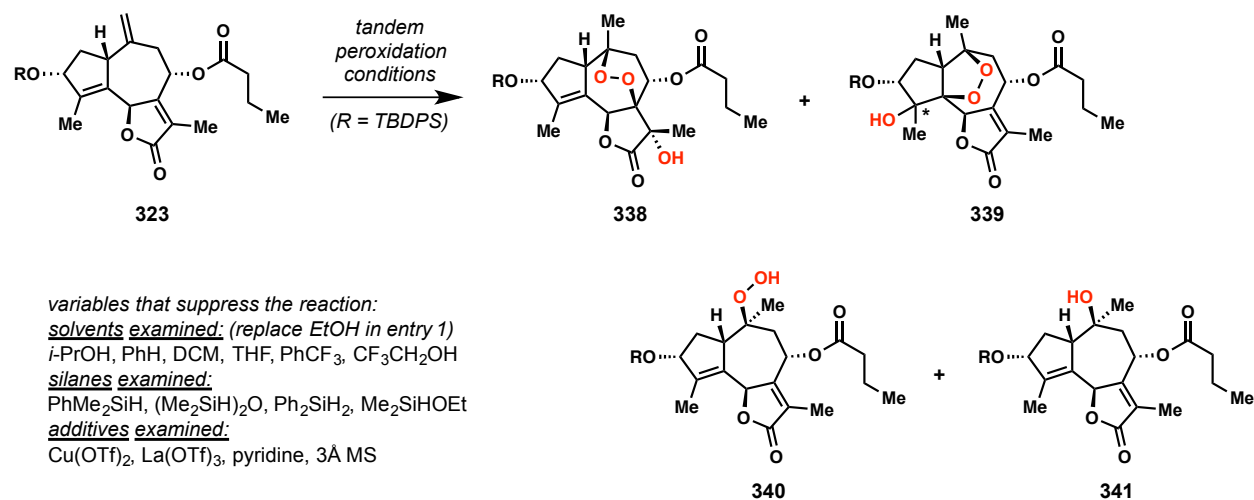
The conditions employing PhSiH_3 as the reductant provided a slightly decreased yield (13%) of the desired endoperoxide **338**, and an increased yield (18%) of the undesired isomer **339** (entry 2). Incorporation of *t*-butyl-hydroperoxide (TBHP) proved ineffective. With catalytic amounts of TBHP added to the reaction, the yield of **338** dropped to 9% (entry 3), whereas stoichiometric amounts of TBHP completely inhibited the formation of the desired endoperoxide (entry 4). Under these conditions (entries 3-4), hydroperoxide **340** was observed as the major component during early stages of the reaction as judged by TLC, and increased amounts of mono-hydration product **341** was isolated over extended reaction time. The hydroperoxidation conditions based on $\text{Mn}(\text{dpm})_3$ and $\text{Fe}(\text{acac})_3$ failed to provide any desired product (entries 5-6). The use of Carreira's catalyst offered a clean hydroperoxidation without cyclization (entry 7).¹¹³ The unstable peroxide **340** could be isolated in moderate yield after a rapid column chromatography employing silica gel pretreated with TBHP (70% in H_2O). Attempts on converting freshly prepared **340** to endoperoxide **338** failed to provide the desired product [SmI_2/O_2 ; di-*tert*-butyl peroxyoxalate (DBPO, prepared *in situ*); or $\text{Pd}(\text{OAc})_2/\text{O}_2$].¹¹⁴ Under condition employing $\text{Co}(\text{modp})_2$ as the catalyst, triethylsilylated **340** was obtained as the major product (entry 8).¹¹⁵

Additionally, variation of solvent or silane suppressed the reactivity of the catalyst system. Incorporation of Lewis acids [$\text{Cu}(\text{OTf})_2$ or $\text{La}(\text{OTf})_3$], base (pyridine), or 3 Å molecular sieve resulted in low conversion of the starting material. Enone **342** was also briefly examined for the tandem peroxidation, however, the desired product **343** was not observed under the conditions listed in Figure 2.20. For the evaluation of this transformation, the product standard of **343** was prepared from endoperoxide **338** via a HF-mediated desilylation followed by oxidation with Dess–Martin periodinane.

The future work in this optimization, in my perspective, could explore the following directions: (i) discovery of an oxidant additive that facilitates the oxidation of the Co(II) catalyst to the Co(III) species, but does not contain a reactive H atom source as in TBHP; (ii) synthesis of an alternative diene substrate with a saturated cyclopentane as the A ring, which may alter the

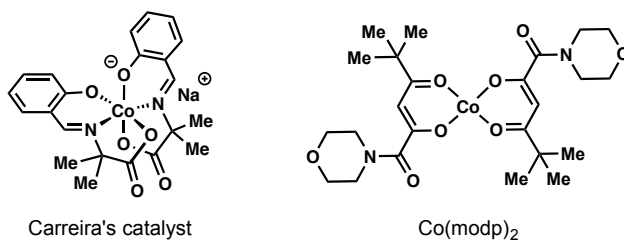
overall geometry of the corresponding intermediate to force the peroxy moiety to uptake an axial configuration, thus facilitating the cyclization.

Table 2.4. Selected examples of optimization for the tandem peroxidation.



Entries	Conditions ^[a]	Isolated Yield [%]			
		338	339	340	341
1 ^[b]	Co(acac) ₂ (0.25 equiv), Et ₃ SiH (5 equiv), EtOH, 48 h	16	10	–	19
2 ^[b]	Co(acac) ₂ (0.25 equiv), PhSiH ₃ (3 equiv), <i>i</i> -PrOH (30 equiv), DCM, 48 h	13	18	–	15
3 ^[b]	Co(acac) ₂ (0.25 equiv), Et ₃ SiH (5 equiv), <i>t</i> -BuOOH (0.25 equiv), EtOH	9	ND	–	ND
4 ^[b]	Co(acac) ₂ (0.25 equiv), Et ₃ SiH (5 equiv), <i>t</i> -BuOOH (1 equiv), EtOH	0	ND	–	ND
5 ^[c]	Mn(dpm) ₃ (0.3 equiv), PhSiH ₃ (3 equiv), <i>i</i> -PrOH (30 equiv), DCM	0	–	–	–
6 ^[c]	Fe(acac) ₃ (0.3 equiv), PhSiH ₃ or Et ₃ SiH, EtOH	0	–	–	–
7 ^[c]	Carreira's catalyst (0.3 equiv), Et ₃ SiH (8 equiv), EtOH, 12 h	0	–	63	–
8 ^[c]	Co(modp) ₂ (0.3 equiv), Et ₃ SiH (5 equiv), DCE ^[d]	0	–	–	–

[a] Reaction performed on a 25-mg scale unless otherwise stated; [b] The silane was added slowly over 24 h via a syringe pump. [c] The silane was added slowly over 8 h via a syringe pump. [d] Triethylsilylated **340** was obtained as the major product.



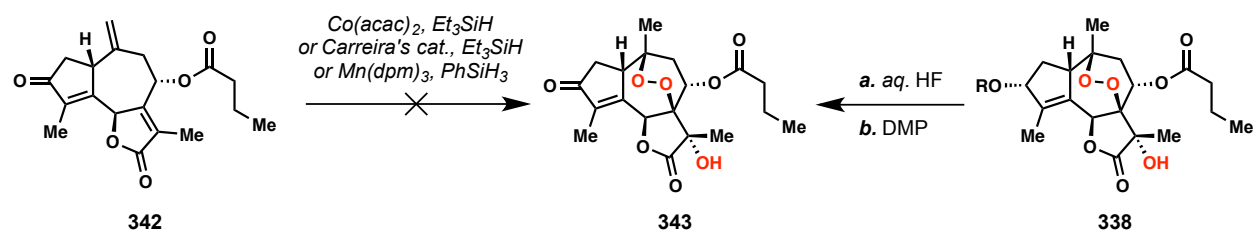


Figure 2.20. Failed peroxidation of enone **342**.

2.7 Synthetic Studies on Guaianolides from the Apiaceae family (*i.e.* Slovanolides)

2.7.1. Introduction

As mentioned in section 2.2, despite the extensive synthetic studies on the Asteraceae guaianolides, the thapsigargin group represents the only members in the Apiaceae family that have been chemically synthesized. Herein, I will discuss my preliminary work towards the synthesis of this neglected family of guaianolides (sections 2.7.2 and 2.7.3), which were also referred to as slovanolides by researchers in the field of natural product isolation.¹¹⁶

During the isolation of slovanolides, Holub and coworkers noticed a distinct chemical property compared to that of guaianolides from the Asteraceae plants, *i.e.* their preference of the lactone position in chemical derivatization (Figure 2.21).¹¹⁷ Global hydrolysis (*aq.* NaOH) followed by regeneration of the lactone (H^+) was commonly conducted to remove the ester moieties of the natural products, thus simplifying structural elucidation, or in some cases providing samples for X-ray diffraction.¹⁹ With different configurations on the seven-membered B ring, slovanolides were found to favor the *trans*-lactonization to give 8,12-lactones (*e.g.* **344**), whereas guaianolides from the Asteraceae typically maintained the 6,12-lactone framework (*e.g.* **345**).

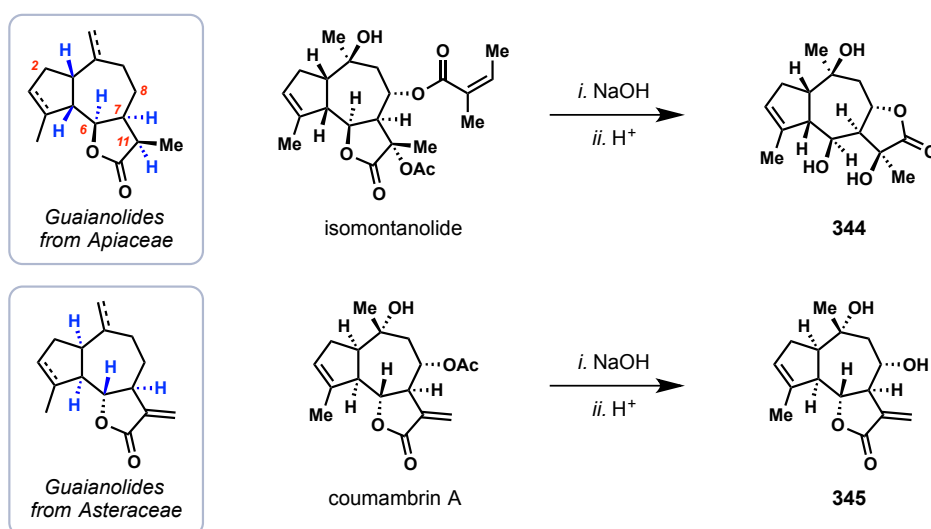
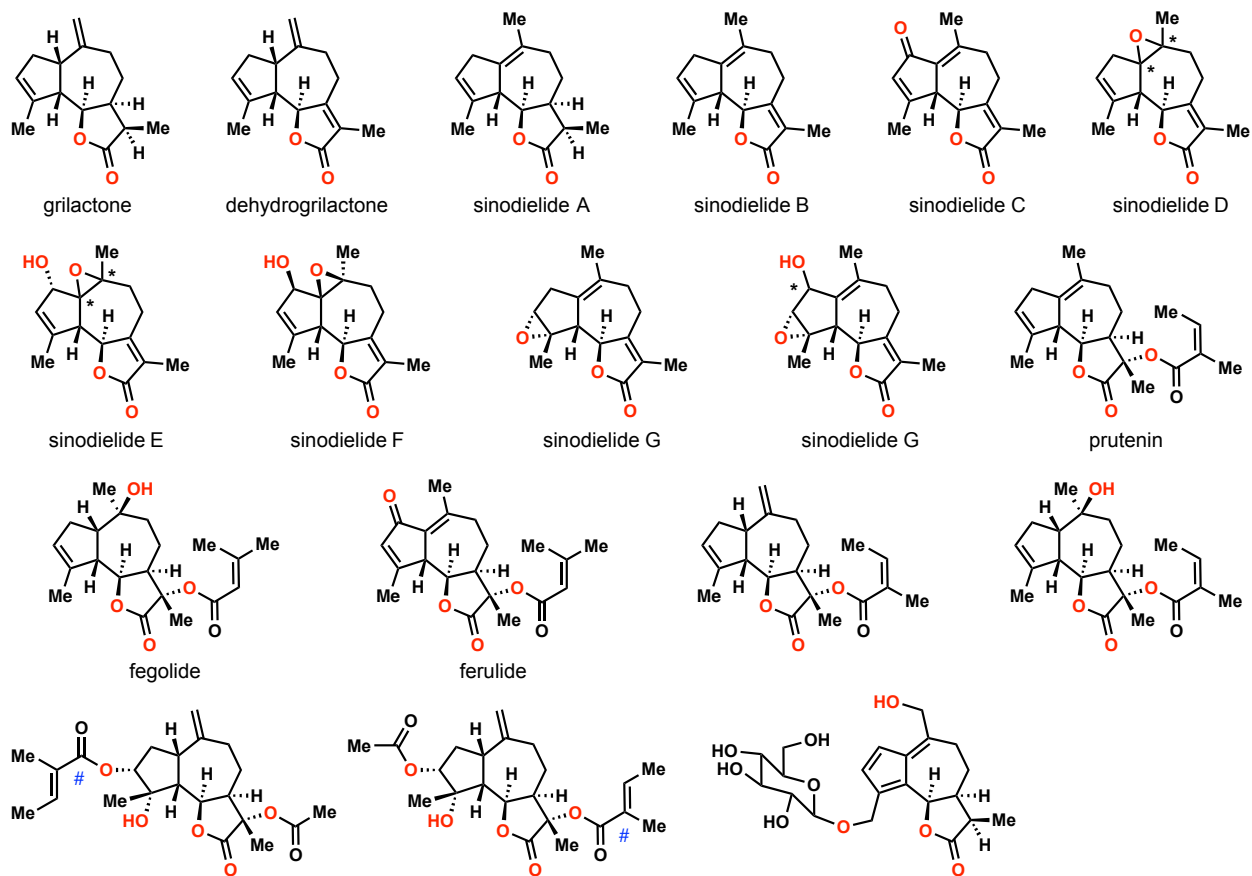


Figure 2.21. Slovanolides and a key chemical property.

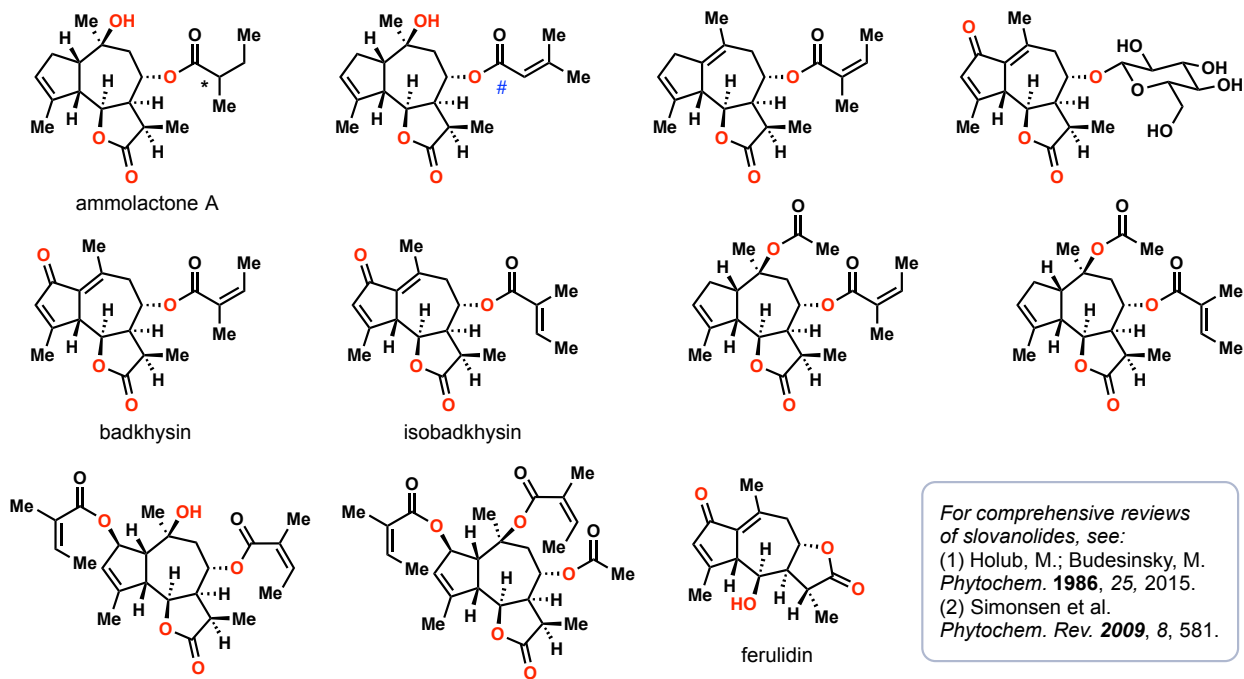
A comprehensive list of guaianolides from the Apiaceae family that I have found during a literature survey in February 2018 are provided in Figure 2.22. The majority of them have also been reviewed by Holub in 1986, and Simonsen in 2009.⁷ It is worth noting that a number of the Apiaceae guaianolides were assigned in their *ent*-form in the original isolation reports based on the absolute configuration of the Asteraceae guaianolides, most of which have been corrected in the aforementioned review.

As shown in Figure 2.22, grilactone and sinodiellide A represent the lowest oxidation level in this family. Subsequent oxygenations at C-2, C-8, C-11 gradually build up the oxidation states in the Apiaceae guaianolides, and after a C-7 oxygenation, ultimately arriving at the trilobolides and thapsigargin.

C-8 non-oxygenated: (# The corresponding angelic ester also exists)



C-8 oxygenated, C-11 non-oxygenated:



For comprehensive reviews of slovanolides, see:
 (1) Holub, M.; Budesinsky, M. *Phytochem.* **1986**, *25*, 2015.
 (2) Simonsen et al. *Phytochem. Rev.* **2009**, *8*, 581.

Figure 2.22. Guaianolides from the Apiaceae family (*stereochemistry not determined)

C-8 oxygenated, C-11 oxygenated: (# The corresponding angelic ester also exists)

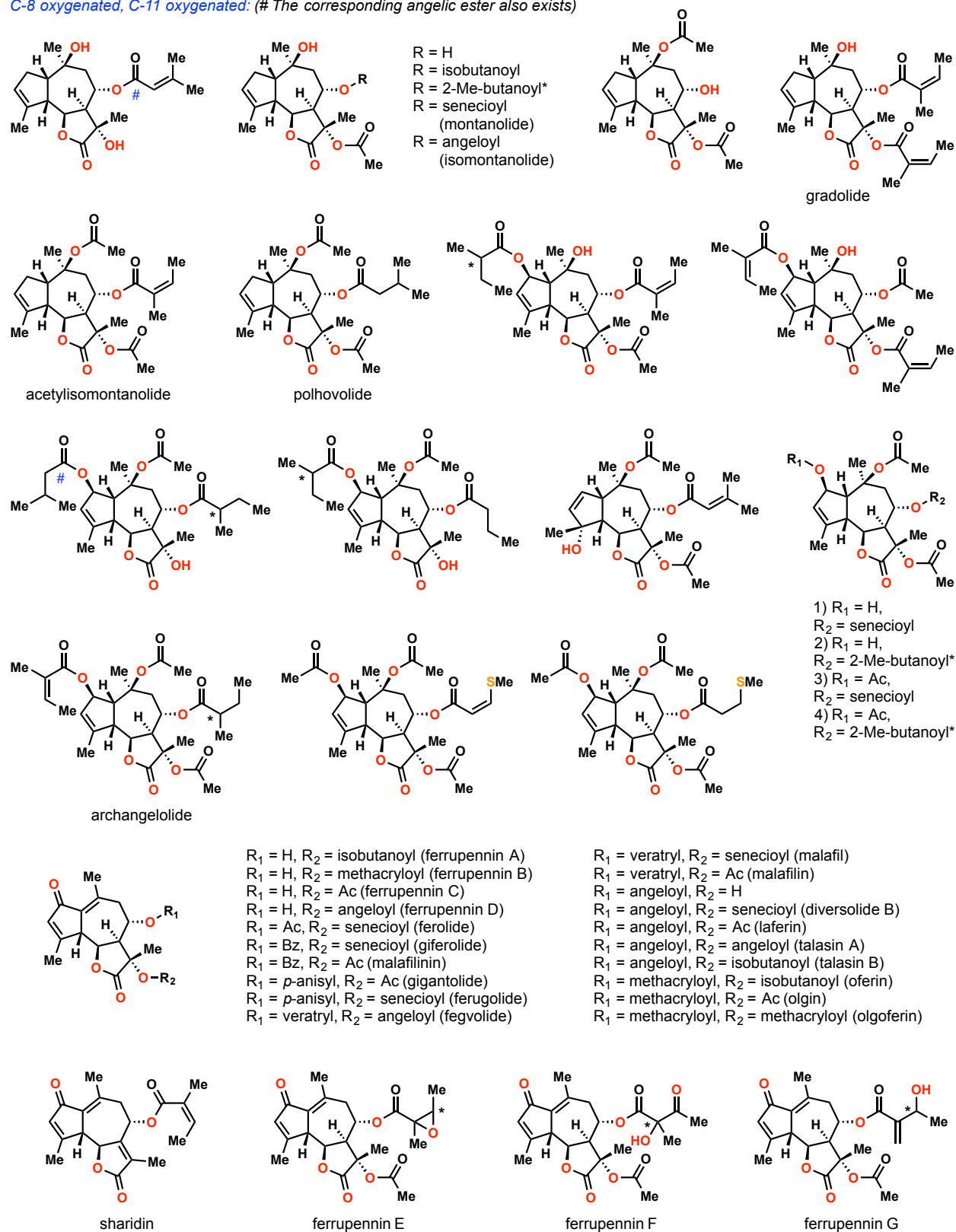


Figure 2.22. Guaianolides from the Apiaceae family (continued) (*stereochem. not determined).

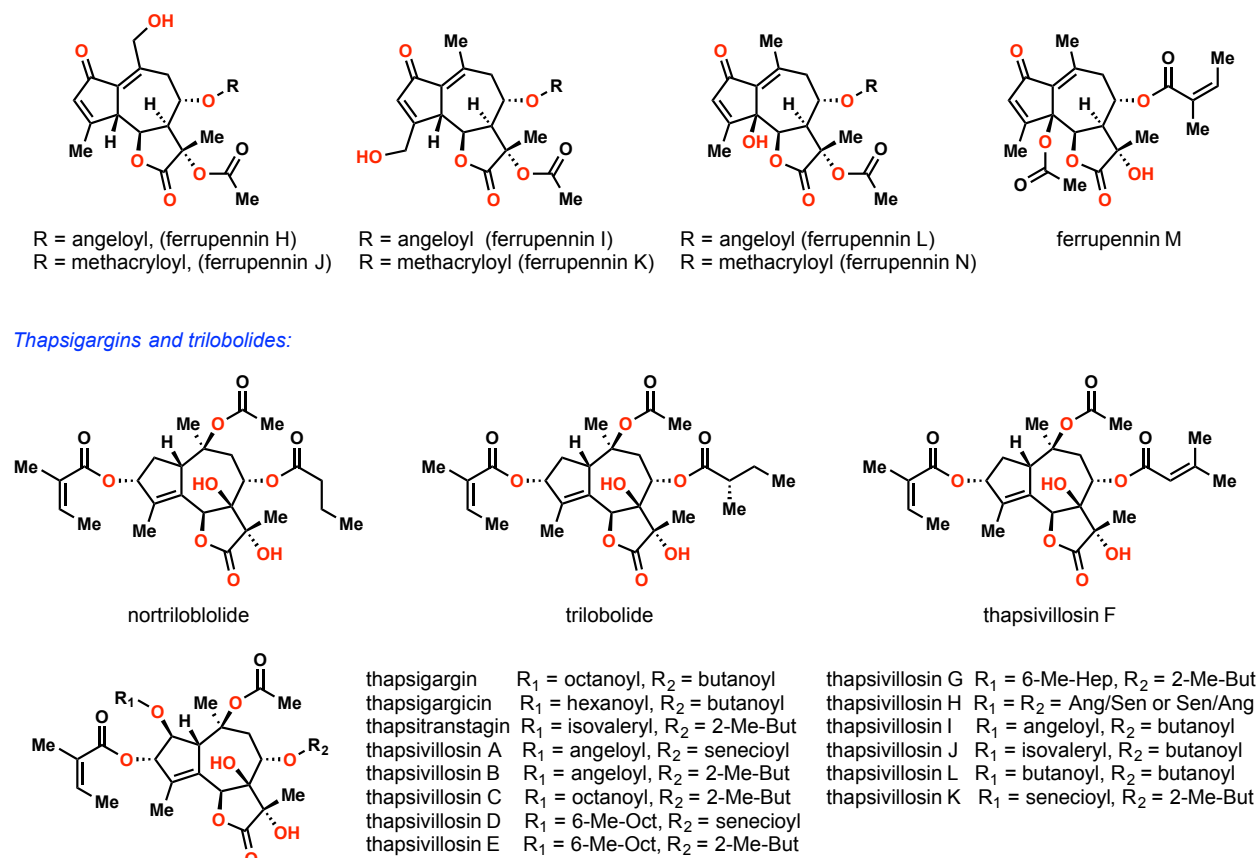


Figure 2.22. Guaianolides from the Apiaceae family (continued).

During a literature survey, a small amount of the Asteraceae guaianolides have also been found to possess a *cis*-fused lactone moiety, and in a few cases, an α -H at C-11 as well (see **346-349**). Possibly, epimerization occurred at some stages of the biosynthetic pathway, especially when the epimerizable stereogenic center was located at an allylic position. In Pedro's synthetic study on the oxidation of kauniolide derivatives, a facile epimerization was also observed associated with the tannunolide's system (Figure 2.23).¹¹⁸

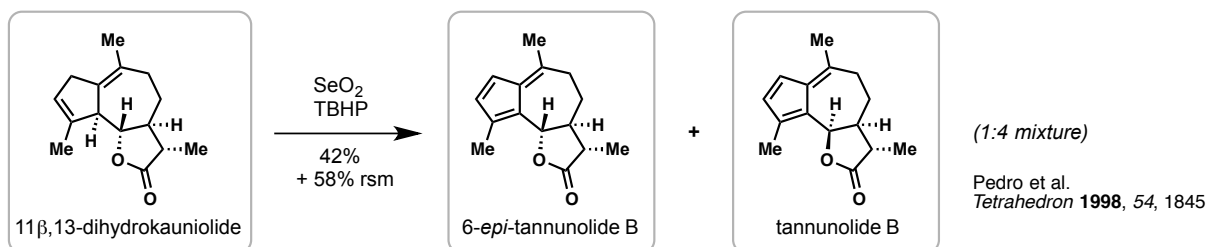


Figure 2.23. Pedro's study on tannunolides and the observation of C-6 epimerization.

A plausible mechanism was proposed based on the study by Pedro and coworkers, for the biosynthesis of guaianolides **346**, **349**, and related isolation artifacts **347**, **348** (Figure 2.24).

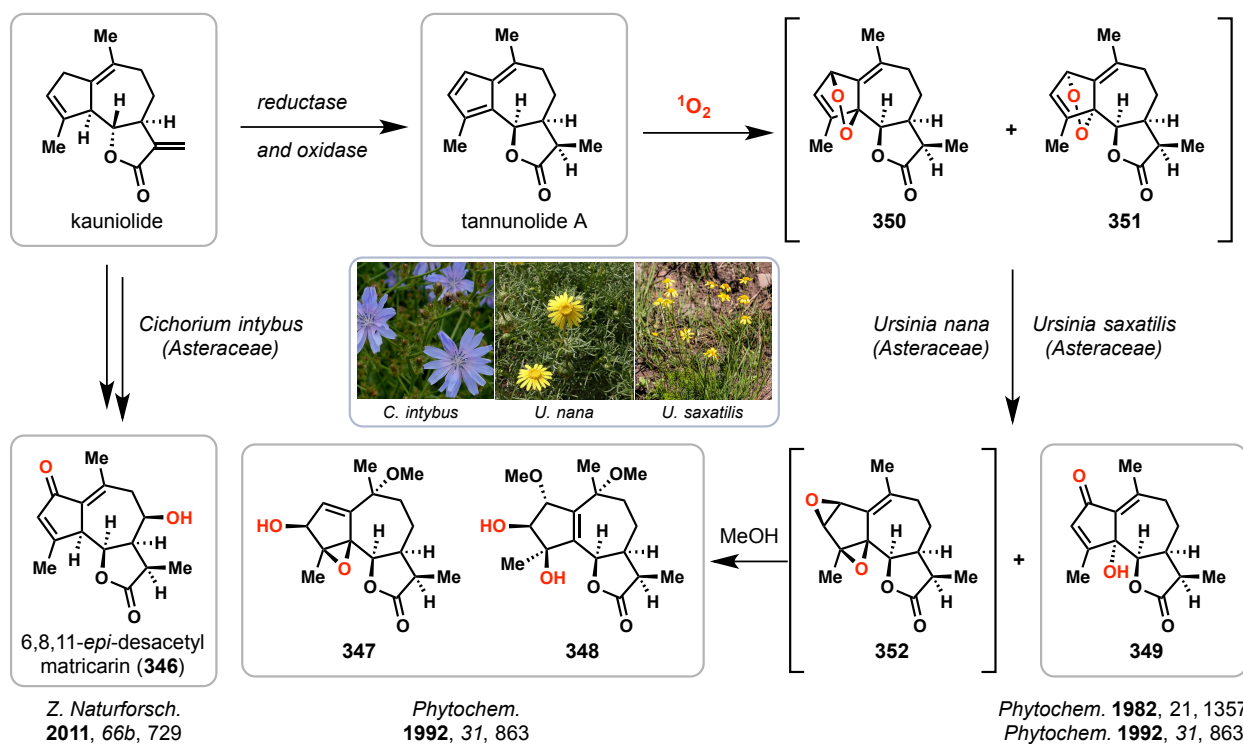


Figure 2.24. Stereochemical patterns of slovanolides found in the Asteraceae family: proposed biosynthetic pathway to 346–349.

2.7.2 Synthesis of C-8 Non-oxygenated Slovanolides

For slovanolides that do not contain the C-8 oxygen, I have completed the total synthesis of grilactone (**353**) and sinodielide A (**354**) from (–)-linalool, featuring a Pauson–Khand reaction in the rapid construction of A ring, and an intramolecular Barbier allylation in the assembly of the seven-membered B ring (Scheme 2.23).

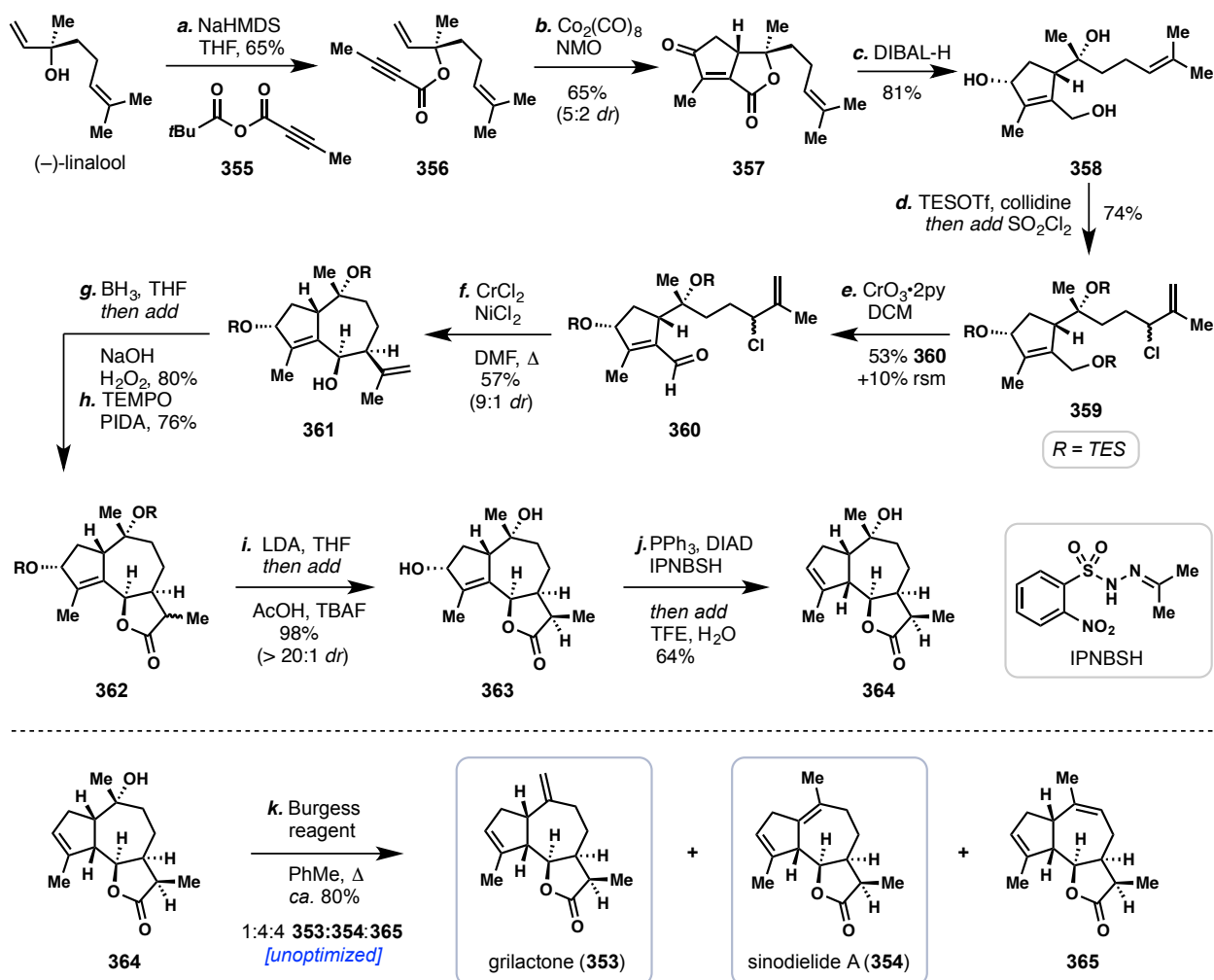
In this synthesis, (–)-linalool was treated with sodium bis(trimethylsilyl)amide (NaHMDS) and mixed anhydride **355**, which was prepared *in situ* by following the protocols developed by Yang and coworkers.¹¹⁹ This forcing acylating condition reproducibly afforded the tertiary ester **356** in 55–75% yields on gram scales. Ester **356** was found to be unstable, and was therefore quickly subjected to the subsequent Pauson–Khand reaction [$\text{Co}_2(\text{CO})_8$, NMO],^{119–120} arriving at the bicyclic enone **357** in 65% yield (5:2 *dr*). Excess amounts of DIBAL-H then cleanly reduced enone **357** to triol **358** in 81% yield. From this intermediate, a one-pot procedure of silylation and allylic chlorination was developed to prepare allylic chloride **359** as a mixture of two diastereomers for the successive ring-forming event. In these studies, it was found that the use of 2,4,6-collidine as base proved imperative for this transformation; when Na_2CO_3 , Et_3N , or pyridine was employed, diminished yields of the desired product were obtained. The mixture of diastereomeric **359** was then treated with the Collins' condition [dipyridine chromium(VI) oxide, CH_2Cl_2], which induced a chemoselective oxidation of the primary triethylsiloxy ether, affording aldehyde **360** in 53% yield. A small amount of silyl ether **359** (10% yield) was also recovered from this reaction. Subsequently, the venerable Nozaki–Hiyama–Kishi condition (CrCl_2 , *cat.* NiCl_2 , 60 °C) successfully provided cycloheptanol **361** in a moderate yield (51%), along with small amounts of its diastereomer (6%) and dechlorinated **360** (<10%). The SnCl_2 -mediated conditions that we have applied in the previous syntheses will be examined for this transformation in the near future.

From the guaianane-type intermediate **361**, a sequence of hydroboration and oxidation was envisioned to assemble the C-ring lactone in grilactone (**353**) and sinodielide (**354**). A two-step procedure employing the standard hydroboration–oxidation (BH_3 –THF, then H_2O_2 , NaOH) and an ensuing oxidation of the alcohol intermediates (TEMPO, PIDA) cleanly afforded lactone **362** as a mixture of two diastereomers. It is worth noting that a one-pot protocol of hydroboration/Collins oxidation was employed in the synthesis of majucin recently reported by our laboratory to convert an alkene to a ketone.¹²¹ These conditions might provide lactone **362** directly from intermediate **361**. The lactone mixture was then deprotonated with LDA followed by the addition of the desilylating agents (TBAF, AcOH). Under this condition, both diastereomers were converted to the desilylated intermediate **363** in near quantitative yield and as a single diastereomer. The requisite $\Delta_{3,4}$ -unsaturation was subsequently unveiled by treating allylic alcohol **363** with the condition developed by Movassaghi and coworkers,¹²² arriving at alkene **364** (64% yield) via a transient allylic diazene intermediate.¹²³ From **364**, I have only examined the Burgess condition for the last elimination step, which unselectively provided grilactone (**353**), sinodielide (**354**), and diene **365**, in an 80% combined yield with a 1:4:4 ratio. The samples obtained from this experiment will serve as standards for the future screening. Nevertheless, this synthesis has clearly demonstrated that we can access slovanolides with the 1st-level oxidation state.

Some initial efforts in this project are presented in Figure 2.25. The minor isomer obtained in the Pauson–Khand reaction (*i.e.* **366**) was functionalized in two steps to the guaianane-type bicycle **367** (Figure 2.25A), which was then globally reduced (DIBAL-H) and

subjected to X-ray crystallographic analysis. The stereogenic center formed in the allylation of the lactone intermediate was confirmed as shown. In contrast, the strategy employing Prins-type cyclization of **366** or its derivative **369** proved unsuccessful (Figure 2.25B). From the major Pauson–Khand product **357**, I also examined the intramolecular Barbier allylation at various stages of the initial studies. Chloro-substituted lactone **370**, methyl ester **371**, or desilylated **360** all failed to provide the corresponding cyclized products. The cyclization of **360** remains the only successful path to the targeted natural products.

The guaianane-type intermediate **361** was also envisioned to access slovanolides bearing higher oxidation states in this series, such as prutenin (**373**) and the unnamed slovanolide **374** (Scheme 2.24). Instead of the hydroboration–oxidation, an asymmetric dihydroxylation followed by the oxidative lactonization of the diol intermediate may provide lactone **375** with the C-11 oxygenation. After assembling the angelic ester moiety and introducing the $\Delta_{3,4}$ -alkene, the resulting intermediate **376** was envisioned to be either dehydrated by Pedro’s condition (TF_2O)^{47c} to afford prutenin (**173**), or subjected to a directed dihydroxylation ($\text{OsO}_4 \cdot \text{TMEDA}$),¹²⁴ followed by alcohol elimination and acetylation, to arrive at **374**.



Scheme 2.23. Total synthesis of grilactone (**353**) and sinodiellide A (**354**) from (-)-linalool.

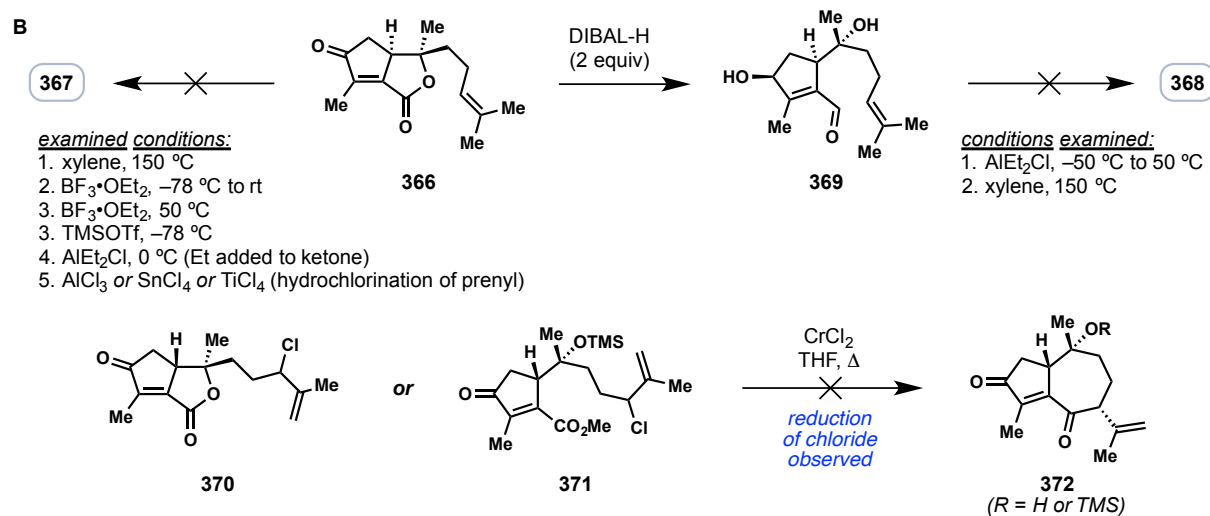
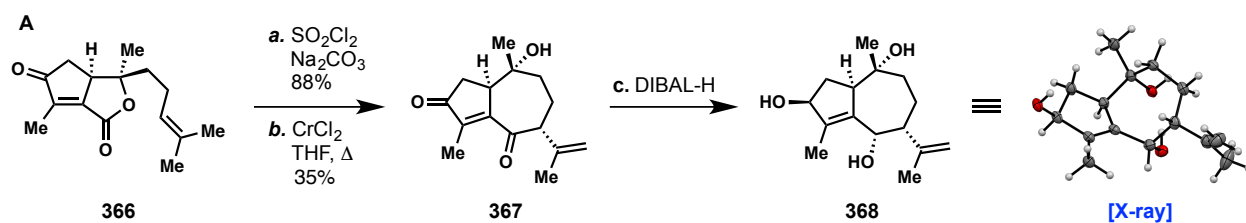
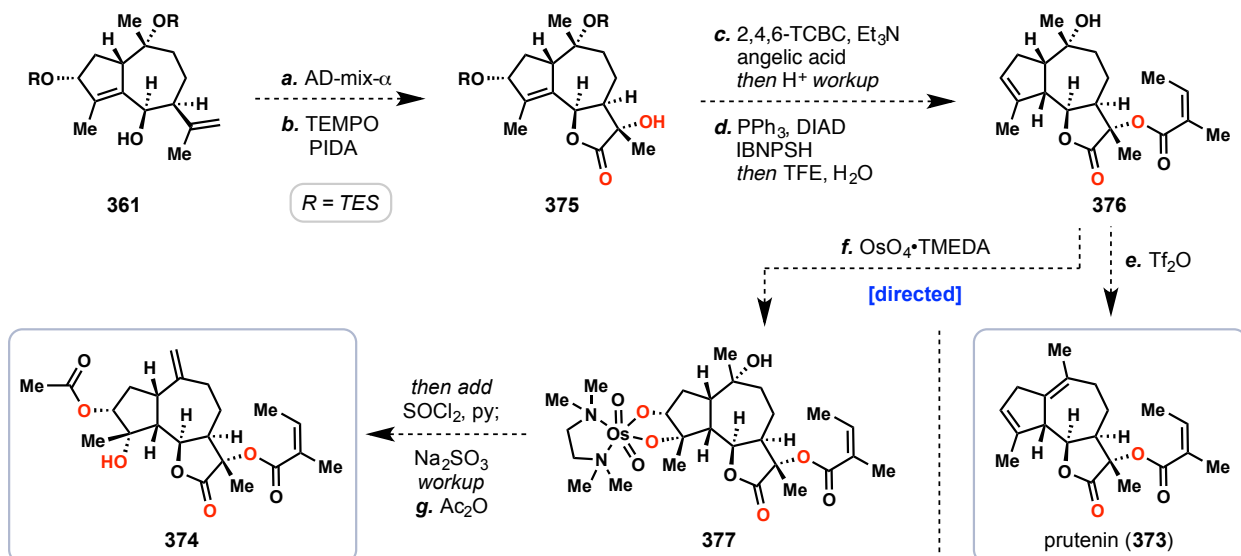


Figure 2.25. A) Functionalization of the minor isomer (**366**) from the Pauson–Khand reaction. B) Selected examples of unsuccessful attempts in the construction of the B ring.



Scheme 2.24. Potential access to two biogenetically related slovanolides prutenin (**373**) and **374**.

2.7.2 Study towards the Synthesis of C-8 Oxygenated Slovanolides

The C-8 oxygenated slovanolides represent the middle level of oxidation states in this family. In the synthetic studies on these targets (Figure 2.26A), intermediate **378** and **379**, which are related to the synthesis of mikanokryptin (**44**), were examined for the preparation of the corresponding aldehydes **380** and **381**. However, both intermediates remained unreactive towards the TESOTf-mediated deacetalization or other Brønsted acid-mediated conditions.

In a key study (Figure 2.26B), α -methylene lactone **320** that is also an intermediate in our synthesis of nortrilobolide (**40**) led to successful construction of the slovanolide's carbon network. From **320**, reduction with NaBH₄ cleanly afforded α -methyl lactone **382** in near quantitative yield. The subsequent DDQ-mediated PMB ether cleavage was found to be sensitive to both reaction time and workup procedure. Under optimal conditions, the reaction mixture was quenched after approximately 2 hours by a mixed aqueous solution of NaHCO₃ and Na₂S₂O₃, and the organic extract was directly filtered through a short column of silica gel. With this procedure, the sensitive alcohol **383** could be obtained in high yield. Conversely, the substantial formation of 8,12-lactone **384** was observed with extension of the reaction time or concentration of the crude mixture. Alcohol **383** was then immediately treated with Dess–Martin periodinane, in which a clean conversion was observed after 30 minutes based on TLC analysis. However, aldehyde **381** was found to be highly unstable as well. Silica gel column chromatography or preparative TLC led to decomposition to a more polar aldehyde, tentatively assigned as **385** based on spectroscopic analysis (*cf.* **332** → **333**, Figure 2.18).

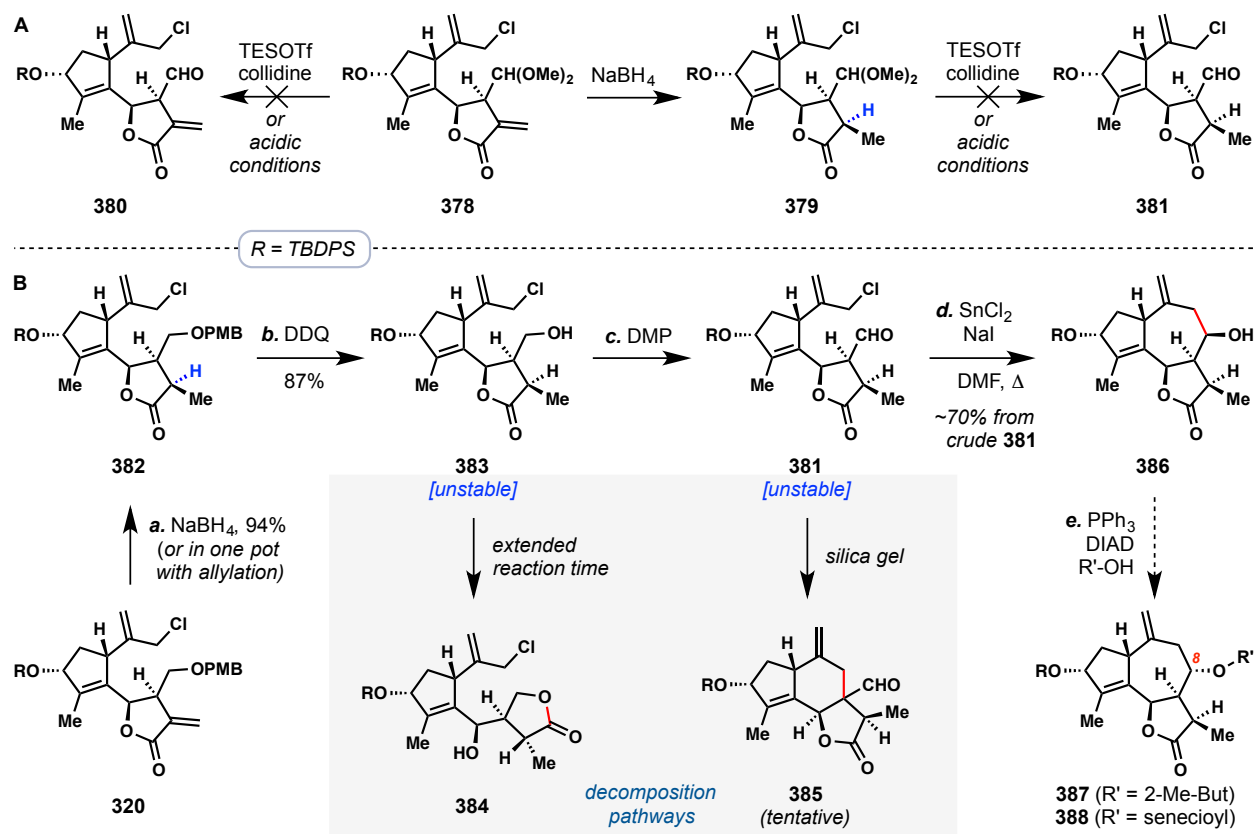
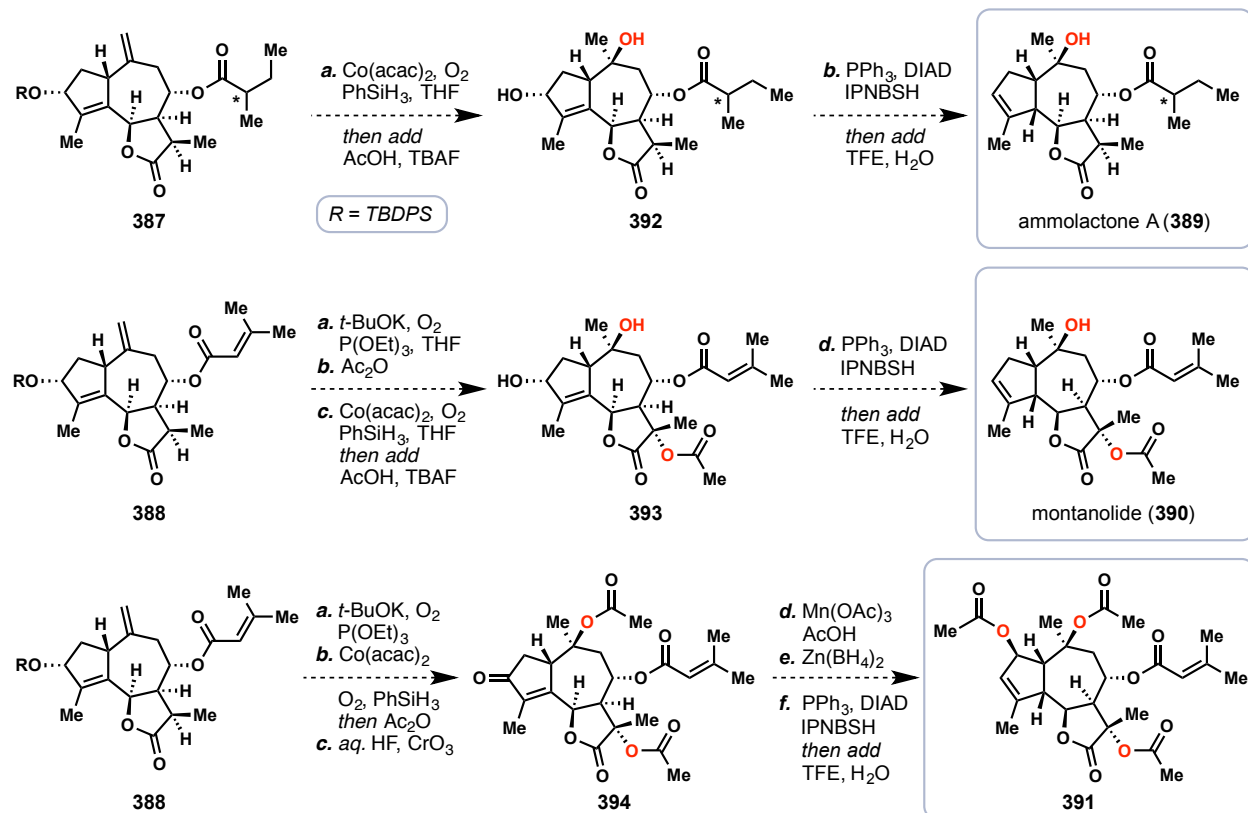


Figure 2.26. Preliminary studies towards the synthesis of C-8 oxygenated slovanolides.

Nevertheless, the SnCl_2 -mediated intramolecular allylation continued to be robust and could cleanly convert the crude aldehyde to the [5,7,5]-fused tricycle **386**. At this stage, intermediate **386** is stable for storage. A subsequent Mitsunobu reaction was envisioned to install the ester moiety at C-8, which was found in most C-8 oxygenated slovanolides. Potentially, from the Mitsunobu products we could access slovanolides with the middle levels of oxidation states, represented by ammollactone A (**389**), montanolide (**390**), and **391** (Scheme 2.25). Future key experiments will involve hydration of the exocyclic alkene [$\text{Co}(\text{acac})_2$, PhSiH_3 , O_2], α -oxygenation of the C-ring lactone [$t\text{-BuOK}$, O_2 , $\text{P}(\text{OEt})_3$], or α -oxygenation of the A-ring enone [$\text{Mn}(\text{OAc})_3$, AcOH],^{56a} in combination with introduction of the $\Delta_{3,4}$ -alkene as the end game.



Scheme 2.25. Potential access to C-8 oxygenated slovanolides with various oxidation states.

In summary, we could potentially access the Apiaceae guaianolides ranging all the oxidation levels, in which I have completed the synthesis of grilactone (**353**) and sinodiellide (**354**) as the first level, nortrilobolide (**40**) and thapsigargin (**41**) as the top levels, and the key intermediates **361** and **386** *en route* to slovanolides **373–374** and **389–391** representing the remaining oxidation states.

2.8 Conclusion and Acknowledgements

In conclusion, we have expanded our oxygen stitching strategy from the synthesis of endoperoxide-containing natural products, to the strategic installation of multiple oxygen atoms in complex sesquiterpenoids. Such a conceptually novel transformation was envisioned to have continued use in the total syntheses of other highly oxygenated terpenoids. For the synthesis of complex guaianolides, we have demonstrated the power of the SnCl₂-mediated intramolecular allylation in the construction of the cycloheptane core. This robust condition may find use in the syntheses of other terpenoids that contain seven-membered carbocyclic rings.

The total syntheses of mikanokryptin, nortrilobolide, grilactone, and sinodielide were designed by Professor Thomas Maimone and myself in a collaborative process. The expansion of the endoperoxide synthesis to the stereocontrolled trihydroxylation was conceptualized and realized by myself with the guidance from Professor Thomas Maimone.

The experiments discussed in sections 2.3, 2.4, 2.6, and 2.7 were conducted solely by me. The synthetic route to mikanokryptin discussed in section 2.5 was explored by myself, while Dr. Silong Xu contributed to the optimization of the ozonolysis–condensation reaction and the indium-mediated allylation reaction, as well as significant assistance with scale-up efforts which enabled my examination of the front-line reactions. All X-ray crystal structures were obtained by Dr. Antonio DiPasquale, and the suitable crystalline samples were prepared and submitted by myself.

Furthermore, undergraduate researcher Yujia Tao and I have completed a 3-step total synthesis of a eudesmane sesquiterpene boariol via the oxygen stitching strategy disclosed in this chapter. The synthesis was designed by me, and the experiments were conducted by Yujia Tao under my guidance.

2.9 References

1. (a) Mahalingam, D.; Wilding, G.; Denmeade, S.; Sarantopoulos, J.; Cosgrove, D.; Cetnar, J.; Azad, N.; Bruce, J.; Kurman, M.; Allgood, V. E.; Carducci, M., *Br. J. Cancer* **2016**, *114*, 986; (b) Mahalingam, D.; Peguero, J.; Cen, P.; Allgood, V.; Shazer, R.; Campos, L., *J. Hepatol.* **2017**, *66*, S207.
2. Rasmussen, U.; Christensen, S. B.; Sandberg, F., *Acta Pharm. Suec.* **1978**, *15*, 133.
3. (a) Thastrup, O.; Cullen, P. J.; Drobak, B. K.; Hanley, M. R.; Dawson, A. P., *Proc. Natl. Acad. Sci. U. S. A.* **1990**, *87*, 2466; (b) Treimana, M.; Caspersena, C.; Christensen, S. B., *Trends Pharmacol. Sci.* **1998**, *19*, 131; (c) Andersen, T. B.; Lopez, C. Q.; Manczak, T.; Martinez, K.; Simonsen, H. T., *Molecules* **2015**, *20*, 6113.
4. (a) Pedersen, B. P.; Buch-Pedersen, M. J.; Morth, J. P.; Palmgren, M. G.; Nissen, P., *Nature* **2007**, *450*, 1111; (b) Quynh Doan, N. T.; Christensen, S. B., *Curr. Pharm. Des.* **2015**, *21*, 5501.
5. Sohoel, H.; Jensen, A. M. L.; Moller, J. V.; Nissen, P.; Denmeade, S. R.; Isaacs, J. T.; Olsen, C. E.; Christensen, S. B., *Bioorg. Med. Chem.* **2006**, *14*, 2810.
6. (a) Simonsen, H. T.; Weitzel, C.; Christensen, S. B., Guaianolide Sesquiterpenoids: Pharmacology and Biosynthesis. In *Natural Products*, Ramawat, K.; Mérillon, J. M., Eds. Springer: Berlin, 2013; (b) Santana, A.; Molinillo, J. M. G.; Macias, F. A., *Eur. J. Org. Chem.* **2015**, 2093; (c) Schall, A.; Reiser, O., *Eur. J. Org. Chem.* **2008**, 2353.
7. (a) Drew, D. P.; Krichau, N.; Reichwald, K.; Simonsen, H. T., *Phytochem. Rev.* **2009**, *8*, 581; (b) Holub, M.; Budesinsky, M., *Phytochemistry* **1986**, *25*, 2015.
8. (a) Padilla-Gonzalez, G. F.; dos Santos, F. A.; Da Costa, F. B., *Crit. Rev. Plant. Sci.* **2016**, *35*, 18; (b) Ghantous, A.; Gali-Muhtasib, H.; Vuorela, H.; Saliba, N. A.; Darwiche, N., *Drug Discovery Today* **2010**, *15*, 668; (c) Ivanescu, B.; Miron, A.; Corciova, A., *J. Anal. Methods. Chem.* **2015**, *2015*, 247685; (d) Chadwick, M.; Trewin, H.; Gawthrop, F.; Wagstaff, C., *Int. J. Mol. Sci.* **2013**, *14*, 12780.
9. (a) Kupchan, S. M.; Fessler, D. C.; Eakin, M. A.; Giacobbe, T. J., *Science* **1970**, *168*, 376; (b) Kupchan, S. M.; Eakin, M. A.; Thomas, A. M., *J. Med. Chem.* **1971**, *14*, 1147; (c) Lee, K. H.; Hall, I. H.; Mar, E. C.; Starnes, C. O.; ElGebaly, S. A.; Waddell, T. G.; Hadgraft, R. I.; Ruffner, C. G.; Weidner, I., *Science* **1977**, *196*, 533; (d) Taylor, P. G.; Dupuy Loo, O. A.; Bonilla, J. A.; Murillo, R., *Fitoterapia* **2008**, *79*, 428; (e) Siedle, B.; Garcia-Pineros, A. J.; Murillo, R.; Schulte-Monting, J.; Castro, V.; Rungeler, P.; Klaas, C. A.; Da Costa, F. B.; Kisiel, W.; Merfort, I., *J. Med. Chem.* **2004**, *47*, 6042; (f) Scotti, M. T.; Fernandes, M. B.; Ferreira, M. J.; Emerenciano, V. P., *Bioorg. Med. Chem.* **2007**, *15*, 2927; (g) Zhang, Q.; Lu, Y.; Ding, Y.; Zhai, J.; Ji, Q.; Ma, W.; Yang, M.; Fan, H.; Long, J.; Tong, Z.; Shi, Y.; Jia, Y.; Han, B.; Zhang, W.; Qiu, C.; Ma, X.; Li, Q.; Shi, Q.; Zhang, H.; Li, D.; Zhang, J.; Lin, J.; Li, L. Y.; Gao, Y.; Chen, Y., *J. Med. Chem.* **2012**, *55*, 8757; (h) Janecka, A.; Wyrebska, A.; Gach, K.; Fichna, J.; Janecki, T., *Drug Discovery Today* **2012**, *17*, 561; (i) Zhang, S.; Won, Y. K.; Ong, C. N.; Shen, H. M., *Curr. Med. Chem. Anticancer Agents* **2005**, *5*, 239; (j) Merfort, I., *Curr. Drug Targets* **2011**, *12*, 1560; (k) Fuchino, H.; Koide, T.; Takahashi, M.; Sekita, S.; Satake, M., *Planta Med.* **2001**, *67*, 647; (l) Rocha, L. G.; Almeida, J. R.; Macedo, R. O.; Barbosa-Filho, J. M., *Phytomedicine* **2005**, *12*, 514; (m) Higuchi, Y.; Shimoma, F.; Ando, M., *J. Nat. Prod.* **2003**, *66*, 810; (n) Ross, J. J.; Arnason, J. T.; Birnboim, H. C., *Planta Med.* **1999**, *65*, 126; (o) Marles, R. J.; Kaminski, J. J.

- Arnason, J. T.; Pazos-Sanou, L.; Heptinstall, S.; Fischer, N. H.; Crompton, C. W.; Kindack, D. G.; Awang, D. V., *J. Nat. Prod.* **1992**, *55*, 1044.
10. (a) Kreuger, M. R. O.; Grootjans, S.; Biavatti, M. W.; Vandenabeele, P.; D'Herde, K., *Anti-Cancer Drugs* **2012**, *23*, 883; (b) Al-Saghir, J.; Al-Ashi, R.; Salloum, R.; Saliba, N. A.; Talhouk, R. S.; Homaidan, F. R., *BMC Complement Altern. Med.* **2009**, *9*, 36.
 11. (a) Hwang, D.; Fischer, N. H.; Jang, B. C.; Tak, H.; Kim, J. K.; Lee, W., *Biochem. Biophys. Res. Commun.* **1996**, *226*, 810; (b) Uchi, H.; Arrighi, J. F.; Aubry, J. P.; Furue, M.; Hauser, C., *J. Allergy Clin. Immunol.* **2002**, *110*, 269.
 12. Chaturvedi, M. M.; Sung, B.; Yadav, V. R.; Kannappan, R.; Aggarwal, B. B., *Oncogene* **2011**, *30*, 1615.
 13. (a) Lyss, G.; Knorre, A.; Schmidt, T. J.; Pahl, H. L.; Merfort, I., *J. Biol. Chem.* **1998**, *273*, 33508; (b) Rungeler, P.; Castro, V.; Mora, G.; Goren, N.; Vichnewski, W.; Pahl, H. L.; Merfort, I.; Schmidt, T. J., *Bioorg. Med. Chem.* **1999**, *7*, 2343; (c) Garcia-Pineros, A. J.; Castro, V.; Mora, G.; Schmidt, T. J.; Strunck, E.; Pahl, H. L.; Merfort, I., *J. Biol. Chem.* **2001**, *276*, 39713; (d) Garcia-Pineros, A. J.; Lindenmeyer, M. T.; Merfort, I., *Life Sci.* **2004**, *75*, 841; (e) Buchele, B.; Zugmaier, W.; Lunov, O.; Syrovets, T.; Merfort, I.; Simmet, T., *Anal. Biochem.* **2010**, *401*, 30.
 14. (a) Hehner, S. P.; Heinrich, M.; Bork, P. M.; Vogt, M.; Ratter, F.; Lehmann, V.; Schulze-Osthoff, K.; Droge, W.; Schmitz, M. L., *J. Biol. Chem.* **1998**, *273*, 1288; (b) Oka, D.; Nishimura, K.; Shiba, M.; Nakai, Y.; Arai, Y.; Nakayama, M.; Takayama, H.; Inoue, H.; Okuyama, A.; Nonomura, N., *Int. J. Cancer* **2007**, *120*, 2576.
 15. Kwok, B. H.; Koh, B.; Ndubuisi, M. I.; Elofsson, M.; Crews, C. M., *Chem. Biol.* **2001**, *8*, 759.
 16. Jin, H. Z.; Lee, J. H.; Lee, D.; Hong, Y. S.; Kim, Y. H.; Lee, J. J., *Phytochemistry* **2004**, *65*, 2247.
 17. Liu, Q. Elucidation of the sesquiterpene lactone biosynthetic pathway in feverfew (*Tanacetum parthenium*). PhD Thesis, Wageningen University, Wageningen, the Netherlands, 2013.
 18. (a) Andersen, T. B.; Martinez-Swatson, K. A.; Rasmussen, S. A.; Boughton, B. A.; Jorgensen, K.; Andersen-Ranberg, J.; Nyberg, N.; Christensen, S. B.; Simonsen, H. T., *Plant Physiol.* **2017**, *174*, 56; (b) Pickel, B.; Drew, D. P.; Manczak, T.; Weitzel, C.; Simonsen, H. T.; Ro, D. K., *Biochem. J.* **2012**, *448*, 261.
 19. Ugliengo, P.; Viterbo, D.; Appendino, G.; Chiari, G., *J. Mol. Struct.* **1992**, *265*, 311.
 20. (a) Ho, T.-L., *Enantioselective Synthesis. Natural Products from Chiral Terpenes*. Wiley: New York, 1992; (b) Gaich, T.; Mulzer, J., *Chiral Pool Synthesis: Starting from Terpenes*. In *Comprehensive Chirality*, Carreira, E. M.; Yamamoto, H., Eds. Elsevier Ltd.: 2012; Vol. 2, pp 163; (c) Brill, Z. G.; Condakes, M. L.; Ting, C. P.; Maimone, T. J., *Chem. Rev.* **2017**, *117*, 11753.
 21. (a) Lee, E.; Yoon, C. H., *J. Chem. Soc., Chem. Commun.* **1994**, 479; (b) Lee, E.; Lim, J. W.; Yoon, C. H.; Sung, Y. S.; Kim, Y. K.; Yun, M.; Kim, S., *J. Am. Chem. Soc.* **1997**, *119*, 8391.
 22. Sanchezviesca, F.; Romo, J., *Tetrahedron* **1963**, *19*, 1285.
 23. Daniewski, W. M.; Danikiewicz, W.; Gumulka, M.; Pankowska, E.; Krajewski, J.; Grabarczyk, H.; Wichlacz, M., *Phytochemistry* **1993**, *34*, 1639.
 24. Hung, K.; Hu, X.; Maimone, T. J., *Nat. Prod. Rep.* **2018**, *35*, 174.

25. (a) Liu, Y.; Zhao, G., *Chin. J. Chem.* **2013**, *31*, 18; (b) Pogrebnoi, S.; Saraber, F. C. E.; Jansen, B. J. M.; de Groot, A., *Tetrahedron* **2006**, *62*, 1743; (c) Zhang, F. Y.; Jia, Y. X., *Tetrahedron* **2009**, *65*, 6840.
26. (a) Oliver, S. F.; Hogenauer, K.; Simic, O.; Antonello, A.; Smith, M. D.; Ley, S. V., *Angew. Chem. Int. Ed.* **2003**, *42*, 5996; (b) Ley, S. V.; Antonello, A.; Balskus, E. P.; Booth, D. T.; Christensen, S. B.; Cleator, E.; Gold, H.; Hogenauer, K.; Hunger, U.; Myers, R. M.; Oliver, S. F.; Simic, O.; Smith, M. D.; Sohoel, H.; Woolford, A. J., *Proc. Natl. Acad. Sci. U. S. A.* **2004**, *101*, 12073.
27. (a) Ball, M.; Andrews, S. P.; Wierschem, F.; Cleator, E.; Smith, M. D.; Ley, S. V., *Org. Lett.* **2007**, *9*, 663; (b) Andrews, S. P.; Ball, M.; Wierschem, F.; Cleator, E.; Oliver, S.; Hogenauer, K.; Simic, O.; Antonello, A.; Hunger, U.; Smith, M. D.; Ley, S. V., *Chem. Eur. J.* **2007**, *13*, 5688.
28. Zhang, S.; Wang, J.; Xue, H.; Deng, Q.; Xing, F.; Ando, M., *J. Nat. Prod.* **2002**, *65*, 1927.
29. Elford, T. G.; Hall, D. G., *J. Am. Chem. Soc.* **2010**, *132*, 1488.
30. Yang, H.; Gao, Y.; Qiao, X.; Xie, L.; Xu, X., *Org. Lett.* **2011**, *13*, 3670.
31. Barbetti, P.; Casinovi, C. G.; Santurbano, B.; Longo, R., *Collect. Czech. Chem. Commun.* **1979**, *44*, 3123.
32. Both enantiomers of **102** were prepared in this work, and *ent*-**102** was found to possess promising antitumor activities.
33. Huo, J.; Yang, S.-P.; Ding, J.; Yue, J.-M., *J. Nat. Prod.* **2004**, *67*, 1470.
34. de Lichtervelde, L.; Boitano, A. E.; Wang, Y.; Krastel, P.; Petersen, F.; Cooke, M. P.; Schultz, P. G., *ACS Chem. Biol.* **2013**, *8*, 866.
35. Johnson, T. C.; Chin, M. R.; Han, T.; Shen, J. P.; Rana, T.; Siegel, D., *J. Am. Chem. Soc.* **2016**, *138*, 6068.
36. Wolinsky, J.; Hutchins, R. O.; Gibson, T. W., *J. Org. Chem.* **1968**, *33*, 407.
37. Barton, D. H. R.; de Mayo, P.; Shafiq, M., *J. Chem. Soc.* **1957**, 929.
38. (a) Trommsdorff, H., *Ann. Chem. Pharm.* **1834**, *11*, 190; (b) Kozlowski, M.; Yoon, T., *J. Org. Chem.* **2016**, *81*, 6895; (c) Natarajan, A.; Tsai, C. K.; Khan, S. I.; McCarren, P.; Houk, K. N.; Garcia-Garibay, M. A., *J. Am. Chem. Soc.* **2007**, *129*, 9846.
39. Rimington, C.; Roets, G., *Onderstepoort J. Vet. Sci.* **1936**, *7*, 507.
40. (a) Barton, D. H. R.; Levisalles, J. E. D., *J. Chem. Soc.* **1958**, 4518; (b) Barton, D. H. R.; Wells, R. J.; Pinhey, J. T., *J. Chem. Soc.* **1964**, 2518; (c) Barton, D. H. R.; Pinhey, J. T., *Proc. Chem. Soc.* **1960**, 279.
41. (a) Hamilton, J. A.; Mcphail, A. T.; Sim, G. A., *J. Chem. Soc.* **1962**, 708; (b) Hamilton, J. A.; Mcphail, A. T.; Sim, G. A., *Proc. Chem. Soc.* **1960**, 278.
42. (a) Holub, M.; Herout, V., *Collect. Czech. Chem. Commun.* **1962**, *27*, 2980; (b) Mariano, M.; Alejandra, M. Z.; Pedro, J. N., *J. Nat. Prod.* **1988**, *51*, 221.
43. (a) White, E. H.; Marx, J. N., *J. Am. Chem. Soc.* **1967**, *89*, 5511; (b) Marx, J. N.; White, E. H., *Tetrahedron* **1969**, *25*, 2117; (c) White, E. H.; Eguchi, S.; Marx, J. N., *Tetrahedron* **1969**, *25*, 2099.
44. Seaman, F. C.; Fischer, N. H.; Mabry, T. J., *Phytochemistry* **1986**, *25*, 2663.
45. Greene, A. E.; Edgar, M. T., *J. Org. Chem.* **1989**, *54*, 1468.
46. Schuster, D. I.; Fabian, A. C., *Tetrahedron Lett.* **1966**, 4093.
47. (a) Blay, G.; Cardona, M. L.; Garcia, B.; Pedro, J. R., *J. Org. Chem.* **1991**, *56*, 6172; (b) Blay, G.; Bargues, V.; Cardona, L.; Garcia, B.; Pedro, J. R., *J. Org. Chem.* **2000**, *65*, 6703;

- (c) Blay, G.; Bargues, V. V.; Cardona, L.; Collado, A. M.; Garcia, B.; Munoz, M. C.; Pedro, J. R., *J. Org. Chem.* **2000**, *65*, 2138.
48. (a) Manzano, F. L.; Guerra, F. M.; Moreno-Dorado, F. J.; Jorge, Z. D.; Massanet, G. M., *Org. Lett.* **2006**, *8*, 2879; (b) Marin-Barrios, R.; Garcia-Cabeza, A. L.; Moreno-Dorado, F. J.; Guerra, F. M.; Massanet, G. M., *J. Org. Chem.* **2014**, *79*, 6501.
49. Chu, H.; Smith, J. M.; Felding, J.; Baran, P. S., *ACS Cent. Sci.* **2017**, *3*, 47.
50. (a) Hu, X.; Xu, S.; Maimone, T. J., *Angew. Chem. Int. Ed.* **2017**, *56*, 1624; (b) Chen, D.; Evans, P. A., *J. Am. Chem. Soc.* **2017**, *139*, 6046.
51. Herz, W.; Srinivasan, A.; Kalyanaraman, P. S., *Phytochemistry* **1975**, *14*, 233.
52. (a) Bovill, M. J.; Guy, M. H. P.; Sim, G. A.; White, D. N. J.; Herz, W., *J. Chem. Soc., Perkin Trans. 2* **1979**, 53; (b) Reynolds, W. F.; Enriquez, R. G.; Chavez, M. A.; Silba, A. L.; Martinez, M. A., *Can. J. Chem.* **1985**, *63*, 849.
53. Zhao, Y. M.; Maimone, T. J., *Angew. Chem. Int. Ed.* **2015**, *54*, 1223.
54. Hoffmann, H. M. R.; Rabe, J., *J. Org. Chem.* **1985**, *50*, 3849.
55. Berdan, C. A.; Ho, R.; Lehtola, H. S.; To, M.; Hu, X.; Huffman, T. R.; Petri, Y.; Demeulenaere, S. G.; Maimone, T. J.; Olzmann, J. A.; Nomura, D. K., *eLife* **2018**, *submitted*.
56. (a) Doan, N. T.; Crestey, F.; Olsen, C. E.; Christensen, S. B., *J. Nat. Prod.* **2015**, *78*, 1406; (b) Crestey, F.; Toma, M.; Christensen, S. B., *Tetrahedron Lett.* **2015**, *56*, 5896.
57. (a) Rigby, J. H.; Wilson, J. Z., *J. Am. Chem. Soc.* **1984**, *106*, 8217; (b) Rigby, J. H.; Senanayake, C., *J. Am. Chem. Soc.* **1987**, *109*, 3147.
58. Demuynck, M.; Devreese, A. A.; Declercq, P. J.; Vandewalle, M., *Tetrahedron Lett.* **1982**, *23*, 2501.
59. Edgar, M. T.; Greene, A. E.; Crabbe, P., *J. Org. Chem.* **1978**, *44*, 159.
60. Ando, M.; Ibayashi, K.; Minami, N.; Yoshimura, H.; Nakamura, T.; Isogai, K., *J. Nat. Prod.* **1994**, *57*, 433.
61. Li, C.; Yu, X.; Lei, X., *Org. Lett.* **2010**, *12*, 4284.
62. Schreiber, J.; Maag, H.; Hashimoto, N.; Eschenmoser, A., *Angew. Chem. Int. Ed.* **1971**, *10*, 330.
63. Rybalko, K. S.; Bankovskii, A. I.; Kibalchin, P. N., *J. Gen. Chem. USSR* **1964**, *34*, 1358.
64. Carret, S.; Depres, J. P., *Angew. Chem. Int. Ed.* **2007**, *46*, 6870.
65. Lone, S. H.; Bhat, K. A.; Khuroo, M. A., *Chem. Biol. Interact.* **2015**, *240*, 180.
66. Adekenov, S. M.; Muchametzhanov, M. N.; Kagarlitskii, A. D.; Kuprianov, A. N., *Khim. Prir. Soedin.* **1982**, 655.
67. Kalidindi, S.; Jeong, W. B.; Schall, A.; Bandichhor, R.; Nosse, B.; Reiser, O., *Angew. Chem. Int. Ed.* **2007**, *46*, 6361.
68. Schall, A. Studies Towards the Total Synthesis of Biological Active γ -Butyrolactones. PhD Thesis, University of Regensburg, Regensburg, Germany, 2007.
69. Zhai, J. D.; Li, D.; Long, J.; Zhang, H. L.; Lin, J. P.; Qiu, C. J.; Zhang, Q.; Chen, Y., *J. Org. Chem.* **2012**, *77*, 7103.
70. (a) Bohlmann, F.; Zdero, C., *Chem. Ber.* **1974**, *107*, 1409; (b) Bohlmann, F.; Zdero, C.; Jakupovic, J.; Rourke, J. P., *Liebigs Ann. Chem.* **1985**, 2342.
71. (a) Barthel, A.; Kaden, F.; Jager, A.; Metz, P., *Org. Lett.* **2016**, *18*, 3298; (b) Knuppel, S.; Rogachev, V. O.; Metz, P., *Eur. J. Org. Chem.* **2010**, 6145.
72. Posner, G. H.; Babiak, K. A.; Loomis, G. L.; Frazee, W. J.; Mittal, R. D.; Karle, I. L., *J. Am. Chem. Soc.* **1980**, *102*, 7498.

73. Umbreit, M. A.; Sharpless, K. B., *Org. Synth.* **1981**, *60*, 29.
74. (a) Shimomaki, K.; Kusama, H.; Iwasawa, N., *Chem. Eur. J.* **2016**, *22*, 9953; (b) Hirose, T.; Miyakoshi, N.; Mukai, C., *J. Org. Chem.* **2008**, *73*, 1061.
75. Delair, P.; Kann, N.; Greene, A. E., *J. Chem. Soc., Perkin Trans. 1* **1994**, 1651.
76. (a) Nakamura, A.; Nakada, M., *Synthesis* **2013**, *45*, 1421; (b) Chen, M. S.; White, M. C., *Science* **2007**, *318*, 783; (c) Chen, M. S.; White, M. C., *J. Am. Chem. Soc.* **2004**, *126*, 1346; (d) Chen, M. S.; Prabakaran, N.; Labenz, N. A.; White, M. C., *J. Am. Chem. Soc.* **2005**, *127*, 6970; (e) Stang, E. M.; White, M. C., *J. Am. Chem. Soc.* **2011**, *133*, 14892; (f) McLaughlin, E. C.; Choi, H.; Wang, K.; Chiou, G.; Doyle, M. P., *J. Org. Chem.* **2009**, *74*, 730.
77. Roberts, B. P., *Chem. Soc. Rev.* **1999**, *28*, 25.
78. (a) Wolinsky, J.; Barker, W., *J. Am. Chem. Soc.* **1960**, *82*, 636; (b) Srikrishna, A.; Babu, N. C., *Tetrahedron Lett.* **2001**, *42*, 4913; (c) Pisoni, D. S.; Silva, D. B.; Schenato, R. A.; Ceschi, M. A., *J. Braz. Chem. Soc.* **2004**, *15*, 652.
79. Elamparuthi, E.; Fellay, C.; Neuburger, M.; Gademann, K., *Angew. Chem. Int. Ed.* **2012**, *51*, 4071.
80. Donohoe, T. J.; Ironmonger, A.; Kershaw, N. M., *Angew. Chem. Int. Ed.* **2008**, *47*, 7314.
81. Royals, E. E.; Robinson, A. G., *J. Am. Chem. Soc.* **1956**, *78*, 4161.
82. Furstner, A., *Chem. Rev.* **1999**, *99*, 991.
83. Han, X.; Peh, G.; Floreancig, P. E., *Eur. J. Org. Chem.* **2013**, 1193.
84. Wuts, P. G. M.; Greene, T. W., Protection for the Carbonyl Group. In *Greene's Protective Groups in Organic Synthesis*, 4 ed.; John Wiley & Sons, Inc: Hoboken, New Jersey, 2006; Vol. 4, pp 431.
85. (a) Graham, T. J.; Doyle, A. G., *Org. Lett.* **2012**, *14*, 1616; (b) Arendt, K. M.; Doyle, A. G., *Angew. Chem. Int. Ed.* **2015**, *54*, 9876.
86. (a) Fujioka, H.; Sawama, Y.; Murata, N.; Okitsu, T.; Kubo, O.; Matsuda, S.; Kita, Y., *J. Am. Chem. Soc.* **2004**, *126*, 11800; (b) Fujioka, H.; Okitsu, T.; Sawama, Y.; Murata, N.; Li, R.; Kita, Y., *J. Am. Chem. Soc.* **2006**, *128*, 5930.
87. (a) Bryan, V. J.; Chan, T. H., *Tetrahedron Lett.* **1996**, *37*, 5341; (b) Iwamoto, M.; Miyano, M.; Utsugi, M.; Kawada, H.; Nakada, M., *Tetrahedron Lett.* **2004**, *45*, 8653; (c) Fleury, L. M.; Kosal, A. D.; Masters, J. T.; Ashfeld, B. L., *J. Org. Chem.* **2013**, *78*, 253.
88. (a) Suzuki, S.; Onishi, T.; Fujita, Y.; Otera, J., *Synth. Commun.* **1985**, *15*, 1123; (b) Tilstam, U.; Weinmann, H., *Org. Process Res. Dev.* **2002**, *6*, 384; (c) Farney, E. P.; Feng, S. S.; Schafers, F.; Reisman, S. E., *J. Am. Chem. Soc.* **2018**, *140*, 1267.
89. Bagirov, V. Y.; Sheichenko, V. I.; Gasanova, R. Y.; Pimenov, M. G., *Chem. Nat. Compd.* **1978**, *14*, 695.
90. (a) Orav, A.; Raal, A.; Arak, E.; Muurisepp, M.; Kailas, T., *Proc. Estonian Acad. Sci. Chem.* **2006**, *55*, 155; (b) Fischer, G., *Adv. Heterocycl. Chem.* **2009**, *97*, 131.
91. Cleary, L.; Pitzen, J.; Brailsford, J. A.; Shea, K. J., *Org. Lett.* **2014**, *16*, 4460.
92. Maury, J.; Feray, L.; Bertrand, M. P., *Org. Lett.* **2011**, *13*, 1884.
93. Beccalli, E. M.; Erba, E.; Trimarco, P., *Synth. Commun.* **2000**, *30*, 629.
94. Kurono, N.; Yamaguchi, M.; Suzuki, K.; Ohkuma, T., *J. Org. Chem.* **2005**, *70*, 6530.
95. Hue, B. Studies towards the Total Synthesis of Solanoclepin A. PhD Thesis, University of Amsterdam, 2005.
96. (a) Chen, M. J.; Narkunan, K.; Liu, R. S., *J. Org. Chem.* **1999**, *64*, 8311; (b) Hoffmann, H. M. R.; Rabe, J., *Angew. Chem. Int. Ed.* **1985**, *24*, 94; (c) Okuda, Y.; Nakatsukasa, S.;

- Oshima, K.; Nozaki, H., *Chem. Lett.* **1985**, 481; (d) Masuyama, Y.; Nimura, Y.; Kurusu, Y., *Tetrahedron Lett.* **1991**, 32, 225.
97. Park, B. R.; Kim, K. H.; Lim, J. W.; Kim, J. N., *Tetrahedron Lett.* **2012**, 53, 36.
98. (a) Nokami, J.; Tamaoka, T.; Ogawa, H.; Wakabayashi, S., *Chem. Lett.* **1986**, 541; (b) Kato, N.; Kusakabe, S.; Wu, X.; Kamitamari, M.; Takeshita, H., *J. Chem. Soc., Chem. Commun.* **1993**, 1002; (c) Boldrini, G. P.; Savoia, D.; Tagliavini, E.; Trombini, C.; Umanironchi, A., *J. Org. Chem.* **1983**, 48, 4108; (d) Boldrini, G. P.; Lodi, L.; Tagliavini, E.; Tarasco, C.; Trombini, C.; Umanironchi, A., *J. Org. Chem.* **1987**, 52, 5447; (e) Nishida, M.; Tozawa, T.; Yamada, K.; Mukaiyama, T., *Chem. Lett.* **1996**, 1125; (f) Petrier, C.; Luche, J. L., *J. Org. Chem.* **1985**, 50, 910; (g) Gao, Y.; Wang, X.; Sun, L.; Xie, L.; Xu, X., *Org. Biomol. Chem.* **2012**, 10, 3991; (h) Foo, K.; Usui, I.; Gotz, D. C.; Werner, E. W.; Holte, D.; Baran, P. S., *Angew. Chem. Int. Ed.* **2012**, 51, 11491; (i) Tanaka, H.; Yamashita, S.; Hamatani, T.; Ikemoto, Y.; Torii, S., *Chem. Lett.* **1986**, 1611; (j) Zhou, J. Y.; Jia, Y.; Sun, G. F.; Wu, S. H., *Synth. Commun.* **1997**, 27, 1899; (k) Tanaka, H.; Nakahata, S.; Watanabe, H.; Zhao, J. F.; Kuroboshi, M.; Torii, S., *Inorg. Chim. Acta* **1999**, 296, 204; (l) Wada, M.; Akiba, K., *Tetrahedron Lett.* **1985**, 26, 4211; (m) Araki, S.; Ito, H.; Butsugan, Y., *J. Organomet. Chem.* **1988**, 347, 5; (n) Araki, S.; Ito, H.; Katsumura, N.; Butsugan, Y., *J. Organomet. Chem.* **1989**, 369, 291.
99. (a) Molander, G. A.; Harris, C. R., *Chem. Rev.* **1996**, 96, 307; (b) Edmonds, D. J.; Johnston, D.; Procter, D. J., *Chem. Rev.* **2004**, 104, 3371; (c) Nicolaou, K. C.; Ellery, S. P.; Chen, J. S., *Angew. Chem. Int. Ed.* **2009**, 48, 7140.
100. (a) Imai, T.; Nishida, S., *Synthesis* **1993**, 395; (b) Breit, B., *Eur. J. Org. Chem.* **1998**, 1123; (c) Smith, A. B.; Sfougataki, C.; Gotchev, D. B.; Shirakami, S.; Bauer, D.; Zhu, W.; Doughty, V. A., *Org. Lett.* **2004**, 6, 3637.
101. Li, C. J.; Chan, T. H., *Organometallics* **1991**, 10, 2548.
102. (a) Buehler, C. A.; Whitehead, F.; Goodge, B. D., *J. Am. Chem. Soc.* **1937**, 59, 2299; (b) Clark, E. P., *J. Am. Chem. Soc.* **1939**, 61, 1836; (c) Ungnade, H. E.; Hendley, E. C., *J. Am. Chem. Soc.* **1948**, 70, 3921.
103. Bordoloi, M.; Sarmah, J. C.; Sharma, R. P., *Tetrahedron* **1989**, 45, 289.
104. Crabtree, R. H.; Davis, M. W., *Organometallics* **1983**, 2, 681.
105. Frimpong, K.; Wzorek, J.; Lawlor, C.; Spencer, K.; Mitzel, T., *J. Org. Chem.* **2009**, 74, 5861.
106. Semmelhack, M. F.; Chou, C. S.; Cortes, D. A., *J. Am. Chem. Soc.* **1983**, 105, 4492.
107. Magnus, P.; Payne, A. H.; Waring, M. J.; Scott, D. A.; Lynch, V., *Tetrahedron Lett.* **2000**, 41, 9725.
108. (a) Crisp, G. T.; Meyer, A. G., *Tetrahedron* **1995**, 51, 5831; (b) Patel, R. M.; Puranik, V. G.; Argade, N. P., *Org. Biomol. Chem.* **2011**, 9, 6312.
109. Wakamatsu, H.; Nishida, M.; Adachi, N.; Mori, M., *J. Org. Chem.* **2000**, 65, 3966.
110. Ito, A.; Kishida, M.; Kurusu, Y.; Masuyama, Y., *J. Org. Chem.* **2000**, 65, 494.
111. (a) Imai, T.; Nishida, S., *J. Chem. Soc., Chem. Commun.* **1994**, 277; (b) Tan, X. H.; Shen, B.; Deng, W.; Zhao, H.; Liu, L.; Guo, Q. X., *Org. Lett.* **2003**, 5, 1833; (c) Chaudhuri, M. K.; Dehury, S. K.; Hussain, S., *Tetrahedron Lett.* **2005**, 46, 6247; (d) Kashyap, B.; Phukan, P., *Tetrahedron Lett.* **2013**, 54, 6324; (e) Masuyama, Y.; Kaneko, Y.; Kurusu, Y., *Tetrahedron Lett.* **2004**, 45, 8969.
112. (a) Masuyama, Y.; Hayashi, R.; Otake, K.; Kurusu, Y., *J. Chem. Soc., Chem. Commun.* **1988**, 44; (b) Masuyama, Y.; Otake, K.; Kurusu, Y., *Tetrahedron Lett.* **1988**, 29, 3563; (c)

- Masuyama, Y.; Takahara, J. P.; Kurusu, Y., *Tetrahedron Lett.* **1989**, *30*, 3437; (d) Masuyama, Y.; Hayakawa, A.; Kurusu, Y., *J. Chem. Soc., Chem. Commun.* **1992**, 1102; (e) Masuyama, Y.; Ito, A.; Kurusu, Y., *Chem. Commun.* **1998**, 315; (f) Marshall, J. A., *Chem. Rev.* **2000**, *100*, 3163.
113. (a) Waser, J.; Gaspar, B.; Nambu, H.; Carreira, E. M., *J. Am. Chem. Soc.* **2006**, *128*, 11693; (b) Michaudel, Q.; Journot, G.; Regueiro-Ren, A.; Goswami, A.; Guo, Z.; Tully, T. P.; Zou, L.; Ramabhadran, R. O.; Houk, K. N.; Baran, P. S., *Angew. Chem. Int. Ed.* **2014**, *53*, 12091.
114. Hu, X.; Maimone, T. J., Peroxy Radical Additions. In *Science of Synthesis, Applications of Domino Transformations in Organic Synthesis*, Snyder, S. A., Ed. Georg Thieme Verlag: Stuttgart, Germany, 2016; Vol. 1, pp 157.
115. Tokuyasu, T.; Kunikawa, S.; Masuyama, A.; Nojima, M., *Org. Lett.* **2002**, *4*, 3595.
116. (a) Rychlewska, U.; Holub, M.; Budesinsky, M.; Smitalova, Z., *Collect. Czech. Chem. Commun.* **1984**, *49*, 2790; (b) Smitalova, Z.; Budesinsky, M.; Saman, D.; Vasickova, S.; Holub, M., *Collect. Czech. Chem. Commun.* **1984**, *49*, 852.
117. Holub, M.; Motl, O.; Samek, Z., *Collect. Czech. Chem. Commun.* **1978**, *43*, 2471.
118. Bargues, V.; Blay, G.; Cardona, L.; Garcia, B.; Pedro, J. R., *Tetrahedron* **1998**, *54*, 1845.
119. Li, Y.; Chen, Z. X.; Xiao, Q.; Ye, Q. D.; Sun, T. W.; Meng, F. K.; Ren, W. W.; You, L.; Xu, L. M.; Wang, Y. F.; Chen, J. H.; Yang, Z., *Chem. Asian J.* **2012**, *7*, 2334.
120. Krafft, M. E.; Romero, R. H.; Scott, I. L., *J. Org. Chem.* **1992**, *57*, 5277.
121. Condakes, M. L.; Hung, K.; Harwood, S. J.; Maimone, T. J., *J. Am. Chem. Soc.* **2017**, *139*, 17783.
122. (a) Movassaghi, M.; Piizzi, G.; Siegel, D. S.; Piersanti, G., *Angew. Chem. Int. Ed.* **2006**, *45*, 5859; (b) Movassaghi, M.; Ahmad, O. K., *J. Org. Chem.* **2007**, *72*, 1838.
123. (a) Wood, J. L.; Porco, J. A.; Taunton, J.; Lee, A. Y.; Clardy, J.; Schreiber, S. L., *J. Am. Chem. Soc.* **1992**, *114*, 5898; (b) Myers, A. G.; Kukkola, P. J., *J. Am. Chem. Soc.* **1990**, *112*, 8208; (c) Myers, A. G.; Movassaghi, M.; Zheng, B., *J. Am. Chem. Soc.* **1997**, *119*, 8572.
124. Hung, K.; Condakes, M. L.; Morikawa, T.; Maimone, T. J., *J. Am. Chem. Soc.* **2016**, *138*, 16616.

Supplementary Information

For

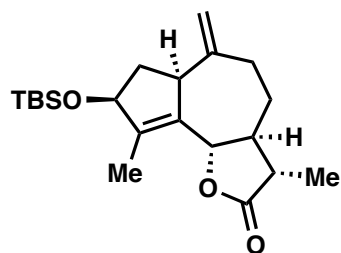
Chapter 2

Expansion of the Oxygen Stitching Strategy: Total Syntheses of
Complex Guaianolides

General Procedures

Unless otherwise stated, all reactions were performed in oven-dried or flame-dried glass round-bottom flask with a rubber septum, or Fisherbrand® borosilicate glass reaction tubes (Fisher Scientific, 1495925A, 13 × 100 mm) with black phenolic screw cap (13-425), under an atmosphere of dry nitrogen or argon. Dry tetrahydrofuran (THF), dichloromethane (DCM), diethyl ether, *N,N*-dimethylformamide (DMF), toluene, and acetonitrile were obtained by passing these previously degassed solvents through activated alumina columns. Anhydrous *N*-methylformamide (NMF) and acetone were purchased from Fisher Chemical and used directly without further purification. Amine and alcohol reagents and solvents were distilled from calcium hydride prior to use. L-Carvone, R-carvone, α -santonin, L-linalool, and 2,2-dimethoxyacetaldehyde (60% in H₂O) were purchased from Sigma-Aldrich and used directly without further purification. Methyl acrylate and 2-butynoic acid were purchased Fisher Chemical and used directly without further purification. Reactions were monitored by thin layer chromatography (TLC) on TLC silica gel 60 F₂₅₄ glass plates (EMD Millipore) and visualized by UV irradiation and staining with *p*-anisaldehyde, phosphomolybdic acid, or potassium permanganate. Volatile solvents were removed under reduced pressure using a rotary evaporator. Flash column chromatography was performed using Silicycle F60 silica gel (60Å, 230-400 mesh, 40-63 μ m). Ethyl acetate and hexanes were purchased from Fisher Chemical and used for chromatography without further purification. Proton nuclear magnetic resonance (¹H NMR) and carbon nuclear magnetic resonance (¹³C NMR) spectra were recorded on Bruker AVB-400, AV-500, AV-600 and AV-700 spectrometers operating at 400, 500, 600, and 700 MHz for ¹H, and 100, 125, 150, and 175 MHz for ¹³C. Chemical shifts are reported in parts per million (ppm) with respect to the residual solvent signal CDCl₃ (¹H NMR: δ = 7.26; ¹³C NMR: δ = 77.16), CD₂Cl₂ (¹H NMR: δ = 5.32; ¹³C NMR: δ = 53.84), DMSO-*d*₆ (¹H NMR: δ = 2.50; ¹³C NMR: δ = 39.52), C₆D₆ (¹H NMR: δ = 7.16; ¹³C NMR: δ = 128.06), and CD₃OD (¹H NMR: δ = 3.31; ¹³C NMR: δ = 49.00). Peak multiplicities are reported as follows: *s* = singlet, *d* = doublet, *t* = triplet, *q* = quartet, *p* = pentet, *dd* = doublet of doublets, *td* = triplet of doublets, *dt* = doublet of triplets, *ddd* = doublet of doublet of doublets, *ddt* = doublet of doublet of triplets, *ddq* = doublet of doublet of quartets, *dddd* = doublet of doublet of doublet of doublets, *m* = multiplet, *br* = broad signal, *app* = apparent. Melting points were determined using MEI-TEMP™ apparatus and are uncorrected. IR spectra were recorded on a Nicolet 380 FT-IR spectrometer. High-resolution mass spectra (HRMS) were obtained by the QB3/chemistry mass spectrometry facility at the University of California, Berkeley using a Thermo LTQ-FT mass spectrometer; and at the Lawrence–Berkeley National Laboratory Catalysis Center using a Perkin Elmer AxION 2 TOF mass spectrometer. Optical rotations were measured on a Perkin-Elmer 241 polarimeter. X-ray crystallographic analyses were performed at the UC-Berkeley College of Chemistry X-ray crystallography facility (MicroSTAR-H APEX II, ChexSTAR: RUA # 1091).

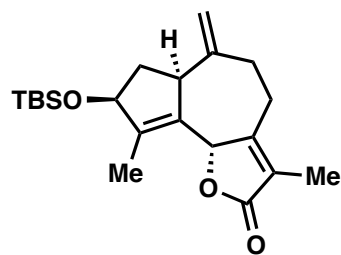
SI-2.3. Model Study



Compound 256: This procedure was adapted from previous conditions reported by Greene and co-workers.¹ The starting enone **120** was prepared by following the procedure reported by Lei and coworkers.² (i) A 100 mL round-bottom flask was charged with a stir bar, enone **120** (1.00 g, 4.06 mmol, 1 equiv), CeCl₃•7H₂O (2.27 g, 6.09 mmol, 1.5 equiv) and ethanol (20 mL). The resulting mixture was stirred at room temperature for 15 minutes and then cooled to –10 °C over an ice/salt bath. NaBH₄ (178 mg, 4.67 mmol, 1.15 equiv)

was added in 4 portions over 0.5 hour, and the reaction mixture was further stirred at –10 °C for 2 hours. After the consumption of the starting material was complete as judged by TLC (Et₂O/hexane, 1:1), the reaction was quenched by addition of *sat.* NH₄Cl (40 mL). The resulting mixture was extracted with EtOAc (40 mL × 3). The combined organic phase was washed with H₂O (50 mL) and brine (50 mL), dried over Na₂SO₄, and concentrated *in vacuo*. The crude mixture was purified by column chromatography (Et₂O/hexane, 1:2 to 2:1), affording the corresponding allylic alcohol (828 mg, 82%) as a colorless oil, the spectra data of which was in agreement with that previously reported.

(ii) A 100 mL round-bottom flask was charged with a stir bar, the aforementioned allylic alcohol (745 mg, 3.00 mmol), TBSCl (900 mg, 6.00 mmol, 2 equiv), imidazole (408 mg, 6.00 mmol, 2 equiv), DMAP (36 mg, 0.30 mmol, 0.2 equiv), and DMF (30 mL). The reaction mixture was stirred at room temperature for 8 hours, and quenched by addition of *aq.* LiCl (40 mL, 10% w/w). The resulting mixture was extracted with EtOAc (40 mL × 3). The combined organic phase was washed with H₂O (50 mL × 2) and brine (50 mL), dried over Na₂SO₄, and concentrated *in vacuo*. The crude mixture was purified by column chromatography (Et₂O/hexane, 1:20), affording **256** (936 mg, 87%) as a colorless oil: $[\alpha]_D^{20} = +101.5^\circ$ (c 0.010 g/mL, CHCl₃); ¹H NMR (600 MHz, CDCl₃) δ 4.91 (app. t, *J* = 1.2 Hz, 1H), 4.88 (s, 1H), 4.75 (app. dq, *J* = 10.9, 1.8 Hz, 1H), 4.57 – 4.51 (m, 1H), 3.32 – 3.24 (m, 1H), 2.45 – 2.34 (m, 2H), 2.27 – 2.18 (m, 1H), 2.17 – 2.09 (m, 1H), 2.11 – 1.97 (m, 2H), 1.82 (app. dt, *J* = 2.6, 1.3 Hz, 3H), 1.60 (ddd, *J* = 12.6, 8.8, 7.3 Hz, 1H), 1.47 – 1.36 (m, 1H), 1.22 (d, *J* = 6.9 Hz, 3H), 0.92 (s, 9H), 0.11 (s, 3H), 0.09 (s, 3H); ¹³C NMR (150 MHz, CDCl₃) δ 178.8, 150.4, 143.0, 133.3, 111.2, 81.2, 78.5, 77.4, 77.16, 77.0, 48.9, 47.9, 41.8, 41.2, 35.9, 31.1, 26.0, 18.4, 12.9, 12.1, –4.3, –4.6; IR (thin film, cm^{–1}) 2955, 2931, 2885, 2857, 1780, 1643, 1461, 1360; HRMS (ESI) *calcd.* for [C₂₁H₃₄O₃SiNa]⁺ (M+Na)⁺: *m/z* 385.2175, found 385.2170.



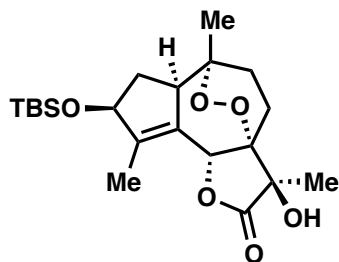
Compound 257: (i) A 100 mL round-bottom flask was charged with a stir bar, a freshly prepared solution of LDA in THF (5 mL, 1 M), and dry THF (20 mL). The reaction mixture was cooled to –78 °C over a dry ice-acetone bath, and compound **256** (1.09 g, 3.00 mmol, 1 equiv) in 5 mL THF was added dropwise. The resulting mixture was allowed to warm up to –50 °C over 1 hour and cooled again to –78 °C. Solid (CBrCl₂)₂ (1.60 g, 5.00 mmol, 1.67 equiv) was added in one portion. The reaction mixture was slowly warmed

¹ Delair, P.; Kann, N.; Greene, A. E., *J. Chem. Soc., Perkin Trans. 1* **1994**, 1651.

² Li, C.; Yu, X.; Lei, X., *Org. Lett.* **2010**, 12, 4284.

to 0 °C over 3 hours and then quenched by addition of *sat.* NH₄Cl (40 mL). The resulting mixture was extracted with EtOAc (40 mL × 3). The combined organic phase was washed with H₂O (50 mL) and brine (50 mL), dried over Na₂SO₄, and concentrated *in vacuo*. The crude mixture was purified by column chromatography (EtOAc/hexane, 1:100 to 1:10), affording the corresponding bromide (1.10 g, 83%) as a colorless oil. This compound is unstable and should be immediately used in the next step without storage.

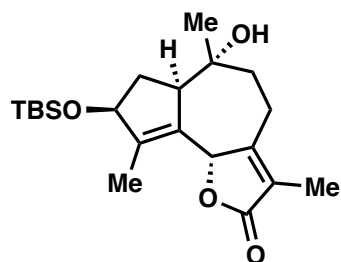
(ii) A 500 mL round-bottom flask was charged with a stir bar, the aforementioned bromide (1.10 g, 2.50 mmol) and DMF (180 mL). Solid LiBr (1.75 g, 20.2 mmol) and Li₂CO₃ (1.50 g, 20.3 mmol) were added to the reaction in one portion. The resulting mixture was stirred at 60 °C for 2 hours, and then cooled to room temperature and quenched by addition of *aq.* LiCl (150 mL, 10% w/w). The resulting mixture was extracted with EtOAc (100 mL × 3). The combined organic phase was washed with H₂O (100 mL × 2) and brine (100 mL), dried over Na₂SO₄, and concentrated *in vacuo*. The crude mixture was purified by column chromatography (EA/hexane, 1:10), affording **257** (510 mg, 56%) as a colorless oil: $[\alpha]_D^{20} = +31^\circ$ (c 0.001 g/mL, CHCl₃); ¹H NMR (600 MHz, CDCl₃) δ 5.56 (s, 1H), 4.78 (s, 1H), 4.76 (s, 1H), 4.51 (app. t, *J* = 6.7 Hz, 1H), 3.13 (app. t, *J* = 7.8 Hz, 1H), 2.78 (ddd, *J* = 14.0, 9.2, 7.4 Hz, 1H), 2.50 (app. dt, *J* = 12.8, 8.2 Hz, 1H), 2.44 – 2.36 (m, 2H), 2.22 (ddd, *J* = 12.8, 7.3, 3.8 Hz, 1H), 1.87 (dd, *J* = 2.3, 1.0 Hz, 3H), 1.77 (app. t, *J* = 1.6 Hz, 3H), 1.44 (app. dt, *J* = 13.3, 6.7 Hz, 1H), 0.91 (s, 9H), 0.10 (s, 3H), 0.08 (s, 3H); ¹³C NMR (175 MHz, CDCl₃) δ 174.9, 160.5, 150.2, 148.1, 131.9, 125.0, 111.3, 78.6, 78.3, 77.3, 77.2, 77.0, 48.6, 41.8, 30.4, 27.3, 26.0, 18.4, 12.0, 8.5, -4.3, -4.6; IR (thin film, cm⁻¹) 2954, 2928, 2856, 1756, 1681, 1463, 1354, 1302; HRMS (ESI) *calcd.* for [C₂₁H₃₂O₃SiNa]⁺ (M+Na)⁺: *m/z* 383.2019, found 383.2021.



Compound 258: A 25 mL round-bottom flask was charged with a stir bar, compound **257** (50.0 mg, 0.139 mmol, 1 equiv), Co(acac)₂ (7.1 mg, 0.028 mmol, 0.2 equiv), *i*-PrOH (0.58 mL) and DCM (3 mL). The reaction mixture was bubbled vigorously with O₂ for 5 minutes and then stirred at room temperature under an atmosphere of oxygen. A solution of PhSiH₃ (43 μL, 2.5 equiv) in DCM (1 mL) was added dropwise to the reaction mixture over 12 hours via syringe pump. After the reaction was complete as judged by TLC (EtOAc/hexane, 1:4), the mixture was diluted with DCM (5 mL) and

H₂O (5 mL), and the aqueous phase was extracted by DCM (5 mL × 2). The combined organic phase was washed with brine (20 mL), dried over Na₂SO₄, and concentrated *in vacuo*. The crude mixture was purified by column chromatography (EA/hexane, 1:10), affording **258** (5.0 mg, 9%) as a white solid: +23° (c 0.002 g/mL, CHCl₃); ¹H NMR (600 MHz, CDCl₃) δ 5.39 (s, 1H), 4.58 (app. t, *J* = 7.7 Hz, 1H), 3.20 (brs, 1H), 2.35 (app. dt, *J* = 12.1, 6.3 Hz, 1H), 2.16 – 2.02 (m, 3H), 1.84 (d, *J* = 2.4 Hz, 3H), 1.81 – 1.74 (m, 1H), 1.66 (dd, *J* = 13.6, 8.6 Hz, 1H), 1.48 (s, 3H), 1.20 – 1.12 (m, 4H), 0.92 (s, 9H), 0.12 (s, 3H), 0.10 (s, 3H); ¹³C NMR (175 MHz, CDCl₃) δ 176.1, 151.71, 130.31, 86.1, 82.3, 80.7, 75.7, 52.6, 38.9, 26.0, 24.9, 23.9, 18.3, 17.8, 16.8, 12.2, -4.3, -4.6; IR (thin film, cm⁻¹) 3414, 2955, 2929, 2856, 1785, 1669, 1606, 1461, 1376, 1360; HRMS (ESI) *calcd.* for [C₂₁H₃₄O₆SiNa]⁺ (M+Na)⁺: *m/z* 433.2023, found 433.2021.

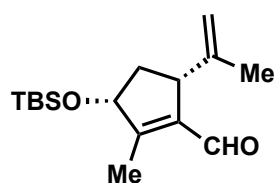
Vapor diffusion of an Et₂O solution of **258** with pentane afforded X-ray quality crystals.



Compound 259: A 10 mL round-bottom flask was charged with a stir bar, compound **257** (11.0 mg, 0.03 mmol, 1 equiv), $\text{Mn}(\text{dpm})_3$ (3.7 mg, 0.0015 mmol, 0.2 equiv), *i*-PrOH (0.13 mL) and DCM (0.6 mL). The reaction mixture was bubbled vigorously with O_2 for 5 minutes and then TBHP (9.5 μL , 5 M in decane) was added. The reaction mixture was stirred at $-10\text{ }^\circ\text{C}$ under an atmosphere of oxygen, and a solution of PhSiH_3 (9.5 μL , 2.5 equiv) in DCM (0.4 mL) was added dropwise over 15 hours via a syringe pump. After

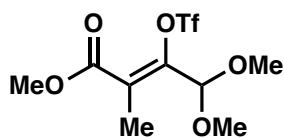
the reaction was complete as judged by TLC (EtOAc/hexane, 1:4), the reaction was quenched by addition of PPh_3 (19 mg), the mixture was diluted with DCM (3 mL) and H_2O (3 mL), and the aqueous phase was extracted by DCM (3 mL \times 2). The combined organic phase was washed with brine (10 mL), dried over Na_2SO_4 , and concentrated *in vacuo*. The crude mixture was purified by column chromatography (EA/hexane, 1:10), affording **259** (3.7 mg, 32%) as a colorless oil: ^1H NMR (400 MHz, CDCl_3) δ 5.50 (brs, 1H), 4.43 (brd, $J = 8.1$ Hz, 1H), 2.79 (ddd, $J = 14.2, 5.9, 3.0$ Hz, 1H), 2.49 (d, $J = 8.9$ Hz, 1H), 2.27 – 2.08 (m, 2H), 2.02 (ddd, $J = 13.4, 5.9, 3.1$ Hz, 1H), 2.01 (ddd, $J = 13.3, 5.8, 3.0$ Hz, 1H), 1.84 (d, $J = 2.0$ Hz, 3H), 1.82 (d, $J = 1.9$ Hz, 3H), 1.76 (dt, $J = 14.8, 2.6$ Hz, 1H), 1.60 (dd, $J = 13.3, 2.9$ Hz, 1H), 1.14 (s, 3H), 0.89 (s, 9H), 0.08 (s, 3H), 0.08 (s, 3H); ^{13}C NMR (125 MHz, CDCl_3) δ 174.9, 161.6, 148.2, 131.1, 123.2, 79.2, 78.0, 74.8, 66.0, 55.2, 43.6, 34.2, 26.0, 25.9, 22.9, 21.9, 18.3, 15.4, 12.8, 8.4, -4.3, -4.7.

SI-2.4 Initial Forays



Aldehyde 263: *Tert*-butyldimethyl silyl *cis*-carveol (**262**) was prepared in 95% yield over 2 steps from L-carvone by following the procedures reported by Gademann and coworkers.¹

A 100 mL round-bottom flask was charged with a stir bar, compound **262** (3.0 g, 11 mmol, 1 equiv), dry pyridine (0.3 mL, 0.3 equiv), DCM (30 mL), and MeOH (30 mL). The resulting mixture was cooled to $-78\text{ }^{\circ}\text{C}$ over a dry ice-acetone bath. The system was purged with O₂ for 5 min, and ozone generation was initiated (5~6 psi, 1.6~1.8 L/min, 90 V). The reaction was monitored carefully by TLC (EtOAc/hexane, 1:30), and disconnected from the ozone generator immediately after complete consumption of the starting material (8~10 min). The reaction mixture was then bubbled with a stream of N₂ for 10 min, followed by the addition of dimethyl sulfide (7.35 mL, 100 mmol). The mixture was allowed to warm up to room temperature gradually and stirred for 8 hours. Piperidine (0.74 mL, 7.6 mmol) and acetic acid (0.58 mL, 10 mmol) were then added to the reaction, which was heated at reflux for 16 hours. After complete conversion of the intermediates, the crude mixture was filtered through a short column of silica gel (washed with DCM), concentrated *in vacuo*, and purified by flash column chromatography (EtOAc/hexane, 1:30) to afford aldehyde **263** (1.1 g, 35%) as a colorless oil: $[\alpha]_{\text{D}}^{20} = +42.4^{\circ}$ (c 0.005 g/mL, CHCl₃); ¹H NMR (400 MHz, C₆D₆) δ 9.85 (s, 1H), 4.95 (brs, 1H), 4.87 (app. t, $J = 1.7$ Hz, 1H), 4.11 (app. ddt, $J = 7.4, 6.1, 1.2$ Hz, 1H), 3.39 – 3.31 (m, 1H), 2.12 (dt, $J = 13.2, 8.0$ Hz, 1H), 1.74 (dd, $J = 2.1, 1.1$ Hz, 3H), 1.66 (app. t, $J = 1.1$ Hz, 3H), 1.50 – 1.40 (m, 1H), 0.92 (s, 9H), -0.01 (s, 3H), -0.03 (s, 3H); ¹³C NMR (100 MHz, C₆D₆) δ 188.4, 159.7, 146.9, 138.5, 111.8, 79.5, 49.3, 39.9, 25.9, 19.8, 18.2, 11.6, -4.4, -4.8; IR (thin film, cm⁻¹) 3076, 2955, 2931, 2887, 2857, 2740, 1722, 1678, 1472, 1469; HRMS (ESI+) *calcd.* for [C₁₆H₂₈O₂SiNa]⁺: m/z 303.1756, found 303.1754.



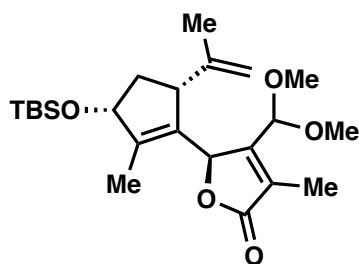
Triflate 265: Methyl 4,4-dimethoxy-2-methyl-3-oxobutanoate was prepared by following the procedure reported by Royals and coworkers.²

A 250 mL round-bottom flask was charged with a stir bar, sodium hydride (463 mg, 95% w/w) and THF (120 mL). A solution of methyl 4,4-dimethoxy-2-methyl-3-oxobutanoate (2.540 g, 13.35 mmol) in THF (13 mL) was then added to the reaction mixture slowly over 15 minutes at 0 °C, and the resulting mixture was then cooled to $-78\text{ }^{\circ}\text{C}$ over a dry ice-acetone batch. Trifluoromethanesulfonic anhydride (2.93 ml, 17.43 mmol, freshly distilled over P₂O₅) was added slowly to the reaction mixture, which was further stirred for 2 hours at $-78\text{ }^{\circ}\text{C}$ and 15 minutes at 0 °C. The reaction was quenched by addition of *sat.* NH₄Cl (50 mL), and the resulting mixture was extracted with EtOAc (100 mL \times 3). The combined organic phase was washed with H₂O (150 mL) and brine (150 mL), dried over Na₂SO₄, and concentrated *in vacuo*. The crude mixture was purified by column chromatography (EtOAc/hexane, 1:30), affording triflate **265** and its *E*-isomer (2.80 g, 65%, 5:2 ratio) as a colorless oil: ¹H NMR (600 MHz, CDCl₃) δ 5.10 (s, 1H), 3.82 (s, 3H), 3.39 (s, 6H), 2.09 (s, 3H); ¹³C NMR (175 MHz, CDCl₃) δ

¹ Elamparuthi, E.; Fellay, C; Neuburger, M.; Gademann K., *Angew. Chem. Int. Ed.* **2012**, *51*, 4071.

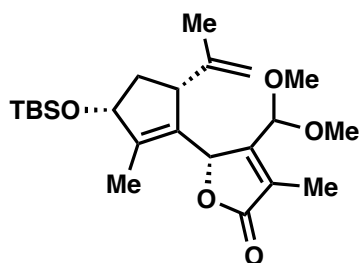
² Royals, E. E.; Robinson, A. G., *J. Am. Chem. Soc.* **1956**, *78*, 4161.

166.0, 144.8, 126.1, 121.3, 119.5, 117.7, 115.9, 99.0, 54.0, 52.7, 14.4; IR (thin film, cm^{-1}) 2958, 2840, 1732, 1417, 1307, 1285; HRMS (ESI) *calcd.* for $[\text{C}_9\text{H}_{13}\text{F}_3\text{NaO}_7\text{S}]^+$ ($\text{M}+\text{Na}$) $^+$: m/z 345.0232, found 345.0237.



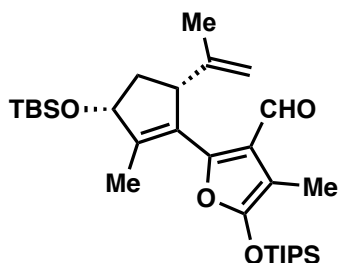
Compound 266: A 100 mL round-bottom flask was charged with a stir bar, anhydrous CrCl_2 (1.092 g, 8.8 mmol, 5 equiv), anhydrous NiCl_2 (20 mg, 0.15 mmol, 0.09 equiv), and dry DMF (20 mL). Aldehyde **263** (479 mg, 1.70 mmol, 1 equiv) and triflate **266** (623 mg, 1.93 mmol, 1.1 equiv) were added as a solution in DMF (5 mL) slowly over 1 hour via a syringe pump. The reaction mixture was stirred at room temperature for 16 hours, and was then diluted with Et_2O (25 mL) and quenched by addition of *aq.*

ethylenediamine (25 mL, 5% v/v). The resulting mixture was diluted with H_2O (100 mL) and extracted with Et_2O (100 mL \times 3). The combined organic phase was washed with H_2O (150 mL) and brine (150 mL), dried over Na_2SO_4 , and concentrated *in vacuo*. The crude mixture was purified by column chromatography (EtOAc /hexane, 1:30 to 1:20), affording compound **266** (323 mg, 45%) as a colorless oil: $[\alpha]_{\text{D}}^{20} = +63.1^\circ$ (c 0.01 g/mL, CHCl_3); ^1H NMR (700 MHz, CDCl_3) δ 5.45 (s, 1H), 5.11 (s, 1H), 4.75 (s, 1H), 4.68 (s, 1H), 4.50 (dd, $J = 7.8, 3.8$ Hz, 1H), 3.36 (brs, 1H), 3.33 (s, 3H), 3.25 (s, 3H), 2.32 (app. dt, $J = 14.0, 7.8$ Hz, 1H), 1.92 (s, 3H), 1.70 (s, 3H), 1.56 (s, 3H), 1.47 (app. dt, $J = 13.0, 3.8$ Hz, 1H), 0.89 (s, 9H), 0.08 (s, 3H), 0.06 (s, 3H); ^{13}C NMR (175 MHz, CDCl_3) δ 174.8, 154.9, 146.6, 143.9, 132.0, 127.8, 113.0, 99.2, 79.8, 78.6, 53.3, 52.0, 51.9, 38.4, 25.9, 18.5, 18.2, 12.1, 9.4, -4.3, -4.7; IR (thin film, cm^{-1}) 2955, 2931, 2857, 1764, 1445, 1361, 1254; HRMS (EI+) *calcd.* for $[\text{C}_{23}\text{H}_{38}\text{O}_5\text{SiNa}]^+$ ($\text{M}+\text{Na}$) $^+$: m/z 445.2381, found 445.2381.



Compound 6-*epi*-266: Obtained from the abovementioned condition as a colorless oil (6% yield): $[\alpha]_{\text{D}}^{20} = -141.1^\circ$ (c 0.01 g/mL, CHCl_3); ^1H NMR (700 MHz, CDCl_3) δ 5.56 (q, $J = 1.9$ Hz, 1H), 5.00 – 4.96 (m, 1H), 4.59 (dd, $J = 2.5, 1.4$ Hz, 1H), 4.50 (d, $J = 2.4$ Hz, 1H), 4.49 – 4.47 (m, 1H), 3.35 (s, 3H), 3.28 (s, 3H), 3.03 – 2.99 (m, 1H), 2.27 (app. dt, $J = 13.5, 8.0$ Hz, 1H), 1.93 (dd, $J = 2.0, 1.0$ Hz, 3H), 1.79 (dd, $J = 2.1, 0.9$ Hz, 3H), 1.67 – 1.64 (m,

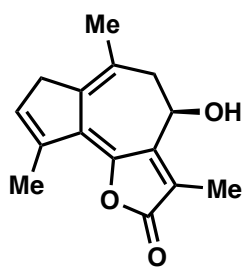
3H), 1.49 (ddd, $J = 13.6, 6.2, 5.1$ Hz, 1H), 0.90 (s, 9H), 0.09 (s, 3H), 0.07 (s, 3H); ^{13}C NMR (175 MHz, CDCl_3) δ 174.2, 153.4, 147.4, 146.1, 130.8, 128.9, 111.6, 99.6, 78.8, 78.2, 53.7, 52.9, 52.0, 38.3, 25.9, 18.2, 17.4, 11.8, 9.4, -4.3, -4.7; IR (thin film, cm^{-1}) 2955, 2930, 2857, 1762, 1445, 1361, 1253.



Compound 269: A reaction tube was charged with a stir bar, compound **266** (11.0 mg, 0.026 mmol, 1 equiv), Et_3N (22 μL , 6 equiv), and DCM (0.5 mL). The resulting mixture was cooled to -78°C over a dry ice-acetone bath, and TIPSOTf (15 μL , 0.056 mmol, 2.1 equiv) was added dropwise. The reaction mixture was stirred at -78°C for 1 hour and was then allowed to warm up to 0°C over 1 hour. At this point, TESOTf (13 μL , 0.057 mmol, 2.2 equiv) was

added dropwise at 0°C . The reaction mixture was further stirred at this temperature for 6 hours, and was then quenched by addition of *sat.* NaHCO_3 (5 mL). The resulting mixture was extracted

with EtOAc (5 mL × 3). The combined organic phase was washed with H₂O (10 mL) and brine (10 mL), dried over Na₂SO₄, and concentrated *in vacuo*. The crude mixture was purified by column chromatography (EtOAc/hexane, 1:30), affording **269** (7.0 mg, 50%) as a colorless oil: $[\alpha]_D^{20} = -106^\circ$ (c 0.001 g/mL, hexane); ¹H NMR (700 MHz, CD₂Cl₂) δ 9.74 (s, 1H), 4.73 – 4.72 (m, 1H), 4.70 – 4.66 (m, 2H), 3.61 (app. ddt, *J* = 8.4, 3.5, 1.8 Hz, 1H), 2.53 (ddd, *J* = 13.2, 8.4, 7.5 Hz, 1H), 2.01 (s, 3H), 1.83 (dd, *J* = 2.2, 1.1 Hz, 3H), 1.60 – 1.57 (m, 1H), 1.56 (t, *J* = 1.1 Hz, 3H), 1.26 (hept, *J* = 7.5 Hz, 3H), 1.09 (d, *J* = 7.5 Hz, 9H), 1.08 (d, *J* = 7.5 Hz, 9H), 0.92 (s, 9H), 0.12 (s, 3H), 0.10 (s, 3H); ¹³C NMR (175 MHz, CD₂Cl₂) δ 187.5, 153.9, 150.6, 148.1, 146.7, 128.2, 124.6, 112.3, 91.6, 80.2, 40.0, 26.0, 18.7, 18.4, 17.7, 14.3, 12.7, 7.9, -4.3, -4.7; IR (thin film, cm⁻¹) 2497, 2929, 2895, 2868, 1680, 1650, 1560, 1463, 1443, 1383; HRMS (ESI+) *calcd.* for [C₃₀H₅₃O₄Si₂⁺] (M+H)⁺: 533.3483, found 533.3481.

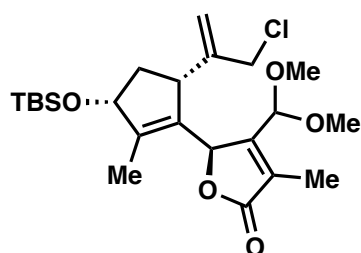


Compound 271: [Procedure A] A reaction tube was charged with a stir bar, compound **266** (10.0 mg, 0.0236 mmol, 1 equiv) and DCM (0.32 mL). A mixture of TFA (0.32 mL) and H₂O (0.16 mL) was added at 0 °C dropwise and the resulting mixture was stirred at 0 °C for 8 hours. After the consumption of the starting material was complete as judged by TLC (EtOAc/hexane, 1:4), the reaction mixture was slowly added to a vigorously stirring mixture of EtOAc (10 mL) and *sat.* NaHCO₃ (20 mL) in a separate flask. The two phases were separated, and the organic phase was washed with *sat.* NaHCO₃ (10 mL), H₂O (10 mL), and brine (10 mL), dried over Na₂SO₄, and concentrated *in vacuo*. The crude mixture was purified by preparative TLC (EtOAc/hexane, 1:1), affording **271** (1.5 mg, 26%) as a bright yellow solid: ¹H NMR (600 MHz, CDCl₃) δ 6.09 (s, 1H), 4.86 – 4.80 (m, 1H), 3.17 (brd, *J* = 8.0 Hz, 2H), 2.81 (dd, *J* = 16.0, 6.7 Hz, 1H), 2.68 (d, *J* = 16.0 Hz, 1H), 2.22 (d, *J* = 2.3 Hz, 3H), 2.05 (s, 3H), 1.97 (s, 3H); ¹³C NMR (151 MHz, CDCl₃) δ 170.7, 149.2, 142.4, 142.2, 136.2, 134.8, 130.1, 129.0, 121.5, 63.1, 40.3, 37.9, 25.1, 17.5, 8.9; IR (thin film, cm⁻¹) 3417, 2928, 2855, 1720, 1653, 1584, 1441, 1367; HRMS (ESI) *calcd.* for [C₁₅H₁₇O₃]⁺ (M+H)⁺: *m/z* 245.1178, found 245.1177.

[Procedure B] A reaction tube was charged with a stir bar, compound **269** (7.0 mg, 0.013 mmol, 1 equiv), and DCM (0.15 mL). The resulting mixture was cooled to -78 °C over a dry ice-acetone bath and a solution of TiCl₂(*i*-PrO)₂ (3 mg) in DCM (0.1 mL) was added dropwise. The reaction mixture was allowed to warm up gradually to -30 °C over 30 minutes and was then quenched by addition of *sat.* NaHCO₃ (5 mL). The aqueous phase was extracted by EtOAc (5 mL × 2) and the combined organic phase was washed with washed with H₂O (10 mL) and brine (10 mL), dried over Na₂SO₄, and concentrated *in vacuo*. The crude mixture was purified by preparative TLC (EtOAc/hexane, 1:1), affording **271** (1.0 mg, 32%) as a bright yellow solid, the spectra data of which was in agreement with that reported in procedure A.

[Procedure C] A reaction tube was charged with a stir bar, compound **270** (5.0 mg, 0.0094 mmol, 1 equiv), and THF (0.1 mL). The resulting mixture was stirred at 0 °C over an ice bath and a solution of TBAF (30 μL, 3 equiv, 1M in THF) was added dropwise. After complete consumption of the starting material as judged by TLC (EtOAc/hexane, 1:10), the reaction mixture was diluted with EtOAc (1 mL) and quenched by addition of *sat.* NaHCO₃ (1 mL). The water phase was extracted by EtOAc (5 mL × 2) and the combined organic phase was washed with washed with H₂O (10 mL) and brine (10 mL), dried over Na₂SO₄, and concentrated *in vacuo*. The crude mixture was purified by preparative TLC (EtOAc/hexane, 1:1), affording a

small amount of **271** as a bright yellow solid, together with a complex mixture of decomposition products. The spectra data of **271** was in agreement with that reported in procedure A. Vapor diffusion of an ethyl acetate solution of **271** with hexane afforded X-ray quality crystals.

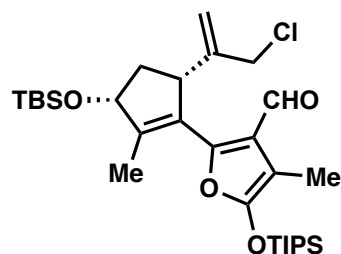


Compound 272: [Procedure A] A reaction tube was charged with a stir bar, compound **266** (30.0 mg, 0.07 mmol, 1 equiv), Na₂CO₃ (30.0 mg, 0.283 mmol, 4 equiv), and DCM (0.4 mL). The resulting mixture was stirred at 0 °C for 20 minutes and freshly distilled SO₂Cl₂ (5.8 μL, 0.07 mmol, 1 equiv) was added in one portion. After the reaction was complete as judged by TLC (EtOAc/hexane, 1:4) (~1 hour), the mixture was diluted with EtOAc (5 mL) and *sat.* NaHCO₃ (10 mL), and the aqueous phase

was extracted by EtOAc (5 mL × 2). The combined organic phase was washed with brine (10 mL), dried over Na₂SO₄, and concentrated *in vacuo*. The crude mixture was purified by column chromatography (EtOAc/hexane, 1:10 to 1:5), affording an inseparable 2.5:1 mixture of **272** and its regioisomer (14.5 mg, 45%) as a colorless oil.

[Procedure B] A reaction tube was charged with a stir bar, compound **266** (28.0 mg, 0.066 mmol, 1 equiv), 4Å molecular sieves (35 mg), and EtOAc (2 mL). The resulting mixture was degassed by bubbling argon for 10 minutes, followed by addition of solid Trichloroisocyanuric acid (16.0 mg, 0.068 mmol, 1 equiv) in one portion. The reaction mixture was stirred at room temperature for 10 minutes, and then quenched by addition of *sat.* Na₂S₂O₃ (4 mL). The aqueous phase was extracted by EtOAc (5 mL × 2) and the combined organic phase was washed with washed with H₂O (10 mL) and brine (10 mL), dried over Na₂SO₄, and concentrated *in vacuo*. The crude mixture was purified by column chromatography (EtOAc/hexane, 1:10 to 1:5), affording an inseparable 6.5:1 mixture of **272** and its regioisomer (20.0 mg, 65%) as a colorless oil: IR (thin film, cm⁻¹) 2955, 2930, 2857, 1762, 1472, 1444, 1361; HRMS (ESI) *calcd.* for [C₂₃H₃₈O₅ClSi]⁺ (M+H)⁺: *m/z* 457.2172, found 457.2170.

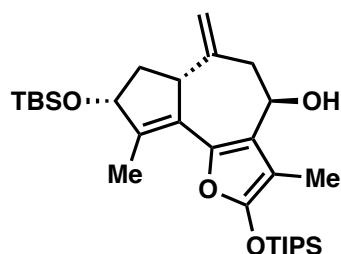
Compound **272** (major): ¹H NMR (700 MHz, CDCl₃) δ 5.48 (d, *J* = 2.2 Hz, 1H), 5.23 – 5.20 (m, 1H), 5.12 (d, *J* = 1.1 Hz, 1H), 5.09 (app. q, *J* = 1.0 Hz, 1H), 4.50 (dd, *J* = 7.4, 2.8 Hz, 1H), 3.99 (dd, *J* = 13.1, 1.2 Hz, 1H), 3.92 – 3.87 (m, 1H), 3.45 – 3.40 (m, 1H), 3.30 (s, 3H), 3.27 (s, 3H), 2.43 (ddd, *J* = 14.0, 8.8, 7.3 Hz, 1H), 1.91 (dd, *J* = 2.1, 1.0 Hz, 3H), 1.73 (dd, *J* = 2.0, 0.8 Hz, 3H), 1.51 (ddd, *J* = 14.0, 3.8, 2.9 Hz, 1H), 0.89 (s, 9H), 0.09 (s, 3H), 0.06 (s, 3H); ¹³C NMR (176 MHz, CDCl₃) δ 174.5, 155.4, 147.2, 144.6, 132.1, 127.9, 116.2, 99.3, 79.9, 78.5, 52.9, 52.7, 48.7, 46.2, 40.2, 36.7, 25.9, 18.1, 12.3, 9.4, -4.3, -4.7.



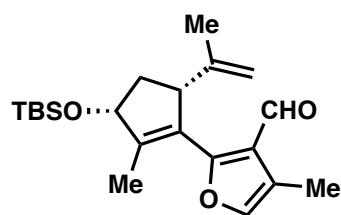
Compound 273: A reaction tube was charged with a stir bar, compound **272** (20.0 mg as a 2.5:1 mixture, 0.0313 mmol of **272**, 1 equiv), Et₃N (mL, 8 equiv), and DCM (0.3 mL). The resulting mixture was cooled to -78 °C over an acetone-dry ice bath, and TIPSOTf (24 μL, 2 equiv) was added dropwise. The reaction mixture was stirred at -78 °C for 1 hour and was allowed to warm up to 0 °C over an additional hour. TESOTf (27 μL, 4 equiv) was then added dropwise at 0 °C. The reaction mixture was stirred at this

temperature for 6 hours, and was then quenched by addition of *sat.* NaHCO₃ (5 mL). The resulting mixture was extracted with EtOAc (5 mL × 3). The combined organic phase was washed with H₂O (10 mL) and brine (10 mL), dried over Na₂SO₄, and concentrated *in vacuo*.

The crude mixture was purified by column chromatography (EtOAc/hexane, 1:30), affording **273** (12 mg, 65%) as a colorless oil: $[\alpha]_D^{20} = -96^\circ$ (c 0.002 g/mL, hexane); $^1\text{H NMR}$ (500 MHz, C_6D_6) δ 9.98 (s, 1H), 5.02 (app. q, $J = 1.2$ Hz, 1H), 4.96 (s, 1H), 4.20 (app. ddt, $J = 7.4, 5.4, 1.1$ Hz, 1H), 3.89 (dd, $J = 12.6, 1.1$ Hz, 1H), 3.82 (dd, $J = 12.6, 1.1$ Hz, 1H), 3.68 (app. t, $J = 7.5$ Hz, 1H), 2.38 (ddd, $J = 13.2, 8.3, 7.4$ Hz, 1H), 2.29 (s, 3H), 1.74 (dd, $J = 2.1, 1.0$ Hz, 3H), 1.60 (ddd, $J = 13.2, 6.4, 5.4$ Hz, 1H), 1.21 – 1.13 (m, 3H), 1.06 (d, $J = 7.3$ Hz, 9H), 1.05 (d, $J = 7.3$ Hz, 9H), 0.93 (s, 9H), 0.01 (s, 3H), 0.00 (s, 3H); $^{13}\text{C NMR}$ (150 MHz, C_6D_6) δ 186.1, 153.9, 150.0, 147.9, 147.1, 127.7, 125.4, 115.8, 92.5, 80.0, 50.0, 46.8, 41.7, 26.0, 18.3, 17.7, 17.7, 14.3, 12.7, 8.1, -4.3, -4.7; IR (thin film, cm^{-1}) 2948, 2928, 2867, 1682, 1650, 1561, 1463, 1443, 1383; HRMS (ESI) *calcd.* for $[\text{C}_{30}\text{H}_{51}\text{ClO}_4\text{Si}_2\text{Na}]^+$ ($\text{M}+\text{Na}$) $^+$: m/z 589.2912, found 589.2917.



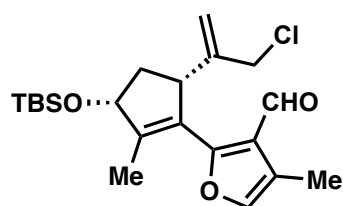
Compound 270: A reaction tube was charged with a stir bar, anhydrous CrCl_2 (89.0 mg, 0.724 mmol, 5 equiv), anhydrous NiCl_2 (2 mg, 0.1 equiv), and dry DMF (1.0 mL). The resulting mixture was stirred at 60°C and a solution of compound **273** (82.0 mg, 0.144 mmol, 1 equiv) in DMF (0.5 mL) was added slowly over 30 minutes via a syringe pump. The reaction mixture was heated at 60°C for an additional 90 minutes, and was then diluted with Et_2O (5 mL) and quenched by addition of *aq.* ethylenediamine (5 mL, 5% v/v). The aqueous phase was extracted by Et_2O (5 mL \times 2) and the combined organic phase was washed with washed with H_2O (10 mL) and brine (10 mL), dried over Na_2SO_4 , and concentrated *in vacuo*. The crude mixture was purified by column chromatography (EtOAc/hexane, 1:20 to 1:10), affording **270** (5.0 mg, 7%) as a colorless oil: $^1\text{H NMR}$ (600 MHz, C_6D_6) δ 4.80 (s, 2H), 4.59 (app. ddt, $J = 8.4, 4.0, 2.2$ Hz, 1H), 4.43 (app. t, $J = 7.5$ Hz, 1H), 3.36 (app. t, $J = 8.8$ Hz, 1H), 2.48 (dd, $J = 12.9, 2.5$ Hz, 1H), 2.29 – 2.22 (m, 2H), 2.19 (dd, $J = 2.5, 1.4$ Hz, 3H), 2.14 (s, 3H), 1.32 – 1.25 (m, 3H), 1.14 (d, $J = 7.4$ Hz, 9H), 1.14 (d, $J = 7.4$ Hz, 9H), 0.99 (s, 9H), 0.09 (s, 3H), 0.06 (s, 3H).



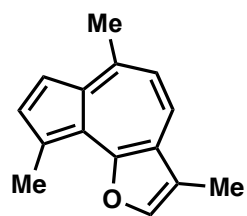
Compound 276: A reaction tube was charged with a stir bar, compound **266** (8.4 mg, 0.02 mmol, 1 equiv) and DCM (0.3 mL). The resulting mixture was cooled to -78°C over a dry ice-acetone bath, and DIBAL-H (22 μL , 1M in hexane) was added dropwise. The reaction mixture was stirred at -78°C for 1 hour and was then quenched by addition of *aq.* potassium sodium tartrate (5 mL, 10% w/w). The aqueous phase was extracted by EtOAc (5 mL \times 2) and the combined organic phase was washed with H_2O (10 mL) and brine (10 mL), dried over Na_2SO_4 , and concentrated *in vacuo*. The crude mixture was used directly to the next step without purification.

The crude lactol (0.02 mmol assumed) was dissolved in acetone (0.6 mL), and amberlyst® 15 (2 mg), H_2O (10 μL) were added. After the reaction was complete as judged by TLC (EtOAc/hexane, 1:4), the reaction was quenched by addition of *sat.* NaHCO_3 (5 mL). The aqueous phase was extracted with EtOAc (5 mL \times 3). The combined organic phase was washed with brine (10 mL), dried over Na_2SO_4 , and concentrated *in vacuo*. The crude mixture was purified by column chromatography (EtOAc/hexane, 1:30), affording **276** (3.5 mg, 49%) as a colorless oil: $[\alpha]_D^{20} = -117^\circ$ (c 0.001 g/ml, CHCl_3); $^1\text{H NMR}$ (700 MHz, CDCl_3) δ 9.85 (d, $J = 0.7$ Hz, 1H), 7.16 – 7.13 (m, 1H), 4.75 (app. dt, $J = 2.3, 0.8$ Hz, 1H), 4.70 – 4.65 (m, 2H), 3.69 (app. tt, $J = 8.6, 2.0$ Hz, 1H), 2.54 (ddd, $J = 13.2, 8.1, 7.5$ Hz, 1H), 2.21 (d, $J = 1.3$ Hz, 3H), 1.84

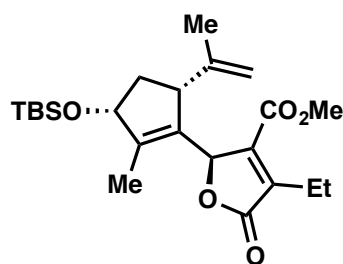
(dd, $J = 2.2, 1.0$ Hz, 3H), 1.63 (ddd, $J = 13.2, 6.9, 5.9$ Hz, 1H), 1.55 (dd, $J = 1.5, 0.8$ Hz, 3H), 0.92 (s, 9H), 0.12 (s, 3H), 0.10 (s, 3H); ^{13}C NMR (150 MHz, CDCl_3) δ 187.3, 161.2, 148.9, 146.0, 140.2, 128.4, 123.0, 120.2, 112.6, 79.9, 53.1, 39.7, 26.0, 18.8, 18.3, 14.1, 9.5, -4.2, -4.6; IR (thin film, cm^{-1}) 2956, 2930, 2886, 2857, 1681, 1546, 1472, 1442, 1412, 1386, 1352; HRMS (ESI) *calcd.* for $[\text{C}_{21}\text{H}_{32}\text{O}_3\text{SiNa}]^+$ ($\text{M}+\text{Na}$) $^+$: m/z 383.2018, found 383.2026.



Compound 278: This compound was prepared from compound **272** (10.0 mg as a 2.5:1 mixture, 0.0156 mmol of **272**) by following the abovementioned procedure, affording **278** (3.0 mg, 49%) as a colorless oil: $[\alpha]_{\text{D}}^{20} = -67^\circ$ (c 0.001 g/mL, CHCl_3); ^1H NMR (700 MHz, CDCl_3) δ 9.84 (d, $J = 0.7$ Hz, 1H), 7.14 (dd, $J = 1.3, 0.7$ Hz, 1H), 5.18 – 5.13 (m, 1H), 5.02 (s, 1H), 4.69 (app. ddt, $J = 7.6, 5.4, 1.1$ Hz, 1H), 4.03 (dd, $J = 12.2, 1.0$ Hz, 1H), 3.95 (dd, $J = 12.2, 1.1$ Hz, 1H), 3.80 (app. t, $J = 7.6$ Hz, 1H), 2.72 (ddd, $J = 13.4, 8.3, 7.4$ Hz, 1H), 2.21 (d, $J = 1.3$ Hz, 3H), 1.85 (dd, $J = 2.2, 0.9$ Hz, 3H), 1.67 (ddd, $J = 13.4, 6.4, 5.4$ Hz, 1H), 0.92 (s, 9H), 0.12 (s, 3H), 0.10 (s, 3H); ^{13}C NMR (175 MHz, CDCl_3) δ 187.1, 160.4, 149.0, 147.0, 140.2, 128.0, 123.3, 120.3, 116.5, 79.9, 49.4, 47.1, 41.7, 25.9, 18.2, 14.3, 9.5, -4.3, -4.6; IR (thin film, cm^{-1}) 2955, 2929, 2857, 1682, 1545, 1472, 1442, 1412, 1386, 1361; HRMS (ESI) *calcd.* for $[\text{C}_{21}\text{H}_{31}\text{O}_3\text{ClSiNa}]^+$ ($\text{M}+\text{Na}$) $^+$: m/z 417.1629, found 417.1628.



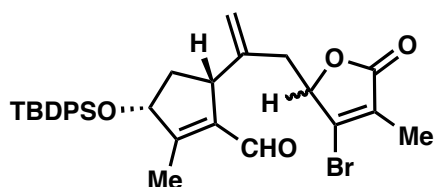
Artemazulene: This compound was obtained as a decomposition product of compound **277**. The crude mixture was re-purified by preparative TLC (EtOAc/hexane, 1:20), affording artemazulene as a blue oil: ^1H NMR (700 MHz, C_6D_6) δ 7.68 (d, $J = 4.2$ Hz, 1H), 7.40 (d, $J = 4.2$ Hz, 1H), 7.26 (d, $J = 10.6$ Hz, 1H), 7.01 (d, $J = 1.4$ Hz, 1H), 6.80 (d, $J = 10.6$ Hz, 1H), 3.13 (s, 3H), 2.70 (s, 3H), 1.80 (d, $J = 1.4$ Hz, 3H); ^{13}C NMR (150 MHz, C_6D_6) δ 158.4, 144.3, 140.2, 139.9, 137.4, 126.5, 124.2, 123.6, 122.5, 120.0, 118.6, 113.8, 25.4, 16.6, 7.6; IR (thin film, cm^{-1}) 2920, 2851, 1738, 1620, 1572, 1452, 1403, 1376, 1336; HRMS (ESI) *calcd.* for $[\text{C}_{15}\text{H}_{15}\text{O}]^+$ ($\text{M}+\text{H}$) $^+$: m/z 211.1123, found 211.1119.



Compound 285: Iodide **284** was prepared by following the procedure reported by Bertrand and coworkers.¹ A 50 mL round-bottom flask was charged with a stir bar, anhydrous CrCl_2 (515 mg, 4.19 mmol, 5 equiv), anhydrous NiCl_2 (10 mg, 0.077 mmol, 0.09 equiv), and dry DMF (8 mL). Aldehyde **263** (285 mg, 1.02 mmol, 1 equiv) and iodide **284** (400 mg, 1.34 mmol, 1.3 equiv) were added dropwise as a solution in DMF (2 mL). The reaction mixture was stirred at room temperature for 2 hours, and was then diluted with Et_2O (25 mL) and quenched by addition of *aq.* ethylenediamine (25 mL, 5% v/v). The resulting mixture was diluted with H_2O (60 mL) and extracted with Et_2O (60 mL \times 3). The combined organic phase was washed with H_2O (100 mL) and brine (100 mL), dried over Na_2SO_4 , and concentrated *in vacuo*. The crude mixture was purified by column chromatography (EtOAc/hexane, 1:20), affording compound **285** and 6-*epi*-**285** (387 mg, 90%, 5.5:1 *dr*) as a colorless oil. Compound **285**: $[\alpha]_{\text{D}}^{20} = +62^\circ$ (c 0.002 g/mL, CHCl_3); ^1H NMR (700 MHz, CDCl_3)

¹ Maury, J.; Feray, L.; Bertrand, M. P., *Org. Lett.* **2011**, *13*, 1884.

δ 5.77 (s, 1H), 4.74 (brs, 1H), 4.61 (app. p, $J = 1.3$ Hz, 1H), 4.53 – 4.48 (m, 1H), 3.82 (s, 3H), 3.34 (brs, 1H), 2.65 – 2.56 (m, 2H), 2.35 – 2.29 (m, 1H), 1.78 (brs, 3H), 1.48 (brs, 3H), 1.46 – 1.41 (m, 1H), 1.13 (td, $J = 7.6, 1.2$ Hz, 3H), 0.88 (s, 9H), 0.08 (s, 3H), 0.05 (s, 3H); ^{13}C NMR (150 MHz, CDCl_3) δ 173.0, 146.7, 145.8, 145.5, 142.5, 130.7, 113.7, 79.7, 78.0, 52.2, 51.5, 38.5, 25.9, 18.6, 18.5, 12.4, 11.8, -4.3, -4.7; IR (thin film, cm^{-1}) 2954, 2930, 2885, 2857, 1767, 1731, 1669, 1644, 1462, 1438; HRMS (ESI) *calcd.* for $[\text{C}_{23}\text{H}_{36}\text{O}_5\text{SiNa}]^+$ ($\text{M}+\text{Na}$) $^+$: m/z 443.2230, found 443.2231.



Compound 305: (i) A 25 mL round-bottom flask was charged with a stir bar, aldehyde *ent*-**173** (132 mg, 0.301 mmol) and LiCl (0.6 mg in 46 μL THF). TMS-CN (42 μL , 0.33 mmol) was then added dropwise, and the reaction mixture was stirred at room temperature for 1 hour. After the reaction was complete as judged by TLC (EtOAc/hexane,

1:4), NaI (450 mg, 3.0 mmol, 10 equiv) in dry acetone (18 mL) was added. The resulting mixture was stirred at room temperature for 16 hours, and then concentrated *in vacuo*. The crude mixture was dissolved in diethyl ether (10 mL), filtered through Celite®, and concentrated *in vacuo*. This process (Et₂O; filtration) was repeated if necessary to remove excess NaI. The crude (0.3 mmol assumed) was then dissolved in DCM (3 mL) and used as a stock solution for the next step.

(ii) A 10 mL round-bottom flask was charged with a stir bar and furan **300** (67 mg, 0.2 mmol). The abovementioned crude solution (2 mL, 0.2 mmol assumed) was added to the reaction flask in one portion. The resulting mixture was cooled to -78 °C over a dry ice-acetone bath, and AgTFA (45 mg, 0.2 mmol) was added in one portion. The reaction mixture was stirred at -78 °C for 4 hours, and was then allowed to gradually warm up to room temperature overnight. The reaction mixture was then filtered through a short column of silica gel (washed with DCM), concentrated *in vacuo*, and purified by flash column chromatography (EtOAc/hexane, 1:20 to 1:10), affording **305** (37 mg, 32%, 1:1 *dr*) as a colorless oil.

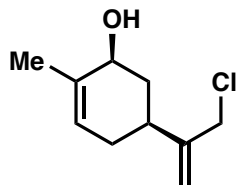
[Note: Reaction set-up, work-up, and purification were all performed in fume hoods. The waste containing cyanide was collected in separate containers under basic conditions, and labeled appropriately.]

Less polar isomer: $[\alpha]_{\text{D}}^{20} = -27^\circ$ (c 0.005 g/mL, CHCl_3); ^1H NMR (600 MHz, CDCl_3) δ 9.94 (s, 1H), 7.71 – 7.61 (m, 4H), 7.47 – 7.42 (m, 2H), 7.42 – 7.37 (m, 4H), 5.07 – 5.01 (m, 3H), 4.63 (app. ddt, $J = 7.8, 5.5, 1.1$ Hz, 1H), 3.37 – 3.30 (m, 1H), 2.82 (ddd, $J = 15.9, 3.1, 1.2$ Hz, 1H), 2.32 – 2.21 (m, 2H), 2.01 (dd, $J = 2.0, 1.0$ Hz, 3H), 1.88 (d, $J = 1.9$ Hz, 3H), 1.60 – 1.52 (m, 1H), 1.07 (s, 9H); ^{13}C NMR (150 MHz, CDCl_3) δ 189.2, 170.9, 162.0, 145.8, 144.2, 139.1, 136.1, 136.1, 133.6, 133.6, 130.1, 129.6, 127.9, 127.9, 114.3, 82.6, 80.4, 47.5, 40.3, 37.8, 27.14, 19.4, 12.3, 10.3; IR (thin film, cm^{-1}) 2956, 2930, 2989, 2857, 1768, 1674, 1590, 1428, 1328; HRMS (ESI) *calcd.* for $[\text{C}_{31}\text{H}_{35}\text{BrO}_4\text{SiNa}]^+$ ($\text{M}+\text{Na}$) $^+$: m/z 601.1386, found 601.1388.

More polar isomer: $[\alpha]_{\text{D}}^{20} = -1^\circ$ (c 0.005 g/mL, CHCl_3); ^1H NMR (700 MHz, CDCl_3) δ 9.92 (s, 1H), 7.70 – 7.63 (m, 4H), 7.47 – 7.43 (m, 2H), 7.42 – 7.37 (m, 4H), 5.06 (s, 1H), 5.04 (app. ddt, $J = 8.5, 3.6, 1.8$ Hz, 1H), 5.01 (s, 1H), 4.64 (app. ddt, $J = 7.7, 5.3, 1.1$ Hz, 1H), 3.27 (app. t, $J = 7.4$ Hz, 1H), 2.82 (ddd, $J = 15.4, 3.1, 1.1$ Hz, 1H), 2.36 – 2.26 (m, 2H), 2.01 (dd, $J = 2.1, 1.0$ Hz, 3H), 1.89 (d, $J = 1.9$ Hz, 3H), 1.61 – 1.55 (m, 1H), 1.08 (s, 9H); ^{13}C NMR (176 MHz, CDCl_3) δ 189.1, 170.9, 161.4, 146.1, 143.9, 139.2, 136.1, 136.1, 133.7, 133.6, 130.1, 130.1, 129.7, 127.9, 127.8, 114.4, 83.0, 80.4, 47.6, 40.3, 38.4, 27.1, 19.4, 12.3, 10.4; IR (thin film, cm^{-1}) 2953, 2930,

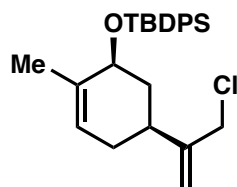
2895, 2857, 1768, 1676, 1590, 1428, 1328; HRMS (ESI) *calcd.* for $[\text{C}_{31}\text{H}_{35}\text{BrO}_4\text{SiNa}]^+$
($\text{M}+\text{Na}$)⁺: m/z 601.1386, found 601.1383.

SI-2.5 Total Synthesis of (+)-Mikanokryptin



Chloro-carveol 307: An oven-dried 3 L three-necked flask equipped with a large stir bar was charged with (+)-carvone (30.0 g, 0.200 mol), sodium carbonate (63.6 g, 0.600 mol), and DCM (1 L). The resulting mixture was stirred vigorously at room temperature for 30 minutes, followed by slow addition of SO₂Cl₂ (20.0 mL, 0.247 mol) over 2 hours via a syringe pump.

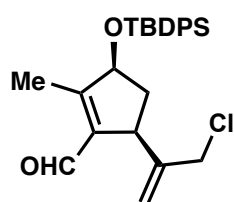
The reaction was monitored by TLC (EtOAc/hexane, 1:4) and additional SO₂Cl₂ was added if necessary. After complete consumption of the starting material, methanol (1 L) and CeCl₃·7H₂O (82.0 g, 0.220 mol) were added and the resulting mixture was stirred at room temperature for 30 minutes. The reaction mixture was then cooled to 0 °C and NaBH₄ (22.8 g, 0.600 mol) was added in 4 portions over 1 hour. After the ketone intermediate was completely consumed as indicated by TLC, the reaction was quenched by addition of 1N aqueous HCl (300 mL) and H₂O (500 mL) sequentially. The aqueous layer was extracted with ethyl acetate (700 mL × 3). The combined organic phase was washed with brine, dried over MgSO₄, and concentrated *in vacuo*. The resulting crude was purified by column chromatography (EtOAc/hexane, 1:10 to 1:5), affording chloro-carveol **307** (29.2 g, 0.156 mol, 78%) as a light yellow oil: $[\alpha]_D^{20} = +37.4^\circ$ (c 0.01 g/mL, CHCl₃); ¹H NMR (600 MHz, CDCl₃) δ 5.53 – 5.49 (m, 1H), 5.19 (s, 1H), 5.03 (s, 1H), 4.27 – 4.21 (m, 1H), 4.11 (s, 2H), 2.55 (ddd, *J* = 15.5, 8.0, 3.5 Hz, 1H), 2.24 (ddt, *J* = 12.2, 5.6, 2.3 Hz, 1H), 2.19 (dddd, *J* = 13.9, 6.9, 3.4, 1.6 Hz, 1H), 1.95 (app. ddq, *J* = 16.6, 10.8, 2.7 Hz, 1H), 1.77 (dd, *J* = 2.8, 1.5 Hz, 3H), 1.53 (app. td, *J* = 12.2, 9.6 Hz, 1H); ¹³C NMR (125 MHz, CDCl₃) δ 148.6, 136.4, 123.6, 113.9, 70.9, 47.6, 38.1, 36.9, 31.5, 19.0; IR (thin film, cm⁻¹) 3324, 2969, 2942, 2916, 2884, 2838, 1716, 1642, 1451, 1434, 1407, 1258; HRMS (EI+) *calcd.* for [C₁₀H₁₅ClO]: *m/z* 186.0811, found 186.0810. [Note: This compound is somewhat volatile and should not be placed under high vacuum for extended periods. On a 1-mmol scale, an 85% yield of product was obtained.]



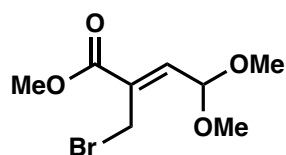
Silyl ether 172: An oven-dried 1 L round-bottom flask was charged with a stir bar, chloro-carveol **307** (18.6 g, 0.100 mol), imidazole (20.4 g, 0.300 mol), and 4-dimethylaminopyridine (0.6 g, 0.005 mol). The flask was placed under vacuum and back-filled with N₂, followed by addition of dry DMF (500 mL). The resulting mixture was cooled to 0 °C, and TBDPSCl (32.8 g, 0.120 mol) was added slowly. The reaction mixture was allowed to warm to

room temperature and stirred overnight. After the reaction was complete as indicated by TLC, the reaction mixture was poured into a separation funnel charged with aqueous LiCl (10% w/w, 1 L). The aqueous layer was extracted with diethyl ether (500 mL × 3) and the combined organic phase was washed with H₂O (500 mL × 2), brine (500 mL), dried over MgSO₄, and concentrated *in vacuo*. The crude mixture was purified by flash column chromatography (EtOAc/hexane, 1:100 to 1:30), affording silyl ether **172** (38.5 g, 0.0906 mol, 91%) as a colorless oil: $[\alpha]_D^{20} = +58.0^\circ$ (c 0.01 g/mL, CHCl₃); ¹H NMR (600 MHz, CDCl₃) δ 7.75 – 7.69 (m, 4H), 7.45 – 7.40 (m, 2H), 7.40 – 7.35 (m, 4H), 5.43 (app. dq, *J* = 5.4, 1.7 Hz, 1H), 5.04 (s, 1H), 4.80 (s, 1H), 4.33 (brs, 1H), 3.92 (dd, *J* = 11.8, 1.0 Hz, 1H), 3.85 (dd, *J* = 11.8, 1.0 Hz, 1H), 2.29 – 2.20 (m, 1H), 2.06 (app. dddt, *J* = 16.9, 5.1, 3.0, 1.7 Hz, 1H), 1.88 (dddd, *J* = 14.4, 11.7, 5.4, 3.0 Hz, 1H), 1.83 (app. ddt, *J* = 12.5, 5.8, 2.3 Hz, 1H), 1.74 (app. dt, *J* = 2.6, 1.3 Hz, 3H), 1.48 (app. td, *J* = 12.5, 10.0 Hz, 1H), 1.08 (s, 9H); ¹³C NMR (150 MHz, CDCl₃) δ 148.6, 137.7, 136.2, 136.2, 135.0, 134.0, 129.8, 129.7, 127.7, 127.5, 122.9, 113.4, 72.8, 47.3, 38.3, 36.2, 31.3, 27.3, 20.2, 19.7; IR (thin

film, cm^{-1}) 3072, 3049, 2999, 2963, 2930, 2889, 2857, 1472, 1449, 1428; HRMS (EI+) calcd. for $[\text{C}_{26}\text{H}_{33}\text{ClOSi}]$: m/z 424.1989, found 424.1990.



Aldehyde 173: An oven-dried 1 L round-bottom flask equipped with a large stir bar was charged with silyl ether **172** (21.3 g, 50.1 mmol), pyridine (1.18 mL, 15.0 mmol), and DCM (500 mL). The reaction flask was connected to a Welsbach ozone generator through plastic tubing and a glass bubbler, and cooled to $-78\text{ }^\circ\text{C}$ over an acetone-dry ice bath. The system was purged with O_2 for 5 min, and ozone generation was initiated (5~6 psi, 1.6~1.8 L/min, 90 V). The reaction was monitored carefully by TLC (EtOAc/hexane, 1:30), and disconnected from the ozone generator immediately after complete consumption of the starting material (20~40 min). The reaction mixture was then bubbled with N_2 for 10 min, followed by the addition of dimethyl sulfide (7.35 mL, 100 mmol). The mixture was allowed to warm up to room temperature gradually and stirred for 8 hours. Piperidine (0.74 mL, 7.6 mmol) and acetic acid (0.58 mL, 10 mmol) were then added to the reaction, which was heated at reflux for 16 hours. After complete conversion of the intermediates, the crude mixture was filtered through a short column of silica gel (washed with DCM), concentrated *in vacuo*, and purified by flash column chromatography (EtOAc/hexane, 1:30) to afford aldehyde **173** (9.16 g, 20.9 mmol, 42%) as a colorless oil: $[\alpha]_{\text{D}}^{20} = -12.3^\circ$ (c 0.01 g/mL, CHCl_3); ^1H NMR (600 MHz, CDCl_3) δ 9.92 (s, 1H), 7.73 – 7.63 (m, 4H), 7.48 – 7.43 (m, 2H), 7.43 – 7.37 (m, 4H), 5.22 (s, 1H), 5.06 (s, 1H), 4.67 (app. ddt, $J = 7.8, 5.5, 1.0$ Hz, 1H), 4.23 (dd, $J = 11.8, 1.2$ Hz, 1H), 4.09 (dd, $J = 11.8, 0.9$ Hz, 1H), 3.36 (ddd, $J = 8.4, 6.0, 2.1$ Hz, 1H), 2.36 (ddd, $J = 13.6, 8.4, 7.8$ Hz, 1H), 2.03 (dd, $J = 2.1, 1.0$ Hz, 3H), 1.69 (ddd, $J = 13.6, 6.0, 5.5$ Hz, 1H), 1.10 (s, 9H); ^{13}C NMR (150 MHz, CDCl_3) δ 189.1, 161.7, 148.2, 139.1, 136.2, 136.1, 133.7, 133.6, 130.1, 130.0, 127.9, 127.8, 115.3, 80.5, 48.4, 44.9, 41.2, 27.1, 19.4, 12.3; IR (thin film, cm^{-1}) 3072, 3050, 2960, 2931, 2892, 2857, 1725, 1674, 1472, 1428; HRMS (EI+) calcd. for $[\text{C}_{26}\text{H}_{31}\text{ClO}_2\text{Si}]$: m/z 438.1782, found 438.1779.



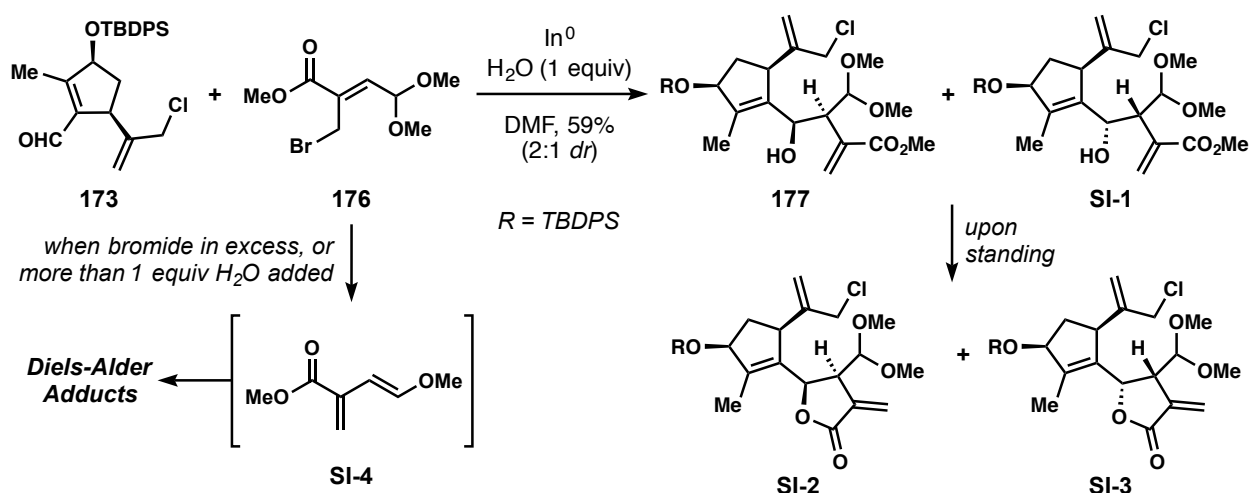
Allylic bromide 176: This procedure was adapted from previous conditions reported by Hoffmann and co-workers.¹ (i) A 250 mL round-bottom flask equipped with a stir bar was charged with 2,2-dimethoxyacetaldehyde (70.0 g, 60% in H_2O , 0.400 mol), methyl acrylate (72.4 mL, 0.800 mol), and DABCO (44.0 g, 0.200 mol). The resulting mixture was stirred at room temperature for 2 days and concentrated *in vacuo*. The resulting oil was diluted with diethyl ether (500 mL) and washed with 1N HCl (300 mL), H_2O (300 mL), and brine (300 mL) sequentially. The organic phase was dried over Na_2SO_4 and concentrated *in vacuo*. The crude mixture was purified by flash column chromatography (EtOAc/hexane, 1:10 – 1:3), affording allylic alcohol **175** (51.0 g, 0.268 mol, 67%) as a colorless oil, spectra data of which was in agreement with that previously reported by Myers and coworkers.²

(ii) A flame-dried 500 mL round-bottom flask was charged with a stir bar, *N*-Bromosuccinimide (22.0 g, 0.124 mol) and DCM (250 mL). The reaction mixture was cooled to $0\text{ }^\circ\text{C}$, followed by the addition of dimethyl sulfide (10.0 mL, 0.139 mol) in DCM (75 mL). The resulting mixture was stirred at $0\text{ }^\circ\text{C}$ for 20 min, and allylic alcohol **175** (20.0 g, 0.105 mol) in DCM (75 mL) was

¹ Martin, H.; Hoffmann, R.; Rabe, J. *J. Org. Chem.* **1985**, *50*, 3849.

² Svenda, J.; Myers, A. G. *Org. Lett.* **2009**, *11*, 2437.

added slowly. The reaction mixture was allowed to warm to room temperature gradually and stirred overnight. After the consumption of the starting material was complete as indicated by TLC (EtOAc/hexane, 1:5), the reaction was quenched by addition of sat. aqueous NaHCO₃ (200 mL). The aqueous phase was extracted with diethyl ether (200 mL × 2). The combined organic phase was washed with H₂O (300 mL) and brine (300 mL) sequentially, dried over Na₂SO₄, and concentrated *in vacuo*. The crude material was purified by flash column chromatography (EtOAc/hexane, 1:15 – 1:5), affording allylic bromide **176** (16.1 g, 0.0636 mol, 61%) as a colorless oil: ¹H NMR (600 MHz, CDCl₃) δ 6.76 (d, *J* = 5.5 Hz, 1H), 5.20 (d, *J* = 5.5 Hz, 1H), 4.30 (s, 2H), 3.82 (s, 3H), 3.36 (s, 6H); ¹³C NMR (150 MHz, CDCl₃) δ 165.7, 141.1, 133.0, 99.0, 52.9, 52.9, 52.6, 23.5; IR (thin film, cm⁻¹) 2997, 2955, 2907, 2832, 1722, 1654, 1438, 1371, 1329; HRMS (ESI) calcd. for [C₈H₁₃⁷⁹BrNaO₄]⁺ (M+Na)⁺: *m/z* 274.9895, found 274.9895, calcd. for [C₈H₁₃⁸¹BrNaO₄]⁺ (M+Na)⁺: 276.9874, found 276.9877.

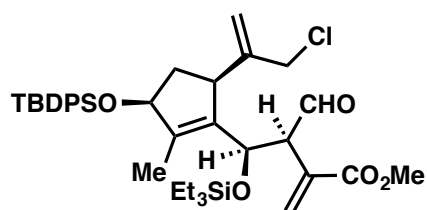


Compound 177 and SI-1: A flame-dried 500 mL round-bottom flask equipped with a stir bar was charged with aldehyde **173** (14.0 g, 31.9 mmol), allylic bromide **176** (6.73 g, 26.6 mmol), and indium shot (4.58 g, 39.9 mmol). The flask was placed under vacuum and back-filled twice with N₂, followed by the addition of DMF (80 mL) and H₂O (0.48 mL, 26.6 mmol). The reaction mixture was stirred vigorously at room temperature while bubbling with N₂ for 1 hour. The resulting mixture was stirred overnight and filtered through a pad of Celite[®]. The filtrate was diluted with H₂O (800 mL) and the aqueous layer was extracted with ethyl acetate (3 × 500 mL). The combined organic phase was washed with H₂O (500 mL × 2) and brine (500 mL), dried over Na₂SO₄, and concentrated *in vacuo*. The crude mixture was purified by flash column chromatography (EtOAc/hexane, 1:20 to 1:10), affording recovered aldehyde **173** along with a mixture of compounds **177** and **SI-1** (11.0 g, 17.9 mmol, 67%, 2:1 *dr*). The diastereomeric ratio (*dr*) of **177** and **SI-1** was determined by ¹H NMR.

The products undergo lactonization upon standing to give **SI-2** and **SI-3**, respectively, and were therefore used immediately to the next step. When allylic bromide **176** was used in excess or more than 1 equivalent of H₂O was added, a mixture of Diels-Alder dimers derived from intermediate **SI-4** was obtained in addition to the aforementioned products. Compounds **177**, **SI-1**, **SI-2**, **SI-3** and the dimerization products from **SI-4** are of similar polarity in various solvent systems, and thus inseparable.

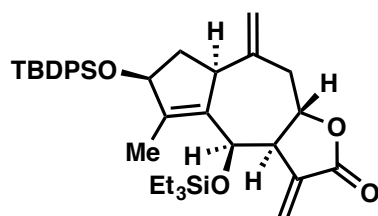
[Notes: Lactonization of **SI-1** is faster than that of the desired diastereomer **177**, which is beneficial for the purpose of product separation in the next step. However, formation of large

amounts of **SI-2** should be avoided. Lactones **SI-2** and **SI-3** are not reactive in the conditions of next step.]



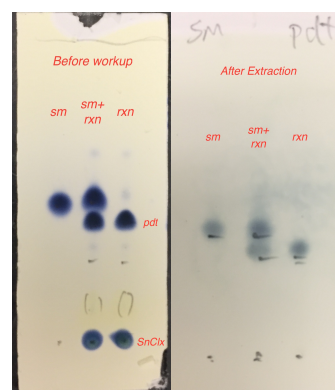
Compound 178: This procedure was adapted from previous conditions reported by Kita and coworkers.¹

A flame-dried 500 mL round-bottom flask equipped with a stir bar was charged with compounds **177** and **SI-1** (12.3 g, 20.1 mmol, 2:1 **177:SI-1**), 2,4,6-collidine (14.5 g, 120 mmol) and DCM (300 mL). The reaction mixture was cooled to -78 °C in an acetone-dry ice bath and TESOTf (21.1 g, 80.0 mmol) was added dropwise. The reaction mixture was allowed to warm gradually and stirred at approximately 0 °C for 24 hours. After complete consumption of the dimethyl acetal intermediate as indicated by TLC, the reaction was quenched by addition of H₂O (50 mL) and stirred at room temperature for 30 min until the disappearance of polar collidine adducts on TLC (EtOAc/hexane, 1:5). The resulting mixture was diluted with H₂O (200 mL) and the aqueous layer was extracted with DCM (200 mL × 3). The combined organic phase was washed with brine (300 mL), dried over MgSO₄, and concentrated *in vacuo*. The crude product was purified by flash column chromatography (EtOAc/hexane, 1:30), affording **178** (7.05 g, 10.4 mmol, 78% from **177**) separated from its diastereomer as a light yellow oil: $[\alpha]_D^{20} = +25.0^\circ$ (c 0.01 g/mL, CHCl₃); ¹H NMR (500 MHz, CDCl₃) δ 9.86 (d, *J* = 2.1 Hz, 1H), 7.68 – 7.62 (m, 4H), 7.45 – 7.41 (m, 2H), 7.39 – 7.35 (m, 4H), 6.17 (s, 1H), 5.58 (s, 1H), 5.36 (s, 1H), 5.27 (s, 1H), 5.18 (d, *J* = 9.9 Hz, 1H), 4.43 (dd, *J* = 7.6, 3.1 Hz, 1H), 4.31 (d, *J* = 12.5 Hz, 1H), 4.14 (d, *J* = 12.5 Hz, 1H), 3.64 (dd, *J* = 9.9, 2.1 Hz, 1H), 3.63 (s, 3H), 3.19 (ddd, *J* = 8.7, 4.3, 1.8 Hz, 1H), 2.09 (ddd, *J* = 14.0, 8.7, 7.6 Hz, 1H), 1.71 (ddd, *J* = 14.0, 4.3, 3.1 Hz, 1H), 1.46 (d, *J* = 1.8 Hz, 3H), 1.07 (s, 9H), 0.95 (t, *J* = 7.9 Hz, 9H), 0.66 – 0.56 (m, 6H); ¹³C NMR (150 MHz, CDCl₃) δ 200.8, 166.1, 148.2, 141.1, 138.1, 136.2, 136.2, 134.7, 134.3, 134.2, 129.9, 129.8, 129.8, 127.7, 127.7, 116.3, 80.0, 68.2, 60.3, 52.3, 47.8, 47.6, 40.1, 27.1, 19.4, 12.7, 7.0, 4.9; IR (thin film, cm⁻¹) 3072, 2956, 2932, 2877, 2857, 1718, 1627, 1590, 1470, 1428; HRMS (ESI) calcd. for [C₃₈H₅₃ClNaO₅Si₂]⁺ (M+Na)⁺: *m/z* 703.3018, found 703.3025.



Compound 179: A flame-dried 500 mL round-bottom flask was charged with a stir bar, NaI (14.9 g, 99.3 mmol) and anhydrous SnCl₂ (9.40 g, 49.6 mmol). The flask was placed under vacuum and back-filled twice

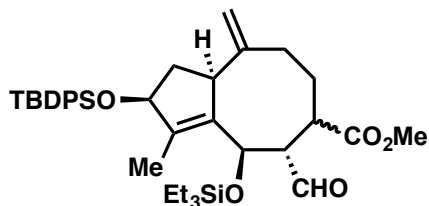
with nitrogen, followed by the addition of degassed dry DMF (250 mL). The resulting mixture was covered by alumina foil to avoid light and stirred at room temperature for 30 min. The starting material **178** (7.60 g, 11.1 mmol) in dry DMF (50 mL) was degassed by bubbling of argon, and transferred to the reaction flask via syringe in one portion. The reaction mixture was stirred in the dark at 60 °C for 12 hours. After complete consumption of the starting material as indicated by TLC (EtOAc/hexane, 1:10,



¹ H. Fujioka, T. Okitsu, Y. Sawama, N. Murata, R. Li, Y. Kita, *J. Am. Chem. Soc.* **2006**, *128*, 5930.

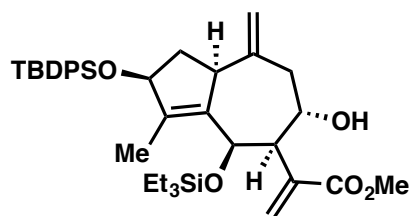
developed twice), the reaction mixture was cooled to room temperature, diluted with ethyl acetate (100 mL), and quenched by addition of *aq.* NH₄F (10% w/w, 100 mL). The resulting mixture was diluted with H₂O (500 mL) and extracted with ethyl acetate (300 mL × 3). The combined organic phase was washed with H₂O (500 mL), brine (500 mL), dried over Na₂SO₄, and concentrated *in vacuo*. The crude mixture was purified by flash column chromatography (EtOAc/hexane, 1:20), affording **179** (6.18 g, 10.0 mmol, 90%) as a colorless oil: $[\alpha]_D^{20} = +57.9^\circ$ (c 0.007 g/mL, CHCl₃); ¹H NMR (600 MHz, CDCl₃) δ 7.74 – 7.67 (m, 4H), 7.47 – 7.41 (m, 2H), 7.42 – 7.35 (m, 4H), 6.28 (d, *J* = 3.4 Hz, 1H), 5.52 (d, *J* = 3.1 Hz, 1H), 5.04 (s, 1H), 4.95 (s, 1H), 4.91 (s, 1H), 4.70 (ddd, *J* = 11.8, 9.8, 4.3 Hz, 1H), 4.57 (app. t, *J* = 7.1 Hz, 1H), 3.06 (dd, *J* = 11.8, 4.3 Hz, 1H), 2.84 – 2.77 (m, 1H), 2.68 (ddd, *J* = 9.8, 3.4, 3.1 Hz, 1H), 2.22 (dd, *J* = 11.8, 11.8 Hz, 1H), 1.96 (ddd, *J* = 11.9, 6.1, 6.1 Hz, 1H), 1.85 (ddd, *J* = 11.9, 11.3, 8.2 Hz, 1H), 1.71 (dd, *J* = 2.5, 1.2 Hz, 3H), 1.11 (s, 9H), 0.89 (t, *J* = 7.9 Hz, 9H), 0.62 – 0.48 (m, 6H); ¹³C NMR (125 MHz, CDCl₃) δ 170.0, 142.4, 140.1, 139.5, 137.6, 136.1, 134.5, 134.2, 129.8, 127.7, 127.7, 119.5, 113.8, 78.6, 77.7, 63.6, 51.8, 48.8, 44.8, 39.3, 27.1, 19.5, 13.1, 7.1, 5.3; IR (thin film, cm⁻¹) 3072, 2963, 2930, 2889, 2857, 1472, 1449, 1428, 1343; HRMS (ESI) calcd. for [C₃₇H₅₀NaO₄Si₂]⁺ (M+Na)⁺: *m/z* 637.3140, found 637.3133.

[Note: This compound is sensitive to nucleophiles; even reagents that are only weakly nucleophilic, such as LDA, form adducts with **179**.]

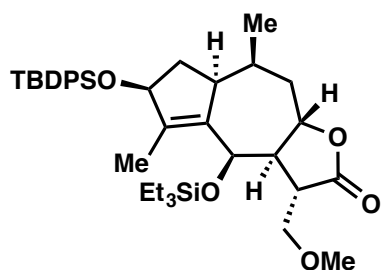


Cyclooctane 309: A flame-dried reaction tube was charged with a stir bar, compound **178** (34.0 mg, 0.0499 mmol), and NaI (75.0 mg, 0.500 mmol). The tube was placed under vacuum and back-filled twice with N₂, followed by addition of dry acetone (6 mL). The resulting mixture was stirred under cover of alumina foil at 40 °C overnight, and then

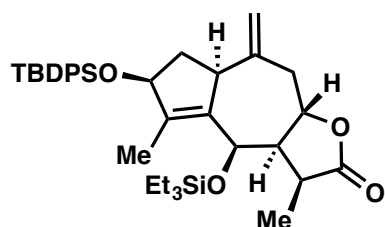
concentrated *in vacuo*. The crude mixture was re-dissolved in dry diethyl ether and filtered through a pad of Celite®. The filtrate was collected in another reaction tube wrapped by alumina foil and concentrated *in vacuo*. Activated zinc powder (32.0 mg, 0.496 mmol) and THF (2 mL) was added to the reaction followed by the addition of degassed saturated *aq.* NH₄Cl (1 mL). The reaction mixture was vigorously stirred for 20 min and the aqueous layer was extracted with ethyl acetate (5 mL × 3). The combined organic phase was washed with H₂O (10 mL), dried over Na₂SO₄, and concentrated *in vacuo*. Flash column chromatography (EtOAc/hexane, 1:20) afforded recovered **178** (11.5 mg, 0.0169 mmol, 34%) and cyclooctane **309** (16.5 mg, 0.0240 mmol, 51%, 5:2 *dr*) as a colorless oil that was an inseparable mixture of two diastereomers: IR (thin film, cm⁻¹) 3072, 2957, 2932, 2877, 2857, 1735, 1635, 1471, 1429; HRMS (EI) calcd. for [C₃₈H₅₄O₅Si₂]: *m/z* 646.3510, found 646.3503; Major diastereomer: ¹H NMR (600 MHz, CDCl₃) δ 9.93 (d, *J* = 2.1 Hz, 1H), 7.72 – 7.65 (m, 4H), 7.46 – 7.34 (m, 6H), 4.85 (app. t, *J* = 1.7 Hz, 1H), 4.83 (br s, 1H), 4.63 – 4.57 (m, 1H), 4.21 (d, *J* = 10.4 Hz, 1H), 3.65 (s, 3H), 3.29 – 3.23 (m, 1H), 3.10 – 3.05 (m, 1H), 2.66 – 2.63 (m, 1H), 2.54 (d, *J* = 10.4 Hz, 1H), 2.12 (d, *J* = 9.2 Hz, 1H), 2.00 (app. dt, *J* = 13.3, 7.5 Hz, 1H), 1.87 (dd, *J* = 2.6, 1.1 Hz, 3H), 1.69 – 1.65 (m, 1H), 1.62 (ddd, *J* = 13.2, 7.9, 6.5 Hz, 1H), 1.59 – 1.54 (m, 1H), 1.09 (s, 9H), 0.81 (t, *J* = 8.0 Hz, 9H), 0.40 (q, *J* = 8.0 Hz, 6H); ¹³C NMR (125 MHz, CDCl₃) δ 206.1, 176.5, 146.9, 140.6, 139.3, 136.2, 136.1, 134.7, 134.2, 129.8, 129.7, 127.7, 127.6, 117.3, 80.5, 71.5, 58.4, 53.3, 52.2, 41.4, 37.6, 34.1, 27.2, 19.4, 12.7, 6.8, 4.6.



[From Entry 7, Table 2.3] Compound **310**, colorless oil: ^1H NMR (500 MHz, CDCl_3) δ 7.71 – 7.65 (m, 4H), 7.45 – 7.40 (m, 2H), 7.40 – 7.34 (m, 4H), 6.30 (s, 1H), 5.80 (s, 1H), 4.95 (d, $J = 1.8$ Hz, 1H), 4.87 (d, $J = 1.8$ Hz, 1H), 4.57 (dd, $J = 7.5$, 6.8 Hz, 1H), 4.34 (d, $J = 3.9$ Hz, 1H), 3.90 (br s, 1H), 3.75 (s, 3H), 3.47 (app. t, $J = 4.0$ Hz, 1H), 3.00 – 2.91 (m, 1H), 2.66 (dd, $J = 13.4$, 2.6 Hz, 1H), 2.26 (dd, $J = 13.4$, 6.7 Hz, 1H), 2.17 (d, $J = 8.0$ Hz, 1H), 2.02 (ddd, $J = 12.6$, 6.8, 6.8 Hz, 1H), 1.68 (br s, 3H), 1.43 (ddd, $J = 12.6$, 9.7, 7.5 Hz, 1H), 1.08 (s, 9H), 0.86 (t, $J = 8.0$ Hz, 9H), 0.49 (qd, $J = 8.0$, 1.7 Hz, 6H); ^{13}C NMR (100 MHz, CDCl_3) δ 169.0, 146.0, 141.9, 140.5, 136.1, 136.1, 136.0, 134.8, 134.3, 129.7, 129.7, 127.7, 127.6, 125.6, 115.2, 80.0, 77.4, 70.1, 69.1, 52.1, 51.3, 50.5, 41.2, 39.3, 27.2, 19.5, 13.4, 6.9, 4.8; IR (thin film, cm^{-1}) 3463, 3072, 3049, 2956, 2932, 2876, 2856, 1775, 1723, 1628, 1470, 1429; HRMS (EI) calcd. for $[\text{C}_{38}\text{H}_{54}\text{O}_5\text{Si}_2]$: m/z 646.3510, found 646.3505.



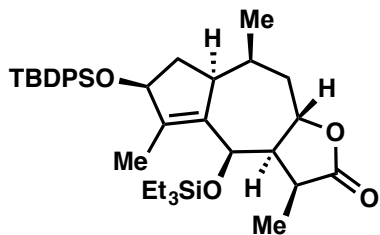
Compound 180: A flame-dried 250 mL round-bottom flask was charged with a stir bar and compound **179** (6.18 g, 10.0 mmol). The flask was placed under vacuum and back-filled twice with nitrogen, followed by the addition of methanol (100 mL) and DCM (35 mL). NaOMe (54 mg, 1.0 mmol) was then added in one portion to the reaction and the resulting mixture was stirred at room temperature for 16 hours. The reaction was monitored by ^1H NMR with an aliquot (0.1 mL) concentrated *in vacuo*. After complete consumption of the starting material, acetic acid (60 mL, 1.0 mmol) and PtO_2 (227 mg, 1.00 mmol) were added sequentially to the reaction. The reaction mixture was bubbled with H_2 until a black suspension formed, and was stirred under 1 atmosphere of H_2 for 6 hours. After the reaction was complete as indicated by ^1H NMR, the reaction mixture was filtered through a pad of Celite[®] and concentrated *in vacuo*. The crude mixture was purified by flash column chromatography (EtOAc/hexane, 1:20), affording **180** (6.23 g, 9.60 mmol, 96%) as a colorless oil: $[\alpha]_D^{20} = +48.8^\circ$ (c 0.01 g/mL, CHCl_3); ^1H NMR (500 MHz, CDCl_3) δ 7.72 – 7.65 (m, 4H), 7.45 – 7.41 (m, 2H), 7.40 – 7.35 (m, 4H), 4.81 (ddd, $J = 12.1$, 10.2, 3.9 Hz, 1H), 4.64 (s, 1H), 4.52 (app. t, $J = 7.4$ Hz, 1H), 3.65 (dd, $J = 9.8$, 4.8 Hz, 1H), 3.59 (dd, $J = 9.8$, 3.5 Hz, 1H), 3.30 (s, 3H), 2.81 (ddd, $J = 12.0$, 4.8, 3.5 Hz, 1H), 2.58 – 2.50 (m, 1H), 2.28 (ddd, $J = 12.7$, 3.9, 3.9 Hz, 1H), 2.14 (dd, $J = 12.0$, 10.2 Hz, 1H), 1.93 (ddd, $J = 12.3$, 7.4, 7.1 Hz, 1H), 1.89 – 1.81 (m, 1H), 1.65 – 1.63 (m, 3H), 1.61 (ddd, $J = 12.7$, 12.1, 3.9 Hz, 1H), 1.51 (ddd, $J = 12.3$, 9.9, 7.4 Hz, 1H), 1.08 (s, 9H), 1.03 (d, $J = 7.3$ Hz, 3H), 0.97 (t, $J = 7.9$ Hz, 9H), 0.72 – 0.57 (m, 6H); ^{13}C NMR (125 MHz, CDCl_3) δ 176.2, 143.1, 139.0, 136.1, 136.1, 134.6, 134.4, 129.7, 129.7, 127.6, 127.6, 79.4, 76.5, 68.9, 63.8, 59.4, 50.2, 50.0, 44.1, 40.9, 39.3, 31.5, 27.1, 19.4, 13.9, 13.0, 7.2, 5.7; IR (thin film, cm^{-1}) 3071, 2958, 2932, 2876, 2857, 1781, 1472, 1428, 1389; HRMS (EI) calcd. for $[\text{C}_{38}\text{H}_{56}\text{O}_5\text{Si}_2]$: m/z 648.3666, found 648.3660.



Compound 308: A flame-dried 25 mL round-bottom flask equipped with a stir bar was charged with compound **179** (560 mg, 0.911 mmol) and Wilkinson's catalyst (83.0 mg, 0.0897 mmol), followed by addition of anhydrous benzene (10 mL). The reaction mixture was bubbled with H_2 for 5 minutes, and was stirred under 1 atmosphere of H_2 for 1 hour. The reaction

mixture was then concentrated *in vacuo* when TLC indicated full conversion of the starting material. The crude mixture was purified by flash column chromatography (EtOAc/hexane, 1:20), affording **308** (304 mg, 0.493 mmol, 54%) as a colorless oil: $[\alpha]_D^{20} = +62.0^\circ$ (c 0.0025 g/mL, CHCl₃); ¹H NMR (500 MHz, CDCl₃) δ 7.73 – 7.67 (m, 4H), 7.46 – 7.41 (m, 2H), 7.40 – 7.36 (m, 4H), 5.01 (s, 1H), 4.90 (s, 1H), 4.90 – 4.84 (m, 1H), 4.72 (s, 1H), 4.59 – 4.53 (m, 1H), 3.06 (dd, *J* = 11.6, 5.0 Hz, 1H), 2.80 (br s, 1H), 2.66 (app p, *J* = 7.8 Hz, 1H), 2.21 (dd, *J* = 10.5, 7.8 Hz, 1H), 2.11 (dd, *J* = 11.6, 11.6 Hz, 1H), 1.93 (app. dt, *J* = 11.6, 6.0 Hz, 1H), 1.83 (app. td, *J* = 11.6, 8.3 Hz, 1H), 1.69 (dd, *J* = 2.5, 1.1 Hz, 3H), 1.32 (d, *J* = 7.8 Hz, 3H), 1.10 (s, 9H), 0.94 (t, *J* = 8.0 Hz, 9H), 0.61 (q, *J* = 8.0 Hz, 6H); ¹³C NMR (100 MHz, CDCl₃) δ 179.6, 142.3, 140.1, 138.5, 136.1, 136.1, 134.6, 134.2, 129.8, 129.8, 127.7, 127.7, 113.4, 78.7, 77.6, 63.9, 49.7, 48.4, 45.4, 39.9, 39.3, 27.1, 19.5, 12.9, 12.4, 7.3, 5.6. IR (thin film, cm⁻¹) 3072, 2957, 2933, 2876, 2856, 1776, 1467, 1589, 1471, 1458; HRMS (EI) calcd. for [C₃₇H₅₂O₄Si₂]: *m/z* 616.3404, found 616.3400.

[When the reaction was not stopped after completion, over reduction could afford 0~10% double-reduction product **SI-5**, which was inseparable from **308**.]

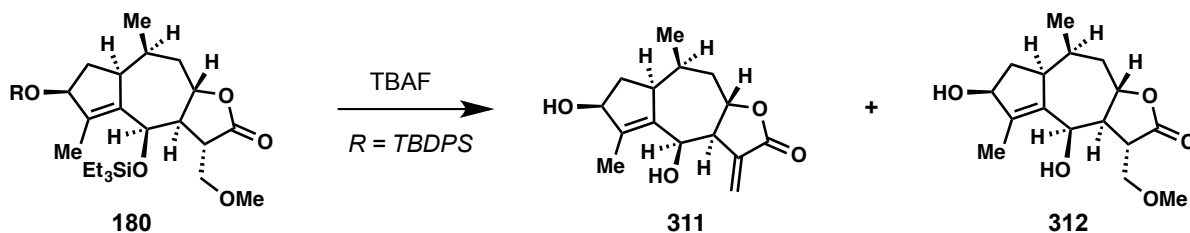


Double-reduction product SI-5: A flame-dried 10 mL round-bottom flask equipped with a stir bar was charged with compound **179** (21.0 mg, 0.0341 mmol) and PtO₂ (1.0 mg, 0.0044 mmol). The flask was placed under vacuum and back-filled with H₂. Anhydrous methanol (0.5 mL) was added and the reaction mixture was cooled to 0 °C. The reaction mixture was bubbled with H₂ until a black suspension formed, and was then

stirred under 1 atmosphere of H₂ for 2 hours. After the reaction was complete as indicated by TLC (EtOAc/hexane, 1:5), the reaction mixture was filtered through a pad of Celite[®] and concentrated *in vacuo*. The crude mixture was purified by flash column chromatography (EtOAc/hexane, 1:20), affording double-reduction product **SI-5** (14.1 mg, 0.0228 mmol, 67%) as a colorless oil: $[\alpha]_D^{20} = +28.4^\circ$ (c 0.005 g/mL, CHCl₃); ¹H NMR (600 MHz, CDCl₃) δ 7.73 – 7.65 (m, 4H), 7.46 – 7.40 (m, 2H), 7.41 – 7.34 (m, 4H), 5.04 (ddd, *J* = 11.5, 10.3, 4.2 Hz, 1H), 4.71 (s, 1H), 4.50 (app. t, *J* = 7.2 Hz, 1H), 2.66 (app. p, *J* = 8.0 Hz, 1H), 2.50 (dddd, *J* = 11.4, 7.0, 2.5, 2.5 Hz, 1H), 2.34 (ddd, *J* = 12.8, 4.2, 4.2 Hz, 1H), 2.08 (dd, *J* = 10.3, 8.7 Hz, 1H), 1.89 – 1.81 (m, 2H), 1.69 (dd, *J* = 2.5, 1.1 Hz, 3H), 1.59 – 1.48 (m, 2H), 1.35 (d, *J* = 7.8 Hz, 3H), 1.09 (s, 9H), 1.06 (d, *J* = 7.3 Hz, 3H), 1.00 (t, *J* = 8.0 Hz, 9H), 0.78 – 0.66 (m, 6H); ¹³C NMR (150 MHz, CDCl₃) δ 179.9, 141.8, 139.7, 136.2, 136.1, 134.7, 134.4, 129.8, 129.7, 127.7, 127.6, 79.3, 77.1, 64.0, 49.7, 49.7, 42.2, 40.1, 39.7, 31.3, 27.1, 19.5, 13.9, 13.5, 13.2, 7.6, 5.9; IR (thin film, cm⁻¹) 3072, 3049, 2958, 2932, 2877, 2856, 1776, 1740, 1458, 1428; HRMS (EI) calcd. for [C₃₇H₅₄O₄Si₂]: *m/z* 618.3561, found 618.3548.

Diol 311: [Condition 1] A reaction tube (Fisher Scientific, 13 × 100 mm) was charged with a stir bar and compound **180** (100 mg, 0.154 mmol) in THF (1 mL). The reaction mixture was cooled to 0 °C and TBAF (0.46 mL, 0.46 mmol, 1M in THF) was added dropwise. The resulting mixture was warmed to room temperature and stirred overnight. After the reaction was complete as indicated by TLC (pure EtOAc), acetic acid (54 μ L) was added to quench the reaction. The reaction mixture was concentrated *in vacuo*, and The crude mixture was purified by flash column chromatography (EtOAc/hexane, 3:1), affording a mixture of **311** and **312** (33.9 mg, 0.128 mmol, 83%, 5:2 ratio). The mixture could be separated by preparative TLC (acetone:toluene 1:4,

developed 3 times).



examined conditions:

1. TBAF, THF
2. TBAF, THF, then add *t*-BuOK
3. *i.* TBAF, THF; *ii.* DBU

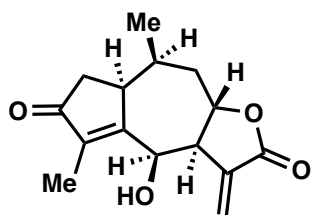
results:

- 60% **311** + 24% **312**
 56% **311**, **312** not observed
 69% **311** with up to 3% **312**

[Condition 2] Compound **180** (28 mg, 0.043 mmol) was treated similarly with TBAF (0.13 mL, 0.13 mmol, 1M in THF) as in Condition 1. After the desilylation was complete as indicated by TLC, the reaction mixture was cooled to 0 °C and LiHMDS (0.13 mL, 0.13 mmol, 1M in THF) was added dropwise. The resulting mixture was further stirred for 20 minutes, followed by addition of acetic acid (25 μ L) to quench the reaction. The crude mixture was purified by flash column chromatography affording diol **311** (6.4 mg, 0.024 mmol, 56%) without any **312** observed.

[Condition 3] A 250 mL round-bottom flask was charged with a stir bar and compound **180** (3.90 g, 6.00 mmol) in THF (100 mL). TBAF (24 mL, 24 mmol, 1 M in THF) was added at 0 °C and the resulting mixture was stirred for 24 hours at room temperature. Acetic acid (0.5 mL) was then added to the reaction. The reaction mixture was concentrated *in vacuo* and then re-dissolved in DCM (20 mL) and toluene (120 mL). DBU (1.0 mL, 6.6 mmol) was added to the reaction and the flask was equipped with a reflux condenser and heated at 120 °C for 24 hours. The crude after concentrating *in vacuo* was purified by flash column chromatography (pure EtOAc), affording diol **311** (1.09 g, 4.12 mmol, 69%) which contained up to 3% **312**.

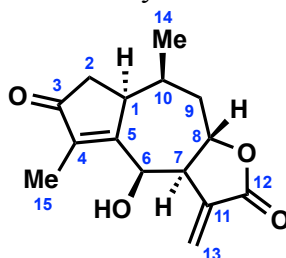
Diol **311**, colorless oil: $[\alpha]_D^{20} = +96.8^\circ$ (c 0.005 g/mL, MeOH); $^1\text{H NMR}$ (600 MHz, CDCl_3) δ 6.37 (d, $J = 3.4$ Hz, 1H), 5.64 (d, $J = 3.1$ Hz, 1H), 4.91 (s, 1H), 4.80 (ddd, $J = 12.6, 9.6, 3.7$ Hz, 1H), 4.52 (dd, $J = 8.0, 5.1$ Hz, 1H), 2.87 – 2.82 (m, 1H), 2.80 (dddd, $J = 9.6, 3.4, 3.1, 1.6$ Hz, 1H), 2.53 (ddd, $J = 14.0, 8.4, 8.0$ Hz, 1H), 2.39 (ddd, $J = 12.6, 3.7, 3.7$ Hz, 1H), 2.06 – 1.99 (m, 1H), 1.90 (d, $J = 2.2$ Hz, 3H), 1.80 (ddd, $J = 12.6, 12.6, 3.7$ Hz, 1H), 1.41 (ddd, $J = 14.0, 6.1, 5.1$ Hz, 1H), 0.98 (d, $J = 7.3$ Hz, 3H); $^{13}\text{C NMR}$ (150 MHz, CDCl_3) δ 169.8, 145.1, 139.4, 137.1, 120.4, 79.0, 75.6, 63.5, 51.2, 50.4, 40.9, 38.8, 32.8, 13.5, 12.6; IR (thin film, cm^{-1}) 3448, 2960, 2924, 2877, 2855, 1748, 1662, 1463, 1404, 1384; HRMS (EI) calcd. for $[\text{C}_{15}\text{H}_{20}\text{O}_4]$: m/z 264.1362, found 264.1355. [Note: Diol **311** is not stable in chloroform at room temperature.]



Mikanokryptin (44): A 100 mL round bottom flask was charged with a stir bar, diol **311** (1.088 g, 4.116 mmol), and DCM (50 mL). Activated MnO_2 (10.7 g, 123 mmol) was added in one portion. The resulting mixture was stirred vigorously at room temperature for 16 hours. The reaction was monitored by TLC (pure EtOAc), and filtered through a pad of Celite[®] when complete conversion was observed. The filtrate was concentrated *in vacuo*, affording spectroscopically pure mikanokryptin (1.051 g, 4.007 mmol, 97%) as a light-yellow to white solid: mp 230.5 –

232.4 °C; $[\alpha]_D^{20} = +235.0^\circ$ (lit. $+264^\circ$, c 0.00098 g/mL, MeOH); ^1H NMR (600 MHz, CDCl_3) δ 6.46 (d, $J = 3.5$ Hz, 1H), 5.70 (d, $J = 3.1$ Hz, 1H), 5.17 (br s, 1H), 4.80 (ddd, $J = 12.6, 9.6, 3.5$ Hz, 1H), 3.15 – 3.10 (m, 1H), 3.06 (dddd, $J = 9.6, 3.5, 3.1, 1.9$ Hz, 1H), 2.67 (ddd, $J = 19.1, 6.9, 1.1$ Hz, 1H), 2.45 (ddd, $J = 12.8, 3.5, 3.5$ Hz, 1H), 2.34 – 2.27 (m, 1H), 2.19 (dd, $J = 19.1, 1.9$ Hz, 1H), 1.94 (ddd, $J = 12.8, 12.6, 4.1$ Hz, 1H), 1.92 (dd, $J = 2.1, 0.9$ Hz, 3H), 0.85 (d, $J = 7.3$ Hz, 3H); ^1H NMR (600 MHz, $\text{DMSO-}d_6$) δ 6.20 (d, $J = 3.4$ Hz, 1H), 5.80 (d, $J = 3.1$ Hz, 1H), 5.74 (d, $J = 6.5$ Hz, 1H), 5.09 (d, $J = 6.5$ Hz, 1H), 4.64 (ddd, $J = 12.5, 9.4, 3.4$ Hz, 1H), 3.24 – 3.14 (m, 2H), 2.55 (dd, $J = 19.0, 6.7$ Hz, 1H), 2.21 (ddd, $J = 12.0, 3.4, 3.4$ Hz, 1H), 2.19 – 2.15 (m, 1H), 2.05 (dd, $J = 19.0, 1.9$ Hz, 1H), 1.94 (ddd, $J = 12.5, 12.0, 4.0$ Hz, 1H), 1.76 (d, $J = 1.0$ Hz, 3H), 0.73 (d, $J = 7.1$ Hz, 3H); ^{13}C NMR (150 MHz, $\text{DMSO-}d_6$) δ 207.2, 172.5, 169.5, 141.5, 136.5, 120.8, 75.0, 62.7, 49.5, 44.2, 40.9, 39.4, 32.4, 12.5, 8.6; IR (thin film, cm^{-1}) 3434, 2961, 2924, 2882, 1762, 1679, 1633, 1450, 1407, 1385, 1325; HRMS (EI) calcd. for $[\text{C}_{15}\text{H}_{18}\text{O}_4]$: m/z 262.1205, found 262.1207.

Table S1. ^1H NMR comparison of natural and synthetic mikanokryptin (**44**).



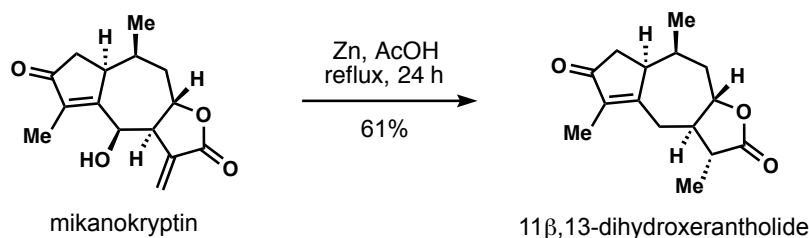
mikanokryptin (**44**)

	mikanokryptin (44) ¹	mikanokryptin (44) this work ²	mikanokryptin (44) ³	mikanokryptin (44) this work
C	90 MHz, <i>d</i> -DMSO	600 MHz, <i>d</i> -DMSO	200 MHz, 95% CDCl ₃ – 5% <i>d</i> -DMSO	600 MHz, CDCl ₃
1	3.16 (m, 1H)	3.19 (m, 1H)	3.12 (dddd, <i>J</i> = 6.8, 2.2, 2.0, 2.0, 1.0 Hz, 1H)	3.12 (m, 1H)
2 α	obscured signal	2.55 (dd, <i>J</i> = 19.0, 6.7 Hz, 1H)	2.65 (ddd, <i>J</i> = 19.1, 6.8, 1.1 Hz, 1H)	2.67 (ddd, <i>J</i> = 19.1, 6.9, 1.1 Hz, 1H)
2 β	obscured signal	2.05 (dd, <i>J</i> = 19.0, 1.9 Hz, 1H)	2.17 (dd, <i>J</i> = 19.1, 2.0 Hz, 1H)	2.19 (dd, <i>J</i> = 19.1, 1.9 Hz, 1H)
6	5.10 (br d, <i>J</i> = 6.2 Hz, 1H)	5.09 (d, <i>J</i> = 6.5 Hz, 1H)	5.13 (dddd, <i>J</i> = 5.6, 3.5, 1.1, 1.0, 0.8 Hz, 1H)	5.17 (br s, 1H)
7	3.16 (m, 1H)	3.19 (m, 1H)	3.01 (dddd, <i>J</i> = 9.6, 3.5, 3.4, 3.0 Hz, 1H)	3.06 (dddd, <i>J</i> = 9.6, 3.5, 3.1, 1.9 Hz, 1H)
8	4.66 (ddd, <i>J</i> = 12, 10, 3.7 Hz, 1H)	4.64 (ddd, <i>J</i> = 12.5, 9.4, 3.4 Hz, 1H)	4.84 (ddd, <i>J</i> = 12.1, 9.6, 3.5 Hz, 1H)	4.80 (ddd, <i>J</i> = 12.6, 9.6, 3.5 Hz, 1H)
9 α	obscured signal	1.94 (ddd, <i>J</i> = 12.5, 12.0, 4.0 Hz, 1H)	1.92 (ddd, <i>J</i> = 12.6, 12.1, 3.9 Hz, 1H)	1.94 (ddd, <i>J</i> = 12.8, 12.6, 4.1 Hz, 1H)
9 β	obscured signal	2.21 (ddd, <i>J</i> = 12.0, 3.4, 3.4 Hz, 1H)	2.42 (ddd, <i>J</i> = 12.6, 3.5, 3.5 Hz, 1H)	2.45 (ddd, <i>J</i> = 12.8, 3.5, 3.5 Hz, 1H)
10	obscured signal	2.17 (m, 1H)	2.29 (dddd, <i>J</i> = 7.3, 3.9, 3.5, 2.2 Hz, 1H)	2.31 (m, 1H)
13 _{cis}	6.24 (d, <i>J</i> = 3.5 Hz, 1H)	6.20 (d, <i>J</i> = 3.4 Hz, 1H)	6.40 (d, <i>J</i> = 3.4 Hz, 1H)	6.46 (d, <i>J</i> = 3.5 Hz, 1H)
13 _{trans}	5.81 (d, <i>J</i> = 3.1 Hz, 1H)	5.80 (d, <i>J</i> = 3.1 Hz, 1H)	5.72 (d, <i>J</i> = 3.0 Hz, 1H)	5.70 (d, <i>J</i> = 3.1 Hz, 1H)
14	0.69 (d, <i>J</i> = 7.2 Hz, 1H)	0.73 (d, <i>J</i> = 7.1 Hz, 3H)	1.90 (dd, <i>J</i> = 2.0, 0.8 Hz, 3H)	1.92 (dd, <i>J</i> = 2.1, 0.9 Hz, 3H)
15	1.74 (dd, <i>J</i> = 1, 0.9 Hz, 1H)	1.76 (d, <i>J</i> = 1.0 Hz, 3H)	0.86 (d, <i>J</i> = 7.3 Hz, 3H)	0.85 (d, <i>J</i> = 7.3 Hz, 3H)
OH	5.60 (d, <i>J</i> = 6.2 Hz, 1H)	5.74 (d, <i>J</i> = 6.5 Hz, 1H)	4.54 (d, <i>J</i> = 5.6 Hz, 1H)	not observed

¹ W. Herz, A. Srinivasan, P. S. Kalyanaraman, *Phytochemistry* **1975**, *14*, 233.

² Crystallographic Analysis of synthetic **44** matches with that reported in: M. J. Bovill, M. H. P. Guy, G. A. Sim, D. N. J. White, W. Herz, *J. Chem. Soc., Perkin Trans. 2* **1979**, 53.

³ W. F. Reynolds, R. G. Enriquez, M. A. Chavez, A. L. Silba, M. A. Martinez, *Can. J. Chem.* **1985**, *63*, 849. Standard inversion-recovery pulse sequence was utilized by choosing a delay time (0.88 s) for which the methyl signal is nulled.

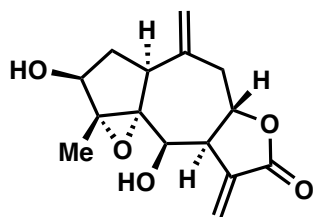


11β,13-dihydroxerantholide: This procedure was adapted from previous conditions reported by Barton and coworkers.¹ 11β,13-dihydroxerantholide has been previously isolated from *Pechuel-Loeschea leibnitziae*.²

A flame-dried reaction tube equipped with a stir bar was charged with mikanokryptin (26.0 mg, 0.0991 mmol) and activated zinc powder (98 mg, 1.5 mmol). The tube was placed under vacuum and back-filled with N₂, followed by the addition of degassed acetic acid (0.8 mL). The reaction mixture was heated at 120 °C for 24 hours, diluted with ethyl acetate and filtered through a pad of Celite[®]. The filtrate was concentrated *in vacuo* and purified by flash column chromatography (EtOAc/hexane, 1:1), affording 11β,13-dihydroxerantholide (15.0 mg, 0.0604 mmol, 61%) as a colorless oil: $[\alpha]_{\text{D}}^{20} = +153.1^{\circ}$ ($c = 0.01$ g/mL, CHCl₃); ¹H NMR (600 MHz, CDCl₃) δ 4.15 (ddd, $J = 12.1, 10.0, 3.7$ Hz, 1H), 3.13 (dq, $J = 6.6, 2.0$ Hz, 1H), 2.98 (ddd, $J = 19.0, 3.2, 1.6$ Hz, 1H), 2.62 (ddd, $J = 19.0, 6.6, 1.2$ Hz, 1H), 2.42 – 2.34 (m, 3H), 2.29 – 2.23 (m, 1H), 2.13 – 2.06 (m, 2H), 1.81 (ddd, $J = 12.1, 12.1, 4.1$ Hz, 1H), 1.70 (q, $J = 1.5$ Hz, 3H), 1.28 (d, $J = 7.0$ Hz, 3H), 0.73 (d, $J = 7.3$ Hz, 3H); ¹³C NMR (125 MHz, CDCl₃) δ 207.2, 178.1, 170.6, 139.5, 81.4, 48.1, 45.2, 42.1, 41.4, 40.5, 33.0, 31.4, 13.0, 13.0, 8.3; IR (thin film, cm⁻¹) 2965, 2931, 2876, 1771, 1695, 1636, 1456, 1383; HRMS (ESI) calcd. for [C₁₅H₂₀NaO₃]⁺ (M+Na)⁺: m/z 271.1310, found 271.1315.

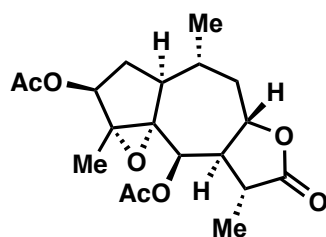
¹ D. H. R. Barton, J. E. D. Levisalles, *J. Chem. Soc.* **1958**, 4518.

² F. Bohlmann, N. Borthakur, *Phytochemistry* **1982**, *21*, 1160.



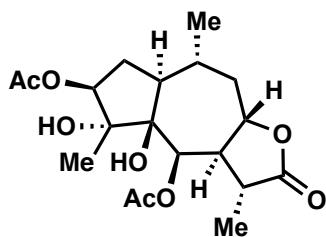
Compound **314**: (i) A 100 mL round-bottom flask was charged with a stir bar, compound **179** (200 mg, 0.325 mmol, 1 equiv), and DCM (6.5 mL). The resulting mixture was cooled to 0 °C over an ice bath, followed by the addition of *m*-CPBA (80 mg, 70% w/w, 1 equiv). The reaction mixture was stirred in a cold room (0-4 °C) for 1 day and quenched by filtration through Celite®. The filtrate was diluted with DCM (40 mL), and then washed with *sat.* NaHCO₃ (40 mL), H₂O (40 mL) and brine (40 mL), dried over Na₂SO₄, and concentrated *in vacuo*. The crude mixture was used directly in the next step without purification.

(ii) The aforementioned crude (0.325 mmol assumed) was dissolved in THF (6 mL) in a 25 mL flask. The resulting mixture was cooled to 0 °C over an ice bath, and TBAF (1 mL in THF, 1 mmol, 3 equiv) was added. The reaction mixture was then stirred at room temperature for 16 hours. After complete consumption of the silylated intermediates as judged by TLC (EtOAc/hexane, 1:1), the reaction was quenched by addition of AcOH (0.2 mL) and diluted with EtOAc (50 mL). The mixture was washed by H₂O (50 mL) and brine (50 mL), dried over Na₂SO₄, and concentrated *in vacuo*. The crude mixture was purified by column chromatography (EtOAc/hexane, 1:1 to pure EtOAc), affording **314** (33.2 mg, 37%) as a colorless oil: $[\alpha]_D^{20} = -39^\circ$ (c 0.003 g/mL, CHCl₃); ¹H NMR (500 MHz, CDCl₃) δ 6.34 (d, *J* = 3.2 Hz, 1H), 5.62 (d, *J* = 3.2 Hz, 1H), 5.48 (d, *J* = 1.0 Hz, 1H), 5.29 – 5.23 (m, 1H), 4.58 (ddd, *J* = 11.7, 9.8, 4.7 Hz, 1H), 4.29 (s, 1H), 4.27 (d, *J* = 6.2 Hz, 1H), 3.22 (app. dtd, *J* = 9.9, 3.3, 1.4 Hz, 1H), 3.15 (dd, *J* = 11.7, 4.7 Hz, 1H), 2.96 (d, *J* = 9.8 Hz, 1H), 2.40 (app. t, *J* = 11.7 Hz, 1H), 2.15 (ddd, *J* = 15.0, 9.9, 6.2 Hz, 1H), 1.82 (dd, *J* = 15.0, 1.4 Hz, 1H), 1.64 (s, 3H); ¹³C NMR (150 MHz, CDCl₃) δ 169.5, 142.2, 136.5, 120.4, 118.8, 77.0, 76.0, 75.2, 71.7, 69.9, 50.1, 48.1, 44.6, 37.8, 13.8; IR (thin film, cm⁻¹) 3446, 2954, 2930, 1752, 1666, 1648, 1448, 1404, 1385; HRMS (ESI) *calcd.* for [C₁₅H₁₉O₅]⁺ (M+H)⁺: *m/z* 279.1233, found 279.1232.



Compound **316**: A 100 mL round-bottom flask was charged with a stir bar, compound **314** (246 mg, 0.884 mmol, 1 equiv), Crabtree's catalyst (71 mg, 0.088 mmol, 0.1 equiv), and DCM (9 mL). The resulting mixture was cooled to 0 °C over an ice bath, and then bubbled with H₂ for 10 minutes. The reaction mixture was further stirred at 0 °C for 8 hours under an atmosphere of H₂, and for another 16 hours at room temperature. After the consumption of the starting material and the mono-reduction intermediate was complete as judged by TLC (EtOAc/hexane, 2:1), pyridine (0.43 mL, 5.3 mmol, 6 equiv), DMAP (11 mg, 0.09 mmol, 0.1 equiv), and acetic anhydride (0.50 mL, 5.3 mmol, 6 equiv) were added sequentially to the reaction. The reaction mixture was stirred at room temperature for 16 hours. After the acetylation is complete as judged by TLC (EtOAc/hexane, 1:1), *sat.* NaHCO₃ (30 mL) was added to quench the reaction. The resulting mixture was extracted with EtOAc (20 mL × 3). The combined organic phase was washed with H₂O (50 mL) and brine (50 mL), dried over Na₂SO₄, and concentrated *in vacuo*. The crude mixture was purified by column chromatography (EtOAc/hexane, 1:2 to 1:1), affording **316** (227 mg, 70%) as a colorless oil: $[\alpha]_D^{20} = +36.1^\circ$ (c 0.010 g/mL, CHCl₃); ¹H NMR (600 MHz, CDCl₃) δ 5.22 (s, 1H), 5.03 (dd, *J* = 6.0, 2.7 Hz, 1H), 4.37 (app. td, *J* = 11.1, 4.4 Hz, 1H), 2.34 (ddd, *J* = 13.0, 4.4, 1.7 Hz, 1H), 2.30 (app. dt, *J* = 13.5, 6.7 Hz, 1H), 2.24 – 2.17 (m, 1H), 2.13 (s, 3H), 2.13 – 2.06 (m, 1H), 2.07 (s, 3H), 2.01 (ddd, *J* = 14.5, 8.7, 6.0 Hz, 1H), 1.87 – 1.79 (m, 1H), 1.72 (ddd, *J* = 14.6, 3.9, 2.6 Hz, 1H), 1.49 (app. q, *J* = 12.0 Hz, 1H), 1.28 – 1.24

(m, 6H), 0.99 (d, $J = 6.8$ Hz, 3H); ^{13}C NMR (150 MHz, CDCl_3) δ 177.2, 170.1, 169.9, 77.2, 76.4, 73.2, 70.4, 70.0, 52.4, 49.2, 43.8, 38.5, 34.3, 29.8, 22.1, 21.2, 20.8, 12.9, 12.5; IR (thin film, cm^{-1}) 2938, 2884, 1774, 1744, 1461, 1431, 1373; HRMS (ESI) *calcd.* for $[\text{C}_{19}\text{H}_{26}\text{O}_7\text{Na}]^+$ ($\text{M}+\text{Na}$) $^+$: m/z 389.1576, found 389.1569.



Compound 318: A reaction tube was charged with a stir bar, compound **316** (11 mg, 0.03 mmol, 1 equiv), and dry toluene (0.3 mL). The resulting mixture was cooled to -78 $^{\circ}\text{C}$, and $\text{BF}_3 \cdot \text{OEt}_2$ (33 μL , 1M in DCM) was added. After the consumption of the starting material is complete as judged by TLC (~ 10 min, EtOAc/hexane, 1:1), the reaction was quenched by addition of *aq.* K_2CO_3 (5mL, 10% w/w). The resulting mixture was extracted with EtOAc (5 mL \times 3).

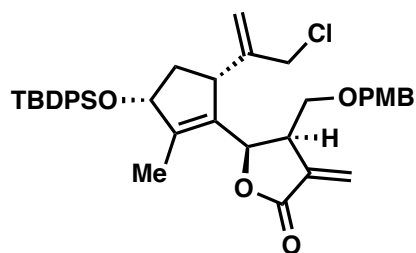
The combined organic phase was washed with H_2O (10 mL) and brine (10 mL), dried over Na_2SO_4 , and concentrated *in vacuo*. The crude mixture was purified by flash column chromatography (EtOAc/hexane, 1:2), affording **318** (11.5 mg, 99%) as a white solid: mp 198.6 – 200.6 $^{\circ}\text{C}$; $[\alpha]_{\text{D}}^{20} = +29.3^{\circ}$ (c 0.010 g/mL, CHCl_3); ^1H NMR (600 MHz, CDCl_3) δ 5.80 (d, $J = 4.1$ Hz, 1H), 4.84 (dd, $J = 8.1, 5.4$ Hz, 1H), 4.58 (ddd, $J = 11.2, 9.7, 3.3$ Hz, 1H), 2.62 (brs, 1H), 2.53 (brs, 1H), 2.44 (app. dt, $J = 13.7, 7.9$ Hz, 1H), 2.35 (app. dt, $J = 13.1, 3.8$ Hz, 1H), 2.18 (s, 3H), 2.25 – 2.04 (m, 4H), 2.07 (s, 3H), 1.57 (ddd, $J = 13.6, 10.3, 5.3$ Hz, 1H), 1.31 – 1.21 (m, 1H), 1.25 (d, $J = 6.8$ Hz, 3H), 1.08 (s, 3H), 0.98 (d, $J = 6.2$ Hz, 3H); ^{13}C NMR (100 MHz, CDCl_3) δ 178.1, 171.3, 169.6, 83.6, 82.9, 80.5, 76.4, 66.6, 53.5, 47.3, 45.1, 37.6, 35.7, 29.1, 21.3, 21.2, 21.1, 17.6, 14.1; IR (thin film, cm^{-1}) 3490, 2934, 2857, 1768, 1673, 1428, 1376, 1332; HRMS (ESI) *calcd.* for $[\text{C}_{19}\text{H}_{28}\text{O}_8\text{Na}]^+$ ($\text{M}+\text{Na}$) $^+$: m/z 407.1682, found 407.1672.

Vapor diffusion of an ethyl acetate solution of **318** with hexane afforded X-ray quality crystals.

SI-2.6. Synthesis of (-)-Nortrilobolide and (-)-Thapsigargin

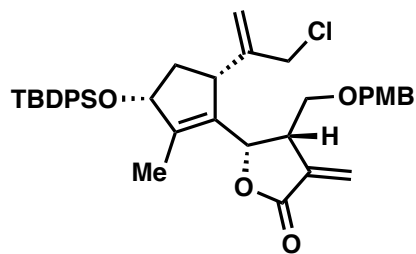
Compounds 320 and 330: Aldehyde *ent*-**173** was prepared from (-)-carvone by following the three-step procedure described in section SI-2.5 (see (+)-carvone → **173**).

A 500 mL round bottom flask was charged with a stir bar, anhydrous ZnCl₂ (200 mg, 1.47 mmol, 0.06 equiv), activated zinc powder (2.43 g, 37.2 mmol, 1.5 equiv), and dry NMF (100 mL). The mixture was degassed by bubbling of argon for 30 minutes. A solution of aldehyde *ent*-**173** (10.9 g, 24.8 mmol, 1 equiv) and allylic chloride **319** (12.3 g, 37.2 mmol, 1.5 equiv) in degassed NMF (50 mL) was then added to the reaction flask. The reaction mixture was stirred at room temperature until the consumption of aldehyde **173** was complete as judged by TLC (EtOAc/hexane, 1:4). The mixture was then diluted with DCM (200 mL) and filtered through Celite®. The filtrate was mixed with H₂O (200 mL) and further stirred at room temperature for 30 minutes. The aqueous phase was extracted with DCM (100 mL × 2), and the combined organic phase was washed with *sat.* NH₄Cl (200 mL), H₂O (200 mL), and brine (200 mL), dried over Na₂SO₄, and concentrated *in vacuo*. The crude mixture was purified by flash column chromatography (EtOAc/hexane, 1:20 to 1:5), affording lactones **320** and **330** (10.65 g, 65%, 2:1 *dr*) as a colorless oil.



Compound 320: $[\alpha]_D^{20} = -46.8^\circ$ (c 0.005 g/mL, CHCl₃); ¹H NMR (600 MHz, CDCl₃) δ 7.70 – 7.61 (m, 4H), 7.46 – 7.36 (m, 6H), 7.09 (d, *J* = 8.3 Hz, 2H), 6.80 (d, *J* = 8.3 Hz, 2H), 6.30 (d, *J* = 2.0 Hz, 1H), 5.70 (d, *J* = 2.0 Hz, 1H), 5.32 (s, 1H), 5.22 (s, 1H), 5.05 (d, *J* = 7.6 Hz, 1H), 4.50 (dd, *J* = 7.4, 2.8 Hz, 1H), 4.26 (d, *J* = 11.3 Hz, 1H), 4.23 (d, *J* = 11.3 Hz, 1H), 4.09 – 4.03 (m, 2H), 3.77 (s, 3H), 3.41 – 3.35 (m, 1H), 3.29

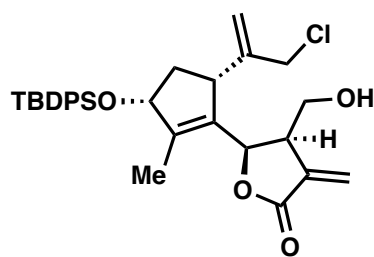
(dd, *J* = 9.2, 7.2 Hz, 1H), 3.23 (dd, *J* = 9.2, 6.7 Hz, 1H), 3.15 (brd, *J* = 8.6 Hz, 1H), 2.07 (app. dt, *J* = 13.9, 8.1 Hz, 1H), 1.66 (brs, 3H), 1.58 (app. dt, *J* = 13.9, 3.4 Hz, 1H), 1.06 (s, 9H); ¹³C NMR (150 MHz, CDCl₃) δ 170.0, 159.5, 147.2, 142.0, 136.8, 136.2, 136.2, 134.4, 134.1, 132.6, 129.9, 129.80, 129.6, 129.4, 127.8, 127.7, 124.0, 117.0, 113.9, 81.7, 77.6, 73.2, 69.9, 55.4, 49.8, 47.2, 43.1, 39.8, 27.1, 19.4, 13.5; IR (thin film, cm⁻¹) 3072, 2932, 2896, 2858, 1769, 1665, 1612, 1587, 1514, 1428; HRMS (ESI+) *calcd.* for [C₃₉H₄₅ClO₅SiNa]⁺ (M+Na)⁺: *m/z* 679.2623, found 679.2624.



Compound 330: $[\alpha]_D^{20} = -31.6^\circ$ (c 0.010 g/mL, CHCl₃); ¹H NMR (600 MHz, C₆D₆) δ 7.81 – 7.74 (m, 4H), 7.27 – 7.20 (m, 6H), 7.00 (d, *J* = 8.3 Hz, 2H), 6.74 (d, *J* = 8.3 Hz, 2H), 6.14 (d, *J* = 2.6 Hz, 1H), 5.33 (s, 1H), 5.20 (s, 1H), 5.09 (d, *J* = 2.6 Hz, 1H), 4.95 (d, *J* = 8.1 Hz, 1H), 4.50 (dd, *J* = 7.6, 2.6 Hz, 1H), 4.30 (d, *J* = 12.5 Hz, 1H), 4.19 (d, *J* = 12.5 Hz, 1H), 4.00 (d, *J* = 11.4 Hz, 1H), 3.89 (d, *J* = 11.4 Hz, 1H), 3.29 (s, 3H),

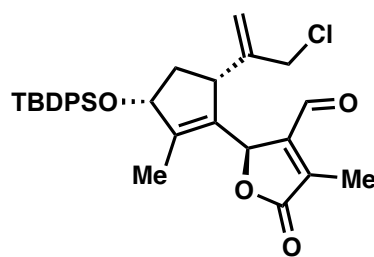
3.04 (d, *J* = 8.3 Hz, 1H), 2.99 (dd, *J* = 9.1, 5.7 Hz, 1H), 2.88 (dd, *J* = 9.1, 6.4 Hz, 1H), 2.82 (app. ddt, *J* = 11.8, 6.1, 3.0 Hz, 1H), 2.06 (app. dt, *J* = 14.0, 8.0 Hz, 1H), 1.90 (app. dt, *J* = 14.0, 3.2 Hz, 1H), 1.43 (s, 3H), 1.19 (s, 9H); ¹³C NMR (150 MHz, CDCl₃) δ 169.8, 159.5, 147.4, 142.9, 136.8, 136.2, 136.2, 136.2, 134.9, 134.1, 129.9, 129.9, 129.5, 129.4, 127.8, 127.7, 122.0, 115.8, 113.9, 80.0, 76.8, 73.4, 68.6, 55.4, 50.0, 46.4, 43.7, 40.1, 27.1, 19.4, 12.6; IR (thin film, cm⁻¹)

3071, 2932, 2894, 2857, 1770, 1664, 1612, 1587, 1514, 1428; HRMS (ESI+) *calcd.* for $[C_{39}H_{45}ClO_5SiNa]^+$ (M+Na) $^+$: m/z 679.2623, found 679.2623.



Compound 331: A 500 mL round-bottom flask was charged with a stir bar, compound **320** (4.0 g, 5.9 mmol, 1 equiv), phosphate buffer (12 mL, pH = 7.5), and DCM (120 mL). 2,3-Dichloro-5,6-dicyano-1,4-benzoquinone (DDQ) (2.7 g, 12 mmol, 2 equiv) was then added in one portion, and the resulting mixture was vigorously stirred at room temperature for 8 hours. After the consumption of the starting material was complete as judged by TLC, the reaction was quenched by addition of *sat.* $N_2S_2O_3$ (80

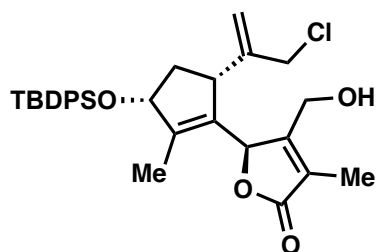
mL). The aqueous phase was extracted with DCM (120 mL \times 2), and the combined organic phase was washed with *sat.* $NaHCO_3$ (200 mL), H_2O (200 mL), and brine (200 mL), dried over Na_2SO_4 , and concentrated *in vacuo*. The crude mixture was purified by flash column chromatography (EtOAc/hexane, 1:4 to 2:1), affording **331** (3.1 g, 94%) as a colorless oil: $[\alpha]_D^{20} = -40^\circ$ (c 0.008 g/mL, $CHCl_3$); 1H NMR (600 MHz, CD_2Cl_2) δ 7.71 – 7.62 (m, 4H), 7.47 – 7.35 (m, 6H), 6.27 (d, $J = 1.9$ Hz, 1H), 5.73 (d, $J = 1.9$ Hz, 1H), 5.36 (s, 1H), 5.27 (s, 1H), 5.05 (d, $J = 7.2$ Hz, 1H), 4.58 (dd, $J = 7.4, 2.9$ Hz, 1H), 4.17 – 4.08 (m, 2H), 3.52 (app. dt, $J = 11.0, 6.4$ Hz, 1H), 3.39 (ddd, $J = 11.0, 7.5, 5.2$ Hz, 1H), 3.26 (app. q, $J = 7.1$ Hz, 1H), 3.20 (brd, $J = 8.8$ Hz, 1H), 2.22 (ddd, $J = 14.0, 8.7, 7.4$ Hz, 1H), 1.71 (dd, $J = 2.0, 0.9$ Hz, 3H), 1.64 (app. dt, $J = 14.1, 3.4$ Hz, 1H), 1.48 (app. t, $J = 5.8$ Hz, 1H), 1.07 (s, 9H); ^{13}C NMR (150 MHz, $CDCl_3$) δ 169.7, 147.2, 142.3, 136.7, 136.2, 136.2, 134.3, 133.9, 132.1, 129.9, 129.8, 127.8, 127.7, 124.2, 117.2, 81.6, 77.5, 77.4, 77.2, 76.9, 62.3, 49.6, 47.3, 45.0, 39.9, 27.1, 19.4, 13.5; IR (thin film, cm^{-1}) 3482, 3072, 3049, 2932, 2890, 2858, 1766, 1662, 1472, 1428; HRMS (ESI+) *calcd.* for $[C_{31}H_{37}ClO_4SiNa]^+$ (M+Na) $^+$: m/z 559.2047, found 559.2060.



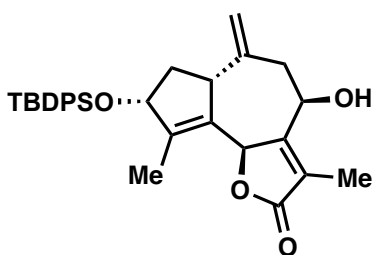
Compound 321: A 100 mL round-bottom flask was charged with a stir bar, compound **331** (1.26 g, 2.34 mmol, 1 equiv), $RuHCl(CO)(PPh_3)_3$ (223 mg, 0.234 mmol, 0.1 equiv), and DCE (24 mL). The mixture was degassed by bubbling of argon for 10 minutes, and then stirred at 60 $^\circ C$ for 16 hours. After the conversion of the starting material to intermediate **336** was complete as judged by TLC (EtOAc/hexane, 1:1), *aq.* $NaHCO_3/Na_2CO_3$ buffer (24 mL, pH = 8.6), KBr (0.28 g, 2.34

mmol, 1 equiv), *aq.* $NaOCl$ (2.4 mL, 14% available chlorine), and (2,2,6,6-tetramethylpiperidin-1-yl)oxyl (TEMPO) (37 mg, 0.24 mmol, 0.1 equiv) were added sequentially to the reaction flask. The reaction mixture was further stirred at room temperature for 1 hour until the reaction was complete as judged by TLC (EtOAc/hexane, 1:2). The mixture was then mixed with *sat.* $N_2S_2O_3$ (50 mL). The resulting mixture was extracted with DCM (50 mL \times 2), and the combined organic phase was washed with *sat.* $NaHCO_3$ (100 mL), H_2O (100 mL), and brine (100 mL), dried over Na_2SO_4 , and concentrated *in vacuo*. The crude mixture was purified by flash column chromatography (EtOAc:DCM/hexane, 1:1:15 to 1:1:5), affording **321** (1.08 g, 86%) as a colorless oil: $[\alpha]_D^{20} = +21.2^\circ$ (c 0.010 g/mL, $CHCl_3$); 1H NMR (600 MHz, $CDCl_3$) δ 10.09 (s, 1H), 7.71 – 7.59 (m, 4H), 7.47 – 7.34 (m, 6H), 5.81 (d, $J = 2.3$ Hz, 1H), 5.20 (s, 1H), 5.06 (s, 1H), 4.58 (dd, $J = 7.5, 2.7$ Hz, 1H), 3.95 (d, $J = 13.3$ Hz, 1H), 3.80 (d, $J = 13.3$ Hz, 1H), 3.35 (d, $J = 8.7$ Hz, 1H), 2.23 – 2.14 (m, 4H), 1.71 (d, $J = 1.8$ Hz, 3H), 1.51 (app. dt, $J = 14.1, 3.4$ Hz,

1H), 1.06 (s, 9H); ¹³C NMR (150 MHz, CDCl₃) δ 186.0, 173.5, 151.0, 147.2, 146.3, 139.5, 136.2, 136.1, 134.0, 133.9, 130.9, 129.9, 129.9, 127.8, 127.8, 116.5, 80.7, 77.3, 47.8, 45.9, 39.4, 27.1, 19.4, 12.8, 9.5; IR (thin film, cm⁻¹) 3072, 3049, 2932, 2892, 2857, 1766, 1688, 1589, 1472, 1458; HRMS (ESI+) *calcd.* for [C₃₁H₃₅ClO₄SiNa]⁺ (M+Na)⁺: m/z 557.1891, found 557.1887.



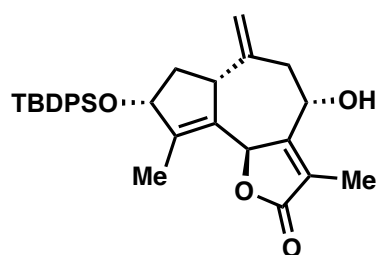
Compound 336: An analytical sample was obtained from an aliquot of the aforementioned reaction mixture, which was purified by preparative TLC (EtOAc/hexane, 1:1), affording **336** as a colorless oil: $[\alpha]_D^{20} = +32.4^\circ$ (c 0.007 g/mL, CHCl₃); ¹H NMR (700 MHz, CDCl₃) δ 7.70 – 7.61 (m, 4H), 7.47 – 7.41 (m, 2H), 7.42 – 7.35 (m, 4H), 5.60 (d, *J* = 2.2 Hz, 1H), 5.24 (s, 1H), 5.18 (s, 1H), 4.60 (dd, *J* = 7.6, 3.2 Hz, 1H), 4.56 – 4.51 (m, 1H), 4.30 (dd, *J* = 14.4, 5.2 Hz, 1H), 3.98 (d, *J* = 13.0 Hz, 1H), 3.94 (d, *J* = 13.0 Hz, 1H), 3.35 (app. q, *J* = 3.9 Hz, 1H), 2.25 (app. dt, *J* = 14.1, 8.1 Hz, 1H), 1.83 (s, 3H), 1.67 (app. t, *J* = 5.6 Hz, 1H), 1.62 – 1.60 (m, 3H), 1.60 – 1.57 (m, 1H), 1.07 (s, 9H); ¹³C NMR (175 MHz, CDCl₃) δ 174.6, 158.8, 147.1, 144.7, 136.1, 134.0, 133.9, 132.6, 130.0, 129.9, 127.8, 127.8, 125.3, 116.3, 80.8, 78.6, 57.6, 48.6, 46.3, 40.1, 27.2, 19.4, 12.6, 9.0; IR (thin film, cm⁻¹) 3451, 3072, 3049, 2932, 2892, 2858, 1738, 1678, 1472, 1428; HRMS (ESI+) *calcd.* for [C₃₁H₃₇ClO₄SiNa]⁺ (M+Na)⁺: m/z 559.2047, found 559.2048.



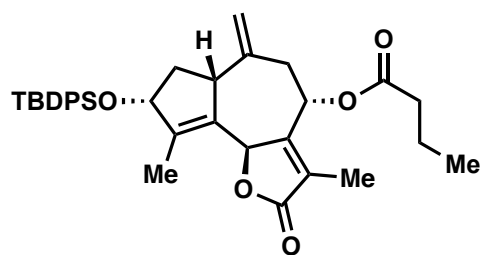
Compound 322: [Procedure A, entry 14, Table 2.3] A reaction tube was charged with a stir bar, anhydrous SnCl₂ (57 mg, 0.3 mmol, 5 equiv), PdCl₂(PhCN)₂ (3.5 mg, 0.0091 mmol, 0.15 equiv), and dry DMF (2 mL). The resulting mixture was stirred at room temperature for 10 minutes and compound **321** (32 mg, 0.06 mmol, 1 equiv) was added in one portion as a solution in dry DMF (1 mL). The reaction mixture was then stirred at 60 °C for 8 hours. After the consumption of the starting material was complete as judged by TLC (EtOAc/hexane, 1:2), the reaction mixture was diluted with EtOAc (10 mL) and quenched by addition of *aq.* NH₄F (10 mL, 5% w/w). The aqueous phase was extracted with EtOAc (10 mL × 2) and the combined organic phase was washed with H₂O (20 mL × 2) and brine (20 mL), dried over Na₂SO₄, and concentrated *in vacuo*. The crude mixture was purified by flash column chromatography (EtOAc/hexane, 1:4), affording **322** (29.0 mg, 95%) as a colorless oil: $[\alpha]_D^{20} = -42.6^\circ$ (c 0.007 g/mL, CHCl₃); ¹H NMR (700 MHz, CDCl₃) δ 7.69 – 7.63 (m, 4H), 7.46 – 7.41 (m, 2H), 7.40 – 7.35 (m, 4H), 5.53 (s, 1H), 4.92 – 4.87 (m, 2H), 4.82 – 4.78 (m, 1H), 4.55 (dd, *J* = 7.0, 6.3 Hz, 1H), 3.07 – 3.00 (m, 1H), 2.84 (dd, *J* = 13.5, 5.1 Hz, 1H), 2.31 (dd, *J* = 13.5, 4.0 Hz, 1H), 2.22 (ddd, *J* = 13.2, 8.0, 7.0 Hz, 1H), 2.07 (d, *J* = 8.5 Hz, 1H), 2.02 (app. t, *J* = 1.8 Hz, 3H), 1.76 (dd, *J* = 2.3, 1.0 Hz, 3H), 1.51 (ddd, *J* = 13.2, 7.2, 6.3 Hz, 1H), 1.11 (s, 9H); ¹³C NMR (150 MHz, CDCl₃) δ 174.5, 159.7, 148.6, 146.8, 136.1, 136.1, 134.2, 133.9, 131.6, 130.0, 129.9, 127.8, 127.7, 126.7, 113.7, 79.0, 76.6, 68.9, 47.5, 42.0, 41.5, 27.2, 19.4, 12.3, 9.9; IR (thin film, cm⁻¹) 3444, 3071, 2956, 2931, 2892, 2857, 1736, 1674, 1472, 1428; HRMS (ESI+) *calcd.* for [C₃₁H₃₇O₄Si]⁺ (M+H)⁺: m/z 501.2461, found 501.2453.

[Note: This condition afforded **322** in 90% yield on a gram scale.]

[Procedure B, entry 1, Table 2.3] From procedure A, the additive PdCl₂(PhCN)₂ (3.5 mg, 0.0091 mmol, 0.15 equiv) was replaced by NaI (45 mg, 0.3 mmol, 5 equiv). Compounds **322** and **337** were obtained (29.3 mg, 97%, 1:1 *dr*) as a colorless oil.



Compound **337**: $[\alpha]_D^{20} = -50.2^\circ$ (c 0.010 g/mL, CHCl₃); ¹H NMR (600 MHz, CDCl₃) δ 7.70 – 7.64 (m, 4H), 7.47 – 7.40 (m, 2H), 7.41 – 7.35 (m, 4H), 5.80 (s, 1H), 5.00 (s, 1H), 4.92 – 4.84 (m, 2H), 4.59 (app. t, *J* = 6.4 Hz, 1H), 2.95 – 2.90 (m, 1H), 2.59 (dd, *J* = 12.7, 6.0 Hz, 1H), 2.53 (dd, *J* = 12.7, 7.3 Hz, 1H), 2.14 (app. dt, *J* = 13.3, 7.6 Hz, 1H), 2.09 (d, *J* = 5.0 Hz, 1H), 1.80 (app. t, *J* = 1.5 Hz, 3H), 1.75 (s, 3H), 1.59 (app. dt, *J* = 13.3, 5.7 Hz, 2H), 1.09 (s, 9H); ¹³C NMR (150 MHz, CDCl₃) δ 174.3, 160.8, 148.0, 145.6, 136.1, 136.1, 134.2, 133.9, 131.7, 129.9, 129.9, 127.8, 127.7, 125.3, 114.5, 79.2, 76.4, 65.7, 48.4, 41.2, 40.7, 27.2, 19.5, 12.4, 8.6; IR (thin film, cm⁻¹) 3434, 3071, 2957, 2931, 2891, 2858, 1758, 1737, 1472, 1428; HRMS (ESI+) *calcd.* for [C₃₁H₃₇O₄Si]⁺ (M+H)⁺: *m/z* 501.2461, found 501.2454.

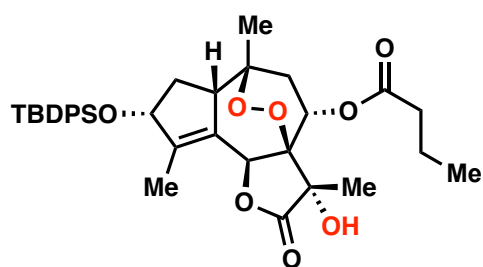


Compound **323**: A 100 mL round-bottom flask was charged with a stir bar, compound **322** (711 mg, 1.42 mmol, 1 equiv), and PPh₃ (1.18 g, 4.26 mmol, 3 equiv). The mixture was azeotropically dried with toluene (20 mL \times 3), and then dissolved in THF (14.2 mL). The reaction mixture was cooled to 0 °C over an ice bath, followed by the addition of *n*-butyric acid (0.4 mL, 4.31 mmol, 3 equiv) and diisopropyl azodicarboxylate (DIAD) (0.84 mL, 4.29, 3 equiv). The resulting mixture was allowed to warm up to room temperature and stirred for 8 hours. After the consumption of the starting material was complete as judged by TLC (EtOAc/hexane, 1:2), the reaction was quenched by addition of *sat.* NaHCO₃ (50 mL). The aqueous phase was extracted with EtOAc (50 mL \times 2), and the combined organic phase was washed with H₂O (20 mL \times 2) and brine (20 mL), dried over Na₂SO₄, and concentrated *in vacuo*. The crude mixture was purified by flash column chromatography (EtOAc/hexane, 1:4), affording **323** (570 mg, 70%) as a colorless oil: $[\alpha]_D^{20} = -67.3^\circ$ (c 0.010 g/mL, CHCl₃); ¹H NMR (700 MHz, CDCl₃) δ 7.71 – 7.63 (m, 4H), 7.50 – 7.40 (m, 2H), 7.41 – 7.35 (m, 4H), 5.78 (app. t, *J* = 8.2 Hz, 1H), 5.68 (brs, 1H), 4.81 (s, 1H), 4.77 (s, 1H), 4.57 (app. tdt, *J* = 6.9, 2.0, 1.0 Hz, 1H), 3.04 – 2.98 (m, 1H), 2.66 (dd, *J* = 12.6, 7.9 Hz, 1H), 2.51 (dd, *J* = 12.6, 8.5 Hz, 1H), 2.33 (td, *J* = 7.4, 2.6 Hz, 2H), 2.16 (ddd, *J* = 12.9, 7.8, 6.9 Hz, 1H), 1.85 (d, *J* = 2.0 Hz, 3H), 1.81 (dd, *J* = 2.4, 1.1 Hz, 3H), 1.67 (app. h, *J* = 7.4 Hz, 2H), 1.46 (ddd, *J* = 12.9, 7.9, 6.9 Hz, 1H), 1.09 (s, 8H), 0.97 (t, *J* = 7.4 Hz, 3H); ¹³C NMR (175 MHz, CDCl₃) δ 173.8, 172.7, 155.5, 149.5, 144.9, 136.1, 134.2, 133.8, 130.9, 130.0, 129.9, 128.6, 127.8, 127.7, 114.2, 78.9, 76.4, 67.3, 47.6, 41.8, 36.2, 35.8, 27.2, 19.4, 18.5, 13.8, 12.2, 8.9; IR (thin film, cm⁻¹) 2961, 2931, 2857, 1762, 1428, 1380, 1359; HRMS (ESI) *calcd.* for [C₃₅H₄₂O₅SiNa]⁺ (M+Na)⁺: *m/z* 593.2699, found 593.2682.

Compounds **338**, **339**, **341**: A reaction tube (Biotage® microwave vial 351521, 2-5 mL) was charged with a stir bar and compound **323** (22.0 mg, 0.0385 mmol, 1 equiv). The tube was sealed, placed under vacuum, and back-filled with O₂. In a separate container, Co(acac)₂ (10 mg, 0.039 mmol) was dissolved in anhydrous ethanol (5 mL), and the mixture was degassed by bubbling of

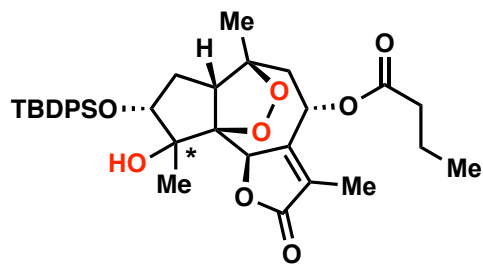
O₂ for 10 minutes assisted by sonication. A portion of this catalyst solution (1 mL, 0.0077 mmol of [Co], 0.2 equiv) was then added to the reaction tube. The resulting mixture was vigorously stirred at room temperature under an atmosphere of O₂ (balloon), while a solution of Et₃SiH (31 μL, 0.19 mmol, 5 equiv) in ethanol (0.5 mL) was slowly added over 24 hours via a syringe pump. After the addition of silane was complete, the reaction mixture was stirred at room temperature for an additional 24 hours, and was then mixed with EtOAc (10 mL) and H₂O (10 mL). The aqueous phase was extracted with EtOAc (10 mL × 3), and the combined organic phase was washed with H₂O (20 mL) and brine (20 mL), dried over Na₂SO₄, and concentrated *in vacuo*. The crude mixture was purified by flash column chromatography (EtOAc/hexane, 1:8 to 1:4), affording **338** (4.0 mg, 16%), **339** (2.5 mg, 10%), and **341** (4.6 mg, 20%).

[Note: Peroxides **338** and **339** are not stable at room temperature.]



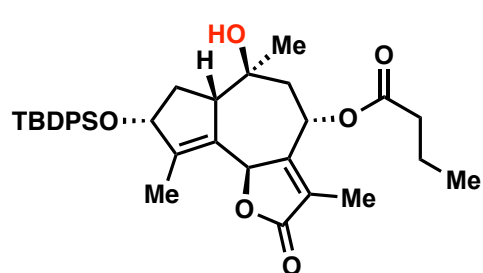
Compound **338** was obtained as a colorless oil: ¹H NMR (600 MHz, CDCl₃) δ 7.73 – 7.65 (m, 4H), 7.48 – 7.35 (m, 6H), 5.72 (app. t, *J* = 8.9 Hz, 1H), 5.65 (s, 1H), 4.63 (app. t, *J* = 7.6 Hz, 1H), 2.98 (brs, 1H), 2.34 – 2.29 (m, 2H), 2.26 (s, 1H), 2.14 (dd, *J* = 13.1, 8.7 Hz, 1H), 2.06 (app. dt, *J* = 12.2, 6.3 Hz, 1H), 1.86 (brs, 3H), 1.74 – 1.63 (m, 4H), 1.53 (s, 3H), 1.11 (s, 9H), 1.03 (s, 3H), 0.98 – 0.95 (m, 3H); ¹³C NMR (150 MHz, CDCl₃) δ

174.6, 172.7, 152.6, 136.1, 136.1, 134.2, 133.5, 130.1, 130.0, 129.7, 127.9, 127.8, 84.6, 83.4, 77.7, 76.9, 76.8, 62.7, 52.0, 38.6, 36.4, 33.9, 27.2, 27.2, 23.6, 19.5, 18.2, 16.7, 13.8, 12.6.



Compound **339** was obtained a colorless oil: (major isomer) ¹H NMR (600 MHz, CDCl₃) δ 7.72 – 7.66 (m, 4H), 7.47 – 7.36 (m, 6H), 5.91 (dd, *J* = 5.5, 2.2 Hz, 1H), 4.76 (d, *J* = 1.9 Hz, 1H), 3.69 (dd, *J* = 11.0, 5.4 Hz, 1H), 2.91 (s, 1H), 2.37 – 2.31 (m, 3H), 2.13 (dd, *J* = 11.2, 7.6 Hz, 1H), 1.96 – 1.88 (m, 4H), 1.68 – 1.61 (m, 3H), 1.38 (s, 3H), 1.12 (s, 3H), 1.09 (s, 9H), 0.94 (t, *J* = 7.4 Hz, 3H); ¹³C NMR (151 MHz, CDCl₃) δ 173.3, 172.0, 156.3,

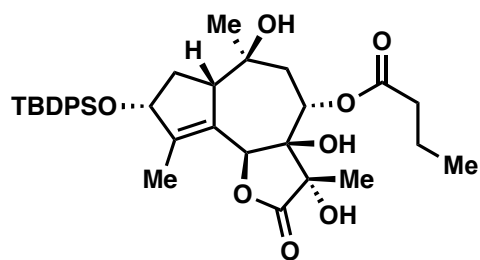
135.9, 135.8, 133.7, 133.0, 129.9, 129.8, 127.8, 127.6, 127.5, 91.5, 85.0, 78.9, 78.3, 78.1, 66.4, 54.9, 44.1, 36.1, 30.6, 26.9, 20.8, 19.3, 18.5, 18.2, 13.6, 8.7.



Compound **341** was obtained a colorless oil: [α]_D²⁰ = –78° (c 0.002 g/mL, CHCl₃); ¹H NMR (600 MHz, CDCl₃) δ 7.70 – 7.60 (m, 4H), 7.47 – 7.41 (m, 2H), 7.44 – 7.35 (m, 4H), 6.00 (app. t, *J* = 4.4 Hz, 1H), 5.62 (s, 1H), 4.58 (d, *J* = 8.3 Hz, 1H), 2.48 (brd, *J* = 8.7 Hz, 1H), 2.39 (dd, *J* = 14.8, 5.7 Hz, 1H), 2.37 – 2.29 (m, 2H), 2.07 (app. dt, *J* = 16.3, 8.7 Hz, 1H), 1.88 (s, 3H), 1.85 – 1.74 (m, 2H), 1.72 – 1.63 (m, 5H), 1.37 – 1.33 (m, 4H), 1.10 (s, 9H), 0.98

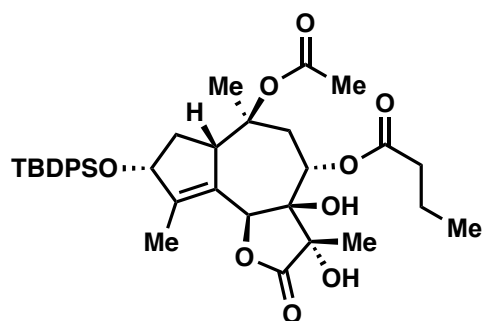
(td, *J* = 7.4, 1.2 Hz, 3H); ¹³C NMR (150 MHz, CDCl₃) δ 173.7, 172.3, 156.9, 147.8, 136.2, 136.1, 134.1, 134.1, 131.1, 130.0, 129.9, 127.8, 127.8, 125.6, 78.9, 76.9, 74.2, 66.2, 54.8, 46.9, 36.3, 33.9, 27.3, 24.8, 19.5, 18.4, 13.9, 12.9, 8.9; IR (thin film, cm⁻¹) 3466, 2961, 2932, 2857,

1742, 1461, 1428, 1381, 1361; HRMS (ESI) *calcd.* for $[C_{35}H_{44}O_6SiNa]^+$ (M+Na) $^+$: m/z 611.2805, found 611.2807.



Compound 325: From the aforementioned condition, the reaction mixture was quenched alternatively by bubbling of N_2 for 10 minutes, followed by the addition of activated zinc powder (7.5 mg) and an aqueous solution of NH_4Cl (10 mg in 75 μL H_2O). The resulting mixture was vigorously stirred at room temperature until the consumption of the endoperoxide intermediates was complete as judged by TLC (EtOAc/hexane, 1:2). The

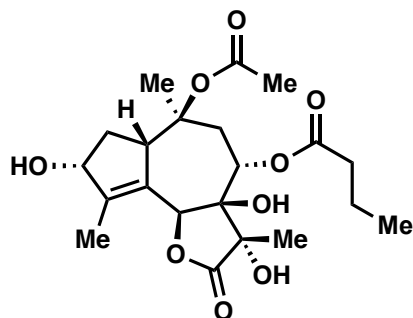
mixture was then filtered through Celite®, and mixed with EtOAc (10 mL) and *sat.* $NaHCO_3$ (10 mL). The aqueous phase was extracted with EtOAc (10 mL \times 3), and the combined organic phase was washed with H_2O (20 mL) and brine (20 mL), dried over Na_2SO_4 , and concentrated *in vacuo*. The crude mixture was purified by flash column chromatography (EtOAc/hexane, 1:1 to pure EtOAc), affording **325** (3.6 mg, 15%) as a colorless oil: $[\alpha]_D^{20} = -38.5^\circ$ (c 0.002 g/mL, $CHCl_3$); 1H NMR (600 MHz, $CDCl_3$) δ 7.72 – 7.66 (m, 4H), 7.45 – 7.41 (m, 2H), 7.40 – 7.35 (m, 4H), 5.74 (s, 1H), 5.53 – 5.49 (m, 1H), 4.62 (app. t, $J = 7.3$ Hz, 1H), 3.07 (brs, 1H), 2.27 (t, $J = 7.5$ Hz, 2H), 2.23 (dd, $J = 14.9, 3.4$ Hz, 1H), 2.13 – 2.06 (m, 2H), 1.94 (dd, $J = 14.9, 4.1$ Hz, 1H), 1.85 – 1.80 (m, 4H), 1.68 – 1.60 (m, 3H), 1.45 (s, 3H), 1.20 (s, 3H), 1.11 (s, 9H), 0.95 (t, $J = 7.4$ Hz, 3H); ^{13}C NMR (150 MHz, $CDCl_3$) δ 175.1, 172.5, 149.1, 136.2, 134.4, 134.0, 129.9, 129.9, 127.8, 127.7, 127.1, 79.0, 78.8, 78.5, 78.4, 73.9, 66.6, 54.3, 44.8, 36.7, 35.3, 27.3, 23.8, 19.5, 18.2, 16.6, 13.9, 13.5; IR (thin film, cm^{-1}) 3435, 3047, 3378, 2955, 2928, 2856, 1767, 1719, 1458, 1428; HRMS (ESI) *calcd.* for $[C_{35}H_{46}O_8SiNa]^+$ (M+Na) $^+$: m/z 645.2860, found 645.2862.



Compound 327: A reaction tube was charged with a stir bar and compound **325** (6.0 mg, 9.6 μmol , 1 equiv). In a separate round-bottom flask, $TsOH \cdot H_2O$ (23 mg, 0.12 mmol) was azeotropically dried with toluene for 3 times, and then dissolved in isopropenyl acetate (1 mL). A portion of this prepared solution (0.1 mL, 0.012 mmol of $TsOH$, 1.2 equiv) was added to the reaction tube at 0 $^\circ C$ over an ice bath. The mixture was allowed to warm up to room temperature, and was stirred for *ca.* 2 hours. The reaction was carefully monitored by TLC (EtOAc/hexane,

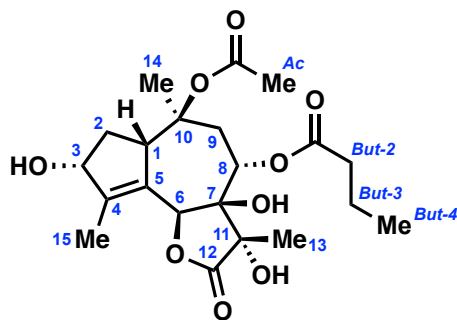
2:1), and after complete consumption of the starting material was observed, the mixture was cooled to 0 $^\circ C$, followed by the addition of EtOAc (5 mL) and *sat.* $NaHCO_3$ (5 mL). The aqueous phase was extracted with EtOAc (5 mL \times 2), and the combined organic phase was washed with H_2O (20 mL) and brine (20 mL), dried over Na_2SO_4 , and concentrated *in vacuo*. The crude mixture was purified by flash column chromatography (EtOAc/hexane, 1:2 to 1:1), affording **327** (5.1 mg, 80%) as a colorless oil: $[\alpha]_D^{20} = -32^\circ$ (c 0.001 g/mL, $CHCl_3$); 1H NMR (600 MHz, $CDCl_3$) δ 7.71 – 7.66 (m, 4H), 7.46 – 7.40 (m, 2H), 7.40 – 7.35 (m, 4H), 5.70 (s, 1H), 5.55 (dd, $J = 4.0, 3.7$ Hz, 1H), 4.67 – 4.60 (m, 1H), 3.87 (brs, 1H), 2.97 (dd, $J = 14.8, 3.7$ Hz, 1H), 2.27 (t, $J = 7.6$ Hz, 2H), 2.18 (dd, $J = 14.8, 4.0$ Hz, 1H), 2.07 (s, 1H), 1.99 (s, 1H), 1.89 (s, 3H), 1.86 – 1.79 (m, 4H), 1.65 (app. h, $J = 7.4$ Hz, 2H), 1.49 (app. dt, $J = 13.3, 6.5$ Hz, 1H), 1.45 (s, 3H), 1.33 (s, 3H), 1.11 (s, 8H), 0.95 (t, $J = 7.4$ Hz, 3H); ^{13}C NMR (150 MHz, $CDCl_3$) δ 174.9, 172.2,

170.2, 148.7, 136.0, 135.9, 134.4, 133.6, 129.7, 129.6, 127.6, 127.5, 126.4, 85.3, 78.8, 78.6, 78.2, 77.9, 66.4, 50.4, 38.6, 36.5, 35.1, 27.1, 22.2, 22.1, 19.3, 18.0, 16.3, 13.7, 13.3; IR (thin film, cm^{-1}) 3425, 2926, 2855, 1787, 1734, 1464, 1368; HRMS (ESI+) *calcd.* for $[\text{C}_{37}\text{H}_{48}\text{O}_9\text{SiNa}]^+$ (M+Na) $^+$: m/z 687.2966, found 687.2969.



Compound 326: A plastic tube was charged with a stir bar, compound **327** (1.4 mg, 2.1 μmol), and a solvent mixture of *aq.* HF and MeCN (0.2 mL, 1:5 v/v). The resulting mixture was stirred at room temperature for 2 hours. After the consumption of the starting material was complete as judged by TLC (EtOAc/hexane, 1:1), the mixture was diluted with EtOAc (5 mL), and was then added dropwise to *sat.* NaHCO_3 (5 mL) in a separate container. The aqueous phase was extracted with EtOAc (5 mL \times 3), and the combined organic phase was washed with H_2O (10 mL) and brine (10 mL), dried

over Na_2SO_4 , and concentrated *in vacuo*. The crude mixture was purified by preparative TLC (EtOAc/hexane, 1:1), affording **326** (0.5 mg, 46%) as a colorless oil, along with its C-3 epimer (*ca.* 35% yield). The spectra data of **326** was in agreement with that previously reported, as shown in Tables S2 and S3.

Table S2. ^1H NMR comparison of common intermediate **326**.

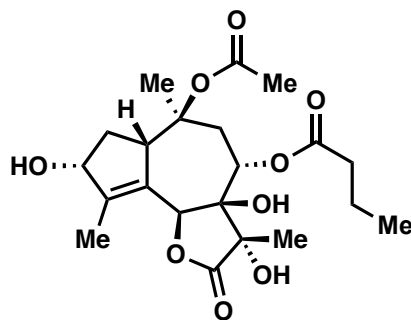
No.	Christensen ¹ (600 MHz, CDCl ₃)	Evans ² (600 MHz, CDCl ₃)	Baran ³ (600 MHz, CDCl ₃)	this work (700 MHz, CDCl ₃)
6	5.69 (1H, s)	5.69 (s, 1H)	5.70 (s, 1H)	5.70 (s, 1H)
8	5.61 (1H, t, $J = 3.6$ Hz)	5.61 (app. t, $J = 3.7$ Hz, 1H)	5.60 (t, $J = 3.8$ Hz, 1H)	5.60 (app. t, $J = 3.8$ Hz, 1H)
3	4.59 (1H, t, $J = 6.8$ Hz)	4.59 (app. q, $J = 6.6$ Hz, 1H)	4.59 (s, 1H)	4.60 (app. q, $J = 6.6$, 1H)
1	4.16 (1H, t, $J = 7.1$ Hz)	4.19 (app. t, $J = 6.9$ Hz, 1H)	4.13 (s, 1H)	4.11 (brs, 1H)
9a	3.08 (1H, dd, $J = 15.0, 3.5$ Hz)	3.10 (dd, $J = 14.9, 3.3$ Hz, 1H)	3.04 (dd, $J = 14.8, 3.5$ Hz, 1H)	3.03 (dd, $J = 14.8, 3.6$ Hz)
OH	2.52 (1H, s)	2.66 (s, 1H)		
2a	2.40 (1H, dt, $J = 13.5, 8.2$ Hz)	2.39 (app. dt, $J = 14.0, 8.2$ Hz, 1H)	2.41 (dt, $J = 14.0, 8.2$ Hz, 1H)	2.42 (app. dt, $J = 14.0, 8.2$, 1H)
But-2 9b OH	2.27 (3H, t, $J = 6.8$ Hz) 2.22 (1H, dd, $J = 14.8, 3.9$ Hz) OH	2.28 (s, 1H) 2.27 (t, $J = 7.7$ Hz, 2H) 2.19 (dd, 14.7, 4.0 Hz, 1H)	2.30 – 2.22 (m, 4H) 2.22 (s, 1H)	2.29 – 2.25 (m, 3H) 2.11 (s, 1H)
OH			2.17 (s, 1H)	2.05 (s, 1H)
Ac	1.97 (3H, s)	1.97 (s, 3H)	1.98 (s, 3H)	1.98 (s, 3H)
15	1.95 (3H, s)	1.95 (s, 3H)	1.96 (s, 3H)	1.96 (s, 3H)
3-OH	1.79 (1H, s)	1.80 (d, $J = 6.3$ Hz, 1H)	1.78 (d, $J = 6.3$ Hz, 1H)	1.77 (d, $J = 6.3$ Hz, 1H)
2b, But-3	1.69–1.53 (3H, m)	1.66-1.59 (m, 3H)	1.63 (dq, $J = 13.5, 7.0, 6.3$ Hz, 3H)	1.68-1.59 (m, 3H)
13	1.49 (3H, s)	1.48 (s, 3H)	1.49 (s, 3H)	1.49 (s, 3H)
14	1.34 (3H, s)	1.33 (s, 3H)	1.35 (s, 3H)	1.36 (s, 3H)
But-4	0.95 (3H, t, $J = 7.4$ Hz)	0.94 (t, $J = 7.4$ Hz, 3H)	0.95 (t, $J = 7.4$ Hz, 3H)	0.95 (t, $J = 7.4$ Hz, 3H)

¹ Doan, N. T.; Crestey, F.; Olsen, C. E.; Christensen, S. B., *J. Nat. Prod.* **2015**, 78, 1406.

² Chen, D.; Evans, P. A., *J. Am. Chem. Soc.* **2017**, 139, 6046.

³ Chu, H.; Smith, J. M.; Felding, J.; Baran, P. S., *ACS Cent. Sci.* **2017**, 3, 47.

Table S3. ^{13}C NMR comparison of common intermediate **326**.



Baran ¹ (150 MHz, CDCl ₃)	This Work (225 MHz, CDCl ₃)
175.1	175.0
172.5	172.5
170.6	170.5
147.6	147.7
128.4	128.2
85.4	85.3
79.0	79.1
78.8	78.8
77.9	77.9
77.7	77.6
66.6	66.5
50.8	50.8
38.8	38.8
36.7	36.7
34.9	34.9
22.5	22.6
22.3	22.2
18.2	18.2
16.5	16.5
13.9	13.9
13.0	13.0

¹ The NMR spectrum was generously provided by Chu, H. (Baran group).

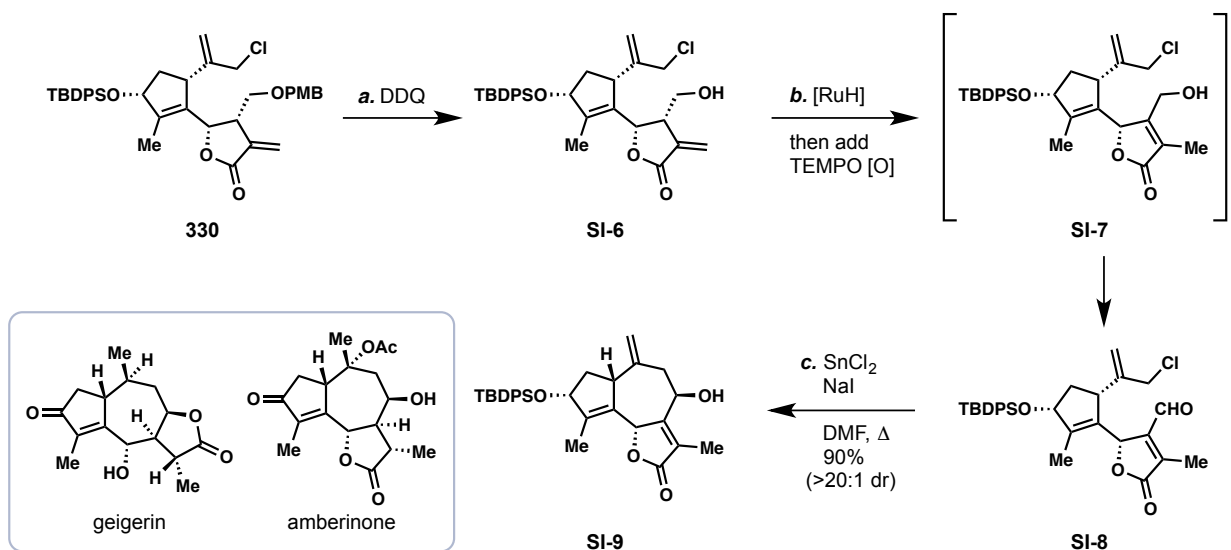
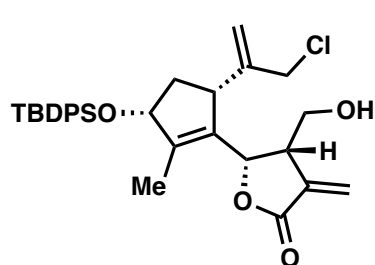
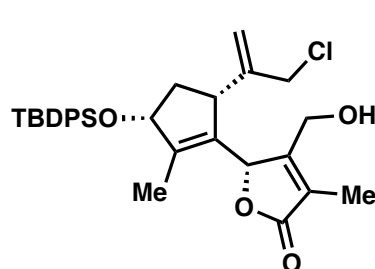


Figure SI-1. Synthesis of tricycle **SI-9** from **330**.

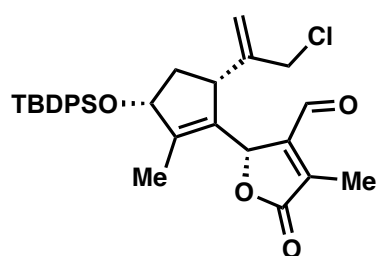
From lactone **330**, Compounds **SI-6**, **SI-7**, **SI-8**, and **SI-9** were prepared similarly as **331**, **336**, **321**, and **322**, by following the aforementioned procedures.



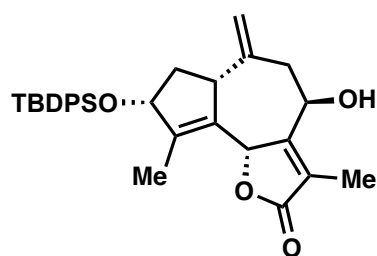
Compound **SI-6** was obtained as a colorless oil: $[\alpha]_D^{20} = -19.4^\circ$ (c 0.005 g/mL, CHCl₃); ¹H NMR (600 MHz, CD₂Cl₂) δ 7.72 – 7.62 (m, 4H), 7.48 – 7.39 (m, 2H), 7.43 – 7.35 (m, 4H), 6.22 (d, *J* = 2.5 Hz, 1H), 5.69 (d, *J* = 2.5 Hz, 1H), 5.45 (d, *J* = 8.1 Hz, 1H), 5.23 (app. q, *J* = 1.3 Hz, 1H), 5.12 (s, 1H), 4.55 (dd, *J* = 7.5, 2.4 Hz, 1H), 4.20 (dd, *J* = 12.8, 1.1 Hz, 1H), 4.15 (dt, *J* = 12.8, 1.1 Hz, 1H), 3.58 – 3.47 (m, 2H), 3.37 – 3.29 (m, 1H), 3.17 (brd, *J* = 8.6 Hz, 1H), 2.20 (dt, *J* = 14.1, 8.7, 7.5 Hz, 1H), 1.67 (app. dt, *J* = 14.1, 2.9 Hz, 1H), 1.63 (d, *J* = 1.9 Hz, 3H), 1.45 (t, *J* = 5.4 Hz, 1H), 1.07 (s, 9H); ¹³C NMR (151 MHz, CD₂Cl₂) δ 169.8, 148.2, 142.5, 137.3, 136.5, 136.4, 135.5, 134.4, 134.3, 130.1, 128.0, 128.0, 122.5, 115.3, 80.4, 77.0, 61.7, 50.3, 47.1, 45.8, 40.4, 27.2, 19.5, 12.7; IR (thin film, cm⁻¹) 3471, 3072, 3049, 2930, 2892, 2857, 1753, 1664, 1472, 1427; HRMS (ESI+) *calcd.* for [C₃₁H₃₇ClO₄SiNa]⁺ (M+Na)⁺: *m/z* 559.2047, found 559.2045.



Compound **SI-7** was obtained as a colorless oil: $[\alpha]_D^{20} = -131.2^\circ$ (c 0.005 g/mL, CHCl₃); ¹H NMR (700 MHz, CDCl₃) δ 7.71 – 7.63 (m, 4H), 7.46 – 7.41 (m, 2H), 7.41 – 7.35 (m, 4H), 5.69 (brs, 1H), 5.18 (s, 1H), 4.96 (s, 1H), 4.54 (dd, *J* = 7.6, 4.5 Hz, 1H), 4.46 (dd, *J* = 14.3, 3.4 Hz, 1H), 4.16 (dd, *J* = 14.3, 5.3 Hz, 1H), 4.08 (d, *J* = 12.5 Hz, 1H), 4.04 (d, *J* = 12.5 Hz, 1H), 3.00 (brs, 1H), 2.16 (app. dt, *J* = 13.9, 8.1 Hz, 1H), 1.82 (app. t, *J* = 1.4 Hz, 3H), 1.74 (d, *J* = 2.1 Hz, 3H), 1.73 – 1.70 (m, 1H), 1.52 (t, *J* = 5.2 Hz, 1H), 1.09 (s, 9H); ¹³C NMR (175 MHz, CDCl₃) δ 174.1, 157.3, 147.6, 147.0, 136.2, 136.2, 134.0, 133.9, 130.9, 129.9, 129.9, 127.8, 127.8, 126.3, 116.6, 79.6, 78.0, 57.4, 49.1, 45.0, 39.4, 27.1, 19.4, 12.4, 9.0; IR (thin film, cm⁻¹) 3452, 3072, 3049, 2932, 2892, 2858, 1736, 1680, 1472, 1428; HRMS (ESI+) *calcd.* For [C₃₁H₃₇ClO₄SiNa]⁺ (M+Na)⁺: *m/z* 559.2047, found 559.2050

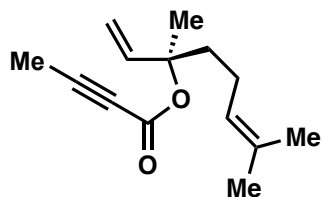


Compound **SI-8** was obtained as a colorless oil: $[\alpha]_D^{20} = -72.5^\circ$ (c 0.004 g/mL, CHCl_3); $^1\text{H NMR}$ (600 MHz, CDCl_3) δ 10.09 (s, 1H), 7.70 – 7.61 (m, 4H), 7.48 – 7.33 (m, 6H), 5.82 (d, $J = 2.4$ Hz, 1H), 5.17 (s, 1H), 4.98 (s, 1H), 4.57 (dd, $J = 7.6, 4.4$ Hz, 1H), 4.01 (d, $J = 12.4$ Hz, 1H), 3.96 (d, $J = 12.4$ Hz, 1H), 2.87 (brs, 1H), 2.20 (d, $J = 2.0$ Hz, 3H), 2.13 (app. dt, $J = 13.9, 8.0$ Hz, 1H), 1.83 – 1.79 (m, 3H), 1.58 (app. dt, $J = 13.9, 4.9$ Hz, 1H), 1.07 (s, 9H); $^{13}\text{C NMR}$ (150 MHz, CDCl_3) δ 186.0, 172.9, 149.7, 149.1, 147.3, 141.6, 136.2, 136.1, 134.1, 133.9, 129.9, 129.9, 129.1, 127.8, 127.7, 116.8, 79.7, 77.0, 48.8, 45.6, 39.7, 27.1, 19.4, 12.6, 9.5; IR (thin film, cm^{-1}) 3072, 3049, 2932, 2891, 2858, 1766, 1688, 1589, 1472, 1458; HRMS (ESI+) *calcd.* for $[\text{C}_{31}\text{H}_{35}\text{ClO}_4\text{SiNa}]^+$ ($\text{M}+\text{Na}$) $^+$: m/z 557.1891, found 557.1889.



Compound **SI-9**: A 500 mL round-bottom flask was charged with a stir bar, anhydrous SnCl_2 (5.20 g, 27.5 mmol, 5 equiv), NaI (4.12 g, 27.5 mmol, 5 equiv), and dry DMF (120 mL). The resulting mixture was stirred at room temperature for 10 minutes and compound **SI-8** (2.90 g, 5.42 mmol, 1 equiv) was added in one portion as a solution in dry DMF (40 mL). The reaction mixture was then stirred at 60 °C for 8 hours. After the consumption of the starting material was complete as judged by TLC (EtOAc/hexane, 1:2), the reaction mixture was diluted with EtOAc (200 mL), and quenched by addition of *aq.* NH_4F (100 mL, 5% w/w). The aqueous phase was extracted with EtOAc (100 mL \times 2) and the combined organic phase was washed with H_2O (300 mL \times 2) and brine (300 mL), dried over Na_2SO_4 , and concentrated *in vacuo*. The crude mixture was purified by flash column chromatography (EtOAc/hexane, 1:4), affording **SI-9** (2.45 g, 90%) as a colorless oil: $[\alpha]_D^{20} = -111.7^\circ$ (c 0.01 g/mL, CHCl_3); $^1\text{H NMR}$ (600 MHz, CDCl_3) δ 7.69 – 7.61 (m, 4H), 7.46 – 7.40 (m, 2H), 7.40 – 7.33 (m, 4H), 5.23 (s, 1H), 5.14 (s, 1H), 4.98 (s, 1H), 4.81 – 4.76 (m, 1H), 4.60 – 4.54 (m, 1H), 3.20 – 3.14 (m, 1H), 2.52 – 2.43 (m, 2H), 2.31 (dd, $J = 9.3, 1.7$ Hz, 1H), 2.13 (app. dt, $J = 12.9, 7.1$ Hz, 1H), 1.95 (app. t, $J = 1.7$ Hz, 3H), 1.69 (s, 3H), 1.37 (app. dt, $J = 12.9, 8.6$ Hz, 1H), 1.06 (s, 9H); $^{13}\text{C NMR}$ (150 MHz, CDCl_3) δ 174.4, 159.9, 143.9, 141.2, 136.1, 136.1, 134.4, 133.8, 129.9, 129.8, 128.3, 127.8, 127.7, 123.3, 118.2, 79.9, 79.5, 62.0, 50.2, 41.3, 35.6, 27.2, 19.4, 12.2, 8.8; IR (thin film, cm^{-1}) 3464, 3072, 2958, 2931, 2891, 2858, 1760, 1743, 1472, 1428; HRMS (ESI+) *calcd.* for $[\text{C}_{31}\text{H}_{36}\text{O}_4\text{SiNa}]^+$ ($\text{M}+\text{Na}$) $^+$: m/z 523.2281, found 523.2281.

SI-2.7. Synthetic Studies on Guaianolides from the Apiaceae family

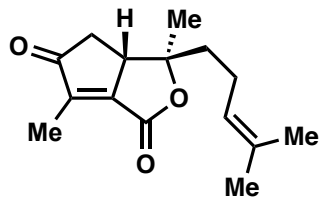


Compound 356: This procedure was adapted from previous conditions reported by Yang and coworkers.¹

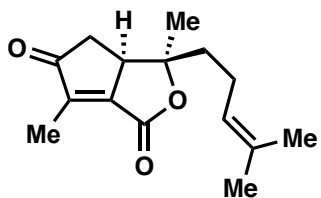
A 250 mL round-bottom flask was charged with a stir bar, 2-butyneic acid (1.80 g, 21.4 mmol, 3 equiv), and THF (72 mL). The mixture was cooled to 0 °C, and NaH (856 mg, 60% w/w, 3 equiv, washed with hexane) was added in three portions. The resulting mixture was stirred at 0 °C for 15 minutes, and then freshly distilled pivaloyl chloride (2.18 mL, 17.7 mmol, 2.5 equiv) was slowly added. The mixture was stirred for 1 hour at 0 °C, and for an additional 15 min at room temperature, which was then cooled to -45 °C over an acetone-dry ice bath. In a separate 100 mL round-bottom flask, L-linalool (1.42 mL, 7.90 mmol, 1 equiv) was dissolved in THF (20 mL), and NaHMDS (15.8 mL, 2 equiv, 1 M) was added in one portion. The mixture was stirred at room temperature for 1 hour, and was then slowly added to the 250 mL flask that contains mixed anhydride via a syringe pump over 3 hours at -45 °C. The reaction mixture was allowed to gradually warm up to room temperature, and was stirred for 8 hours. After the consumption of the starting material was complete as judged by TLC (EtOAc/hexane, 1:10), the reaction mixture was diluted with EtOAc (100 mL) and quenched by addition of *sat.* NaHCO₃ (100 mL). The aqueous phase was extracted by Et₂O (100 mL × 2) and the combined organic phase was washed with washed with brine (200 mL), dried over Na₂SO₄, and concentrated *in vacuo*. The crude mixture was purified by column chromatography (Et₂O/hexane, 1:100 to 1:20), affording ester **356** (1.13 g, 65%) as a colorless oil: $[\alpha]_D^{20} = -20.3^\circ$ (c 0.007 g/mL, CHCl₃); ¹H NMR (700 MHz, CDCl₃) δ 5.98 (dd, *J* = 17.5, 11.0 Hz, 1H), 5.20 (dd, *J* = 17.5, 0.8 Hz, 1H), 5.16 (dd, *J* = 11.0, 0.8 Hz, 1H), 5.11 – 5.05 (m, 1H), 2.03 – 1.96 (m, 2H), 1.96 (s, 3H), 1.91 – 1.84 (m, 1H), 1.85 – 1.78 (m, 1H), 1.67 (d, *J* = 1.3 Hz, 3H), 1.59 (brs, 3H), 1.57 (s, 3H); ¹³C NMR (150 MHz, CDCl₃) δ 152.5, 141.0, 132.2, 123.7, 114.1, 85.5, 83.5, 73.6, 39.7, 25.8, 23.7, 22.5, 17.8, 3.9; IR (thin film, cm⁻¹) 2969, 2924, 2856, 2242, 1700, 1449, 1376; HRMS (ESI) *calcd.* for [C₁₄H₂₀O₂Na]⁺ (M+Na)⁺: *m/z* 243.1361, found 243.1364. [Note: This compound is not stable in chloroform at room temperature.]

Compound 357 and 366: A 250 mL round-bottom flask was charged with a stir bar, ester **356** (0.67 g, 3.0 mmol, 1 equiv), Co₂(CO)₈ (1.15 g, 3.36 mmol, 1.1 equiv) and DCM (120 mL). The resulting solution was stirred at room temperature for 1 hour and then cooled to 0 °C over an ice bath. 4-Methylmorpholine *N*-oxide (3.35 g, 28.6 mmol, 9.5 equiv) was added in 5 portions over 1 hour at 0 °C. After complete consumption of the starting material as judged by TLC (EtOAc/hexane, 1:10), the reaction was quenched by addition of *sat.* Na₂S₂O₃ (100 mL). The aqueous phase was extracted by DCM (100 mL × 2) and the combined organic phase was washed with washed with *sat.* Na₂S₂O₃ (100 mL) and brine (100 mL), dried over Na₂SO₄, and concentrated *in vacuo* to a *ca.* 40 mL solution. The solution was filtered through a short silica gel column and washed with Et₂O. The filtrate was concentrated *in vacuo* and purified by column chromatography (EtOAc/hexane, 1:10 to 1:5), affording enones **356** and **366** (0.56 g, 65%, 5:2 *dr*) as a white foam.

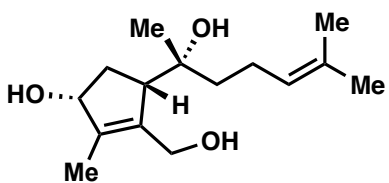
¹ Li, Y.; Chen, Z. X.; Xiao, Q.; Ye, Q. D.; Sun, T. W.; Meng, F. K.; Ren, W. W.; You, L.; Xu, L. M.; Wang, Y. F.; Chen, J. H.; Yang, Z., *Chem. Asian J.* **2012**, *7*, 2334.



Compound 356 (major): $[\alpha]_D^{20} = +153.3^\circ$ (c 0.010 g/mL, CHCl_3); ^1H NMR (600 MHz, CDCl_3) δ 5.00 (app. tt, $J = 7.1, 1.6$ Hz, 1H), 3.33 (ddq, $J = 6.5, 3.5, 3.1$ Hz, 1H), 2.72 (dd, $J = 18.3, 6.5$ Hz, 1H), 2.37 (dd, $J = 18.3, 3.5$ Hz, 1H), 2.16 – 2.04 (m, 2H), 2.02 (d, $J = 3.1$ Hz, 3H), 1.65 (d, $J = 1.5$ Hz, 3H), 1.58 (s, 3H), 1.57 (s, 3H), 1.41 (ddd, $J = 14.0, 10.8, 5.9$ Hz, 1H), 1.38 – 1.32 (m, 1H); ^{13}C NMR (151 MHz, CDCl_3) δ 208.2, 165.4, 157.5, 143.7, 133.1, 122.8, 88.5, 51.2, 38.6, 35.6, 25.7, 25.5, 21.8, 17.8, 9.0; IR (thin film, cm^{-1}) 2977, 2932, 2860, 1750, 1722, 1681, 1456, 1438; HRMS (ESI) *calcd.* for $[\text{C}_{15}\text{H}_{20}\text{O}_3\text{Na}]^+$ ($\text{M}+\text{Na}$) $^+$: m/z 271.1310, found 271.1312.

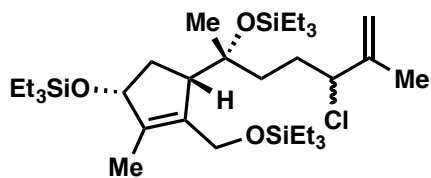


Compound 366 (minor): $[\alpha]_D^{20} = -41.9^\circ$ (c 0.010 g/mL, CHCl_3); ^1H NMR (600 MHz, CDCl_3) δ 5.07 (app. t, $J = 7.2$ Hz, 1H), 3.32 (dt, $J = 6.5, 3.3$ Hz, 1H), 2.69 (dd, $J = 18.4, 6.5$ Hz, 1H), 2.28 (dd, $J = 18.4, 3.4$ Hz, 1H), 2.15 – 2.04 (m, 2H), 2.02 (d, $J = 3.0$ Hz, 3H), 1.94 – 1.79 (m, 2H), 1.68 (s, 3H), 1.60 (s, 3H), 1.18 (s, 3H); ^{13}C NMR (150 MHz, CDCl_3) δ 208.2, 165.2, 157.5, 143.9, 133.0, 122.7, 89.5, 48.9, 41.1, 39.2, 25.8, 22.7, 20.0, 17.8, 8.9; IR (thin film, cm^{-1}) 2972, 2927, 2859, 1764, 1722, 1682, 1439, 1408; HRMS (ESI) *calcd.* for $[\text{C}_{15}\text{H}_{20}\text{O}_3\text{Na}]^+$ ($\text{M}+\text{Na}$) $^+$: m/z 271.1310, found 271.1305.

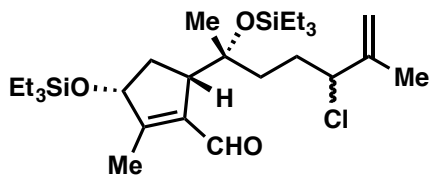


Compound 358: A 25 mL round-bottom flask was charged with a stir bar, enone **356** (112 mg, 0.451 mmol, 1 equiv), and DCM (5 mL). The resulting mixture was cooled to -78°C over an acetone–dry ice bath, and DIBAL-H (1.2 mL, 1.5 M in toluene, 4 equiv) was slowly added over 1 hour via a syringe pump. The reaction mixture was then allowed to warm up to room temperature, and was further stirred for 16 hours. After the consumption of the reduction intermediates was complete as judged by TLC (EtOAc/hexane, 1:1), the reaction was quenched by addition of *aq.* Rochelle salt (15 mL, 10% w/w). The mixture was stirred at room temperature for 30 minutes, and was then extracted with DCM (20 mL \times 3). The organic phase was washed with *sat.* NaHCO_3 (30 mL), H_2O (30 mL), and brine (30 mL), dried over Na_2SO_4 , and concentrated *in vacuo*. The crude mixture was purified by column chromatography (EtOAc/hexane, 1:1), affording triol **358** (93 mg, 81%) and the corresponding diol aldehyde (5 mg, 4%).

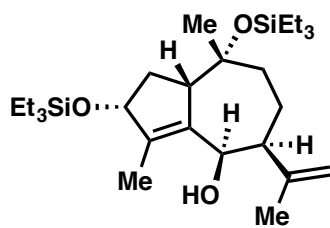
Compound 358: a white foam, $[\alpha]_D^{20} = +28.5^\circ$ (c 0.010 g/ml CH_2Cl_2); ^1H NMR (600 MHz, CD_3OD) δ 5.13 (app. tt, $J = 7.3, 1.6$ Hz, 1H), 4.38 (dd, $J = 7.9, 5.2$ Hz, 1H), 4.31 (d, $J = 12.7$ Hz, 1H), 4.10 (d, $J = 12.7$ Hz, 1H), 2.80 – 2.73 (m, 1H), 2.34 (dt, $J = 13.7, 8.3$ Hz, 1H), 2.14 (tt, $J = 12.5, 5.7$ Hz, 1H), 2.01 (tt, $J = 13.0, 6.2$ Hz, 1H), 1.73 (brs, 3H), 1.66 (s, 3H), 1.61 (s, 3H), 1.51 (ddd, $J = 14.0, 11.9, 5.3$ Hz, 1H), 1.43 (ddd, $J = 14.1, 12.0, 4.9$ Hz, 1H), 1.37 (ddd, $J = 13.7, 6.5, 5.0$ Hz, 1H), 1.19 (s, 3H); ^{13}C NMR (150 MHz, CD_3OD) δ 141.5, 138.7, 131.9, 126.1, 79.0, 75.1, 59.4, 57.8, 37.7, 36.5, 26.0, 25.9, 23.2, 17.6, 11.6; IR (thin film, cm^{-1}) 3296, 2968, 2916, 2859, 1692, 1650, 1439, 1377; HRMS (ESI) *calcd.* for $[\text{C}_{15}\text{H}_{26}\text{O}_3\text{Na}]^+$ ($\text{M}+\text{Na}$) $^+$: m/z 277.1780, found 277.1770.



Compound 359: A reaction tube was charged with a stir bar, triol **358** (23 mg, 0.09 mmol, 1 equiv), and DCM (2 mL). The mixture was cooled to $-78\text{ }^{\circ}\text{C}$ over an acetone–dry ice bath. 2,4,6-Collidine (0.13 mL, 0.99 mmol, 10 equiv) and TESOTf (0.1 mL, 0.44 mmol, 5 equiv) was added sequentially to the reaction mixture. The reaction mixture was allowed to gradually warm up to room temperature, and was stirred until the consumption of the starting material, and the mono- and di-silylated intermediates were complete as judged by TLC (EtOAc/hexane, 1:5). The reaction mixture was then cooled to $-78\text{ }^{\circ}\text{C}$, and SO_2Cl_2 (9 μL , 1.2 equiv) was added in one portion. The resulting mixture was allowed to gradually warm up to room temperature. After the chlorination of the intermediate to was complete as judged by TLC (EtOAc/hexane, 1:10), the reaction was quenched by addition of *sat.* $\text{Na}_2\text{S}_2\text{O}_3$ (5 mL) and *sat.* NaHCO_3 (5 mL). The aqueous phase was extracted by EtOAc (15 mL \times 2) and the combined organic phase was washed with washed with H_2O (20 mL) and brine (20 mL), dried over Na_2SO_4 , and concentrated *in vacuo*. The crude mixture was purified by flash column chromatography (Et₂O/hexane, 1:100 to 1:20), affording allylic chloride **359** (42 mg, 74%) as a mixture of two diastereomers. Both diastereomers were subjected to the next step without further purification.

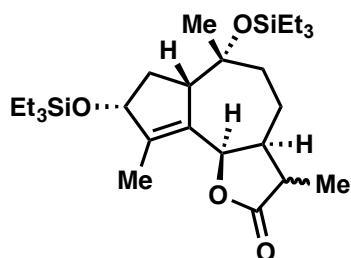


Compound 360: A 25 mL round-bottom flask was charged with a stir bar, allylic chloride **359** (431 mg, 0.682 mmol, 1 equiv), and DCM (6.8 mL). The mixture was cooled to $0\text{ }^{\circ}\text{C}$ over an ice bath, and $\text{CrO}_3\cdot 2\text{py}$ (530 mg, 2.05 mmol, 3 equiv) was added in one portion. The reaction mixture was stirred in a cold room ($0 - 4\text{ }^{\circ}\text{C}$) until the consumption of the starting material was near completion as judged by TLC (EtOAc/hexane, 1:10). The mixture was then filtered through a short column of silica gel (washed with Et₃N/DCM, 1:10). The filtrate was concentrated *in vacuo*, and The crude mixture was purified by column chromatography (EtOAc/hexane, 1:20), affording recovered allylic chloride **359** (42 mg, 10%), as well as aldehyde **360** (186 mg, 53%) as a mixture of two diastereomers. Both diastereomers were subjected to the next step without further purification.



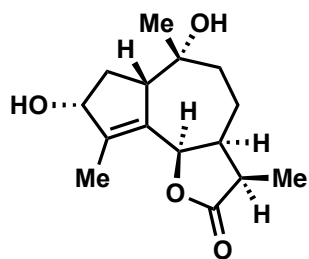
Compound 361: A 50 mL round-bottom flask was charged with a stir bar, anhydrous CrCl_2 (222 mg, 1.81 mmol, 5 equiv), anhydrous NiCl_2 (4 mg, 0.03 mmol, 0.1 equiv), and dry DMF (12 mL). The resulting mixture was heated at $60\text{ }^{\circ}\text{C}$, while a solution of aldehyde **360** (186 mg, 0.361 mmol, 1 equiv) in DMF (6 mL) was slowly added over 30 minutes via a syringe pump. After the addition was complete, the reaction mixture was further stirred at $60\text{ }^{\circ}\text{C}$ for 1 hour. After the consumption of the starting material was complete as judged by TLC (EtOAc/hexane, 1:5), the reaction mixture was cooled to room temperature, and quenched by addition of Et₂O (20 mL) and *aq.* $(\text{NH}_2\text{CH}_2)_2$ (10 mL, 10% w/w). The mixture was stirred at room temperature for 10 minutes, and was then extracted with Et₂O (30 mL \times 3). The organic phase was washed with H_2O (50 mL \times 2) and brine (50 mL), dried over Na_2SO_4 , and concentrated *in vacuo*. The crude mixture was purified by column chromatography (EtOAc/hexane, 1:10 to 1:5), affording cycloheptanol **361** (98 mg, 57%, 9:1 *dr*) as a colorless oil: $^1\text{H NMR}$ (500 MHz, CDCl_3) δ 4.86 –

4.80 (m, 2H), 4.70 (s, 1H), 4.42 (app. t, $J = 7.4$ Hz, 1H), 2.66 – 2.58 (m, 1H), 2.49 (dd, $J = 11.1$, 5.6 Hz, 1H), 2.22 (app. dt, $J = 12.3$, 7.4 Hz, 1H), 1.90 – 1.76 (m, 6H), 1.69 – 1.62 (m, 5H), 1.33 (s, 3H), 1.00 – 0.90 (m, 18H), 0.65 – 0.55 (m, 12H); ^{13}C NMR (150 MHz, CDCl_3) δ 149.6, 139.5, 138.8, 110.0, 77.8, 76.6, 70.1, 54.9, 48.5, 39.5, 36.7, 30.6, 24.5, 22.8, 11.6, 7.4, 7.1, 7.0, 5.1.



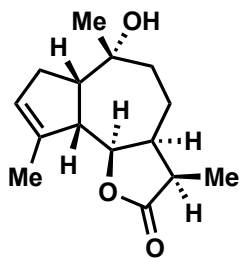
Compound 362: (i) A reaction tube was charged with a stir bar, cycloheptanol **361** (9.0 mg, 0.019 mmol, 1 equiv), and THF (0.2 mL). The mixture was cooled to 0 °C over an ice bath, and $\text{BH}_3\text{-THF}$ (34 μL , 1 M in THF, 1.8 equiv) was added in one portion. The reaction mixture was stirred in a cold room (0 – 4 °C) for *ca.* 16 hours. After the consumption of the starting material was complete as judged by TLC (EtOAc/hexane, 1:8), *aq.* NaOH (25 μL) and *aq.* H_2O_2 (4 μL , 30% w/w) were added sequentially to the reaction. The reaction mixture was stirred at room temperature until the consumption of the borane adducts was complete as judged by TLC (EtOAc/hexane, 1:8), and was then mixed with *sat.* $\text{Na}_2\text{S}_2\text{O}_3$ (5 mL) and EtOAc (5 mL). The resulting mixture was extracted with EtOAc (10 mL \times 3), and the combined organic phase was washed with brine (30 mL), dried over Na_2SO_4 , and concentrated *in vacuo*. The crude mixture was purified by column chromatography (EtOAc/hexane, 1:5 to 1:1), affording the corresponding primary alcohol (7.5 mg, 80%) as a mixture of two diastereomers (5:4 *dr*). Both diastereomers were subjected to the next step without further purification.

(ii) The aforementioned primary alcohol (7.5 mg, 0.015 mmol, 1 equiv) was dissolved in DCM (0.1 mL) in a reaction tube that was charged with a stir bar. A solution of TEMPO (2.3 mg, 0.015 mmol, 1 equiv) and PIDA (48 mg, 0.15 mmol, 10 equiv) in DCM (0.1 mL) was added to the reaction in one portion. The resulting mixture was stirred at room temperature for 8 hours. After the consumption of the starting material was complete as judged by TLC (EtOAc/hexane, 1:4), the reaction was quenched by addition of *sat.* $\text{Na}_2\text{S}_2\text{O}_3$ (5 mL), and diluted with EtOAc (5 mL). The resulting mixture was extracted with EtOAc (10 mL \times 3), and the combined organic phase was washed with brine (30 mL), dried over Na_2SO_4 , and concentrated *in vacuo*. The crude mixture was purified by column chromatography (EtOAc/hexane, 1:5 to 1:1), affording lactone **362** (5.8 mg, 78%) as a mixture of two diastereomers (5:4 *dr*). Both diastereomers were subjected to the next step without further purification.



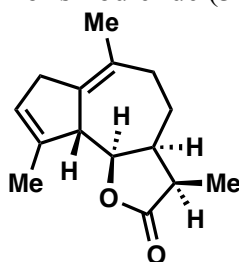
Compound 363: A reaction tube was charged with a stir bar, lactone **362** (8.0 mg, 0.016 mmol, 1 equiv) as a mixture of two diastereomers (5:4 *dr*), and dry THF (0.3 mL). The mixture was cooled to – 78 °C over an acetone–dry ice bath, and a solution of freshly prepared lithium diisopropylamide (LDA) (64 μL , 0.5 M in THF) was added dropwise. The reaction mixture was stirred at – 78 °C for 30 minutes and was allowed to warm to – 40 °C over 1 hour. The reaction mixture was then cooled back to – 78 °C, followed by the addition of acetic acid (5 μL , 5 equiv) and TBAF (0.1 mL, 1M in THF, 6 equiv). The mixture was further stirred at room temperature for 8 hours until the consumption of the silyl ether intermediates was complete as judged by TLC (EtOAc/hexane, 1:1). The reaction was then quenched by addition of *sat.* NH_4Cl (5 mL). The resulting mixture was extracted with EtOAc (10 mL \times 3), and the combined organic phase was washed with brine (30 mL), dried over Na_2SO_4 , and concentrated *in vacuo*.

The crude mixture was purified by column chromatography (EtOAc/hexane, 1:5 to 1:1), affording diol **363** (4.2 mg, 98%) as a white solid: $[\alpha]_D^{20} = +17.4^\circ$ (c 0.0016 g/ml CHCl₃); ¹H NMR (700 MHz, CDCl₃) δ 5.36 (d, $J = 6.6$ Hz, 1H), 4.30 (d, $J = 6.9$ Hz, 1H), 2.92 – 2.85 (m, 2H), 2.69 (dddd, $J = 9.0, 5.7, 5.7, 3.2$ Hz, 1H), 2.15 (ddd, $J = 15.0, 8.6, 6.9$ Hz, 1H), 1.92 (ddd, $J = 16.1, 10.8, 5.5$ Hz, 1H), 1.88 (d, $J = 14.2$ Hz, 1H), 1.80 (s, 3H), 1.56 (dd, $J = 15.0, 8.7$ Hz, 1H), 1.50 (dd, $J = 15.0, 10.8$ Hz, 1H), 1.45 (ddd, $J = 15.7, 8.9, 3.2$ Hz, 1H), 1.27 (s, 3H), 1.22 (d, $J = 7.3$ Hz, 3H); ¹³C NMR (125 MHz, CDCl₃) δ 180.0, 142.9, 134.4, 79.4, 79.2, 71.4, 52.2, 41.6, 38.2, 37.2, 34.9, 31.4, 19.1, 12.1, 10.3; IR (thin film, cm⁻¹) 3352, 3273, 2966, 2929, 2873, 2858, 1766, 1559, 1457, 1379; HRMS (ESI) *calcd.* for [C₁₅H₂₂O₄Na]⁺ (M+Na)⁺: m/z 289.1416, found 289.1437.



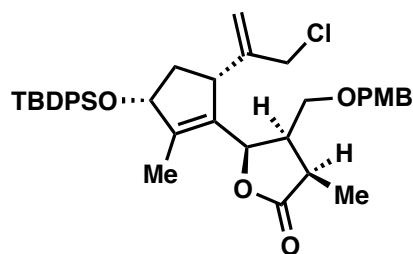
Compound 364: A reaction tube was charged with a stir bar, diol **363** (2.0 mg, 7.5 μ mol, 1 equiv), PPh₃ (6.0 mg, 23 μ mol, 3 equiv), and *N*-isopropylidene-*N'*-2-nitrobenzenesulfonyl hydrazine (IPNBSH) (5.8 mg, 23 μ mol, 3 equiv). The mixture was azeotropically dried with toluene (2 mL \times 3), and then dissolved in dry THF (0.15 mL). The reaction mixture was then cooled to 0 °C over an ice bath, and a solution of diisopropyl azodicarboxylate (DIAD) (4.5 μ L, 3 equiv) in THF (50 μ L) was added dropwise. The resulting mixture was stirred at 0 °C for 1 hour, and then at room temperature for additional 6 hours. After the consumption of the starting material was complete as judged by TLC (EtOAc/hexane, 1:1), the reaction mixture was diluted with DCM (2 mL), and filtered through a short column of silica gel (washed with EtOAc). The filtrate was concentrated *in vacuo*, and the crude mixture was purified by preparative TLC (EtOAc/hexane, 1:1), affording recovered diol **363**, as well as alkene **364** (1.2 mg, 64%) as a white solid, $[\alpha]_D^{20} = -54^\circ$ (c 0.0005 g/ml CHCl₃); ¹H NMR (600 MHz, CDCl₃) δ 5.46 (dd, $J = 3.2, 1.6$ Hz, 1H), 4.88 (dd, $J = 10.6, 7.8$ Hz, 1H), 3.37 – 3.29 (m, 1H), 2.83 – 2.74 (m, 1H), 2.58 (app. q, $J = 9.4$ Hz, 1H), 2.48 – 2.41 (m, 1H), 2.36 – 2.30 (m, 1H), 1.90 (app. dt, $J = 13.1, 7.1$ Hz, 1H), 1.86 – 1.84 (m, 3H), 1.83 – 1.71 (m, 2H), 1.65 – 1.59 (m, 1H), 1.20 (s, 3H), 1.18 (s, 1H), 1.16 (d, $J = 7.6$ Hz, 3H); ¹³C NMR (151 MHz, CDCl₃) δ 180.3, 143.4, 125.3, 85.2, 73.4, 52.1, 50.2, 40.0, 37.7, 37.7, 33.5, 32.5, 21.0, 18.2, 11.7; IR (thin film, cm⁻¹) 3488, 2920, 2852, 1746, 1669, 1594, 1565, 1455, 1378, 1348; HRMS (ESI) *calcd.* for [C₁₅H₂₂O₃Na]⁺ (M+Na)⁺: m/z 273.1467, found 273.1467.

Grilactone (**353**), Sinodielide A (**354**), and compound **365**: A reaction tube was charged with a stir bar, alkene **364** (2.0 mg, 8.0 μ mol, 1 equiv), and toluene (0.4 mL). The Burgess reagent (7.6 mg, 32 μ mol, 4 equiv) was then added in one portion to the solution, and the reaction mixture was stirred at 60 °C for 2 hours. After the consumption of the starting material was complete as judged by TLC (EtOAc/hexane, 1:1), the reaction was quenched by addition of aqueous phosphate buffer (2 mL, pH = 7.5). The resulting mixture was extracted with EtOAc (3 mL \times 2), and the combined organic phase was washed with brine (5 mL), dried over Na₂SO₄, and concentrated *in vacuo*. The crude mixture was purified by preparative TLC (EtOAc/hexane, 1:4), affording grilactone (**353**) and sinodielide A (**354**) as an inseparable mixture (1:4 ratio), as well as the alkene isomer **365**, in a combined *ca.* 80% yield.

Table S4. ^1H and ^{13}C NMR comparison of sinodiellide (**344**).

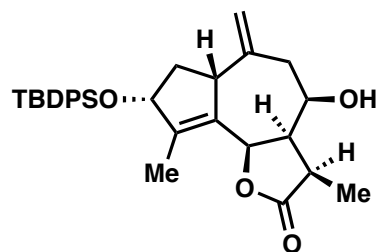
^1H NMR of natural 344 Wang et al. ¹ (500 MHz, CDCl_3)	^1H NMR of synthetic 344 this work (700 MHz, CDCl_3)	^{13}C NMR of natural 344 Wang et al. (125 MHz, CDCl_3)	^{13}C NMR of synthetic 344 this work (225 MHz, CDCl_3)
5.44 (tq, $J = 5.3, 1.6$ Hz)	5.44 (brs, 1H)	179.46	179.7
4.37 (dd, $J = 9.8, 5.8$ Hz, 1H)	4.37 (dd, $J = 10.1, 6.0$ Hz, 1H)	142.00	142.2
3.56 (brd, $J = 9.8$ Hz, 1H)	3.56 (brd, $J = 10.1$ Hz, 1H)	130.98	131.2
2.95 (brs, 2H)	2.95 (brs, 2H)	127.55	127.7
2.79 (dq, $J = 7.3, 7.3$ Hz, 1H)	2.79 (dq, $J = 7.5, 7.5$ Hz, 1H)	124.15	124.3
2.56 (m, 2H)	2.60 – 2.53 (m, 2H)	86.13	86.3
2.09 (m, 1H)	2.12 – 2.04 (m, 1H)	50.71	50.9
1.83 (dd, $J = 1.6, 0.9$ Hz, 3H)	1.83 (brs, 3H)	42.14	42.3
1.78 (m, 1H)	1.81 – 1.76 (m, 1H)	38.55	38.7
1.56 (brs, 3H)	1.56 (brs, 3H)	38.06	38.2
1.54 (m, 1H)	1.54 (m, 1H)	36.39	36.6
1.19 (d, $J = 7.3$ Hz, 3H)	1.18 (d, $J = 7.3$ Hz, 3H)	21.34	21.5
		18.92	19.1
		16.77	17.0
		10.33	10.5

¹ Wang, N.; Taniguchi, M.; Tsuji, D.; Doi, M.; Ohishi, H.; Yoza, K.; and Baba, K. *Chem. Pharm. Bull.* **2003**, *51*, 68.



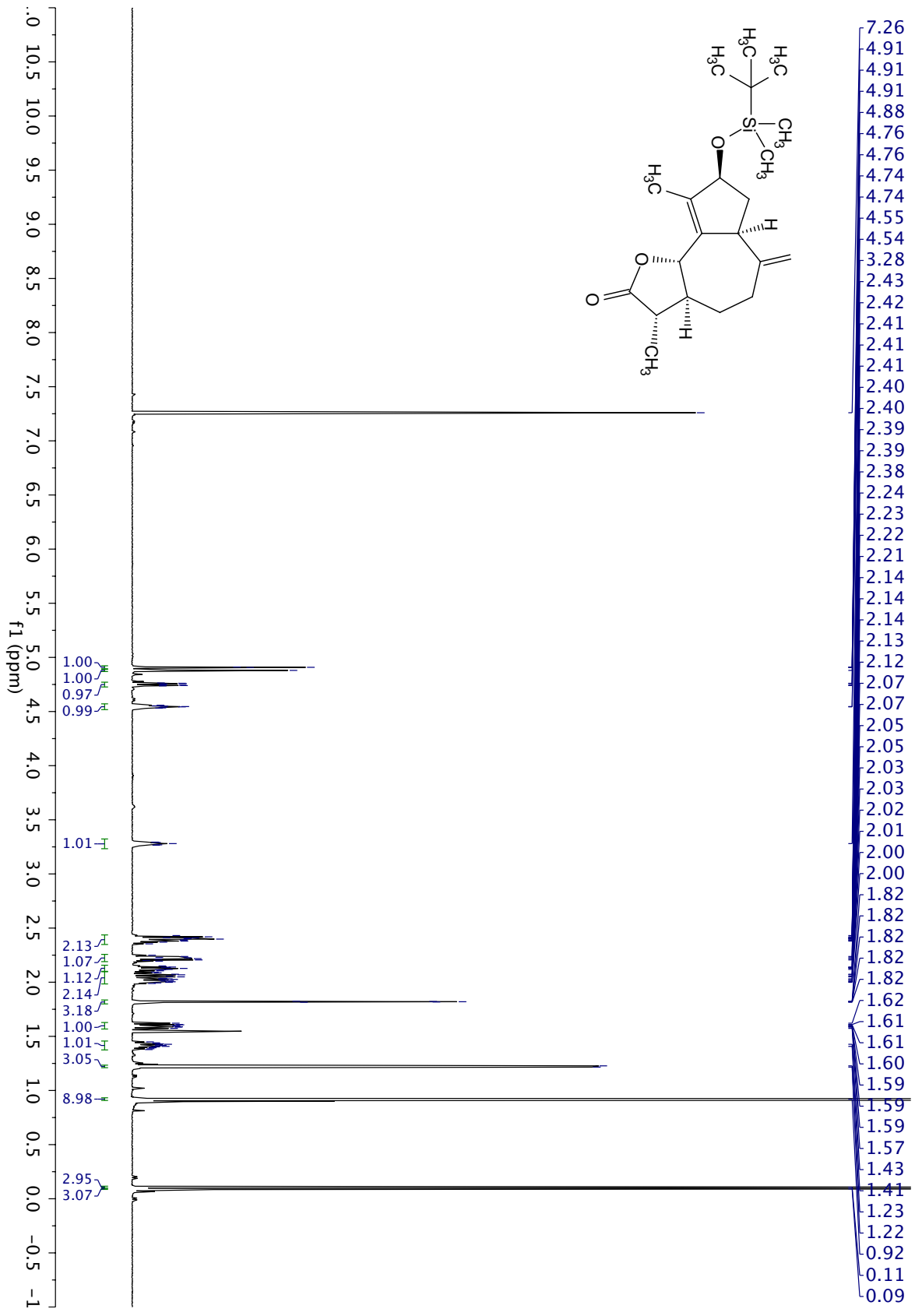
Compound 382: A reaction tube was charged with a stir bar, lactone **320** (19 mg, 0.029 mmol, 1 equiv), and anhydrous methanol (0.3 mL). The resulting mixture was cooled to 0 °C over an ice bath, and NaBH₄ (1.7 mg, 0.044 mmol, 1.5 equiv) was added in one portion. The reaction mixture was stirred at 0 °C until the consumption of the starting material was complete as judged by TLC (EtOAc/hexane, 1:4). The reaction

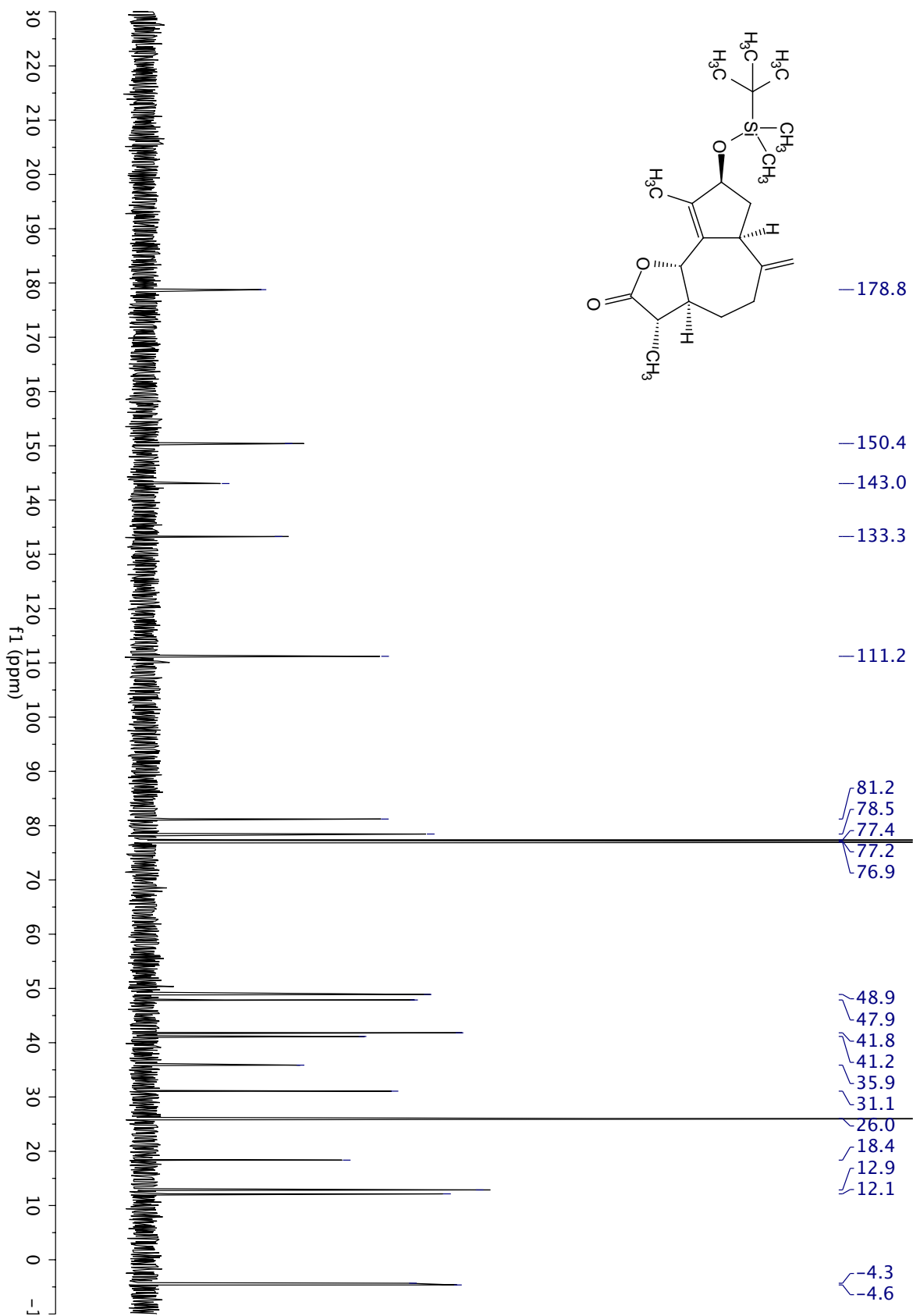
was then quenched by addition of *sat.* NH₄Cl (5 mL), and the resulting mixture was extracted by EtOAc (5 mL × 3). The combined organic phase was washed with H₂O (10 mL) and brine (10 mL), dried over Na₂SO₄, and concentrated *in vacuo*. The crude mixture was purified by column chromatography (EtOAc/hexane, 1:8 to 1:4), affording the reduced product **382** (18 mg, 94%) as a colorless oil: $[\alpha]_D^{20} = -27^\circ$ (c 0.003 g/ml CHCl₃); ¹H NMR (600 MHz, CDCl₃) δ 7.70 – 7.62 (m, 4H), 7.46 – 7.35 (m, 6H), 7.04 (d, *J* = 8.6 Hz, 2H), 6.75 (d, *J* = 8.6 Hz, 2H), 5.30 (s, 1H), 5.23 (s, 1H), 4.92 (d, *J* = 5.5 Hz, 1H), 4.49 (dd, *J* = 7.4, 2.7 Hz, 1H), 4.19 (d, *J* = 11.6 Hz, 1H), 4.13 (d, *J* = 11.6 Hz, 1H), 4.09 (d, *J* = 12.2 Hz, 1H), 4.05 (d, *J* = 12.2 Hz, 1H), 3.75 (s, 3H), 3.24 (dd, *J* = 9.7, 4.0 Hz, 1H), 3.15 (dd, *J* = 9.7, 3.4 Hz, 1H), 3.01 (brd, *J* = 8.6 Hz, 1H), 2.75 (dq, *J* = 7.7, 7.2 Hz, 1H), 2.60 (dddd, *J* = 7.7, 5.5, 4.0, 3.4 Hz, 1H), 2.07 – 1.99 (m, 1H), 1.77 (s, 3H), 1.57 – 1.51 (m, 1H), 1.23 (d, *J* = 7.2 Hz, 3H), 1.05 (s, 9H); ¹³C NMR (150 MHz, CDCl₃) δ 178.6, 159.3, 147.3, 141.6, 136.2, 136.2, 134.5, 134.1, 131.2, 129.8, 129.8, 129.6, 129.2, 127.7, 127.7, 116.8, 113.8, 82.0, 79.4, 73.2, 65.7, 55.4, 49.3, 47.1, 43.4, 39.7, 38.1, 27.1, 19.4, 10.1; IR (thin film, cm⁻¹) 2930, 2980, 2856, 1773, 1612, 1513, 1427; HRMS (ESI) *calcd.* for [C₃₉H₄₇ClO₅SiNa]⁺ (M+Na)⁺: *m/z* 681.2779, found 681.2776.

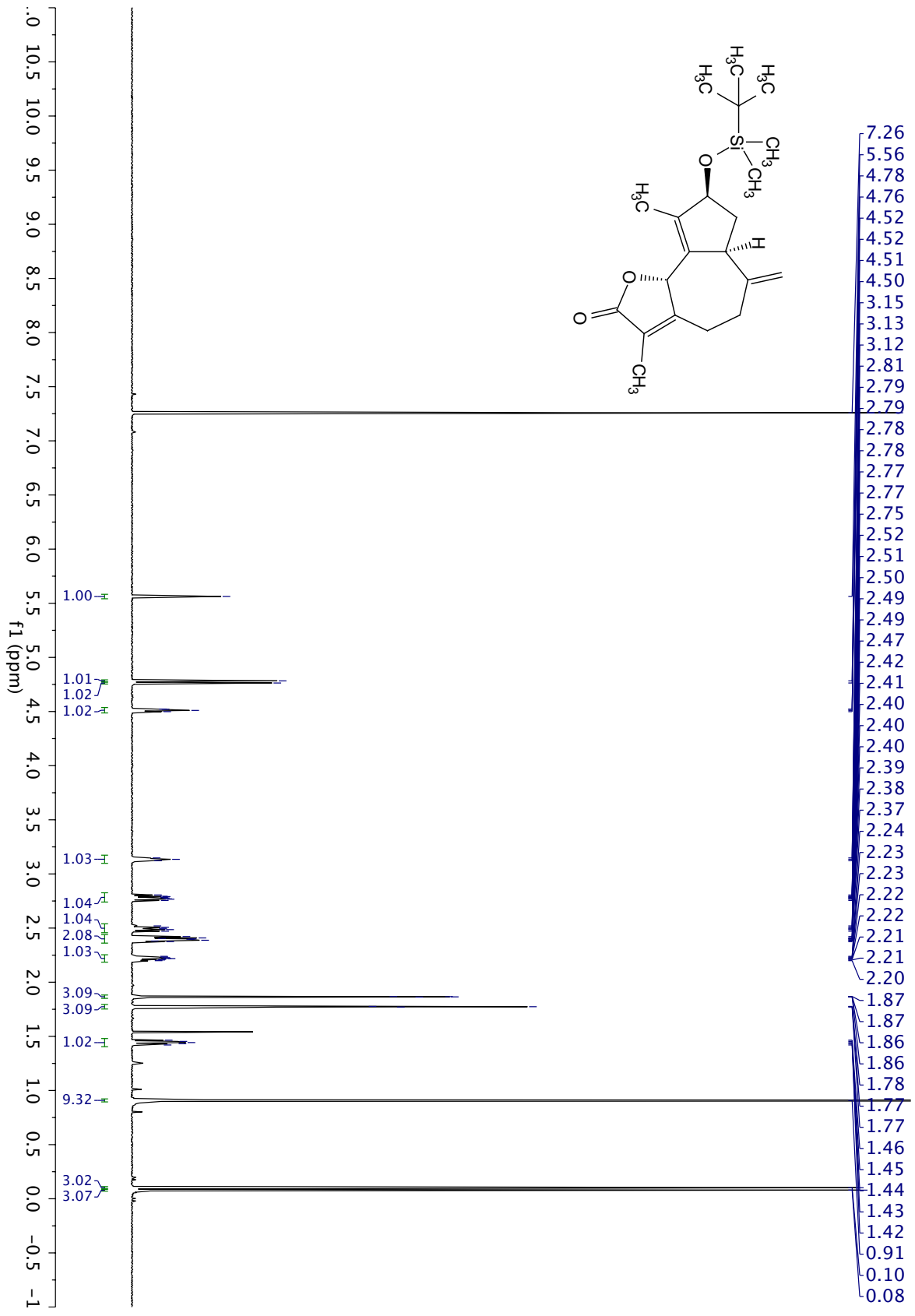


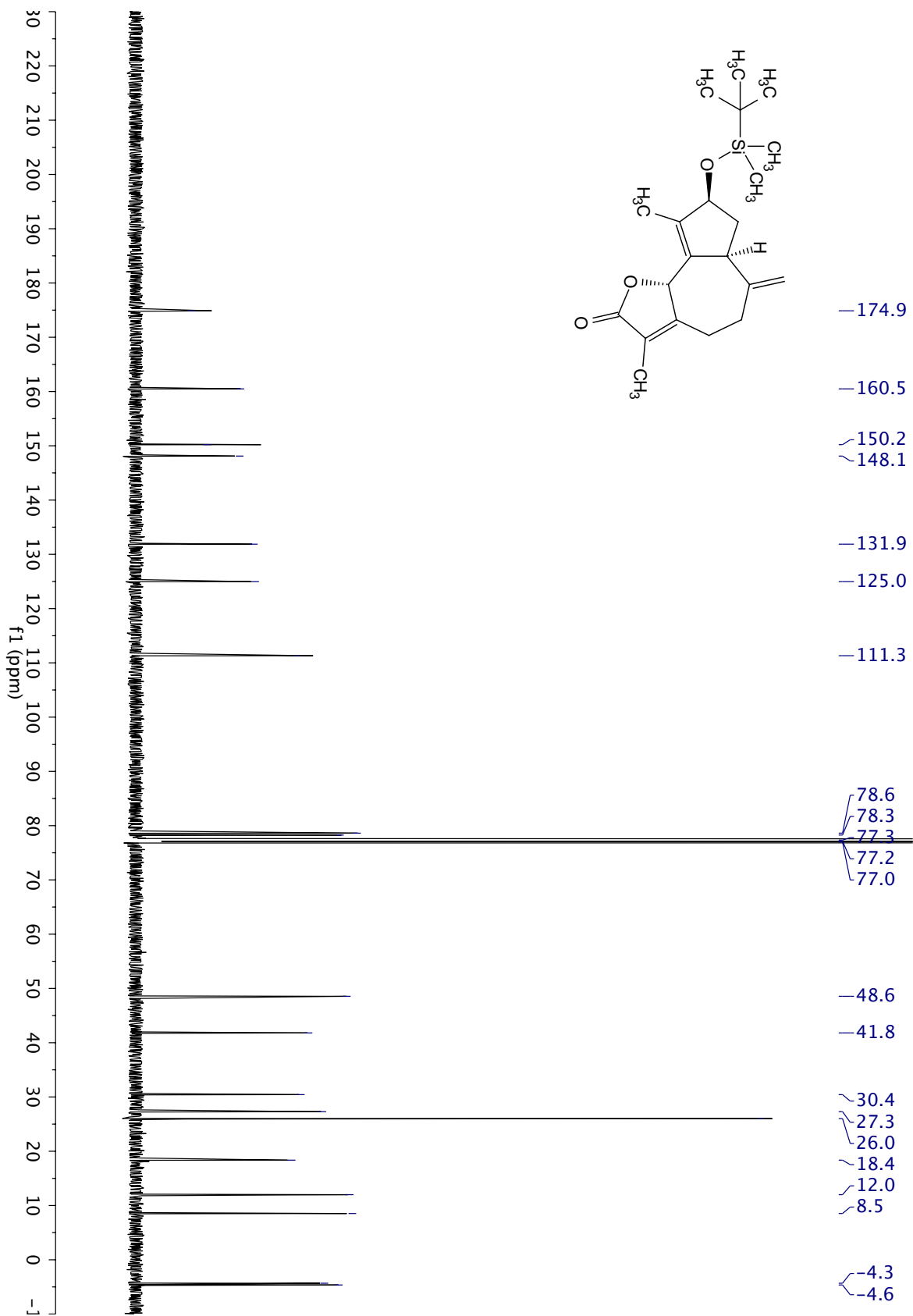
Compound 386: A reaction tube was charged with a stir bar, SnCl₂ (2.3 mg, 12 μmol, 5 equiv), and NaI (1.8 mg, 12 μmol, 5 equiv). A solution of crude aldehyde **381** (1.3 mg, 2.4 μmol, ~90% pure) in DMF (0.1 mL) was then added, and the resulting mixture was stirred at 60 °C for 3 hours. After the consumption of the starting material was complete as judged by TLC (EtOAc/hexane, 1:4), the reaction mixture was cooled to room temperature followed by the addition of *aq.* NH₄F (3 mL, 5%

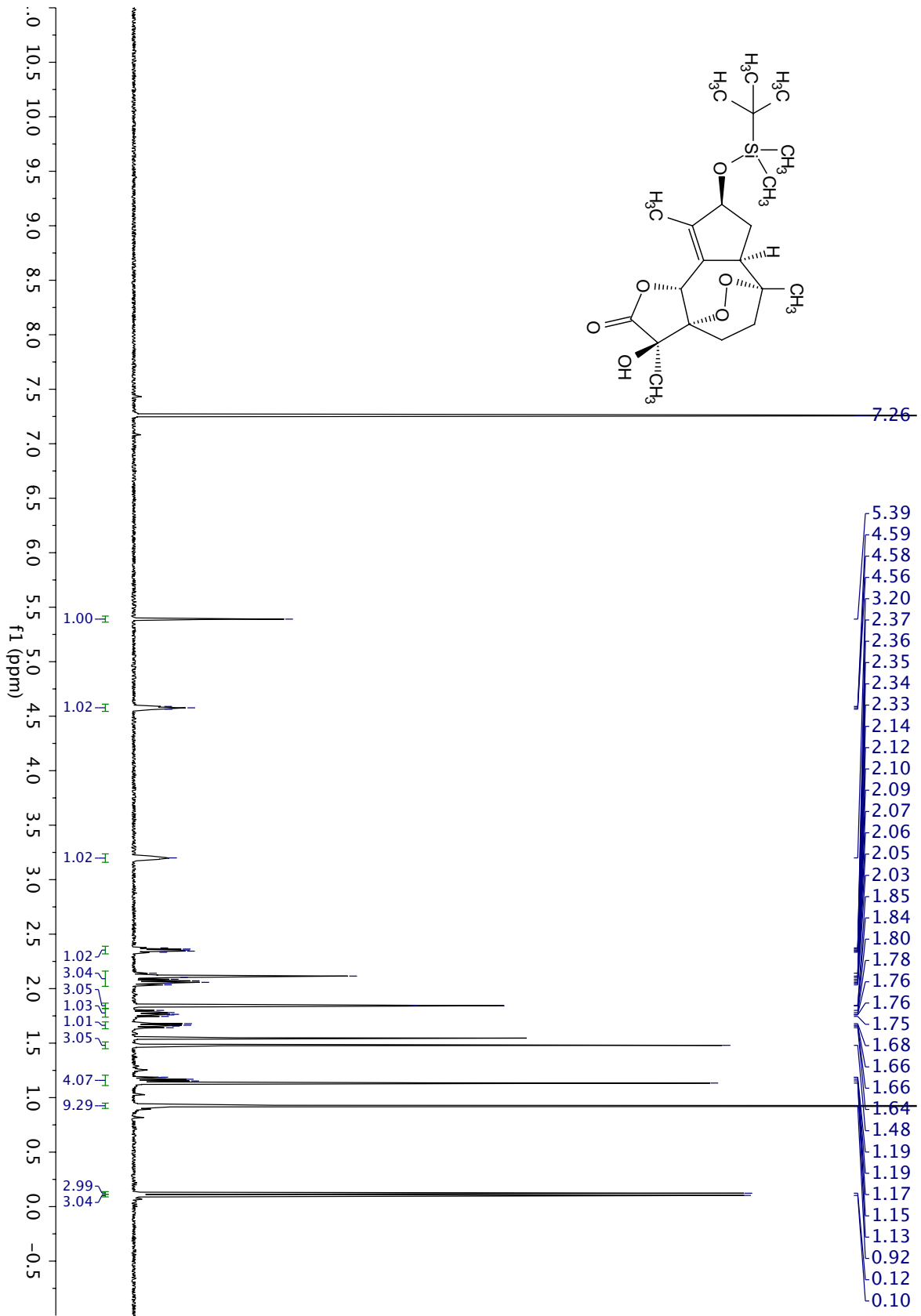
w/w). The mixture was extracted with ethyl acetate (3 mL × 3), and the combined organic phase was washed with H₂O (5 mL), brine (5 mL), dried over Na₂SO₄, and concentrated *in vacuo*. The crude mixture was purified by preparative TLC (EtOAc/hexane, 1:2), affording cycloheptanol **386** (0.8 mg, *ca.* 70%) as a colorless oil: ¹H NMR (700 MHz, CDCl₃) δ 7.70 – 7.63 (m, 4H), 7.45 (s, 2H), 7.41 – 7.36 (m, 4H), 5.12 (d, *J* = 4.2 Hz, 1H), 5.07 (brs, 1H), 4.94 (s, 1H), 4.57 (app. t, *J* = 6.6 Hz, 1H), 4.11 – 4.06 (m, 1H), 3.44 – 3.38 (m, 1H), 2.81 (qd, *J* = 6.8, 5.8 Hz, 1H), 2.63 (d, *J* = 13.2 Hz, 1H), 2.53 (dd, *J* = 13.2, 7.7 Hz, 1H), 2.31 (ddd, *J* = 6.8, 4.9, 4.2 Hz, 1H), 2.29 – 2.25 (m, 1H), 2.04 (d, *J* = 8.4 Hz, 1H), 1.67 (dd, *J* = 2.2, 1.0 Hz, 3H), 1.59 – 1.52 (m, 1H), 1.46 (d, *J* = 6.8 Hz, 3H), 1.07 (s, 9H); ¹³C NMR (175 MHz, CDCl₃) δ 179.6, 146.3, 136.1, 136.1, 133.9, 131.6, 129.9, 129.9, 127.8, 127.8, 127.7, 117.5, 79.6, 78.4, 64.6, 50.2, 46.9, 43.3, 41.3, 37.8, 27.2, 19.4, 12.3, 10.2; IR (thin film, cm⁻¹) 3505, 3071, 2930, 2857, 1769, 1666, 1469, 1428, 1358; HRMS (ESI) *calcd.* for [C₃₁H₃₈O₄SiNa]⁺ (M+Na)⁺: *m/z* 525.2432, found 525.2442.

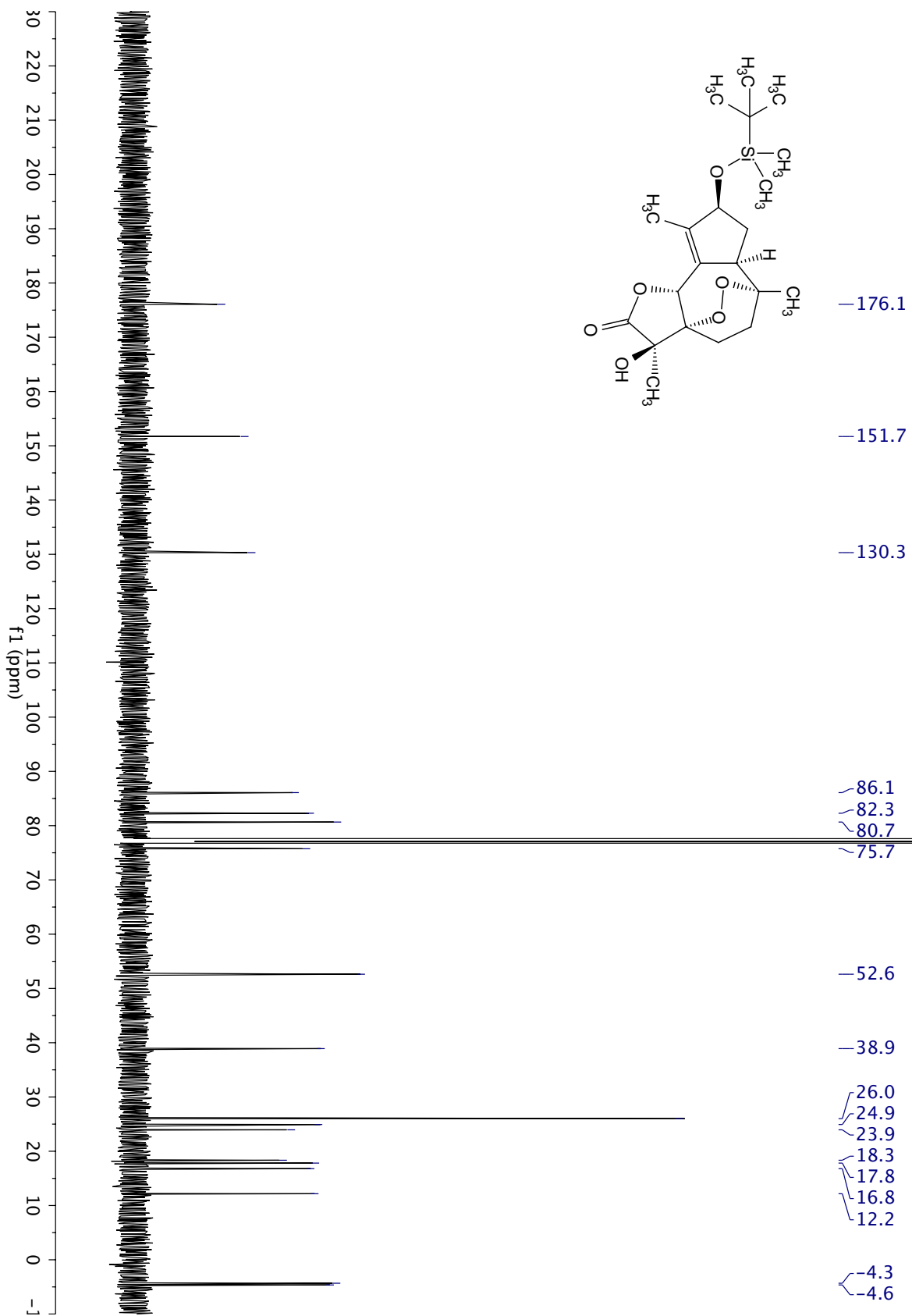


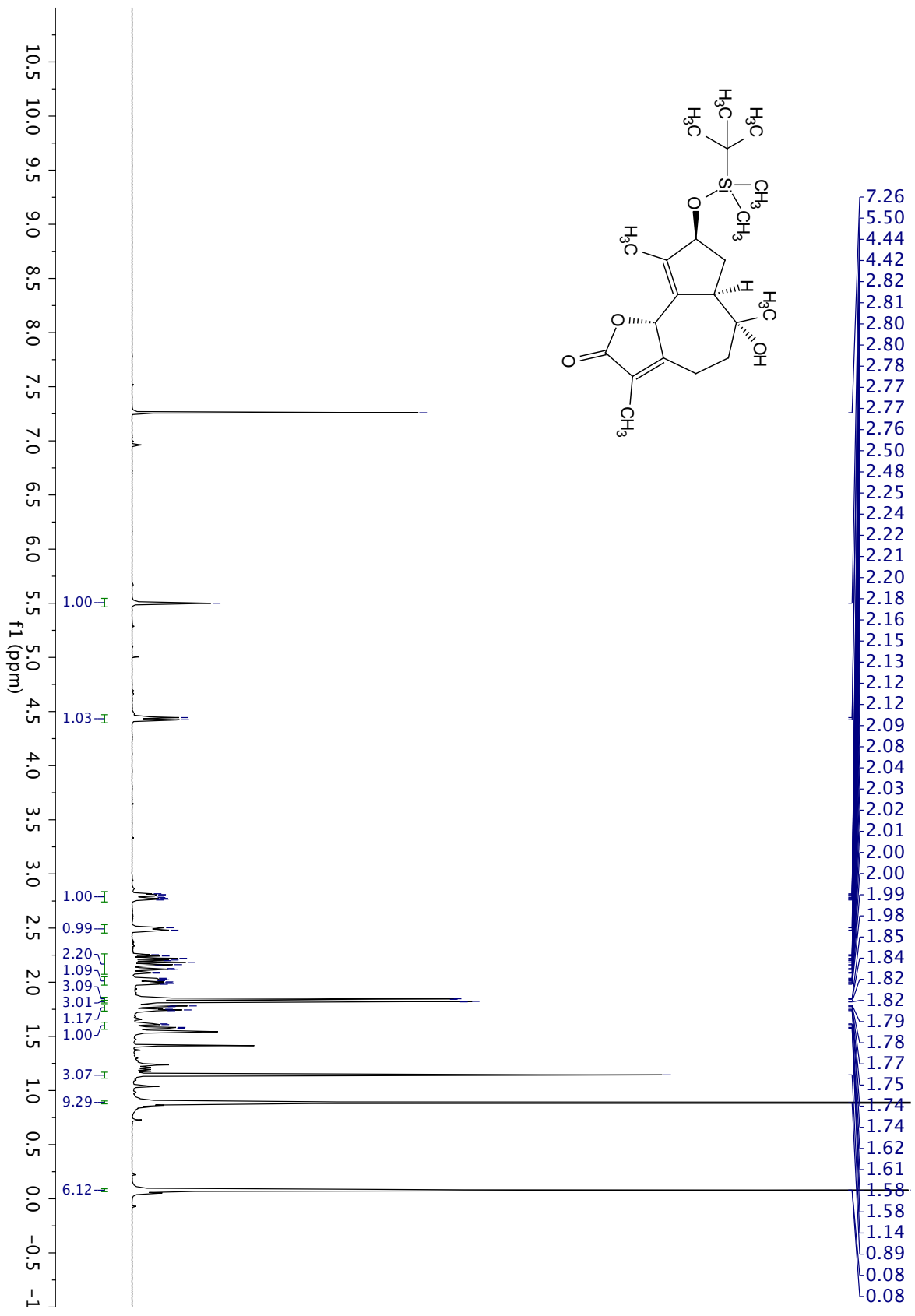


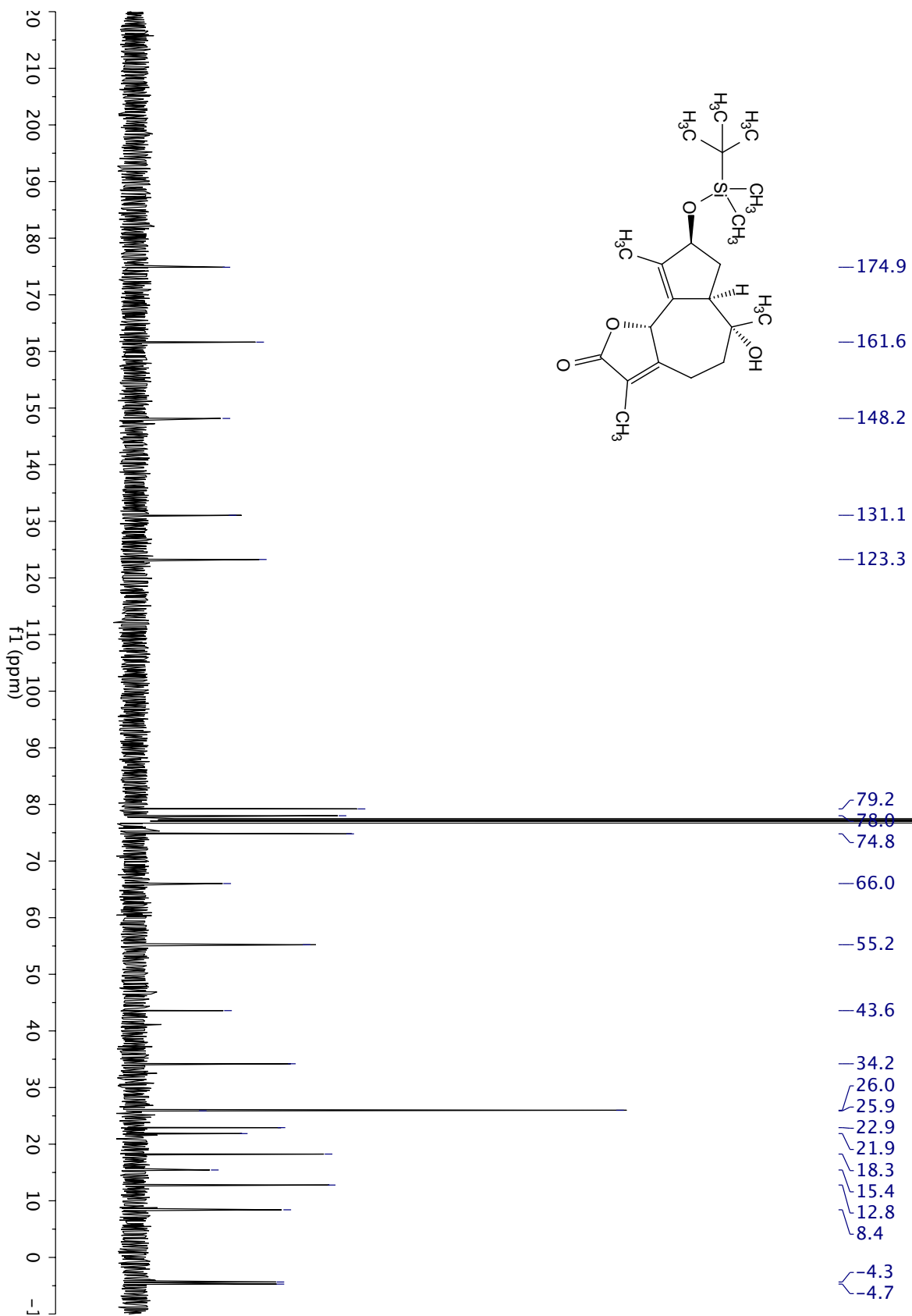


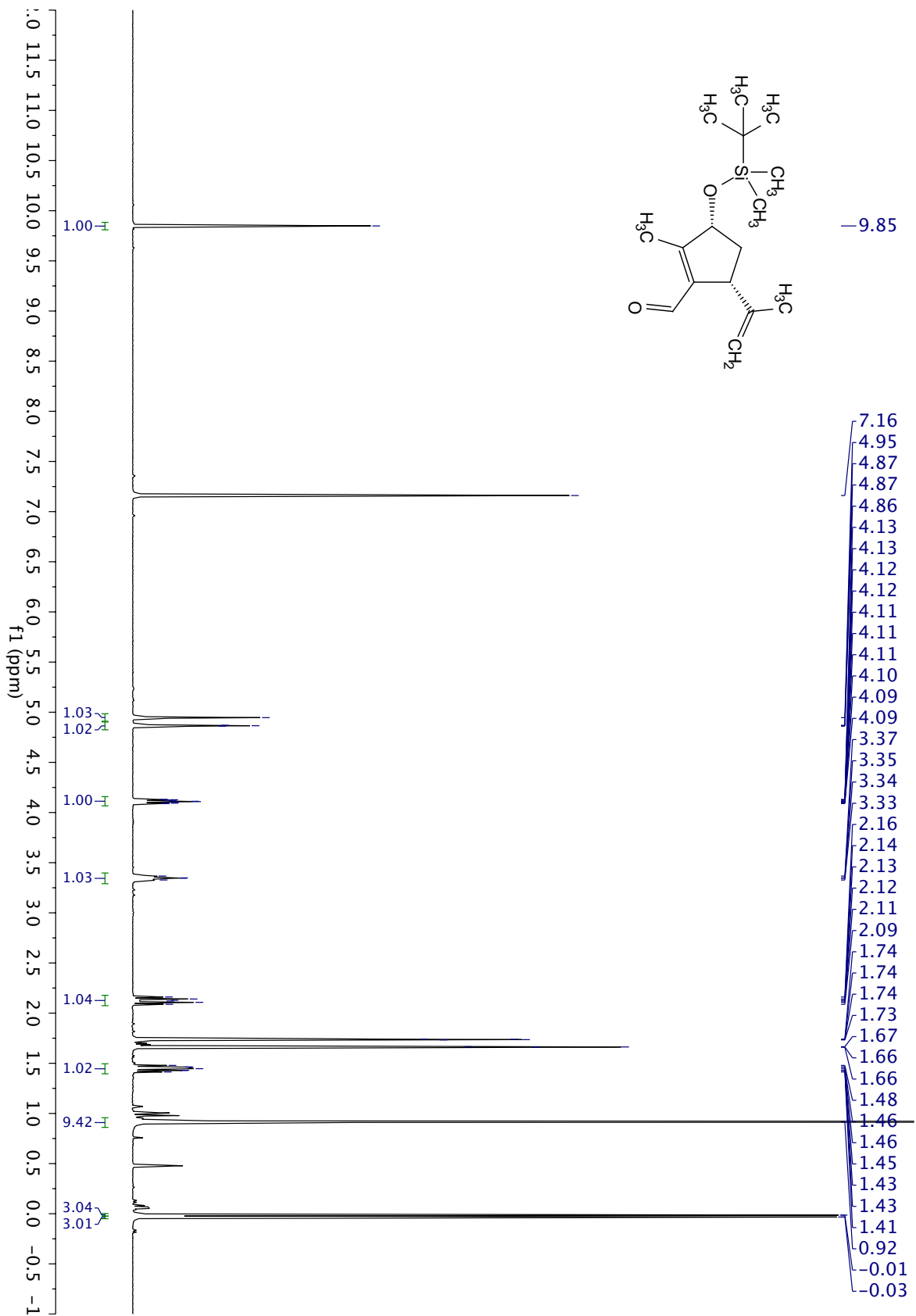


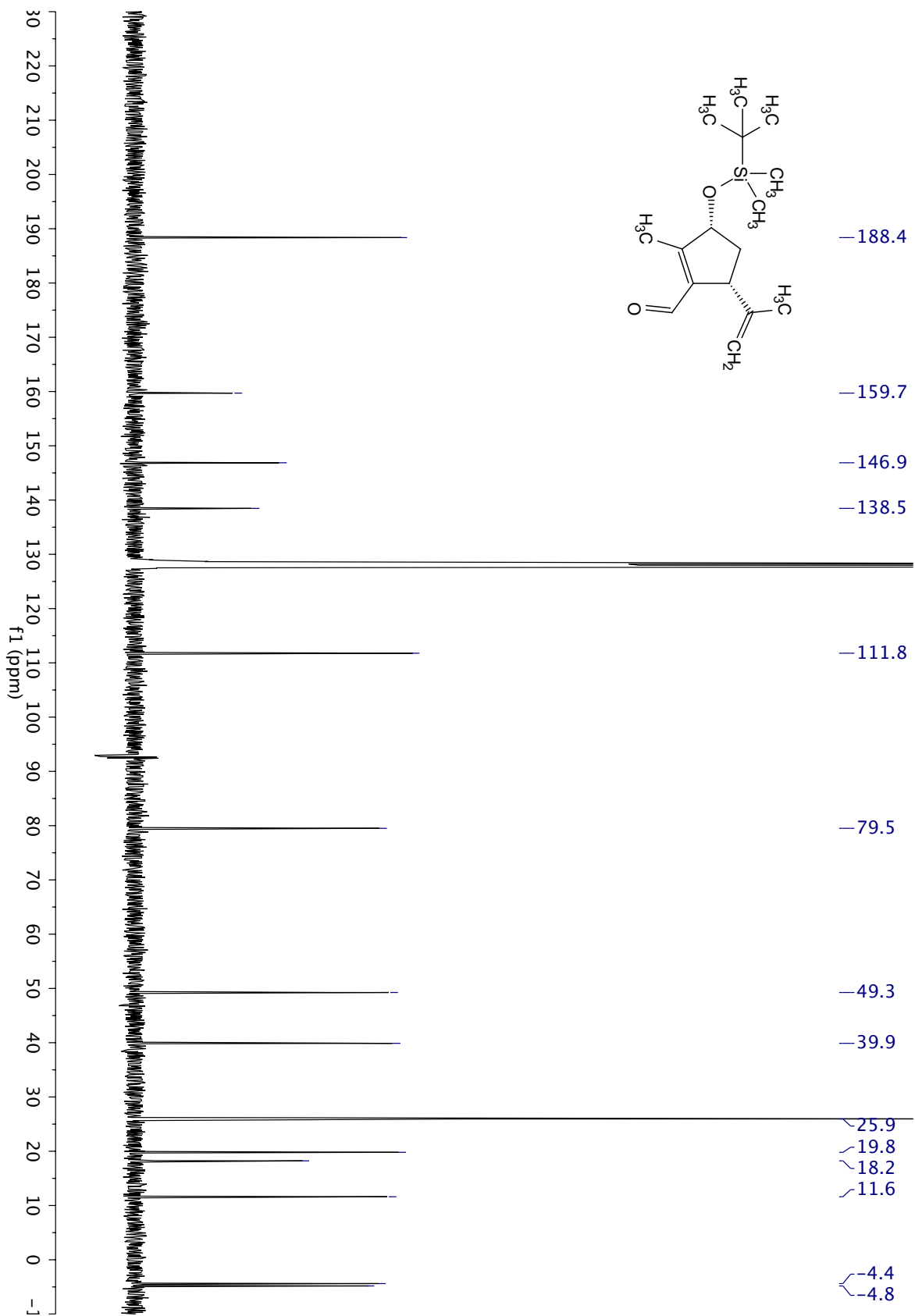


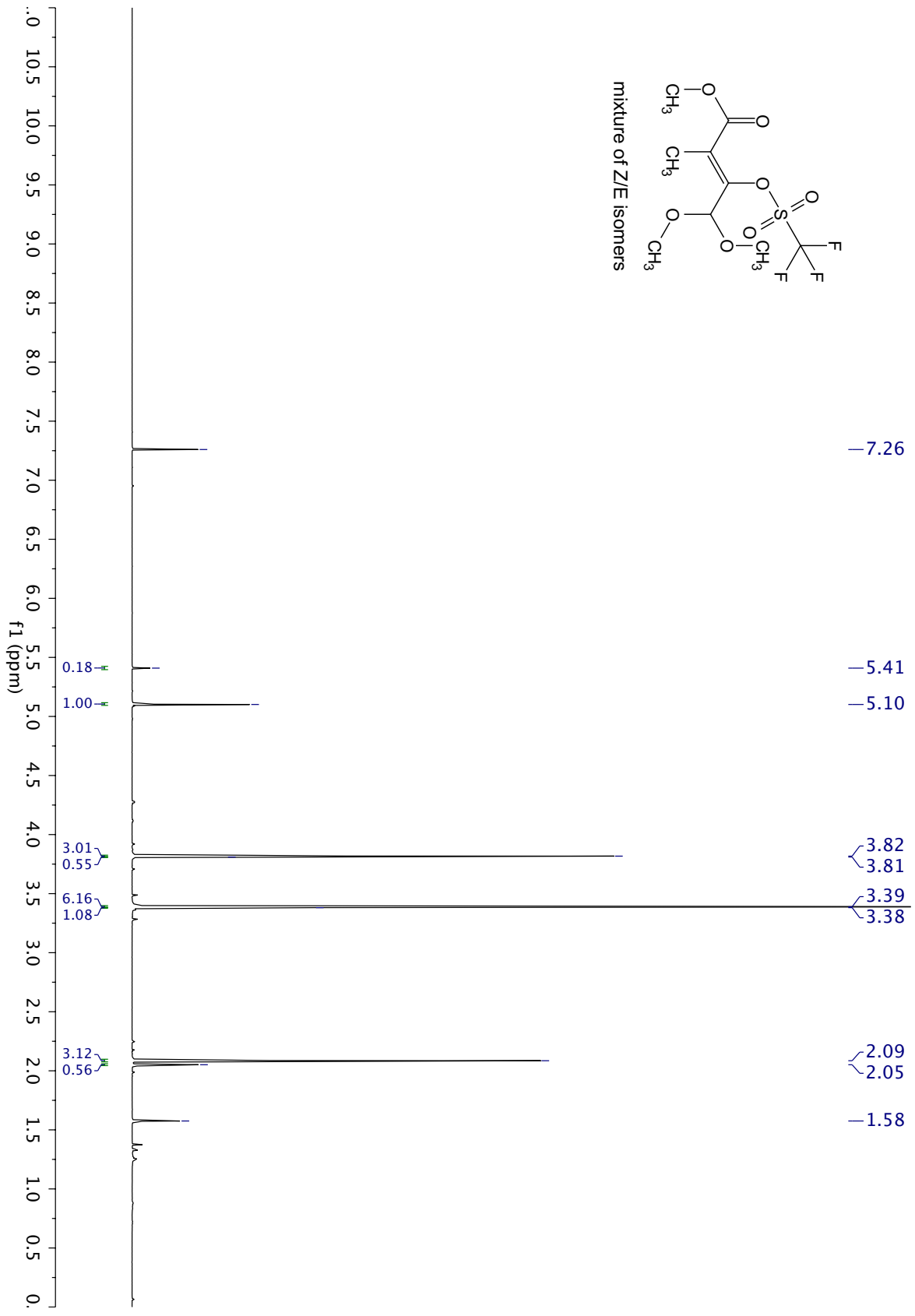
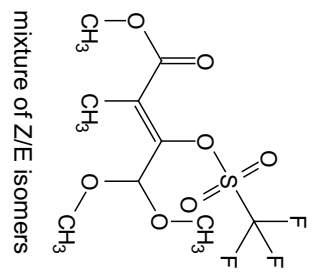


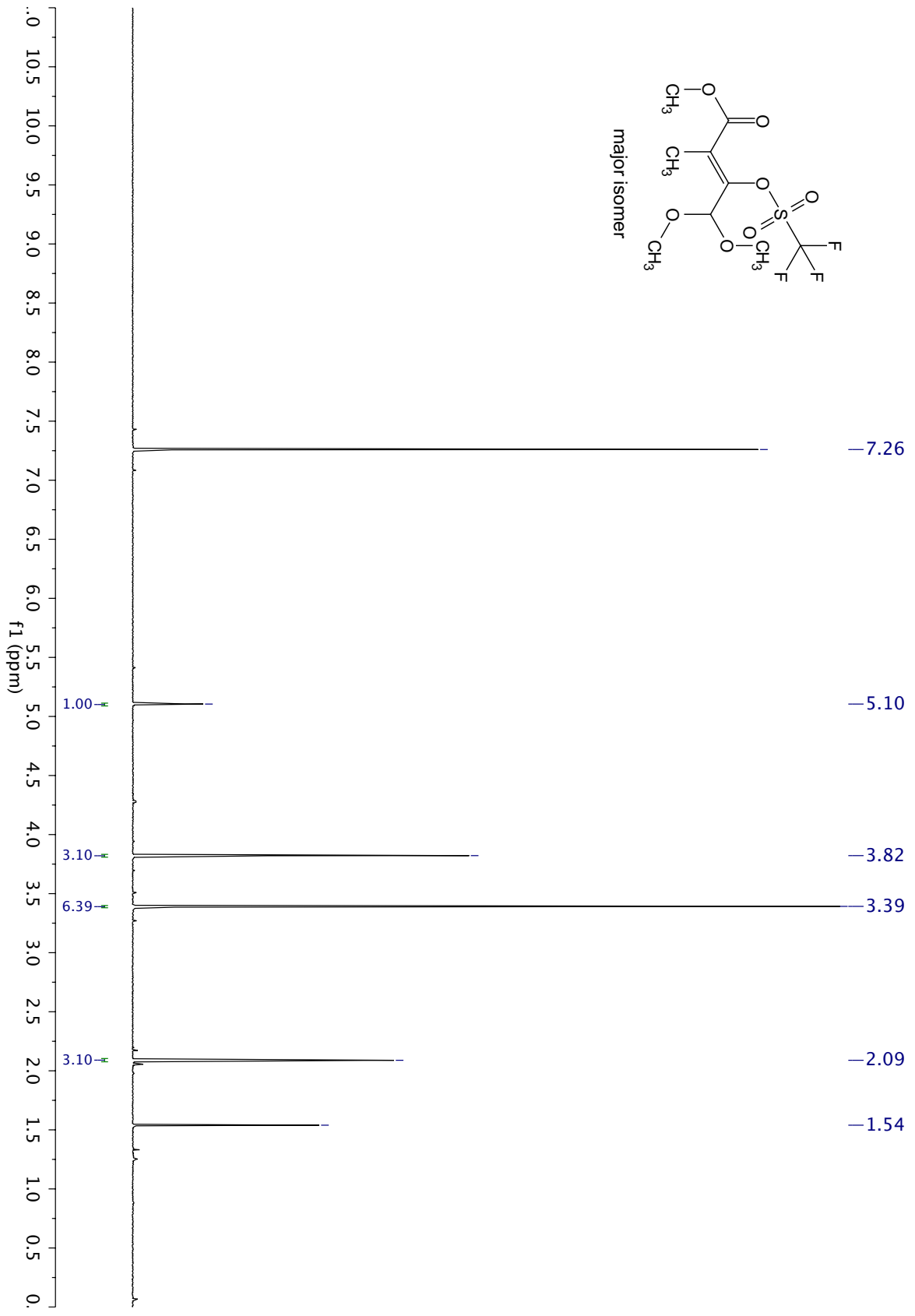
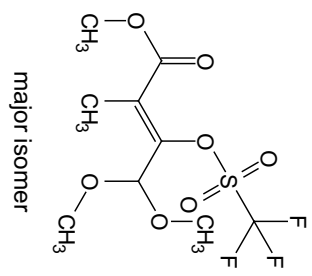


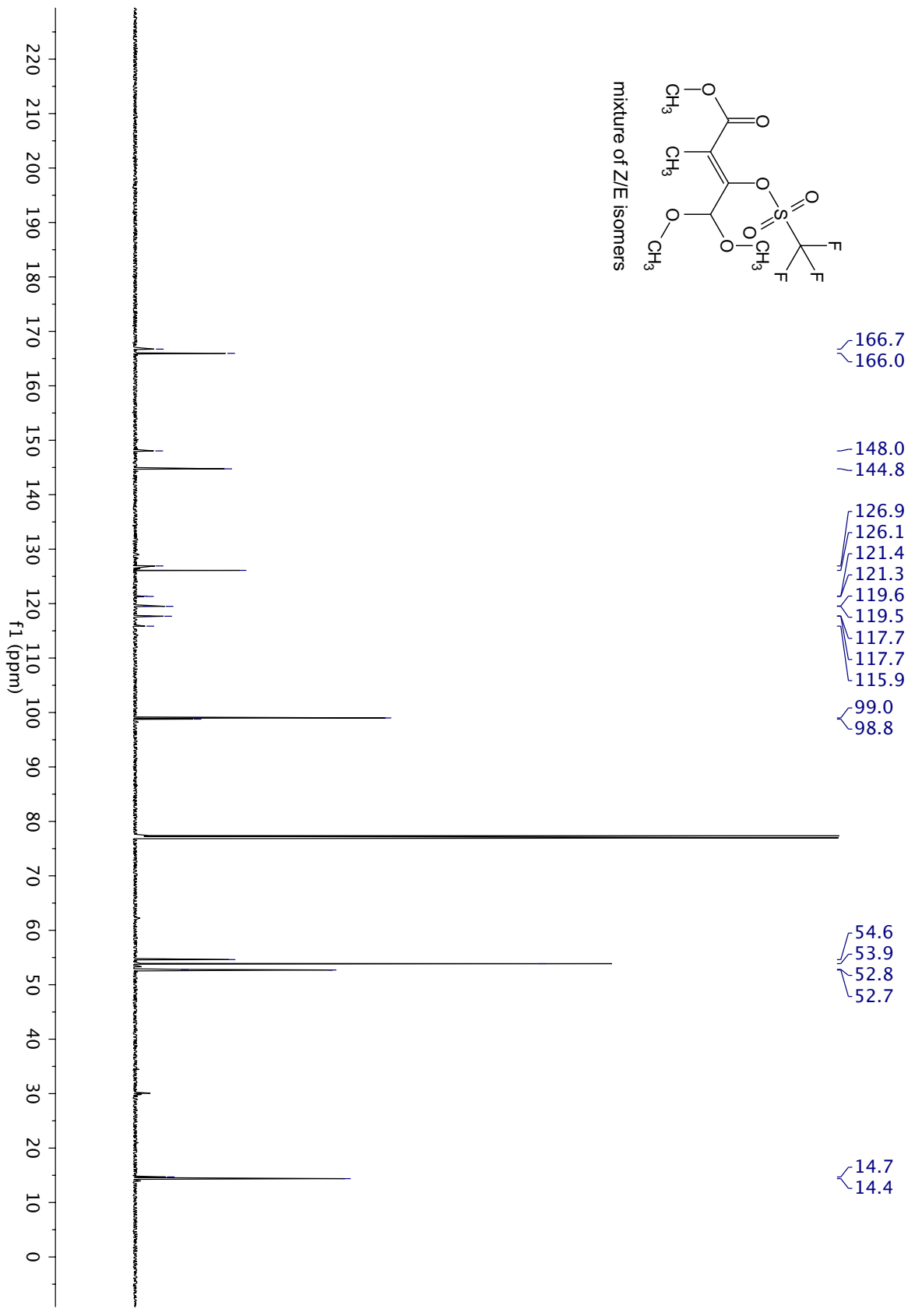
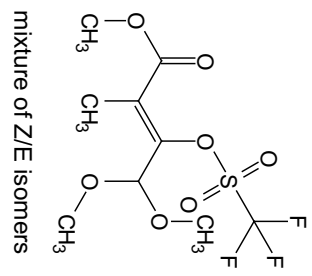


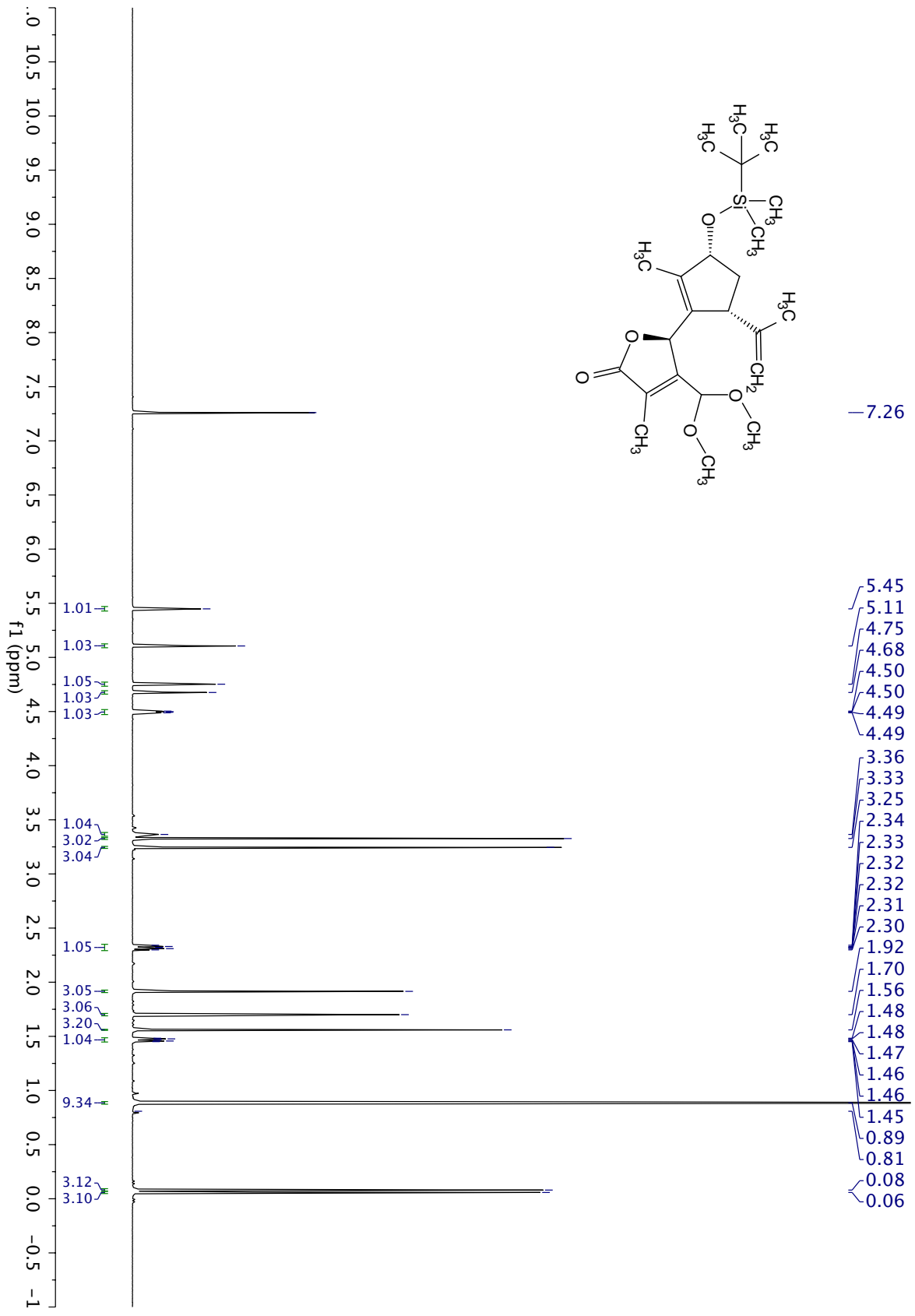


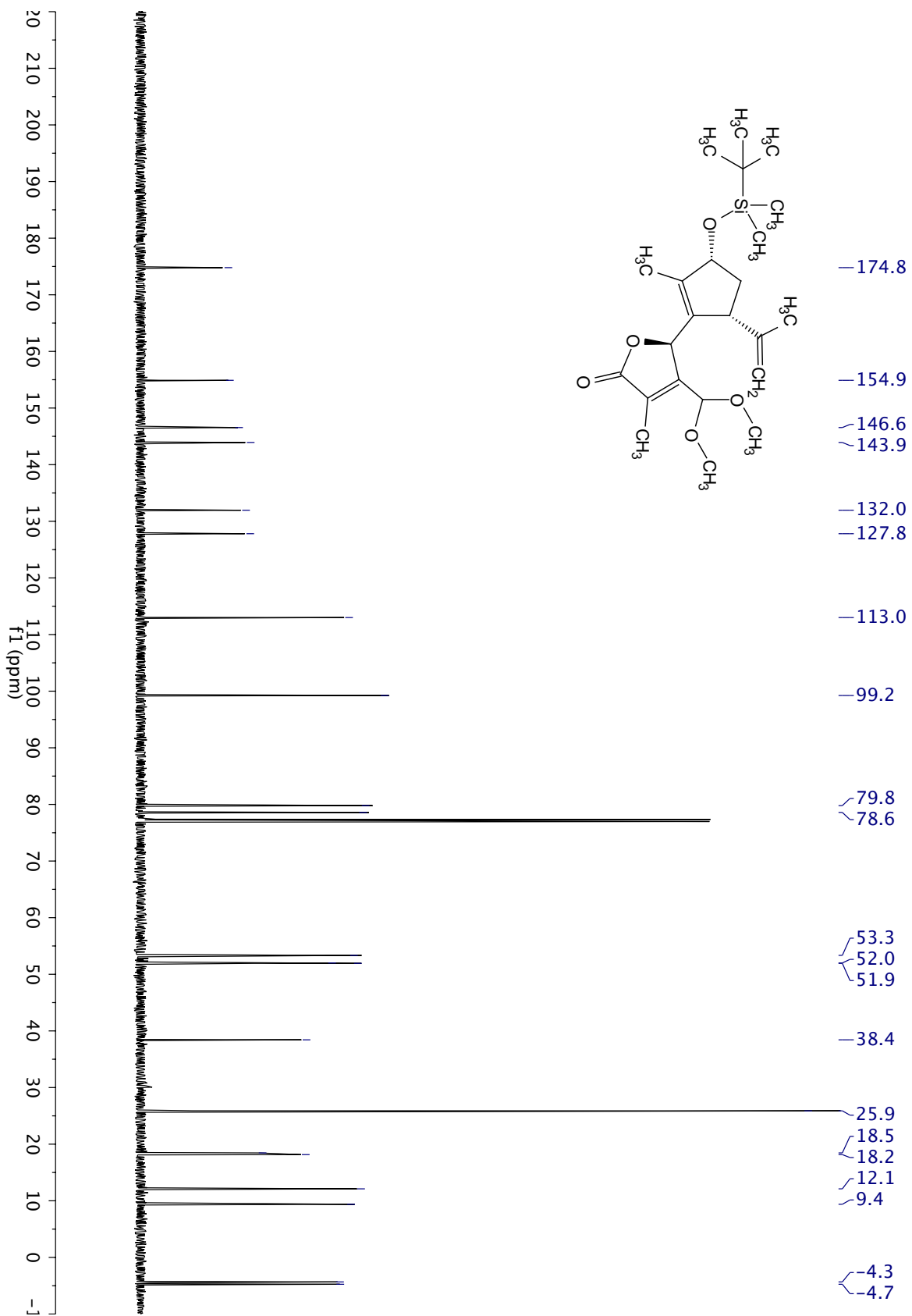


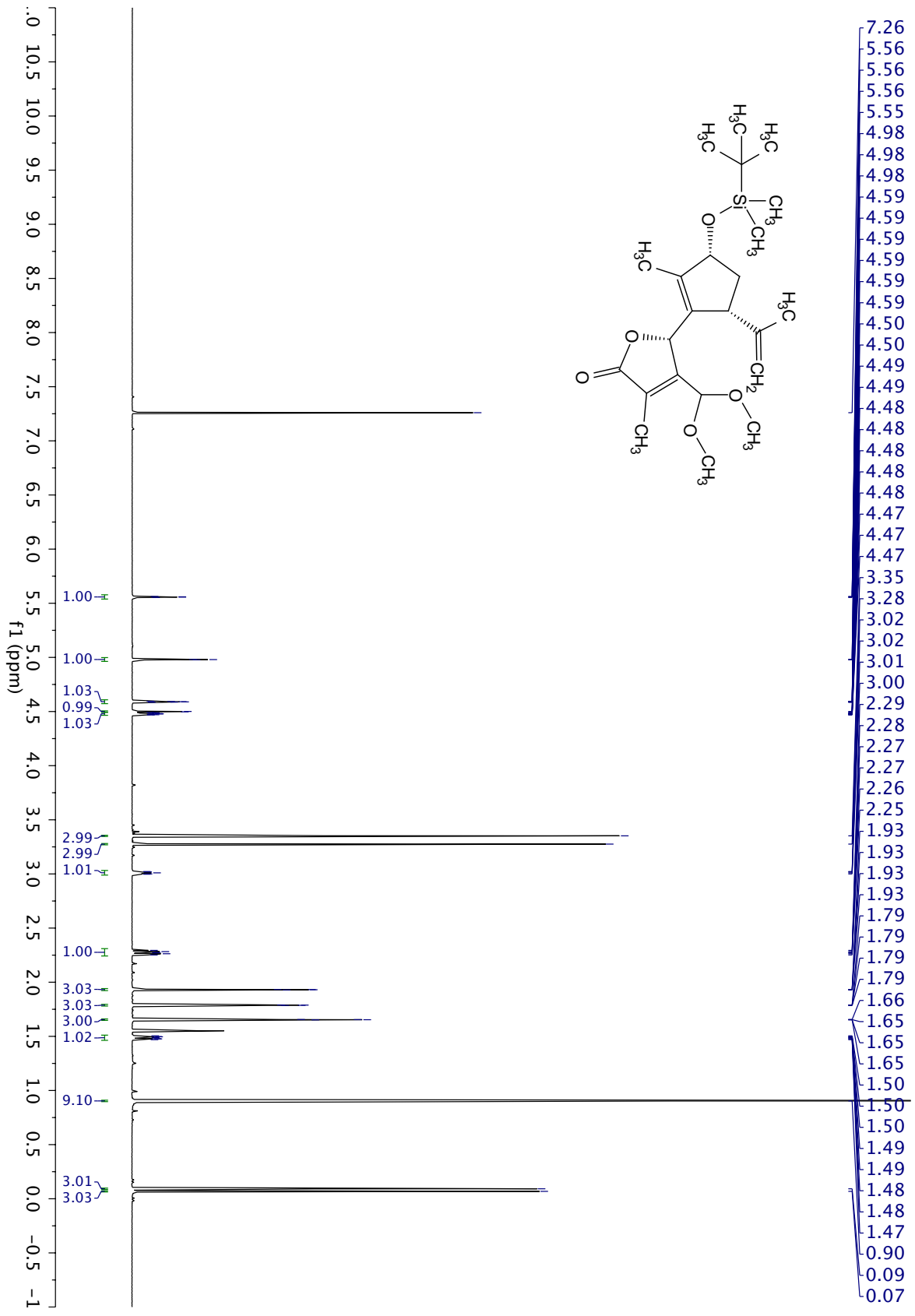


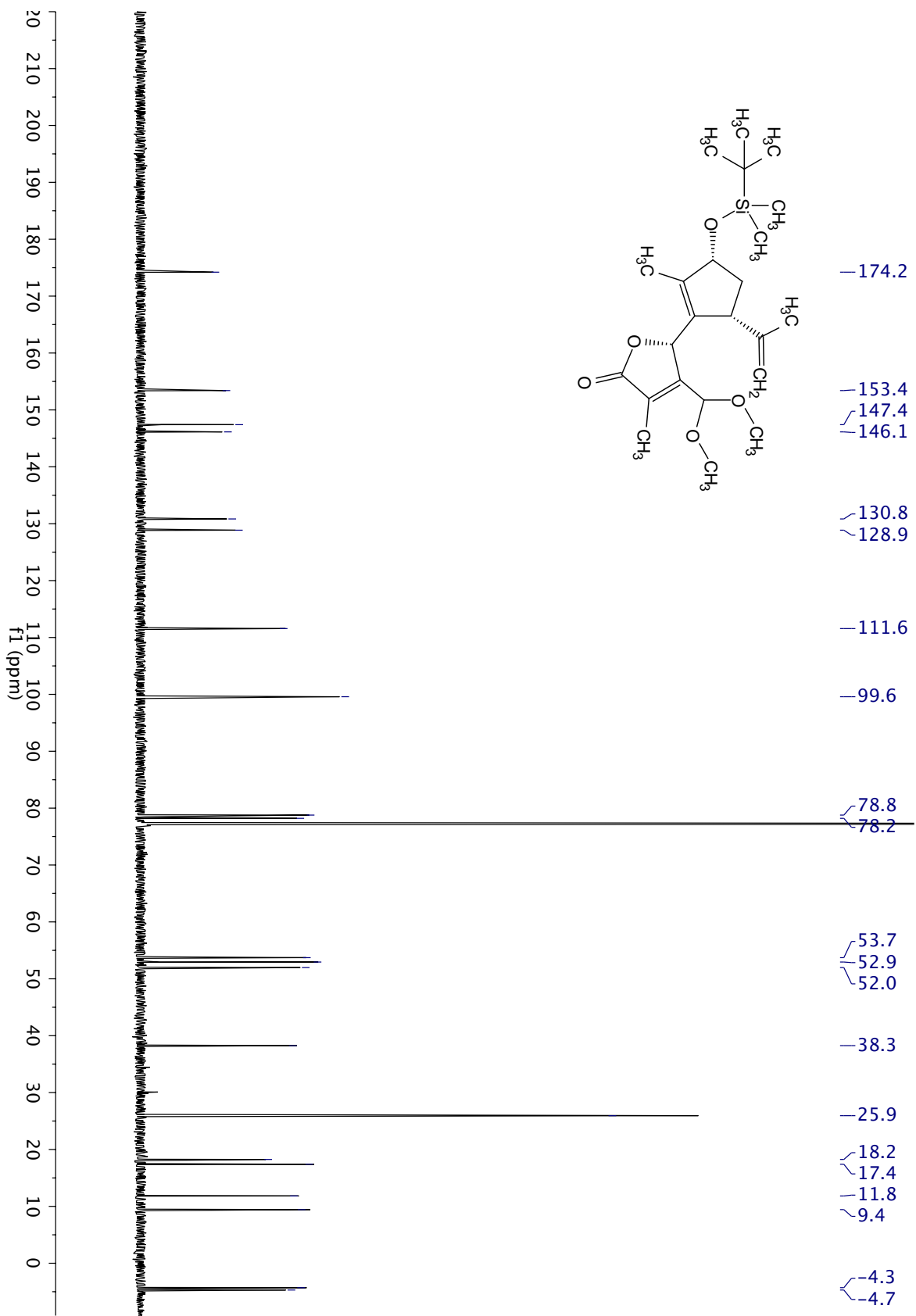


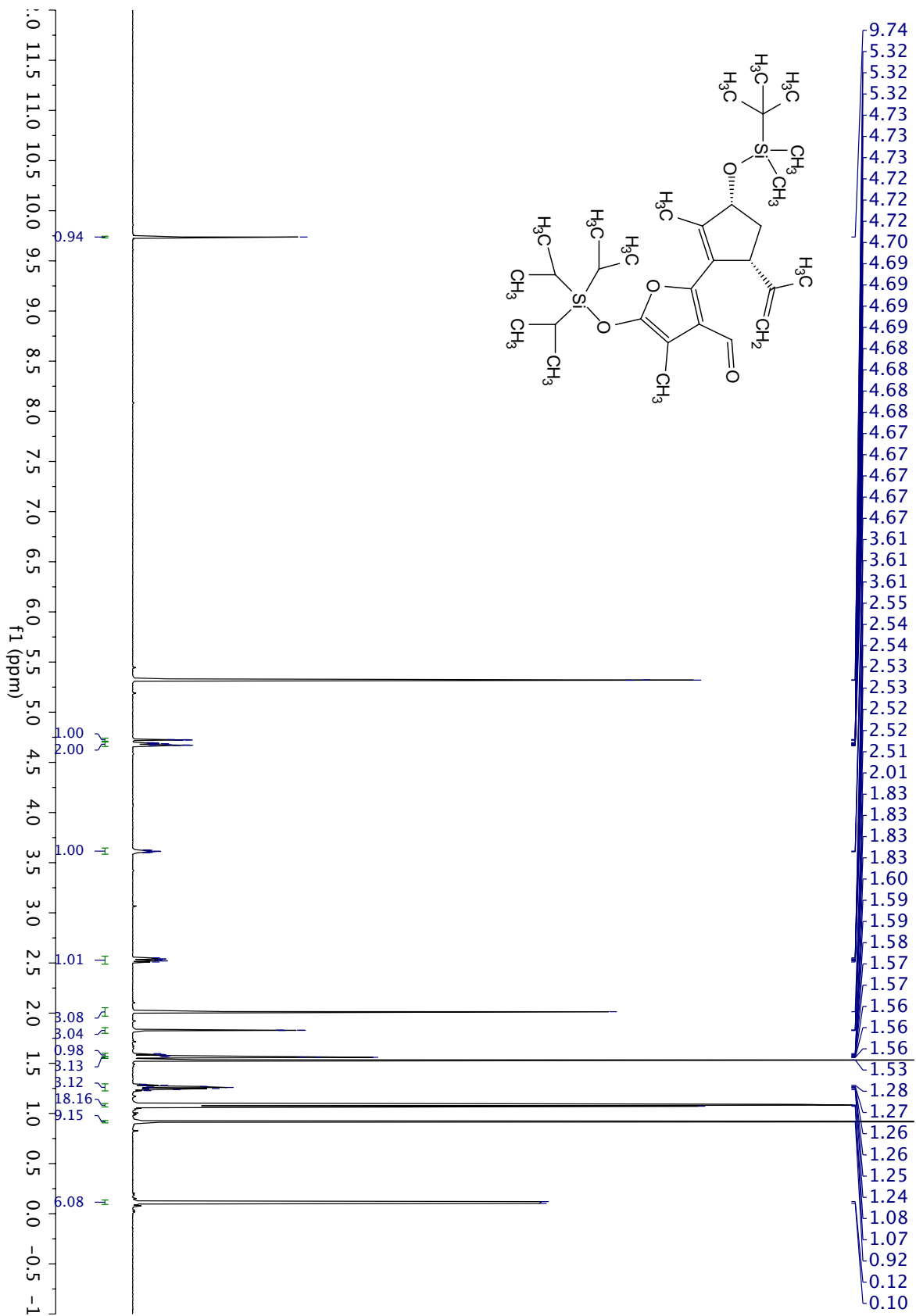


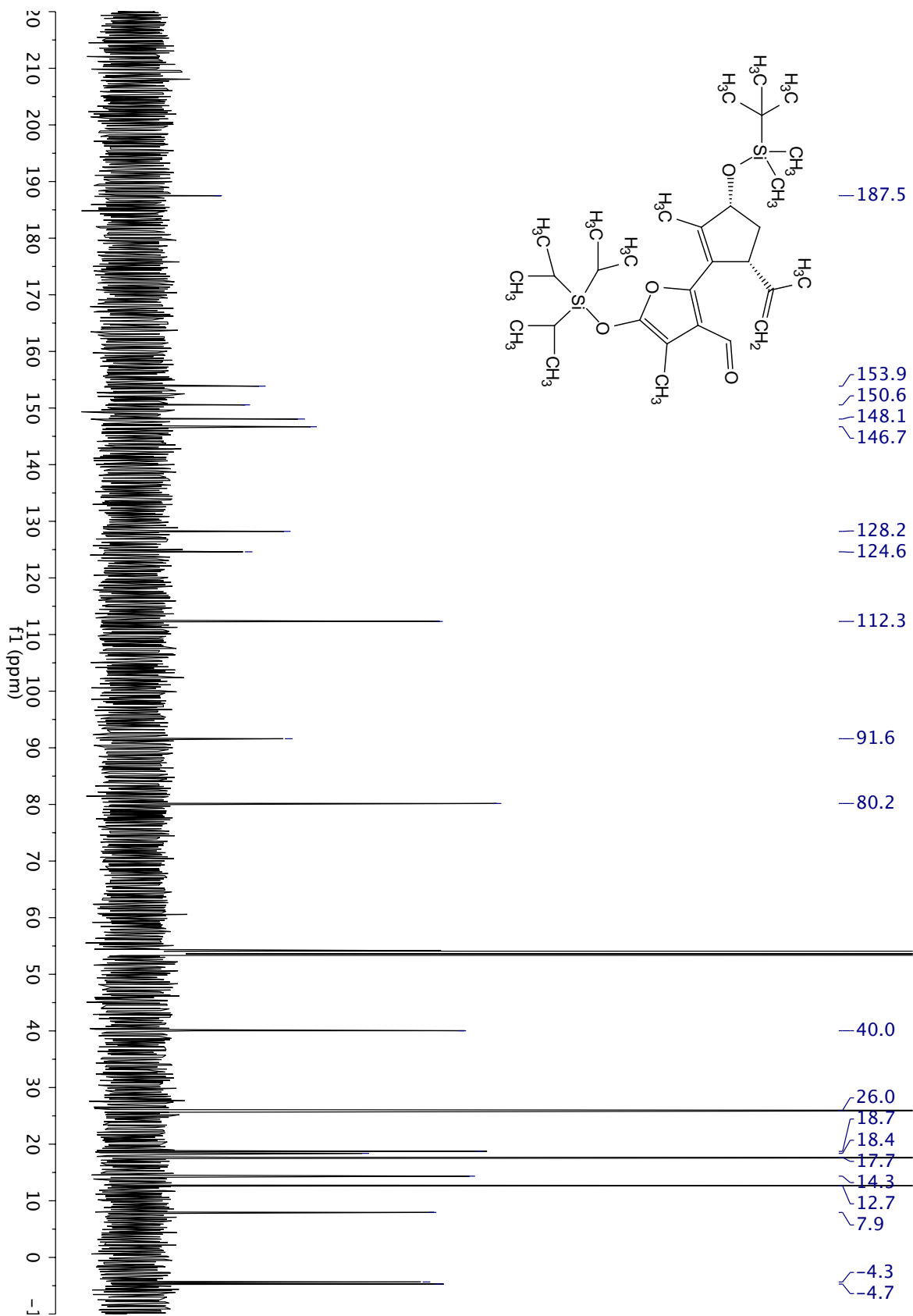


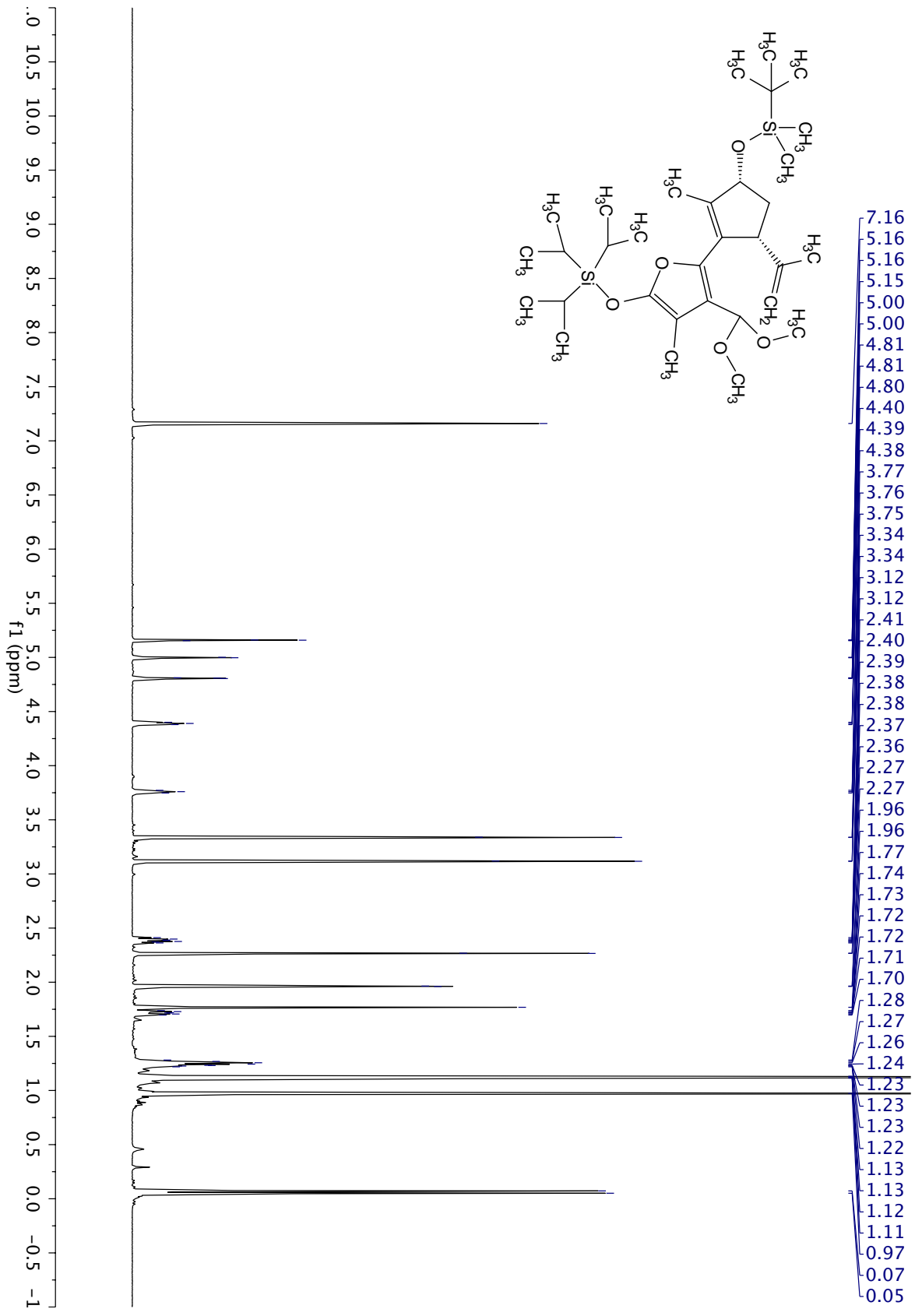


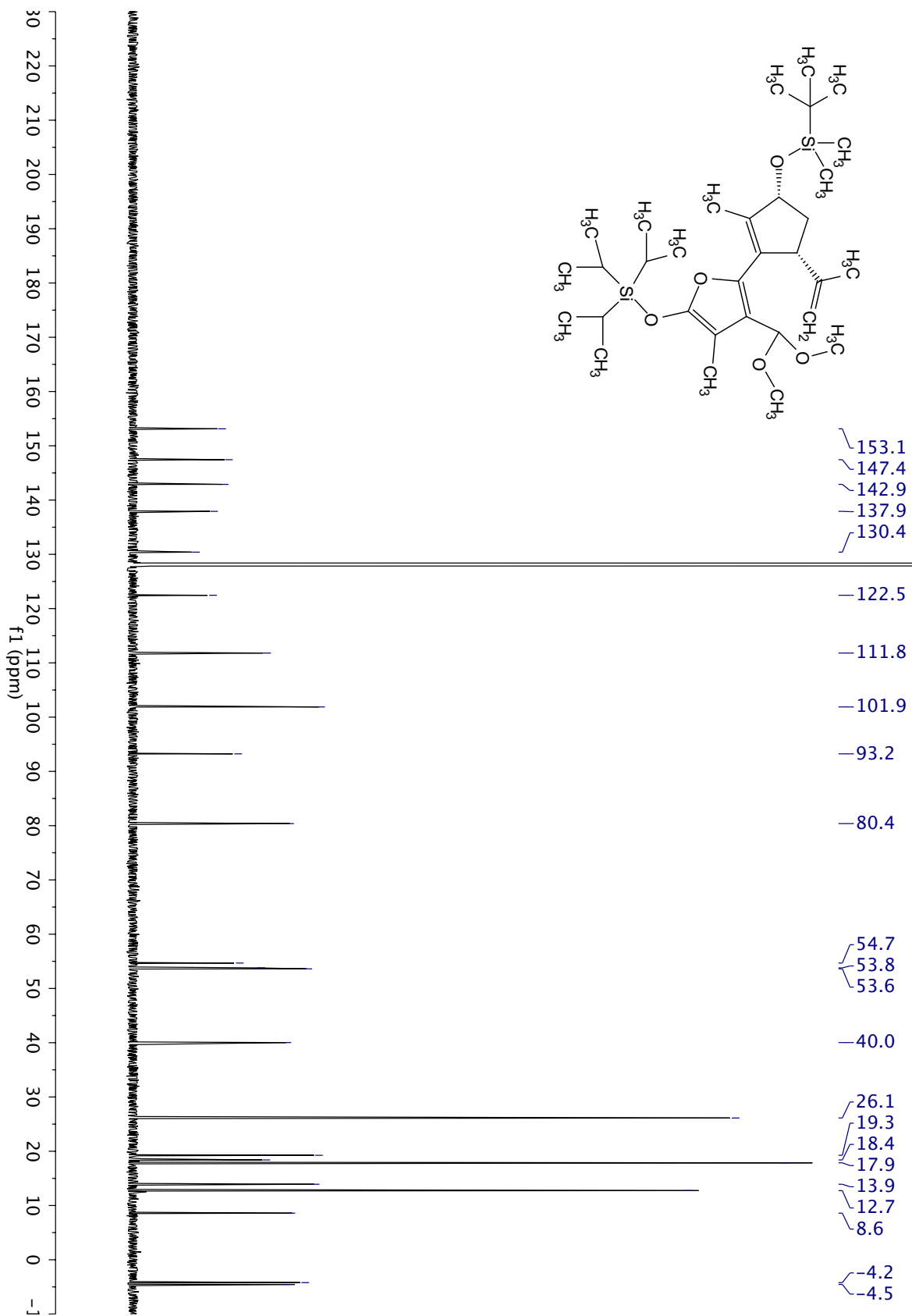


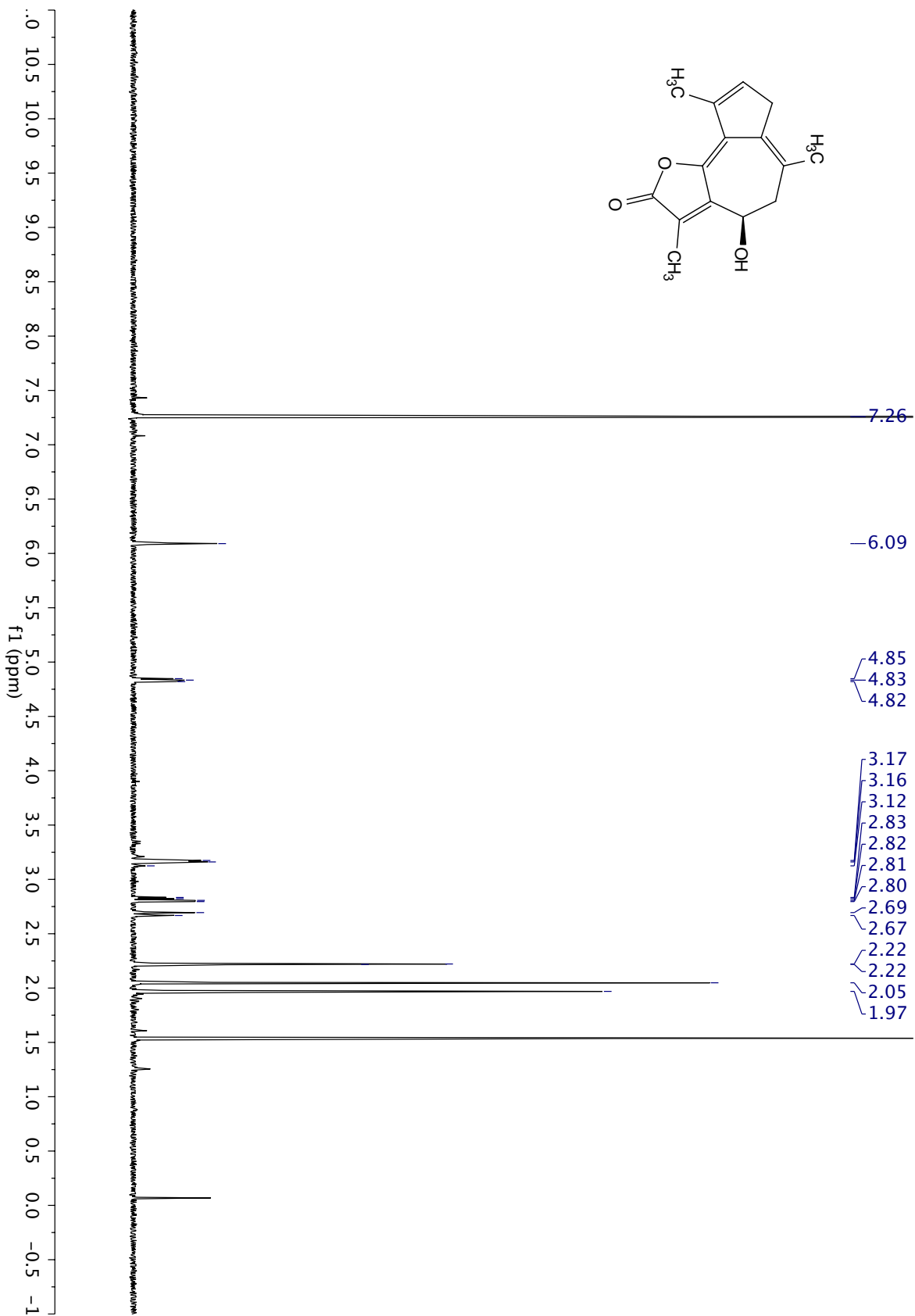
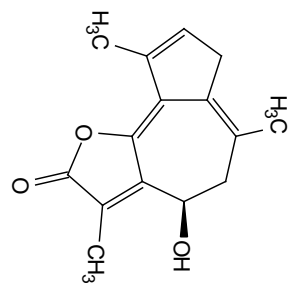


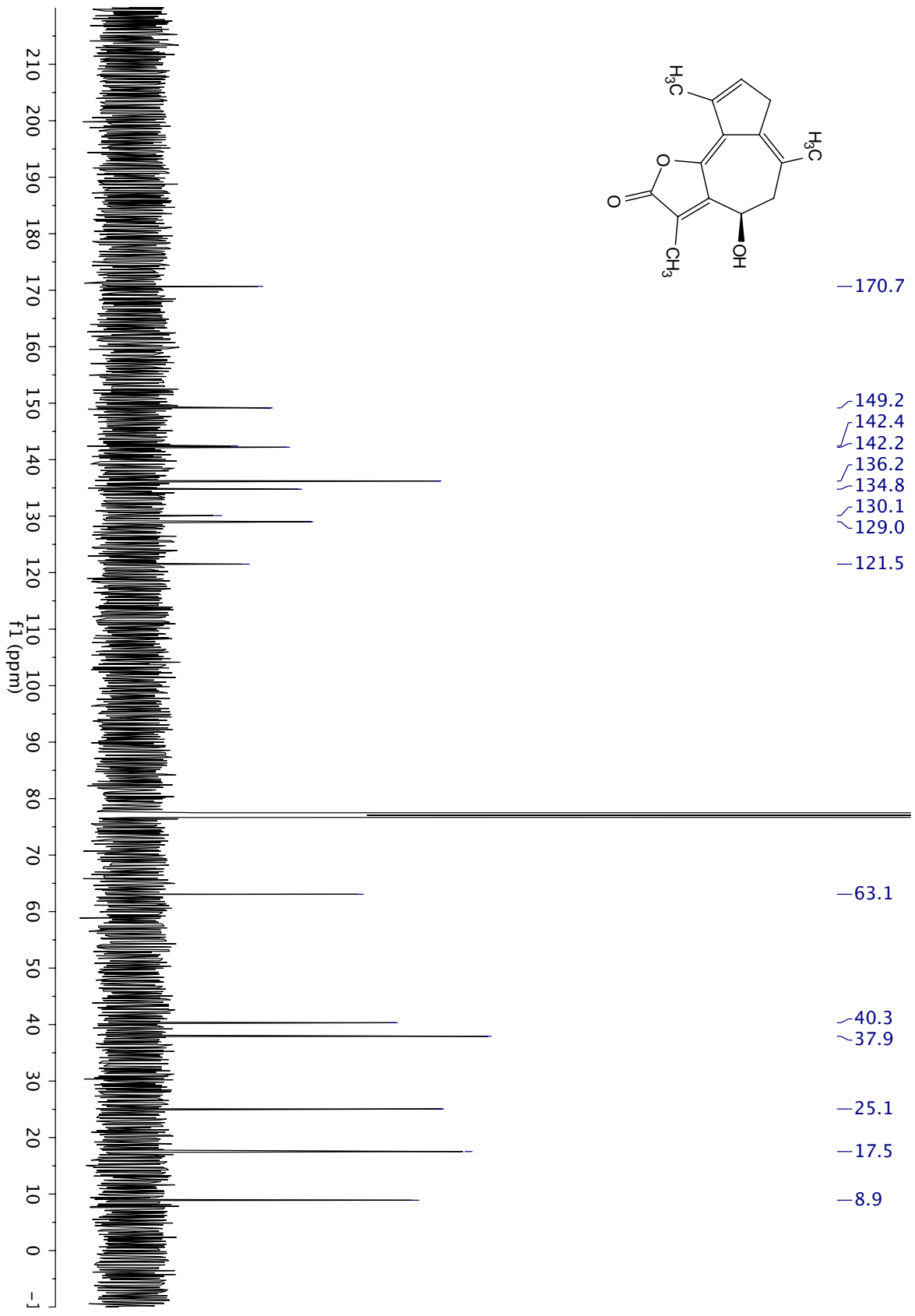


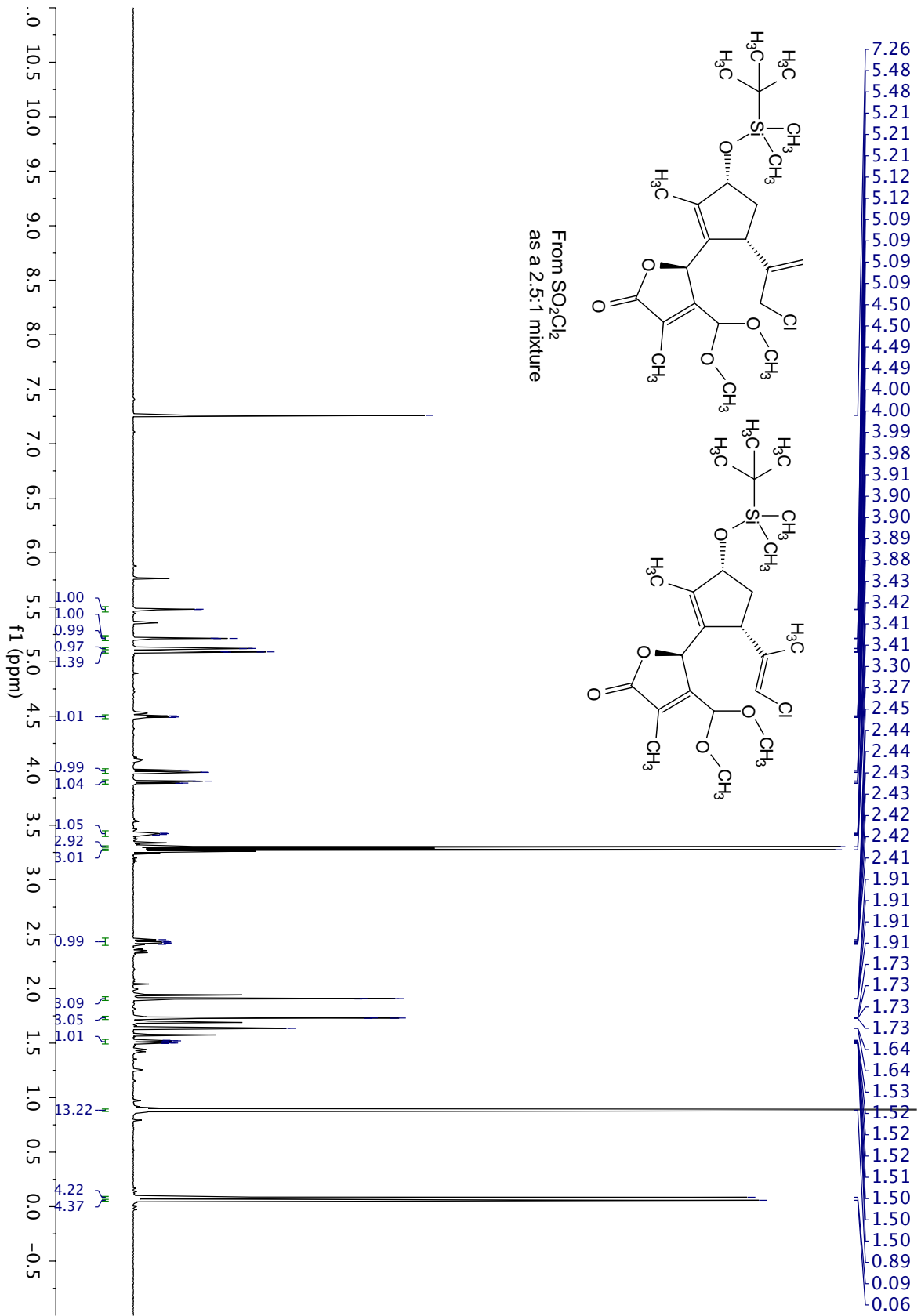


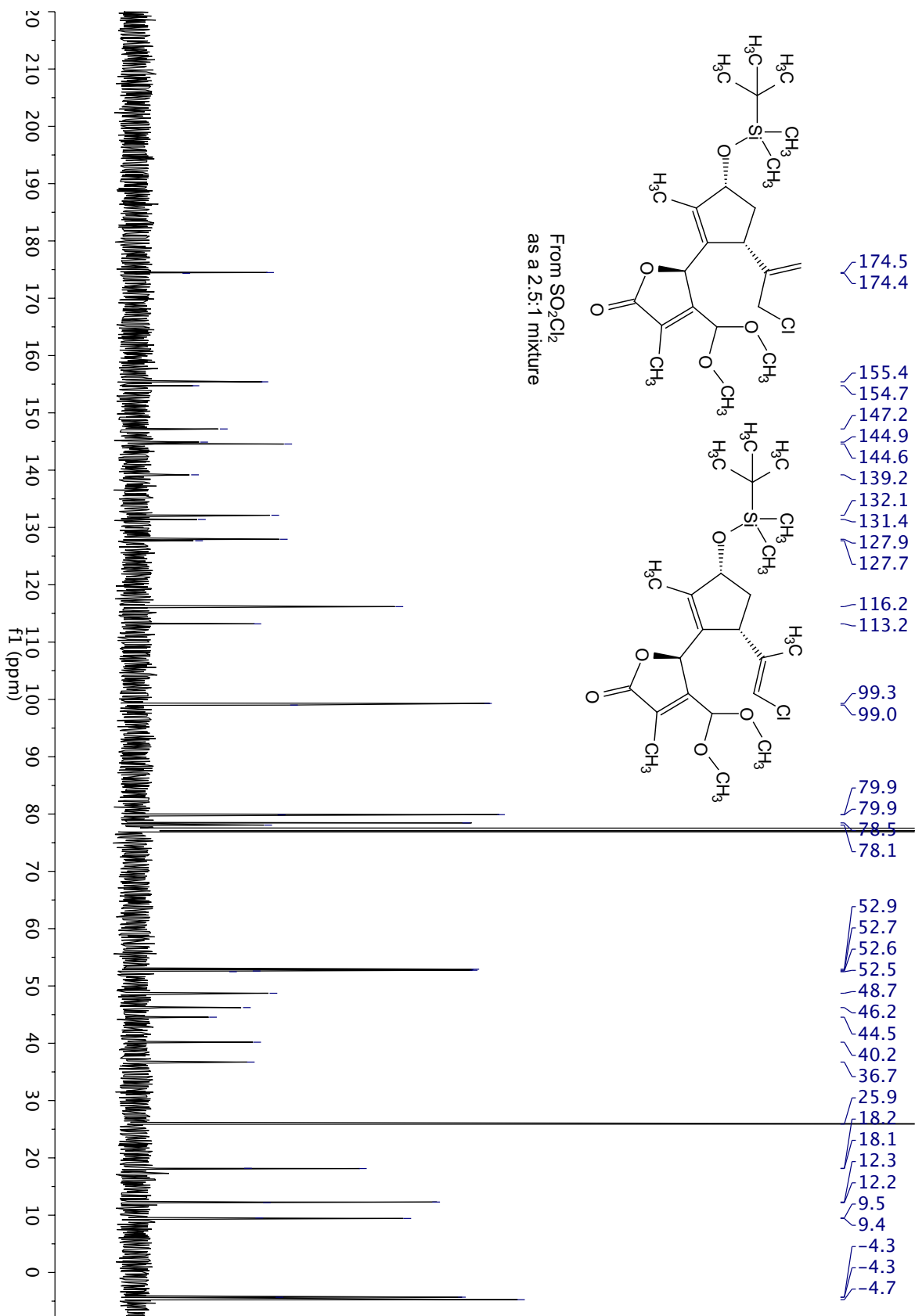


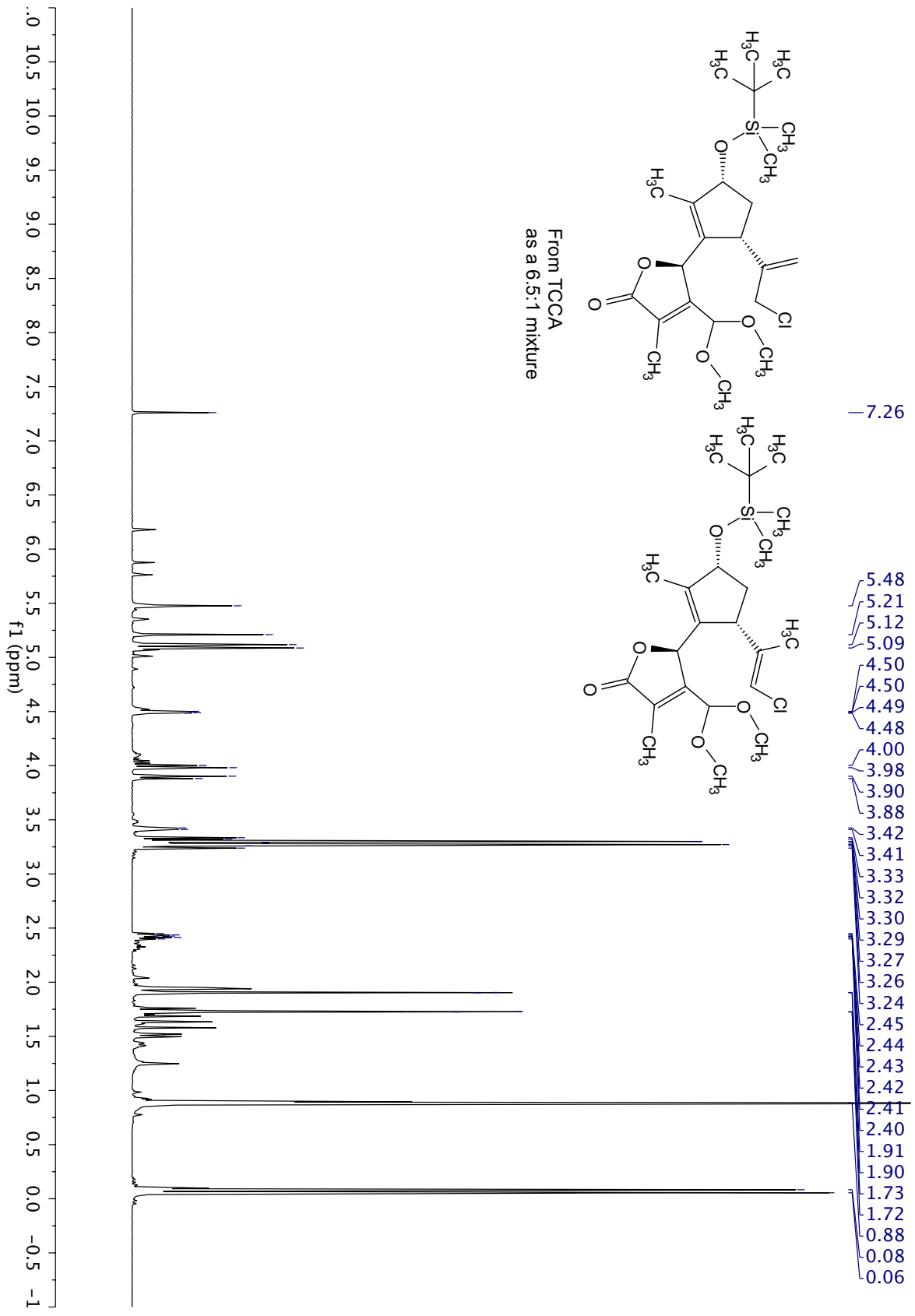


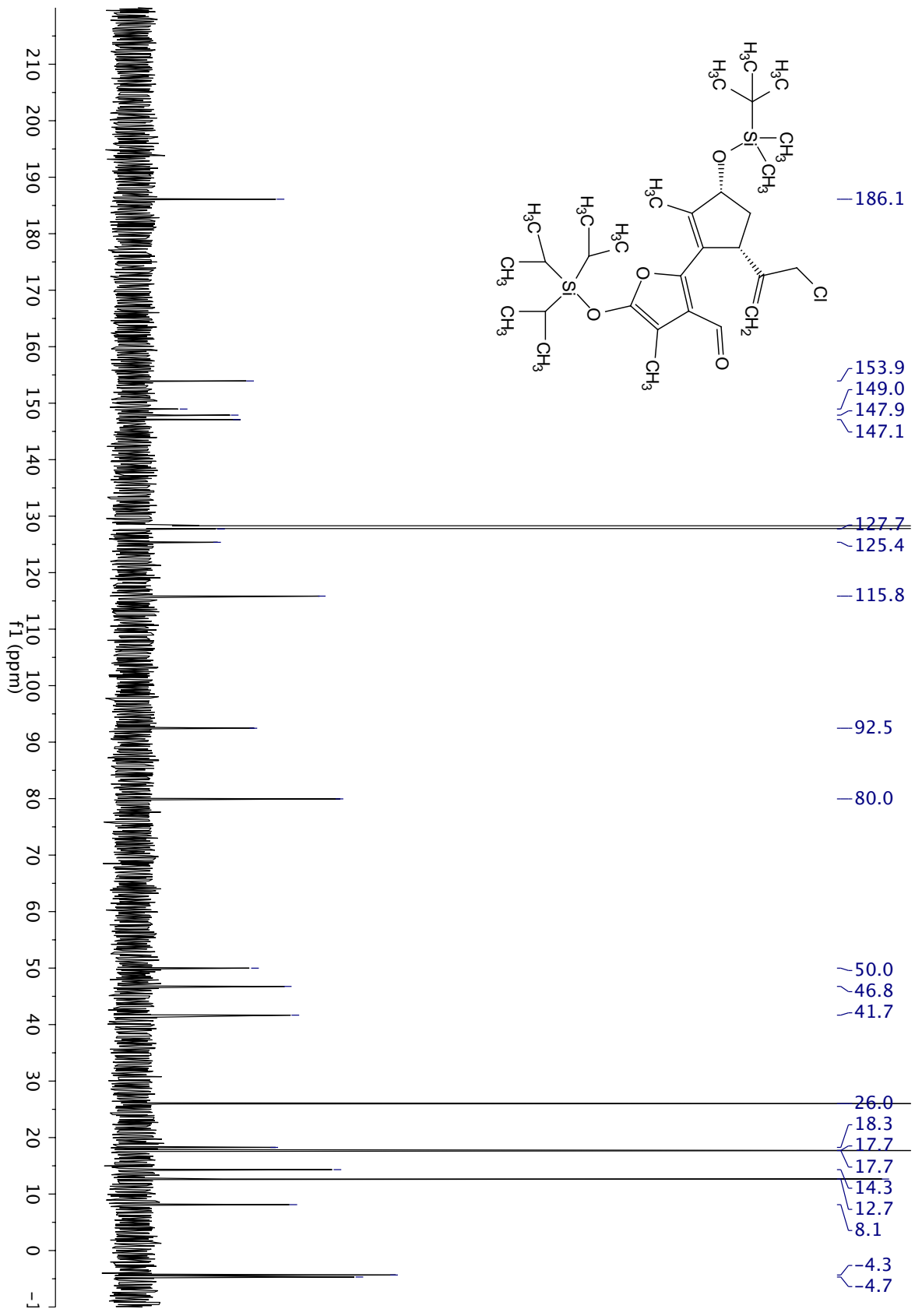


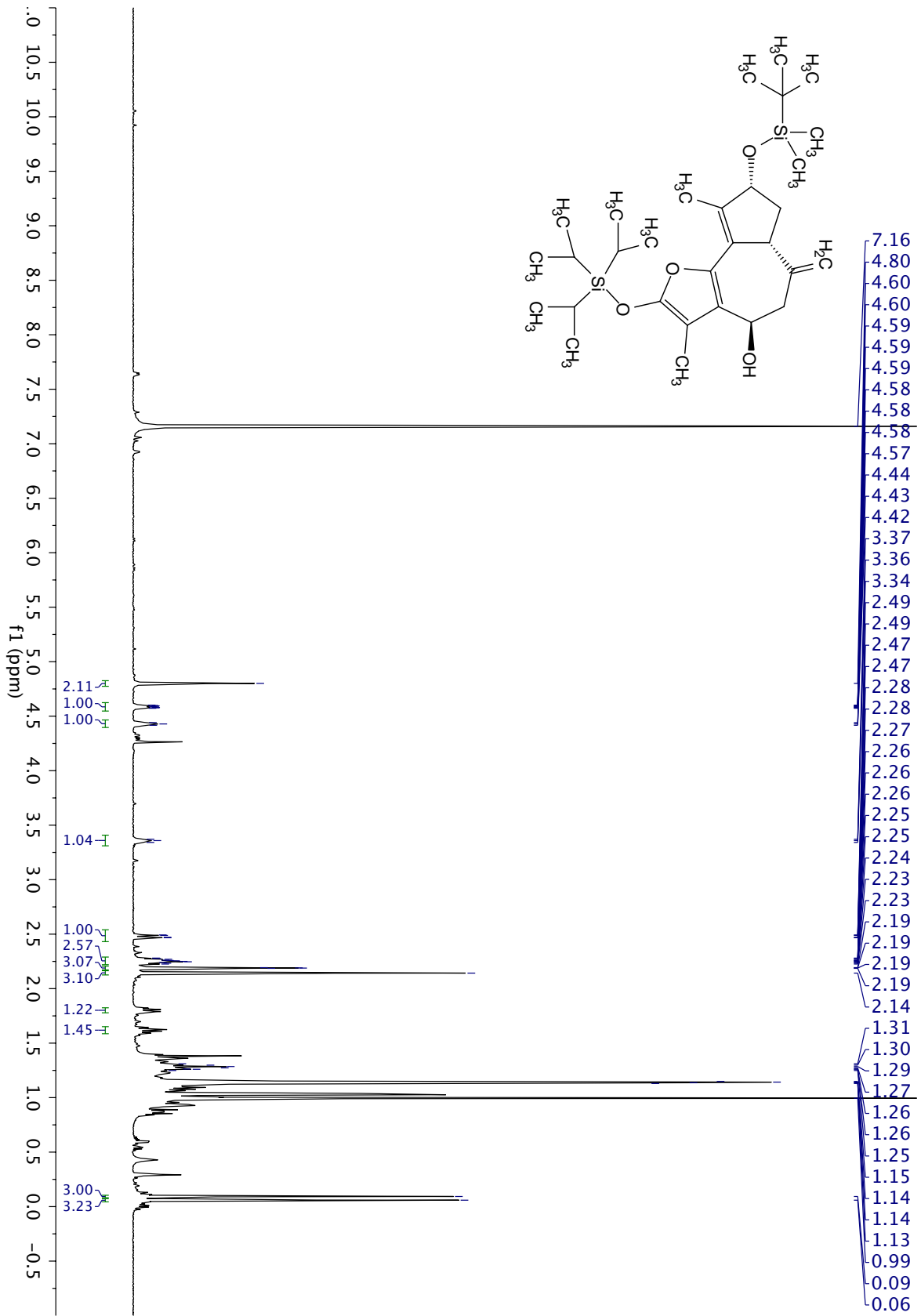


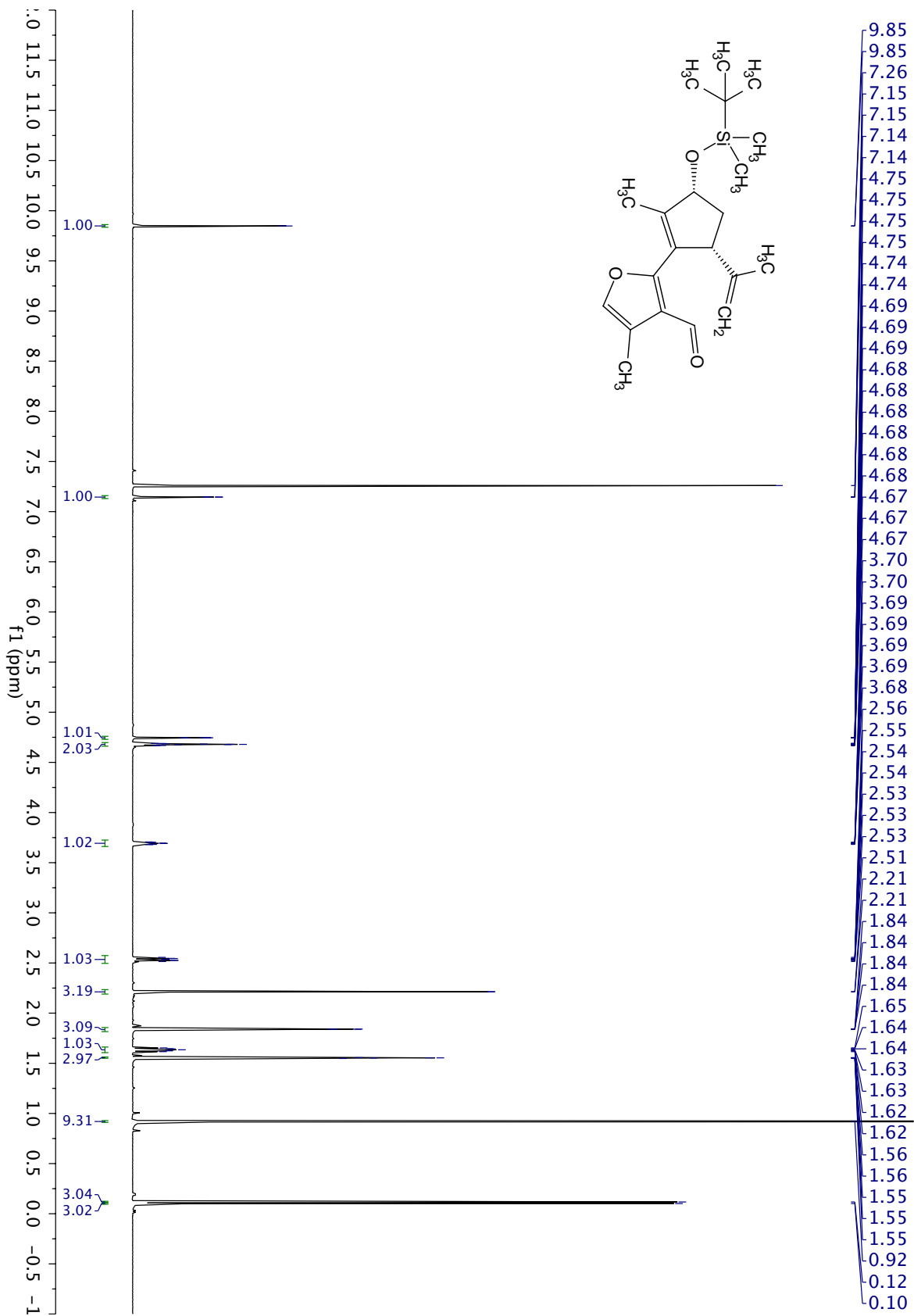


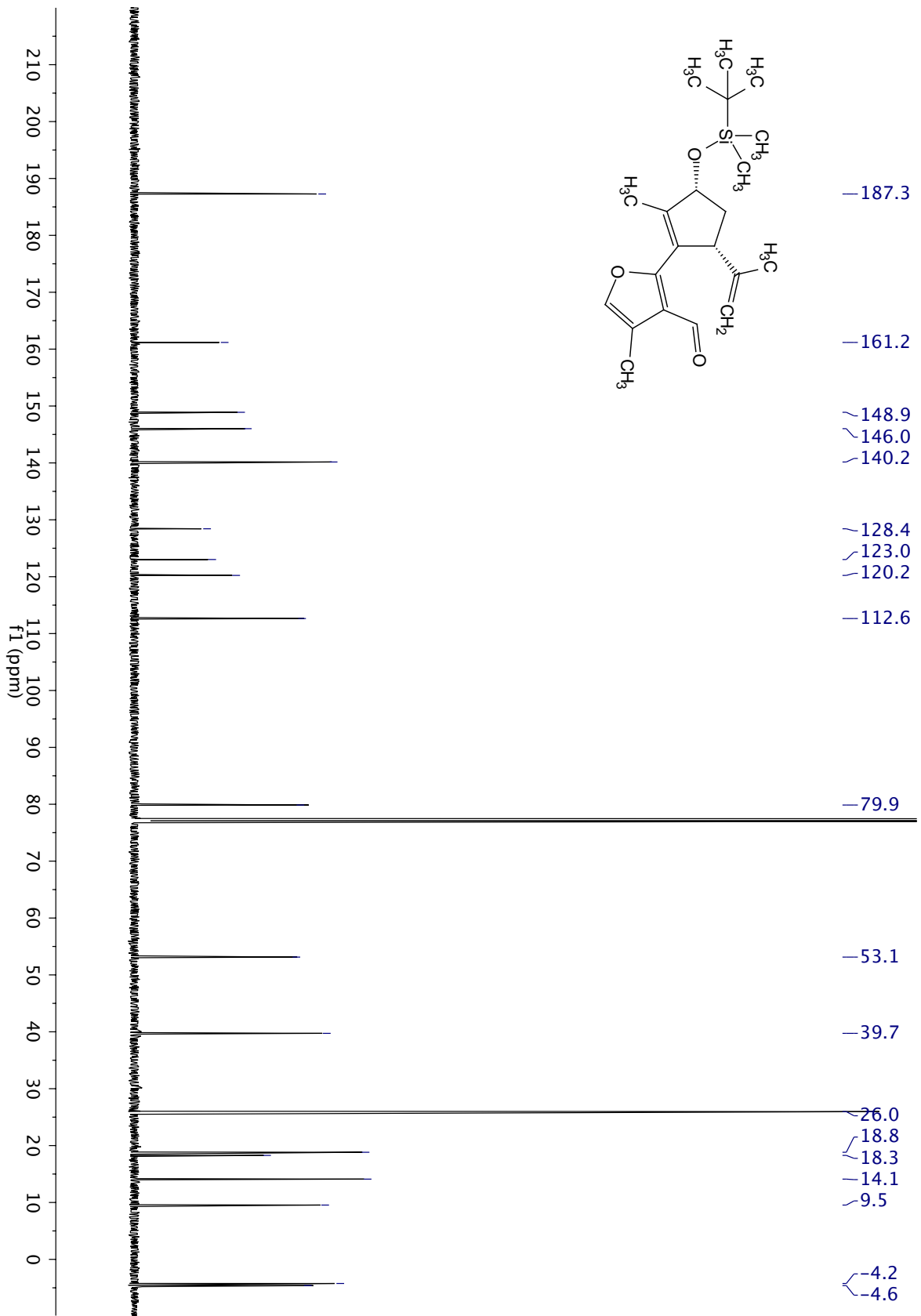


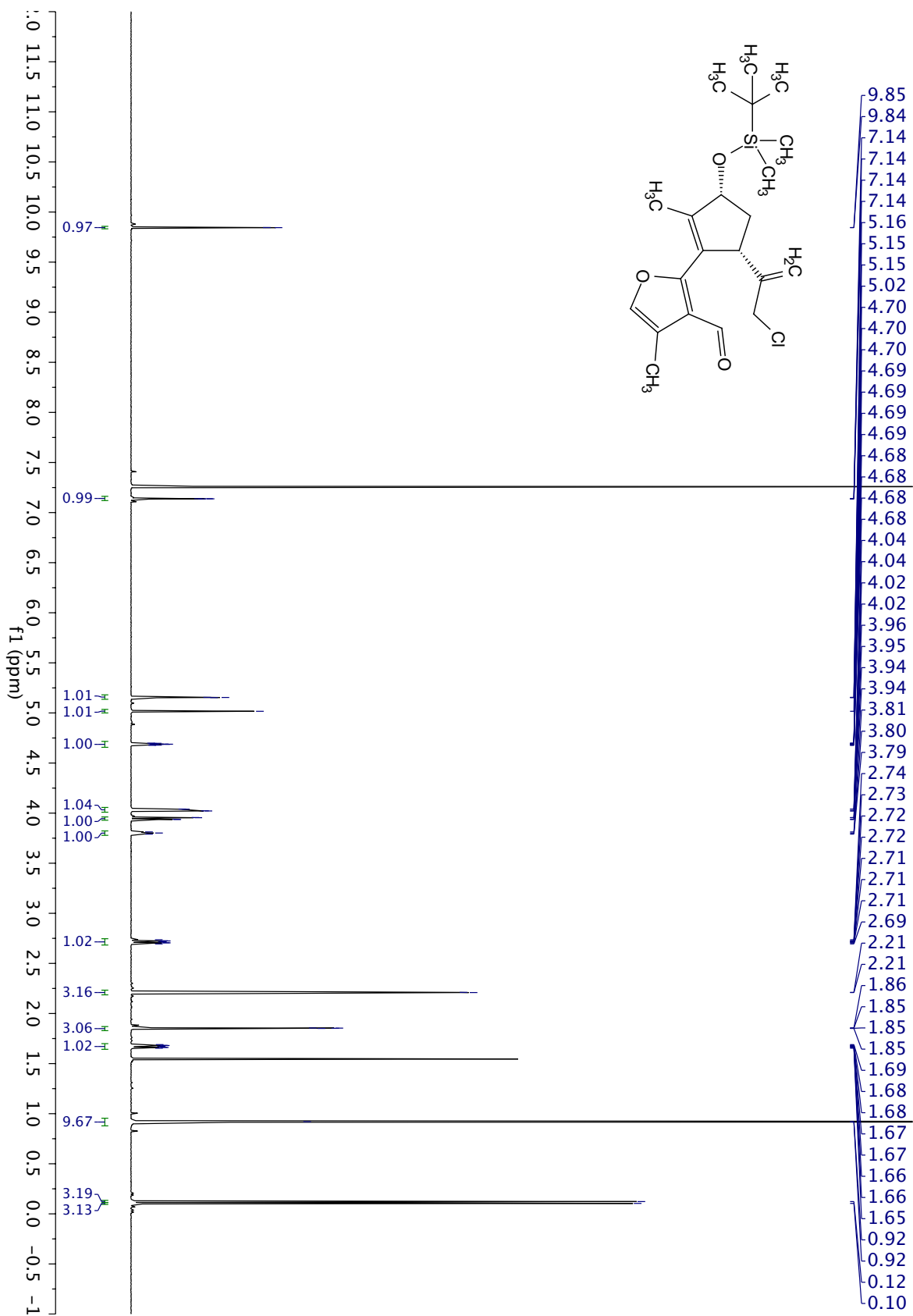


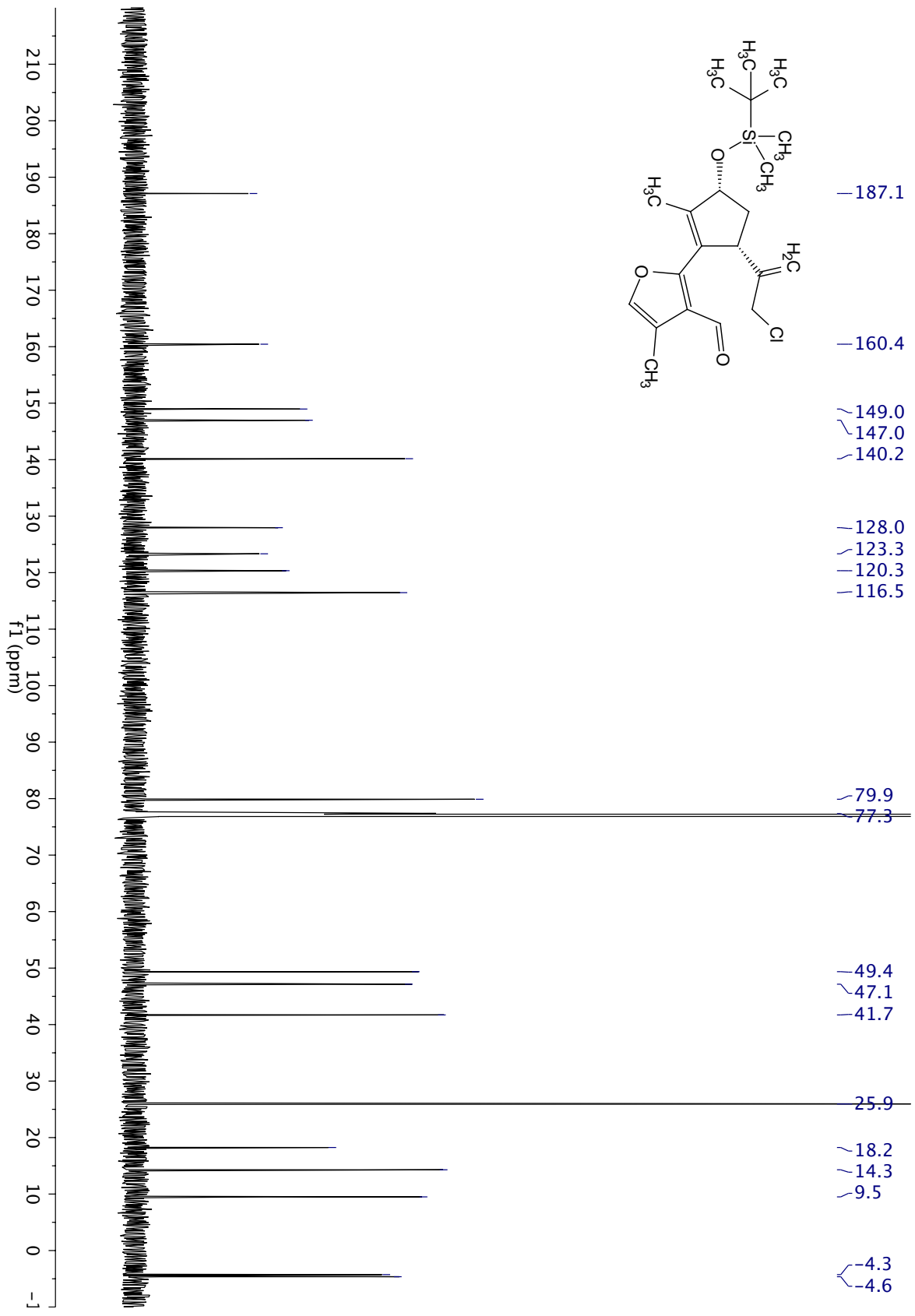


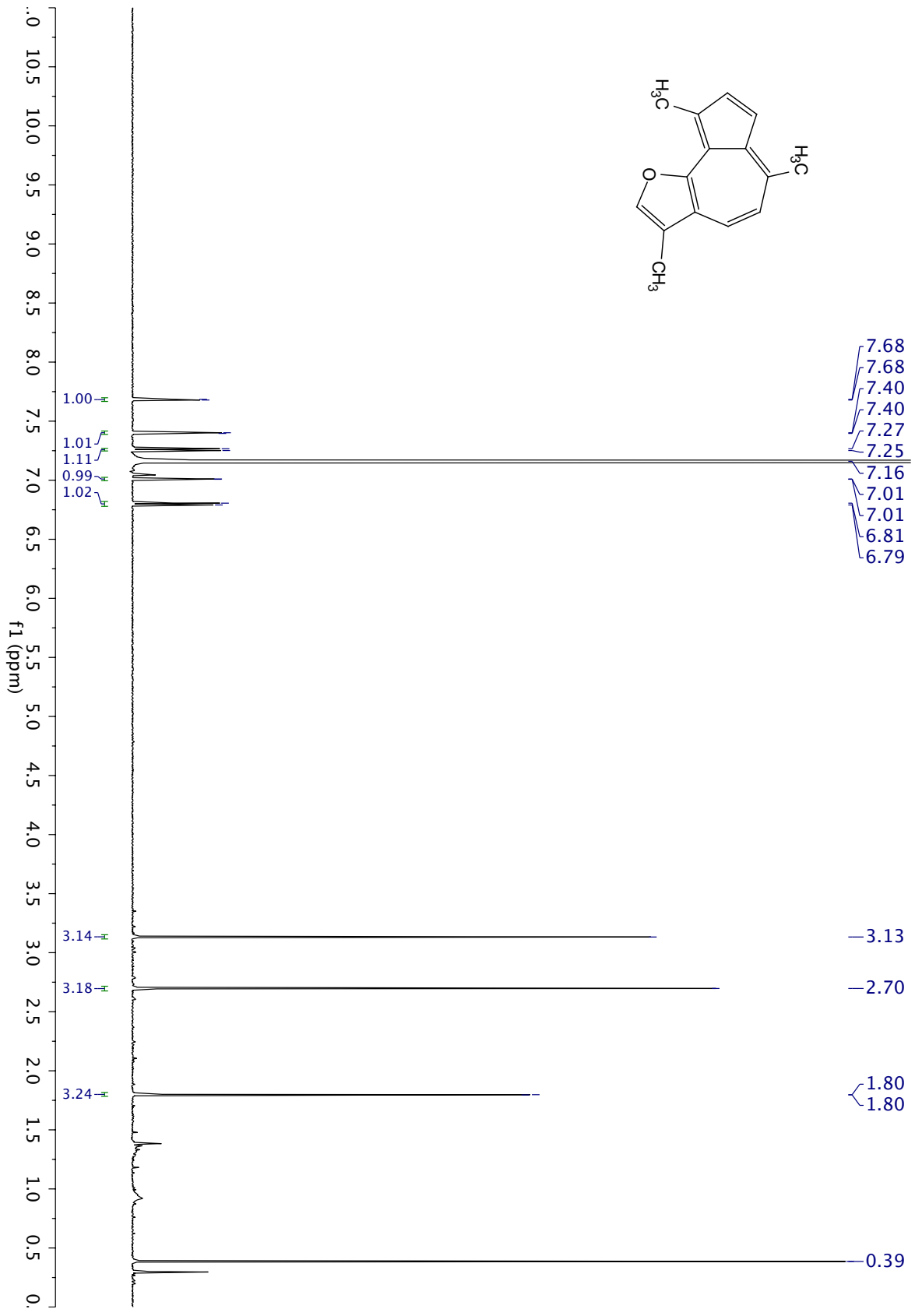


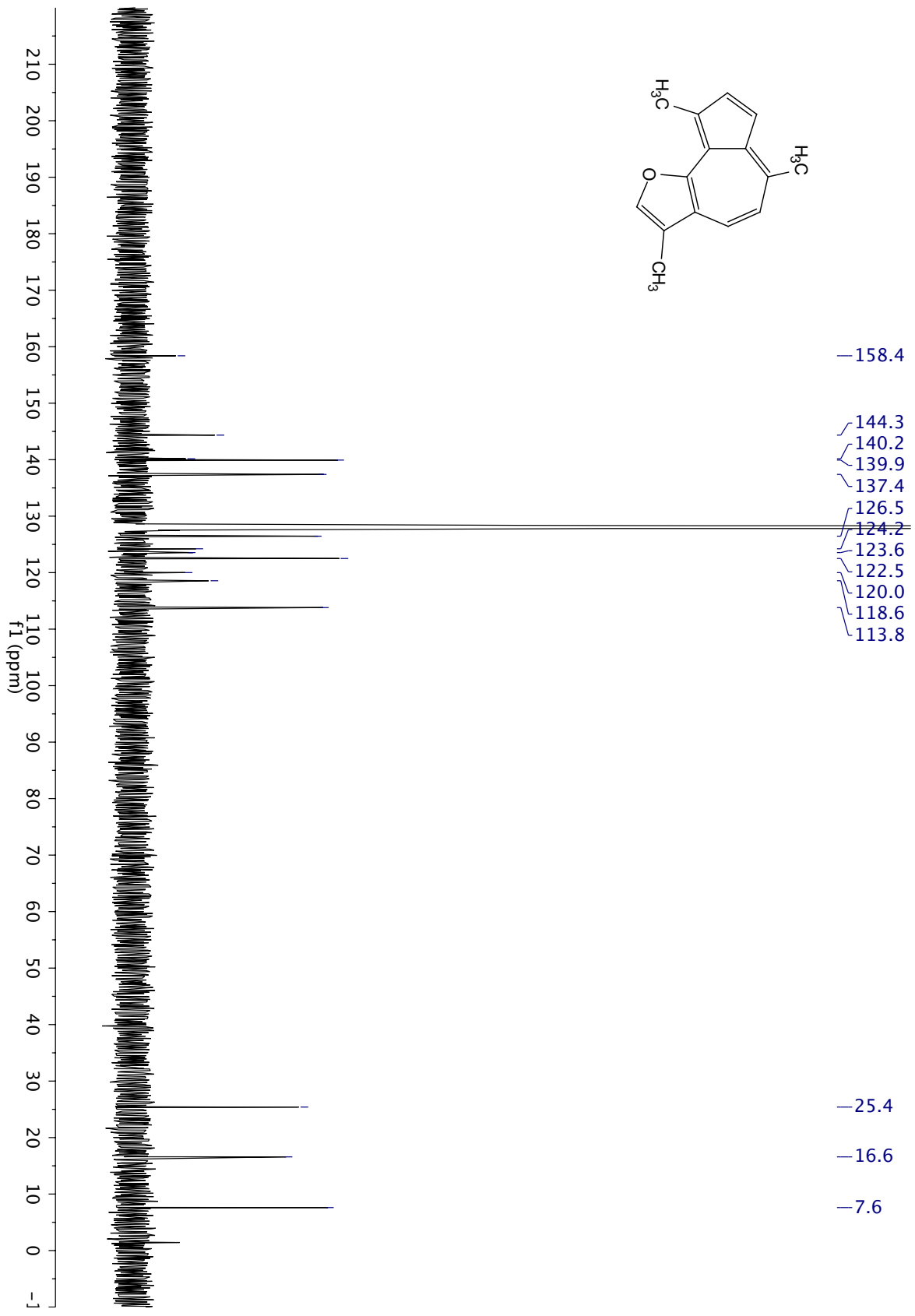


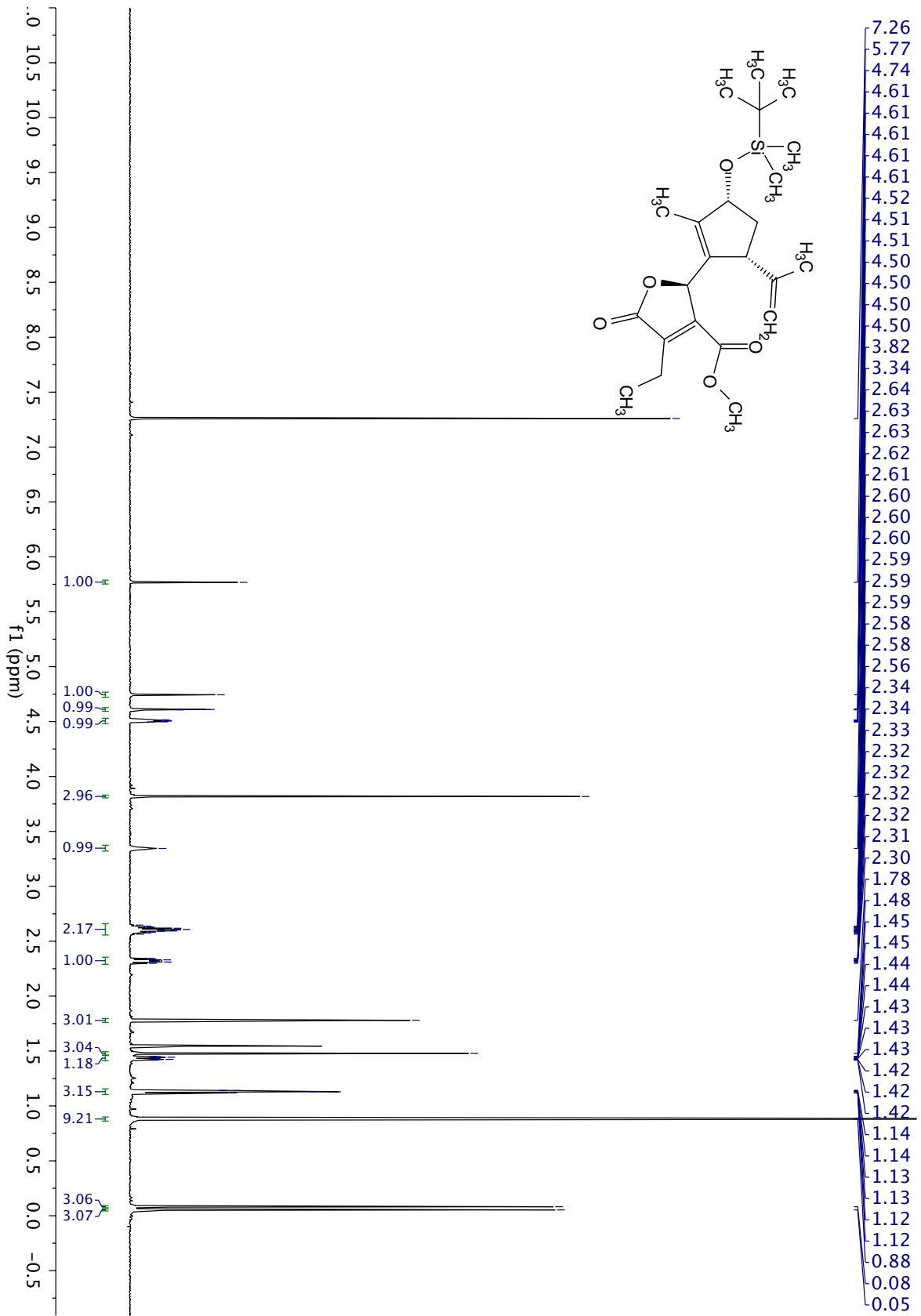


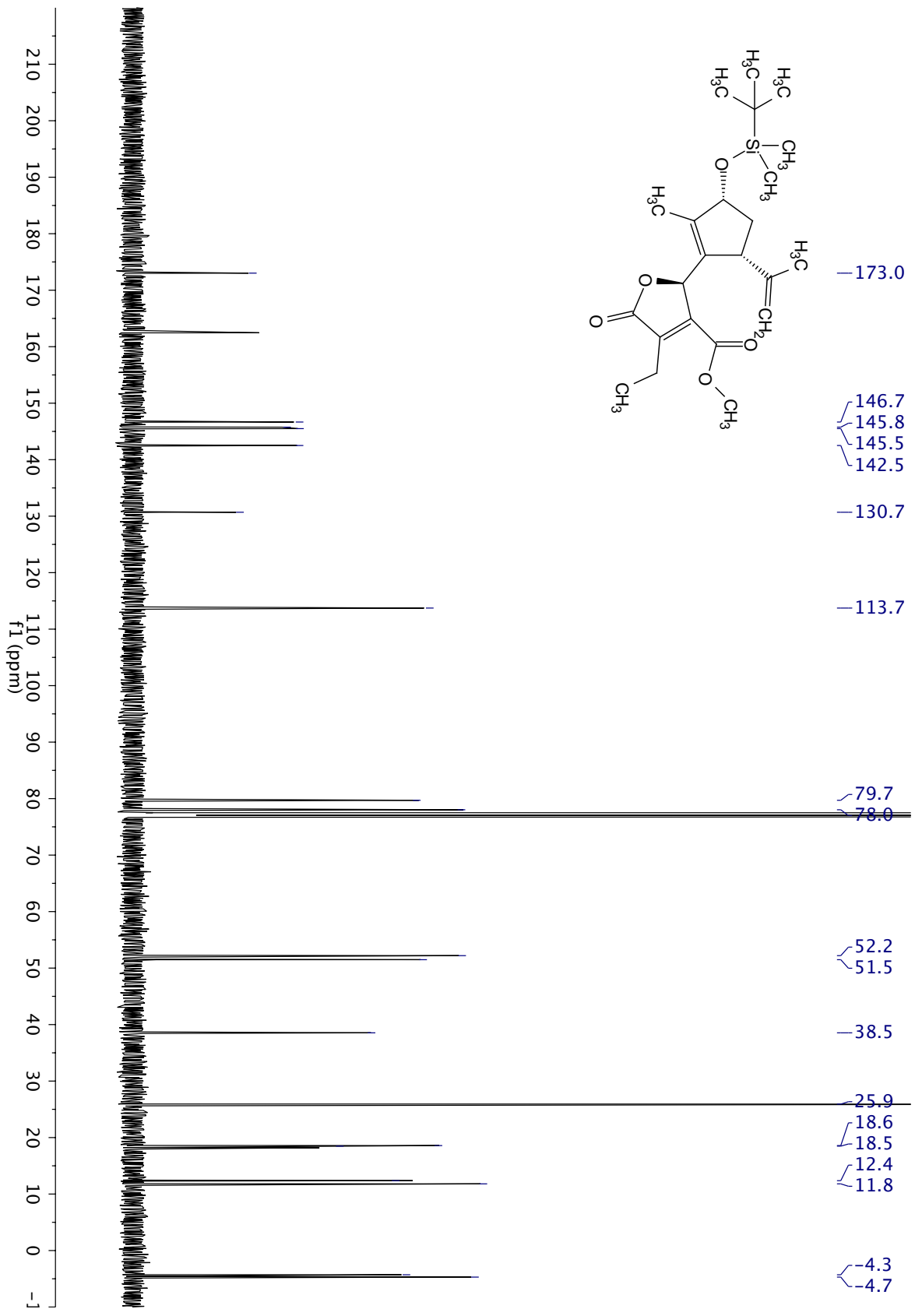


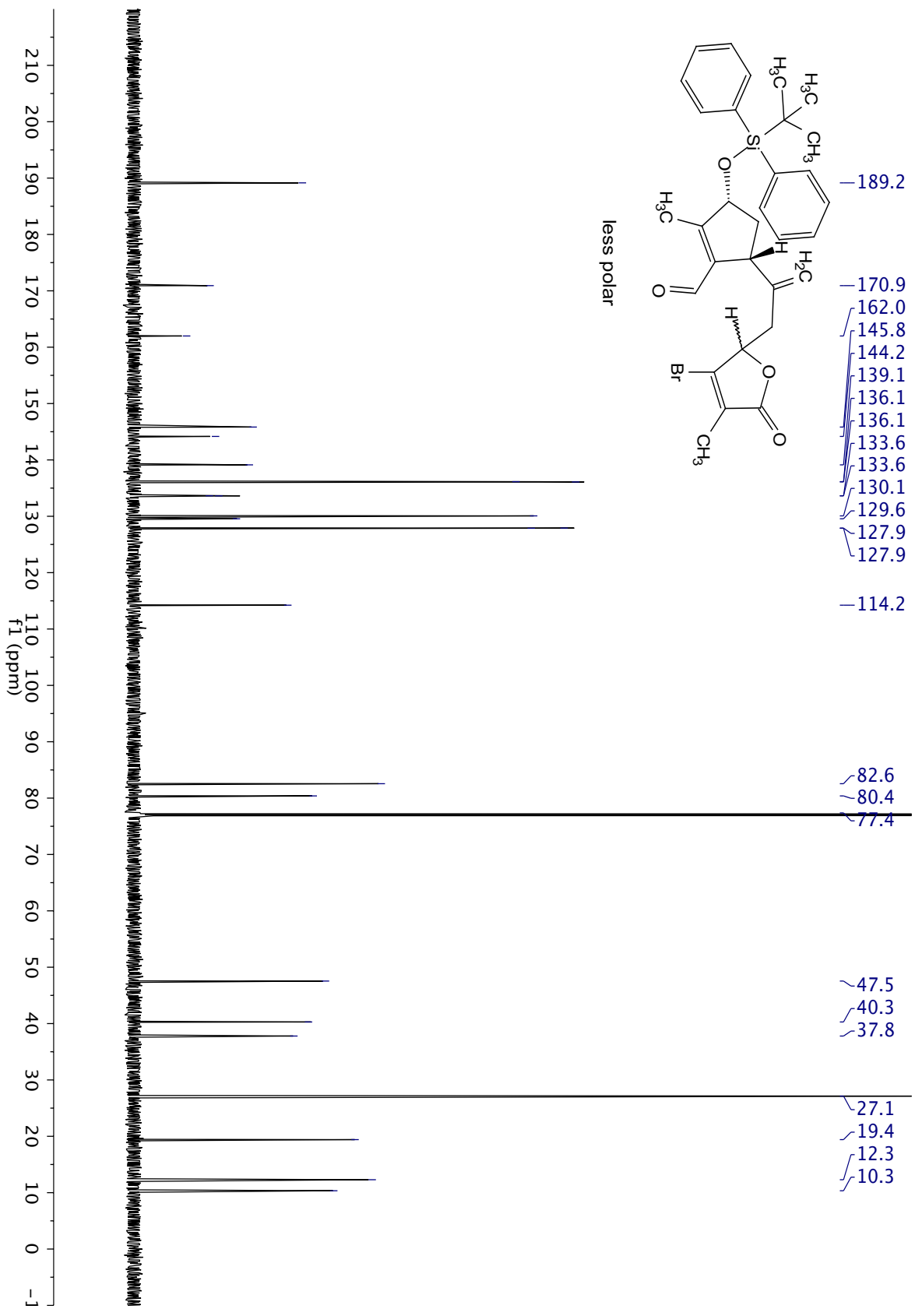


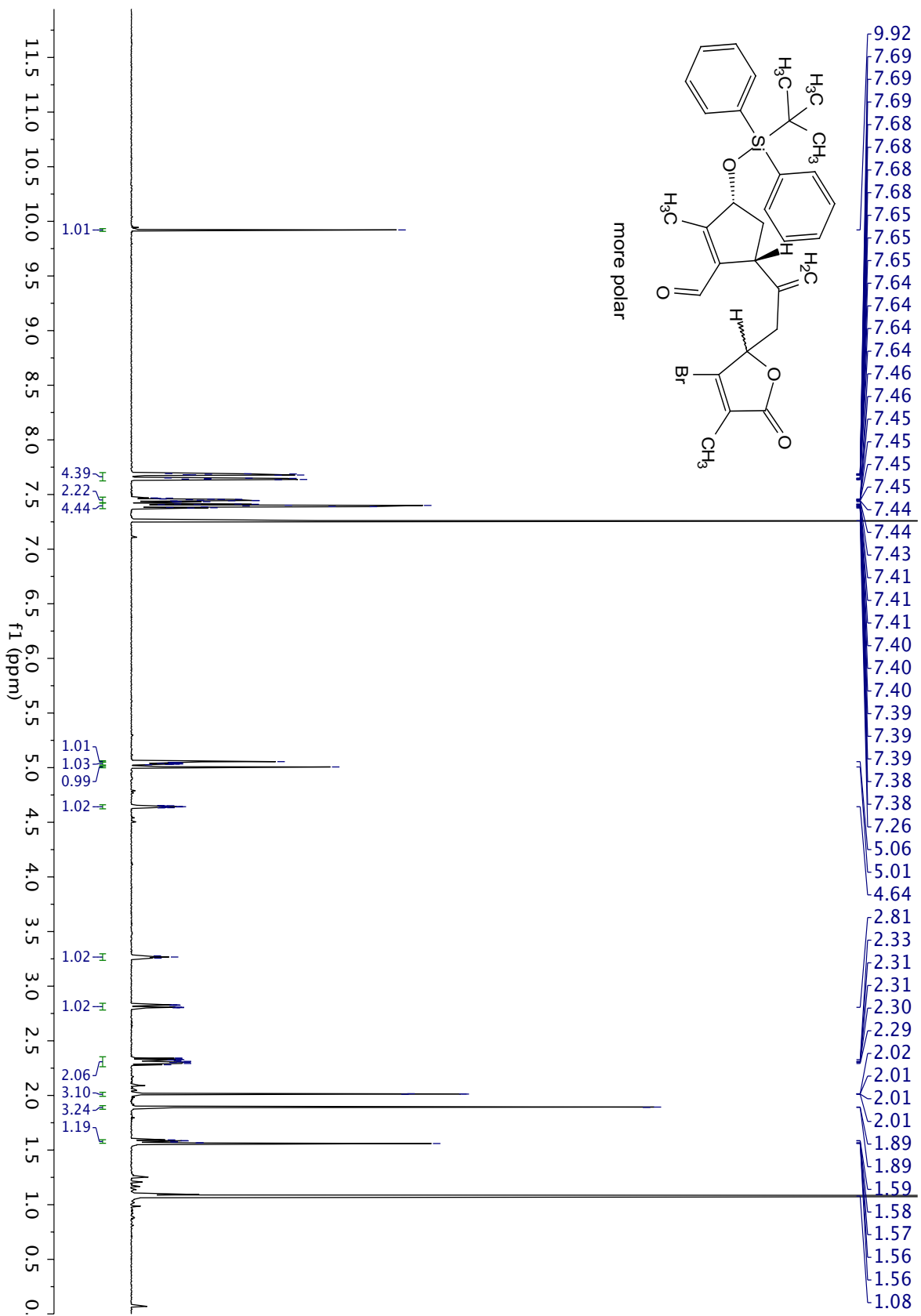


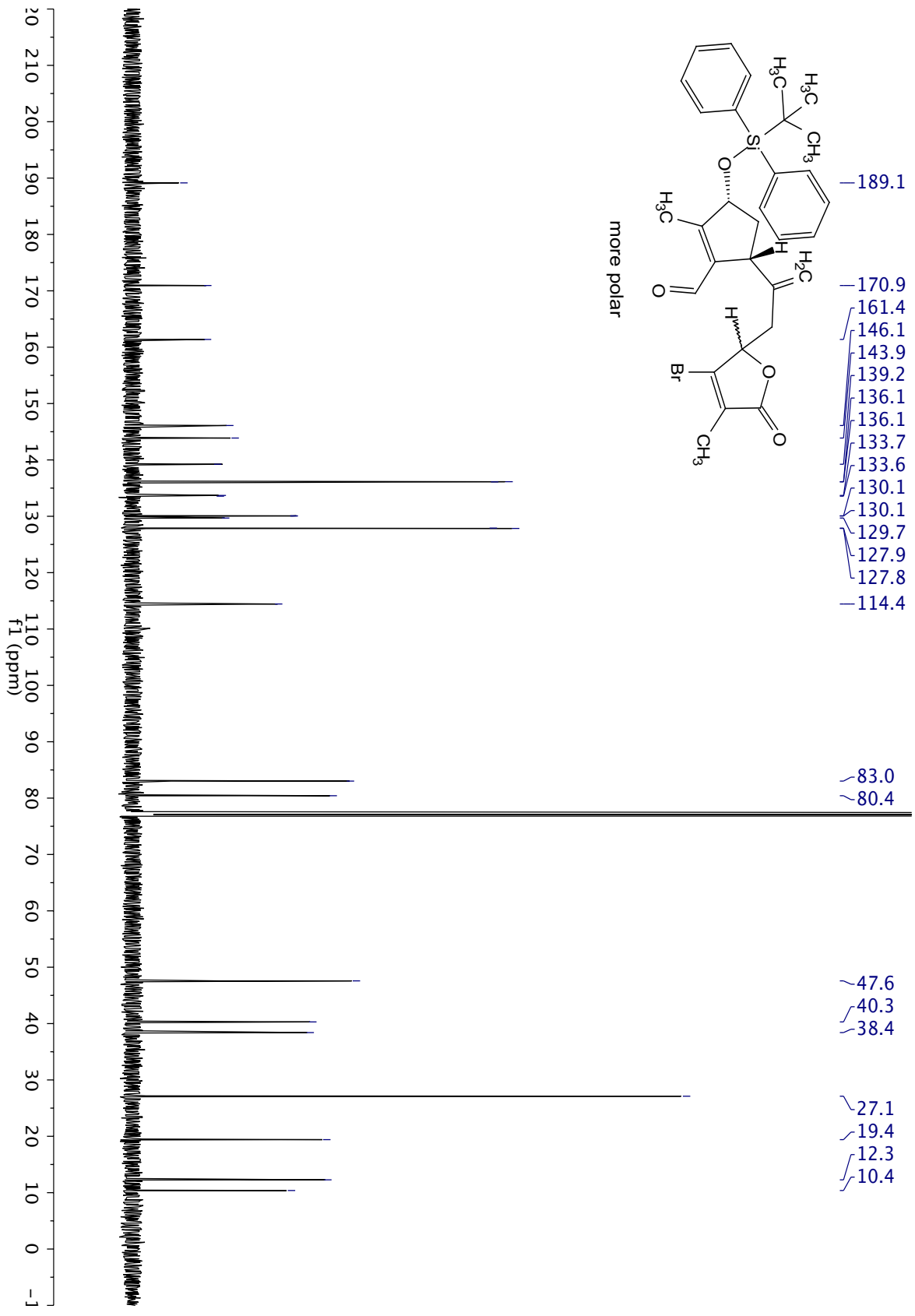


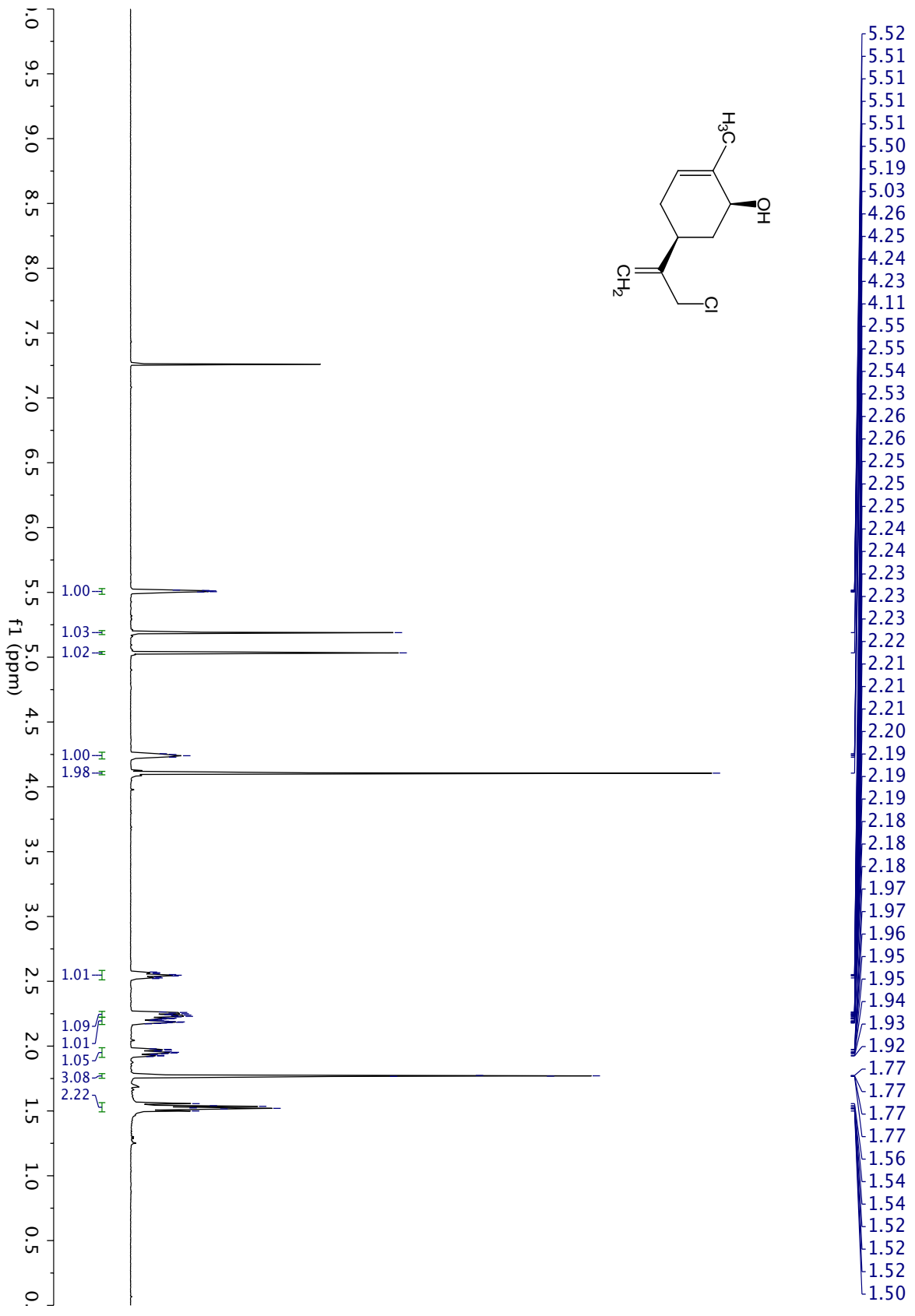




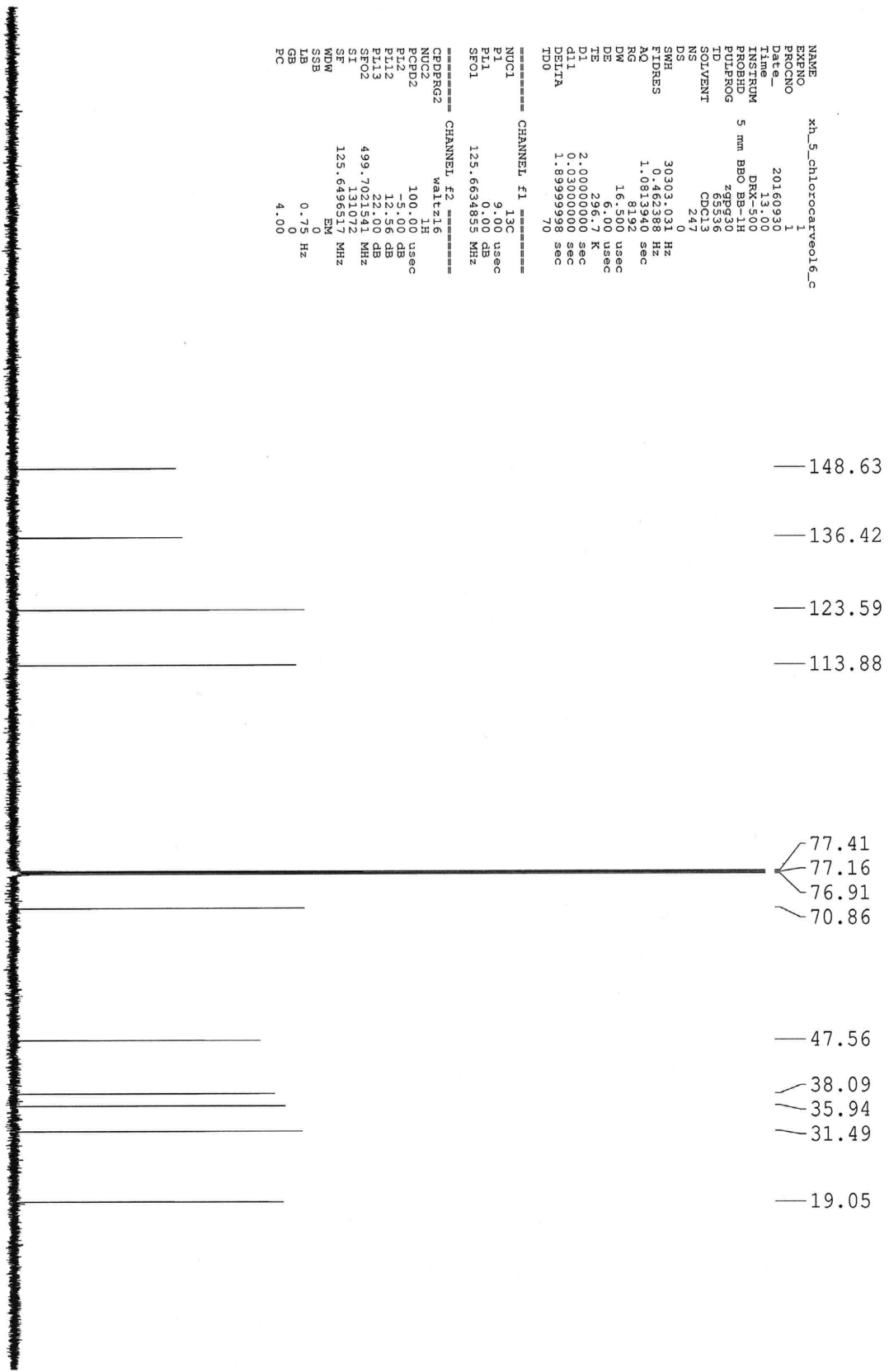






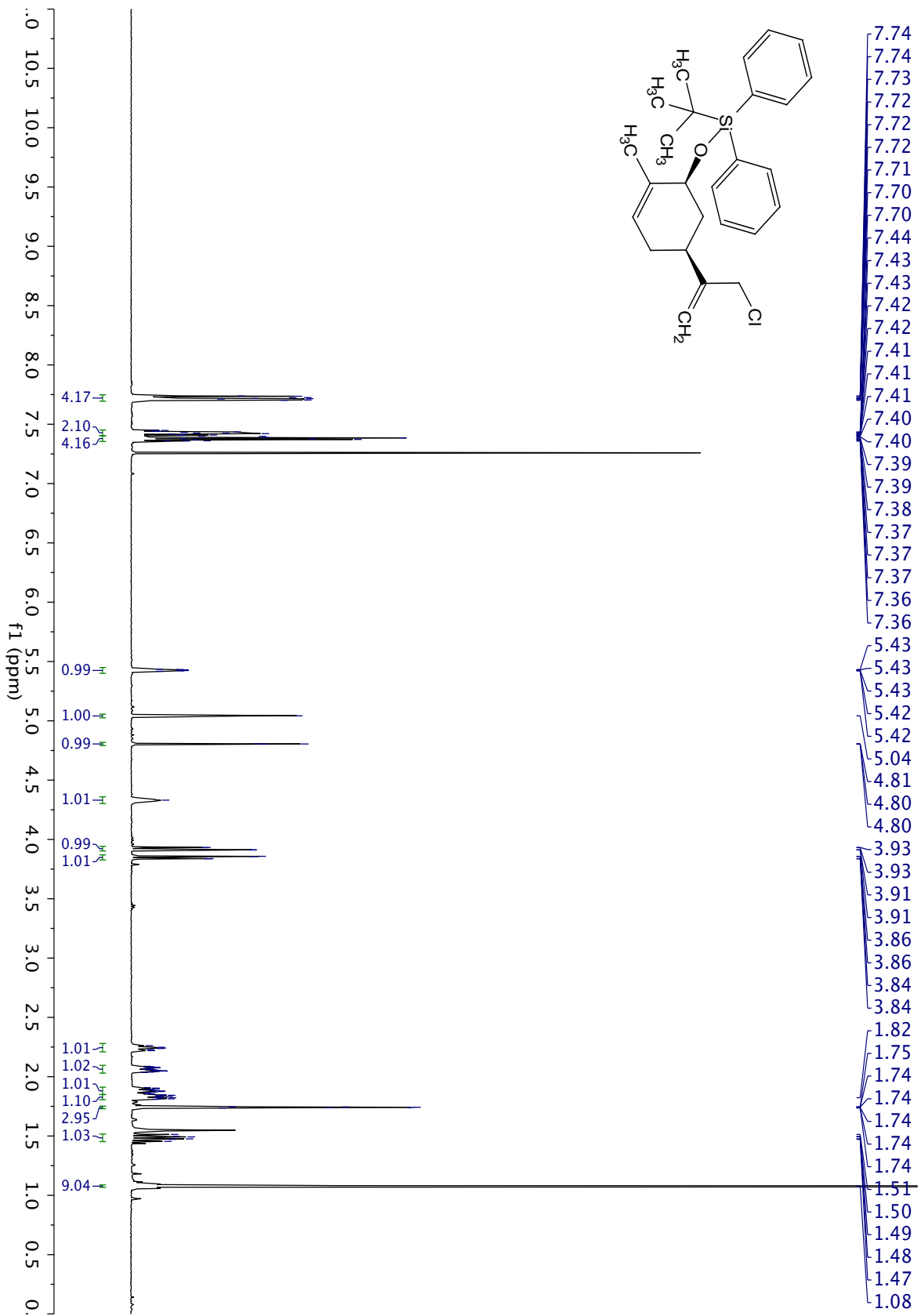


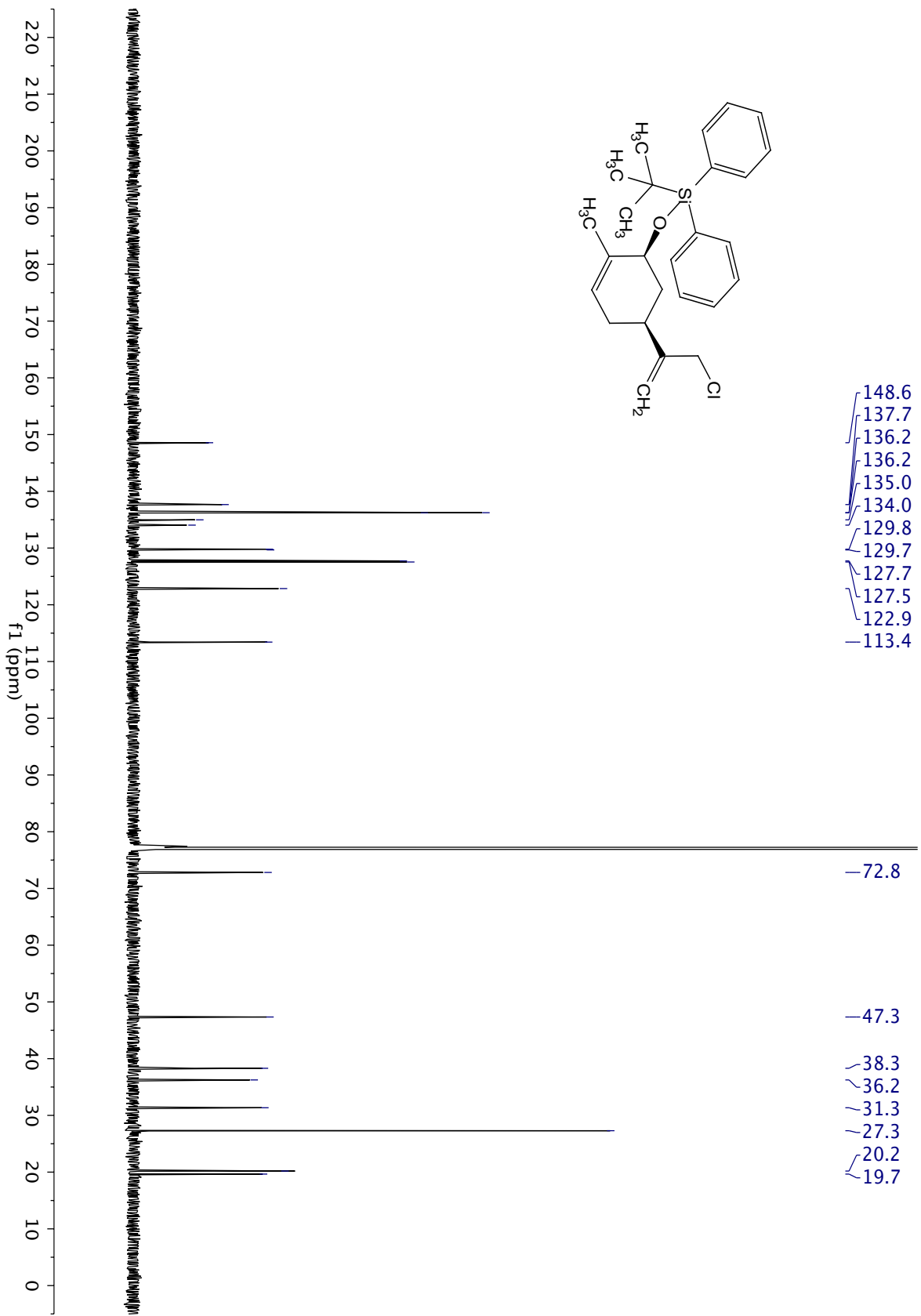
220 210 200 190 180 170 160 150 140 130 120 110 100 90 80 70 60 50 40 30 20 10 0 ppm

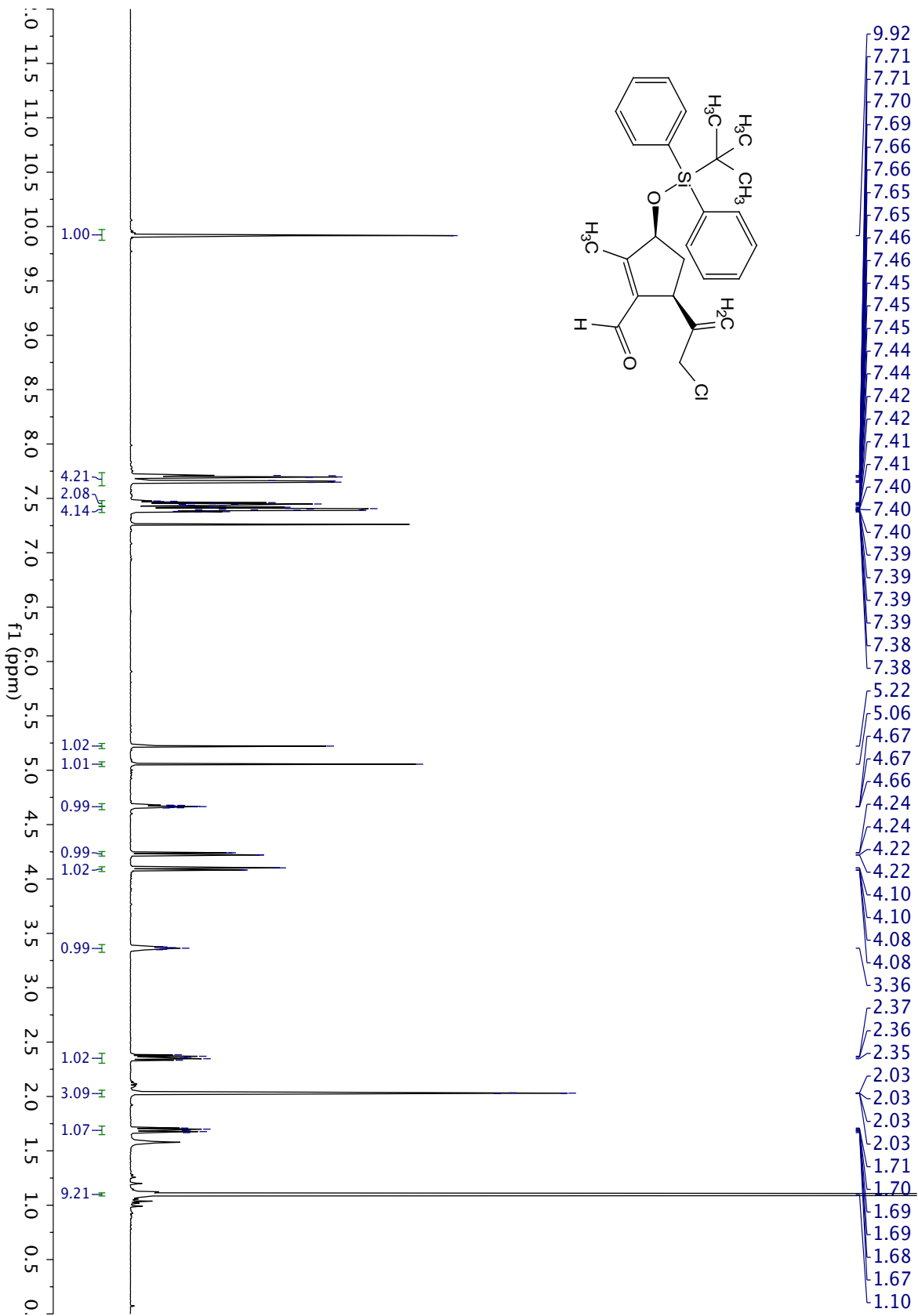


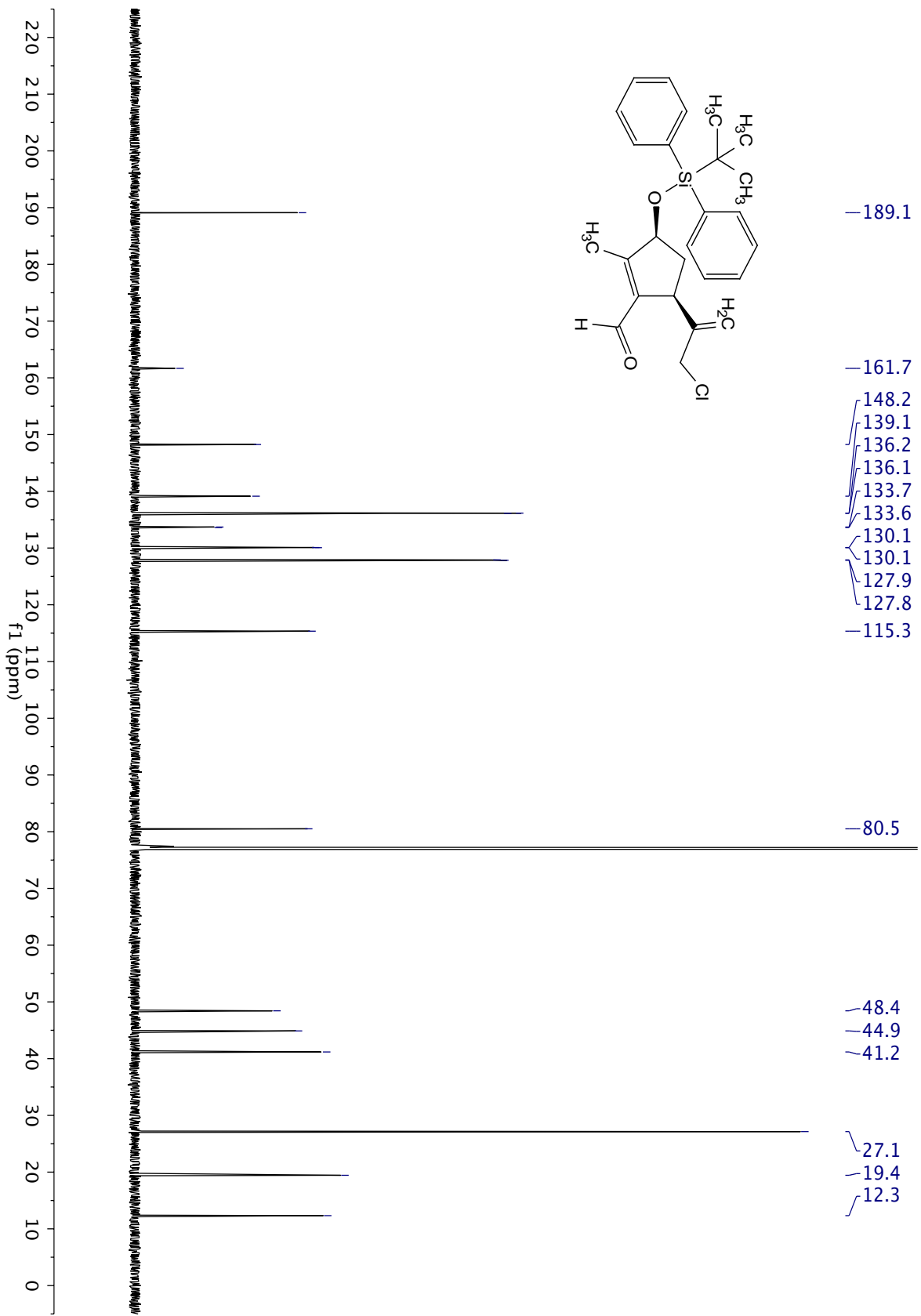
```

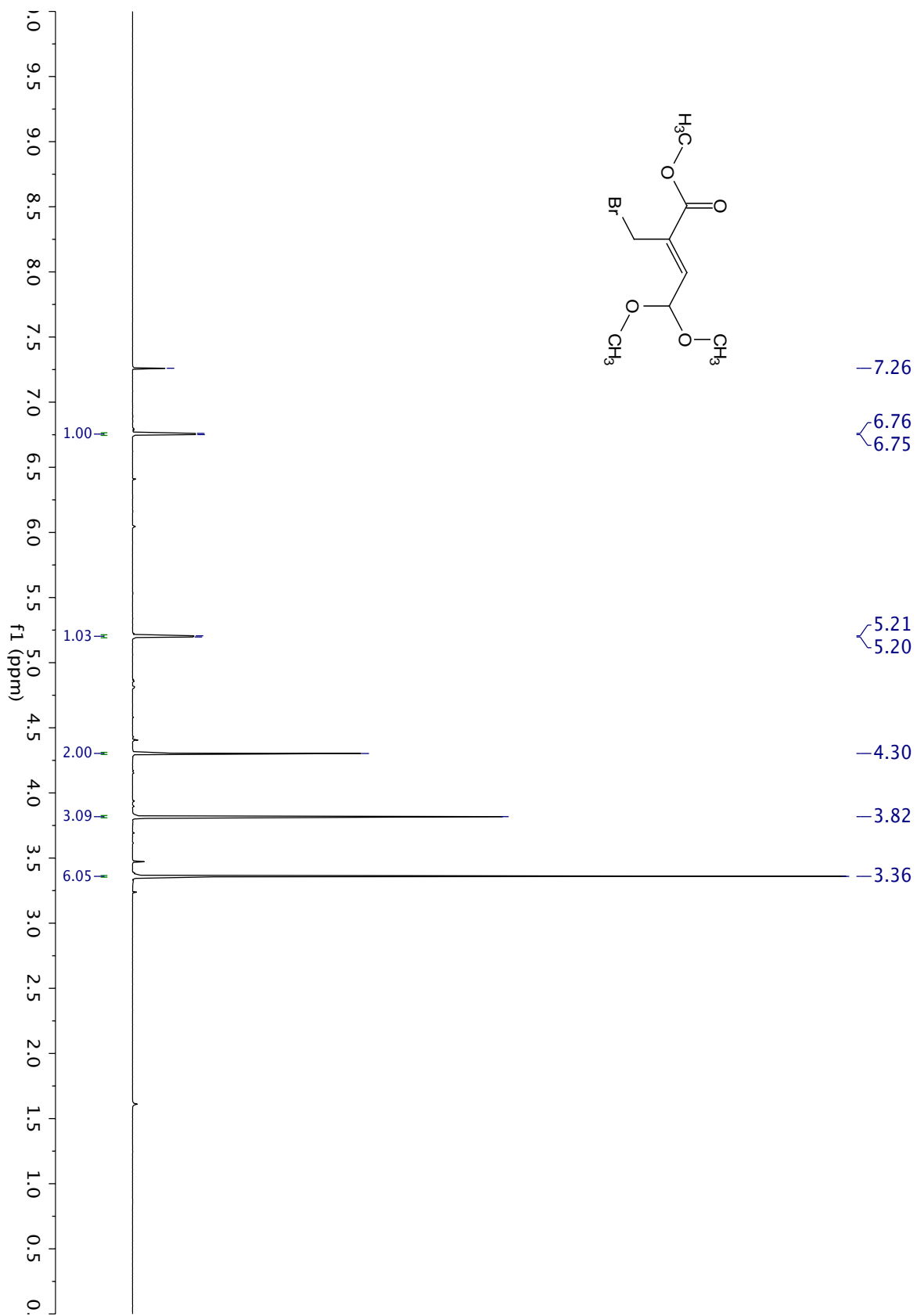
NAME kh_5-chlorocarveol6_c
EXPNO 1
PROCNO 1
Date_ 20160930
Time 13.00
INSTRUM 5 mm BBO BB-1H
PROBHD 4mm1H
PULPROG zgpg30
TD 65536
SOLVENT CDCl3
NS 247
DS 0
SWH 30303.031 Hz
FIDRES 0.462388 Hz
AQ 1.0813940 sec
RG 8192
DM 16.500 usec
DE 6.00 usec
TE 296.7 K
NUC1 13C
NUC2 13C
PCPD2 100.00 usec
PI1 9.00 usec
PI2 5.00 dB
PI3 12.56 dB
SFO2 499.7021541 MHz
SI 131072
SF 125.6496517 MHz
WDW EM
SSB 0
LB 0
GB 0
FC 4.00
  
```

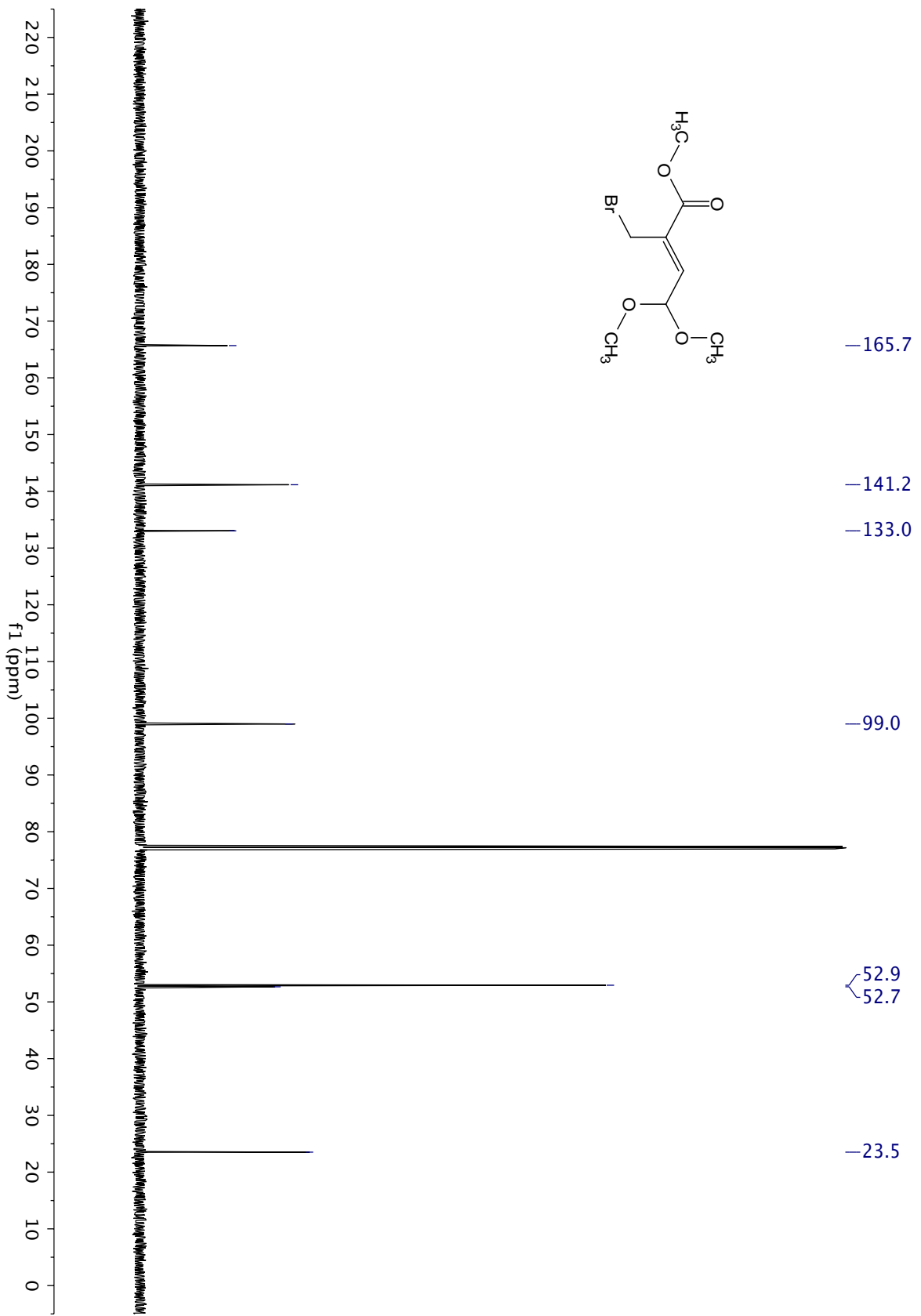


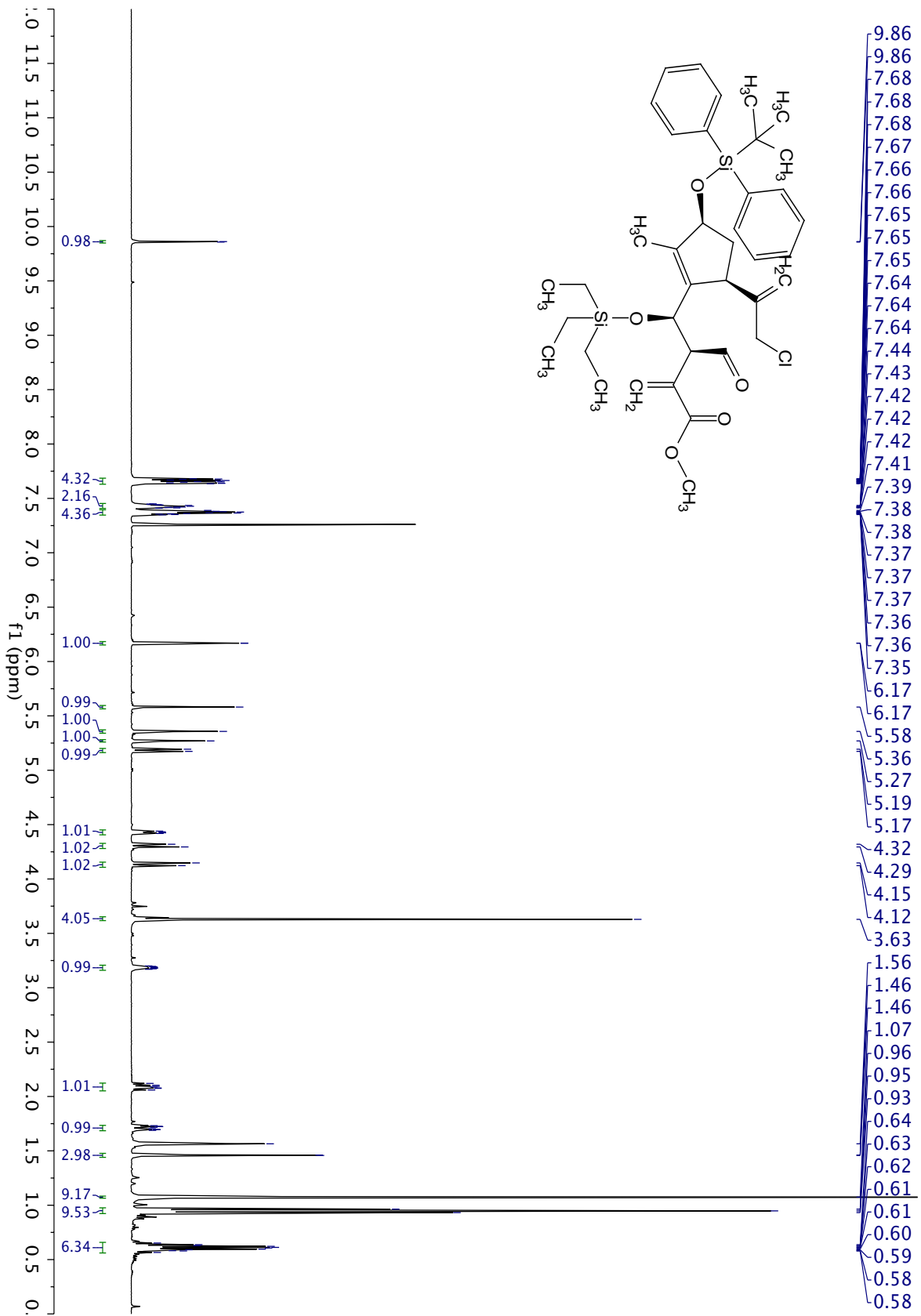


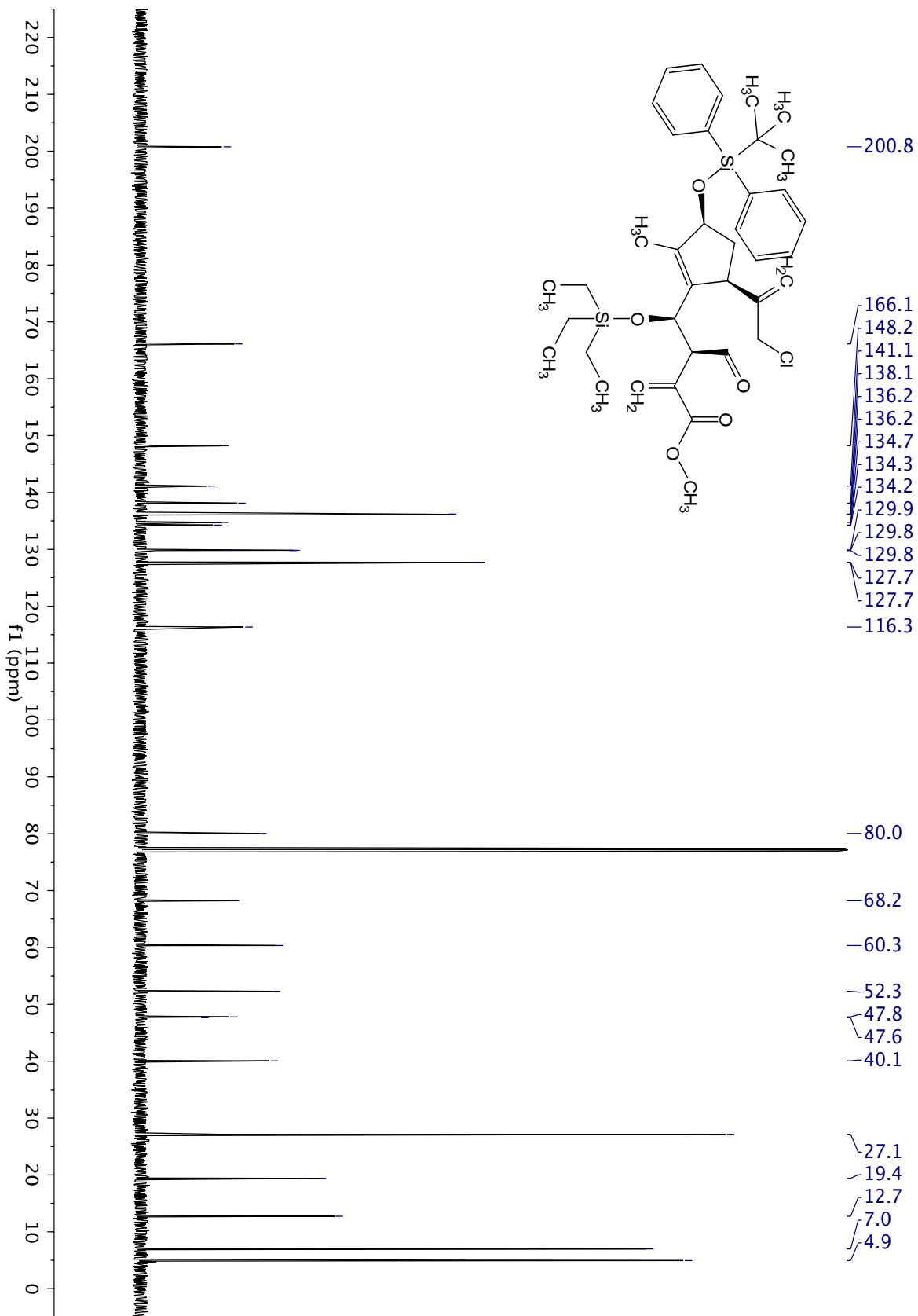


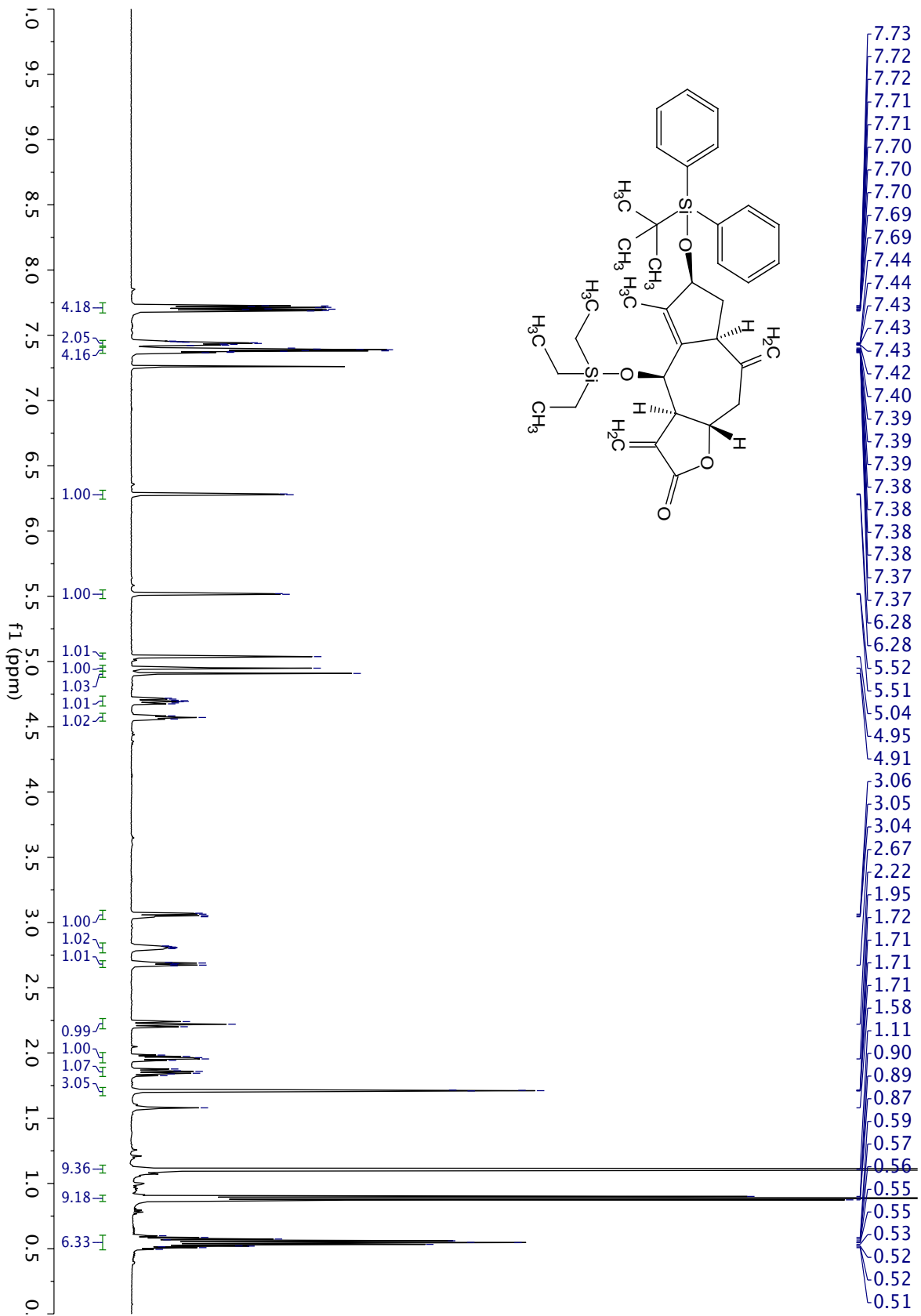


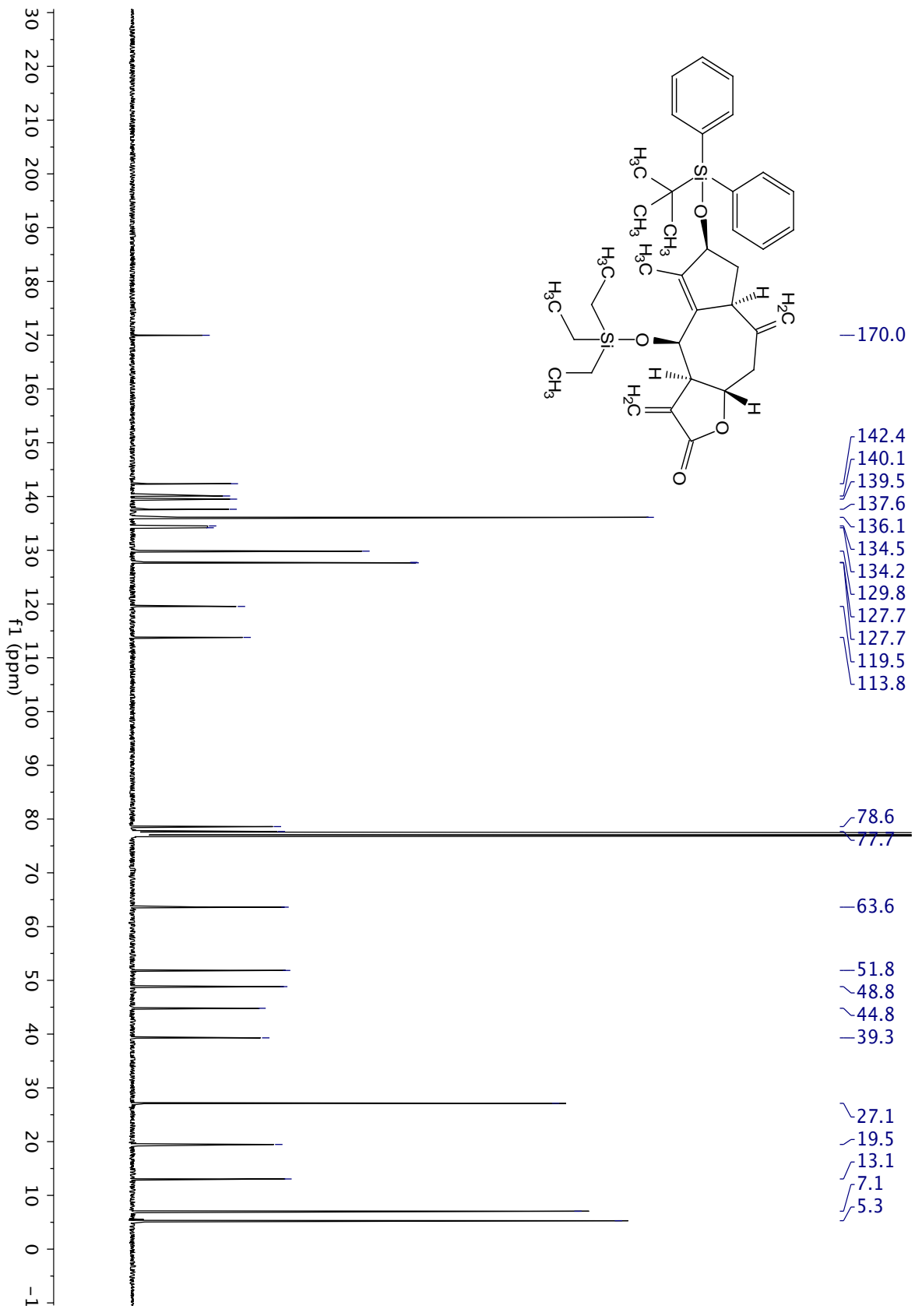


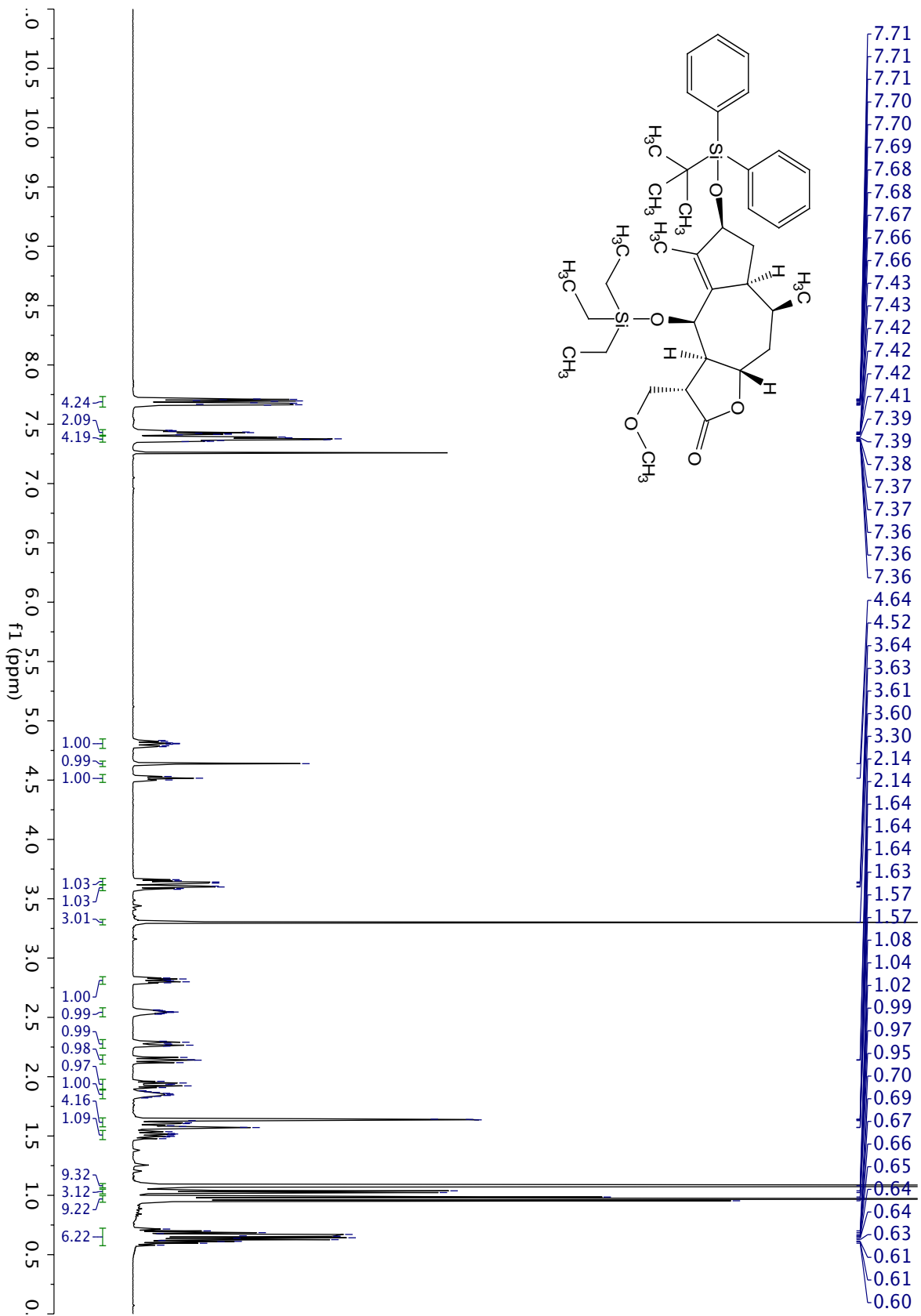


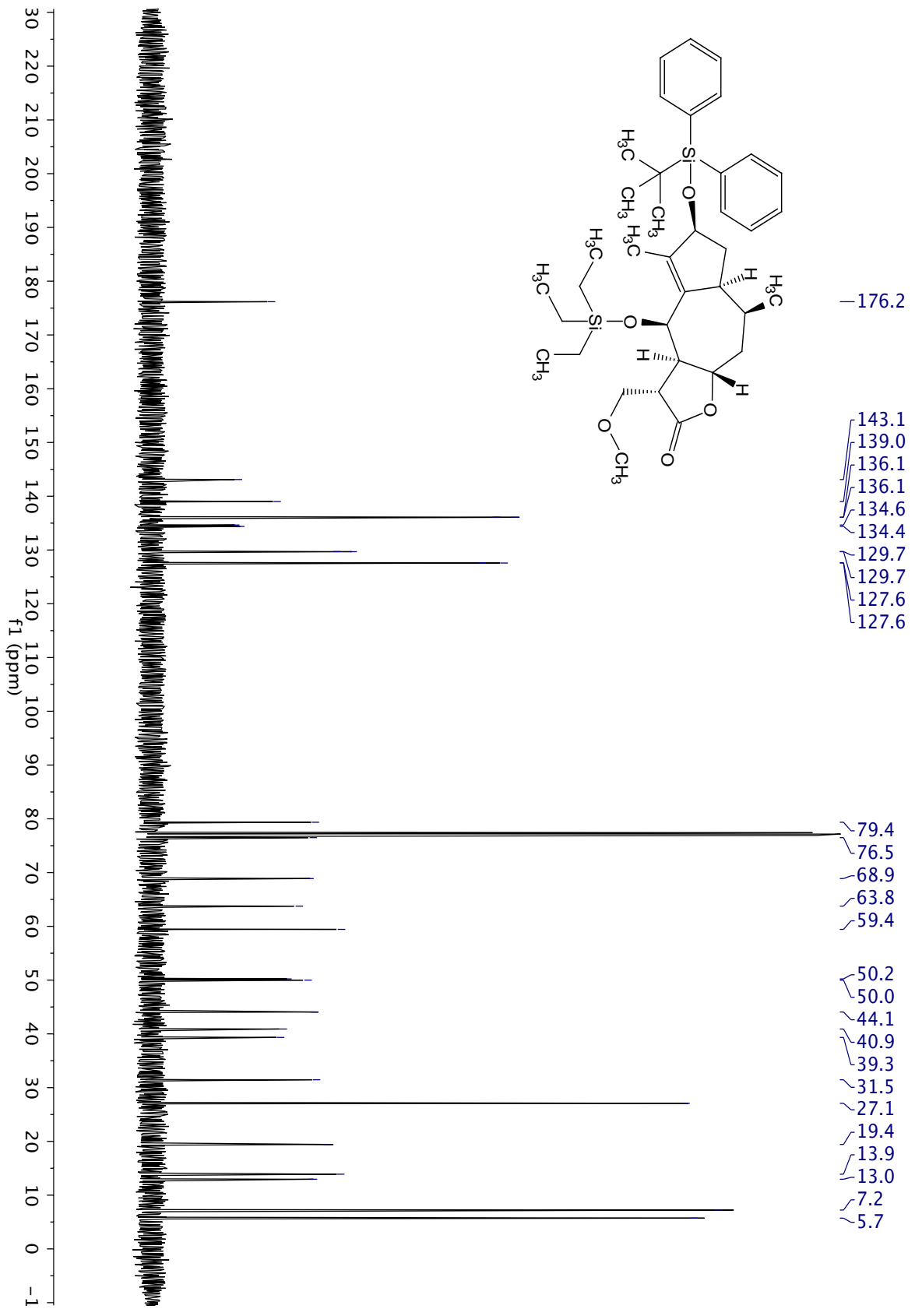


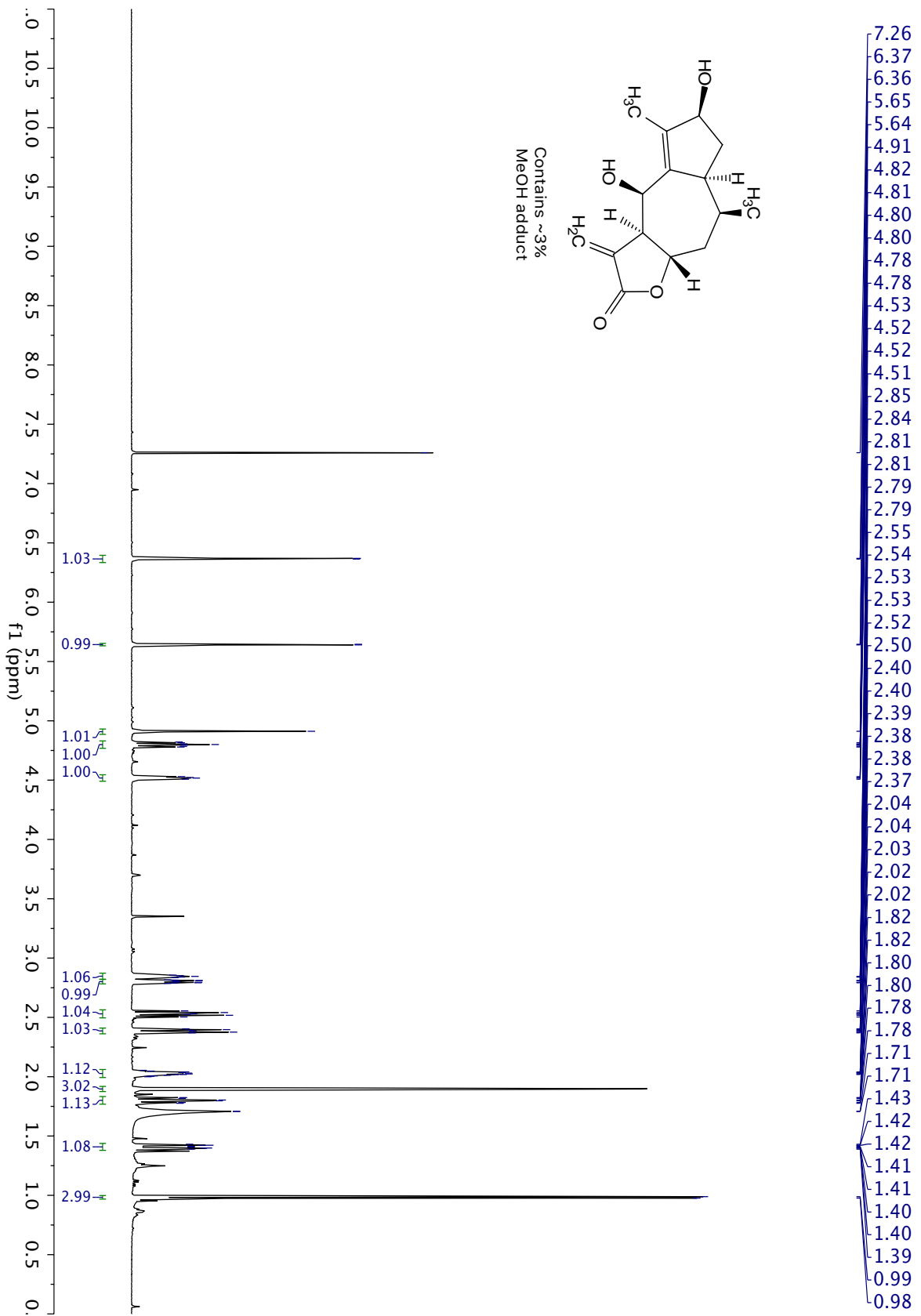


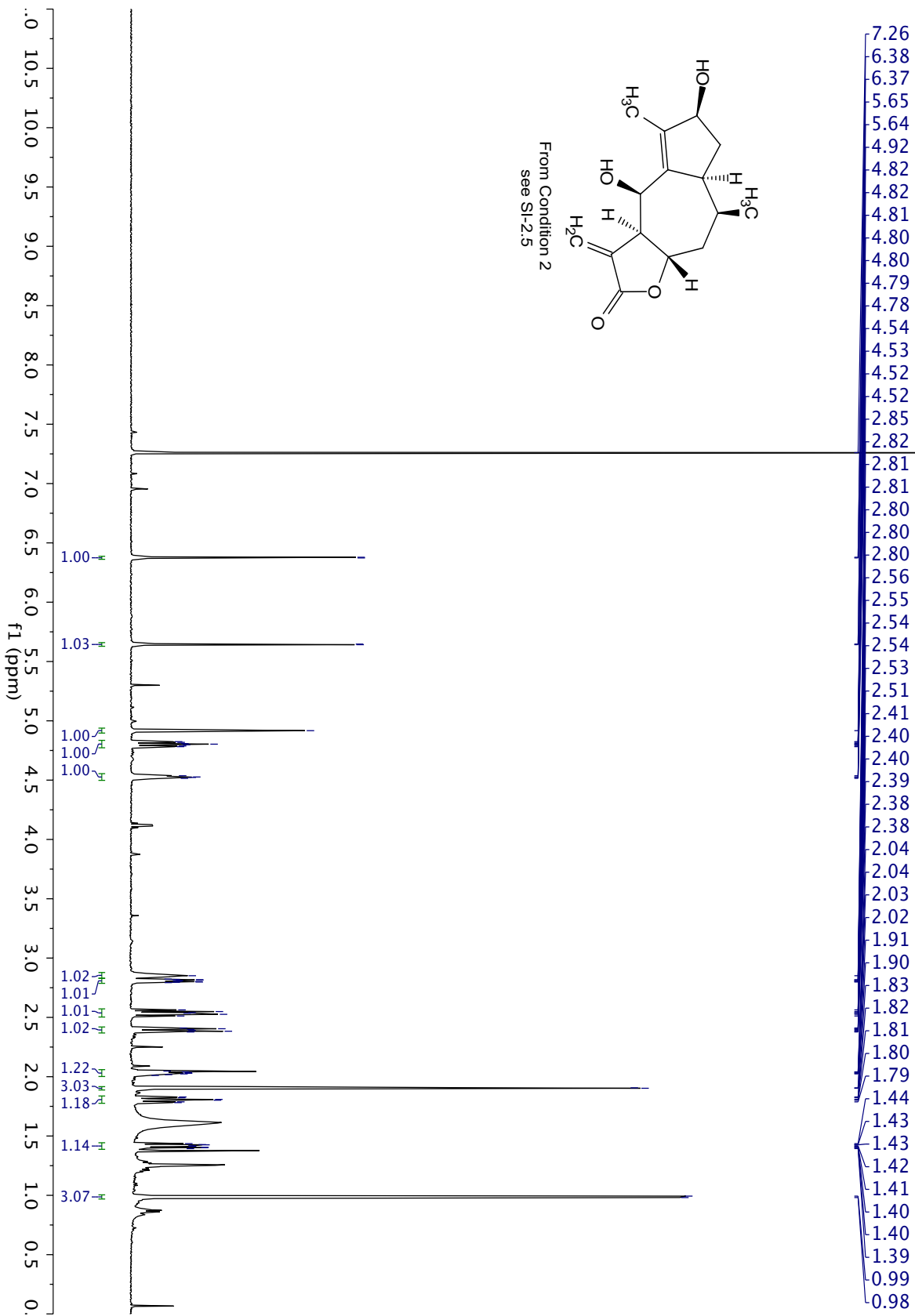


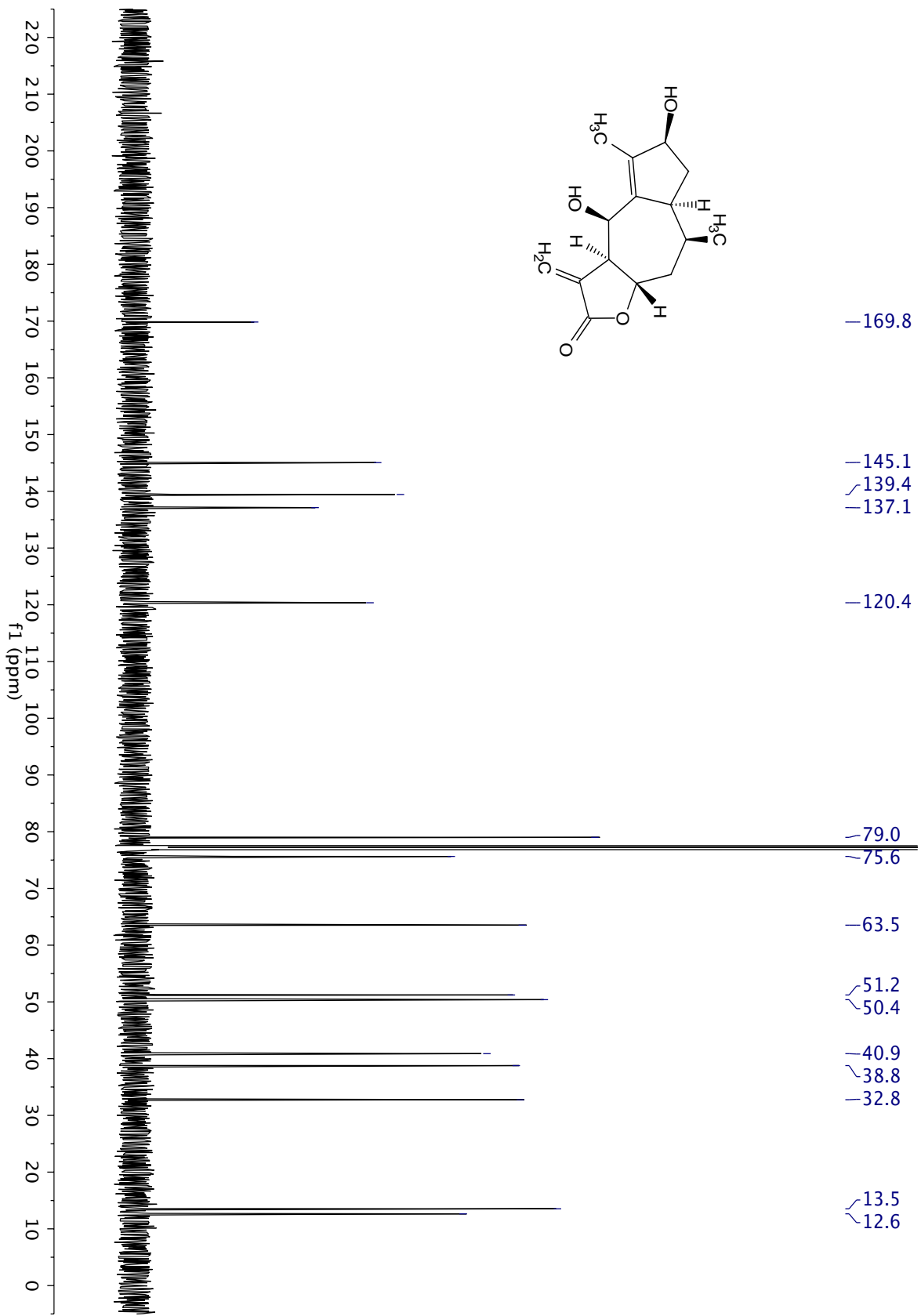


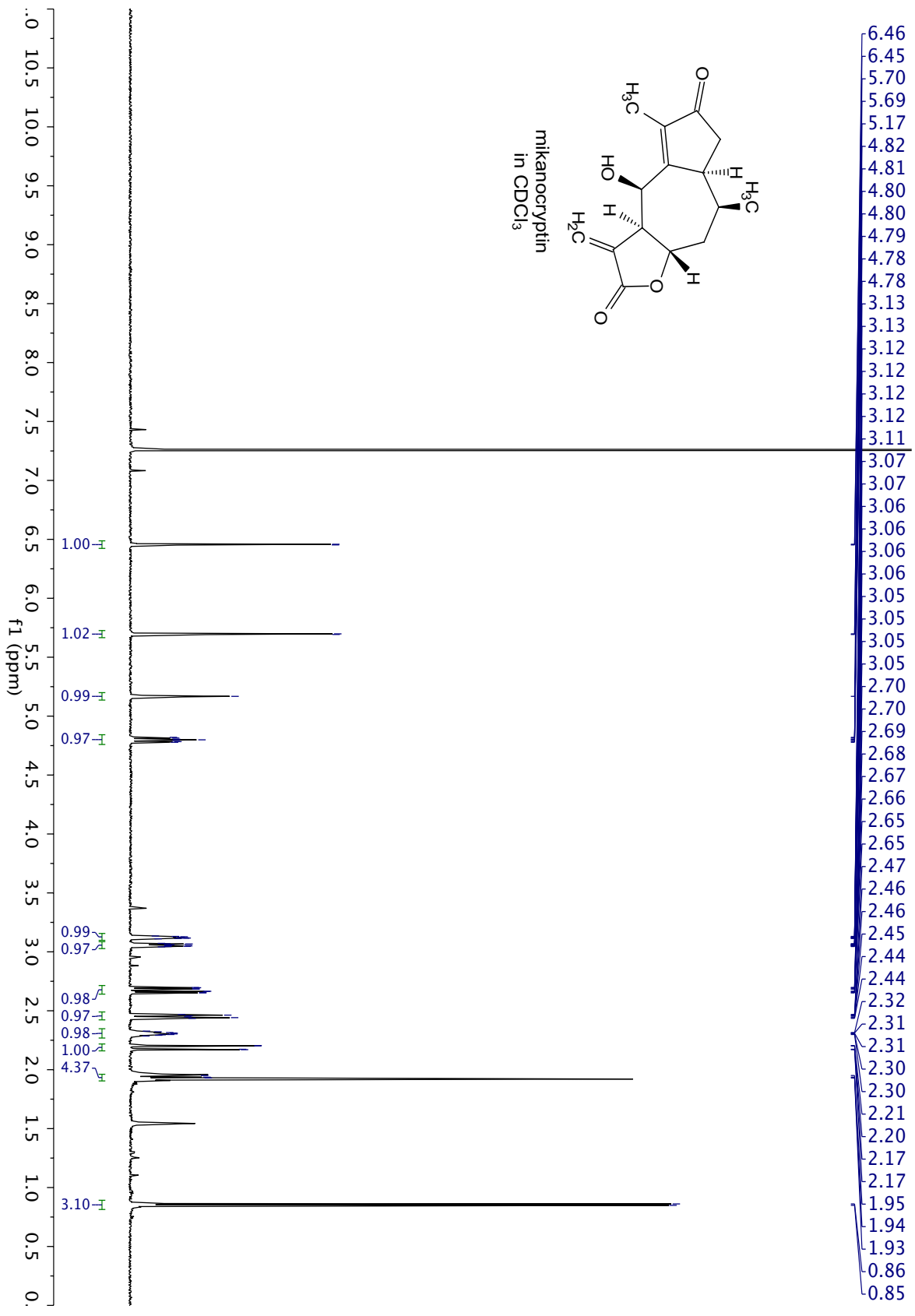


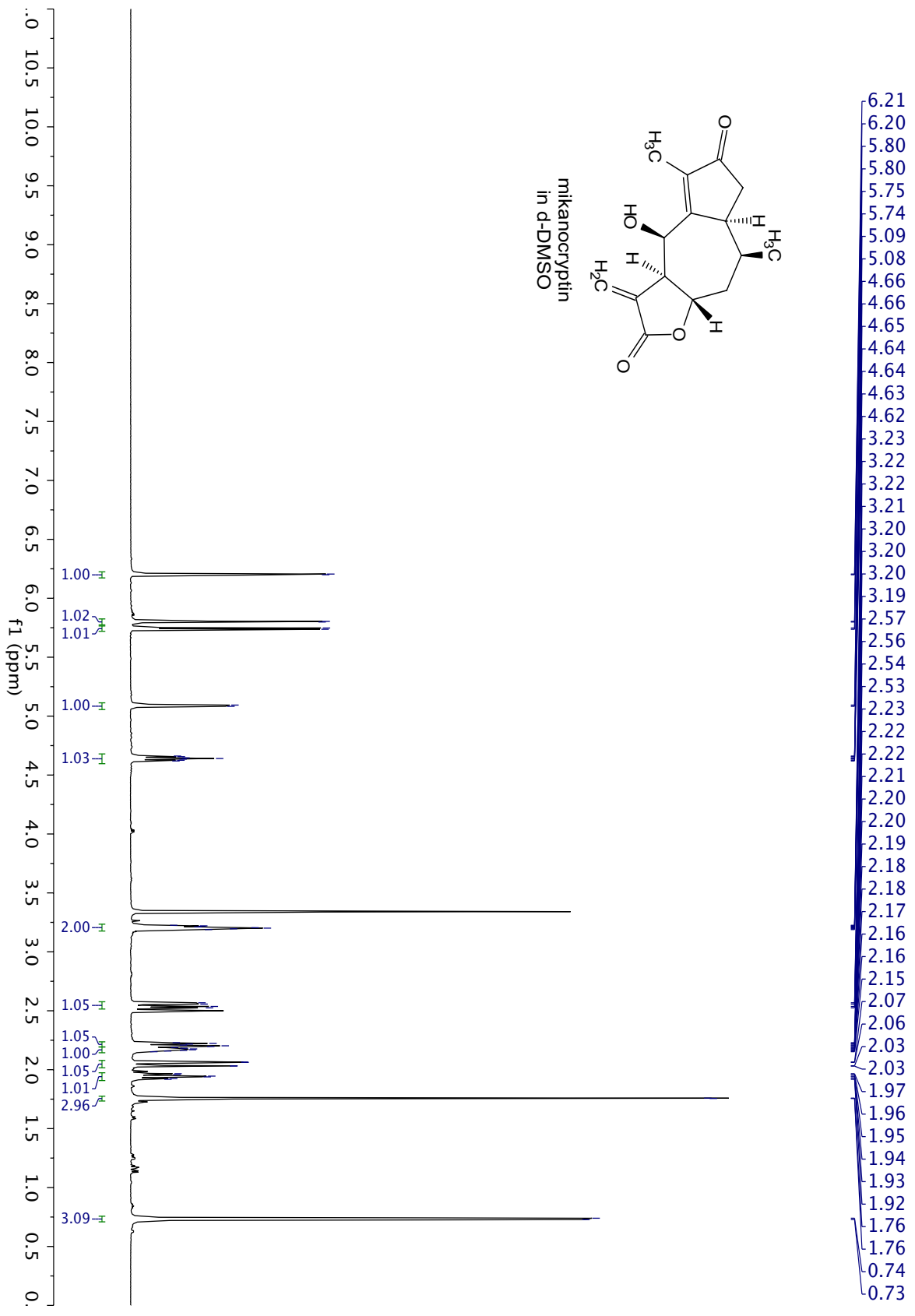


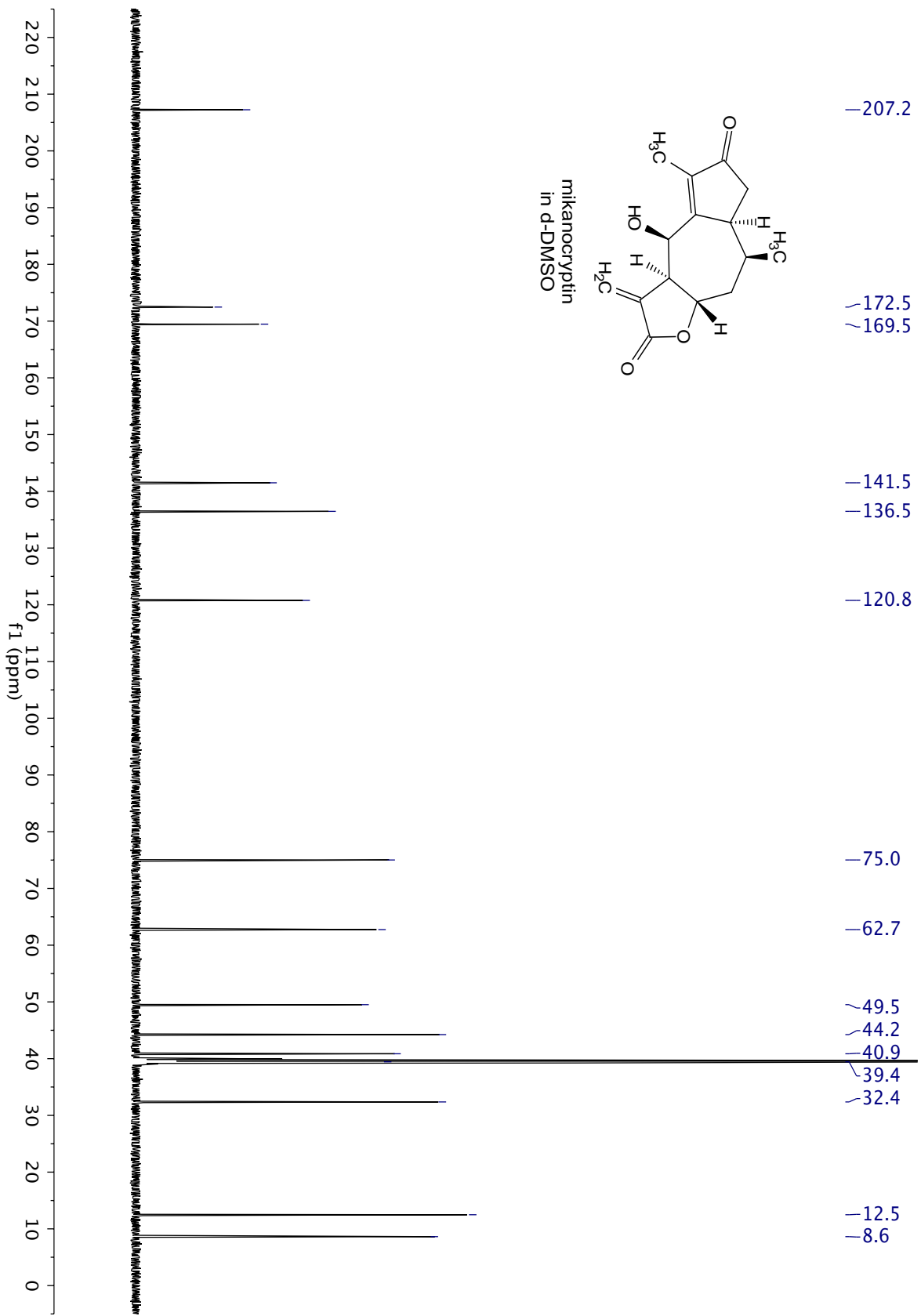


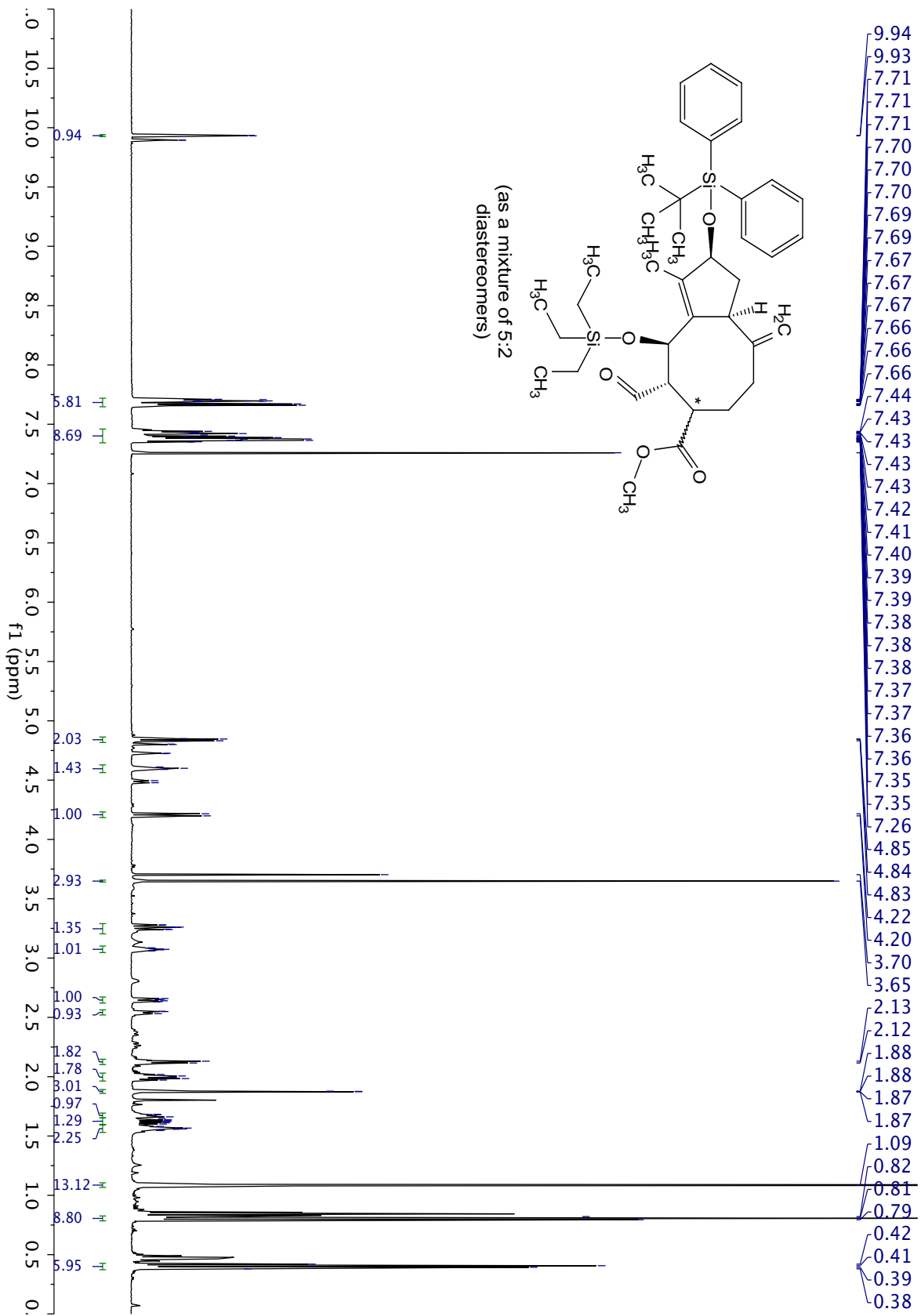


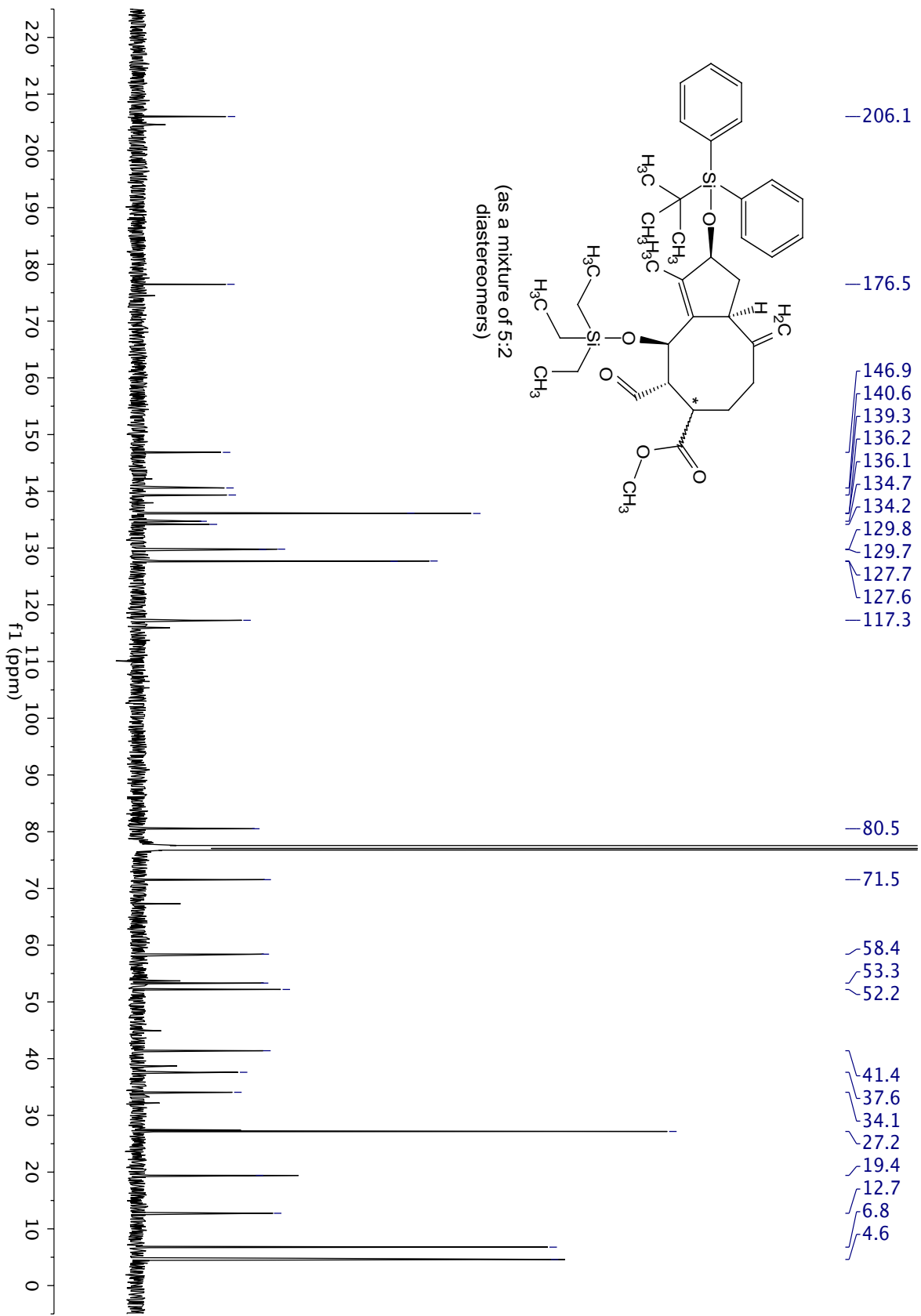


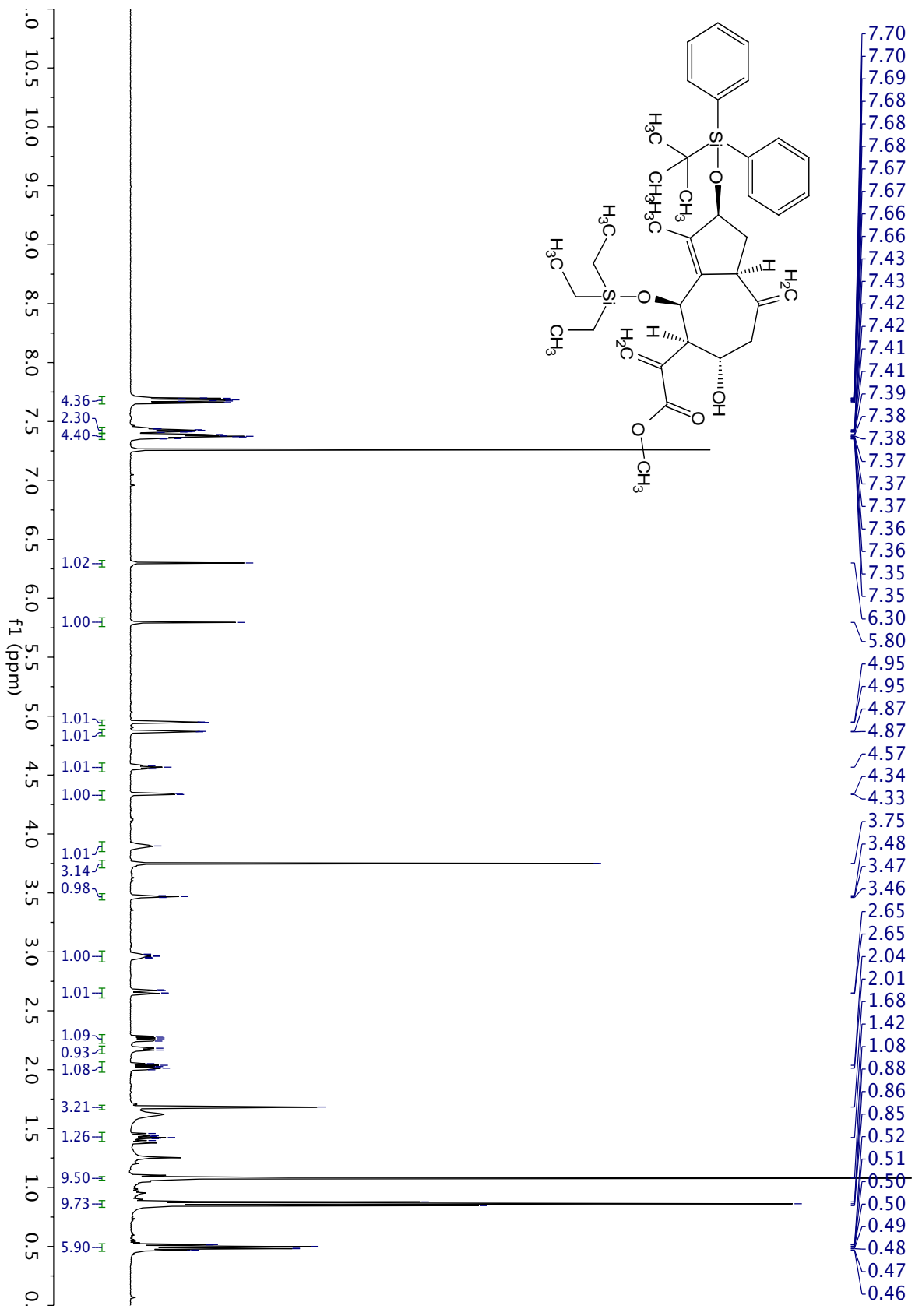


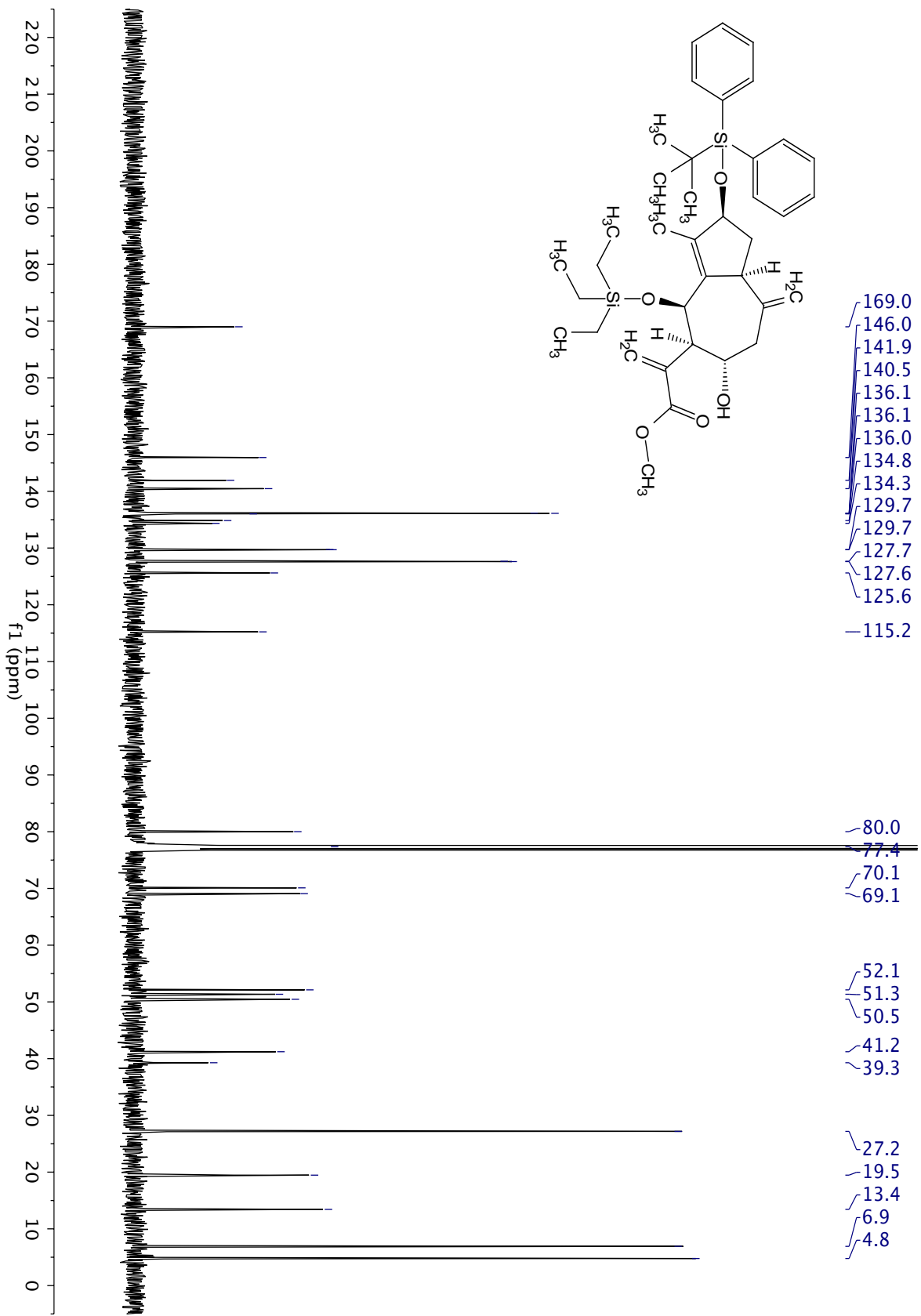


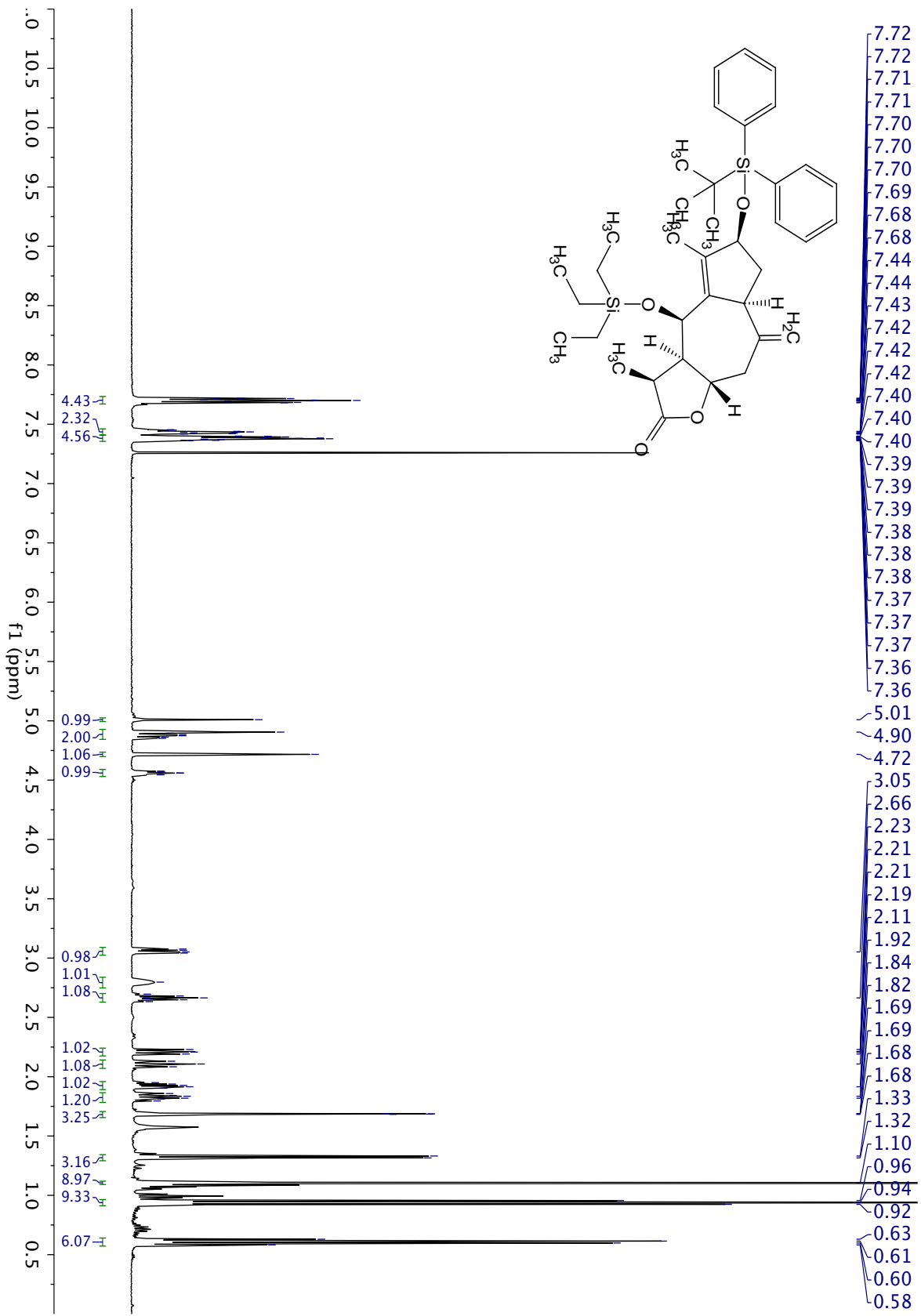


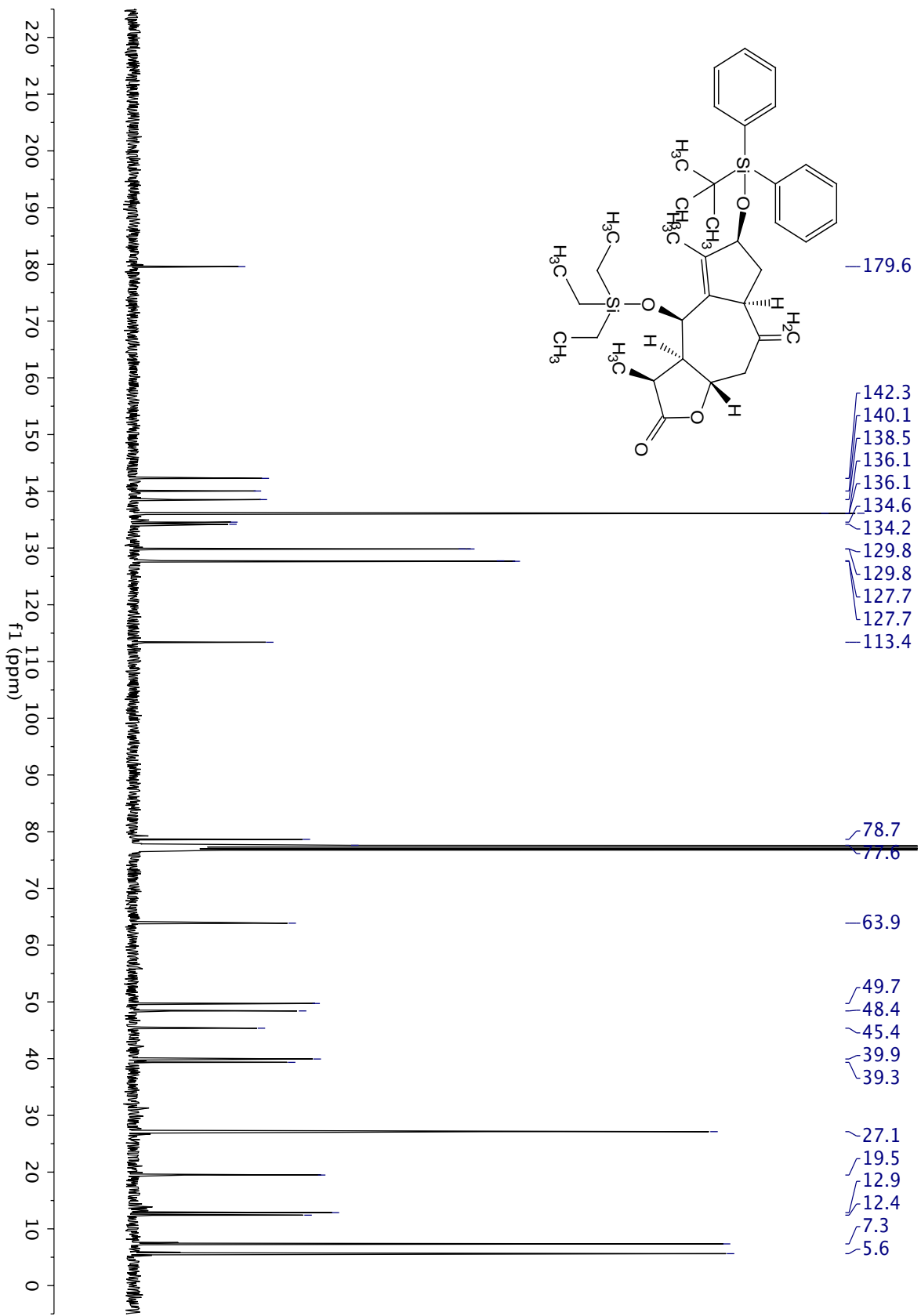


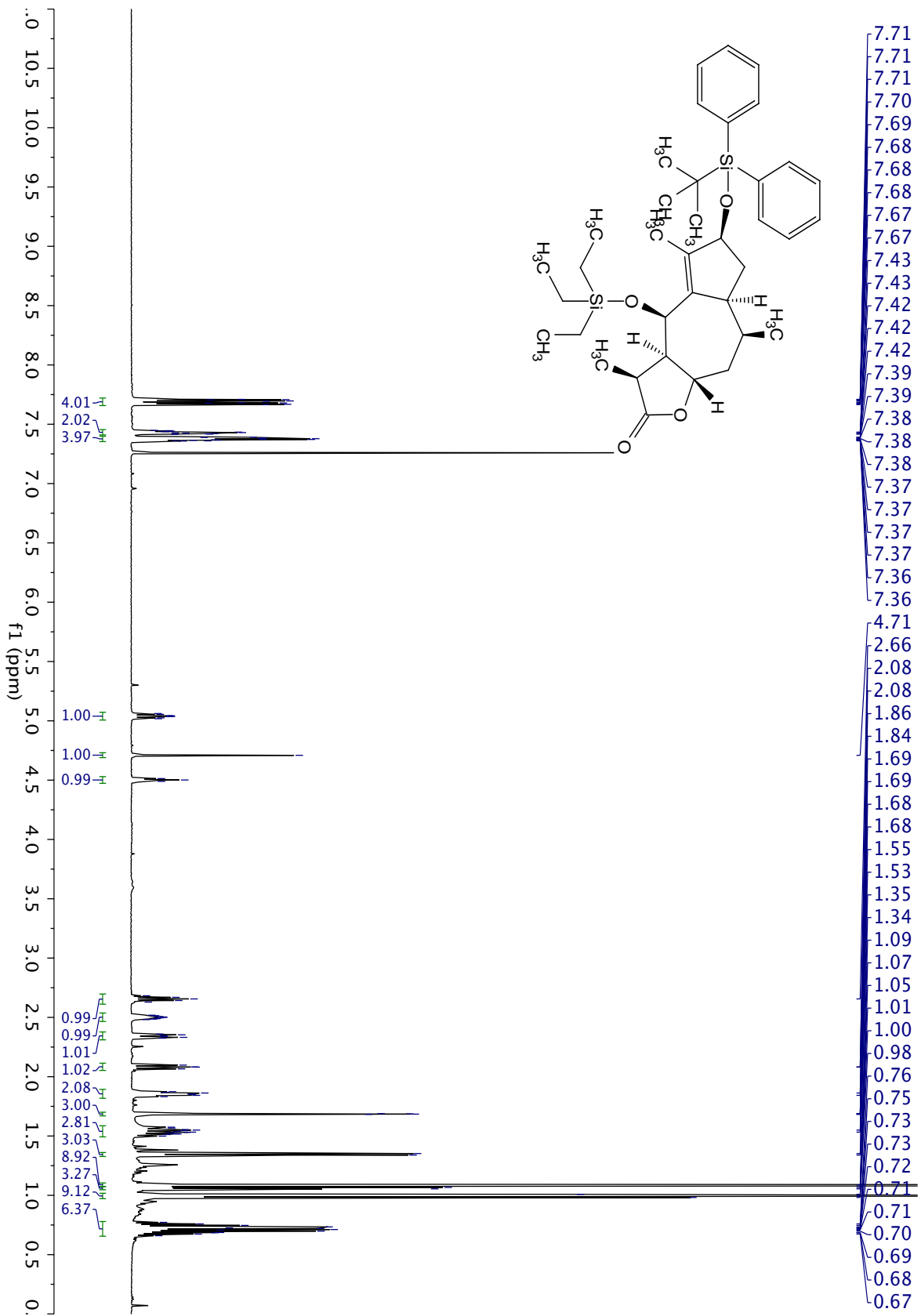


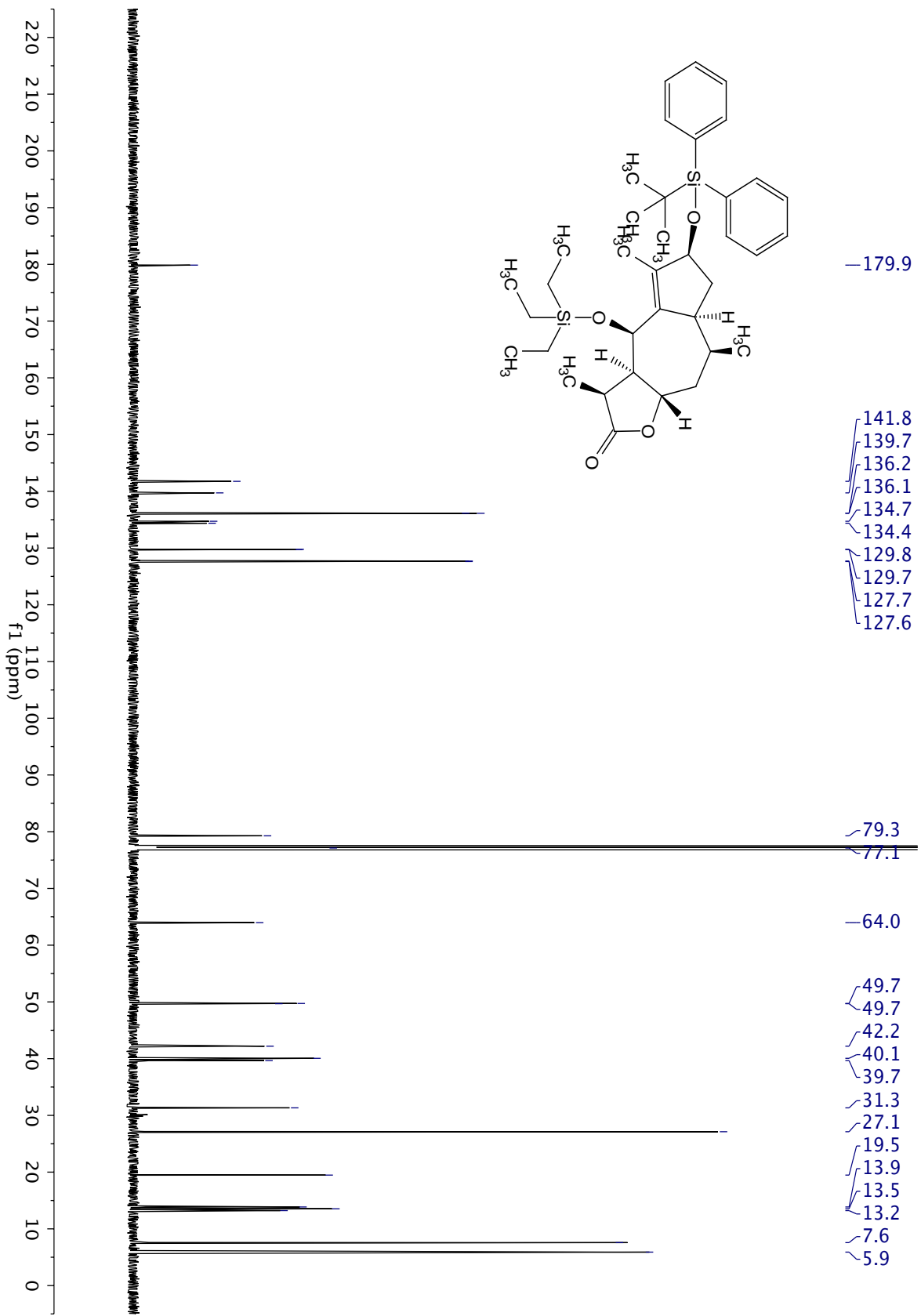


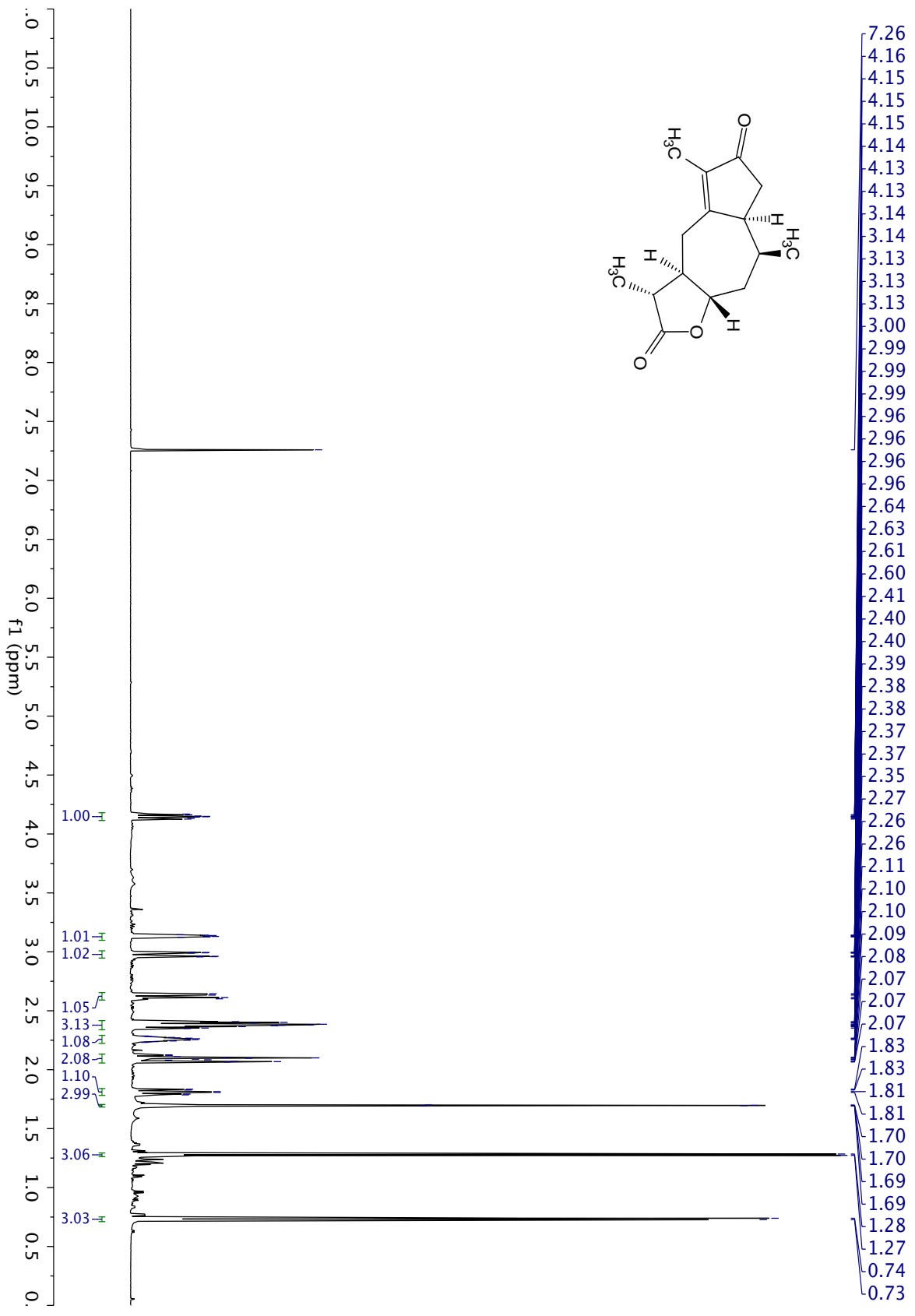


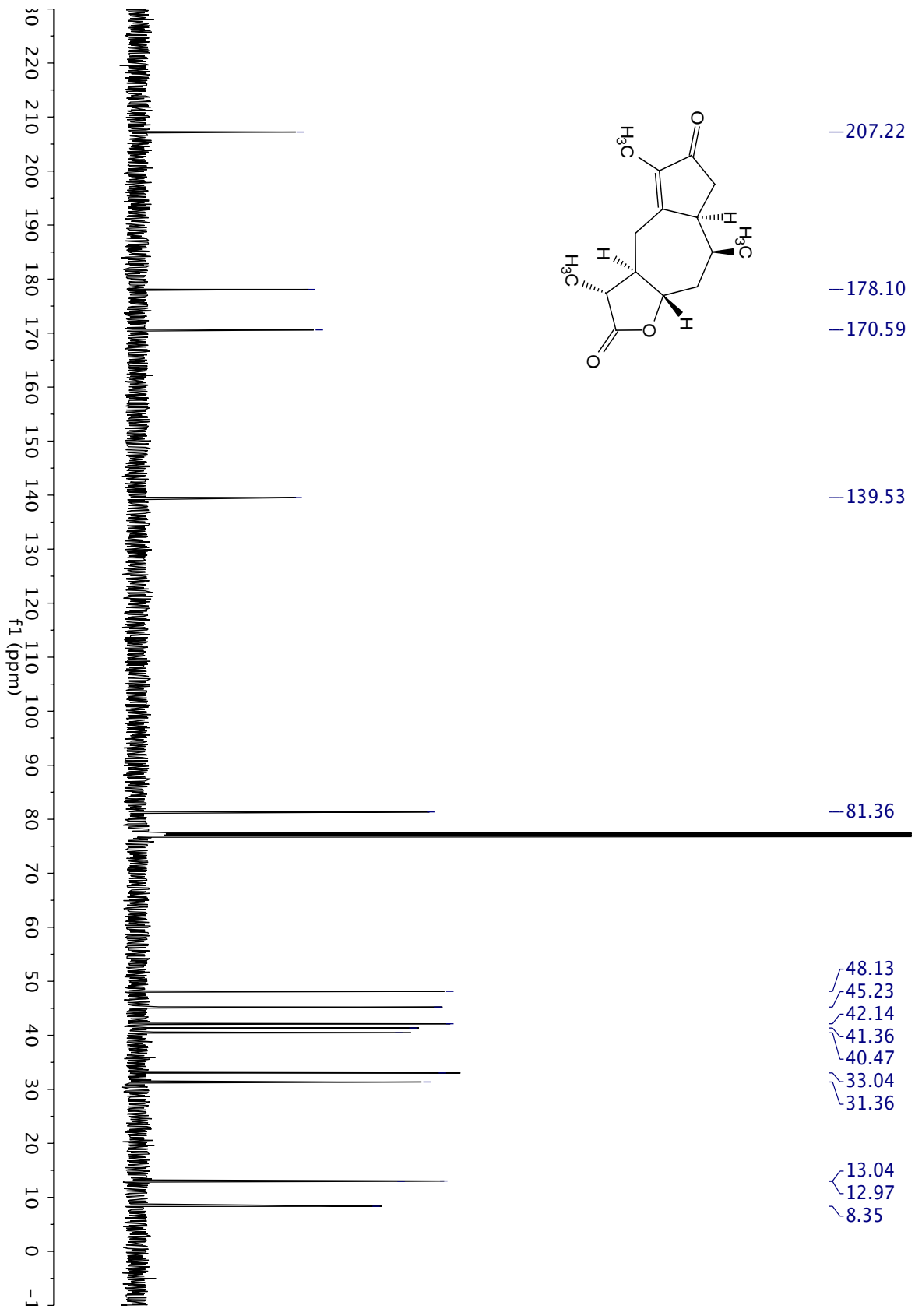


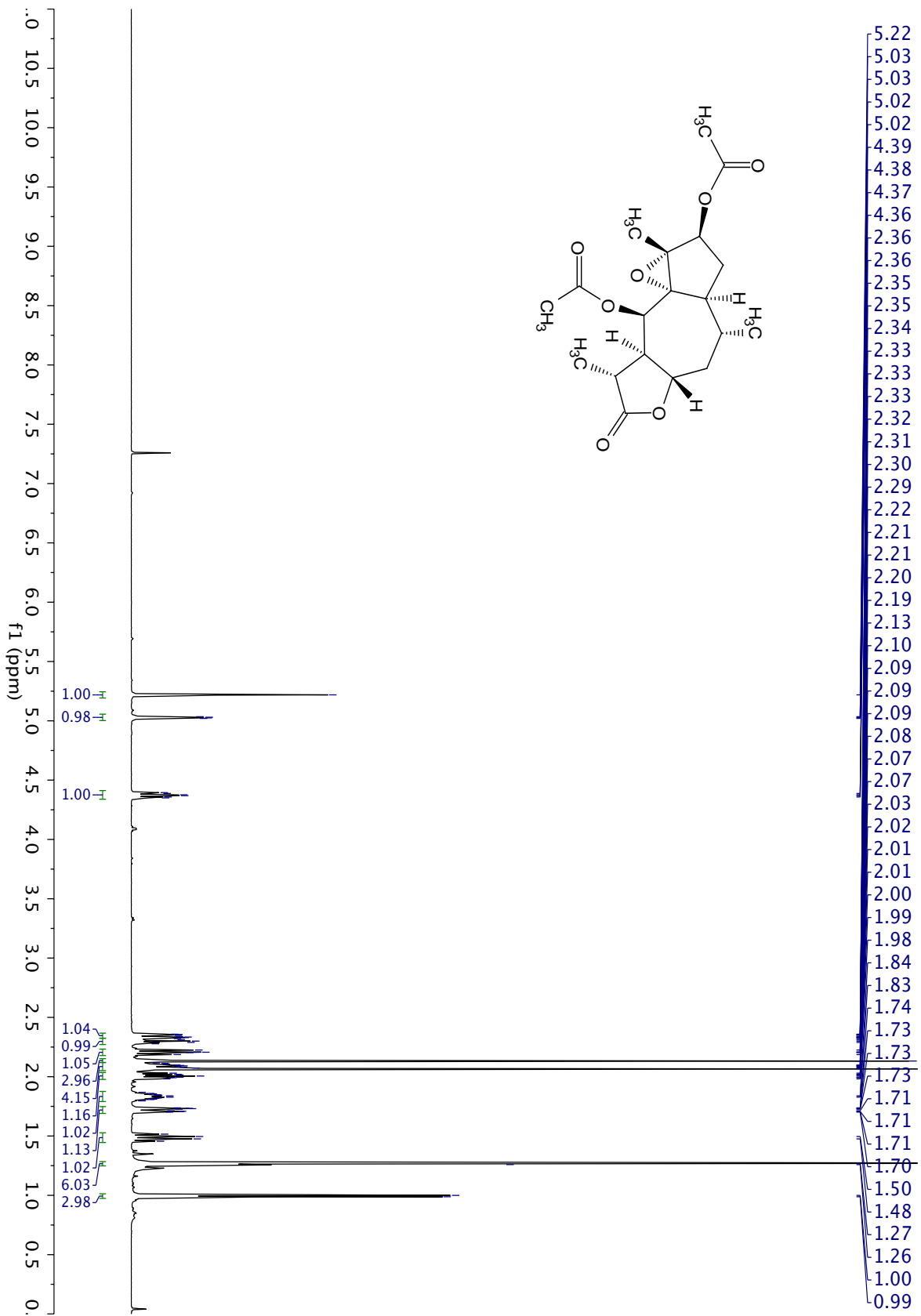


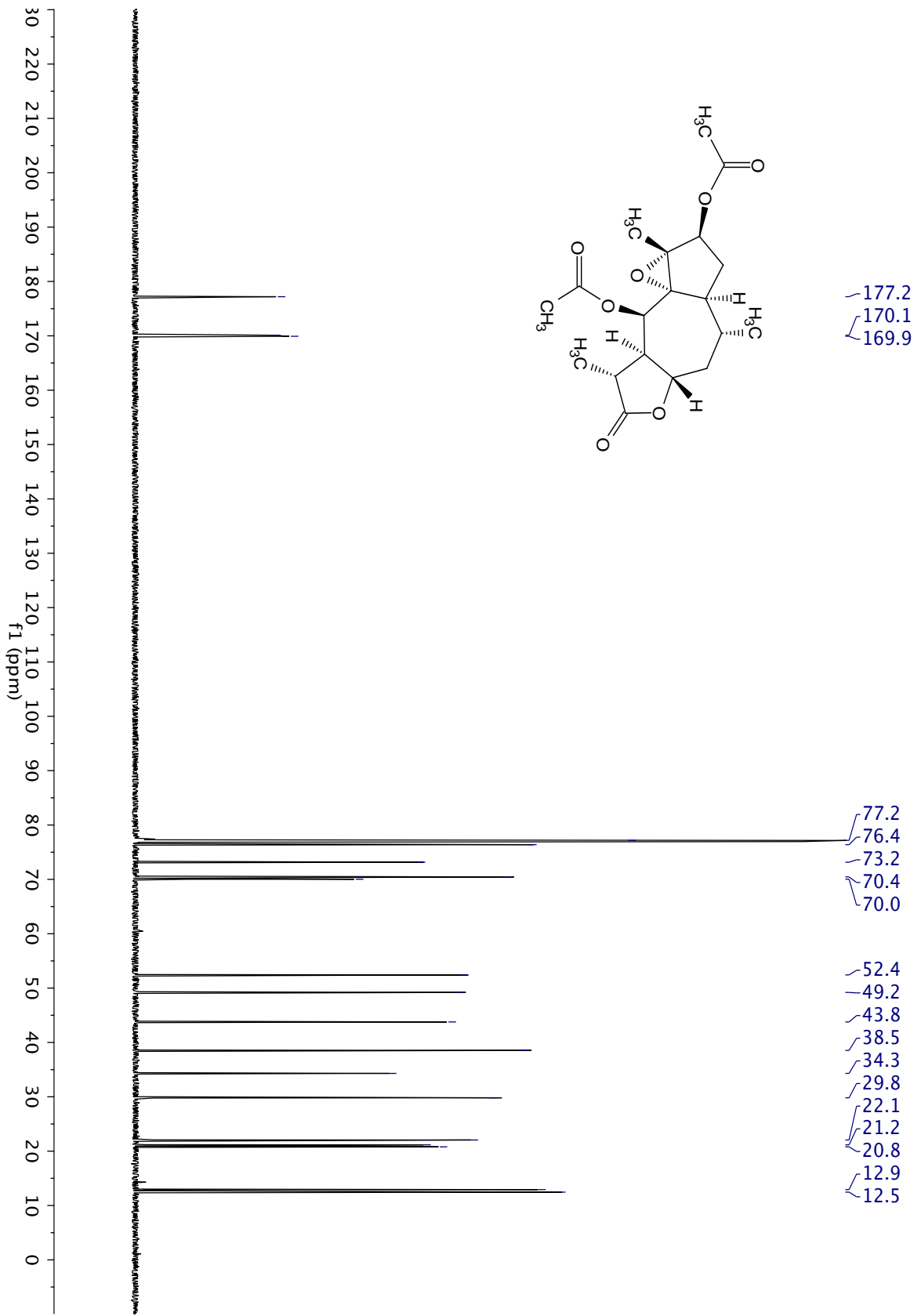


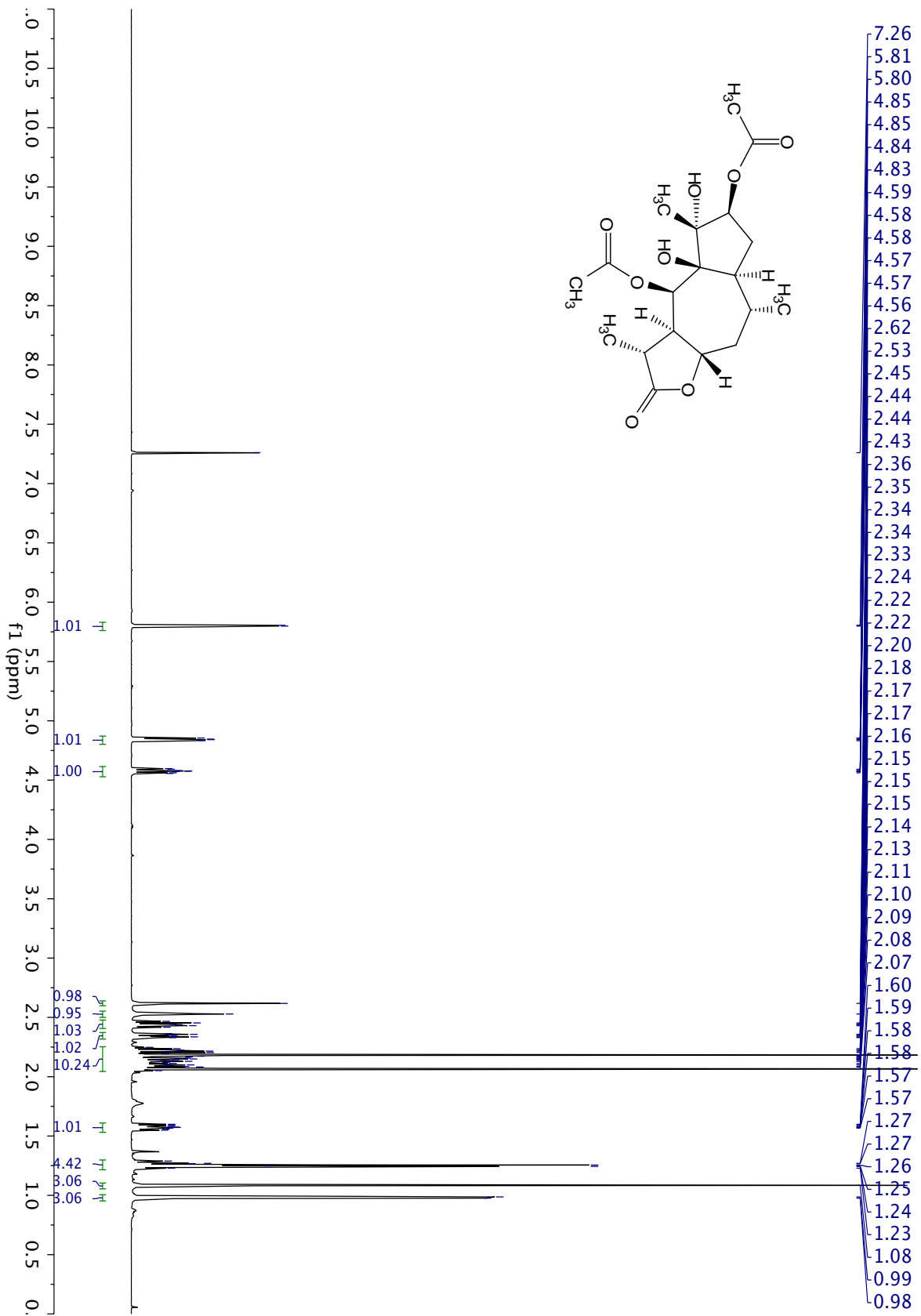


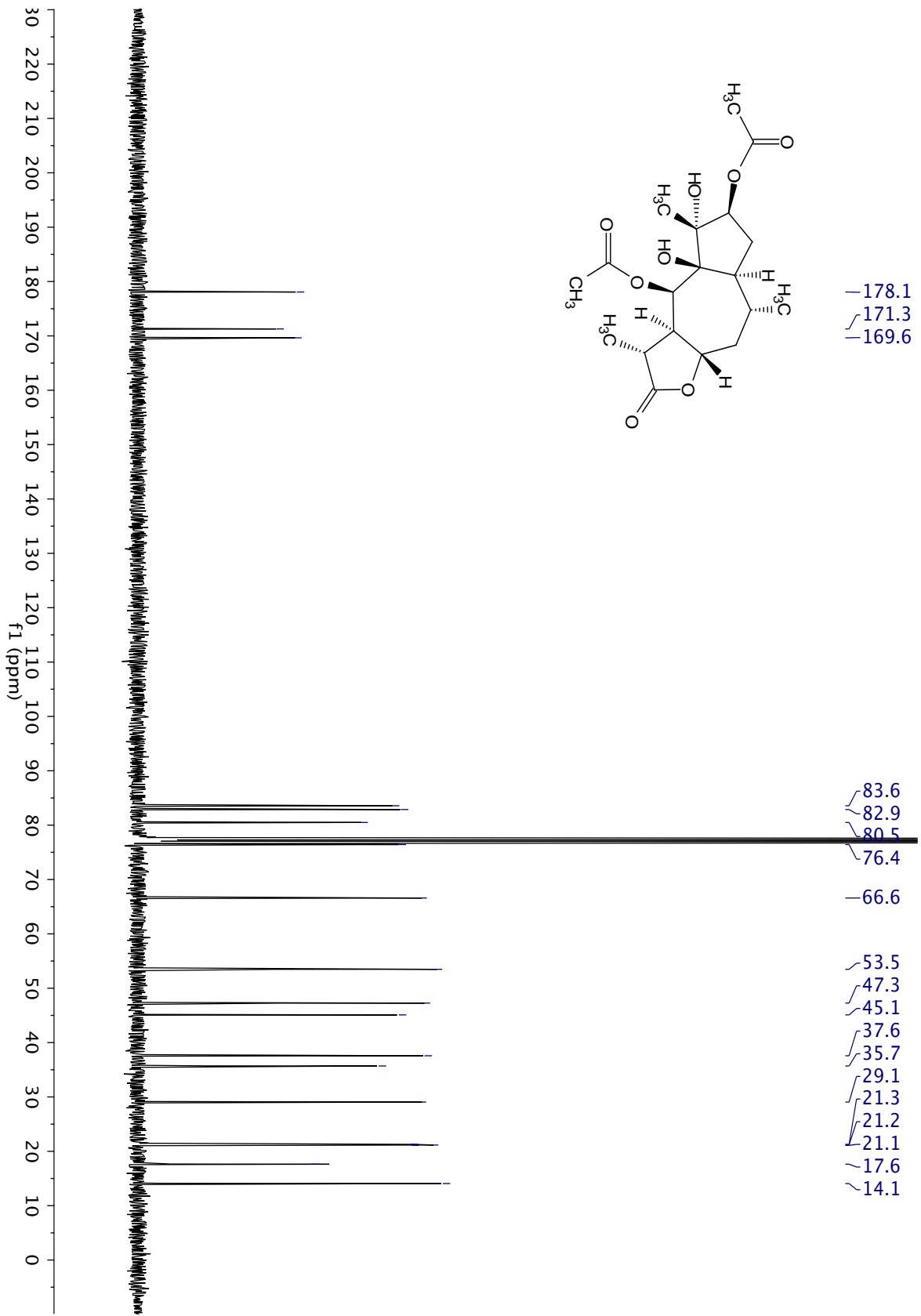


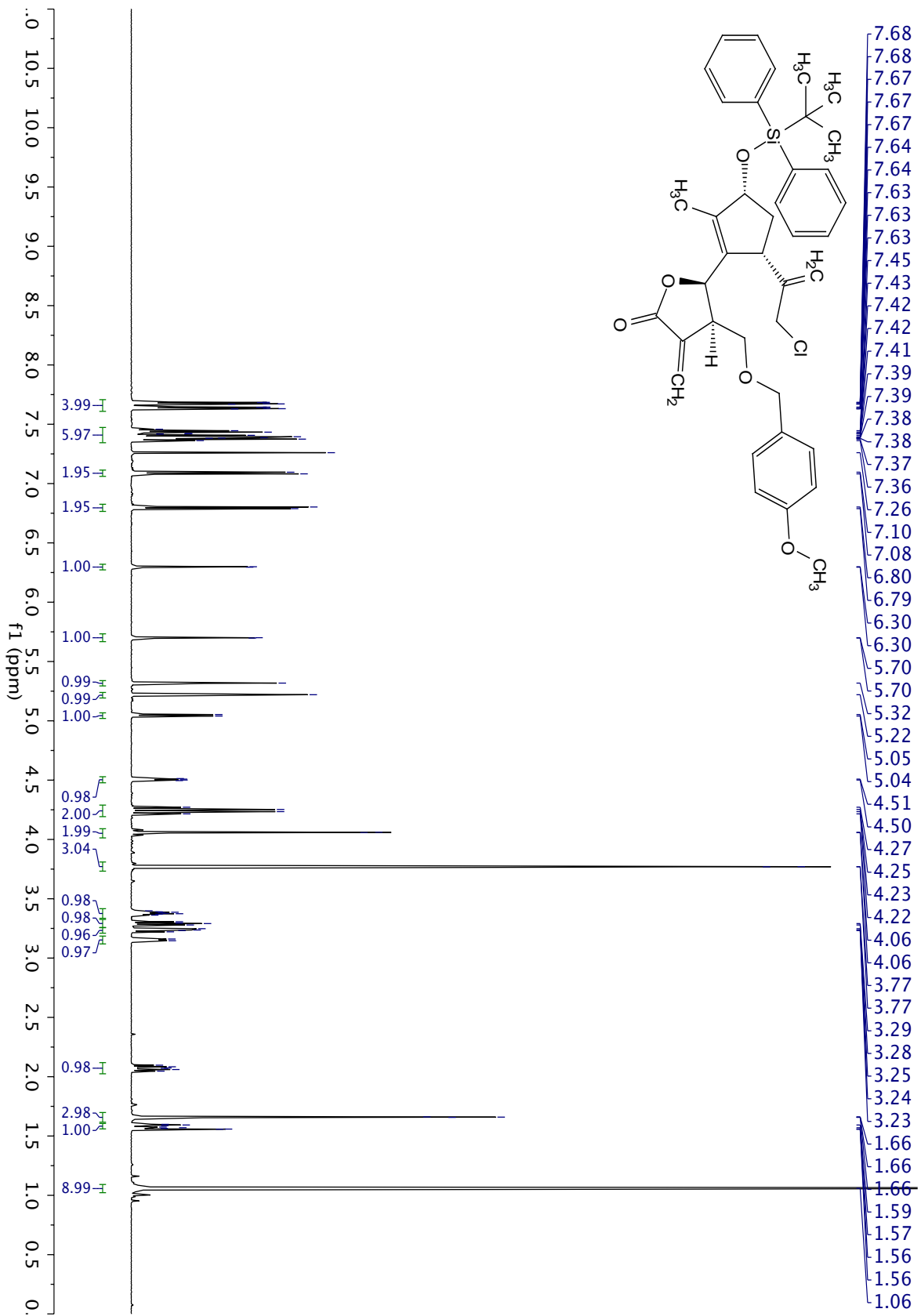


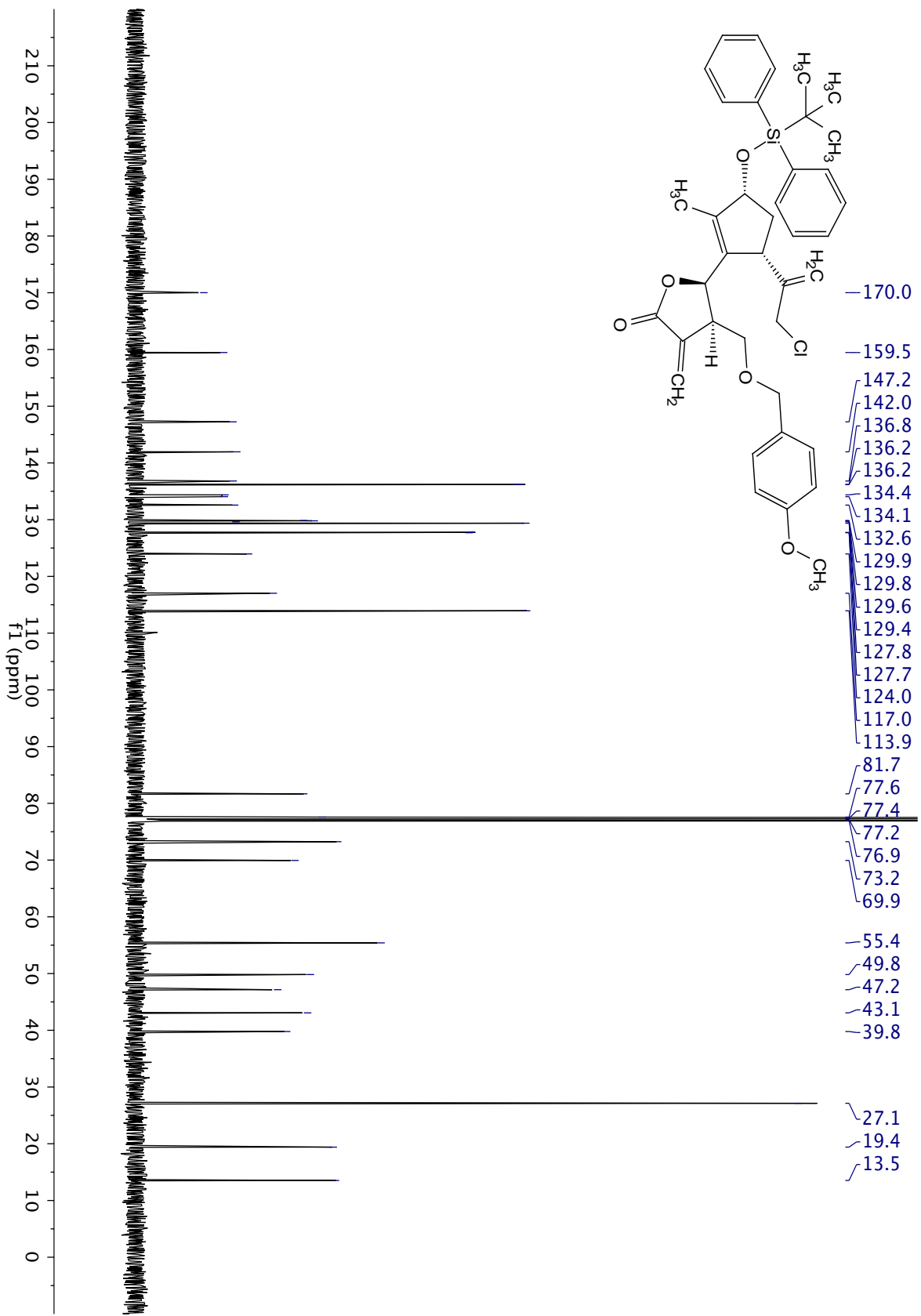


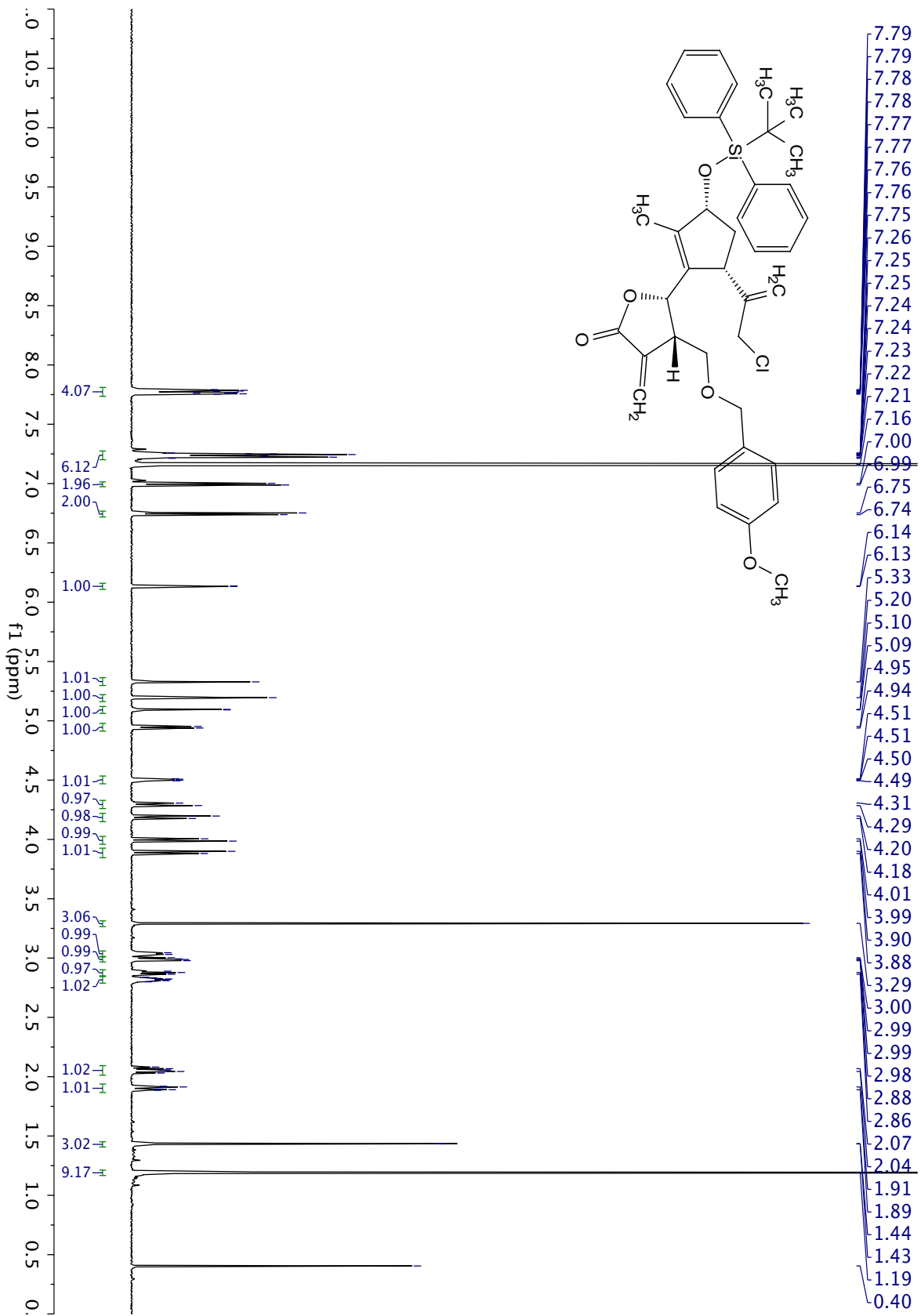


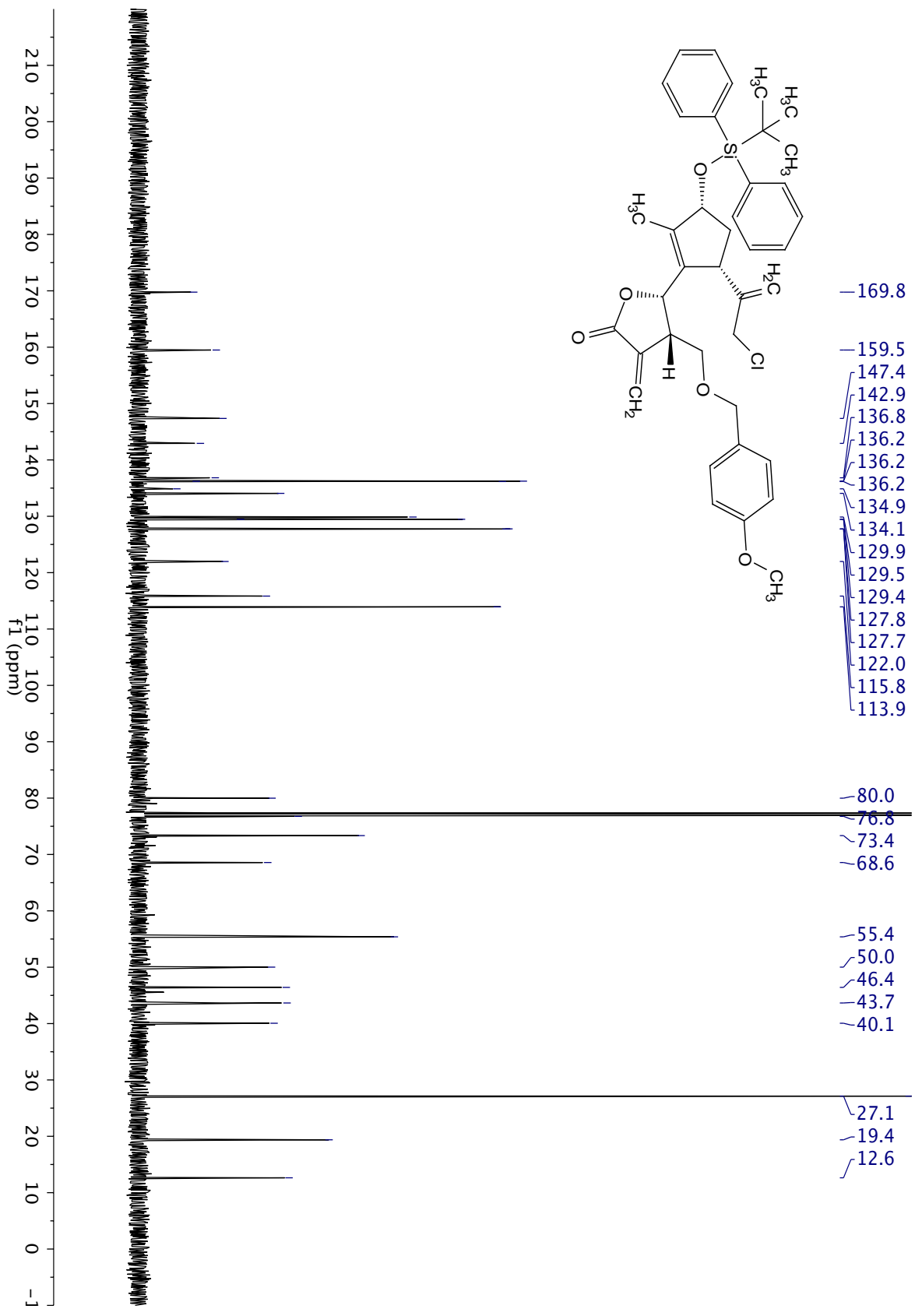


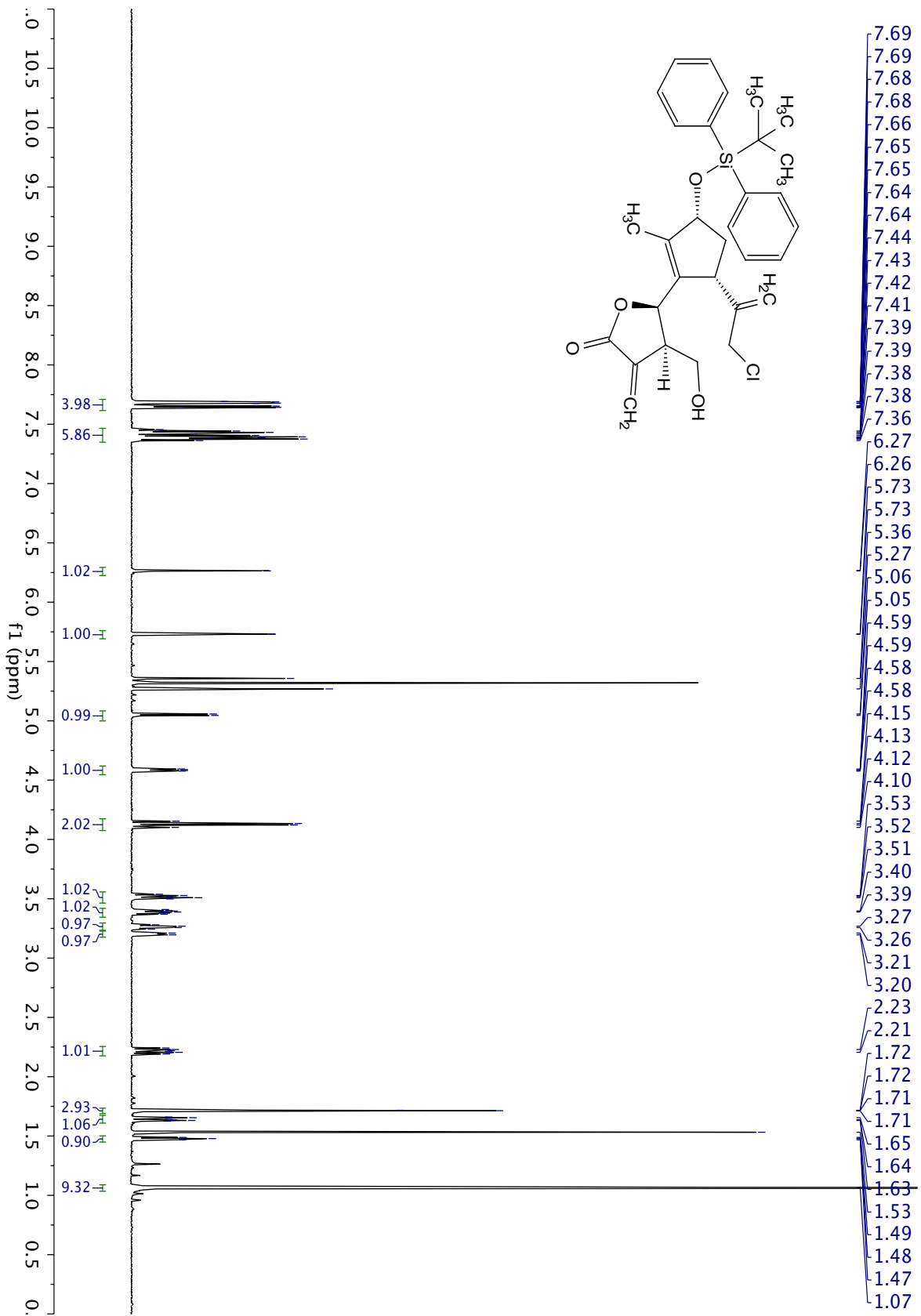


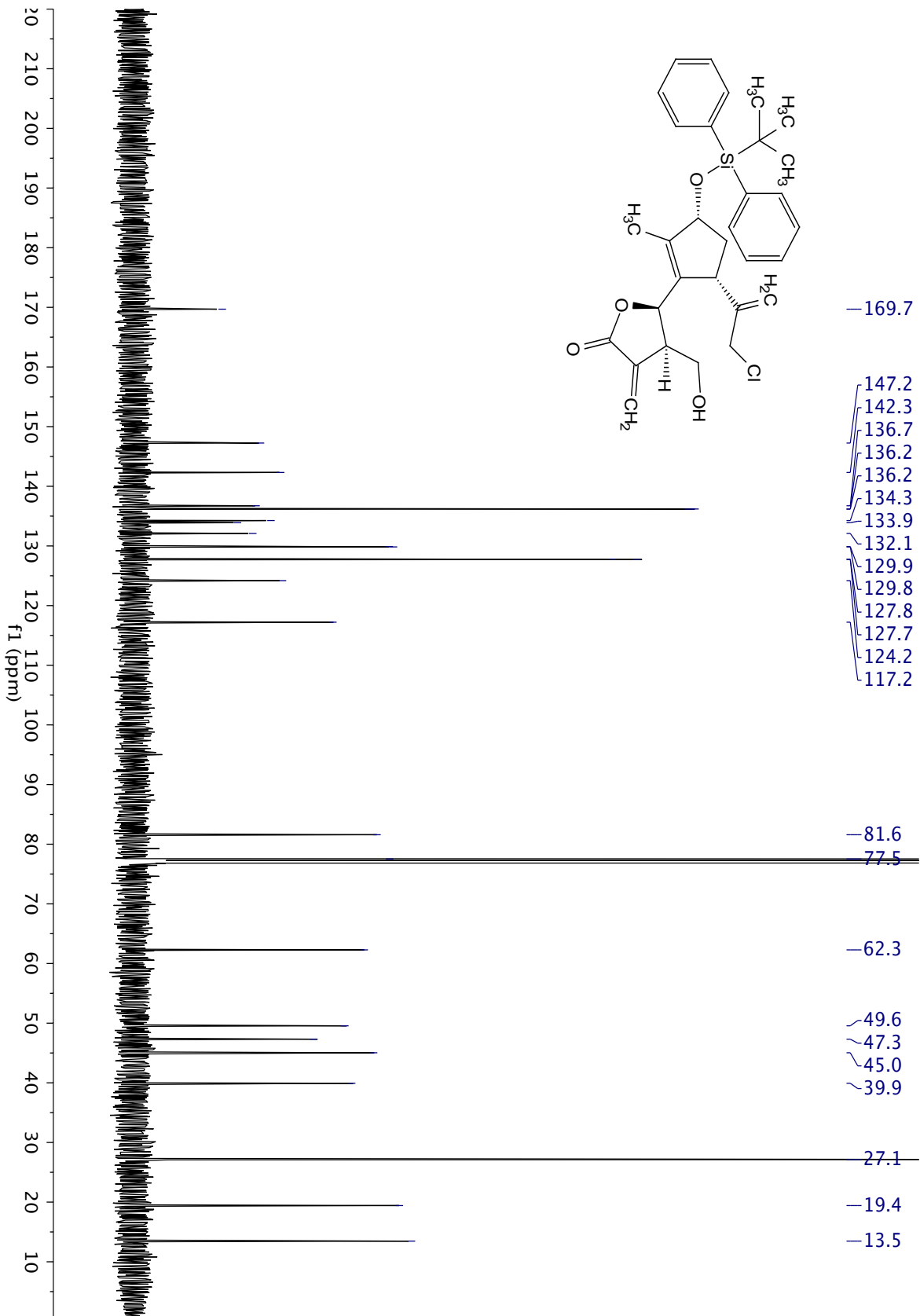


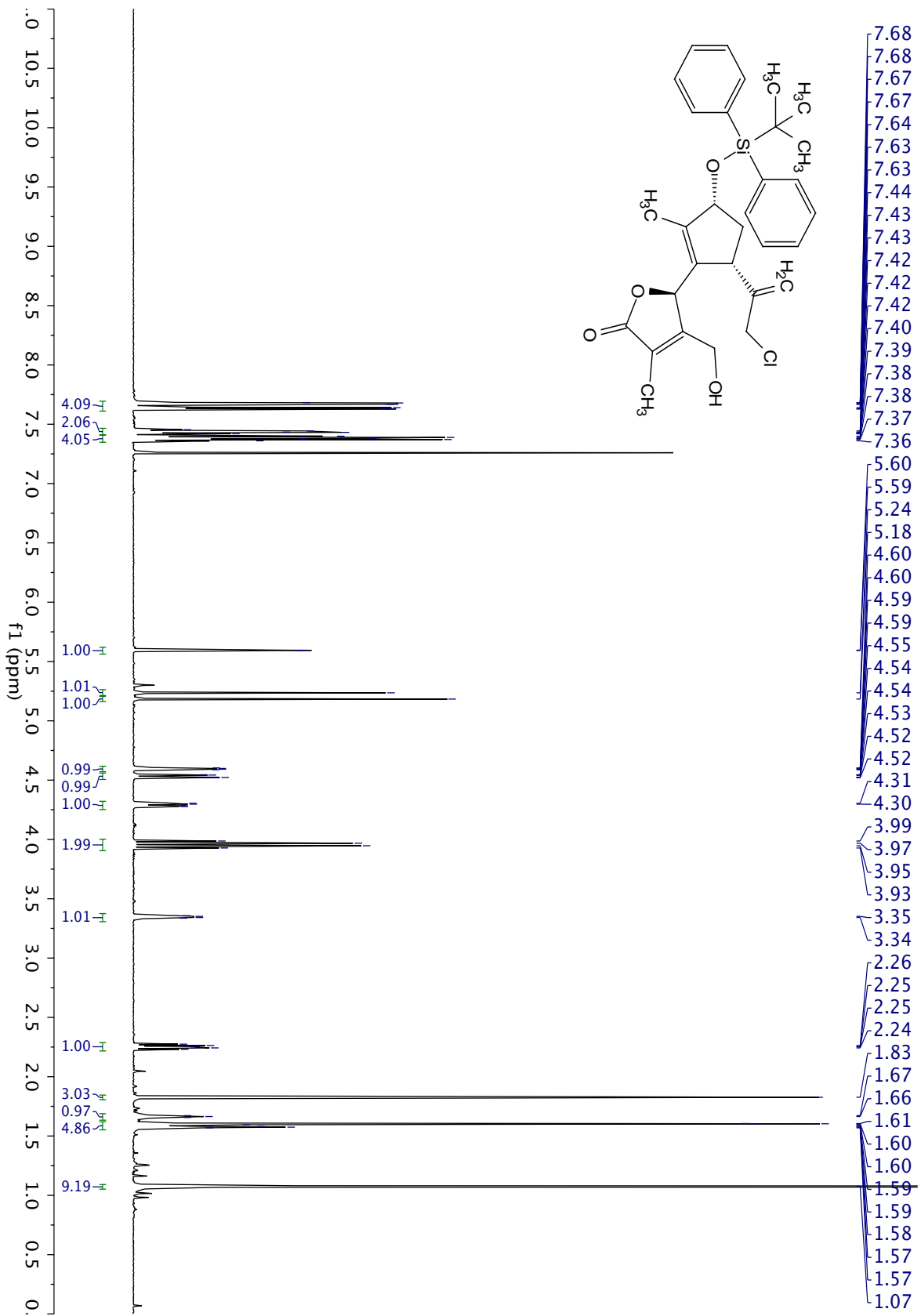


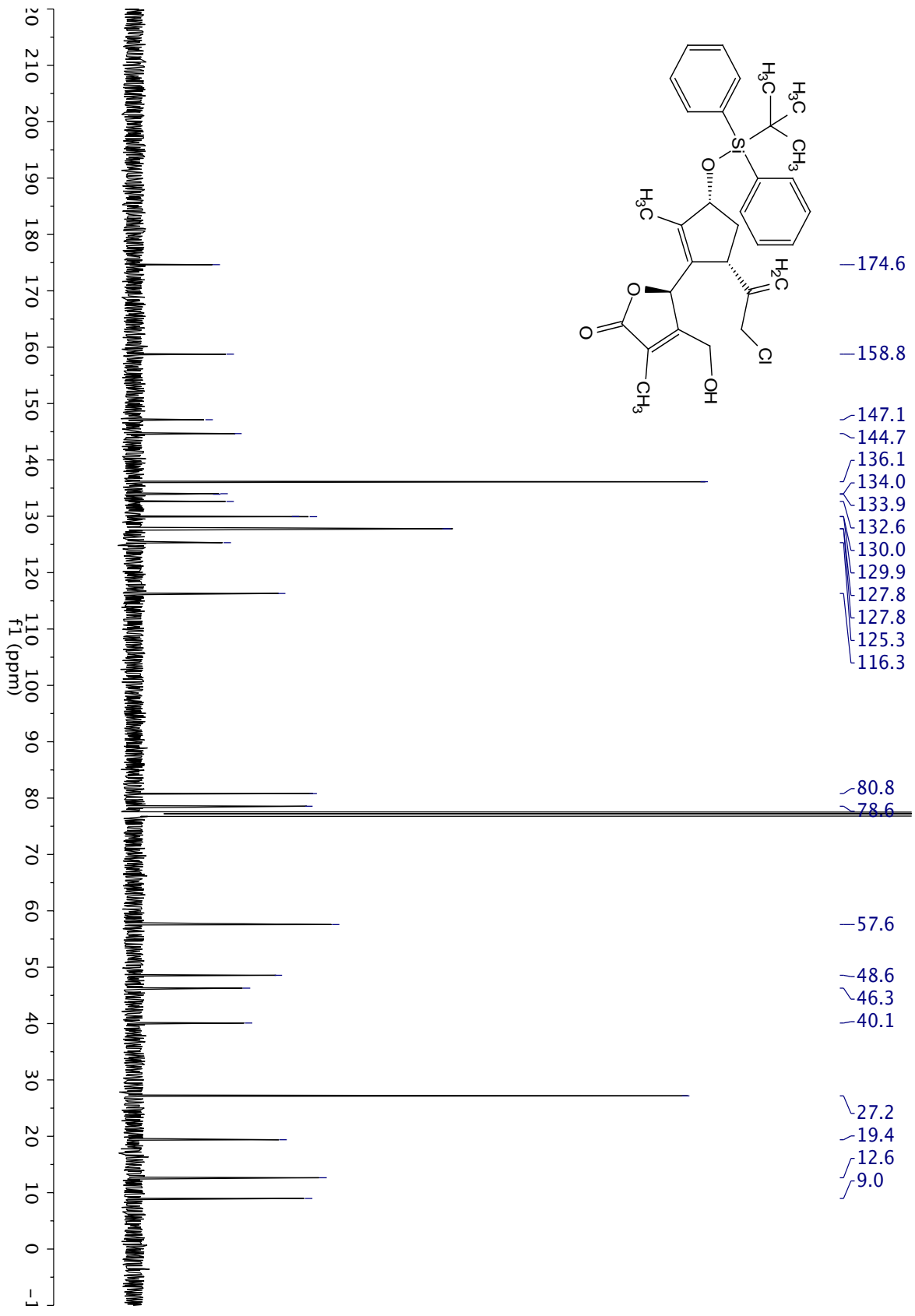


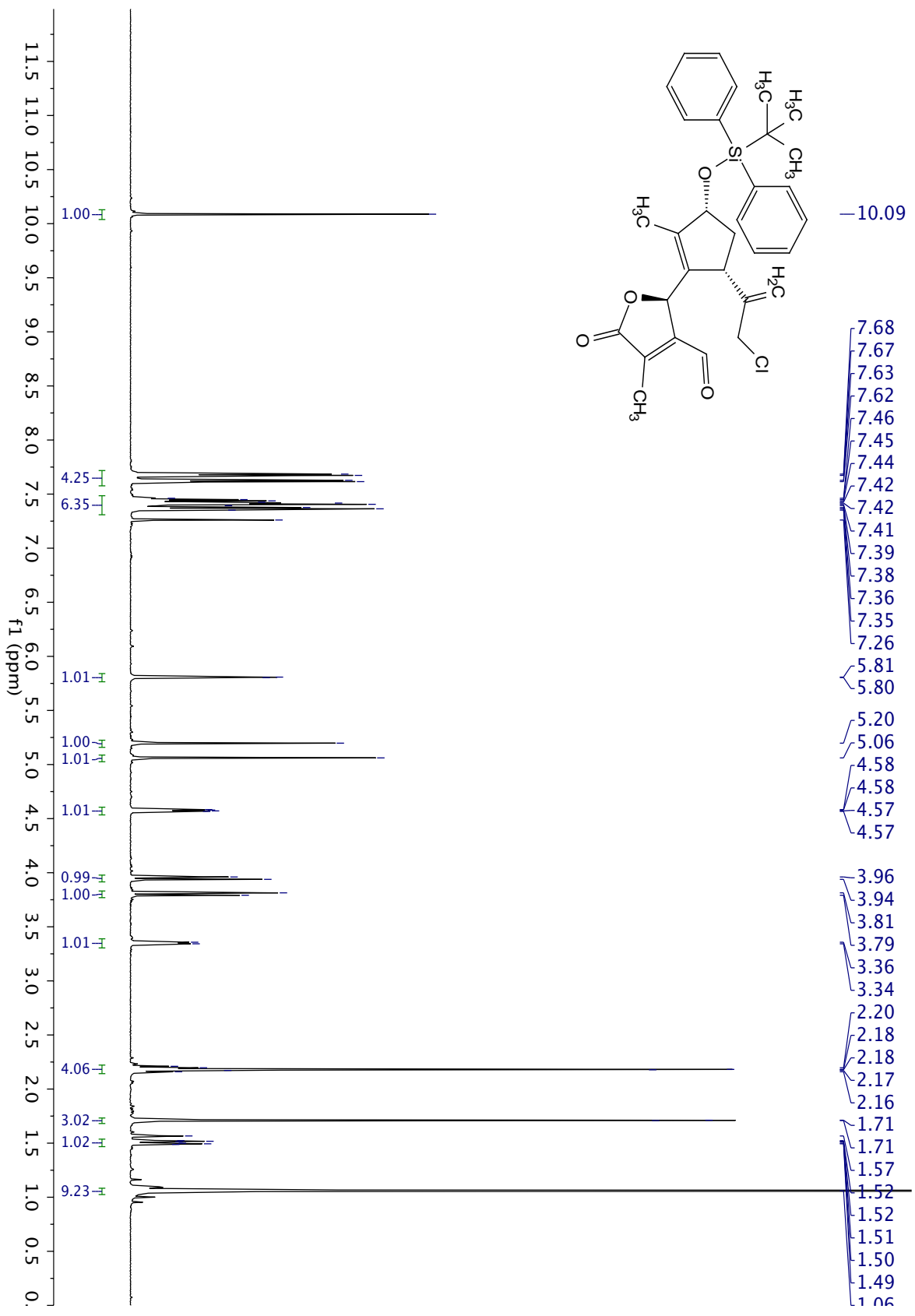


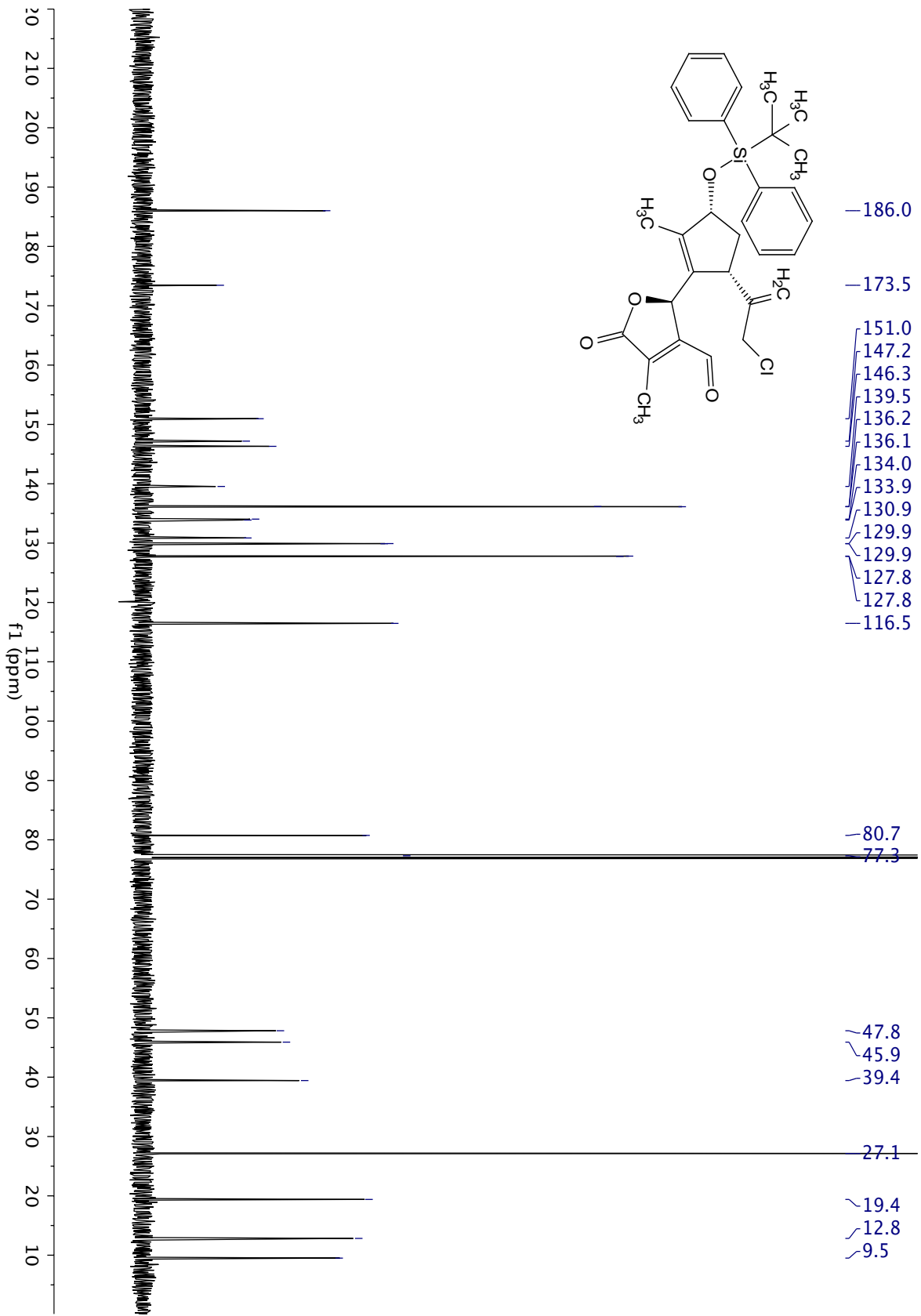


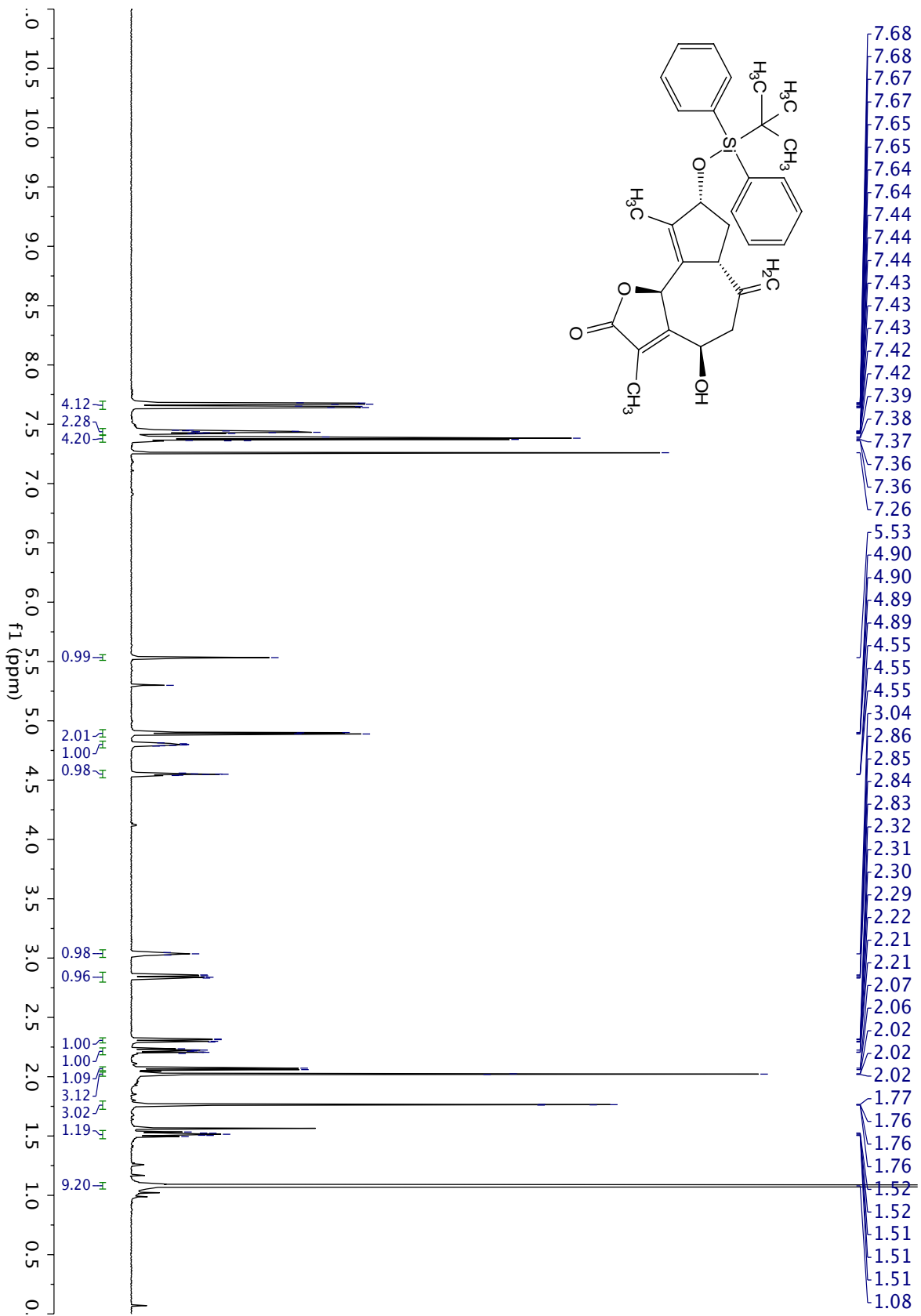


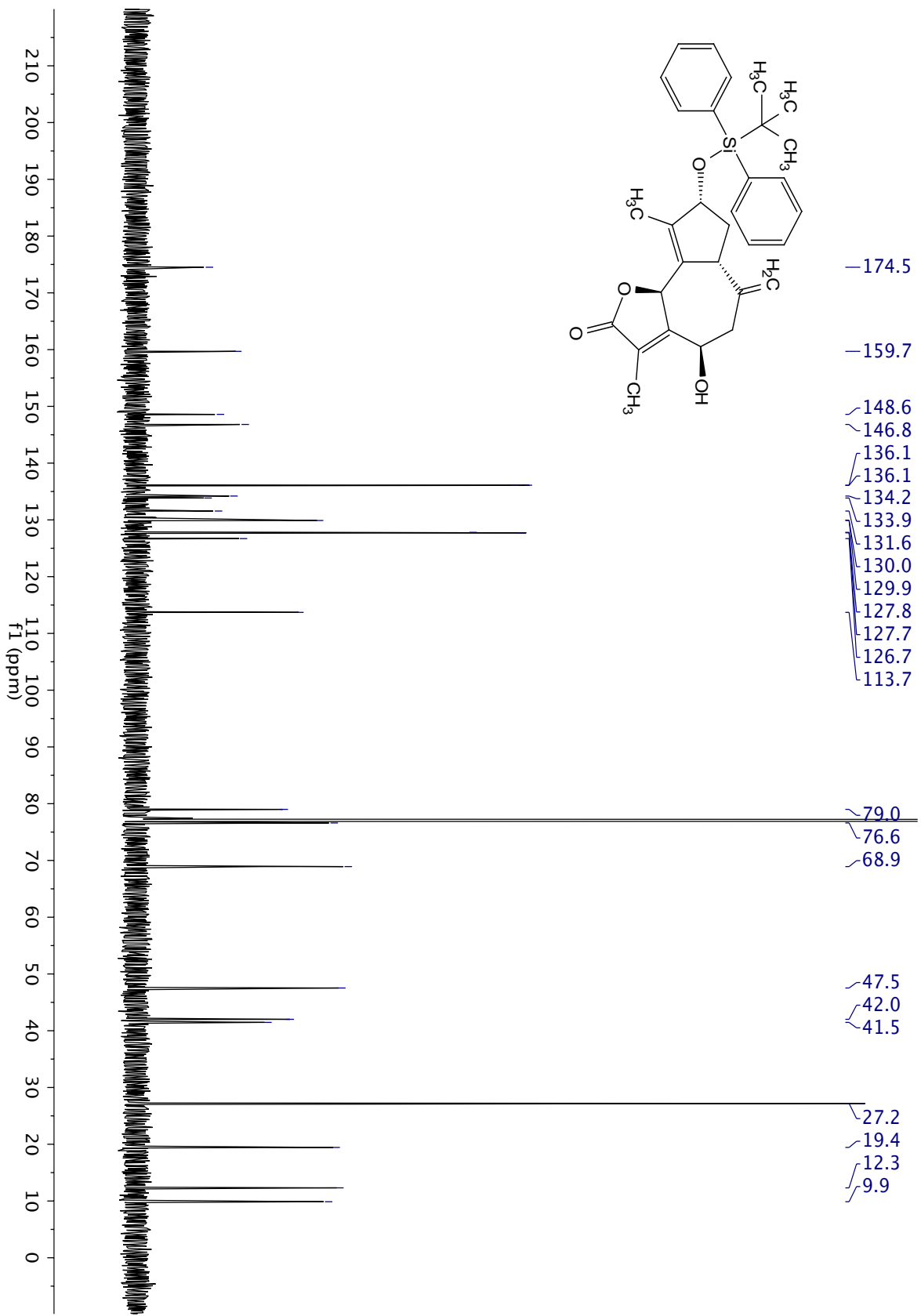


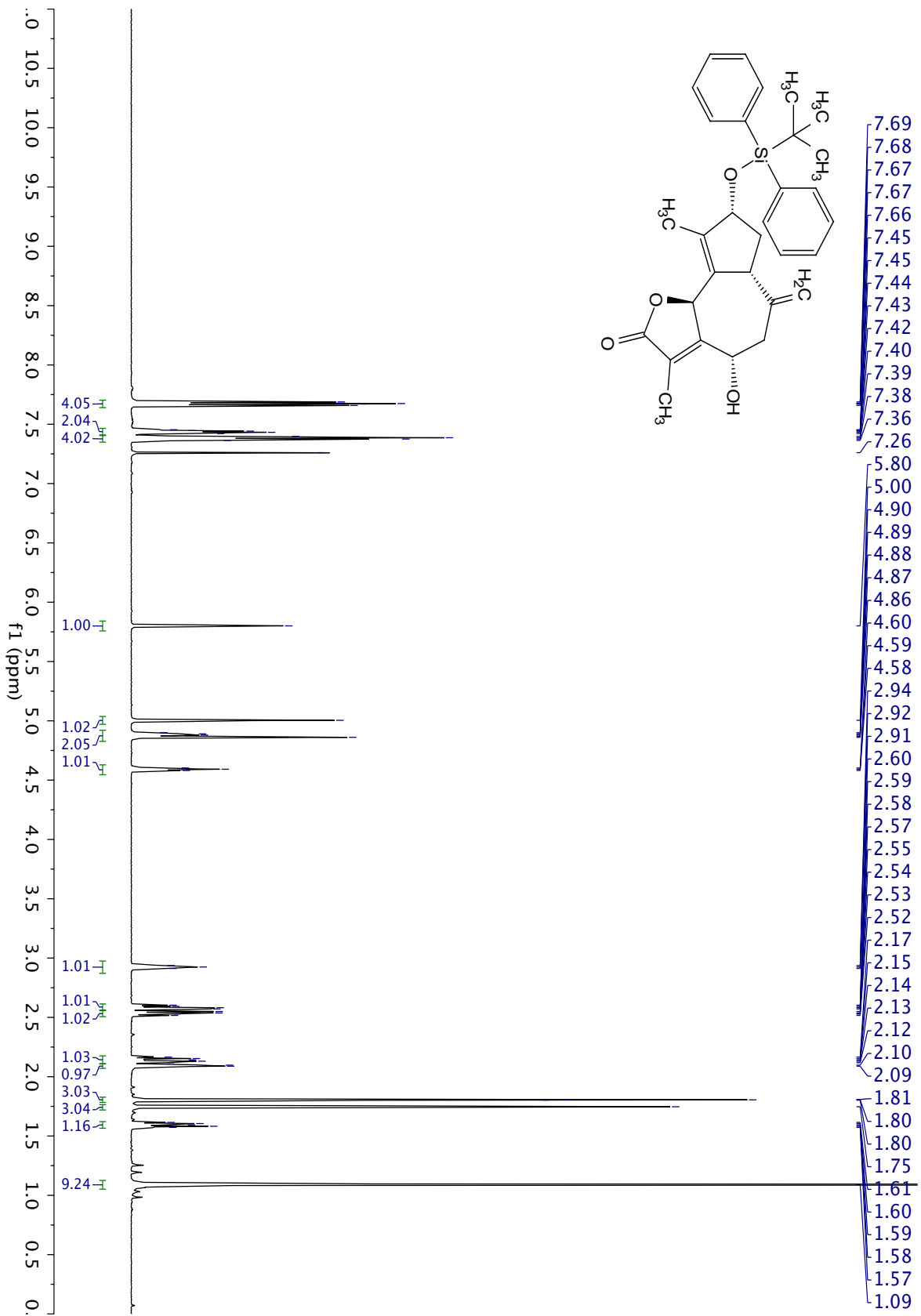


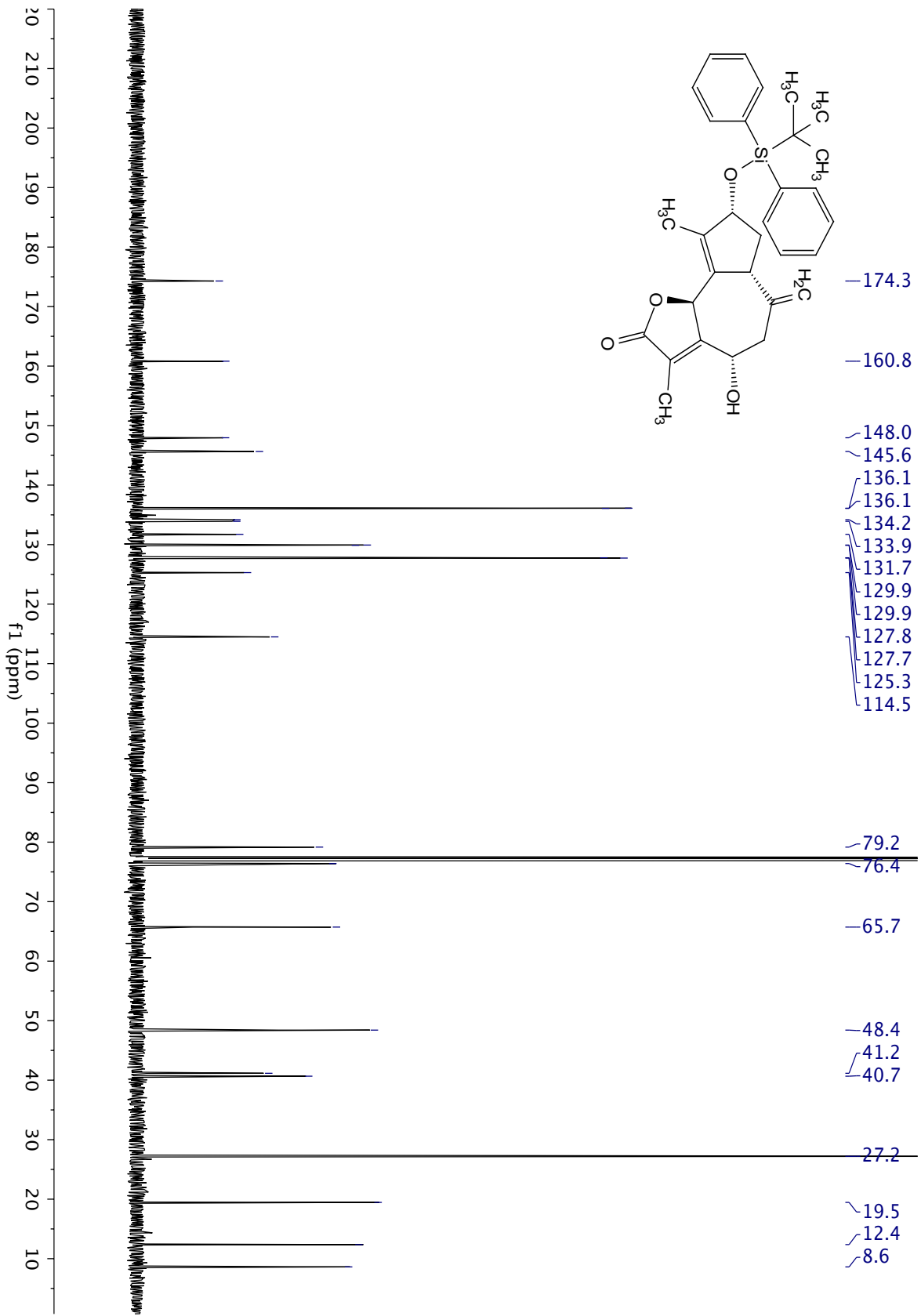


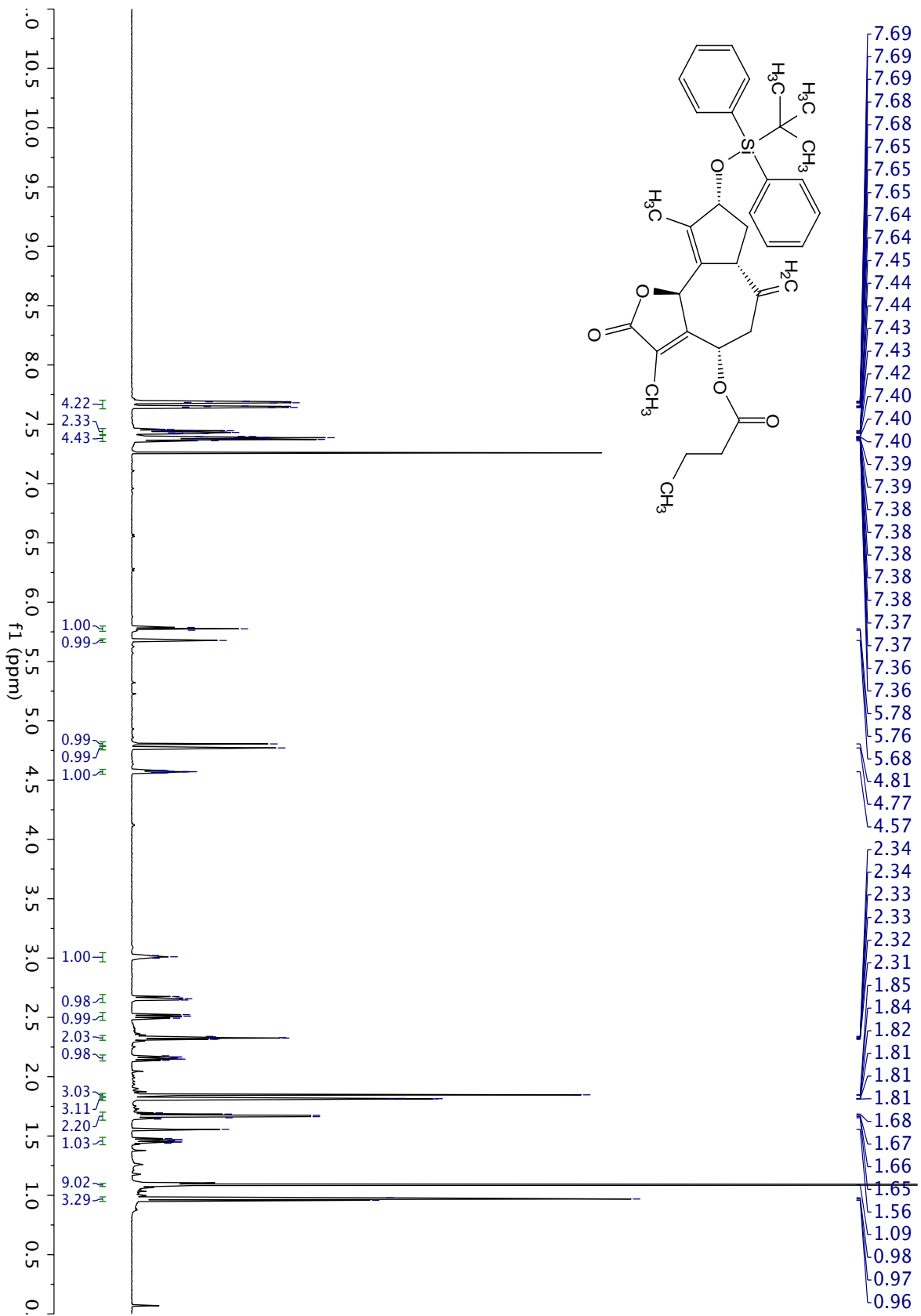


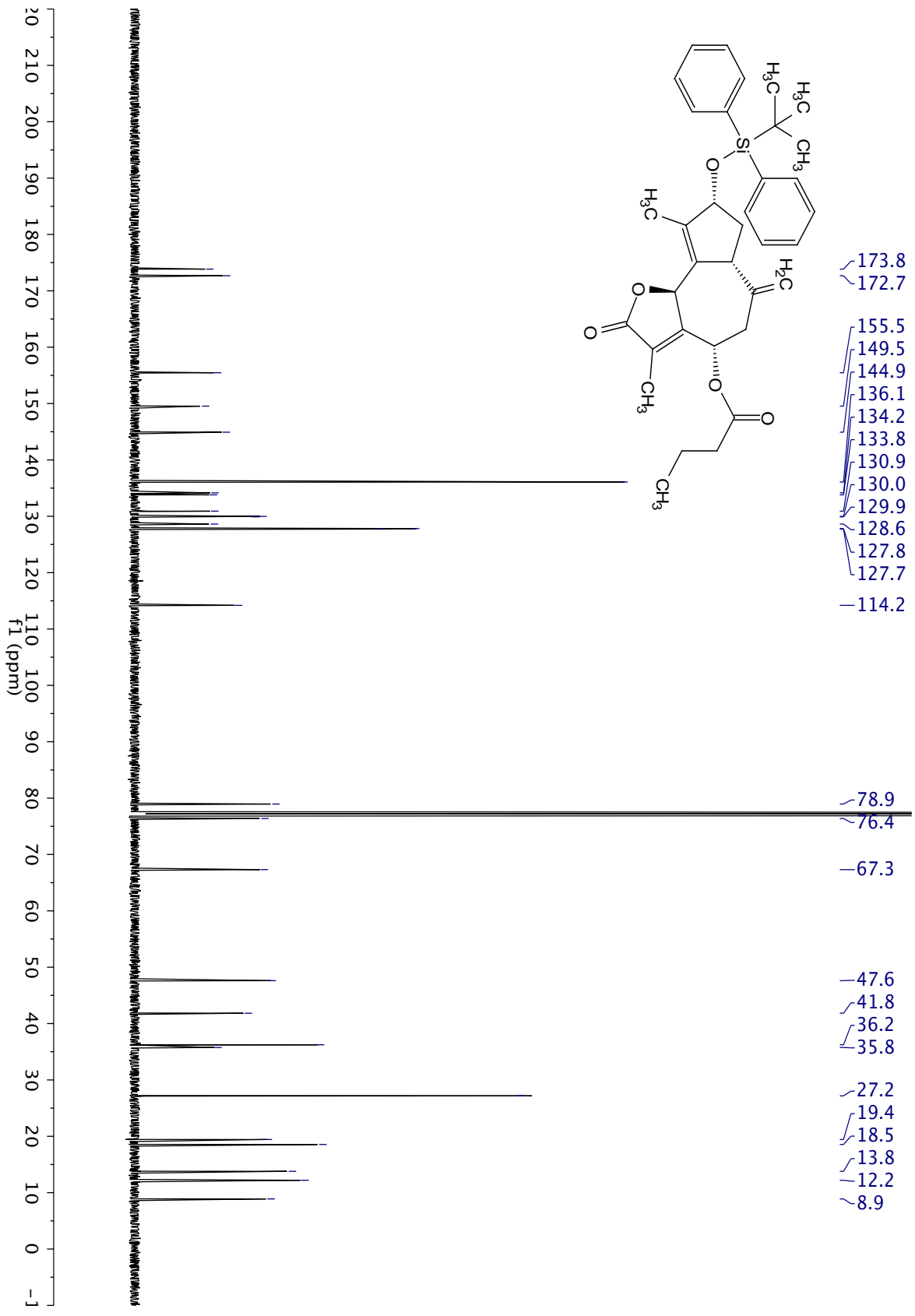


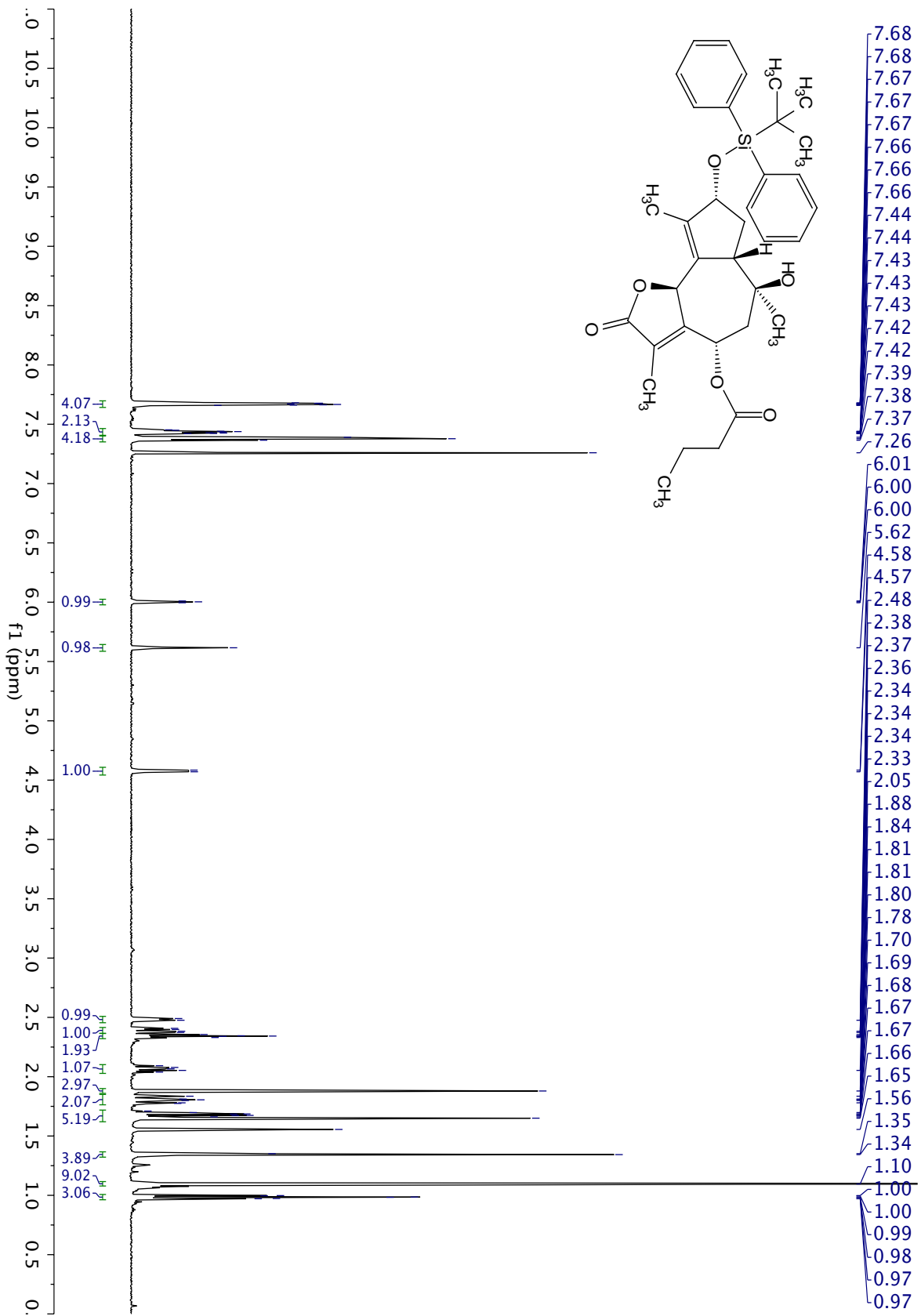


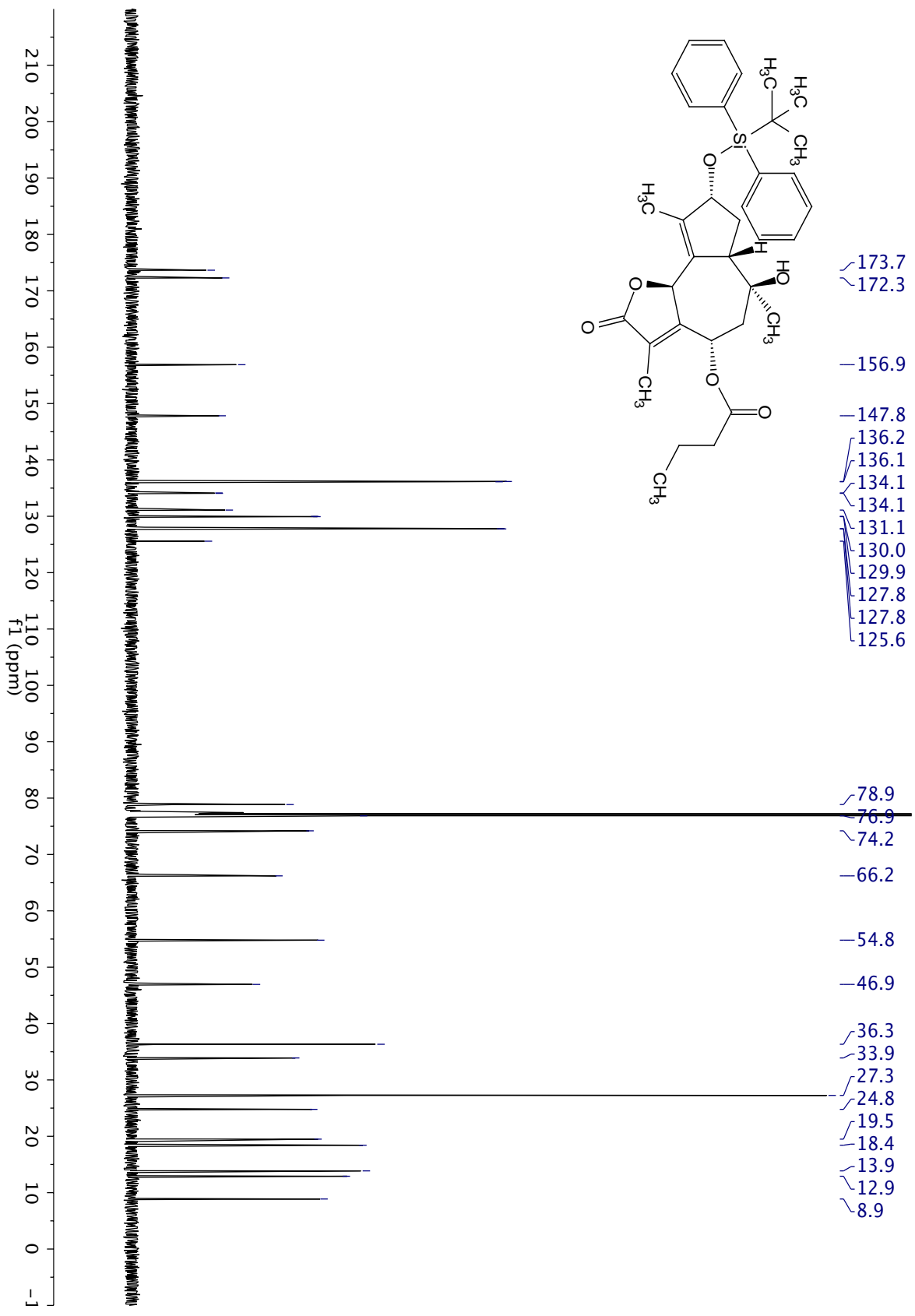


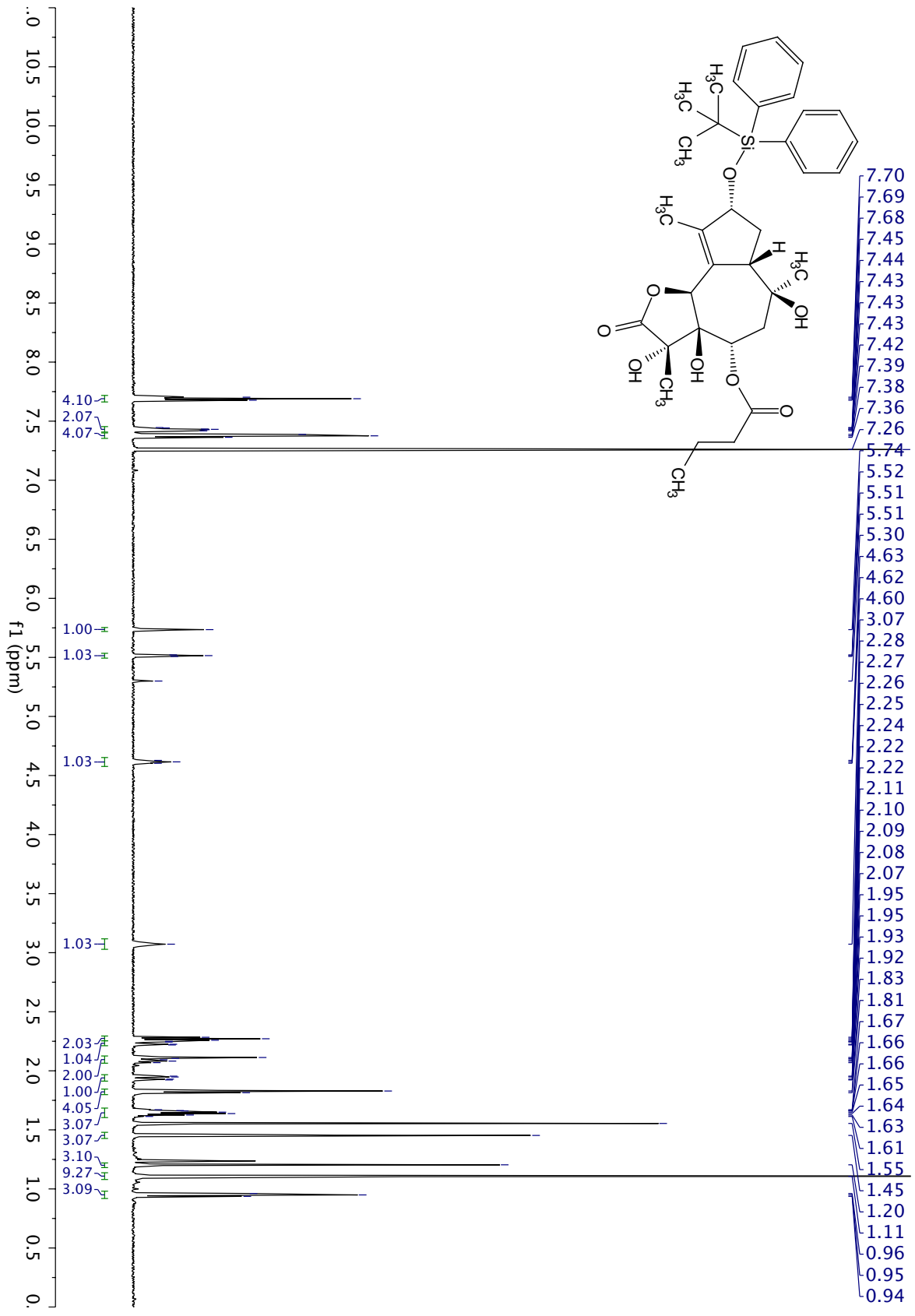


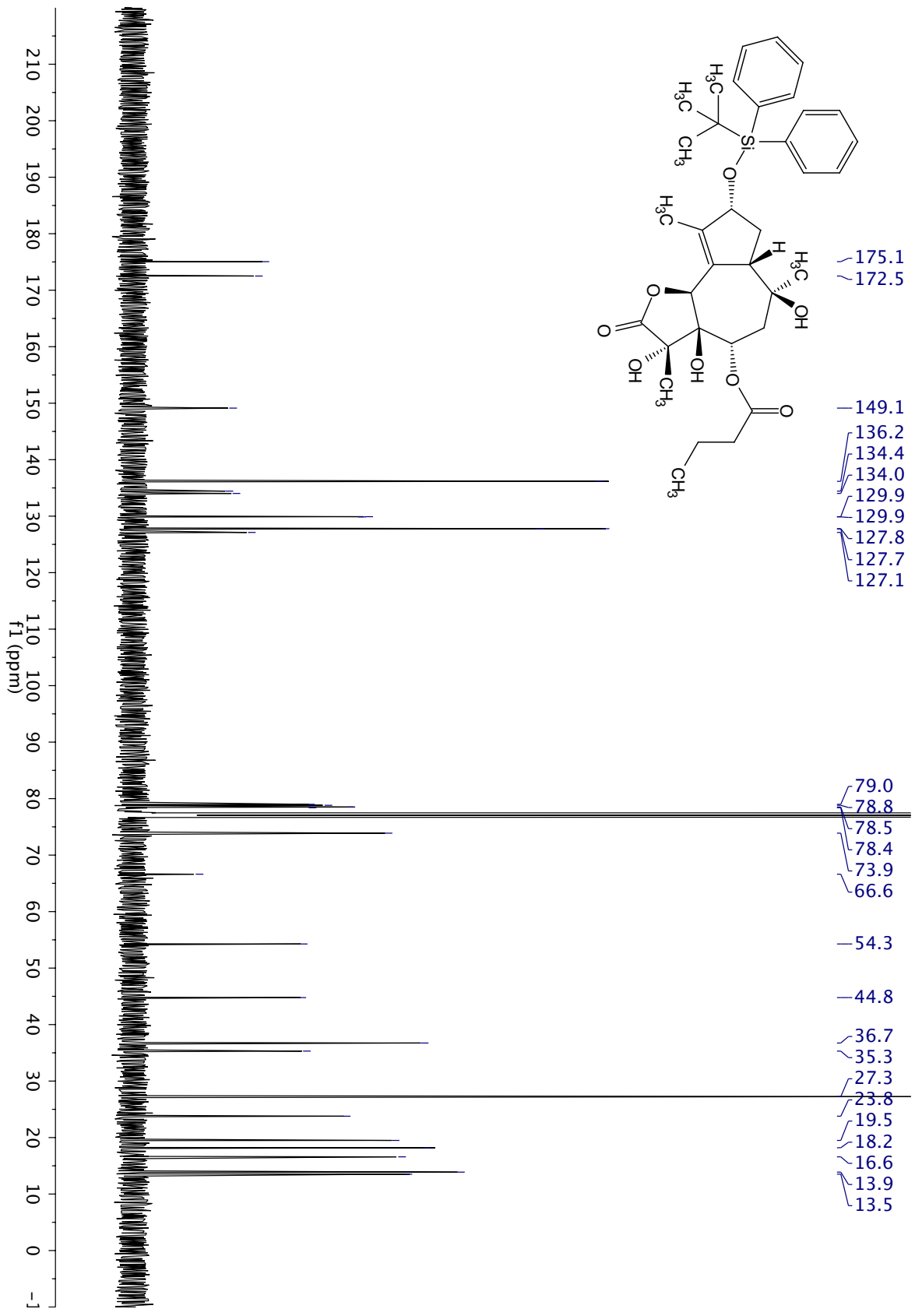


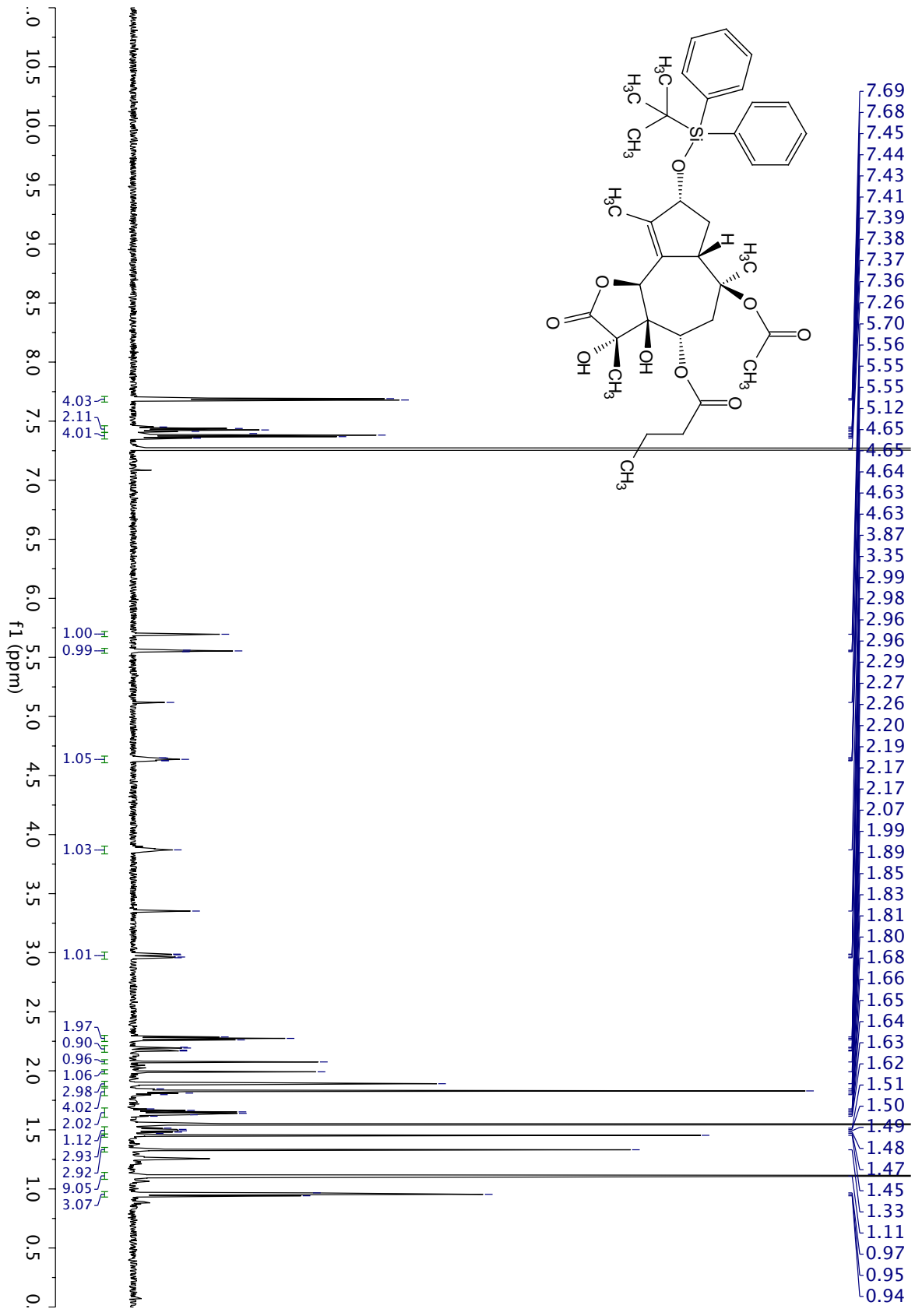


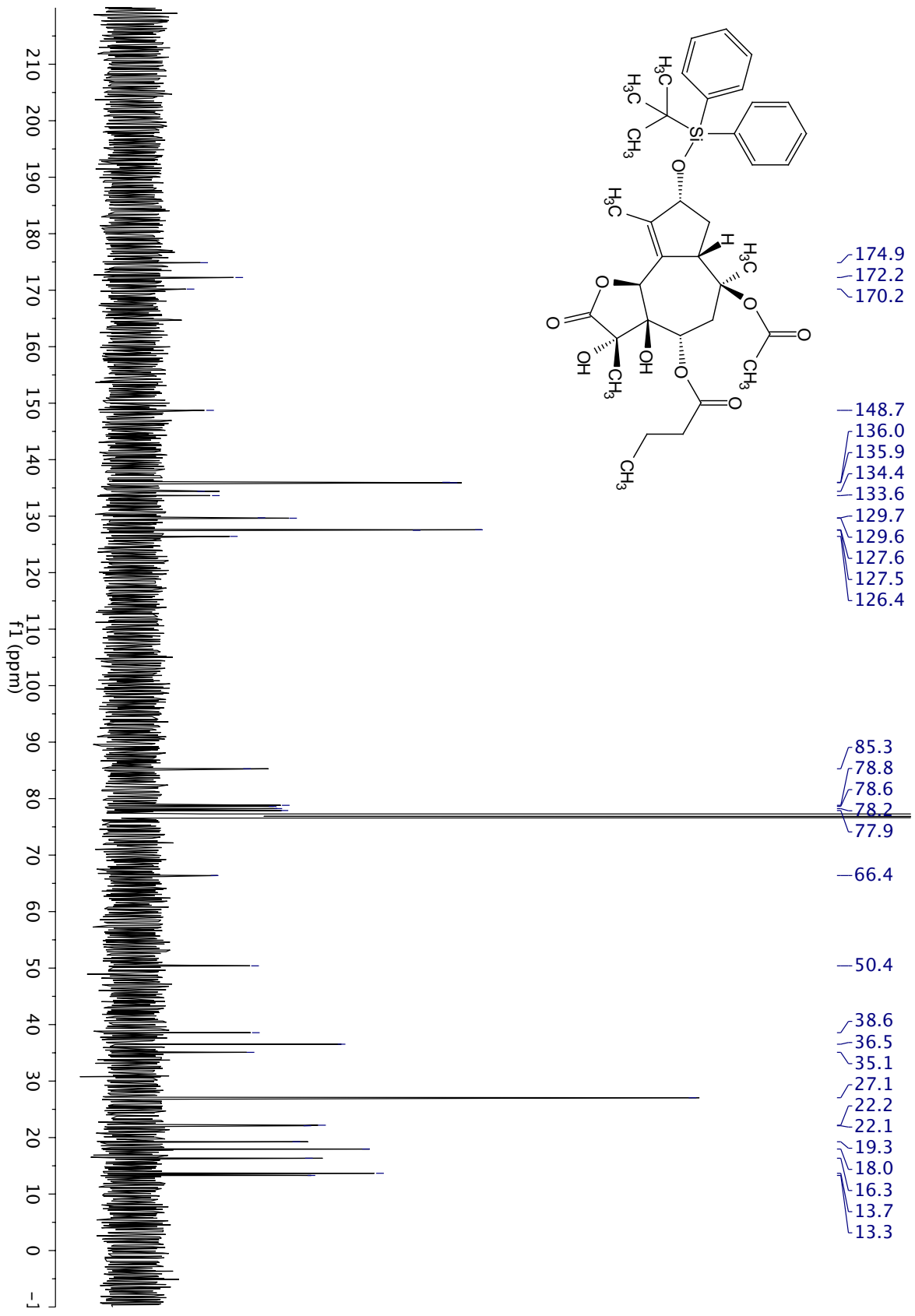


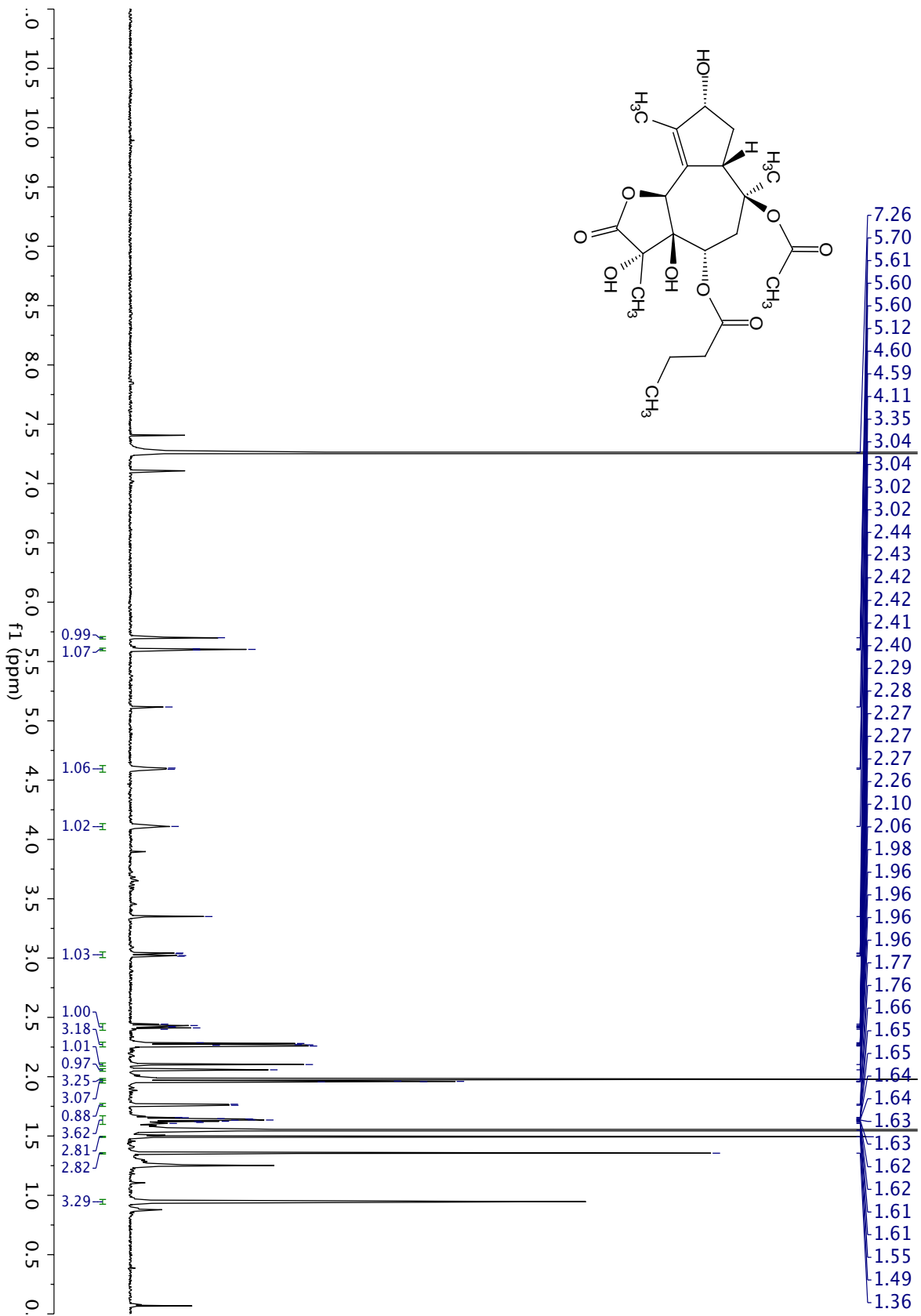


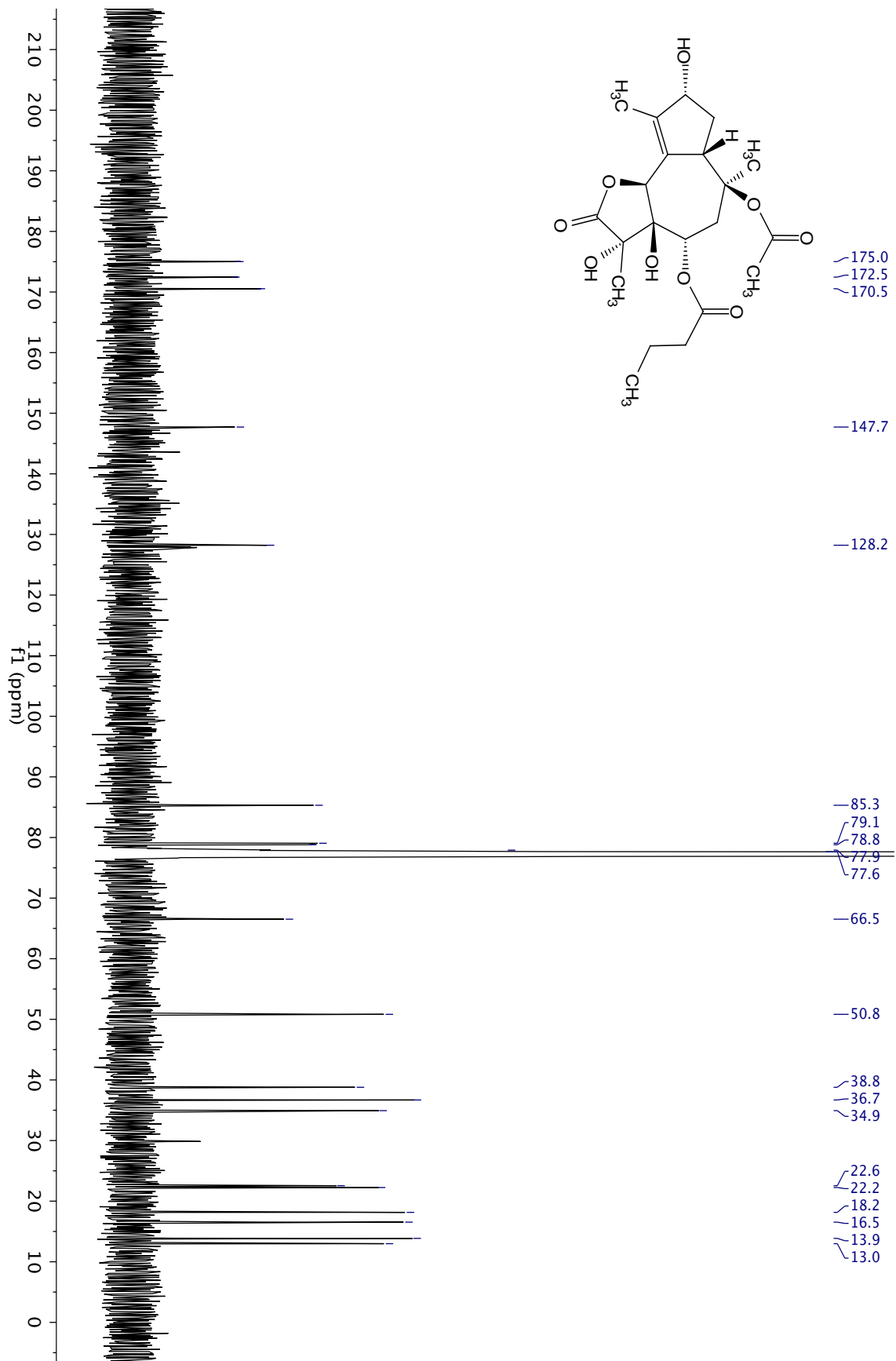


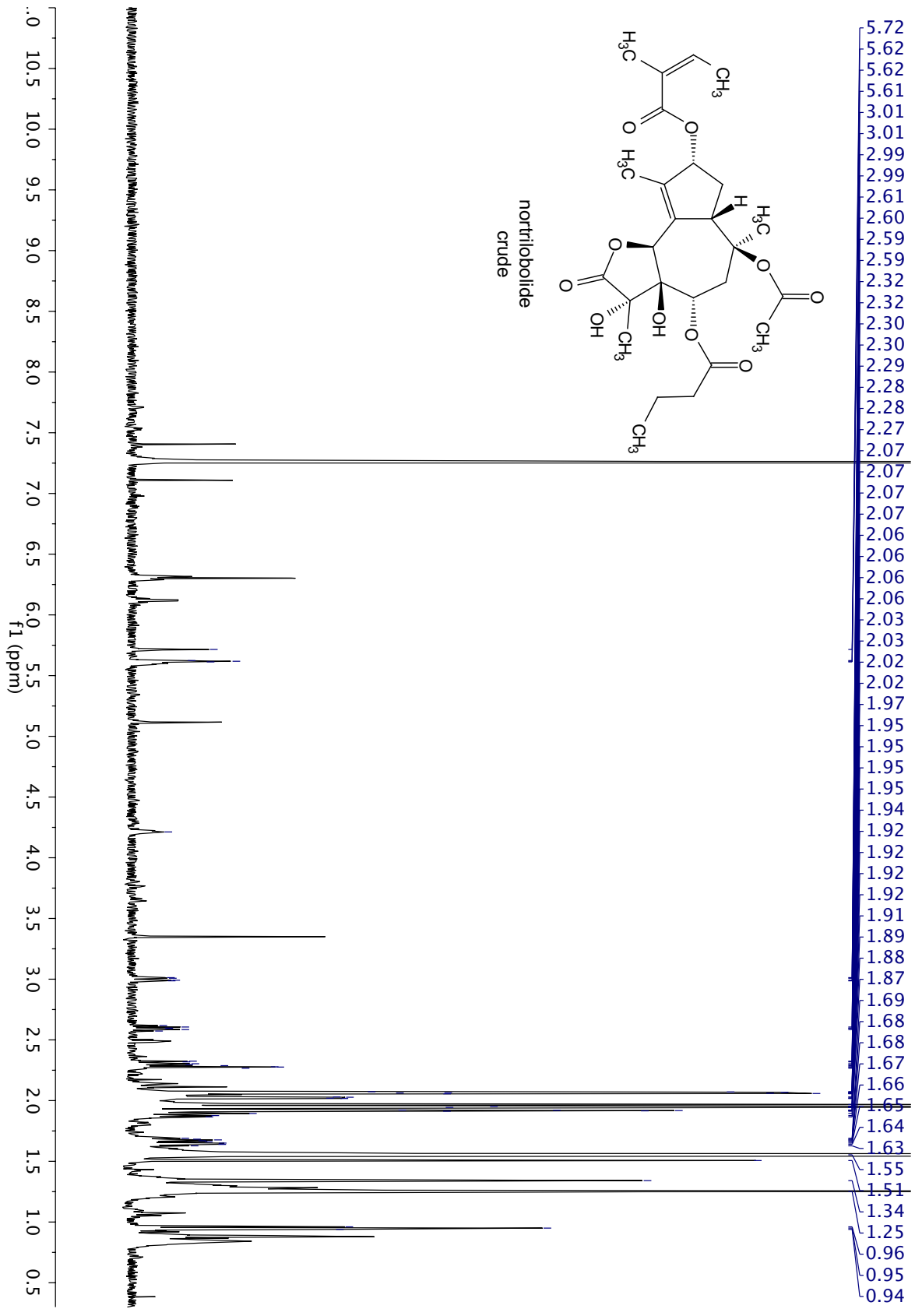


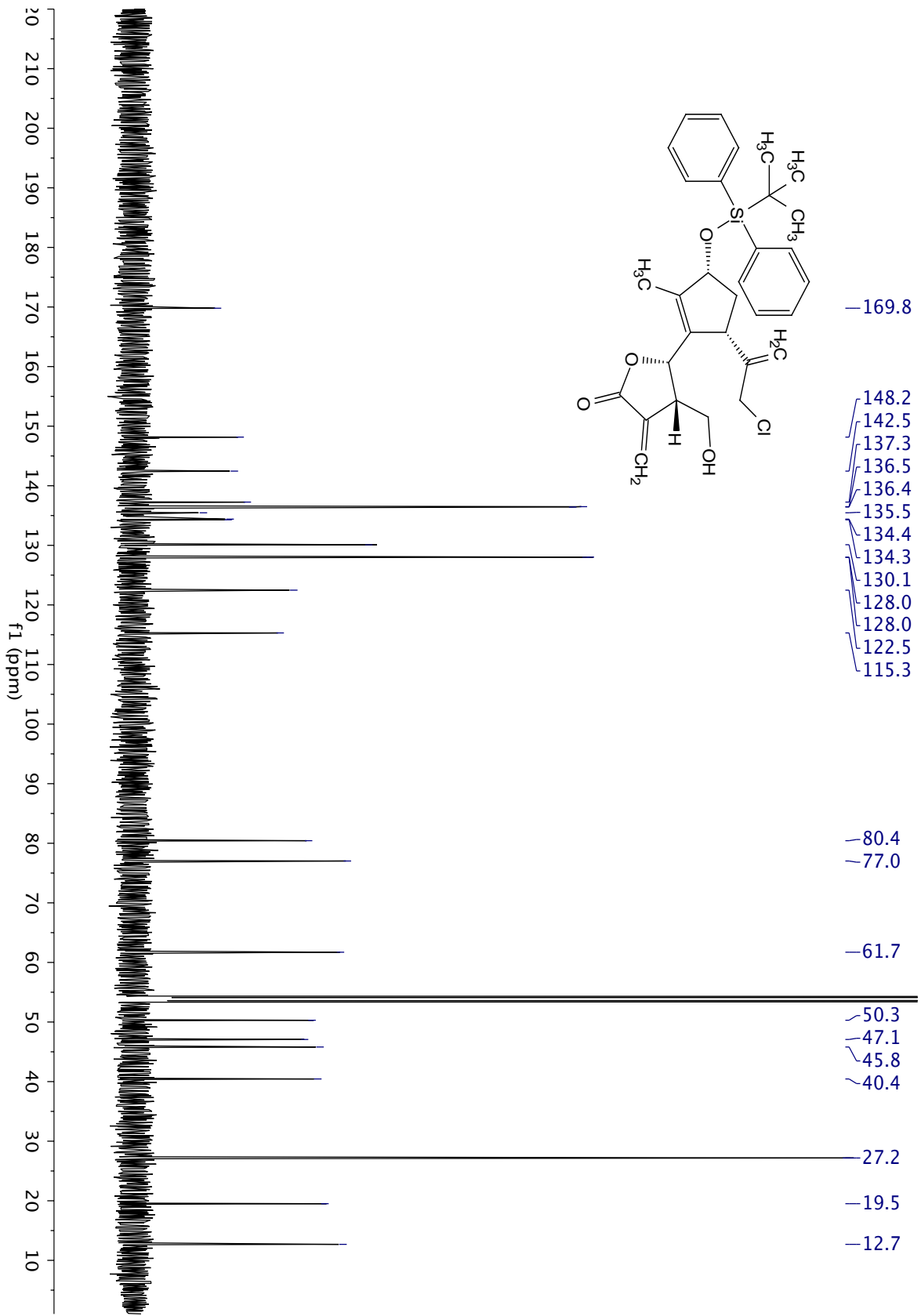


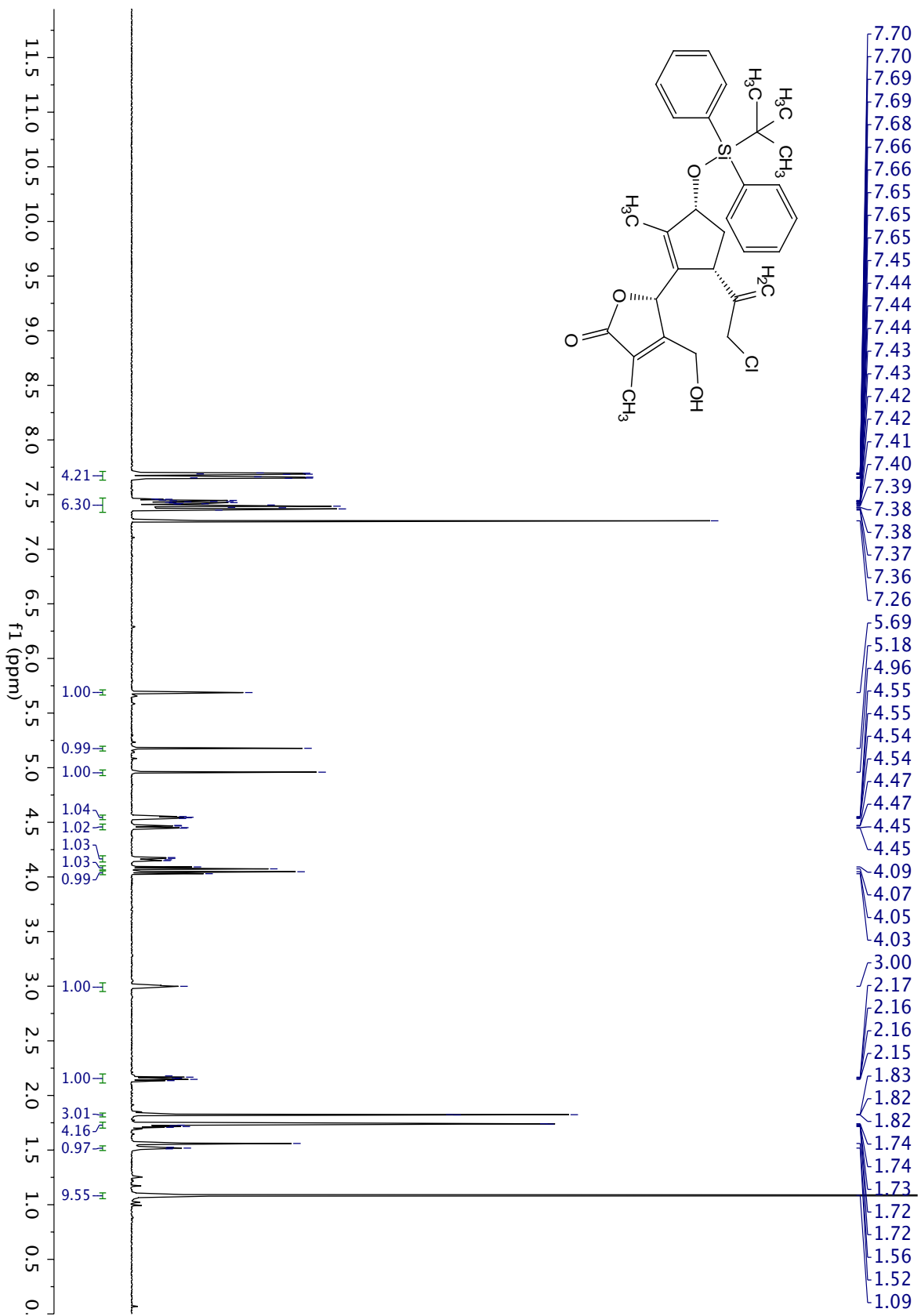


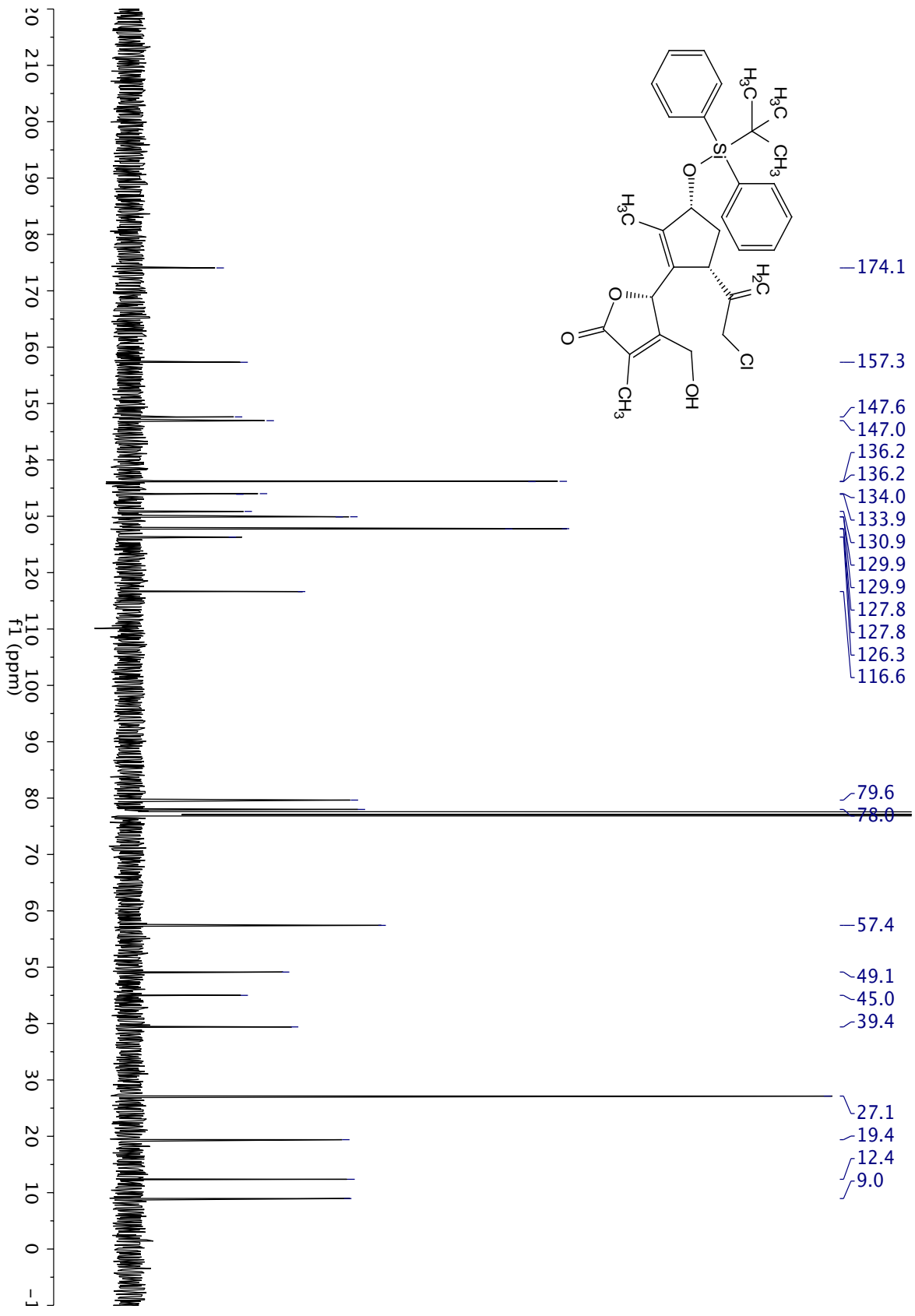


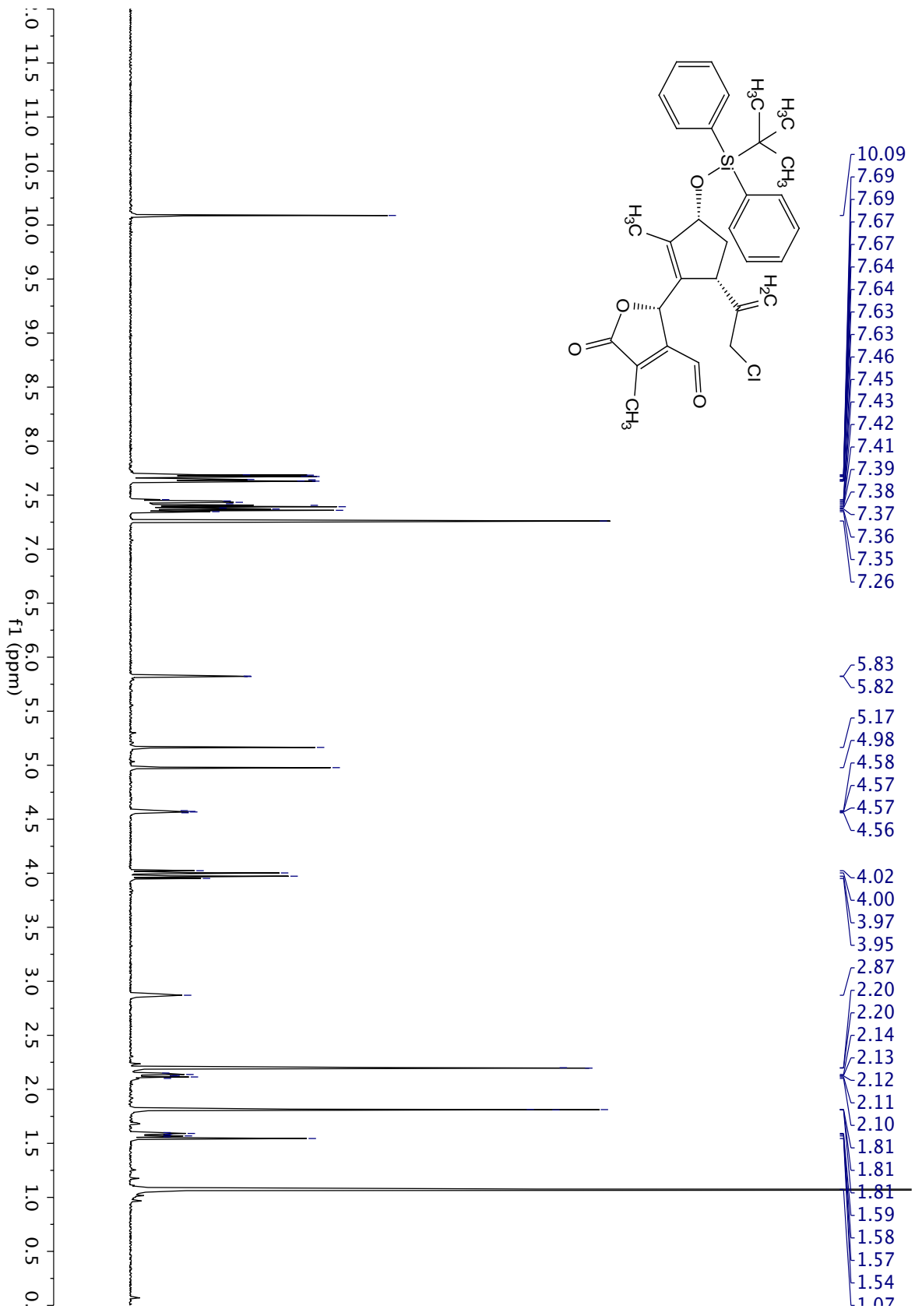


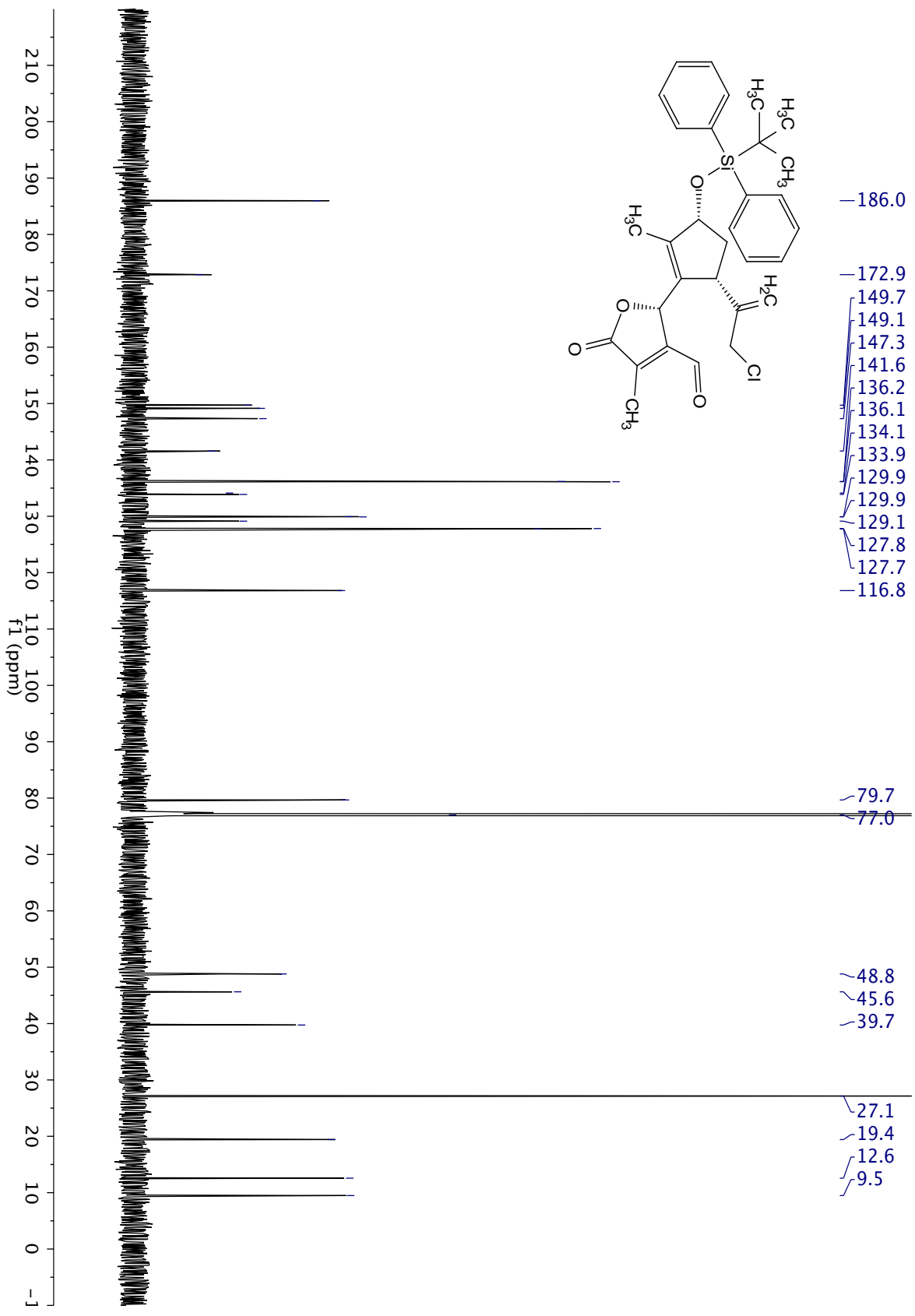


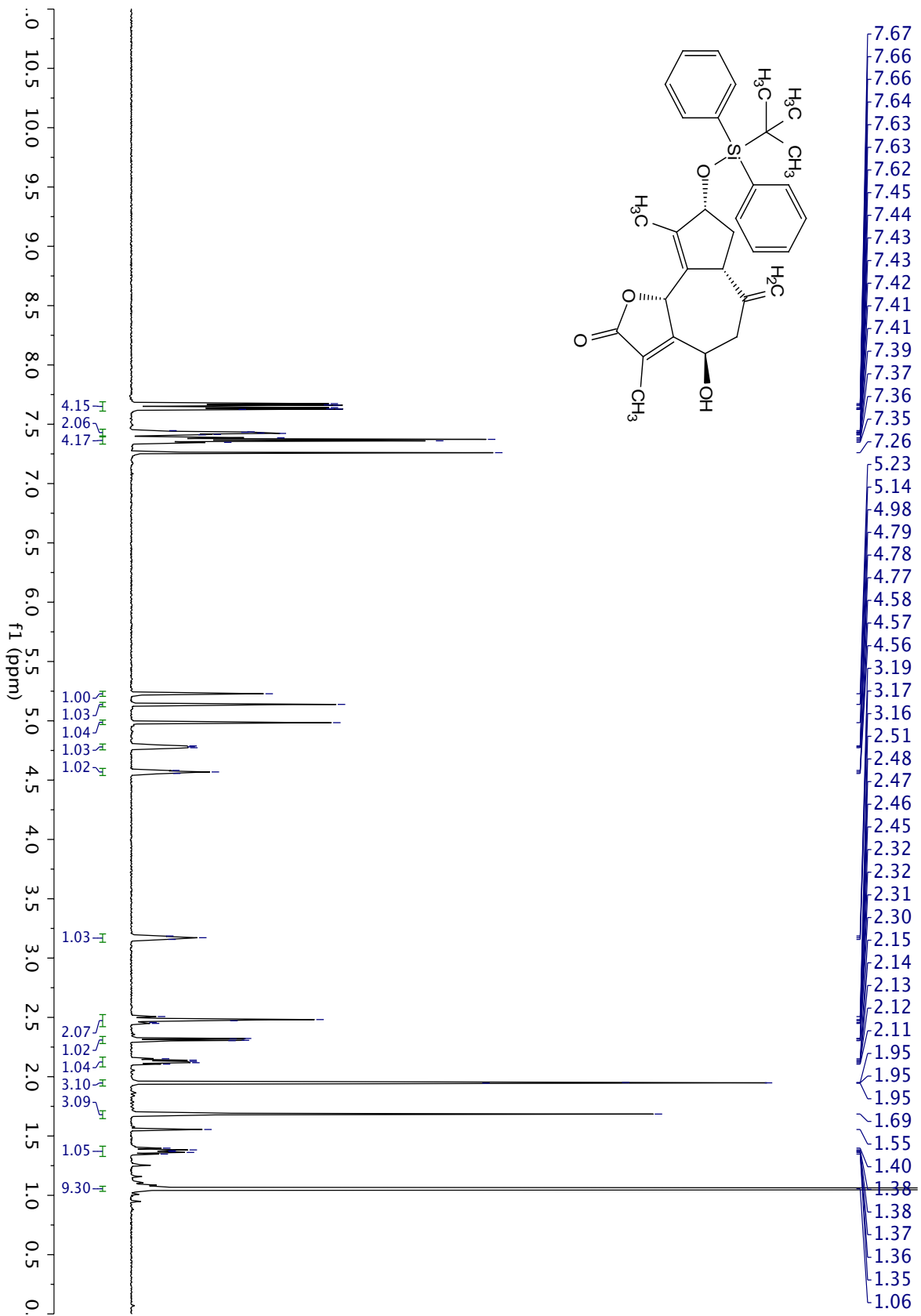


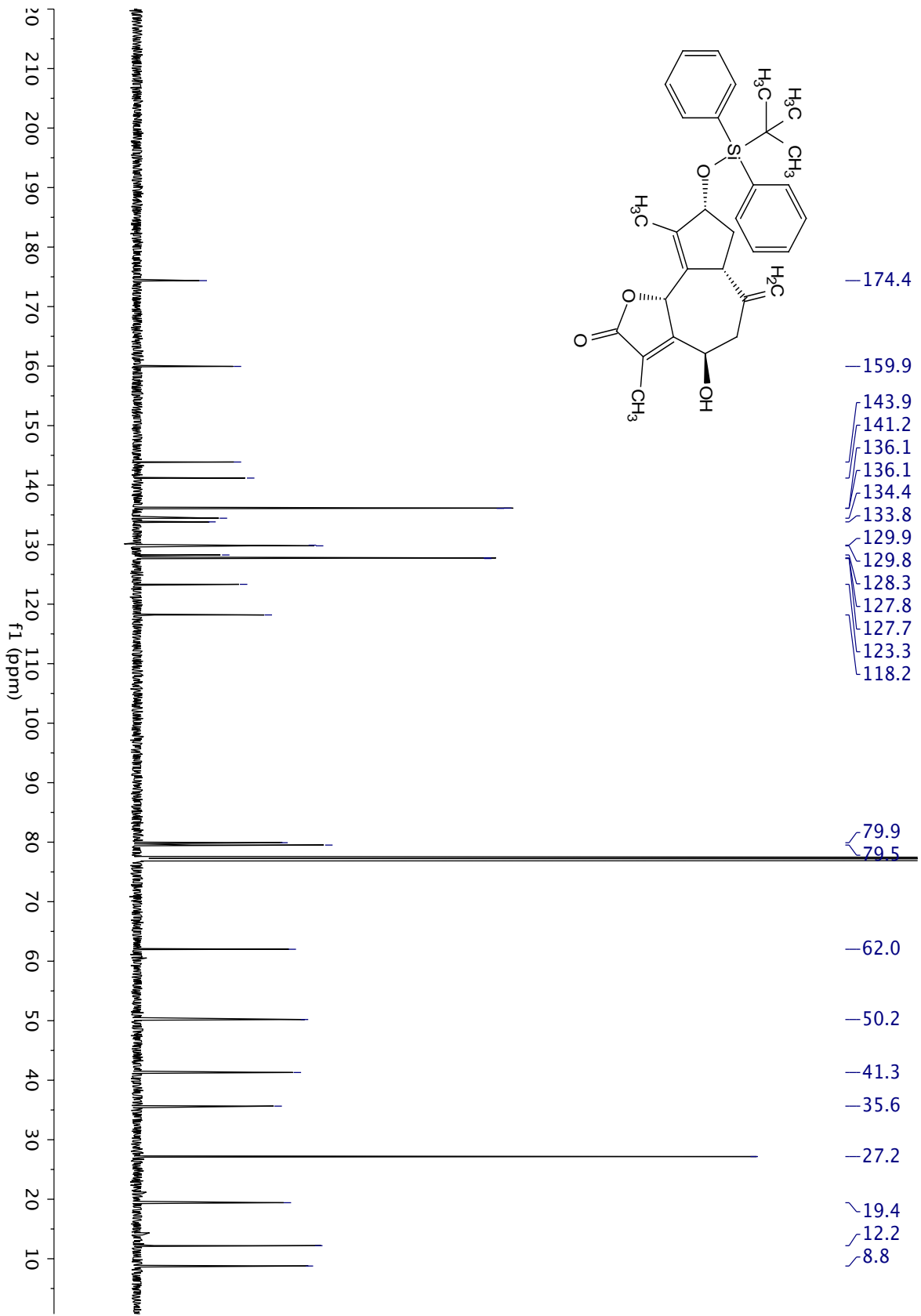


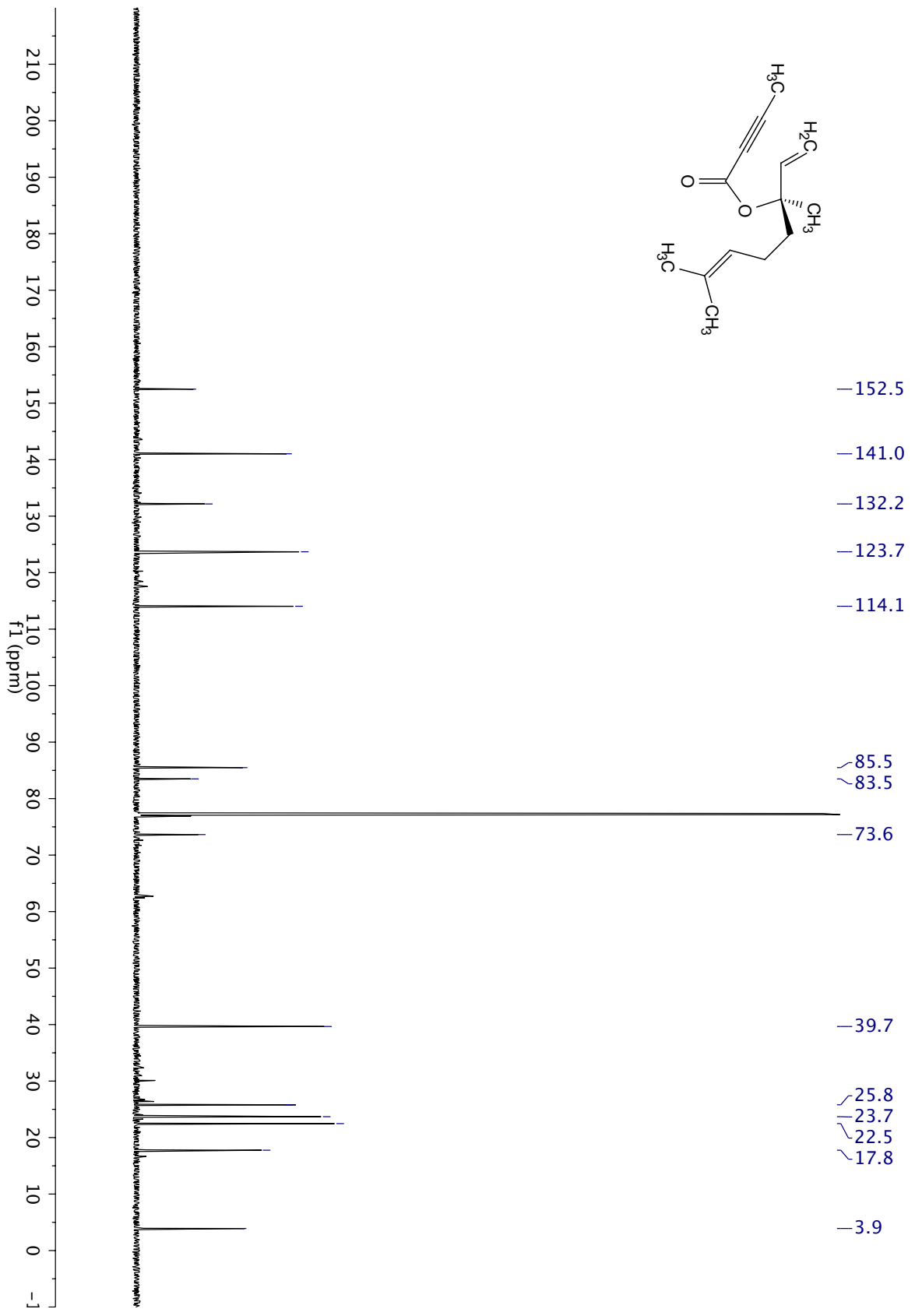
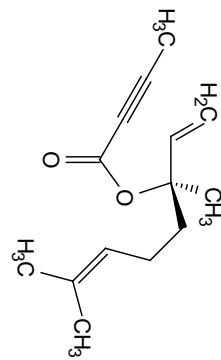


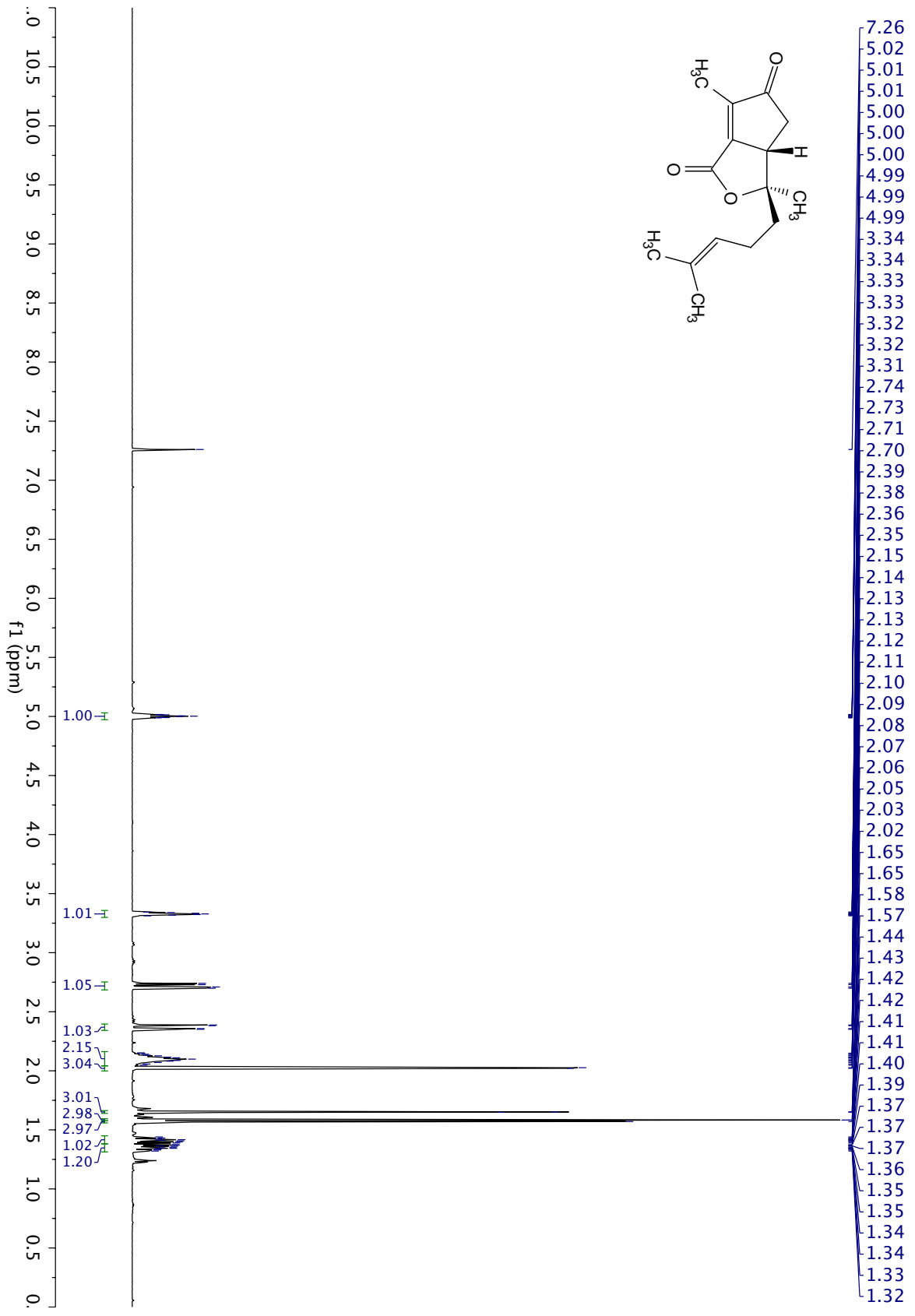


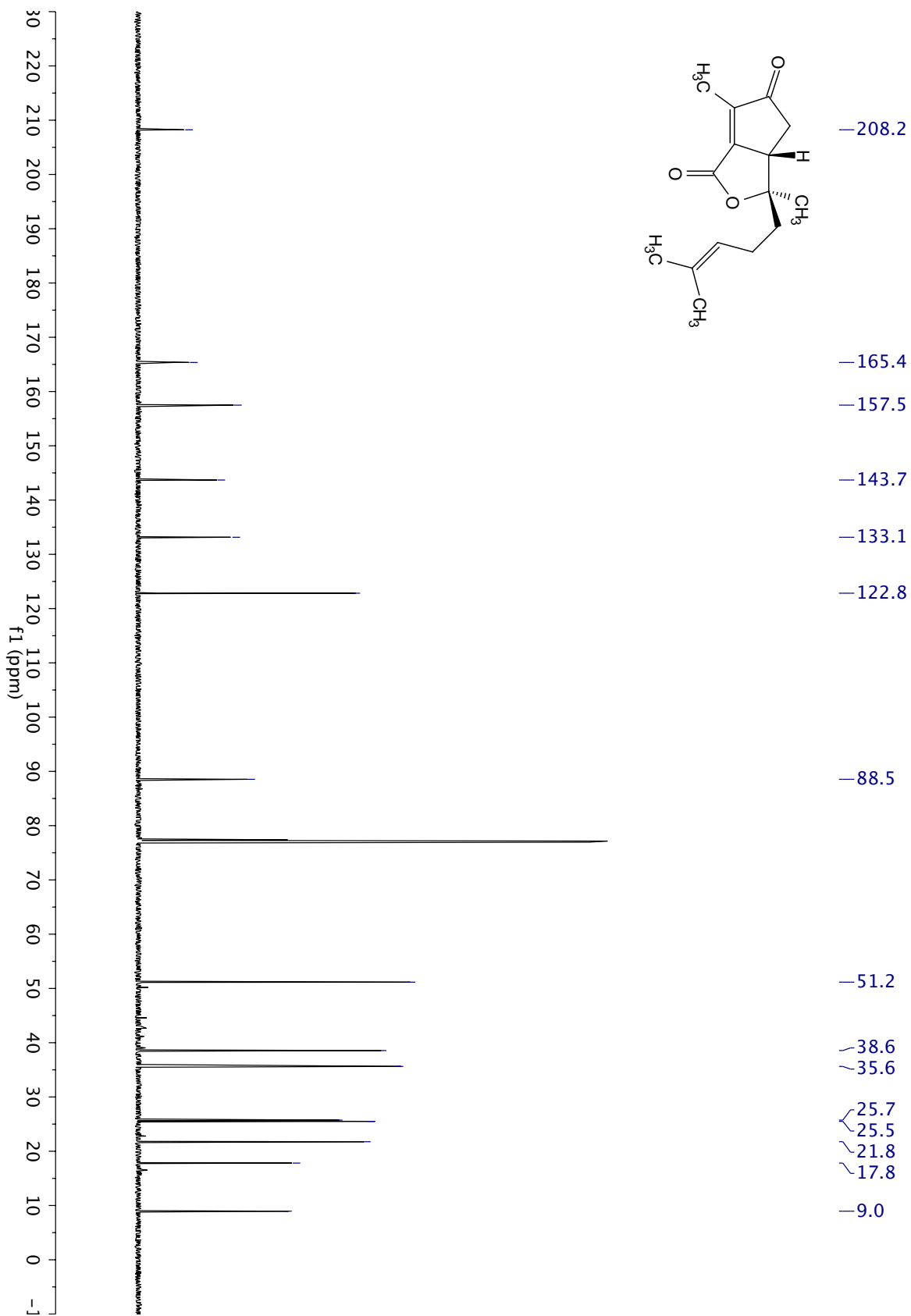


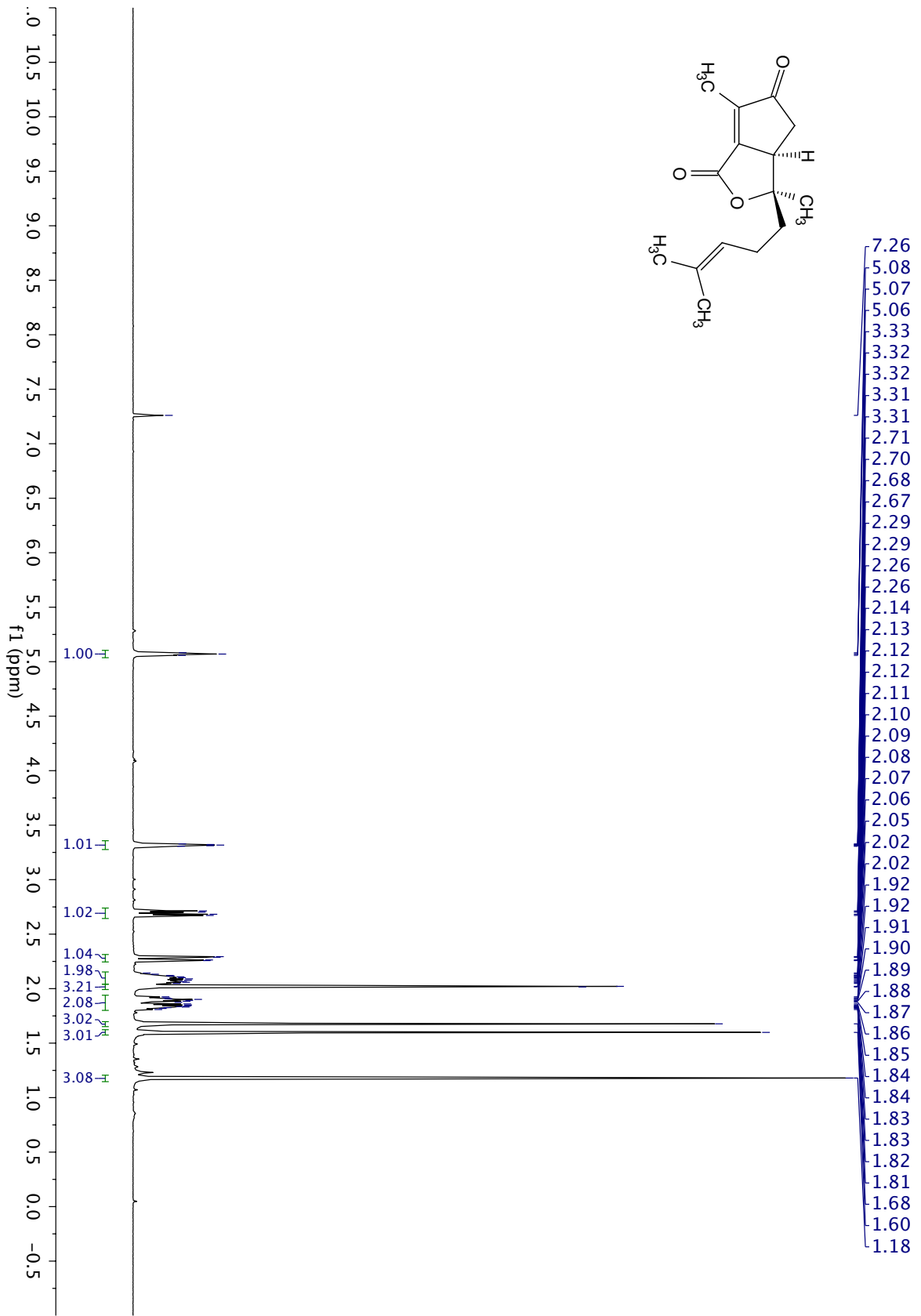


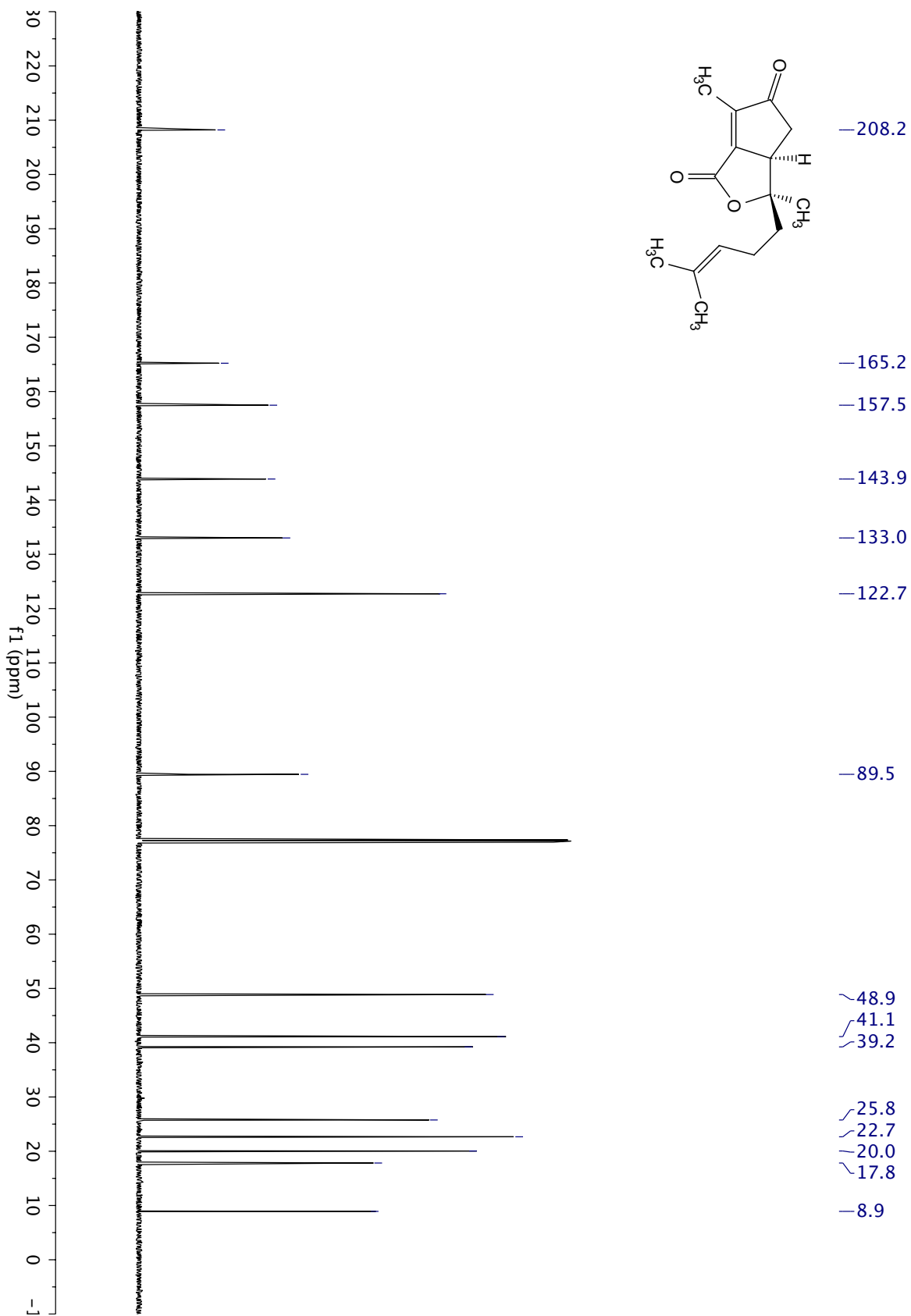


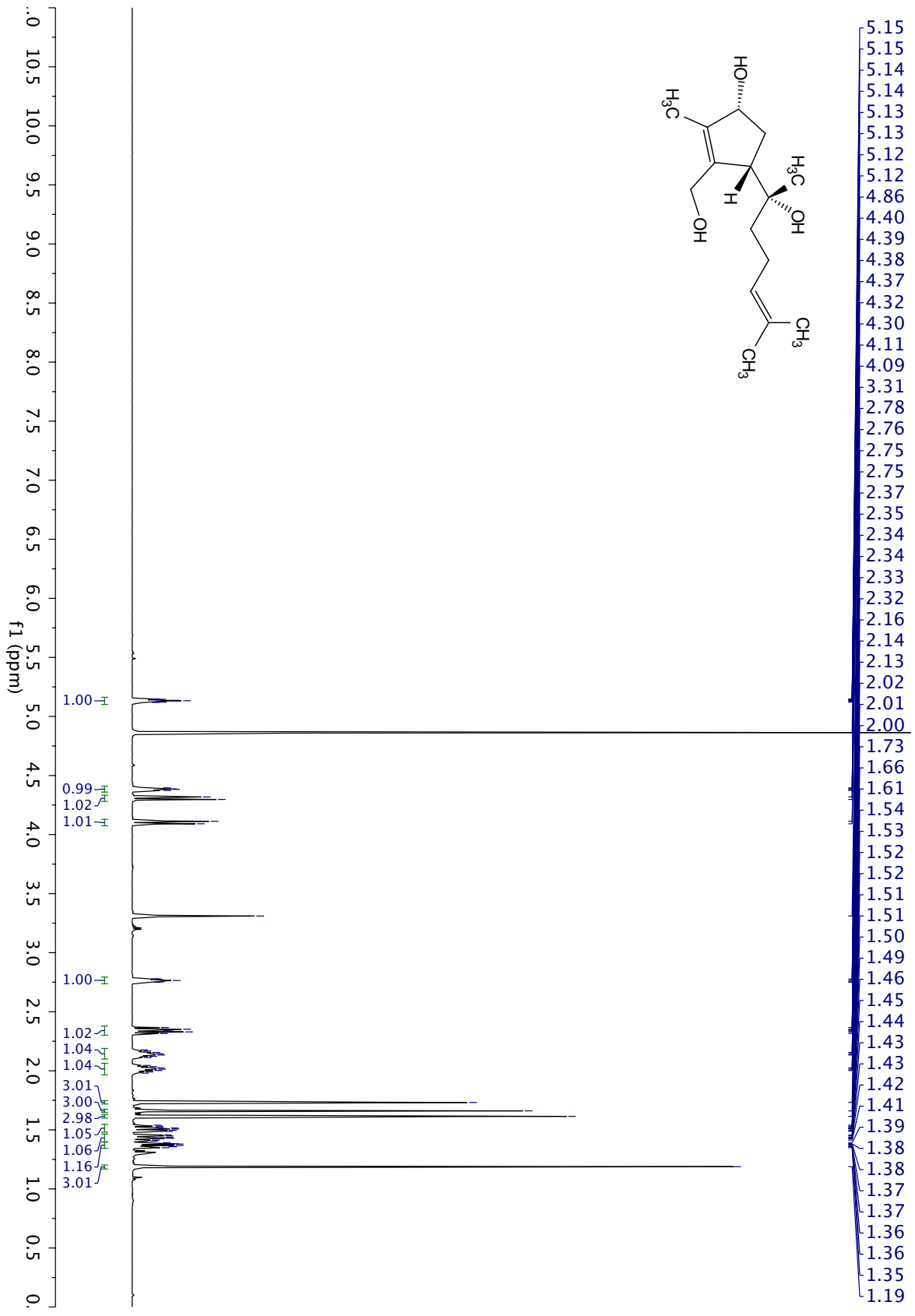


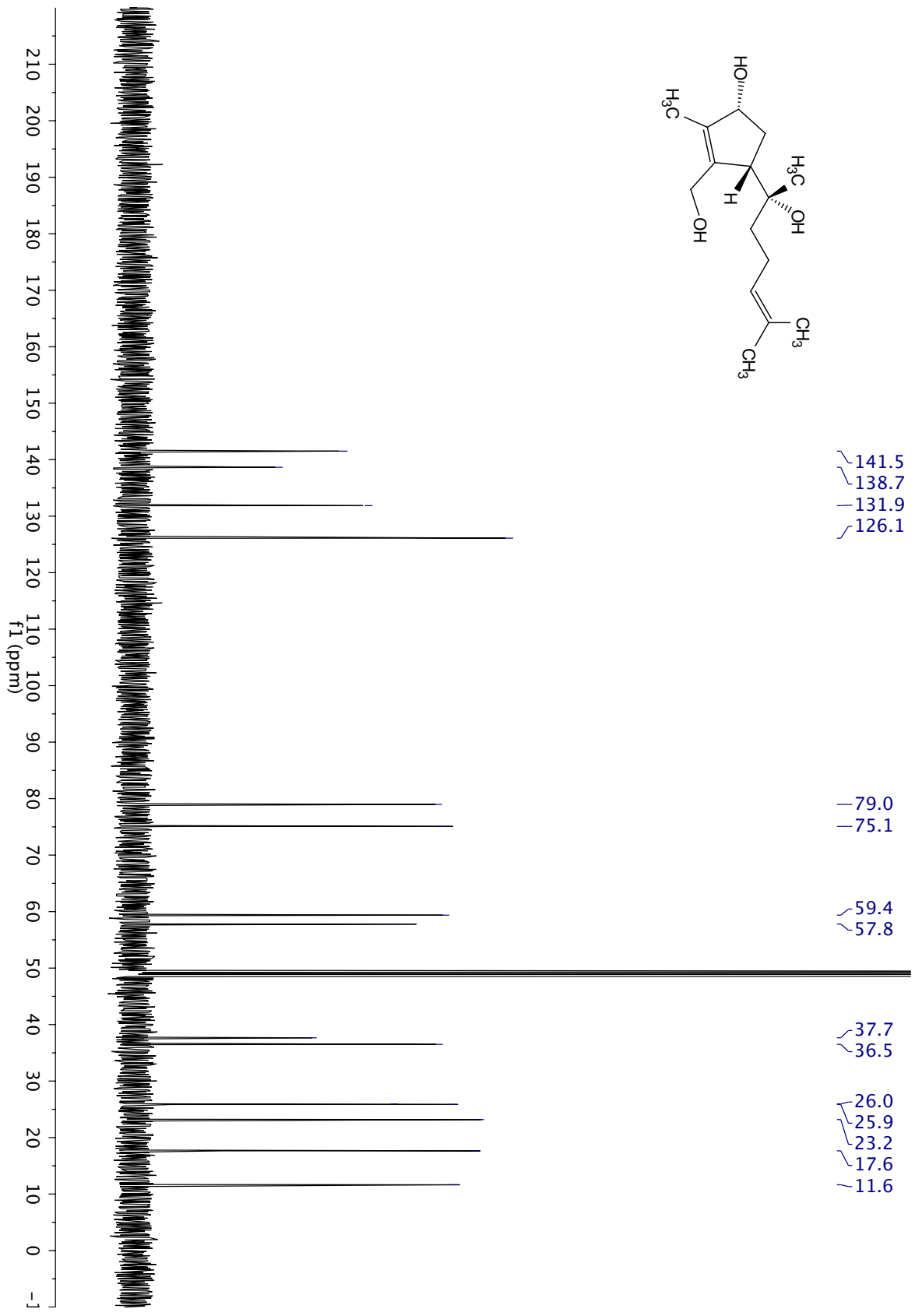


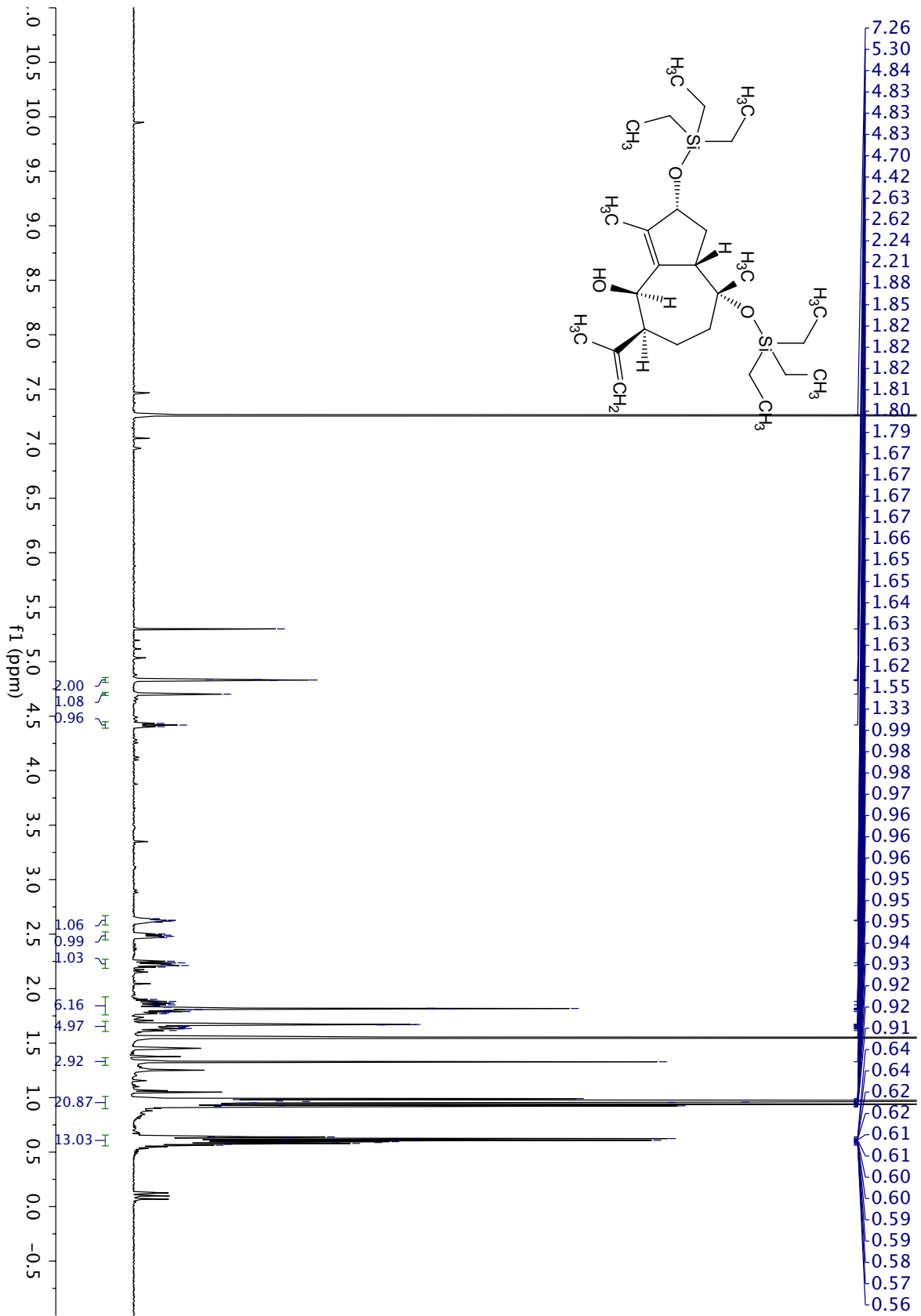


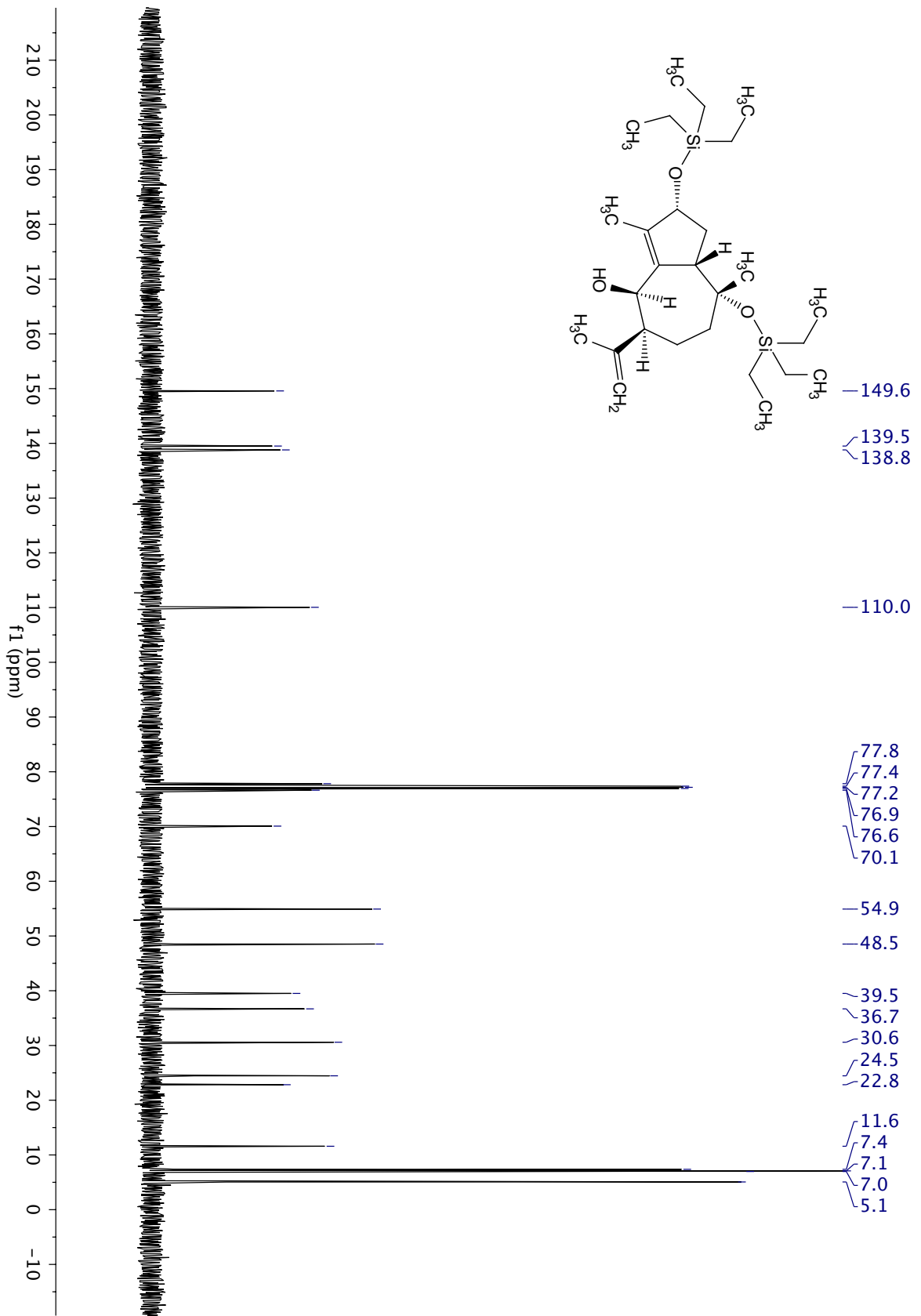


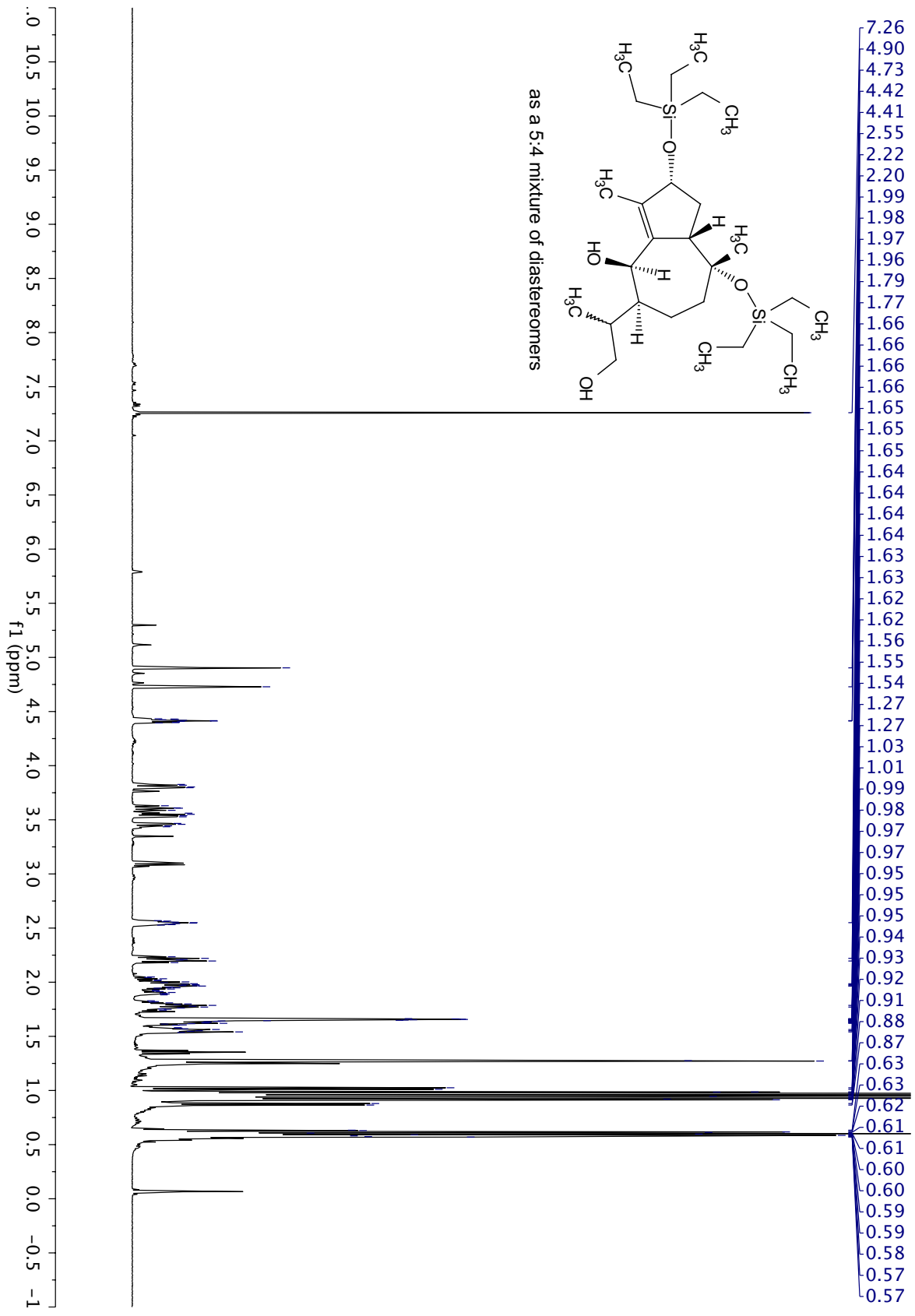


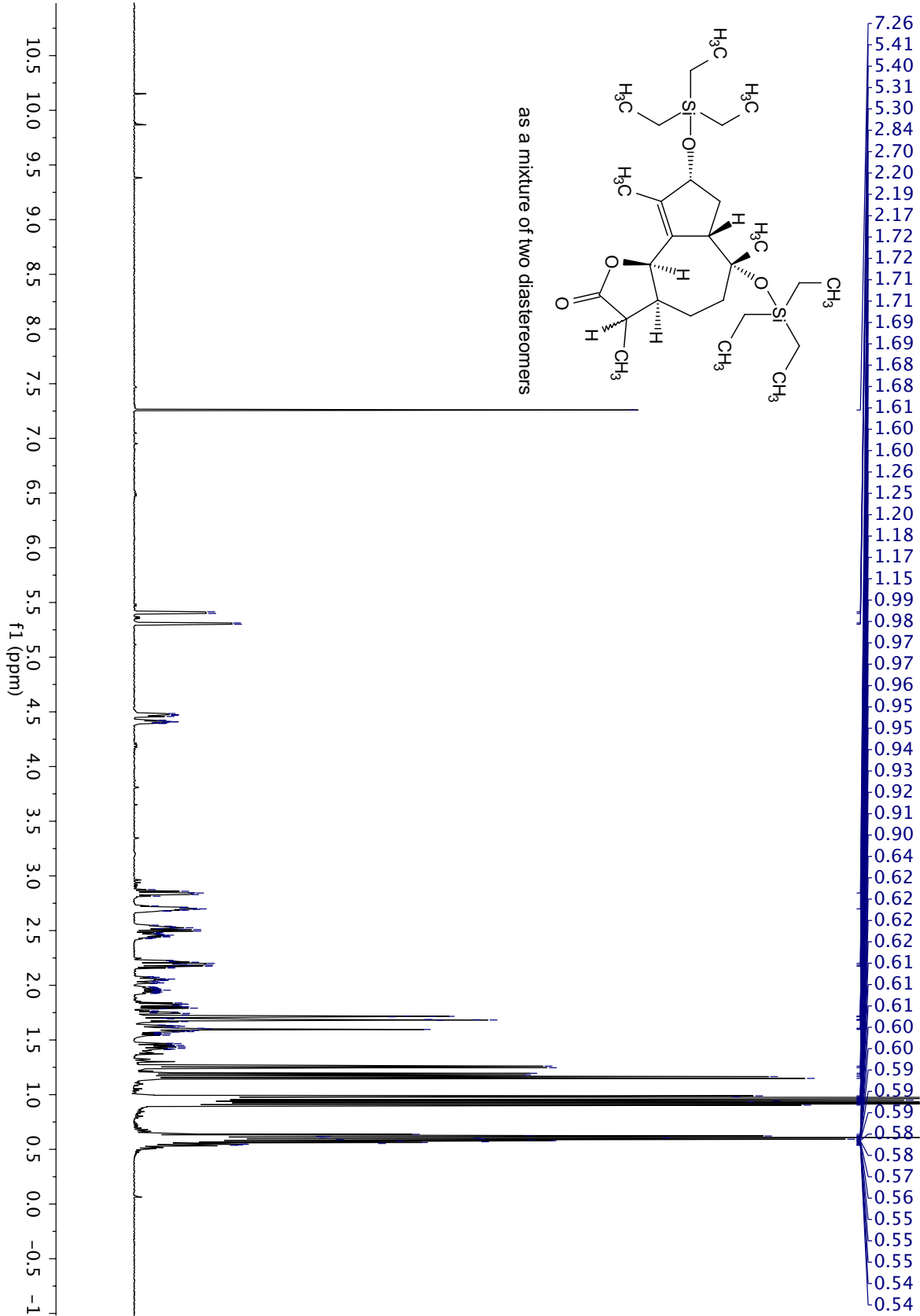


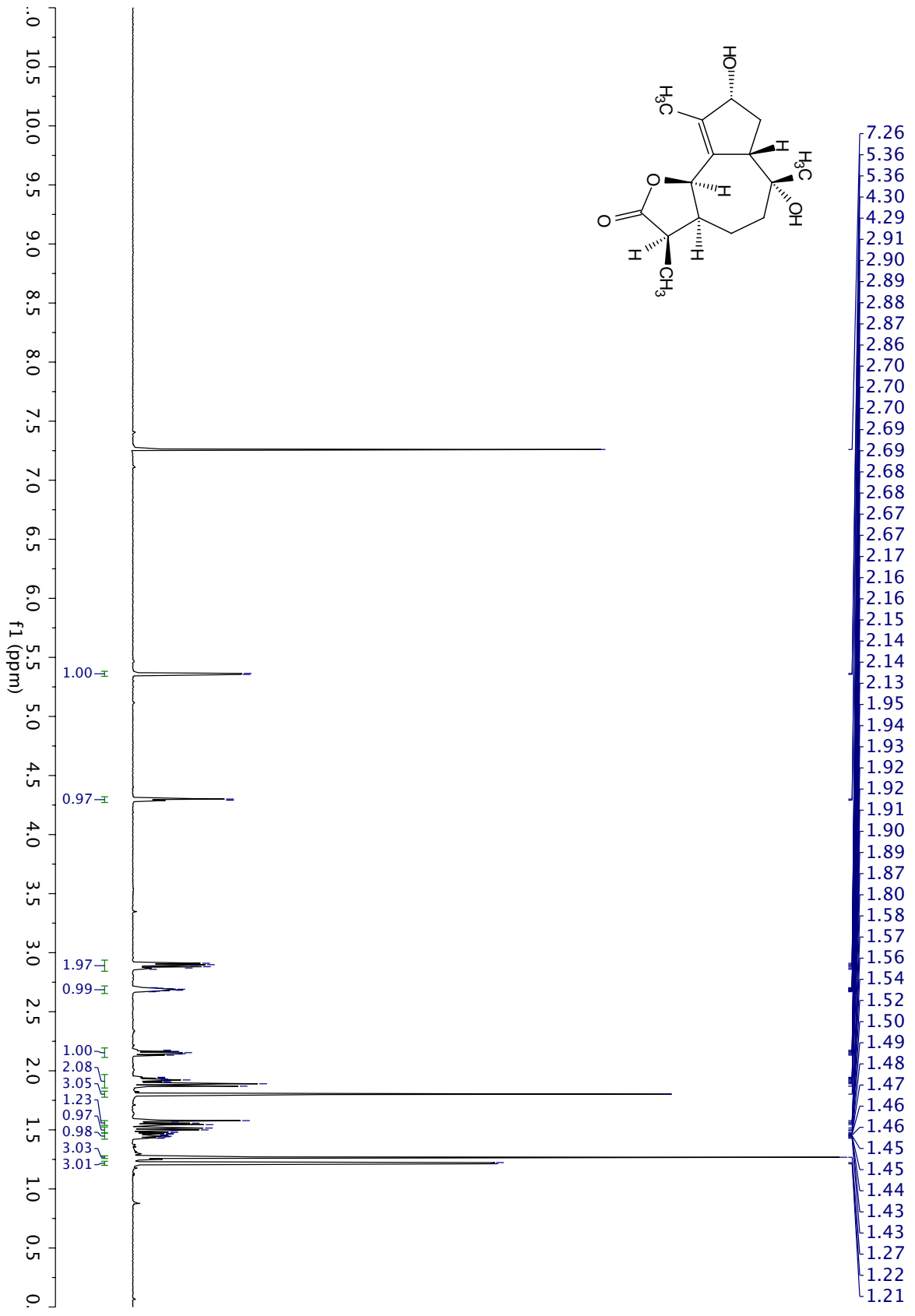


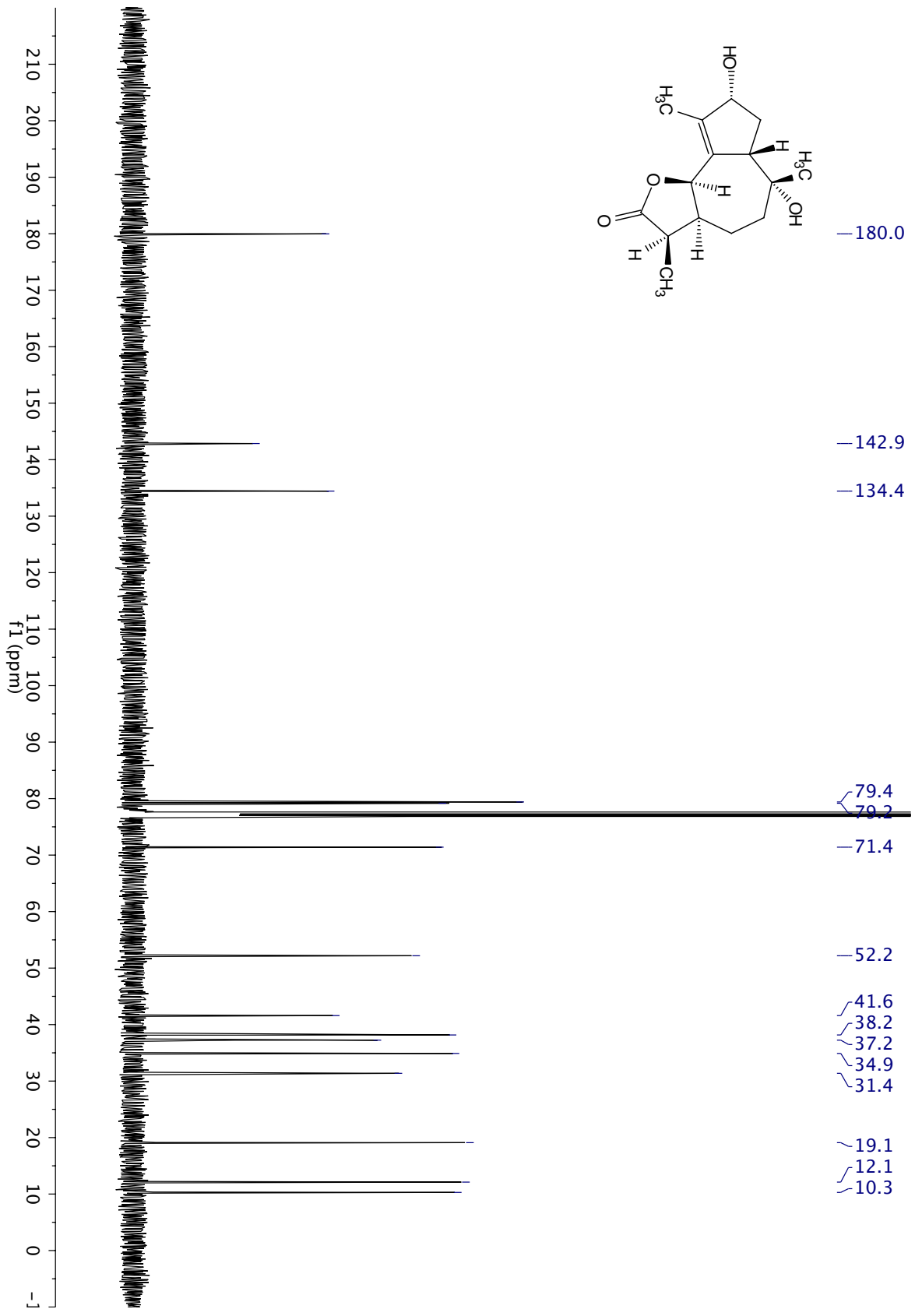


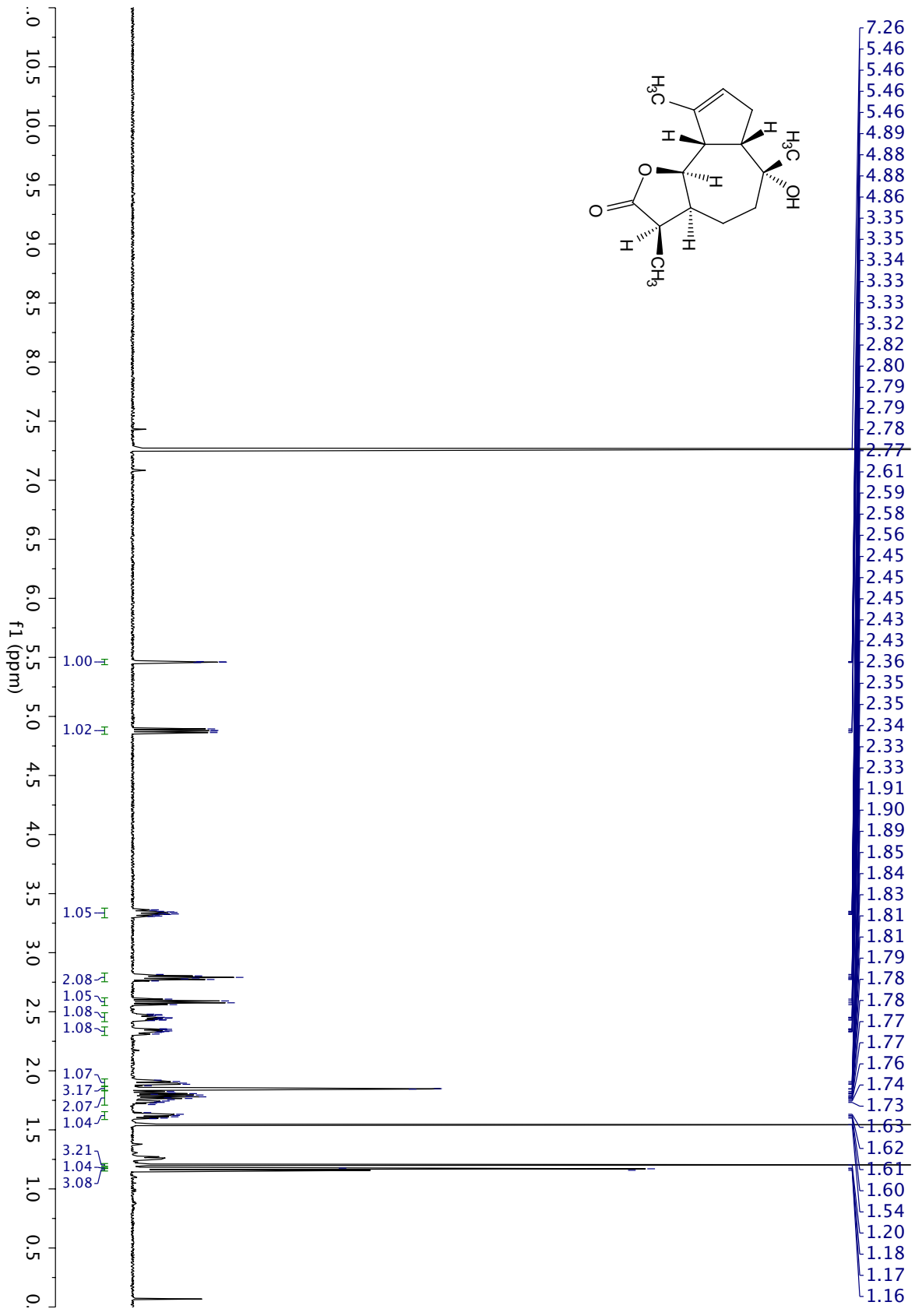


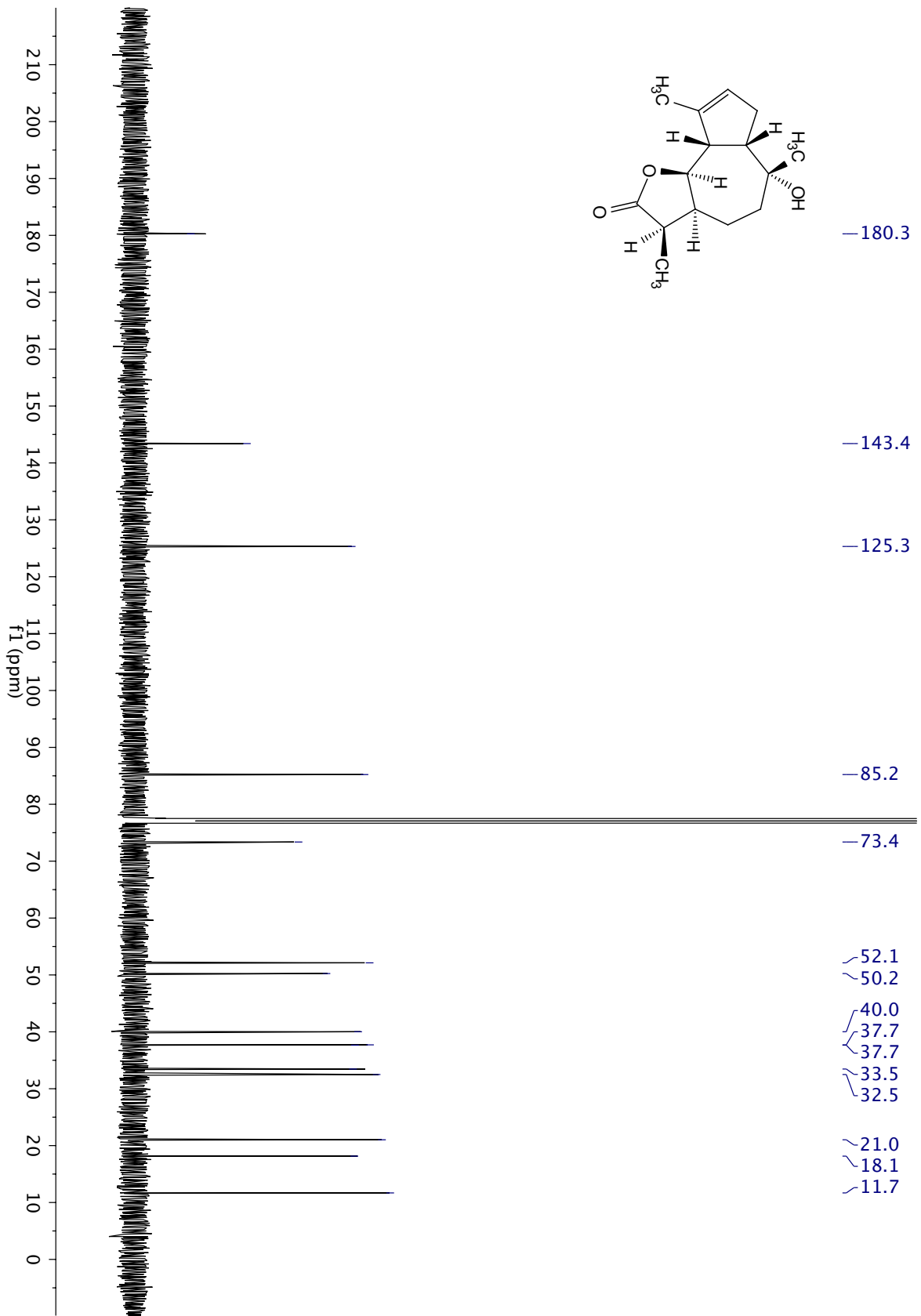


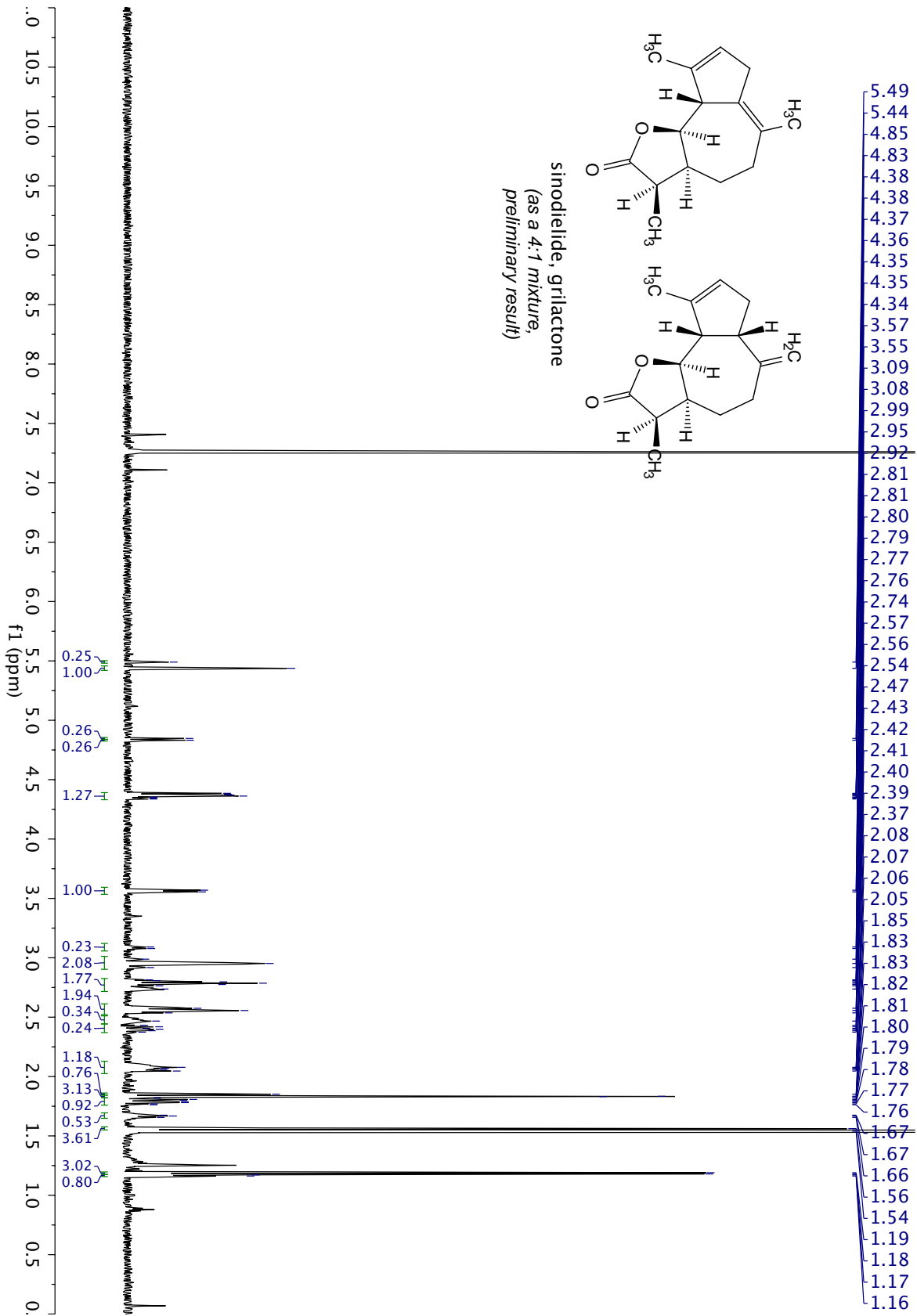


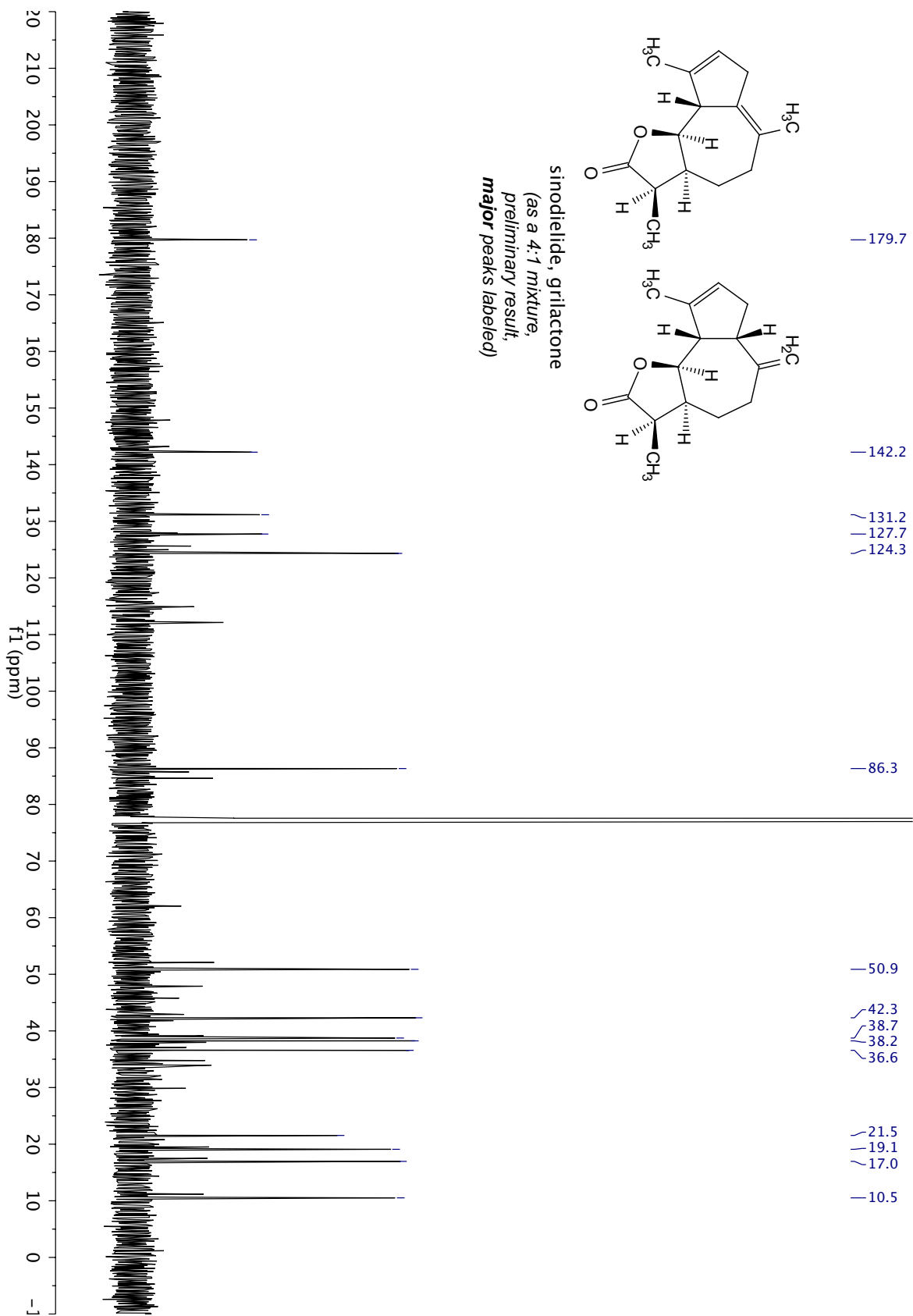


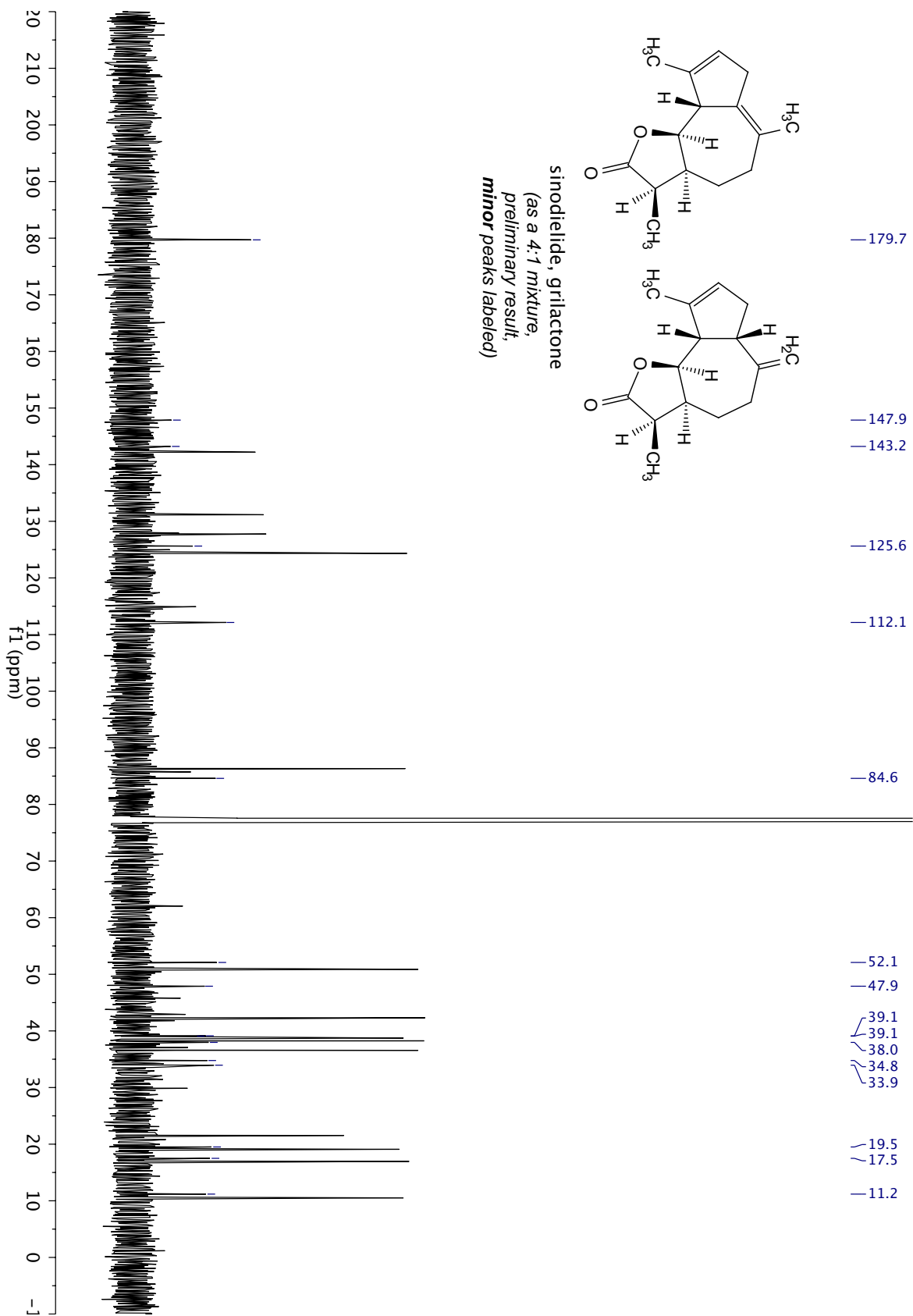


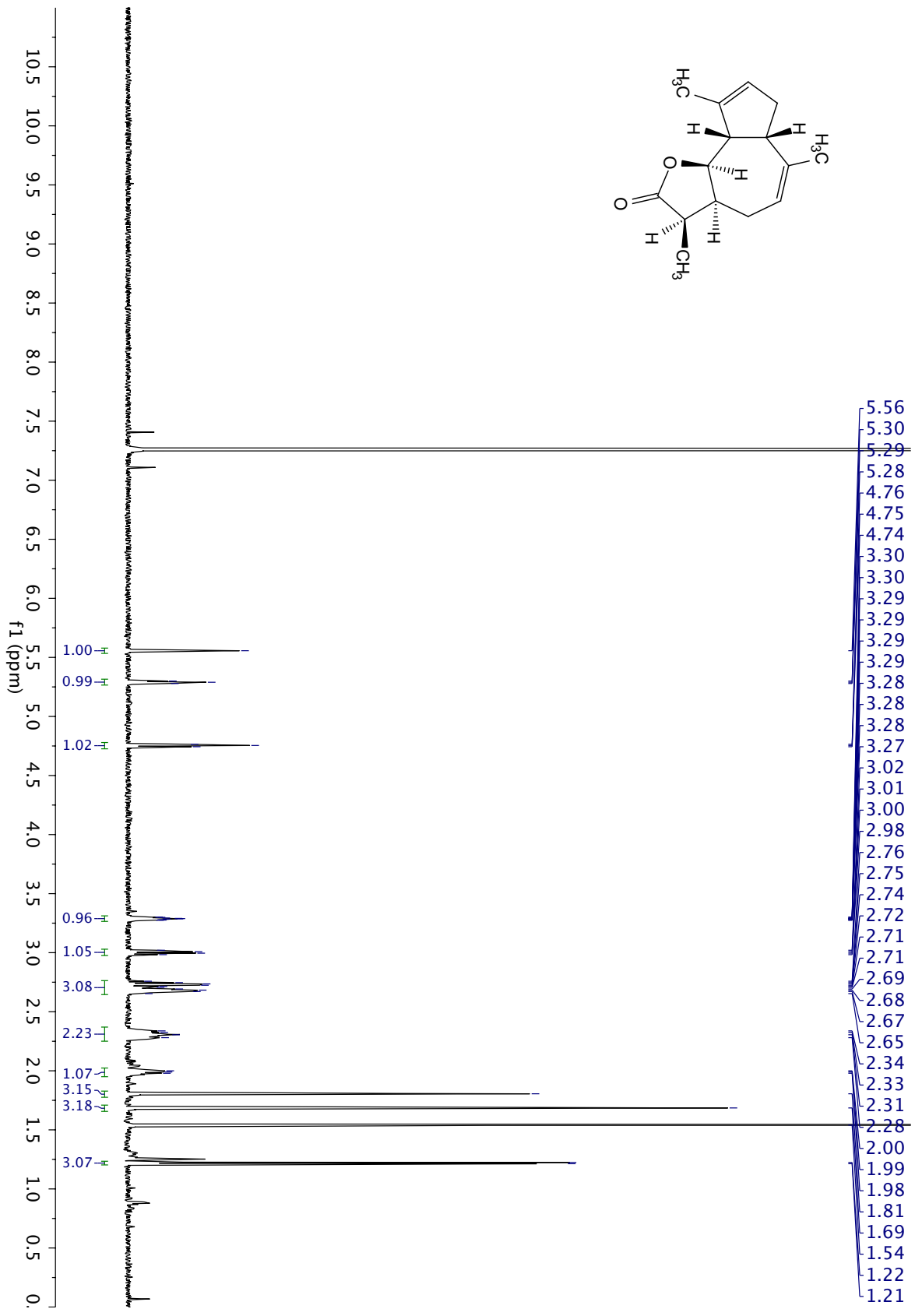


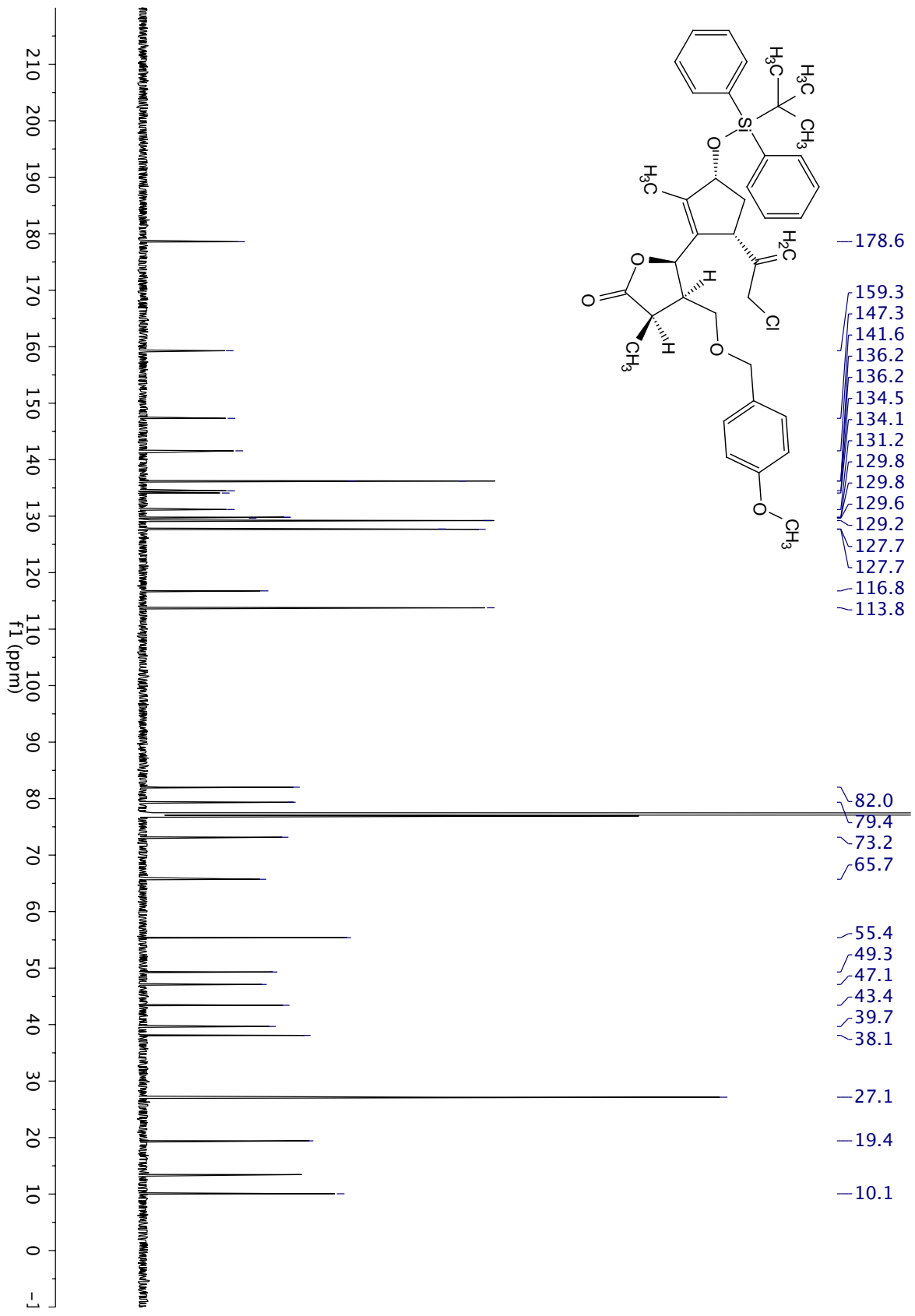


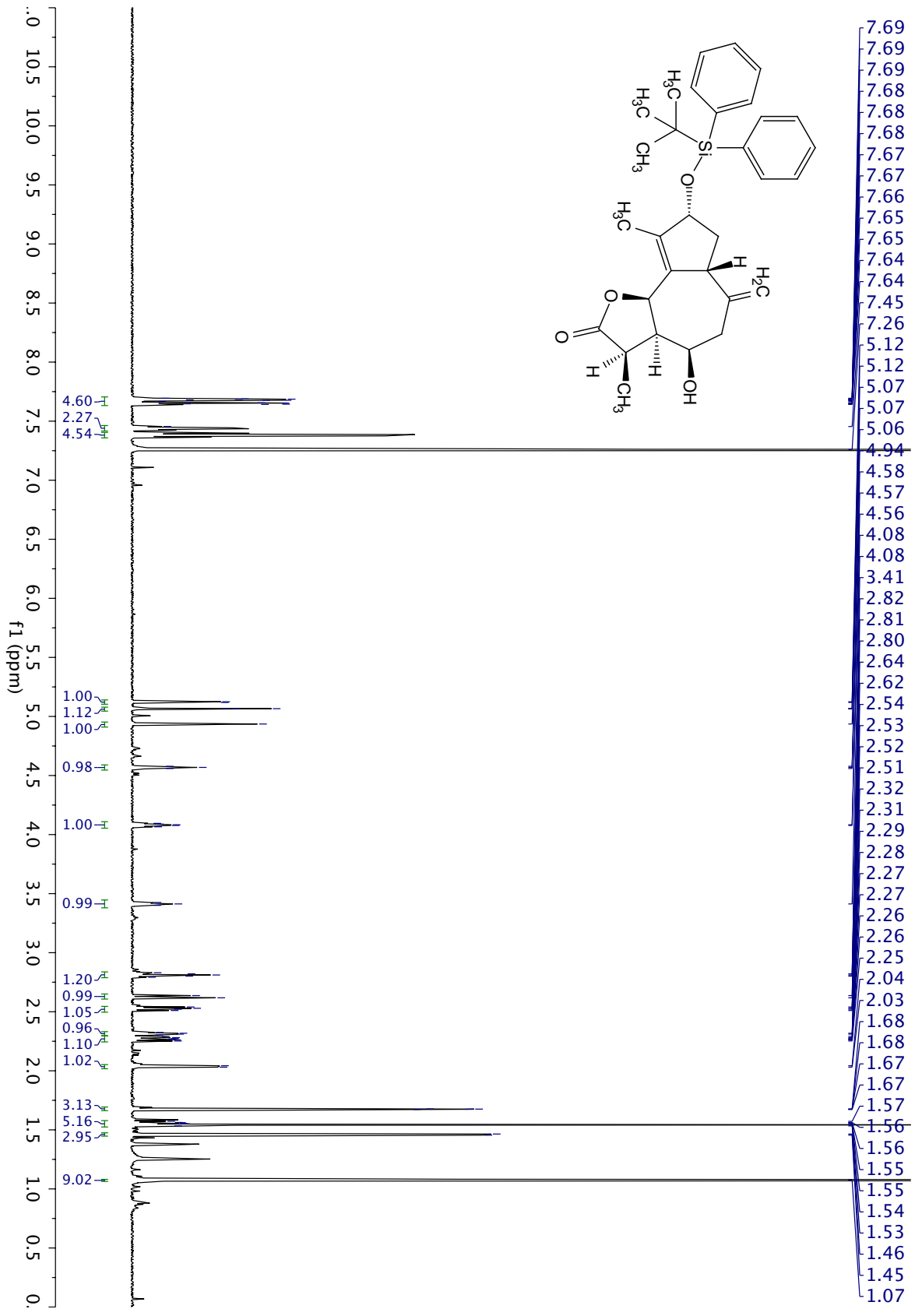


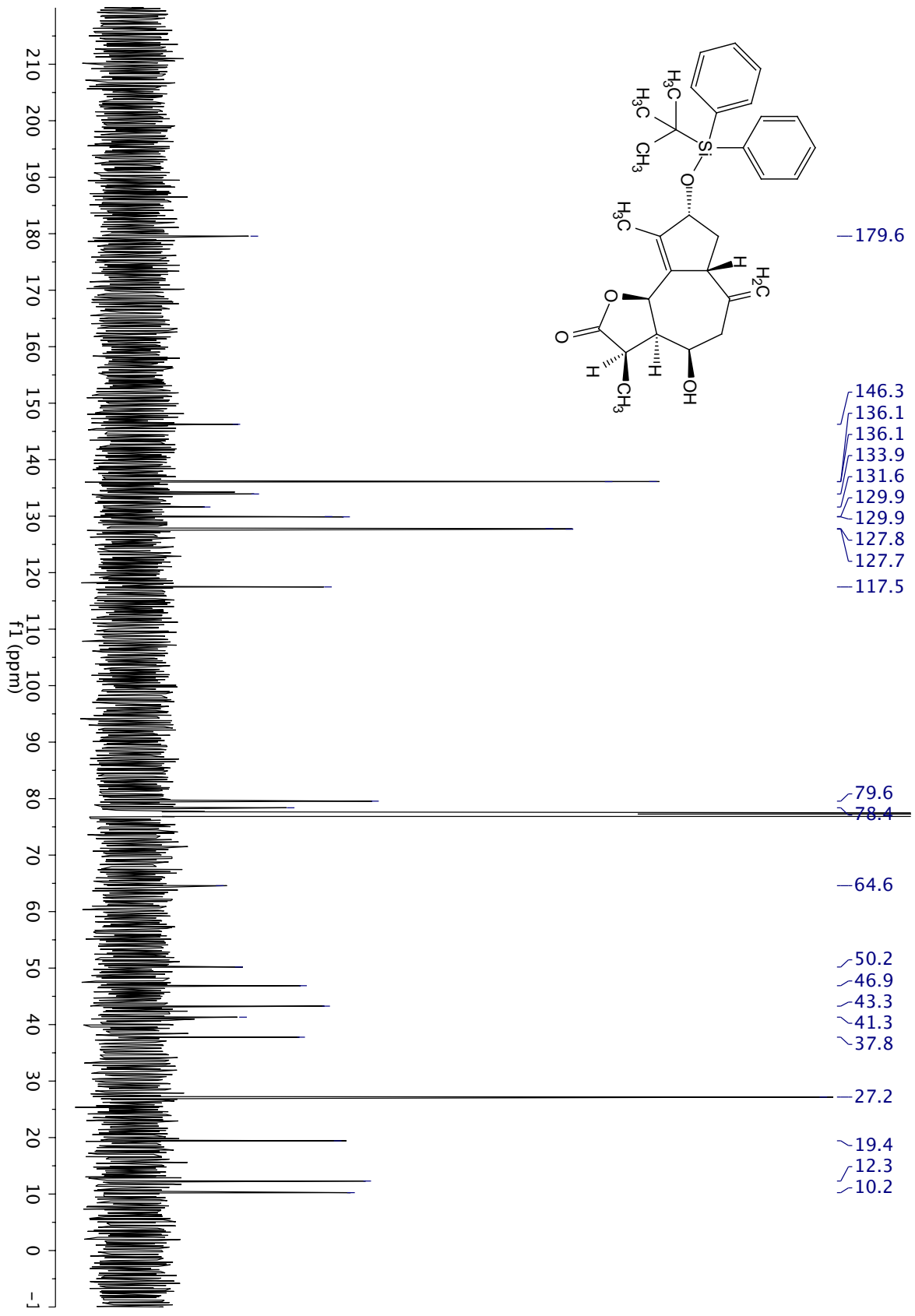


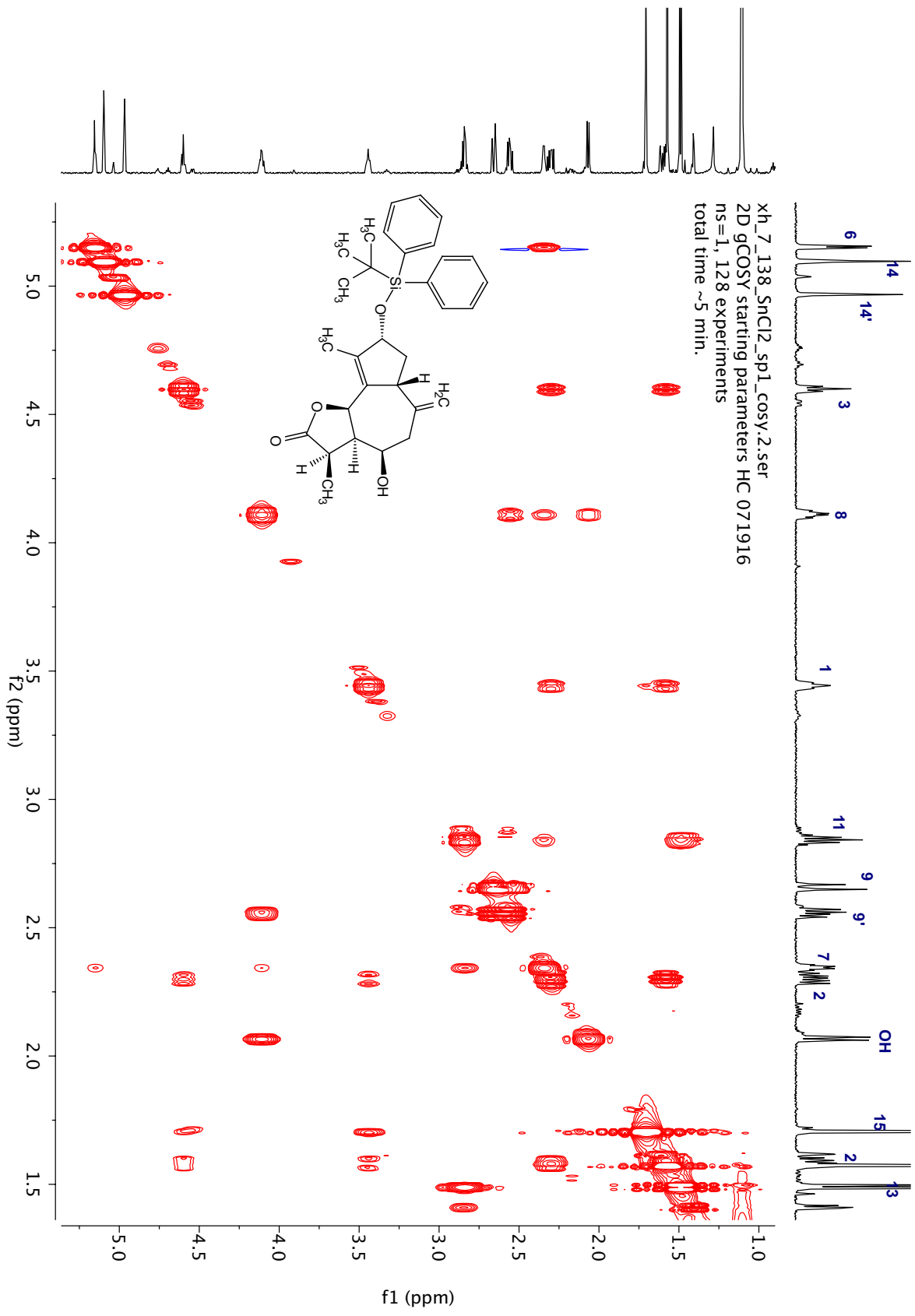




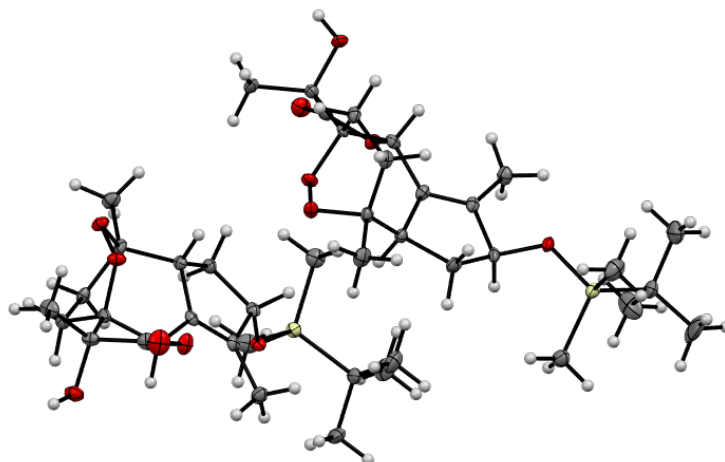








X-Ray crystallographic Analysis of Compound 258



A colorless block 0.060 x 0.030 x 0.030 mm in size was mounted on a Cryoloop with Paratone oil. Data were collected in a nitrogen gas stream at 100(2) K using phi and omega scans. Crystal-to-detector distance was 60 mm and exposure time was 10 seconds per frame using a scan width of 0.5°. Data collection was 98.8% complete to 25.000° in θ . A total of 17778 reflections were collected covering the indices, $-15 \leq h \leq 15$, $-11 \leq k \leq 11$, $-23 \leq l \leq 23$. 17778 reflections were found to be symmetry independent, with an R_{int} of 0.0405. Indexing and unit cell refinement indicated a primitive, monoclinic lattice. The space group was found to be P 21 (No. 4). The data were integrated using the Bruker SAINT software program and scaled using the TWINABS software program. Solution by iterative methods (SHELXT) produced a complete heavy-atom phasing model consistent with the proposed structure. All non-hydrogen atoms were refined anisotropically by full-matrix least-squares (SHELXL-2014). All hydrogen atoms were placed using a riding model. Their positions were constrained relative to their parent atom using the appropriate HFIX command in SHELXL-2014. Absolute stereochemistry was unambiguously determined to be *R* at C3, C4, C8, C10, C24, C25, C29, and C31, and *S* at C1, C7, C22, and C28, respectively.

Table 1. Crystal data and structure refinement for compound **258**.

X-ray ID	maimone42	
Sample/notebook ID	XH_392_Co_01	
Empirical formula	C21 H34 O6 Si	
Formula weight	410.57	
Temperature	100(2) K	
Wavelength	0.71073 Å	
Crystal system	Monoclinic	
Space group	P 21	
Unit cell dimensions	a = 12.5559(4) Å	$\alpha = 90^\circ$.
	b = 9.3020(3) Å	$\beta = 100.830(2)^\circ$.
	c = 19.5456(6) Å	$\gamma = 90^\circ$.
Volume	2242.17(12) Å ³	
Z	4	
Density (calculated)	1.216 Mg/m ³	
Absorption coefficient	0.137 mm ⁻¹	
F(000)	888	
Crystal size	0.060 x 0.030 x 0.030 mm ³	
Theta range for data collection	1.061 to 25.412°.	
Index ranges	-15 ≤ h ≤ 15, -11 ≤ k ≤ 11, -23 ≤ l ≤ 23	
Reflections collected	17778	
Independent reflections	17778 [R(int) = 0.0405]	
Completeness to theta = 25.000°	98.8 %	
Absorption correction	Semi-empirical from equivalents	
Max. and min. transmission	0.928 and 0.768	
Refinement method	Full-matrix least-squares on F ²	
Data / restraints / parameters	17778 / 1 / 524	
Goodness-of-fit on F ²	1.034	
Final R indices [I > 2σ(I)]	R1 = 0.0382, wR2 = 0.0967	
R indices (all data)	R1 = 0.0415, wR2 = 0.0989	
Absolute structure parameter	-0.01(6)	
Extinction coefficient	n/a	
Largest diff. peak and hole	0.224 and -0.271 e.Å ⁻³	

Table 2. Atomic coordinates ($\times 10^4$) and equivalent isotropic displacement parameters ($\text{\AA}^2 \times 10^3$) for maimone42. $U(\text{eq})$ is defined as one third of the trace of the orthogonalized U^{ij} tensor.

	x	y	z	$U(\text{eq})$
C(1)	3170(3)	3813(5)	1587(2)	14(1)
C(2)	4230(3)	3040(5)	1891(2)	17(1)
C(3)	5148(3)	4081(5)	1799(2)	13(1)
C(4)	6208(3)	3336(5)	1709(2)	14(1)
C(5)	6208(3)	2893(5)	954(2)	16(1)
C(6)	6698(3)	4109(5)	581(2)	15(1)
C(7)	6406(3)	5552(5)	840(2)	11(1)
C(8)	6807(3)	6904(5)	520(2)	15(1)
C(9)	6046(3)	8039(5)	731(2)	16(1)
C(10)	5184(3)	5844(5)	726(2)	13(1)
C(11)	4592(3)	5008(5)	1190(2)	13(1)
C(12)	3510(3)	4896(5)	1092(2)	14(1)
C(13)	6513(4)	2126(5)	2229(2)	21(1)
C(14)	8001(3)	7272(5)	745(2)	18(1)
C(15)	2688(3)	5726(5)	596(2)	18(1)
C(16)	1949(3)	1716(6)	2488(2)	21(1)
C(17)	1804(4)	-90(6)	1161(3)	29(1)
C(18)	145(3)	2356(5)	1235(2)	21(1)
C(19)	-635(4)	1302(8)	1491(3)	53(2)
C(20)	-143(4)	2442(6)	439(2)	32(1)
C(21)	24(4)	3845(6)	1539(3)	38(2)
C(22)	7268(3)	6226(5)	3403(2)	13(1)
C(23)	8146(3)	7002(5)	3098(2)	14(1)
C(24)	9120(3)	5975(5)	3190(2)	13(1)
C(25)	10224(3)	6748(5)	3300(2)	14(1)
C(26)	10626(3)	7218(5)	4054(2)	15(1)
C(27)	11338(3)	6021(5)	4454(2)	15(1)
C(28)	10950(3)	4564(5)	4176(2)	13(1)
C(29)	11557(3)	3227(5)	4510(2)	15(1)
C(30)	10722(4)	2057(5)	4261(2)	20(1)
C(31)	9787(3)	4204(5)	4256(2)	15(1)

C(32)	8922(3)	5033(5)	3791(2)	13(1)
C(33)	7894(3)	5137(5)	3889(2)	13(1)
C(34)	10223(3)	7994(5)	2786(2)	20(1)
C(35)	12662(3)	2940(5)	4342(2)	20(1)
C(36)	7366(3)	4298(5)	4386(2)	19(1)
C(37)	5996(4)	10045(5)	3857(2)	25(1)
C(38)	5499(3)	8337(6)	2502(2)	21(1)
C(39)	4400(3)	7493(5)	3720(2)	18(1)
C(40)	3451(4)	8542(7)	3507(2)	31(1)
C(41)	4582(4)	7279(6)	4519(2)	28(1)
C(42)	4111(4)	6038(6)	3361(3)	29(1)
O(1)	7109(2)	4332(3)	1920(1)	16(1)
O(2)	6824(2)	5724(3)	1583(1)	15(1)
O(3)	5120(2)	7404(3)	835(1)	15(1)
O(4)	6503(2)	6714(4)	-215(1)	19(1)
O(5)	6184(3)	9313(4)	776(2)	24(1)
O(6)	2381(2)	2851(3)	1193(1)	15(1)
O(7)	11045(2)	5820(3)	3105(1)	16(1)
O(8)	10991(2)	4411(3)	3440(1)	16(1)
O(9)	9713(2)	2647(3)	4114(2)	20(1)
O(10)	11606(2)	3392(4)	5243(1)	21(1)
O(11)	10870(3)	793(4)	4209(2)	29(1)
O(12)	6699(2)	7180(3)	3793(1)	14(1)
Si(1)	1581(1)	1718(2)	1523(1)	16(1)
Si(2)	5665(1)	8243(1)	3465(1)	14(1)

Table 3. Bond lengths [\AA] and angles [$^\circ$] for maimone42.

C(1)-O(6)	1.446(5)	C(13)-H(13C)	0.9800
C(1)-C(12)	1.512(6)	C(14)-H(14A)	0.9800
C(1)-C(2)	1.531(6)	C(14)-H(14B)	0.9800
C(1)-H(1)	1.0000	C(14)-H(14C)	0.9800
C(2)-C(3)	1.542(6)	C(15)-H(15A)	0.9800
C(2)-H(2A)	0.9900	C(15)-H(15B)	0.9800
C(2)-H(2B)	0.9900	C(15)-H(15C)	0.9800
C(3)-C(11)	1.528(6)	C(16)-Si(1)	1.856(4)
C(3)-C(4)	1.540(6)	C(16)-H(16A)	0.9800
C(3)-H(3)	1.0000	C(16)-H(16B)	0.9800
C(4)-O(1)	1.461(5)	C(16)-H(16C)	0.9800
C(4)-C(13)	1.517(6)	C(17)-Si(1)	1.866(5)
C(4)-C(5)	1.532(6)	C(17)-H(17A)	0.9800
C(5)-C(6)	1.536(6)	C(17)-H(17B)	0.9800
C(5)-H(5A)	0.9900	C(17)-H(17C)	0.9800
C(5)-H(5B)	0.9900	C(18)-C(21)	1.527(7)
C(6)-C(7)	1.503(6)	C(18)-C(20)	1.532(6)
C(6)-H(6A)	0.9900	C(18)-C(19)	1.535(7)
C(6)-H(6B)	0.9900	C(18)-Si(1)	1.881(4)
C(7)-O(2)	1.458(5)	C(19)-H(19A)	0.9800
C(7)-C(8)	1.531(6)	C(19)-H(19B)	0.9800
C(7)-C(10)	1.533(6)	C(19)-H(19C)	0.9800
C(8)-O(4)	1.425(5)	C(20)-H(20A)	0.9800
C(8)-C(14)	1.521(5)	C(20)-H(20B)	0.9800
C(8)-C(9)	1.532(6)	C(20)-H(20C)	0.9800
C(9)-O(5)	1.199(6)	C(21)-H(21A)	0.9800
C(9)-O(3)	1.353(5)	C(21)-H(21B)	0.9800
C(10)-O(3)	1.471(5)	C(21)-H(21C)	0.9800
C(10)-C(11)	1.495(6)	C(22)-O(12)	1.445(5)
C(10)-H(10)	1.0000	C(22)-C(33)	1.505(6)
C(11)-C(12)	1.341(5)	C(22)-C(23)	1.529(6)
C(12)-C(15)	1.492(6)	C(22)-H(22)	1.0000
C(13)-H(13A)	0.9800	C(23)-C(24)	1.536(6)
C(13)-H(13B)	0.9800	C(23)-H(23A)	0.9900

C(23)-H(23B)	0.9900	C(35)-H(35C)	0.9800
C(24)-C(32)	1.523(6)	C(36)-H(36A)	0.9800
C(24)-C(25)	1.540(6)	C(36)-H(36B)	0.9800
C(24)-H(24)	1.0000	C(36)-H(36C)	0.9800
C(25)-O(7)	1.450(5)	C(37)-Si(2)	1.857(5)
C(25)-C(26)	1.530(6)	C(37)-H(37A)	0.9800
C(25)-C(34)	1.533(6)	C(37)-H(37B)	0.9800
C(26)-C(27)	1.545(6)	C(37)-H(37C)	0.9800
C(26)-H(26A)	0.9900	C(38)-Si(2)	1.858(4)
C(26)-H(26B)	0.9900	C(38)-H(38A)	0.9800
C(27)-C(28)	1.507(7)	C(38)-H(38B)	0.9800
C(27)-H(27A)	0.9900	C(38)-H(38C)	0.9800
C(27)-H(27B)	0.9900	C(39)-C(40)	1.535(6)
C(28)-O(8)	1.456(5)	C(39)-C(42)	1.536(7)
C(28)-C(31)	1.535(6)	C(39)-C(41)	1.549(6)
C(28)-C(29)	1.538(6)	C(39)-Si(2)	1.885(4)
C(29)-O(10)	1.431(5)	C(40)-H(40A)	0.9800
C(29)-C(35)	1.508(6)	C(40)-H(40B)	0.9800
C(29)-C(30)	1.525(7)	C(40)-H(40C)	0.9800
C(30)-O(11)	1.198(6)	C(41)-H(41A)	0.9800
C(30)-O(9)	1.361(5)	C(41)-H(41B)	0.9800
C(31)-O(9)	1.474(5)	C(41)-H(41C)	0.9800
C(31)-C(32)	1.493(6)	C(42)-H(42A)	0.9800
C(31)-H(31)	1.0000	C(42)-H(42B)	0.9800
C(32)-C(33)	1.344(6)	C(42)-H(42C)	0.9800
C(33)-C(36)	1.494(6)	O(1)-O(2)	1.466(4)
C(34)-H(34A)	0.9800	O(4)-H(4)	0.8400
C(34)-H(34B)	0.9800	O(6)-Si(1)	1.667(3)
C(34)-H(34C)	0.9800	O(7)-O(8)	1.473(4)
C(35)-H(35A)	0.9800	O(10)-H(10A)	0.8400
C(35)-H(35B)	0.9800	O(12)-Si(2)	1.662(3)
O(6)-C(1)-C(12)	108.6(3)	C(12)-C(1)-H(1)	110.8
O(6)-C(1)-C(2)	112.0(4)	C(2)-C(1)-H(1)	110.8
C(12)-C(1)-C(2)	103.5(3)	C(1)-C(2)-C(3)	105.9(4)
O(6)-C(1)-H(1)	110.8	C(1)-C(2)-H(2A)	110.6

C(3)-C(2)-H(2A)	110.6	C(14)-C(8)-C(7)	116.7(4)
C(1)-C(2)-H(2B)	110.6	O(4)-C(8)-C(9)	107.1(3)
C(3)-C(2)-H(2B)	110.6	C(14)-C(8)-C(9)	113.5(4)
H(2A)-C(2)-H(2B)	108.7	C(7)-C(8)-C(9)	100.8(3)
C(11)-C(3)-C(4)	116.3(3)	O(5)-C(9)-O(3)	122.5(4)
C(11)-C(3)-C(2)	101.7(3)	O(5)-C(9)-C(8)	127.8(4)
C(4)-C(3)-C(2)	114.3(4)	O(3)-C(9)-C(8)	109.6(4)
C(11)-C(3)-H(3)	108.0	O(3)-C(10)-C(11)	112.2(3)
C(4)-C(3)-H(3)	108.0	O(3)-C(10)-C(7)	103.6(3)
C(2)-C(3)-H(3)	108.0	C(11)-C(10)-C(7)	114.7(4)
O(1)-C(4)-C(13)	101.3(3)	O(3)-C(10)-H(10)	108.7
O(1)-C(4)-C(5)	107.6(3)	C(11)-C(10)-H(10)	108.7
C(13)-C(4)-C(5)	113.6(4)	C(7)-C(10)-H(10)	108.7
O(1)-C(4)-C(3)	108.8(4)	C(12)-C(11)-C(10)	124.1(4)
C(13)-C(4)-C(3)	111.8(3)	C(12)-C(11)-C(3)	111.7(4)
C(5)-C(4)-C(3)	112.8(3)	C(10)-C(11)-C(3)	124.1(3)
C(4)-C(5)-C(6)	109.3(4)	C(11)-C(12)-C(15)	127.7(4)
C(4)-C(5)-H(5A)	109.8	C(11)-C(12)-C(1)	111.1(4)
C(6)-C(5)-H(5A)	109.8	C(15)-C(12)-C(1)	121.2(3)
C(4)-C(5)-H(5B)	109.8	C(4)-C(13)-H(13A)	109.5
C(6)-C(5)-H(5B)	109.8	C(4)-C(13)-H(13B)	109.5
H(5A)-C(5)-H(5B)	108.3	H(13A)-C(13)-H(13B)	109.5
C(7)-C(6)-C(5)	110.7(3)	C(4)-C(13)-H(13C)	109.5
C(7)-C(6)-H(6A)	109.5	H(13A)-C(13)-H(13C)	109.5
C(5)-C(6)-H(6A)	109.5	H(13B)-C(13)-H(13C)	109.5
C(7)-C(6)-H(6B)	109.5	C(8)-C(14)-H(14A)	109.5
C(5)-C(6)-H(6B)	109.5	C(8)-C(14)-H(14B)	109.5
H(6A)-C(6)-H(6B)	108.1	H(14A)-C(14)-H(14B)	109.5
O(2)-C(7)-C(6)	111.6(3)	C(8)-C(14)-H(14C)	109.5
O(2)-C(7)-C(8)	103.4(3)	H(14A)-C(14)-H(14C)	109.5
C(6)-C(7)-C(8)	118.5(3)	H(14B)-C(14)-H(14C)	109.5
O(2)-C(7)-C(10)	106.7(3)	C(12)-C(15)-H(15A)	109.5
C(6)-C(7)-C(10)	114.2(3)	C(12)-C(15)-H(15B)	109.5
C(8)-C(7)-C(10)	101.0(3)	H(15A)-C(15)-H(15B)	109.5
O(4)-C(8)-C(14)	112.4(3)	C(12)-C(15)-H(15C)	109.5
O(4)-C(8)-C(7)	105.3(3)	H(15A)-C(15)-H(15C)	109.5

H(15B)-C(15)-H(15C)	109.5	H(21B)-C(21)-H(21C)	109.5
Si(1)-C(16)-H(16A)	109.5	O(12)-C(22)-C(33)	109.3(3)
Si(1)-C(16)-H(16B)	109.5	O(12)-C(22)-C(23)	112.3(4)
H(16A)-C(16)-H(16B)	109.5	C(33)-C(22)-C(23)	103.6(3)
Si(1)-C(16)-H(16C)	109.5	O(12)-C(22)-H(22)	110.5
H(16A)-C(16)-H(16C)	109.5	C(33)-C(22)-H(22)	110.5
H(16B)-C(16)-H(16C)	109.5	C(23)-C(22)-H(22)	110.5
Si(1)-C(17)-H(17A)	109.5	C(22)-C(23)-C(24)	106.1(4)
Si(1)-C(17)-H(17B)	109.5	C(22)-C(23)-H(23A)	110.5
H(17A)-C(17)-H(17B)	109.5	C(24)-C(23)-H(23A)	110.5
Si(1)-C(17)-H(17C)	109.5	C(22)-C(23)-H(23B)	110.5
H(17A)-C(17)-H(17C)	109.5	C(24)-C(23)-H(23B)	110.5
H(17B)-C(17)-H(17C)	109.5	H(23A)-C(23)-H(23B)	108.7
C(21)-C(18)-C(20)	109.0(4)	C(32)-C(24)-C(23)	101.9(3)
C(21)-C(18)-C(19)	109.6(4)	C(32)-C(24)-C(25)	115.7(3)
C(20)-C(18)-C(19)	108.7(4)	C(23)-C(24)-C(25)	113.7(4)
C(21)-C(18)-Si(1)	109.3(3)	C(32)-C(24)-H(24)	108.4
C(20)-C(18)-Si(1)	110.5(3)	C(23)-C(24)-H(24)	108.4
C(19)-C(18)-Si(1)	109.6(3)	C(25)-C(24)-H(24)	108.4
C(18)-C(19)-H(19A)	109.5	O(7)-C(25)-C(26)	107.5(3)
C(18)-C(19)-H(19B)	109.5	O(7)-C(25)-C(34)	101.1(3)
H(19A)-C(19)-H(19B)	109.5	C(26)-C(25)-C(34)	112.0(4)
C(18)-C(19)-H(19C)	109.5	O(7)-C(25)-C(24)	110.6(4)
H(19A)-C(19)-H(19C)	109.5	C(26)-C(25)-C(24)	113.2(3)
H(19B)-C(19)-H(19C)	109.5	C(34)-C(25)-C(24)	111.8(3)
C(18)-C(20)-H(20A)	109.5	C(25)-C(26)-C(27)	109.7(4)
C(18)-C(20)-H(20B)	109.5	C(25)-C(26)-H(26A)	109.7
H(20A)-C(20)-H(20B)	109.5	C(27)-C(26)-H(26A)	109.7
C(18)-C(20)-H(20C)	109.5	C(25)-C(26)-H(26B)	109.7
H(20A)-C(20)-H(20C)	109.5	C(27)-C(26)-H(26B)	109.7
H(20B)-C(20)-H(20C)	109.5	H(26A)-C(26)-H(26B)	108.2
C(18)-C(21)-H(21A)	109.5	C(28)-C(27)-C(26)	110.4(3)
C(18)-C(21)-H(21B)	109.5	C(28)-C(27)-H(27A)	109.6
H(21A)-C(21)-H(21B)	109.5	C(26)-C(27)-H(27A)	109.6
C(18)-C(21)-H(21C)	109.5	C(28)-C(27)-H(27B)	109.6
H(21A)-C(21)-H(21C)	109.5	C(26)-C(27)-H(27B)	109.6

H(27A)-C(27)-H(27B)	108.1	H(35A)-C(35)-H(35B)	109.5
O(8)-C(28)-C(27)	112.0(4)	C(29)-C(35)-H(35C)	109.5
O(8)-C(28)-C(31)	106.8(3)	H(35A)-C(35)-H(35C)	109.5
C(27)-C(28)-C(31)	114.1(4)	H(35B)-C(35)-H(35C)	109.5
O(8)-C(28)-C(29)	103.5(3)	C(33)-C(36)-H(36A)	109.5
C(27)-C(28)-C(29)	118.3(3)	C(33)-C(36)-H(36B)	109.5
C(31)-C(28)-C(29)	100.7(4)	H(36A)-C(36)-H(36B)	109.5
O(10)-C(29)-C(35)	111.7(3)	C(33)-C(36)-H(36C)	109.5
O(10)-C(29)-C(30)	107.1(3)	H(36A)-C(36)-H(36C)	109.5
C(35)-C(29)-C(30)	114.2(4)	H(36B)-C(36)-H(36C)	109.5
O(10)-C(29)-C(28)	105.2(3)	Si(2)-C(37)-H(37A)	109.5
C(35)-C(29)-C(28)	116.9(4)	Si(2)-C(37)-H(37B)	109.5
C(30)-C(29)-C(28)	100.7(3)	H(37A)-C(37)-H(37B)	109.5
O(11)-C(30)-O(9)	122.1(4)	Si(2)-C(37)-H(37C)	109.5
O(11)-C(30)-C(29)	128.2(4)	H(37A)-C(37)-H(37C)	109.5
O(9)-C(30)-C(29)	109.7(4)	H(37B)-C(37)-H(37C)	109.5
O(9)-C(31)-C(32)	112.3(3)	Si(2)-C(38)-H(38A)	109.5
O(9)-C(31)-C(28)	102.8(3)	Si(2)-C(38)-H(38B)	109.5
C(32)-C(31)-C(28)	115.0(4)	H(38A)-C(38)-H(38B)	109.5
O(9)-C(31)-H(31)	108.8	Si(2)-C(38)-H(38C)	109.5
C(32)-C(31)-H(31)	108.8	H(38A)-C(38)-H(38C)	109.5
C(28)-C(31)-H(31)	108.8	H(38B)-C(38)-H(38C)	109.5
C(33)-C(32)-C(31)	123.9(4)	C(40)-C(39)-C(42)	109.4(4)
C(33)-C(32)-C(24)	111.7(4)	C(40)-C(39)-C(41)	108.4(4)
C(31)-C(32)-C(24)	124.2(3)	C(42)-C(39)-C(41)	108.9(4)
C(32)-C(33)-C(36)	127.6(4)	C(40)-C(39)-Si(2)	110.0(3)
C(32)-C(33)-C(22)	111.1(4)	C(42)-C(39)-Si(2)	110.1(3)
C(36)-C(33)-C(22)	121.2(3)	C(41)-C(39)-Si(2)	110.0(3)
C(25)-C(34)-H(34A)	109.5	C(39)-C(40)-H(40A)	109.5
C(25)-C(34)-H(34B)	109.5	C(39)-C(40)-H(40B)	109.5
H(34A)-C(34)-H(34B)	109.5	H(40A)-C(40)-H(40B)	109.5
C(25)-C(34)-H(34C)	109.5	C(39)-C(40)-H(40C)	109.5
H(34A)-C(34)-H(34C)	109.5	H(40A)-C(40)-H(40C)	109.5
H(34B)-C(34)-H(34C)	109.5	H(40B)-C(40)-H(40C)	109.5
C(29)-C(35)-H(35A)	109.5	C(39)-C(41)-H(41A)	109.5
C(29)-C(35)-H(35B)	109.5	C(39)-C(41)-H(41B)	109.5

H(41A)-C(41)-H(41B)	109.5	C(28)-O(8)-O(7)	111.5(3)
C(39)-C(41)-H(41C)	109.5	C(30)-O(9)-C(31)	109.5(3)
H(41A)-C(41)-H(41C)	109.5	C(29)-O(10)-H(10A)	109.5
H(41B)-C(41)-H(41C)	109.5	C(22)-O(12)-Si(2)	126.2(2)
C(39)-C(42)-H(42A)	109.5	O(6)-Si(1)-C(16)	109.94(18)
C(39)-C(42)-H(42B)	109.5	O(6)-Si(1)-C(17)	106.20(19)
H(42A)-C(42)-H(42B)	109.5	C(16)-Si(1)-C(17)	110.9(2)
C(39)-C(42)-H(42C)	109.5	O(6)-Si(1)-C(18)	107.35(18)
H(42A)-C(42)-H(42C)	109.5	C(16)-Si(1)-C(18)	110.2(2)
H(42B)-C(42)-H(42C)	109.5	C(17)-Si(1)-C(18)	112.0(2)
C(4)-O(1)-O(2)	108.8(3)	O(12)-Si(2)-C(37)	106.25(19)
C(7)-O(2)-O(1)	111.3(3)	O(12)-Si(2)-C(38)	110.44(18)
C(9)-O(3)-C(10)	109.7(3)	C(37)-Si(2)-C(38)	110.5(2)
C(8)-O(4)-H(4)	109.5	O(12)-Si(2)-C(39)	108.30(18)
C(1)-O(6)-Si(1)	126.0(2)	C(37)-Si(2)-C(39)	111.1(2)
C(25)-O(7)-O(8)	108.6(3)	C(38)-Si(2)-C(39)	110.2(2)

Symmetry transformations used to generate equivalent atoms:

Table 4. Anisotropic displacement parameters ($\text{\AA}^2 \times 10^3$) for maimone42. The anisotropic displacement factor exponent takes the form: $-2\pi^2 [h^2 a^{*2} U^{11} + \dots + 2 h k a^* b^* U^{12}]$

	U^{11}	U^{22}	U^{33}	U^{23}	U^{13}	U^{12}
C(1)	10(2)	18(3)	15(2)	-6(2)	3(2)	-4(2)
C(2)	16(2)	17(3)	19(2)	5(2)	4(2)	-3(2)
C(3)	14(2)	13(3)	14(2)	-1(2)	4(2)	-4(2)
C(4)	13(2)	12(3)	17(2)	0(2)	1(2)	-4(2)
C(5)	14(2)	11(3)	21(2)	1(2)	2(2)	0(2)
C(6)	11(2)	17(3)	18(2)	-2(2)	2(2)	0(2)
C(7)	13(2)	13(3)	6(2)	-3(2)	0(2)	-4(2)
C(8)	15(2)	16(3)	12(2)	1(2)	1(2)	-3(2)
C(9)	22(2)	16(3)	9(2)	2(2)	0(2)	-3(2)
C(10)	18(2)	8(3)	11(2)	-1(2)	0(2)	0(2)
C(11)	14(2)	8(3)	17(2)	-1(2)	5(2)	-1(2)
C(12)	12(2)	13(3)	16(2)	-5(2)	4(2)	-1(2)
C(13)	19(2)	17(3)	28(3)	6(2)	3(2)	0(2)
C(14)	15(2)	21(3)	17(2)	5(2)	3(2)	-6(2)
C(15)	15(2)	16(3)	22(2)	2(2)	2(2)	1(2)
C(16)	20(2)	22(3)	21(2)	3(2)	5(2)	-1(2)
C(17)	33(3)	19(3)	37(3)	-6(2)	14(2)	-7(2)
C(18)	12(2)	29(3)	22(2)	1(2)	5(2)	-2(2)
C(19)	16(3)	80(6)	64(4)	25(4)	12(3)	-8(3)
C(20)	16(2)	47(4)	31(3)	1(3)	-1(2)	2(2)
C(21)	26(3)	46(4)	37(3)	-7(3)	-2(2)	23(3)
C(22)	13(2)	14(3)	13(2)	-3(2)	2(2)	1(2)
C(23)	12(2)	16(3)	14(2)	2(2)	1(2)	1(2)
C(24)	12(2)	14(3)	13(2)	0(2)	2(2)	2(2)
C(25)	7(2)	17(3)	19(2)	4(2)	3(2)	3(2)
C(26)	14(2)	10(3)	21(2)	1(2)	5(2)	-2(2)
C(27)	14(2)	17(3)	13(2)	0(2)	1(2)	-1(2)
C(28)	10(2)	18(3)	12(2)	0(2)	1(2)	1(2)
C(29)	18(2)	13(3)	13(2)	2(2)	4(2)	4(2)
C(30)	23(2)	16(3)	20(2)	5(2)	4(2)	5(2)
C(31)	17(2)	10(3)	18(2)	-2(2)	4(2)	0(2)

C(32)	15(2)	10(2)	12(2)	-4(2)	0(2)	0(2)
C(33)	13(2)	9(3)	16(2)	-5(2)	2(2)	-2(2)
C(34)	18(2)	19(3)	22(2)	7(2)	5(2)	2(2)
C(35)	18(2)	22(3)	20(2)	1(2)	2(2)	9(2)
C(36)	17(2)	19(3)	21(2)	5(2)	4(2)	-1(2)
C(37)	35(3)	17(3)	23(3)	0(2)	7(2)	4(2)
C(38)	25(2)	14(3)	23(2)	-1(2)	4(2)	1(2)
C(39)	12(2)	27(3)	16(2)	2(2)	2(2)	1(2)
C(40)	15(2)	45(4)	35(3)	9(3)	6(2)	13(2)
C(41)	17(2)	48(4)	20(2)	8(2)	7(2)	-2(2)
C(42)	24(3)	27(3)	38(3)	0(3)	11(2)	-9(2)
O(1)	15(2)	12(2)	19(2)	7(1)	-2(1)	-1(1)
O(2)	21(2)	11(2)	12(2)	4(1)	1(1)	-2(1)
O(3)	17(2)	10(2)	17(2)	2(1)	4(1)	-2(1)
O(4)	21(2)	23(2)	13(2)	4(2)	5(1)	-6(2)
O(5)	33(2)	13(2)	24(2)	1(2)	4(1)	-5(2)
O(6)	12(1)	16(2)	16(2)	-3(1)	4(1)	-5(1)
O(7)	16(2)	15(2)	17(2)	5(1)	6(1)	2(1)
O(8)	21(2)	14(2)	14(2)	3(1)	5(1)	4(1)
O(9)	17(2)	11(2)	31(2)	2(2)	3(1)	-1(1)
O(10)	19(2)	29(2)	14(2)	5(2)	2(1)	7(2)
O(11)	31(2)	14(2)	42(2)	2(2)	5(2)	4(2)
O(12)	13(1)	15(2)	13(2)	-2(1)	3(1)	4(1)
Si(1)	14(1)	15(1)	18(1)	-1(1)	6(1)	-2(1)
Si(2)	14(1)	14(1)	15(1)	1(1)	3(1)	2(1)

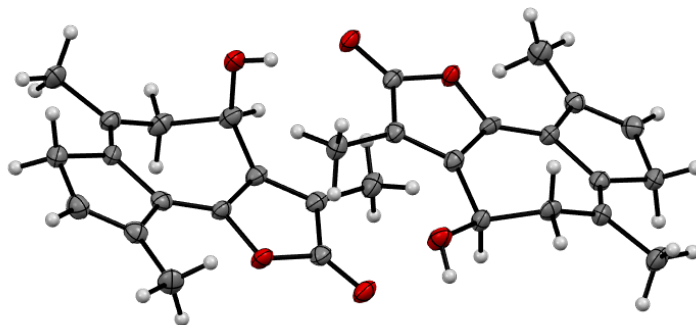
Table 5. Hydrogen coordinates ($\times 10^4$) and isotropic displacement parameters ($\text{\AA}^2 \times 10^3$) for maimone42.

	x	y	z	U(eq)
H(1)	2865	4307	1961	17
H(2A)	4290	2128	1640	21
H(2B)	4262	2822	2391	21
H(3)	5311	4706	2222	16
H(5A)	5457	2697	711	19
H(5B)	6640	2004	946	19
H(6A)	7497	4007	665	18
H(6B)	6425	4041	73	18
H(10)	4858	5622	230	15
H(13A)	7265	1837	2236	32
H(13B)	6031	1304	2094	32
H(13C)	6438	2456	2694	32
H(14A)	8443	6467	634	27
H(14B)	8161	7451	1248	27
H(14C)	8169	8134	497	27
H(15A)	2421	6528	842	27
H(15B)	2081	5095	402	27
H(15C)	3022	6101	217	27
H(16A)	2704	1406	2631	31
H(16B)	1473	1052	2678	31
H(16C)	1864	2687	2664	31
H(17A)	1617	-59	652	43
H(17B)	1346	-799	1338	43
H(17C)	2568	-362	1305	43
H(19A)	-493	1289	2001	79
H(19B)	-527	336	1316	79
H(19C)	-1385	1608	1319	79
H(20A)	-881	2818	299	48
H(20B)	-101	1481	241	48
H(20C)	368	3084	268	48

H(21A)	493	4528	1354	56
H(21B)	233	3805	2048	56
H(21C)	-733	4159	1411	56
H(22)	6746	5734	3026	16
H(23A)	8349	7916	3348	17
H(23B)	7885	7218	2598	17
H(24)	9053	5363	2763	15
H(26A)	9999	7411	4281	18
H(26B)	11054	8114	4063	18
H(27A)	12101	6160	4404	18
H(27B)	11305	6078	4956	18
H(31)	9717	4372	4751	18
H(34A)	10971	8274	2775	30
H(34B)	9834	8815	2936	30
H(34C)	9862	7689	2320	30
H(35A)	13152	3732	4518	30
H(35B)	12602	2864	3836	30
H(35C)	12949	2039	4562	30
H(36A)	7923	3811	4725	28
H(36B)	6876	3582	4127	28
H(36C)	6951	4951	4630	28
H(37A)	6050	9986	4363	37
H(37B)	5423	10726	3663	37
H(37C)	6689	10373	3752	37
H(38A)	6159	8732	2376	31
H(38B)	4882	8957	2316	31
H(38C)	5368	7369	2305	31
H(40A)	3317	8679	3001	47
H(40B)	3631	9468	3740	47
H(40C)	2799	8148	3646	47
H(41A)	3909	6940	4650	42
H(41B)	4797	8194	4753	42
H(41C)	5156	6566	4661	42
H(42A)	3451	5660	3495	44
H(42B)	4709	5360	3505	44
H(42C)	3990	6165	2855	44

H(4)	6912	7209	-416	28
H(10A)	12144	2941	5461	31

X-Ray crystallographic Analysis of Compound 271



A yellow plate 0.050 x 0.030 x 0.020 mm in size was mounted on a Cryoloop with Paratone oil. Data were collected in a nitrogen gas stream at 100(2) K using phi and omega scans. Crystal-to-detector distance was 60 mm and exposure time was 10 seconds per frame using a scan width of 2.0°. Data collection was 98.6% complete to 67.000° in θ . A total of 15860 reflections were collected covering the indices, $-8 \leq h \leq 8$, $-11 \leq k \leq 11$, $-11 \leq l \leq 12$. 4019 reflections were found to be symmetry independent, with an R_{int} of 0.0387. Indexing and unit cell refinement indicated a primitive, triclinic lattice. The space group was found to be P 1 (No. 1). The data were integrated using the Bruker SAINT software program and scaled using the SADABS software program. Solution by iterative methods (SHELXT) produced a complete heavy-atom phasing model consistent with the proposed structure. All non-hydrogen atoms were refined anisotropically by full-matrix least-squares (SHELXL-2014). All hydrogen atoms were placed using a riding model. Their positions were constrained relative to their parent atom using the appropriate HFIX command in SHELXL-2014. Absolute stereochemistry was unambiguously determined to be *R* at C5 and C20, respectively.

Table 1. Crystal data and structure refinement for compound **271**.

X-ray ID	maimone66	
Sample/notebook ID	XH_TBAF	
Empirical formula	C ₁₅ H ₁₆ O ₃	
Formula weight	244.28	
Temperature	100(2) K	
Wavelength	1.54178 Å	
Crystal system	Triclinic	
Space group	P 1	
Unit cell dimensions	a = 6.96280(10) Å	α = 112.9050(10)°.
	b = 9.4090(2) Å	β = 91.6060(10)°.
	c = 9.9765(2) Å	γ = 94.4850(10)°.
Volume	598.99(2) Å ³	
Z	2	
Density (calculated)	1.354 Mg/m ³	
Absorption coefficient	0.758 mm ⁻¹	
F(000)	260	
Crystal size	0.050 x 0.030 x 0.020 mm ³	
Theta range for data collection	4.822 to 68.518°.	
Index ranges	-8 ≤ h ≤ 8, -11 ≤ k ≤ 11, -11 ≤ l ≤ 12	
Reflections collected	15860	
Independent reflections	4019 [R(int) = 0.0387]	
Completeness to theta = 67.000°	98.6 %	
Absorption correction	Semi-empirical from equivalents	
Max. and min. transmission	0.929 and 0.840	
Refinement method	Full-matrix least-squares on F ²	
Data / restraints / parameters	4019 / 3 / 333	
Goodness-of-fit on F ²	1.045	
Final R indices [I > 2σ(I)]	R1 = 0.0333, wR2 = 0.0830	
R indices (all data)	R1 = 0.0379, wR2 = 0.0859	
Absolute structure parameter	0.04(12)	
Extinction coefficient	n/a	
Largest diff. peak and hole	0.230 and -0.151 e.Å ⁻³	

Table 2. Atomic coordinates ($\times 10^4$) and equivalent isotropic displacement parameters ($\text{\AA}^2 \times 10^3$) for maimone66. $U(\text{eq})$ is defined as one third of the trace of the orthogonalized U^{ij} tensor.

	x	y	z	$U(\text{eq})$
C(1)	2395(5)	6876(4)	7031(4)	19(1)
C(2)	2390(5)	4400(4)	5418(4)	22(1)
C(3)	2739(5)	5435(4)	4635(4)	21(1)
C(4)	2735(5)	6915(4)	5629(4)	21(1)
C(5)	3149(6)	8373(4)	5366(4)	23(1)
C(6)	1849(6)	9626(4)	6160(4)	26(1)
C(7)	2232(5)	10430(4)	7787(4)	23(1)
C(8)	2413(5)	9705(4)	8703(4)	21(1)
C(9)	2586(6)	10530(4)	10360(4)	24(1)
C(10)	2474(6)	9235(4)	10865(4)	27(1)
C(11)	2335(5)	7835(4)	9774(4)	24(1)
C(12)	2351(5)	8030(4)	8373(4)	21(1)
C(13)	3037(6)	4807(4)	3049(4)	27(1)
C(14)	2318(6)	12158(4)	8338(4)	29(1)
C(15)	2297(6)	6323(4)	9940(4)	28(1)
C(16)	7660(5)	3130(4)	2968(4)	19(1)
C(17)	7732(5)	5588(4)	4560(4)	21(1)
C(18)	7321(5)	4602(4)	5344(4)	20(1)
C(19)	7268(5)	3112(4)	4367(4)	20(1)
C(20)	6769(6)	1623(4)	4548(4)	20(1)
C(21)	8161(6)	416(4)	3790(4)	21(1)
C(22)	7784(5)	-414(4)	2167(4)	21(1)
C(23)	7586(5)	315(4)	1250(4)	20(1)
C(24)	7425(6)	-500(4)	-402(4)	22(1)
C(25)	7570(5)	819(4)	-881(4)	24(1)
C(26)	7722(5)	2204(4)	234(4)	21(1)
C(27)	7675(5)	1989(4)	1612(4)	18(1)
C(28)	7030(6)	5307(4)	6949(4)	24(1)
C(29)	7693(6)	-2152(4)	1617(4)	29(1)
C(30)	7778(6)	3721(4)	62(4)	28(1)
O(1)	2191(3)	5323(3)	6865(3)	23(1)

O(2)	2287(4)	3012(3)	4985(3)	28(1)
O(3)	5098(3)	9018(2)	5838(2)	28(1)
O(4)	7931(3)	4679(2)	3128(2)	20(1)
O(5)	7868(4)	6996(3)	4962(3)	26(1)
O(6)	6765(3)	1929(2)	6062(2)	27(1)

Table 3. Bond lengths [\AA] and angles [$^\circ$] for maimone66.

C(1)-C(12)	1.360(5)	C(15)-H(15C)	0.9800
C(1)-O(1)	1.401(4)	C(16)-C(27)	1.362(5)
C(1)-C(4)	1.439(5)	C(16)-O(4)	1.400(4)
C(2)-O(2)	1.201(4)	C(16)-C(19)	1.435(5)
C(2)-O(1)	1.383(4)	C(17)-O(5)	1.220(4)
C(2)-C(3)	1.477(5)	C(17)-O(4)	1.368(4)
C(3)-C(4)	1.359(5)	C(17)-C(18)	1.445(5)
C(3)-C(13)	1.486(5)	C(18)-C(19)	1.358(5)
C(4)-C(5)	1.502(5)	C(18)-C(28)	1.503(5)
C(5)-O(3)	1.430(4)	C(19)-C(20)	1.497(5)
C(5)-C(6)	1.522(5)	C(20)-O(6)	1.424(4)
C(5)-H(5)	1.0000	C(20)-C(21)	1.531(5)
C(6)-C(7)	1.506(5)	C(20)-H(20)	1.0000
C(6)-H(6A)	0.9900	C(21)-C(22)	1.503(5)
C(6)-H(6B)	0.9900	C(21)-H(21A)	0.9900
C(7)-C(8)	1.345(5)	C(21)-H(21B)	0.9900
C(7)-C(14)	1.496(5)	C(22)-C(23)	1.350(5)
C(8)-C(12)	1.475(5)	C(22)-C(29)	1.505(5)
C(8)-C(9)	1.525(5)	C(23)-C(27)	1.469(5)
C(9)-C(10)	1.486(5)	C(23)-C(24)	1.520(5)
C(9)-H(9A)	0.9900	C(24)-C(25)	1.490(5)
C(9)-H(9B)	0.9900	C(24)-H(24A)	0.9900
C(10)-C(11)	1.338(5)	C(24)-H(24B)	0.9900
C(10)-H(10)	0.9500	C(25)-C(26)	1.339(5)
C(11)-C(12)	1.480(5)	C(25)-H(25)	0.9500
C(11)-C(15)	1.493(5)	C(26)-C(27)	1.466(5)
C(13)-H(13A)	0.9800	C(26)-C(30)	1.500(5)
C(13)-H(13B)	0.9800	C(28)-H(28A)	0.9800
C(13)-H(13C)	0.9800	C(28)-H(28B)	0.9800
C(14)-H(14A)	0.9800	C(28)-H(28C)	0.9800
C(14)-H(14B)	0.9800	C(29)-H(29A)	0.9800
C(14)-H(14C)	0.9800	C(29)-H(29B)	0.9800
C(15)-H(15A)	0.9800	C(29)-H(29C)	0.9800
C(15)-H(15B)	0.9800	C(30)-H(30A)	0.9800

C(30)-H(30B)	0.9800	O(3)-H(3)	0.8400
C(30)-H(30C)	0.9800	O(6)-H(6)	0.8400
C(12)-C(1)-O(1)	120.2(3)	C(10)-C(9)-H(9B)	111.1
C(12)-C(1)-C(4)	131.6(3)	C(8)-C(9)-H(9B)	111.1
O(1)-C(1)-C(4)	108.1(3)	H(9A)-C(9)-H(9B)	109.0
O(2)-C(2)-O(1)	121.8(3)	C(11)-C(10)-C(9)	113.4(3)
O(2)-C(2)-C(3)	130.6(3)	C(11)-C(10)-H(10)	123.3
O(1)-C(2)-C(3)	107.6(3)	C(9)-C(10)-H(10)	123.3
C(4)-C(3)-C(2)	107.3(3)	C(10)-C(11)-C(12)	108.8(3)
C(4)-C(3)-C(13)	131.4(3)	C(10)-C(11)-C(15)	125.7(4)
C(2)-C(3)-C(13)	121.3(3)	C(12)-C(11)-C(15)	125.4(3)
C(3)-C(4)-C(1)	108.6(3)	C(1)-C(12)-C(8)	126.4(3)
C(3)-C(4)-C(5)	126.8(3)	C(1)-C(12)-C(11)	125.9(3)
C(1)-C(4)-C(5)	124.5(3)	C(8)-C(12)-C(11)	107.7(3)
O(3)-C(5)-C(4)	110.7(3)	C(3)-C(13)-H(13A)	109.5
O(3)-C(5)-C(6)	107.2(3)	C(3)-C(13)-H(13B)	109.5
C(4)-C(5)-C(6)	113.3(3)	H(13A)-C(13)-H(13B)	109.5
O(3)-C(5)-H(5)	108.5	C(3)-C(13)-H(13C)	109.5
C(4)-C(5)-H(5)	108.5	H(13A)-C(13)-H(13C)	109.5
C(6)-C(5)-H(5)	108.5	H(13B)-C(13)-H(13C)	109.5
C(7)-C(6)-C(5)	116.5(3)	C(7)-C(14)-H(14A)	109.5
C(7)-C(6)-H(6A)	108.2	C(7)-C(14)-H(14B)	109.5
C(5)-C(6)-H(6A)	108.2	H(14A)-C(14)-H(14B)	109.5
C(7)-C(6)-H(6B)	108.2	C(7)-C(14)-H(14C)	109.5
C(5)-C(6)-H(6B)	108.2	H(14A)-C(14)-H(14C)	109.5
H(6A)-C(6)-H(6B)	107.3	H(14B)-C(14)-H(14C)	109.5
C(8)-C(7)-C(14)	121.4(4)	C(11)-C(15)-H(15A)	109.5
C(8)-C(7)-C(6)	124.9(3)	C(11)-C(15)-H(15B)	109.5
C(14)-C(7)-C(6)	113.7(3)	H(15A)-C(15)-H(15B)	109.5
C(7)-C(8)-C(12)	129.3(3)	C(11)-C(15)-H(15C)	109.5
C(7)-C(8)-C(9)	124.1(3)	H(15A)-C(15)-H(15C)	109.5
C(12)-C(8)-C(9)	106.5(3)	H(15B)-C(15)-H(15C)	109.5
C(10)-C(9)-C(8)	103.5(3)	C(27)-C(16)-O(4)	118.9(3)
C(10)-C(9)-H(9A)	111.1	C(27)-C(16)-C(19)	132.9(3)
C(8)-C(9)-H(9A)	111.1	O(4)-C(16)-C(19)	108.0(3)

O(5)-C(17)-O(4)	119.8(3)	H(24A)-C(24)-H(24B)	109.1
O(5)-C(17)-C(18)	131.2(4)	C(26)-C(25)-C(24)	113.0(3)
O(4)-C(17)-C(18)	109.0(3)	C(26)-C(25)-H(25)	123.5
C(19)-C(18)-C(17)	107.3(3)	C(24)-C(25)-H(25)	123.5
C(19)-C(18)-C(28)	132.6(4)	C(25)-C(26)-C(27)	109.5(3)
C(17)-C(18)-C(28)	120.1(3)	C(25)-C(26)-C(30)	124.1(3)
C(18)-C(19)-C(16)	108.1(3)	C(27)-C(26)-C(30)	126.3(3)
C(18)-C(19)-C(20)	130.4(3)	C(16)-C(27)-C(26)	126.2(3)
C(16)-C(19)-C(20)	121.3(3)	C(16)-C(27)-C(23)	126.6(3)
O(6)-C(20)-C(19)	109.1(3)	C(26)-C(27)-C(23)	107.2(3)
O(6)-C(20)-C(21)	111.0(3)	C(18)-C(28)-H(28A)	109.5
C(19)-C(20)-C(21)	111.7(3)	C(18)-C(28)-H(28B)	109.5
O(6)-C(20)-H(20)	108.3	H(28A)-C(28)-H(28B)	109.5
C(19)-C(20)-H(20)	108.3	C(18)-C(28)-H(28C)	109.5
C(21)-C(20)-H(20)	108.3	H(28A)-C(28)-H(28C)	109.5
C(22)-C(21)-C(20)	115.3(3)	H(28B)-C(28)-H(28C)	109.5
C(22)-C(21)-H(21A)	108.4	C(22)-C(29)-H(29A)	109.5
C(20)-C(21)-H(21A)	108.4	C(22)-C(29)-H(29B)	109.5
C(22)-C(21)-H(21B)	108.4	H(29A)-C(29)-H(29B)	109.5
C(20)-C(21)-H(21B)	108.4	C(22)-C(29)-H(29C)	109.5
H(21A)-C(21)-H(21B)	107.5	H(29A)-C(29)-H(29C)	109.5
C(23)-C(22)-C(21)	123.8(3)	H(29B)-C(29)-H(29C)	109.5
C(23)-C(22)-C(29)	121.6(3)	C(26)-C(30)-H(30A)	109.5
C(21)-C(22)-C(29)	114.6(3)	C(26)-C(30)-H(30B)	109.5
C(22)-C(23)-C(27)	128.1(3)	H(30A)-C(30)-H(30B)	109.5
C(22)-C(23)-C(24)	124.2(3)	C(26)-C(30)-H(30C)	109.5
C(27)-C(23)-C(24)	107.4(3)	H(30A)-C(30)-H(30C)	109.5
C(25)-C(24)-C(23)	102.8(3)	H(30B)-C(30)-H(30C)	109.5
C(25)-C(24)-H(24A)	111.2	C(2)-O(1)-C(1)	108.4(3)
C(23)-C(24)-H(24A)	111.2	C(5)-O(3)-H(3)	109.5
C(25)-C(24)-H(24B)	111.2	C(17)-O(4)-C(16)	107.6(3)
C(23)-C(24)-H(24B)	111.2	C(20)-O(6)-H(6)	109.5

Symmetry transformations used to generate equivalent atoms:

Table 4. Anisotropic displacement parameters ($\text{\AA}^2 \times 10^3$) for maimone66. The anisotropic displacement factor exponent takes the form: $-2\pi^2 [h^2 a^{*2} U^{11} + \dots + 2 h k a^* b^* U^{12}]$

	U ¹¹	U ²²	U ³³	U ²³	U ¹³	U ¹²
C(1)	20(2)	13(2)	25(2)	8(2)	1(2)	1(2)
C(2)	20(2)	18(2)	25(2)	6(2)	0(2)	-1(2)
C(3)	19(2)	17(2)	26(2)	8(2)	-2(2)	1(2)
C(4)	20(2)	17(2)	24(2)	7(2)	-2(2)	-2(2)
C(5)	30(2)	18(2)	22(2)	9(1)	-1(2)	-2(2)
C(6)	30(2)	17(2)	31(2)	11(2)	-2(2)	1(2)
C(7)	18(2)	16(2)	33(2)	10(2)	3(2)	2(2)
C(8)	20(2)	15(2)	23(2)	2(2)	4(2)	1(1)
C(9)	23(2)	20(2)	26(2)	5(2)	4(2)	2(2)
C(10)	28(2)	29(2)	22(2)	10(2)	5(2)	3(2)
C(11)	20(2)	26(2)	26(2)	11(2)	2(2)	3(2)
C(12)	14(2)	21(2)	29(2)	11(2)	2(2)	2(2)
C(13)	31(2)	20(2)	26(2)	3(2)	-1(2)	1(2)
C(14)	36(2)	16(2)	36(2)	12(2)	10(2)	5(2)
C(15)	38(2)	26(2)	28(2)	17(2)	5(2)	5(2)
C(16)	19(2)	12(2)	25(2)	7(2)	-2(2)	-1(2)
C(17)	16(2)	14(2)	29(2)	6(2)	-1(2)	1(1)
C(18)	19(2)	18(2)	22(2)	5(2)	0(2)	1(2)
C(19)	19(2)	17(2)	23(2)	7(2)	0(2)	4(1)
C(20)	28(2)	15(2)	17(2)	6(1)	2(1)	2(2)
C(21)	26(2)	15(2)	24(2)	11(1)	3(2)	4(2)
C(22)	24(2)	16(2)	23(2)	5(2)	4(2)	3(2)
C(23)	17(2)	19(2)	25(2)	7(2)	1(2)	1(1)
C(24)	23(2)	18(2)	23(2)	4(2)	3(2)	1(2)
C(25)	24(2)	24(2)	22(2)	9(2)	1(2)	1(2)
C(26)	19(2)	20(2)	23(2)	9(2)	2(2)	2(2)
C(27)	20(2)	14(2)	19(2)	6(1)	1(2)	1(1)
C(28)	32(2)	19(2)	21(2)	5(2)	1(2)	5(2)
C(29)	39(2)	17(2)	30(2)	6(2)	5(2)	2(2)
C(30)	39(2)	25(2)	23(2)	11(2)	2(2)	2(2)
O(1)	26(1)	14(1)	29(1)	9(1)	2(1)	0(1)

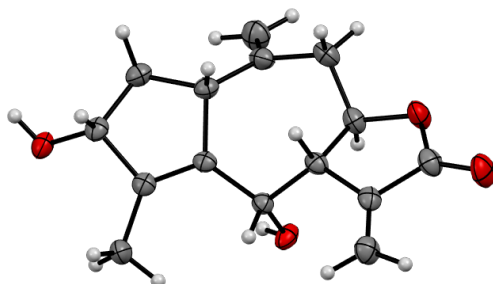
O(2)	29(2)	14(1)	36(2)	7(1)	0(1)	0(1)
O(3)	29(1)	16(1)	37(1)	9(1)	10(1)	3(1)
O(4)	28(1)	12(1)	20(1)	5(1)	2(1)	3(1)
O(5)	28(1)	12(1)	35(2)	6(1)	2(1)	2(1)
O(6)	42(1)	20(1)	20(1)	9(1)	3(1)	-3(1)

Table 5. Hydrogen coordinates ($\times 10^4$) and isotropic displacement parameters ($\text{\AA}^2 \times 10^3$) for maimone66.

	x	y	z	U(eq)
H(5)	2965	8111	4295	28
H(6A)	1968	10421	5738	31
H(6B)	496	9154	5957	31
H(9A)	3831	11181	10699	29
H(9B)	1517	11189	10714	29
H(10)	2499	9388	11865	32
H(13A)	1785	4443	2497	41
H(13B)	3840	3941	2808	41
H(13C)	3683	5624	2795	41
H(14A)	2476	12603	9405	43
H(14B)	1119	12455	8027	43
H(14C)	3415	12549	7942	43
H(15A)	2261	6505	10975	43
H(15B)	3457	5821	9552	43
H(15C)	1148	5652	9402	43
H(20)	5438	1199	4096	24
H(21A)	9490	937	3992	25
H(21B)	8100	-365	4229	25
H(24A)	8489	-1165	-756	27
H(24B)	6175	-1140	-751	27
H(25)	7556	689	-1875	28
H(28A)	6074	4637	7192	37
H(28B)	6568	6332	7202	37
H(28C)	8257	5411	7500	37
H(29A)	6491	-2552	1892	44
H(29B)	8797	-2446	2048	44
H(29C)	7730	-2591	553	44
H(30A)	7783	3533	-975	42
H(30B)	8948	4377	578	42
H(30C)	6639	4244	472	42

H(3)	5838	8310	5551	41
H(6)	6244	1149	6173	41

X-Ray crystallographic Analysis of Desilylated *ent*-179



A colorless blade 0.070 x 0.040 x 0.020 mm in size was mounted on a Cryoloop with Paratone oil. Data were collected in a nitrogen gas stream at 100(2) K using ω scans. Crystal-to-detector distance was 60 mm and exposure time was 5 seconds per frame using a scan width of 2.0°. Data collection was 100.0% complete to 67.000° in θ . A total of 22793 reflections were collected covering the indices, $-8 \leq h \leq 8$, $-9 \leq k \leq 9$, $-15 \leq l \leq 14$. 2366 reflections were found to be symmetry independent, with an R_{int} of 0.0609. Indexing and unit cell refinement indicated a primitive, monoclinic lattice. The space group was found to be P 21 (No. 4). The data were integrated using the Bruker SAINT software program and scaled using the SADABS software program. Solution by iterative methods (SHELXT-2014) produced a complete heavy-atom phasing model consistent with the proposed structure. All non-hydrogen atoms were refined anisotropically by full-matrix least-squares (SHELXL-2014). All hydrogen atoms were placed using a riding model. Their positions were constrained relative to their parent atom using the appropriate HFIX command in SHELXL-2014. Absolute stereochemistry was unambiguously determined to be *R* at C1, C3, C7, and C10, and *S* at C6, respectively.

Table 1. Crystal data and structure refinement for desilylated *ent*-179.

X-ray ID	maimone75	
Sample/notebook ID	XH_183_tbaF	
Empirical formula	C ₁₅ H ₁₈ O ₄	
Formula weight	262.29	
Temperature	100(2) K	
Wavelength	1.54178 Å	
Crystal system	Monoclinic	
Space group	P 21	
Unit cell dimensions	a = 6.7293(2) Å	α = 90°.
	b = 7.8229(2) Å	β = 101.647(2)°.
	c = 12.5521(4) Å	γ = 90°.
Volume	647.17(3) Å ³	
Z	2	
Density (calculated)	1.346 Mg/m ³	
Absorption coefficient	0.796 mm ⁻¹	
F(000)	280	
Crystal size	0.070 x 0.040 x 0.020 mm ³	
Theta range for data collection	3.595 to 68.310°.	
Index ranges	-8 ≤ h ≤ 8, -9 ≤ k ≤ 9, -15 ≤ l ≤ 14	
Reflections collected	22793	
Independent reflections	2366 [R(int) = 0.0609]	
Completeness to theta = 67.000°	100.0 %	
Absorption correction	Semi-empirical from equivalents	
Max. and min. transmission	0.929 and 0.795	
Refinement method	Full-matrix least-squares on F ²	
Data / restraints / parameters	2366 / 1 / 175	
Goodness-of-fit on F ²	1.070	
Final R indices [I > 2σ(I)]	R1 = 0.0391, wR2 = 0.0958	
R indices (all data)	R1 = 0.0420, wR2 = 0.0980	
Absolute structure parameter	0.07(10)	
Extinction coefficient	n/a	
Largest diff. peak and hole	0.245 and -0.147 e.Å ⁻³	

Table 2. Atomic coordinates ($\times 10^4$) and equivalent isotropic displacement parameters ($\text{\AA}^2 \times 10^3$) for maimone75. $U(\text{eq})$ is defined as one third of the trace of the orthogonalized U^{ij} tensor.

	x	y	z	$U(\text{eq})$
C(1)	3592(4)	2776(3)	2431(2)	24(1)
C(2)	4225(4)	1126(3)	3061(2)	27(1)
C(3)	2723(4)	934(3)	3818(2)	25(1)
C(4)	2224(4)	2767(3)	4032(2)	23(1)
C(5)	2657(4)	3791(3)	3254(2)	22(1)
C(6)	2056(4)	5653(3)	3144(2)	22(1)
C(7)	1731(4)	6226(3)	1953(2)	23(1)
C(8)	592(4)	7864(4)	1641(2)	25(1)
C(9)	1523(4)	8701(4)	802(2)	31(1)
C(10)	3699(4)	6517(4)	1540(2)	27(1)
C(11)	4542(4)	4963(4)	1075(2)	30(1)
C(12)	5241(4)	3644(4)	1951(2)	27(1)
C(13)	1249(4)	3212(4)	4963(2)	30(1)
C(14)	-1064(4)	8497(4)	1939(2)	32(1)
C(15)	7196(5)	3252(4)	2233(3)	39(1)
O(1)	3213(3)	7836(3)	702(2)	33(1)
O(2)	3494(3)	19(2)	4790(2)	29(1)
O(3)	3510(3)	6735(2)	3824(2)	30(1)
O(4)	963(3)	9956(3)	265(2)	41(1)

Table 3. Bond lengths [\AA] and angles [$^\circ$] for maimone75.

C(1)-C(12)	1.525(4)	C(8)-C(9)	1.483(4)
C(1)-C(2)	1.529(4)	C(9)-O(4)	1.207(4)
C(1)-C(5)	1.534(4)	C(9)-O(1)	1.351(4)
C(1)-H(1)	1.0000	C(10)-O(1)	1.463(3)
C(2)-C(3)	1.528(4)	C(10)-C(11)	1.509(4)
C(2)-H(2A)	0.9900	C(10)-H(10)	1.0000
C(2)-H(2B)	0.9900	C(11)-C(12)	1.512(4)
C(3)-O(2)	1.420(3)	C(11)-H(11A)	0.9900
C(3)-C(4)	1.509(4)	C(11)-H(11B)	0.9900
C(3)-H(3)	1.0000	C(12)-C(15)	1.327(4)
C(4)-C(5)	1.340(4)	C(13)-H(13A)	0.9800
C(4)-C(13)	1.492(4)	C(13)-H(13B)	0.9800
C(5)-C(6)	1.511(4)	C(13)-H(13C)	0.9800
C(6)-O(3)	1.438(3)	C(14)-H(14A)	0.9500
C(6)-C(7)	1.533(4)	C(14)-H(14B)	0.9500
C(6)-H(6)	1.0000	C(15)-H(15A)	0.9500
C(7)-C(8)	1.503(4)	C(15)-H(15B)	0.9500
C(7)-C(10)	1.533(3)	O(2)-H(2)	0.8400
C(7)-H(7)	1.0000	O(3)-H(3A)	0.8400
C(8)-C(14)	1.339(4)		
C(12)-C(1)-C(2)	115.6(2)	O(2)-C(3)-C(2)	114.3(2)
C(12)-C(1)-C(5)	117.7(2)	C(4)-C(3)-C(2)	102.5(2)
C(2)-C(1)-C(5)	101.4(2)	O(2)-C(3)-H(3)	109.1
C(12)-C(1)-H(1)	107.1	C(4)-C(3)-H(3)	109.1
C(2)-C(1)-H(1)	107.1	C(2)-C(3)-H(3)	109.1
C(5)-C(1)-H(1)	107.1	C(5)-C(4)-C(13)	128.7(3)
C(3)-C(2)-C(1)	104.7(2)	C(5)-C(4)-C(3)	110.4(2)
C(3)-C(2)-H(2A)	110.8	C(13)-C(4)-C(3)	120.7(2)
C(1)-C(2)-H(2A)	110.8	C(4)-C(5)-C(6)	123.3(2)
C(3)-C(2)-H(2B)	110.8	C(4)-C(5)-C(1)	111.1(2)
C(1)-C(2)-H(2B)	110.8	C(6)-C(5)-C(1)	125.2(2)
H(2A)-C(2)-H(2B)	108.9	O(3)-C(6)-C(5)	112.1(2)
O(2)-C(3)-C(4)	112.4(2)	O(3)-C(6)-C(7)	110.7(2)

C(5)-C(6)-C(7)	110.7(2)	C(10)-C(11)-H(11A)	109.5
O(3)-C(6)-H(6)	107.7	C(12)-C(11)-H(11A)	109.5
C(5)-C(6)-H(6)	107.7	C(10)-C(11)-H(11B)	109.5
C(7)-C(6)-H(6)	107.7	C(12)-C(11)-H(11B)	109.5
C(8)-C(7)-C(6)	117.9(2)	H(11A)-C(11)-H(11B)	108.1
C(8)-C(7)-C(10)	102.4(2)	C(15)-C(12)-C(11)	119.9(3)
C(6)-C(7)-C(10)	114.2(2)	C(15)-C(12)-C(1)	123.5(3)
C(8)-C(7)-H(7)	107.2	C(11)-C(12)-C(1)	116.5(2)
C(6)-C(7)-H(7)	107.2	C(4)-C(13)-H(13A)	109.5
C(10)-C(7)-H(7)	107.2	C(4)-C(13)-H(13B)	109.5
C(14)-C(8)-C(9)	122.0(3)	H(13A)-C(13)-H(13B)	109.5
C(14)-C(8)-C(7)	130.7(3)	C(4)-C(13)-H(13C)	109.5
C(9)-C(8)-C(7)	107.1(2)	H(13A)-C(13)-H(13C)	109.5
O(4)-C(9)-O(1)	121.9(3)	H(13B)-C(13)-H(13C)	109.5
O(4)-C(9)-C(8)	128.8(3)	C(8)-C(14)-H(14A)	120.0
O(1)-C(9)-C(8)	109.2(2)	C(8)-C(14)-H(14B)	120.0
O(1)-C(10)-C(11)	109.7(2)	H(14A)-C(14)-H(14B)	120.0
O(1)-C(10)-C(7)	105.4(2)	C(12)-C(15)-H(15A)	120.0
C(11)-C(10)-C(7)	115.4(2)	C(12)-C(15)-H(15B)	120.0
O(1)-C(10)-H(10)	108.7	H(15A)-C(15)-H(15B)	120.0
C(11)-C(10)-H(10)	108.7	C(9)-O(1)-C(10)	110.9(2)
C(7)-C(10)-H(10)	108.7	C(3)-O(2)-H(2)	109.5
C(10)-C(11)-C(12)	110.7(2)	C(6)-O(3)-H(3A)	109.5

Symmetry transformations used to generate equivalent atoms:

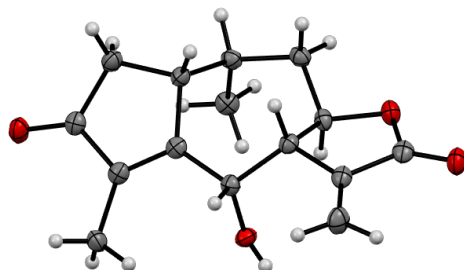
Table 4. Anisotropic displacement parameters ($\text{\AA}^2 \times 10^3$) for maimone75. The anisotropic displacement factor exponent takes the form: $-2\pi^2 [h^2 a^{*2} U^{11} + \dots + 2 h k a^* b^* U^{12}]$

	U ¹¹	U ²²	U ³³	U ²³	U ¹³	U ¹²
C(1)	25(1)	24(1)	23(1)	-4(1)	4(1)	0(1)
C(2)	28(1)	25(1)	28(2)	-5(1)	4(1)	2(1)
C(3)	28(1)	23(1)	22(1)	-2(1)	-1(1)	-3(1)
C(4)	22(1)	24(1)	21(1)	-1(1)	0(1)	-1(1)
C(5)	21(1)	24(1)	18(1)	-3(1)	2(1)	-2(1)
C(6)	25(1)	22(1)	19(1)	0(1)	4(1)	-1(1)
C(7)	24(1)	27(1)	18(1)	-1(1)	2(1)	-2(1)
C(8)	29(1)	27(1)	17(1)	0(1)	-2(1)	-3(1)
C(9)	31(1)	37(2)	22(1)	5(1)	1(1)	-1(1)
C(10)	27(1)	31(1)	23(1)	5(1)	5(1)	-1(1)
C(11)	30(1)	37(2)	24(1)	1(1)	9(1)	-2(1)
C(12)	29(1)	30(1)	25(1)	-4(1)	10(1)	-1(1)
C(13)	39(1)	26(1)	25(1)	4(1)	10(1)	3(1)
C(14)	32(1)	35(2)	27(1)	5(1)	1(1)	4(1)
C(15)	33(2)	41(2)	44(2)	4(2)	12(1)	0(1)
O(1)	36(1)	38(1)	28(1)	12(1)	11(1)	3(1)
O(2)	36(1)	20(1)	29(1)	1(1)	0(1)	-1(1)
O(3)	42(1)	20(1)	23(1)	-2(1)	-4(1)	1(1)
O(4)	44(1)	43(1)	34(1)	18(1)	5(1)	7(1)

Table 5. Hydrogen coordinates ($\times 10^4$) and isotropic displacement parameters ($\text{\AA}^2 \times 10^3$) for maimone75.

	x	y	z	U(eq)
H(1)	2463	2478	1810	29
H(2A)	4135	139	2560	33
H(2B)	5632	1213	3484	33
H(3)	1471	351	3417	30
H(6)	734	5778	3383	27
H(7)	967	5295	1500	28
H(10)	4753	6974	2152	32
H(11A)	5699	5304	744	36
H(11B)	3484	4459	497	36
H(13A)	993	4446	4962	44
H(13B)	2152	2889	5647	44
H(13C)	-39	2595	4891	44
H(14A)	-1676	9512	1609	38
H(14B)	-1625	7931	2479	38
H(15A)	8152	3799	1885	46
H(15B)	7639	2424	2784	46
H(2)	3567	-1025	4647	43
H(3A)	4422	6129	4199	44

X-Ray crystallographic Analysis of (-)-Mikanokryptin (*ent*-44)



A colorless plate 0.050 x 0.040 x 0.020 mm in size was mounted on a Cryoloop with Paratone oil. Data were collected in a nitrogen gas stream at 100(2) K using ω scans. Crystal-to-detector distance was 60 mm and exposure time was 10 seconds per frame using a scan width of 2.0°. Data collection was 99.4% complete to 67.000° in θ . A total of 33715 reflections were collected covering the indices, $-8 \leq h \leq 11$, $-12 \leq k \leq 12$, $-16 \leq l \leq 16$. 2328 reflections were found to be symmetry independent, with an R_{int} of 0.0306. Indexing and unit cell refinement indicated a primitive, orthorhombic lattice. The space group was found to be P 21 21 21 (No. 19). The data were integrated using the Bruker SAINT software program and scaled using the SADABS software program. Solution by iterative methods (SHELXT-2014) produced a complete heavy-atom phasing model consistent with the proposed structure. All non-hydrogen atoms were refined anisotropically by full-matrix least-squares (SHELXL-2014). All hydrogen atoms were placed using a riding model. Their positions were constrained relative to their parent atom using the appropriate HFIX command in SHELXL-2014. Absolute stereochemistry was unambiguously determined to be *R* at C1, C7, C10, and C12, and *S* at C6, respectively.

Table 1. Crystal data and structure refinement for compound *ent-44*.

X-ray ID	maimone80	
Sample/notebook ID	XH_5_MK	
Empirical formula	C ₁₅ H ₁₈ O ₄	
Formula weight	262.29	
Temperature	100(2) K	
Wavelength	1.54178 Å	
Crystal system	Orthorhombic	
Space group	P 21 21 21	
Unit cell dimensions	a = 9.3552(7) Å	α = 90°.
	b = 10.2688(8) Å	β = 90°.
	c = 13.2963(11) Å	γ = 90°.
Volume	1277.33(17) Å ³	
Z	4	
Density (calculated)	1.364 Mg/m ³	
Absorption coefficient	0.807 mm ⁻¹	
F(000)	560	
Crystal size	0.050 x 0.040 x 0.020 mm ³	
Theta range for data collection	5.443 to 68.347°.	
Index ranges	-8 ≤ h ≤ 11, -12 ≤ k ≤ 12, -16 ≤ l ≤ 16	
Reflections collected	33715	
Independent reflections	2328 [R(int) = 0.0306]	
Completeness to theta = 67.000°	99.4 %	
Absorption correction	Semi-empirical from equivalents	
Max. and min. transmission	0.929 and 0.891	
Refinement method	Full-matrix least-squares on F ²	
Data / restraints / parameters	2328 / 0 / 175	
Goodness-of-fit on F ²	1.061	
Final R indices [I > 2σ(I)]	R1 = 0.0277, wR2 = 0.0733	
R indices (all data)	R1 = 0.0280, wR2 = 0.0736	
Absolute structure parameter	0.06(3)	
Extinction coefficient	n/a	
Largest diff. peak and hole	0.216 and -0.134 e.Å ⁻³	

Table 2. Atomic coordinates ($\times 10^4$) and equivalent isotropic displacement parameters ($\text{\AA}^2 \times 10^3$) for maimone80. $U(\text{eq})$ is defined as one third of the trace of the orthogonalized U^{ij} tensor.

	x	y	z	$U(\text{eq})$
C(1)	6651(2)	8272(2)	4010(1)	19(1)
C(2)	5999(2)	8121(2)	5067(1)	22(1)
C(3)	6217(2)	6714(2)	5361(1)	20(1)
C(4)	7002(2)	6068(2)	4545(1)	19(1)
C(5)	7277(2)	6927(2)	3809(1)	18(1)
C(6)	8167(2)	6600(2)	2892(1)	18(1)
C(7)	8424(2)	7775(2)	2212(1)	18(1)
C(8)	9426(2)	7537(2)	1344(1)	21(1)
C(9)	8866(2)	8303(2)	480(1)	22(1)
C(10)	7072(2)	8261(2)	1686(1)	19(1)
C(11)	6222(2)	9273(2)	2252(1)	20(1)
C(12)	5539(2)	8746(2)	3223(1)	20(1)
C(13)	7433(2)	4665(2)	4608(1)	24(1)
C(14)	10588(2)	6812(2)	1299(2)	28(1)
C(15)	4406(2)	7707(2)	3000(2)	23(1)
O(1)	7597(1)	8839(1)	740(1)	23(1)
O(2)	5846(2)	6217(1)	6156(1)	26(1)
O(3)	7478(1)	5564(1)	2367(1)	22(1)
O(4)	9391(2)	8479(1)	-335(1)	28(1)

Table 3. Bond lengths [\AA] and angles [$^\circ$] for maimone80.

C(1)-C(5)	1.524(2)	C(9)-O(4)	1.204(2)
C(1)-C(2)	1.539(2)	C(9)-O(1)	1.354(2)
C(1)-C(12)	1.554(2)	C(10)-O(1)	1.475(2)
C(1)-H(1)	1.0000	C(10)-C(11)	1.510(3)
C(2)-C(3)	1.511(3)	C(10)-H(10)	1.0000
C(2)-H(2A)	0.9900	C(11)-C(12)	1.539(3)
C(2)-H(2B)	0.9900	C(11)-H(11A)	0.9900
C(3)-O(2)	1.224(2)	C(11)-H(11B)	0.9900
C(3)-C(4)	1.469(2)	C(12)-C(15)	1.533(3)
C(4)-C(5)	1.343(3)	C(12)-H(12)	1.0000
C(4)-C(13)	1.498(3)	C(13)-H(13A)	0.9800
C(5)-C(6)	1.514(2)	C(13)-H(13B)	0.9800
C(6)-O(3)	1.426(2)	C(13)-H(13C)	0.9800
C(6)-C(7)	1.527(2)	C(14)-H(14A)	0.9500
C(6)-H(6)	1.0000	C(14)-H(14B)	0.9500
C(7)-C(8)	1.507(3)	C(15)-H(15A)	0.9800
C(7)-C(10)	1.529(2)	C(15)-H(15B)	0.9800
C(7)-H(7)	1.0000	C(15)-H(15C)	0.9800
C(8)-C(14)	1.320(3)	O(3)-H(3)	0.8400
C(8)-C(9)	1.488(3)		
C(5)-C(1)-C(2)	102.79(14)	O(2)-C(3)-C(2)	125.74(17)
C(5)-C(1)-C(12)	115.01(14)	C(4)-C(3)-C(2)	107.98(15)
C(2)-C(1)-C(12)	112.37(15)	C(5)-C(4)-C(3)	109.69(17)
C(5)-C(1)-H(1)	108.8	C(5)-C(4)-C(13)	128.42(17)
C(2)-C(1)-H(1)	108.8	C(3)-C(4)-C(13)	121.86(16)
C(12)-C(1)-H(1)	108.8	C(4)-C(5)-C(6)	123.08(16)
C(3)-C(2)-C(1)	106.20(15)	C(4)-C(5)-C(1)	113.23(16)
C(3)-C(2)-H(2A)	110.5	C(6)-C(5)-C(1)	123.65(15)
C(1)-C(2)-H(2A)	110.5	O(3)-C(6)-C(5)	108.13(14)
C(3)-C(2)-H(2B)	110.5	O(3)-C(6)-C(7)	111.78(14)
C(1)-C(2)-H(2B)	110.5	C(5)-C(6)-C(7)	112.80(15)
H(2A)-C(2)-H(2B)	108.7	O(3)-C(6)-H(6)	108.0
O(2)-C(3)-C(4)	126.24(18)	C(5)-C(6)-H(6)	108.0

C(7)-C(6)-H(6)	108.0	H(11A)-C(11)-H(11B)	107.7
C(8)-C(7)-C(6)	115.03(15)	C(15)-C(12)-C(11)	111.65(15)
C(8)-C(7)-C(10)	102.52(14)	C(15)-C(12)-C(1)	112.06(15)
C(6)-C(7)-C(10)	113.49(14)	C(11)-C(12)-C(1)	113.37(15)
C(8)-C(7)-H(7)	108.5	C(15)-C(12)-H(12)	106.4
C(6)-C(7)-H(7)	108.5	C(11)-C(12)-H(12)	106.4
C(10)-C(7)-H(7)	108.5	C(1)-C(12)-H(12)	106.4
C(14)-C(8)-C(9)	123.56(18)	C(4)-C(13)-H(13A)	109.5
C(14)-C(8)-C(7)	129.77(18)	C(4)-C(13)-H(13B)	109.5
C(9)-C(8)-C(7)	106.68(16)	H(13A)-C(13)-H(13B)	109.5
O(4)-C(9)-O(1)	121.86(18)	C(4)-C(13)-H(13C)	109.5
O(4)-C(9)-C(8)	129.12(19)	H(13A)-C(13)-H(13C)	109.5
O(1)-C(9)-C(8)	109.02(16)	H(13B)-C(13)-H(13C)	109.5
O(1)-C(10)-C(11)	108.87(15)	C(8)-C(14)-H(14A)	120.0
O(1)-C(10)-C(7)	104.25(14)	C(8)-C(14)-H(14B)	120.0
C(11)-C(10)-C(7)	115.55(14)	H(14A)-C(14)-H(14B)	120.0
O(1)-C(10)-H(10)	109.3	C(12)-C(15)-H(15A)	109.5
C(11)-C(10)-H(10)	109.3	C(12)-C(15)-H(15B)	109.5
C(7)-C(10)-H(10)	109.3	H(15A)-C(15)-H(15B)	109.5
C(10)-C(11)-C(12)	113.30(15)	C(12)-C(15)-H(15C)	109.5
C(10)-C(11)-H(11A)	108.9	H(15A)-C(15)-H(15C)	109.5
C(12)-C(11)-H(11A)	108.9	H(15B)-C(15)-H(15C)	109.5
C(10)-C(11)-H(11B)	108.9	C(9)-O(1)-C(10)	110.28(14)
C(12)-C(11)-H(11B)	108.9	C(6)-O(3)-H(3)	109.5

Symmetry transformations used to generate equivalent atoms:

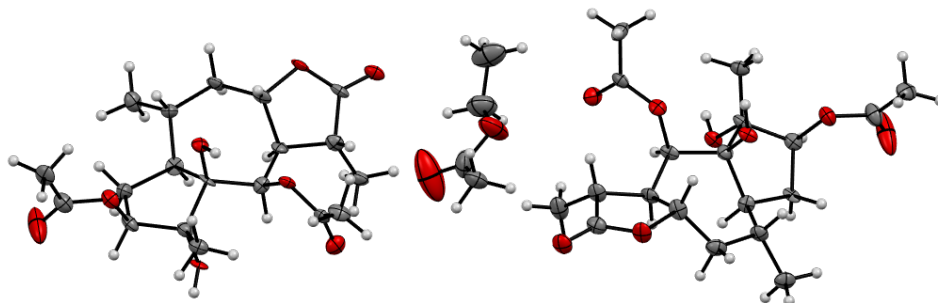
Table 4. Anisotropic displacement parameters ($\text{\AA}^2 \times 10^3$) for maimone80. The anisotropic displacement factor exponent takes the form: $-2\pi^2 [h^2 a^{*2} U^{11} + \dots + 2 h k a^* b^* U^{12}]$

	U^{11}	U^{22}	U^{33}	U^{23}	U^{13}	U^{12}
C(1)	19(1)	20(1)	17(1)	-2(1)	0(1)	1(1)
C(2)	24(1)	24(1)	19(1)	-2(1)	2(1)	4(1)
C(3)	16(1)	25(1)	19(1)	0(1)	-2(1)	-1(1)
C(4)	15(1)	24(1)	19(1)	-1(1)	-1(1)	1(1)
C(5)	14(1)	22(1)	19(1)	-1(1)	-3(1)	0(1)
C(6)	16(1)	20(1)	18(1)	0(1)	-1(1)	0(1)
C(7)	18(1)	20(1)	18(1)	-1(1)	0(1)	-1(1)
C(8)	21(1)	23(1)	18(1)	-1(1)	0(1)	-6(1)
C(9)	23(1)	22(1)	21(1)	-1(1)	-1(1)	-7(1)
C(10)	20(1)	20(1)	17(1)	3(1)	-1(1)	-4(1)
C(11)	21(1)	18(1)	22(1)	2(1)	-3(1)	1(1)
C(12)	20(1)	19(1)	21(1)	0(1)	-2(1)	3(1)
C(13)	27(1)	22(1)	22(1)	4(1)	2(1)	3(1)
C(14)	24(1)	35(1)	25(1)	2(1)	7(1)	1(1)
C(15)	18(1)	25(1)	27(1)	1(1)	0(1)	1(1)
O(1)	25(1)	26(1)	18(1)	5(1)	-1(1)	-2(1)
O(2)	26(1)	31(1)	21(1)	4(1)	6(1)	2(1)
O(3)	25(1)	19(1)	21(1)	-4(1)	3(1)	-1(1)
O(4)	32(1)	33(1)	20(1)	4(1)	3(1)	-5(1)

Table 5. Hydrogen coordinates ($\times 10^4$) and isotropic displacement parameters ($\text{\AA}^2 \times 10^3$) for maimone80.

	x	y	z	U(eq)
H(1)	7449	8919	4044	22
H(2A)	6484	8706	5551	27
H(2B)	4968	8338	5056	27
H(6)	9117	6277	3129	22
H(7)	8818	8500	2631	22
H(10)	6441	7502	1527	23
H(11A)	5459	9612	1808	25
H(11B)	6860	10009	2425	25
H(12)	5022	9495	3539	24
H(13A)	6589	4112	4517	35
H(13B)	7859	4492	5268	35
H(13C)	8133	4473	4080	35
H(14A)	11116	6759	690	33
H(14B)	10898	6342	1875	33
H(15A)	4843	6992	2620	35
H(15B)	3633	8093	2602	35
H(15C)	4020	7371	3634	35
H(3)	8074	5185	1996	32

X-Ray crystallographic Analysis of Compound 318



A colorless plate 0.070 x 0.040 x 0.020 mm in size was mounted on a Cryoloop with Paratone oil. Data were collected in a nitrogen gas stream at 100(2) K using and scans. Crystal-to-detector distance was 60 mm and exposure time was 10 seconds per frame using a scan width of 2.0°. Data collection was 98.3% complete to 67.000° in θ . A total of 6547 reflections were collected covering the indices, $-5 \leq h \leq 6$, $-11 \leq k \leq 11$, $-25 \leq l \leq 25$. 6547 reflections were found to be symmetry independent, with an R_{int} of 0.0684. Indexing and unit cell refinement indicated a primitive, triclinic lattice. The space group was found to be P 1 (No. 1). The data were integrated using the Bruker SAINT software program and scaled using the SADABS software program. Solution by iterative methods (SHELXT-2014) produced a complete heavy-atom phasing model consistent with the proposed structure. All non-hydrogen atoms were refined anisotropically by full-matrix least-squares (SHELXL-2016). All hydrogen atoms were placed using a riding model. Their positions were constrained relative to their parent atom using the appropriate HFIX command in SHELXL-2016.

Table 1. Crystal data and structure refinement for compound **318**.

X-ray ID	maimone86	
Sample/notebook ID	XH_5_196_BF3	
Empirical formula	C42 H64 O18	
Formula weight	856.93	
Temperature	100(2) K	
Wavelength	1.54178 Å	
Crystal system	Triclinic	
Space group	P 1	
Unit cell dimensions	a = 5.4815(3) Å	$\alpha = 79.224(3)^\circ$.
	b = 9.8145(5) Å	$\beta = 84.209(3)^\circ$.
	c = 20.8636(11) Å	$\gamma = 73.901(3)^\circ$.
Volume	1057.96(10) Å ³	
Z	1	
Density (calculated)	1.345 Mg/m ³	
Absorption coefficient	0.878 mm ⁻¹	
F(000)	460	
Crystal size	0.070 x 0.040 x 0.020 mm ³	
Theta range for data collection	2.158 to 68.382°.	
Index ranges	-5 ≤ h ≤ 6, -11 ≤ k ≤ 11, -25 ≤ l ≤ 25	
Reflections collected	6547	
Independent reflections	6547 [R(int) = 0.0684]	
Completeness to theta = 67.000°	98.3 %	
Absorption correction	Semi-empirical from equivalents	
Max. and min. transmission	0.929 and 0.696	
Refinement method	Full-matrix least-squares on F ²	
Data / restraints / parameters	6547 / 3 / 558	
Goodness-of-fit on F ²	1.066	
Final R indices [I > 2σ(I)]	R1 = 0.0643, wR2 = 0.1775	
R indices (all data)	R1 = 0.0706, wR2 = 0.1830	
Absolute structure parameter	0.37(19)	
Extinction coefficient	n/a	
Largest diff. peak and hole	0.734 and -0.355 e.Å ⁻³	

Table 2. Atomic coordinates ($\times 10^4$) and equivalent isotropic displacement parameters ($\text{\AA}^2 \times 10^3$) for maimone86. $U(\text{eq})$ is defined as one third of the trace of the orthogonalized U^{ij} tensor.

	x	y	z	$U(\text{eq})$
C(1)	8296(14)	3588(8)	2701(3)	19(2)
C(2)	7328(17)	4316(8)	3299(4)	23(2)
C(3)	5840(14)	5781(7)	2989(3)	19(2)
C(4)	6383(16)	4386(8)	2181(3)	21(2)
C(5)	7672(15)	4709(8)	1499(3)	21(2)
C(6)	9013(15)	3410(8)	1167(3)	22(2)
C(7)	10656(15)	2071(8)	1602(3)	17(2)
C(8)	12130(16)	876(8)	1195(3)	25(2)
C(9)	11725(15)	-543(8)	1557(3)	21(2)
C(10)	10779(15)	-276(8)	2258(3)	21(2)
C(11)	8808(15)	1956(8)	2803(3)	19(2)
C(12)	9159(13)	1324(7)	2164(3)	14(2)
C(13)	9353(16)	4336(8)	3737(4)	27(2)
C(14)	10679(17)	3976(9)	593(4)	27(2)
C(15)	10530(18)	-1568(9)	750(4)	29(2)
C(16)	8412(18)	-1860(8)	447(4)	30(2)
C(17)	9486(15)	-1399(8)	2632(3)	22(2)
C(18)	7052(16)	904(8)	3822(3)	22(2)
C(19)	4957(16)	287(9)	4108(4)	26(2)
C(20)	4026(16)	6306(7)	7305(3)	22(2)
C(21)	4287(16)	5576(8)	6704(3)	23(2)
C(22)	4027(17)	4092(9)	7002(4)	26(2)
C(23)	2519(17)	5474(8)	7821(3)	23(2)
C(24)	3578(17)	5172(9)	8490(4)	28(2)
C(25)	3382(16)	6457(8)	8834(3)	23(2)
C(26)	4060(15)	7779(8)	8399(3)	18(2)
C(27)	4000(13)	8954(7)	8808(3)	15(1)
C(28)	2468(16)	10400(8)	8451(3)	20(2)
C(29)	2337(15)	10166(8)	7752(3)	19(2)
C(30)	2228(15)	8558(9)	7837(3)	21(2)
C(31)	3027(14)	7939(7)	7199(3)	17(2)

C(32)	6753(19)	5499(9)	6284(4)	35(2)
C(33)	5159(17)	5904(8)	9407(4)	27(2)
C(34)	-458(19)	11497(10)	9252(4)	32(2)
C(35)	-3051(16)	11724(10)	9553(4)	33(2)
C(36)	225(16)	11274(8)	7383(3)	24(2)
C(37)	1011(15)	8952(8)	6176(3)	19(2)
C(38)	-1458(17)	9685(10)	5897(3)	30(2)
C(39)	3090(20)	3652(11)	5116(4)	46(3)
C(40)	1810(20)	2576(10)	5463(4)	40(2)
C(41)	2600(30)	6126(12)	4834(6)	62(3)
C(42)	590(30)	7318(13)	4588(6)	65(4)
O(1)	5257(10)	5796(5)	2386(2)	25(1)
O(2)	5235(10)	6862(6)	3238(2)	24(1)
O(3)	9768(11)	-934(6)	1264(2)	24(1)
O(4)	12697(16)	-1877(12)	540(4)	74(3)
O(5)	13036(9)	-298(5)	2570(2)	18(1)
O(6)	6783(10)	1425(6)	1927(2)	19(1)
O(7)	6732(10)	1480(5)	3179(2)	19(1)
O(8)	8867(11)	907(6)	4104(3)	29(1)
O(9)	2936(12)	4070(5)	7612(2)	28(1)
O(10)	4658(12)	3005(6)	6760(3)	31(1)
O(11)	-88(11)	10769(6)	8749(3)	27(1)
O(12)	1207(16)	11819(13)	9442(5)	81(4)
O(13)	4763(10)	10194(6)	7440(2)	21(1)
O(14)	-246(10)	8437(5)	8080(2)	18(1)
O(15)	768(10)	8404(5)	6819(2)	21(1)
O(16)	3108(11)	8856(6)	5889(2)	27(1)
O(17)	4800(30)	3440(14)	4747(7)	120(5)
O(18)	1758(16)	4989(8)	5201(4)	65(2)

Table 3. Bond lengths [\AA] and angles [$^\circ$] for maimone86.

C(1)-C(11)	1.525(10)	C(13)-H(13A)	0.9800
C(1)-C(2)	1.529(10)	C(13)-H(13B)	0.9800
C(1)-C(4)	1.532(10)	C(13)-H(13C)	0.9800
C(1)-H(1)	1.0000	C(14)-H(14A)	0.9800
C(2)-C(3)	1.503(10)	C(14)-H(14B)	0.9800
C(2)-C(13)	1.513(12)	C(14)-H(14C)	0.9800
C(2)-H(2)	1.0000	C(15)-O(4)	1.200(12)
C(3)-O(2)	1.218(9)	C(15)-O(3)	1.315(10)
C(3)-O(1)	1.325(9)	C(15)-C(16)	1.494(13)
C(4)-O(1)	1.474(9)	C(16)-H(16A)	0.9800
C(4)-C(5)	1.541(10)	C(16)-H(16B)	0.9800
C(4)-H(4)	1.0000	C(16)-H(16C)	0.9800
C(5)-C(6)	1.535(9)	C(17)-H(17A)	0.9800
C(5)-H(5A)	0.9900	C(17)-H(17B)	0.9800
C(5)-H(5B)	0.9900	C(17)-H(17C)	0.9800
C(6)-C(14)	1.546(11)	C(18)-O(8)	1.207(10)
C(6)-C(7)	1.556(10)	C(18)-O(7)	1.362(8)
C(6)-H(6)	1.0000	C(18)-C(19)	1.467(12)
C(7)-C(12)	1.551(9)	C(19)-H(19A)	0.9800
C(7)-C(8)	1.568(10)	C(19)-H(19B)	0.9800
C(7)-H(7)	1.0000	C(19)-H(19C)	0.9800
C(8)-C(9)	1.517(11)	C(20)-C(31)	1.524(9)
C(8)-H(8A)	0.9900	C(20)-C(21)	1.532(9)
C(8)-H(8B)	0.9900	C(20)-C(23)	1.540(10)
C(9)-O(3)	1.456(10)	C(20)-H(20)	1.0000
C(9)-C(10)	1.547(9)	C(21)-C(22)	1.513(11)
C(9)-H(9)	1.0000	C(21)-C(32)	1.527(12)
C(10)-O(5)	1.448(10)	C(21)-H(21)	1.0000
C(10)-C(17)	1.524(11)	C(22)-O(10)	1.214(10)
C(10)-C(12)	1.562(9)	C(22)-O(9)	1.350(9)
C(11)-O(7)	1.452(9)	C(23)-O(9)	1.474(9)
C(11)-C(12)	1.546(9)	C(23)-C(24)	1.513(11)
C(11)-H(11)	1.0000	C(23)-H(23)	1.0000
C(12)-O(6)	1.410(9)	C(24)-C(25)	1.537(11)

C(24)-H(24A)	0.9900	C(35)-H(35A)	0.9800
C(24)-H(24B)	0.9900	C(35)-H(35B)	0.9800
C(25)-C(33)	1.540(11)	C(35)-H(35C)	0.9800
C(25)-C(26)	1.550(10)	C(36)-H(36A)	0.9800
C(25)-H(25)	1.0000	C(36)-H(36B)	0.9800
C(26)-C(27)	1.549(9)	C(36)-H(36C)	0.9800
C(26)-C(30)	1.564(10)	C(37)-O(16)	1.229(9)
C(26)-H(26)	1.0000	C(37)-O(15)	1.356(9)
C(27)-C(28)	1.531(10)	C(37)-C(38)	1.467(11)
C(27)-H(27A)	0.9900	C(38)-H(38A)	0.9800
C(27)-H(27B)	0.9900	C(38)-H(38B)	0.9800
C(28)-O(11)	1.451(10)	C(38)-H(38C)	0.9800
C(28)-C(29)	1.530(10)	C(39)-O(17)	1.150(13)
C(28)-H(28)	1.0000	C(39)-O(18)	1.347(13)
C(29)-O(13)	1.426(9)	C(39)-C(40)	1.467(15)
C(29)-C(36)	1.512(10)	C(40)-H(40A)	0.9800
C(29)-C(30)	1.571(11)	C(40)-H(40B)	0.9800
C(30)-O(14)	1.428(10)	C(40)-H(40C)	0.9800
C(30)-C(31)	1.539(10)	C(41)-O(18)	1.393(14)
C(31)-O(15)	1.457(9)	C(41)-C(42)	1.421(17)
C(31)-H(31)	1.0000	C(41)-H(41A)	0.9900
C(32)-H(32A)	0.9800	C(41)-H(41B)	0.9900
C(32)-H(32B)	0.9800	C(42)-H(42A)	0.9800
C(32)-H(32C)	0.9800	C(42)-H(42B)	0.9800
C(33)-H(33A)	0.9800	C(42)-H(42C)	0.9800
C(33)-H(33B)	0.9800	O(5)-H(5)	0.8400
C(33)-H(33C)	0.9800	O(6)-H(6A)	0.8400
C(34)-O(12)	1.171(13)	O(13)-H(13)	0.8400
C(34)-O(11)	1.345(10)	O(14)-H(14)	0.8400
C(34)-C(35)	1.470(13)		
C(11)-C(1)-C(2)	117.0(6)	C(4)-C(1)-H(1)	106.8
C(11)-C(1)-C(4)	114.0(6)	C(3)-C(2)-C(13)	114.3(7)
C(2)-C(1)-C(4)	104.8(6)	C(3)-C(2)-C(1)	101.5(6)
C(11)-C(1)-H(1)	106.8	C(13)-C(2)-C(1)	115.6(7)
C(2)-C(1)-H(1)	106.8	C(3)-C(2)-H(2)	108.4

C(13)-C(2)-H(2)	108.4	O(3)-C(9)-C(10)	108.7(6)
C(1)-C(2)-H(2)	108.4	C(8)-C(9)-C(10)	105.4(6)
O(2)-C(3)-O(1)	121.8(6)	O(3)-C(9)-H(9)	110.6
O(2)-C(3)-C(2)	126.1(7)	C(8)-C(9)-H(9)	110.6
O(1)-C(3)-C(2)	112.1(6)	C(10)-C(9)-H(9)	110.6
O(1)-C(4)-C(1)	103.6(6)	O(5)-C(10)-C(17)	111.4(6)
O(1)-C(4)-C(5)	105.7(6)	O(5)-C(10)-C(9)	104.8(6)
C(1)-C(4)-C(5)	112.7(6)	C(17)-C(10)-C(9)	112.9(6)
O(1)-C(4)-H(4)	111.5	O(5)-C(10)-C(12)	105.6(6)
C(1)-C(4)-H(4)	111.5	C(17)-C(10)-C(12)	116.9(6)
C(5)-C(4)-H(4)	111.5	C(9)-C(10)-C(12)	104.2(5)
C(6)-C(5)-C(4)	116.6(6)	O(7)-C(11)-C(1)	111.4(6)
C(6)-C(5)-H(5A)	108.1	O(7)-C(11)-C(12)	105.8(6)
C(4)-C(5)-H(5A)	108.1	C(1)-C(11)-C(12)	114.4(5)
C(6)-C(5)-H(5B)	108.1	O(7)-C(11)-H(11)	108.4
C(4)-C(5)-H(5B)	108.1	C(1)-C(11)-H(11)	108.4
H(5A)-C(5)-H(5B)	107.3	C(12)-C(11)-H(11)	108.4
C(5)-C(6)-C(14)	105.8(6)	O(6)-C(12)-C(11)	110.8(5)
C(5)-C(6)-C(7)	116.9(6)	O(6)-C(12)-C(7)	106.9(5)
C(14)-C(6)-C(7)	110.0(6)	C(11)-C(12)-C(7)	114.2(6)
C(5)-C(6)-H(6)	107.9	O(6)-C(12)-C(10)	109.6(6)
C(14)-C(6)-H(6)	107.9	C(11)-C(12)-C(10)	111.8(6)
C(7)-C(6)-H(6)	107.9	C(7)-C(12)-C(10)	103.1(5)
C(12)-C(7)-C(6)	115.1(6)	C(2)-C(13)-H(13A)	109.5
C(12)-C(7)-C(8)	106.0(6)	C(2)-C(13)-H(13B)	109.5
C(6)-C(7)-C(8)	112.1(5)	H(13A)-C(13)-H(13B)	109.5
C(12)-C(7)-H(7)	107.8	C(2)-C(13)-H(13C)	109.5
C(6)-C(7)-H(7)	107.8	H(13A)-C(13)-H(13C)	109.5
C(8)-C(7)-H(7)	107.8	H(13B)-C(13)-H(13C)	109.5
C(9)-C(8)-C(7)	107.4(6)	C(6)-C(14)-H(14A)	109.5
C(9)-C(8)-H(8A)	110.2	C(6)-C(14)-H(14B)	109.5
C(7)-C(8)-H(8A)	110.2	H(14A)-C(14)-H(14B)	109.5
C(9)-C(8)-H(8B)	110.2	C(6)-C(14)-H(14C)	109.5
C(7)-C(8)-H(8B)	110.2	H(14A)-C(14)-H(14C)	109.5
H(8A)-C(8)-H(8B)	108.5	H(14B)-C(14)-H(14C)	109.5
O(3)-C(9)-C(8)	110.9(6)	O(4)-C(15)-O(3)	123.9(9)

O(4)-C(15)-C(16)	123.0(8)	O(10)-C(22)-C(21)	128.3(7)
O(3)-C(15)-C(16)	113.1(7)	O(9)-C(22)-C(21)	111.4(6)
C(15)-C(16)-H(16A)	109.5	O(9)-C(23)-C(24)	106.6(6)
C(15)-C(16)-H(16B)	109.5	O(9)-C(23)-C(20)	104.8(5)
H(16A)-C(16)-H(16B)	109.5	C(24)-C(23)-C(20)	112.1(7)
C(15)-C(16)-H(16C)	109.5	O(9)-C(23)-H(23)	111.0
H(16A)-C(16)-H(16C)	109.5	C(24)-C(23)-H(23)	111.0
H(16B)-C(16)-H(16C)	109.5	C(20)-C(23)-H(23)	111.0
C(10)-C(17)-H(17A)	109.5	C(23)-C(24)-C(25)	118.0(7)
C(10)-C(17)-H(17B)	109.5	C(23)-C(24)-H(24A)	107.8
H(17A)-C(17)-H(17B)	109.5	C(25)-C(24)-H(24A)	107.8
C(10)-C(17)-H(17C)	109.5	C(23)-C(24)-H(24B)	107.8
H(17A)-C(17)-H(17C)	109.5	C(25)-C(24)-H(24B)	107.8
H(17B)-C(17)-H(17C)	109.5	H(24A)-C(24)-H(24B)	107.1
O(8)-C(18)-O(7)	122.7(7)	C(24)-C(25)-C(33)	106.9(6)
O(8)-C(18)-C(19)	125.8(7)	C(24)-C(25)-C(26)	115.7(6)
O(7)-C(18)-C(19)	111.5(7)	C(33)-C(25)-C(26)	109.4(7)
C(18)-C(19)-H(19A)	109.5	C(24)-C(25)-H(25)	108.2
C(18)-C(19)-H(19B)	109.5	C(33)-C(25)-H(25)	108.2
H(19A)-C(19)-H(19B)	109.5	C(26)-C(25)-H(25)	108.2
C(18)-C(19)-H(19C)	109.5	C(27)-C(26)-C(25)	111.1(5)
H(19A)-C(19)-H(19C)	109.5	C(27)-C(26)-C(30)	105.0(6)
H(19B)-C(19)-H(19C)	109.5	C(25)-C(26)-C(30)	115.2(7)
C(31)-C(20)-C(21)	116.9(6)	C(27)-C(26)-H(26)	108.4
C(31)-C(20)-C(23)	115.8(6)	C(25)-C(26)-H(26)	108.4
C(21)-C(20)-C(23)	104.3(6)	C(30)-C(26)-H(26)	108.4
C(31)-C(20)-H(20)	106.3	C(28)-C(27)-C(26)	108.3(6)
C(21)-C(20)-H(20)	106.3	C(28)-C(27)-H(27A)	110.0
C(23)-C(20)-H(20)	106.3	C(26)-C(27)-H(27A)	110.0
C(22)-C(21)-C(32)	111.4(6)	C(28)-C(27)-H(27B)	110.0
C(22)-C(21)-C(20)	102.5(6)	C(26)-C(27)-H(27B)	110.0
C(32)-C(21)-C(20)	116.1(7)	H(27A)-C(27)-H(27B)	108.4
C(22)-C(21)-H(21)	108.9	O(11)-C(28)-C(29)	109.2(6)
C(32)-C(21)-H(21)	108.9	O(11)-C(28)-C(27)	110.0(6)
C(20)-C(21)-H(21)	108.9	C(29)-C(28)-C(27)	105.3(6)
O(10)-C(22)-O(9)	120.4(7)	O(11)-C(28)-H(28)	110.7

C(29)-C(28)-H(28)	110.7	C(34)-C(35)-H(35B)	109.5
C(27)-C(28)-H(28)	110.7	H(35A)-C(35)-H(35B)	109.5
O(13)-C(29)-C(36)	111.2(6)	C(34)-C(35)-H(35C)	109.5
O(13)-C(29)-C(28)	105.8(6)	H(35A)-C(35)-H(35C)	109.5
C(36)-C(29)-C(28)	113.5(6)	H(35B)-C(35)-H(35C)	109.5
O(13)-C(29)-C(30)	105.5(6)	C(29)-C(36)-H(36A)	109.5
C(36)-C(29)-C(30)	116.2(7)	C(29)-C(36)-H(36B)	109.5
C(28)-C(29)-C(30)	103.8(6)	H(36A)-C(36)-H(36B)	109.5
O(14)-C(30)-C(31)	111.5(6)	C(29)-C(36)-H(36C)	109.5
O(14)-C(30)-C(26)	106.4(6)	H(36A)-C(36)-H(36C)	109.5
C(31)-C(30)-C(26)	113.1(6)	H(36B)-C(36)-H(36C)	109.5
O(14)-C(30)-C(29)	110.2(6)	O(16)-C(37)-O(15)	121.6(7)
C(31)-C(30)-C(29)	111.9(6)	O(16)-C(37)-C(38)	126.3(7)
C(26)-C(30)-C(29)	103.4(6)	O(15)-C(37)-C(38)	112.1(6)
O(15)-C(31)-C(20)	110.5(6)	C(37)-C(38)-H(38A)	109.5
O(15)-C(31)-C(30)	105.8(6)	C(37)-C(38)-H(38B)	109.5
C(20)-C(31)-C(30)	113.7(6)	H(38A)-C(38)-H(38B)	109.5
O(15)-C(31)-H(31)	108.9	C(37)-C(38)-H(38C)	109.5
C(20)-C(31)-H(31)	108.9	H(38A)-C(38)-H(38C)	109.5
C(30)-C(31)-H(31)	108.9	H(38B)-C(38)-H(38C)	109.5
C(21)-C(32)-H(32A)	109.5	O(17)-C(39)-O(18)	122.5(11)
C(21)-C(32)-H(32B)	109.5	O(17)-C(39)-C(40)	125.6(10)
H(32A)-C(32)-H(32B)	109.5	O(18)-C(39)-C(40)	111.2(9)
C(21)-C(32)-H(32C)	109.5	C(39)-C(40)-H(40A)	109.5
H(32A)-C(32)-H(32C)	109.5	C(39)-C(40)-H(40B)	109.5
H(32B)-C(32)-H(32C)	109.5	H(40A)-C(40)-H(40B)	109.5
C(25)-C(33)-H(33A)	109.5	C(39)-C(40)-H(40C)	109.5
C(25)-C(33)-H(33B)	109.5	H(40A)-C(40)-H(40C)	109.5
H(33A)-C(33)-H(33B)	109.5	H(40B)-C(40)-H(40C)	109.5
C(25)-C(33)-H(33C)	109.5	O(18)-C(41)-C(42)	113.4(12)
H(33A)-C(33)-H(33C)	109.5	O(18)-C(41)-H(41A)	108.9
H(33B)-C(33)-H(33C)	109.5	C(42)-C(41)-H(41A)	108.9
O(12)-C(34)-O(11)	121.5(9)	O(18)-C(41)-H(41B)	108.9
O(12)-C(34)-C(35)	125.1(9)	C(42)-C(41)-H(41B)	108.9
O(11)-C(34)-C(35)	113.2(8)	H(41A)-C(41)-H(41B)	107.7
C(34)-C(35)-H(35A)	109.5	C(41)-C(42)-H(42A)	109.5

C(41)-C(42)-H(42B)	109.5	C(12)-O(6)-H(6A)	109.5
H(42A)-C(42)-H(42B)	109.5	C(18)-O(7)-C(11)	118.2(6)
C(41)-C(42)-H(42C)	109.5	C(22)-O(9)-C(23)	110.8(6)
H(42A)-C(42)-H(42C)	109.5	C(34)-O(11)-C(28)	117.1(7)
H(42B)-C(42)-H(42C)	109.5	C(29)-O(13)-H(13)	109.5
C(3)-O(1)-C(4)	111.2(5)	C(30)-O(14)-H(14)	109.5
C(15)-O(3)-C(9)	115.5(6)	C(37)-O(15)-C(31)	118.4(6)
C(10)-O(5)-H(5)	109.5	C(39)-O(18)-C(41)	116.8(9)

Symmetry transformations used to generate equivalent atoms:

Table 4. Anisotropic displacement parameters ($\text{\AA}^2 \times 10^3$) for maimone86. The anisotropic displacement factor exponent takes the form: $-2\pi^2 [h^2 a^{*2} U^{11} + \dots + 2 h k a^* b^* U^{12}]$

	U ¹¹	U ²²	U ³³	U ²³	U ¹³	U ¹²
C(1)	8(4)	21(4)	24(3)	-3(3)	-3(3)	2(3)
C(2)	26(5)	16(4)	28(3)	-2(3)	0(3)	-7(3)
C(3)	10(4)	10(4)	33(3)	-4(3)	2(3)	0(3)
C(4)	23(5)	7(3)	33(4)	-5(3)	-4(3)	-3(3)
C(5)	22(4)	10(4)	28(3)	-1(3)	-1(3)	2(3)
C(6)	22(4)	20(4)	20(3)	-1(3)	-4(3)	1(3)
C(7)	17(4)	18(4)	25(3)	-4(3)	-2(3)	-16(3)
C(8)	25(5)	24(4)	21(3)	-2(3)	0(3)	1(3)
C(9)	13(4)	19(4)	33(4)	-10(3)	3(3)	-3(3)
C(10)	17(4)	20(4)	24(3)	-4(3)	0(3)	-1(3)
C(11)	19(4)	20(4)	19(3)	-1(3)	0(3)	-11(3)
C(12)	4(4)	8(3)	29(3)	-4(2)	2(2)	1(3)
C(13)	28(5)	15(4)	37(4)	-7(3)	-11(3)	2(3)
C(14)	28(5)	23(4)	30(4)	-5(3)	8(3)	-10(4)
C(15)	27(5)	25(4)	35(4)	-7(3)	3(3)	-7(4)
C(16)	45(6)	12(4)	35(4)	-7(3)	-2(4)	-10(4)
C(17)	18(4)	17(4)	31(3)	-2(3)	-1(3)	-6(3)
C(18)	25(5)	14(4)	24(3)	-5(3)	0(3)	2(3)
C(19)	14(4)	24(4)	41(4)	-1(3)	2(3)	-7(3)
C(20)	26(5)	9(3)	30(3)	-5(3)	-3(3)	-3(3)
C(21)	30(5)	12(4)	28(3)	-2(3)	4(3)	-11(3)
C(22)	25(5)	19(4)	35(4)	-5(3)	-3(3)	-8(3)
C(23)	28(5)	16(4)	31(4)	-6(3)	5(3)	-15(3)
C(24)	28(5)	20(4)	32(4)	2(3)	-2(3)	-6(4)
C(25)	27(5)	13(4)	26(3)	-1(3)	1(3)	-6(3)
C(26)	21(4)	16(4)	22(3)	-3(2)	0(3)	-12(3)
C(27)	4(4)	15(4)	30(3)	-7(3)	0(2)	-5(3)
C(28)	18(4)	17(4)	28(3)	-4(3)	1(3)	-9(3)
C(29)	13(4)	12(4)	33(4)	-6(3)	3(3)	-3(3)
C(30)	15(4)	24(4)	22(3)	-3(3)	1(3)	-3(3)
C(31)	15(4)	9(3)	31(3)	-3(2)	-2(3)	-7(3)

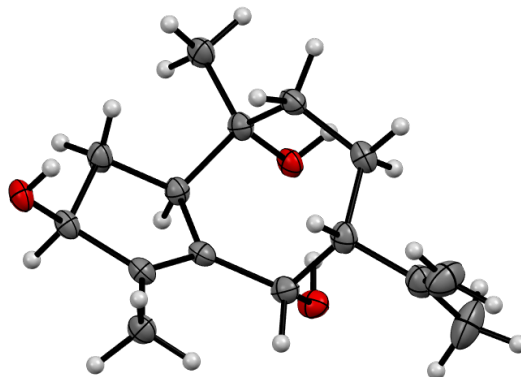
C(32)	51(6)	20(4)	32(4)	-4(3)	14(4)	-11(4)
C(33)	31(5)	19(4)	29(3)	4(3)	-2(3)	-9(4)
C(34)	30(6)	32(5)	40(4)	-19(4)	3(4)	-11(4)
C(35)	17(5)	41(6)	33(4)	-2(3)	3(3)	0(4)
C(36)	23(5)	15(4)	31(3)	-3(3)	-4(3)	-3(3)
C(37)	18(4)	12(4)	29(3)	-7(3)	0(3)	-3(3)
C(38)	29(5)	42(5)	18(3)	-3(3)	-6(3)	-9(4)
C(39)	67(7)	45(6)	29(4)	-16(4)	9(4)	-18(5)
C(40)	41(6)	25(5)	47(5)	-4(3)	-6(4)	3(4)
C(41)	67(8)	40(6)	65(6)	8(5)	-9(6)	-3(6)
C(42)	87(10)	37(6)	71(7)	14(5)	-28(6)	-26(6)
O(1)	19(3)	14(3)	32(3)	-3(2)	1(2)	9(2)
O(2)	22(3)	13(3)	36(3)	-2(2)	-1(2)	-3(2)
O(3)	23(3)	20(3)	32(3)	-8(2)	1(2)	-9(2)
O(4)	37(5)	131(9)	72(5)	-74(6)	9(4)	-19(5)
O(5)	6(3)	13(3)	30(2)	-1(2)	-2(2)	3(2)
O(6)	14(3)	21(3)	23(2)	-2(2)	-1(2)	-5(2)
O(7)	17(3)	11(2)	25(2)	-1(2)	-2(2)	1(2)
O(8)	32(4)	30(3)	26(2)	1(2)	0(2)	-13(3)
O(9)	41(4)	13(3)	31(3)	-3(2)	4(2)	-13(3)
O(10)	39(4)	16(3)	36(3)	-5(2)	2(2)	-8(3)
O(11)	24(3)	26(3)	32(3)	-12(2)	3(2)	-4(2)
O(12)	38(5)	139(10)	102(7)	-95(7)	31(5)	-46(6)
O(13)	20(3)	15(3)	27(2)	0(2)	6(2)	-6(2)
O(14)	12(3)	14(3)	31(2)	-3(2)	0(2)	-7(2)
O(15)	14(3)	23(3)	27(2)	-5(2)	-1(2)	-8(2)
O(16)	22(3)	32(3)	26(2)	0(2)	3(2)	-8(2)
O(17)	126(11)	107(9)	155(10)	-78(8)	90(9)	-73(8)
O(18)	61(5)	34(4)	76(5)	8(4)	19(4)	8(4)

Table 5. Hydrogen coordinates ($\times 10^4$) and isotropic displacement parameters ($\text{\AA}^2 \times 10^3$) for maimone86.

	x	y	z	U(eq)
H(1)	9945	3817	2544	23
H(2)	6114	3814	3566	28
H(4)	5062	3865	2169	25
H(5A)	6364	5362	1209	26
H(5B)	8937	5235	1538	26
H(6)	7684	3100	980	27
H(7)	11942	2391	1802	21
H(8A)	11475	1089	752	30
H(8B)	13965	830	1152	30
H(9)	13353	-1320	1564	25
H(11)	10388	1521	3050	23
H(13A)	10571	4817	3482	41
H(13B)	10243	3347	3918	41
H(13C)	8558	4857	4094	41
H(14A)	9622	4804	316	40
H(14B)	11452	3214	334	40
H(14C)	12020	4269	765	40
H(16A)	8701	-1716	-29	45
H(16B)	6797	-1201	565	45
H(16C)	8348	-2855	607	45
H(17A)	10596	-2363	2609	33
H(17B)	7874	-1288	2437	33
H(17C)	9158	-1266	3090	33
H(19A)	5143	-21	4579	40
H(19B)	4996	-542	3905	40
H(19C)	3334	1014	4030	40
H(20)	5776	6077	7466	26
H(21)	2817	6081	6425	27
H(23)	670	5992	7835	28
H(24A)	5398	4649	8451	33

H(24B)	2705	4513	8780	33
H(25)	1599	6774	9018	27
H(26)	5820	7459	8201	22
H(27A)	3198	8728	9248	19
H(27B)	5752	8994	8860	19
H(28)	3332	11172	8455	24
H(31)	4374	8372	6956	21
H(32A)	8203	4976	6550	53
H(32B)	6895	6475	6111	53
H(32C)	6742	4996	5920	53
H(33A)	6931	5746	9237	40
H(33B)	4885	4996	9648	40
H(33C)	4791	6617	9700	40
H(35A)	-3073	11977	9987	49
H(35B)	-3596	10840	9595	49
H(35C)	-4210	12507	9279	49
H(36A)	374	12240	7397	35
H(36B)	-1423	11174	7585	35
H(36C)	354	11128	6928	35
H(38A)	-2308	10497	6121	45
H(38B)	-2516	9009	5953	45
H(38C)	-1201	10038	5431	45
H(40A)	198	2709	5265	60
H(40B)	1481	2689	5923	60
H(40C)	2902	1610	5433	60
H(41A)	3722	5779	4463	74
H(41B)	3629	6450	5110	74
H(42A)	-289	7042	4268	97
H(42B)	1294	8118	4378	97
H(42C)	-606	7616	4949	97
H(5)	13800	-1152	2715	27
H(6A)	5971	964	2208	29
H(13)	4622	10954	7166	32
H(14)	-1347	9056	7852	27

X-Ray crystallographic Analysis of Compound 368



A colorless rod 0.050 x 0.030 x 0.020 mm in size was mounted on a Cryoloop with Paratone oil. Data were collected in a nitrogen gas stream at 100(2) K using phi and omega scans. Crystal-to-detector distance was 60 mm and exposure time was 5 seconds per frame using a scan width of 2.0°. Data collection was 100.0% complete to 67.000° in θ . A total of 71772 reflections were collected covering the indices, $-11 \leq h \leq 11$, $-11 \leq k \leq 11$, $-29 \leq l \leq 29$. 2579 reflections were found to be symmetry independent, with an R_{int} of 0.0569. Indexing and unit cell refinement indicated a primitive, trigonal lattice. The space group was found to be P 32 2 1 (No. 154). The data were integrated using the Bruker SAINT software program and scaled using the SADABS software program. Solution by iterative methods (SIR-2014) produced a complete heavy-atom phasing model consistent with the proposed structure. All non-hydrogen atoms were refined anisotropically by full-matrix least-squares (SHELXL-2014). All hydrogen atoms were placed using a riding model. Their positions were constrained relative to their parent atom using the appropriate HFIX command in SHELXL-2014. Absolute stereochemistry was unambiguously determined to be *R* at C3, C6, and C7, and *S* at C2 and C9, respectively.

Table 1. Crystal data and structure refinement for compound **368**.

X-ray ID	maimone54	
Sample/notebook ID	XH_479	
Empirical formula	C15 H24 O3	
Formula weight	252.34	
Temperature	100(2) K	
Wavelength	1.54178 Å	
Crystal system	Trigonal	
Space group	P 32 2 1	
Unit cell dimensions	a = 10.0004(2) Å	$\alpha = 90^\circ$.
	b = 10.0004(2) Å	$\beta = 90^\circ$.
	c = 24.4006(4) Å	$\gamma = 120^\circ$.
Volume	2113.32(9) Å ³	
Z	6	
Density (calculated)	1.190 Mg/m ³	
Absorption coefficient	0.646 mm ⁻¹	
F(000)	828	
Crystal size	0.050 x 0.030 x 0.020 mm ³	
Theta range for data collection	5.107 to 68.441°.	
Index ranges	-11 ≤ h ≤ 11, -11 ≤ k ≤ 11, -29 ≤ l ≤ 29	
Reflections collected	71772	
Independent reflections	2579 [R(int) = 0.0569]	
Completeness to theta = 67.000°	100.0 %	
Absorption correction	Semi-empirical from equivalents	
Max. and min. transmission	0.929 and 0.847	
Refinement method	Full-matrix least-squares on F ²	
Data / restraints / parameters	2579 / 0 / 169	
Goodness-of-fit on F ²	1.057	
Final R indices [I > 2σ(I)]	R1 = 0.0344, wR2 = 0.0817	
R indices (all data)	R1 = 0.0358, wR2 = 0.0826	
Absolute structure parameter	0.04(5)	
Extinction coefficient	n/a	
Largest diff. peak and hole	0.247 and -0.169 e.Å ⁻³	

Table 2. Atomic coordinates ($\times 10^4$) and equivalent isotropic displacement parameters ($\text{\AA}^2 \times 10^3$) for maimone54. $U(\text{eq})$ is defined as one third of the trace of the orthogonalized U^{ij} tensor.

	x	y	z	$U(\text{eq})$
C(1)	1429(2)	6260(2)	10026(1)	20(1)
C(2)	480(2)	6771(3)	10348(1)	23(1)
C(3)	1521(3)	8358(3)	10621(1)	25(1)
C(4)	2507(3)	8284(3)	11090(1)	24(1)
C(5)	3571(3)	7635(3)	10954(1)	23(1)
C(6)	2808(2)	5877(3)	10873(1)	22(1)
C(7)	2124(2)	5363(2)	10290(1)	21(1)
C(8)	3307(3)	5526(3)	9854(1)	24(1)
C(9)	2694(3)	5771(2)	9311(1)	22(1)
C(10)	1761(2)	6501(2)	9492(1)	21(1)
C(11)	649(3)	9158(3)	10807(1)	30(1)
C(12)	1170(3)	10622(3)	10674(1)	42(1)
C(13)	-767(4)	8284(4)	11149(1)	49(1)
C(14)	3949(3)	5331(3)	11003(1)	27(1)
C(15)	1293(3)	7322(3)	9088(1)	26(1)
O(1)	-488(2)	5610(2)	10734(1)	26(1)
O(2)	1512(2)	5073(2)	11241(1)	22(1)
O(3)	3883(2)	6639(2)	8923(1)	24(1)

Table 3. Bond lengths [\AA] and angles [$^\circ$] for maimone54.

C(1)-C(10)	1.338(3)	C(8)-H(8B)	0.9900
C(1)-C(2)	1.504(3)	C(9)-O(3)	1.425(2)
C(1)-C(7)	1.524(3)	C(9)-C(10)	1.510(3)
C(2)-O(1)	1.432(2)	C(9)-H(9)	1.0000
C(2)-C(3)	1.548(3)	C(10)-C(15)	1.499(3)
C(2)-H(2A)	1.0000	C(11)-C(12)	1.325(4)
C(3)-C(11)	1.517(3)	C(11)-C(13)	1.493(4)
C(3)-C(4)	1.536(3)	C(12)-H(12A)	0.9500
C(3)-H(3A)	1.0000	C(12)-H(12B)	0.9500
C(4)-C(5)	1.534(3)	C(13)-H(13A)	0.9800
C(4)-H(4A)	0.9900	C(13)-H(13B)	0.9800
C(4)-H(4B)	0.9900	C(13)-H(13C)	0.9800
C(5)-C(6)	1.539(3)	C(14)-H(14A)	0.9800
C(5)-H(5A)	0.9900	C(14)-H(14B)	0.9800
C(5)-H(5B)	0.9900	C(14)-H(14C)	0.9800
C(6)-O(2)	1.446(2)	C(15)-H(15A)	0.9800
C(6)-C(14)	1.525(3)	C(15)-H(15B)	0.9800
C(6)-C(7)	1.551(3)	C(15)-H(15C)	0.9800
C(7)-C(8)	1.538(3)	O(1)-H(1)	0.8400
C(7)-H(7)	1.0000	O(2)-H(2)	0.8400
C(8)-C(9)	1.528(3)	O(3)-H(3)	0.8400
C(8)-H(8A)	0.9900		
C(10)-C(1)-C(2)	126.1(2)	C(4)-C(3)-C(2)	112.96(18)
C(10)-C(1)-C(7)	111.83(19)	C(11)-C(3)-H(3A)	106.3
C(2)-C(1)-C(7)	122.08(17)	C(4)-C(3)-H(3A)	106.3
O(1)-C(2)-C(1)	110.73(18)	C(2)-C(3)-H(3A)	106.3
O(1)-C(2)-C(3)	112.53(16)	C(5)-C(4)-C(3)	117.24(17)
C(1)-C(2)-C(3)	110.94(18)	C(5)-C(4)-H(4A)	108.0
O(1)-C(2)-H(2A)	107.5	C(3)-C(4)-H(4A)	108.0
C(1)-C(2)-H(2A)	107.5	C(5)-C(4)-H(4B)	108.0
C(3)-C(2)-H(2A)	107.5	C(3)-C(4)-H(4B)	108.0
C(11)-C(3)-C(4)	110.78(17)	H(4A)-C(4)-H(4B)	107.2
C(11)-C(3)-C(2)	113.58(19)	C(4)-C(5)-C(6)	117.26(18)

C(4)-C(5)-H(5A)	108.0	C(1)-C(10)-C(9)	110.78(18)
C(6)-C(5)-H(5A)	108.0	C(15)-C(10)-C(9)	120.72(17)
C(4)-C(5)-H(5B)	108.0	C(12)-C(11)-C(13)	121.1(2)
C(6)-C(5)-H(5B)	108.0	C(12)-C(11)-C(3)	119.8(2)
H(5A)-C(5)-H(5B)	107.2	C(13)-C(11)-C(3)	119.1(2)
O(2)-C(6)-C(14)	107.08(16)	C(11)-C(12)-H(12A)	120.0
O(2)-C(6)-C(5)	110.45(16)	C(11)-C(12)-H(12B)	120.0
C(14)-C(6)-C(5)	110.43(18)	H(12A)-C(12)-H(12B)	120.0
O(2)-C(6)-C(7)	105.20(16)	C(11)-C(13)-H(13A)	109.5
C(14)-C(6)-C(7)	110.97(17)	C(11)-C(13)-H(13B)	109.5
C(5)-C(6)-C(7)	112.45(17)	H(13A)-C(13)-H(13B)	109.5
C(1)-C(7)-C(8)	101.48(15)	C(11)-C(13)-H(13C)	109.5
C(1)-C(7)-C(6)	116.53(18)	H(13A)-C(13)-H(13C)	109.5
C(8)-C(7)-C(6)	114.27(17)	H(13B)-C(13)-H(13C)	109.5
C(1)-C(7)-H(7)	108.0	C(6)-C(14)-H(14A)	109.5
C(8)-C(7)-H(7)	108.0	C(6)-C(14)-H(14B)	109.5
C(6)-C(7)-H(7)	108.0	H(14A)-C(14)-H(14B)	109.5
C(9)-C(8)-C(7)	105.49(17)	C(6)-C(14)-H(14C)	109.5
C(9)-C(8)-H(8A)	110.6	H(14A)-C(14)-H(14C)	109.5
C(7)-C(8)-H(8A)	110.6	H(14B)-C(14)-H(14C)	109.5
C(9)-C(8)-H(8B)	110.6	C(10)-C(15)-H(15A)	109.5
C(7)-C(8)-H(8B)	110.6	C(10)-C(15)-H(15B)	109.5
H(8A)-C(8)-H(8B)	108.8	H(15A)-C(15)-H(15B)	109.5
O(3)-C(9)-C(10)	115.33(17)	C(10)-C(15)-H(15C)	109.5
O(3)-C(9)-C(8)	113.22(18)	H(15A)-C(15)-H(15C)	109.5
C(10)-C(9)-C(8)	102.68(16)	H(15B)-C(15)-H(15C)	109.5
O(3)-C(9)-H(9)	108.4	C(2)-O(1)-H(1)	109.5
C(10)-C(9)-H(9)	108.4	C(6)-O(2)-H(2)	109.5
C(8)-C(9)-H(9)	108.4	C(9)-O(3)-H(3)	109.5
C(1)-C(10)-C(15)	128.5(2)		

Symmetry transformations used to generate equivalent atoms:

Table 4. Anisotropic displacement parameters ($\text{\AA}^2 \times 10^3$) for maimone54. The anisotropic displacement factor exponent takes the form: $-2\pi^2 [h^2 a^{*2} U^{11} + \dots + 2 h k a^* b^* U^{12}]$

	U ¹¹	U ²²	U ³³	U ²³	U ¹³	U ¹²
C(1)	19(1)	20(1)	19(1)	-2(1)	-4(1)	7(1)
C(2)	22(1)	28(1)	18(1)	3(1)	1(1)	12(1)
C(3)	30(1)	28(1)	19(1)	2(1)	2(1)	16(1)
C(4)	29(1)	23(1)	19(1)	-3(1)	-1(1)	12(1)
C(5)	23(1)	28(1)	17(1)	-2(1)	-3(1)	11(1)
C(6)	23(1)	27(1)	14(1)	2(1)	1(1)	12(1)
C(7)	24(1)	22(1)	17(1)	-1(1)	0(1)	12(1)
C(8)	32(1)	31(1)	16(1)	0(1)	0(1)	20(1)
C(9)	26(1)	21(1)	15(1)	-1(1)	0(1)	10(1)
C(10)	22(1)	20(1)	18(1)	-2(1)	-3(1)	8(1)
C(11)	37(1)	34(1)	23(1)	-2(1)	-1(1)	22(1)
C(12)	35(2)	35(1)	60(2)	0(1)	2(1)	21(1)
C(13)	54(2)	46(2)	58(2)	4(1)	22(1)	34(2)
C(14)	34(1)	38(1)	16(1)	0(1)	-2(1)	23(1)
C(15)	29(1)	32(1)	18(1)	2(1)	-1(1)	17(1)
O(1)	21(1)	29(1)	23(1)	4(1)	3(1)	10(1)
O(2)	26(1)	26(1)	13(1)	1(1)	1(1)	12(1)
O(3)	29(1)	23(1)	16(1)	-2(1)	3(1)	10(1)

Table 5. Hydrogen coordinates ($\times 10^4$) and isotropic displacement parameters ($\text{\AA}^2 \times 10^3$) for maimone54.

	x	y	z	U(eq)
H(2A)	-210	6899	10083	27
H(3A)	2261	9034	10332	30
H(4A)	3154	9341	11236	29
H(4B)	1802	7649	11387	29
H(5A)	4338	7936	11253	28
H(5B)	4146	8144	10616	28
H(7)	1301	4251	10308	25
H(8A)	4337	6419	9937	29
H(8B)	3391	4581	9838	29
H(9)	1975	4737	9149	26
H(12A)	641	11132	10798	50
H(12B)	2074	11160	10456	50
H(13A)	-1124	8984	11273	73
H(13B)	-529	7843	11467	73
H(13C)	-1579	7451	10930	73
H(14A)	4241	5524	11391	41
H(14B)	4873	5895	10775	41
H(14C)	3468	4223	10928	41
H(15A)	537	7544	9257	39
H(15B)	833	6666	8765	39
H(15C)	2205	8291	8977	39
H(1)	60	5421	10945	39
H(2)	1795	5386	11563	33
H(3)	4467	7530	9047	36